Keller-Segel-Type Models and Kinetic Equations for Interacting Particles: Long-Time Asymptotic Analysis

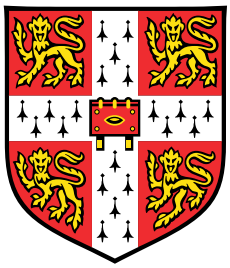

presented by

Franca Karoline Olga HOFFMANN

Member of Christ's College

University of Cambridge

Centre for Mathematical Sciences

Cambridge Centre for Analysis (CCA)

submitted April 2017

Supervised by

José Antonio Carrillo and Clément Mouhot

This dissertation is submitted for the degree of

Doctor of Philosophy (Mathematics).

Dissertation Summary

Franca Karoline Olga HOFFMANN

Keller-Segel-Type Models and Kinetic Equations for Interacting Particles: Long-Time Asymptotic Analysis

This thesis consists of three parts: The first and second parts focus on long-time asymptotics of macroscopic and kinetic models respectively, while in the third part we connect these regimes using different scaling approaches.

Keller–Segel-type aggregation-diffusion equations
We study a Keller–Segel-type model with non-linear power-law diffusion and non-local particle interaction: Does the system admit equilibria? If yes, are they unique? Which solutions converge to them? Can we determine an explicit rate of convergence? To answer these questions, we make use of the special gradient flow structure of the equation and its associated free energy functional for which the overall convexity properties are not known. Special cases of this family of models have been investigated in previous works, and this part of the thesis represents a contribution towards a complete characterisation of the asymptotic behaviour of solutions.

Hypocoercivity techniques for a fibre lay-down model
We show existence and uniqueness of a stationary state for a kinetic Fokker-Planck equation modelling the fibre lay-down process in non-woven textile production. Further, we prove convergence to equilibrium with an explicit rate. This part of the thesis is an extension of previous work which considered the case of a stationary conveyor belt. Adding the movement of the belt, the global equilibrium state is not known explicitly and a more general hypocoercivity estimate is needed. Although we focus here on a particular application, this approach can be used for any equation with a similar structure as long as it can be understood as a certain perturbation of a system for which the global Gibbs state is known.

Scaling approaches for collective animal behaviour models
We study the multi-scale aspects of self-organised biological aggregations using various scaling techniques. Not many previous studies investigate how the dynamics of the initial models are preserved via these scalings. Firstly, we consider two scaling approaches (parabolic and grazing collision limits) that can be used to reduce a class of non-local kinetic 1D and 2D models to simpler models existing in the literature. Secondly, we investigate how some of the kinetic spatio-temporal patterns are preserved via these scalings using asymptotic preserving numerical methods.

Remerciements

Mwanzo wa chanzo ni chane mbili...

It was at a seminar talk by Vincent Calvez one late afternoon in December 2011 at the ENS Lyon that I first heard about the study of biological aggregation by means of partial differential equations. I was amazed how very theoretical mathematical arguments from PDE Theory and Functional Analysis can contribute directly to the understanding of complicated phenomena we observe in nature. And I was fascinated by the videos of moving bands of *E. coli* . As the lecturer of my first PDE course and guiding my first research steps in a summer internship, it was Vincent who inspired my interest in PDE Analysis and who put me in touch with José Antonio Carrillo, who then took me on as a master student in the topic. Thanks to José Antonio's enjoyable supervision style and his infectious passion for the subject, I stayed on for a PhD, co-supervised together with Clément Mouhot at the University of Cambridge. I am extremely grateful to the Cambridge Centre for Analysis (CCA), especially James Norris, for allowing me to pursue an unusual PhD arrangement based jointly at University of Cambridge and Imperial College London under the supervision of José Antonio and Clément. It is a real honour to work with these two great mathematicians, to learn from them, and to be part of their academic family.

It is thanks to Clément that I was able to stay in my cohort at the Cambridge Centre of Analysis and be part of his very active research group in Cambridge, whilst continuing to work with José Antonio in London. I am very grateful for his support and generosity during the years of my thesis, for introducing me to the world of kinetic theory and passing on his enthusiasm for the subject. Thank you for suggesting a research problem that I am passionate about, for making the very enjoyable collaboration with Émeric Bouin possible and for handling many administrative challenges related to my PhD arrangement.

Most of my thesis has been supervised by José Antonio, who has been a role model to me both on an academic and on a personal level. His clairvoyance and problem solving skills (mathematical and otherwise), as well as his pedagogical and organisational skills are exceptional. Discussions with him are highly enjoyable and rewarding, his stamina to explain things is astounding, and he always brings with him a positive attitude and a smile. He believes in the research abilities of his students and sees them as actual assets, rather than burdens. I am ∞-ly grateful for the numerous opportunities that he provided during my PhD by suggesting collaborations, research programs and conferences, inspiring me to take up an academic research career and fostering my development towards a mathematical globetrotter in the process. It is for good reasons that he was awarded the 'Best Supervision Award 2016' by the Imperial College Union following our nomination, since, in Markus' words, "he puts the *super* in supervisor". I cannot thank you enough for all

your time, your support, your mentorship, your availability, your patience and encouragements, your open ear, for sharing your mathematical thought process in a way that is both inspiring and educational, for your advice and help in navigating the academic world, for accepting to supervise me under several rather unconventional arrangements, for never stopping to believe in me, for putting up with my sometimes crazy plans, interests and adventures (be it exchanging my office for a bus on a bumpy road in Kenya, being taken up by wardening duties, or trying Swedish Surströmming), and thank you for making my PhD such an enjoyable experience.
Another person who has played a significant role for the shaping of this thesis and my decision to continue in academia is Vincent Calvez. Thank you for being a great mentor, for all your support, your encouragements and your patience, they were invaluable. Thank you for taking care of me as if I would be one of your own students and for giving me the possibility to return to the beautiful city of Lyon so many times.
During the time of my PhD, I had the chance to meet, learn from and work with many talented mathematicians that have shaped my idea of what it means to be a researcher. It is through bouncing off ideas, seeing a problem through somebody else's eyes and being able to ask questions that mathematics comes alive. As I've learned in Kenya:

Iwapo unataka kwenda haraka, nenda peke yako;
Iwapo mnataka kwenda mbali, nendeni pamoja.[1]

I'm especially grateful to my collaborators and mentors Raluca Eftimie, Émeric Bouin, Eric Carlen, Jean Dolbeault, Bruno Volzone, Edoardo Mainini and Peter Dobbins – thank you for fruitful discussions, virtual and in front of blackboards, and for teaching me new interesting mathematics. Finally, I thank my examiners Adrien Blanchet and Carola Schönlieb, who accepted to read all these words.

My time as a PhD student was an exciting, eventful, diverse, sometimes challenging, and mostly enjoyable journey shaped by people from all around the globe. First of all, let me mention my PhD brothers and sisters Francesco, Markus, Rafa and Sergio from the London side, and Ludovic, Jo, Megan, Helge, Tom, Sara and Marc from the Cambridge side, my office mates in London Marina, Marco, Tom, Sam, Nik, Onur, Maddy, Urbain, Anna, Cezary, Massi, Luca, Silvia and Martin, and my fellow CCAers in Cambridge Adam, Harold, Karen, Ellen, Ben, David, Dominik, Davide, Eavan and Sam, and the many mathematicians that I had the chance working, travelling and conferencing with Pedro, Esther, Ewelina, Émeric, Amit, Ariane, Yao, Gaspard, Mikaela, Oliver, Álvaro, Nils, José Alfredo, Simone, Young-Pil, Yanghong, Aneta, Claudia, Francesco, Anna, Gabi, Katrin, Susanne ... and many others. The PhD ride was so much more enjoyable sharing it with

[1] If you want to go quickly, go alone; If you want to go far, go together.

you, from all sorts of dinners to self-organised office seminars, spontaneous dancing sessions and conference laser quest.
Further, thanks to the 2015-16 Imperial College SIAM chapter team Michael, Juvid, Hanne, Alex, Adam, Marina and Arman, and the Imperial College Maths Helpdesk team Alexis, Michael, Tom, Isaac and Sam for all your enthusiasm and for putting up with me in so many meetings, not to forget the resourceful Anderson Santos for battling Imperial College administration on our behalf and always lending an open ear.
Turning the task of taking care of hundreds of freshers (trust me, a recommendable life training) into an enjoyable challenge, I was lucky to live with the most amazing warden teams João, Arash, Mirko, Abi, Stu, Tas, Sei and Ben. You are my South Kensington family. Thanks to several energetic warden and hall senior teams for uncountable 8 am meetings, dinners, parties, BBQs, eventful freshers fortnights and for putting up with all my travel plans, (and yes, it's a djembe, not a bongo!).
A big influence on the kind of proverbs and quotes in this thesis comes from unforgettable moments spent on the African continent thanks to the amazing people of AMI and SAMI, and the many volunteers from all around the world that put their time, brains, sweat and hearts into making maths camps and other educational initiatives happen across Africa and in the UK. I'm grateful to have found you and to be part of this very inspiring network of people, you have changed my view on the world. And of course, all of this would have never been possible without José Antonio and Clément being supportive of my different parallel lifes.

Last but not least, thanks to all the special people in my life who are always there for me, no matter where, no matter when, it is impossible to name you all, but you know who you are. I thank my adopted families the Heepe-Sullivans and the Bichets who gave me a home away from home, vous avez pour toujours une place très spéciale dans mon cœur. For their friendship and support for many years, I am grateful to Ileana, Ronja Räubertochter, Natalia, Féfé, Terja, Céleste, Janine, Judith, Dobriyana, Julie, Srinjan, Njoki, Wafa, Marina, Marco (pineapple on pizza?), to Markus for special party and Spätzle-making skills and his unbeatable sense of humour, and of course to my beloved *String Theory* people. How could I ever forget the hours of music around mountains of cheese only topped by Uruguayan asado? Thanks to Kin for helping me to keep up and progress on the viola and for unforgettable duo performances in Lyon, Stockholm, London and Cambridge, to Agustin Omwami for a unique goat experience and so much more, to David Stern for important life advice, to Arieh Iserles for several philosphical coffees, to Juan Luis Vázquez Suárez for perspicacious stories on the life as a mathematician, to my maths teacher Michael Mannheims for his inspiring way of teaching, to our Mathe-LK of which certain people manage to generate, year after year, entertaining Christmas stories, and to my kizomberos and salseros, who make sure I'm

staying (in)sane.
Wer mich am meisten zu Verrücktheiten inspiriert und mich davor bewahrt gar zu verrückt zu werden ist meine Familie. Danke an Opa Jörg, der es immer wieder schafft, die Großfamilie zusammen zu führen, an meine Eltern, die mir Flügel und einen sicheren Hafen schenken, an meinen talentierten Bruder, unseren Fisch-Experten, der immer für mich da ist, an Lisa, an meine Onkels und Cousinen mit Familie, die immer ein offenes Ohr für mich haben und mit denen ich gerne mehr Zeit verbringen würde. Meine Familie hat es nach mehr oder weniger erfolgreichen Erklärungsversuchen inzwischen aufgegegeben, zu verstehen, was ich nun eigentlich genau in meiner Doktorarbeit erforsche, und dennoch geben sie mir immer neue Energie und Motivation. Wie mein Papa so oft sagt, wenn er sieht wie ich Integrale auf's Papier werfe: "Also, ich kann das jetzt nur ästhetisch beurteilen..."

Statement of Originality

I hereby declare that my dissertation entitled 'Keller-Segel-Type Models and Kinetic Equations for Interacting Particles: Long-Time Asymptotic Analysis' is not substantially the same as any that I have submitted, or, is being concurrently submitted for a degree or diploma or other qualification at the University of Cambridge or any other University or similar institution. I further state that no substantial part of my dissertation has already been submitted, or, is being concurrently submitted for any such degree, diploma or other qualification at the University of Cambridge or any other University or similar institution, except as declared in this text. This dissertation is the result of my own work and includes nothing which is the outcome of work done in collaboration except where specifically indicated in this text.

Chapter 1 motivates the research problems investigated in this thesis, gives an overview of the mathematical methods and techniques that are relevant for Chapters 2-6, provides an overview of the literature and states the main results of this thesis. The literature review was done under the guidance, explanations and supervision of Professor José A. Carrillo[2] and Professor Clément Mouhot[3].

The original research problem that led to the results in Part I (Chapters 2-4) was suggested by Professor José A. Carrillo. Chapters 2 and 3 are original research work produced in collaboration with Professor José A. Carrillo and Professor Vincent Calvez[4]. Chapter 4 is original research work produced in collaboration with Professor José A. Carrillo, Professor Edoardo Mainini[5] and Professor Bruno Volzone[6]. Professor José A. Carrillo was the one who suggested the collaborations. The radiality proof in Section 2.1 of Chapter 4 was contributed by Professor José A. Carrillo and Professor Bruno Volzone, but has been included here for completeness.

Part II (Chapter 5) is original research work produced in collaboration with Professor Clément Mouhot and Doctor Emeric Bouin[7]. Professor Clément Mouhot suggested the research problem and the collaboration.

[2]Department of Mathematics, Imperial College London, South Kensington Campus, London SW7 2AZ, UK.
[3]DPMMS, Centre for Mathematical Sciences, University of Cambridge, Wilberforce Road, Cambridge CB3 0WA, UK.
[4]Unité de Mathématiques Pures et Appliquées, CNRS UMR 5669 and équipe-projet INRIA NUMED, École Normale Supérieure de Lyon, Lyon, France.
[5]Dipartimento di Ingegneria Meccanica, Università degli Studi di Genova, Genova, Italia.
[6]Dipartimento di Ingegneria, Università degli Studi di Napoli "Parthenope", Napoli, Italia.
[7]CEREMADE - Université Paris-Dauphine, UMR CNRS 7534, Paris, France.

Part III (Chapter 6) is original research work produced in collaboration with Professor José A. Carrillo and Professor Raluca Eftimie[8]. The collaboration was suggested by Professor José A. Carrillo. Section 2.2 in Chapter 6 was contributed by Professor Raluca Eftimie. Section 3.2 in Chapter 6 was contributed by Professor José A. Carrillo. Some of the results presented in Chapter 6 were already part of my master thesis, namely: (1) a special case of Remark 2.2, (2) the parabolic drift-diffusion limit in Section 3.1, and (3) a theoretical development of the AP scheme used in Section 4, all for the case $\lambda_1 = 0$. These parts have been included in this dissertation to allow for a comprehensive and self-contained presentation of Chapter 6.

[8] Division of Mathematics, University of Dundee, Dundee, UK.

Dzigbodi wotso koa anyidi
dide hafi kpona efe doka.

If you patiently dissect an ant,
you will see its entrails [9].

Ghanaian proverb (Ewe)

[9] With patience, you can accomplish the most difficult task.

Für Margarita & Freimut, meine Eltern,
die fast alle Verrücktheiten ihrer Tochter mitmachen
und mich bedingungslos unterstützen.

Contents

Preamble

This thesis is centered around the analysis of non-linear partial differential equations arising naturally from models in physics, mathematical biology, fluid mechanics, chemistry, engineering and social science. Often, these models have hidden connections across applications, and the structural similarities in their dynamics allow us to apply the same mathematical techniques in very different physical contexts. Non-linearities and long-range interactions in addition to local effects pose analytical challenges that cannot be tackled with conventional PDE methods. This thesis focuses on developing new mathematical tools to understand the behaviour of these models, in particular their asymptotics.

The first chapter is an introduction, presenting the mathematical context, motivations and necessary tools for the chapters to follow. The introduction is structured by parts (Part I: Chapters 2-4, Part II: Chapter 5, Part III: Chapter 6) and provides and overview of the results obtained in this thesis. All following chapters each correspond to an article or book chapter.

List of works contained in this thesis:

- Chapter 2: article [63], in collaboration with Vincent Calvez[4] and José A. Carrillo[1], published in the special issue "Advances in Reaction-Cross-Diffusion Systems" of *Nonlinear Analysis TMA*.
- Chapter 3: book chapter [64], in collaboration with Vincent Calvez[4] and José A. Carrillo[1], to appear in "Nonlocal and Nonlinear Diffusions and Interactions: New Methods and Directions" as part of the C.I.M.E. Foundation Subseries "Lecture Notes in Mathematics" at *Springer*.
- Chapter 4: article [90], in collaboration with José A. Carrillo[1], Edoardo Mainini[5] and Bruno Volzone[6], submitted for publication.
- Chapter 5: article [49], in collaboration with Emeric Bouin[7] and Clément Mouhot[3], accepted for publication in *SIAM Journal on Mathematical Analysis*.
- Chapter 6: article [84], in collaboration with José A. Carrillo[1] and Raluca Eftimie[8], published in *Kinetic and Related Models*.

How to read this thesis

Each chapter is written to be self-contained. The logical relations between the chapters are the following: Chapter 3 builds on the results in Chapter 2. Chapter 4 is tackling similar questions to Chapter 2, but in a different regime, and using different tools in some cases. For part I, an overview of the different regimes and their definitions can be found in Chapter 1. Chapters 5 and 6 are each fully self-contained. The logical order of reading this thesis would be the order it is presented, or changing the order of any of the parts I-III. A short overview of conclusions and perspectives can be found at the very end of the thesis.

In order to keep the notation simple, equations are numbered by section number in each chapter. For example, when reading Section 3 of Chapter 4, the first equation in that section would be numbered (3.1). Cross-references to equations in other chapters are explicitly mentioned. When reading Chapter 2, the same equation would be referenced as "equation (3.1) in Chapter 4". The same holds true for (sub)sections, theorems, definitions, propositions, corollaries, lemmata and remarks. Figures however are numbered per chapter, e.g. Figure 3.14 refers to the 14^{th} figure in Chapter 3. References are listed together for all chapters at the end of the thesis in a general bibliography.

All historical footnotes about mathematicians are taken either from [174], or from wikipedia[10].

Funding

This thesis would not have been possible without the financial support that allowed its realisation. It was supported by EPSRC grant number EP/H023348/1 (for the Cambridge Centre for Analysis), ERC Grant MATKIT (ERC-2011-StG) and EPSRC Grant Number EP/P031587/1, in addition to funding from a number of organisations that supported me in the attendance of conferences, workshops and research programs over the course of my Ph.D[11]. I would also like to thank Professor Vincent Calvez, who generously supported numerous research visits to the ENS Lyon, resulting in fruitful collaborations.

[10] www.wikipedia.org/.

[11] Centro Internazionale Matematico Estivo (Italy), Christ's College (Cambridge, UK), CNRS-PAN Mathematics Summer Institute (Cracow, Poland), Gran Sasso Science Institute (L'Aquila, Italy), Gruppo Nazionale per la Fisica Matematica (Italy), Hausdorff Center for Mathematics (Bonn, Germany), Institute of Mathematics of Polish Academy of Sciences (Warsaw, Poland)), KI-Net Research Network in Mathematical Sciences (US), Mittag-Leffler Institute (Stockholm, Sweden), Santander (UK).

Chapter 1

Introduction

Chapter Content

Most applied mathematicians spend their time developing, improving, analysing and testing mathematical models – equations that describe a physical phenomenon – trying to make sense of the (physical and/or mathematical) world. Of course, mathematical models will never be able to capture the full reality and complexity of nature. Most of the models we currently use are based on simplifying assumptions that are rarely satisfied in practice. This is not to say that simplification renders a model less useful as a tool to understand the world. On the contrary, it is this simplifying aspect that gives us powerful information about the dominant dynamics at play. Good mathematical models find a reasonable trade-off between simplicity, complexity and mathematical difficulty. If a model is too simple, important physical features may be lost. If it is too complex on the other hand, incorporating many details of the observed phenomena, we may not be able to handle the analysis and so no useful information can be extracted from the model. It is when we are able to successfully analyse a model that provides a reasonable approximation to a complicated real world process that we can claim to have understood the dominant driving principles – a powerful source of information for applications. In order to build the mathematical tools and theories that allow us to handle the analysis of a particular equation, it is often useful to start with a master equation – the simplest model one can think of that is representative for a more general class of models and still incorporates the common structural difficulties. One such master equation for the class of models analysed in this thesis is the non-linear heat equation $\partial_t \rho = \Delta \rho^m$, $m > 0$ which appears in a number of applications across physics, chemistry, biology and engineering (see Section 2.1 for more details). It extends the structural difficulty of another master equation, the heat equation ($m = 1$), by adding the non-linearity to the diffusion. Historically, it has often been thanks to a representative master equation generating a rich mathematical theory that more complex and therefore more realistic models could be tackled. What is so fascinating is that models of similar mathematical form and difficulty can appear in the context of very different applications. Understanding more about their general structure gives us new insights about nature's laws, allowing us to see the beautiful unifying patterns that surround us.

This thesis is centered around the analysis of non-linear partial differential equations arising naturally from models in physics, mathematical biology, fluid mechanics, chemistry, engineering and social science. Often, these models have hidden connections across applications, and the structural similarities in their dynamics allow us to apply the same mathematical techniques in very different physical contexts. Non-linearities and long-range interactions in addition to local effects pose analytical challenges that cannot be tackled with conventional PDE methods. This thesis focuses on developing new mathematical tools to understand the behaviour of these models, in particular their asymptotics.

The choice of title for this thesis and the sense in which it is to be understood deserve a few explanatory words. First of all, the term *interacting particles* should be taken in a very broad interpretation. Here, the 'particles' can represent for example molecules of a gas, single-cell organisms such as bacteria, stars in a galaxy, lay-down points of polymer fibres, insects, fish, birds, ungulates, or even humans. Correspondingly, the interaction of particles with each other, or with their environment, could be via molecular forces, chemical signals[1], gravitational forces, an external force describing the coiling properties of the polymer fibres, or - in the case of animals and humans - visual, auditory or tactile signals. The type of interaction could be linear or non-linear, local or non-local. Both linear local interactions (Chapter 5) and non-linear non-local interactions (Chapters 2, 3, 4 and 6) are considered in this thesis.

Secondly, let me comment on what I mean by *asymptotic analysis*. Two types of asymptotics have to be distinguished:

(1) the behaviour of solutions predicted by the model after a very long time $t \to \infty$ which we call *long-time asymptotic behaviour* or ergodic properties (Chapters 2-5), and

(2) the limiting equations obtained by letting certain parameters of a model be either very big or very small (Chapter 6).

As suggested by the title, the main focus lies in the long-time asymptotic analysis, but we also consider limiting processes.

In case (1), we want to know whether solutions converge to an asymptotic profile and if yes, in which sense and how fast. What do these asymptotic profiles look like? How many are there, and what is their basin of attraction? The natural candidates amongst which to look for asymptotic profiles are the equilibrium states of the model under consideration. This means that the first

[1]The ability of certain types of bacteria to respond to chemical gradients is known as *bacterial chemotaxis*, see Section 1.

logical step towards understanding the asymptotic behaviour of solutions is often to study the stationary problem instead, which is our focus in Chapters 2, 3 and 4. It is only in Chapters 3 and 5 that we actually study the evolution problem with the aim of finding explicit rates of convergence.

Case (2) makes the connection between different observation scales, using a set of methods called *multiscale analysis* or *scaling process* or *limiting process*. Let us take the example of a monoatomic gas. Using Newton's[2] laws, one can write down an equation for n interacting gas particles located at positions $X_1(t), \dots, X_n(t)$. This type of model is usually referred to as a *particle-based model*, or *Individual Based Model* (IBM) in the case where the particles represent living organisms, see Section 2.2.2. In practice however, it is often hopeless to attempt to describe the position and velocity of every particle if the number of particles is large[3]. Using statistical ideas, we can instead describe the evolution of the probability density $f(t, x, v)$ of a certain particle to be at location x and travelling with velocity v at time t. One example of such a model is the *Boltzmann equation* modelling the particle distribution of a monoatomic rarefied gas, see Section 8. This level of description is called *kinetic* since the function f depends not only on space and time, but also on velocities. There are several techniques that allow us to go from a particle description to a kinetic description of the same evolution process, but this interesting and still developing mathematical field is not the focus of this thesis[4]. We may also want to make a connection between different kinetic descriptions, for example when the difference between velocities before and after a collision is small, known as *grazing collisions*, see Section 8.1. In Chapter 6, we use this idea applied to animals turning only a small angle upon interactions with neighbours such as migratory birds following favourable winds or magnetic fields.

In practise however, all that our typical observation can detect are changes in the macroscopic state of the gas, described by quantities such as density, bulk velocity, temperature, stresses, and heat flow, and these are related to some suitable averages of quantities depending on the kinetic probability density. It is therefore desirable to be able to describe the dynamics at a macroscopic scale, using for example a *hydrodynamic scaling*[5]. The idea is to rescale time and space by the change of variables $(t, x, v) \mapsto (t/\varepsilon^\gamma, x/\varepsilon, v)$ for a small scaling parameter $\varepsilon \ll 1$, together with certain scaling assumptions specifying how the interaction term behaves in the limit $\varepsilon \to 0$. The

[2] Isaac Newton (1642-1727) was an English mathematician, astronomer, and physicist who is widely recognised as one of the most influential scientists of all time and a key figure in the scientific revolution. His three laws of motion were first published in *PhilosophiæNaturalis Principia Mathematica* in 1687. Beyond his work on the mathematical sciences, Newton dedicated much of his time to the study of alchemy and biblical chronology. In a manuscript from 1704 he estimated that the world would end no earlier than 2060.

[3] The number of air molecules at atmospheric pressure and at 0° C temperature is around 2.7×10^{19} per cm^3, a lot more than what would be feasible to keep track of.

[4] Some of the more common regimes are *low density limits*, *weak coupling limits* or *mean-field limits*, see for example [259, 263], or Section 2.2.4 for the latter.

[5] For more details on the techniques involved, see Sections 6.2.3 and 8.

two main scaling approaches are *parabolic limits* ($\gamma = 2$) for which diffusive forces dominate, and *hyperbolic limits* ($\gamma = 1$), which are convective.

In terms of modelling perspective, Part I (Chapters 2-4) deals with a macroscopic model, Part II (Chapter 5) is concerned with a kinetic model, and Part III (Chapter 6) focuses on the connection between different kinetic and macroscopic regimes using parabolic and grazing collision limits.

Finally, the term *Keller–Segel-type models* in the title of this thesis refers to models that are close variations of what is known as the classical Keller–Segel model, which we describe in more detail in the next section.

This introductory chapter is structured into 9 sections: Section 1 describes the classical Keller–Segel model, and subsequent sections correspond to Part I (Sections 2-4), Part II (Sections 5-7) and Part III (Sections 8-9) of this thesis. For each part, we explain the relevant mathematical tools, introduce the models we are analysing in this thesis together with the most important notation, give some motivation and context of the problem, and last but not least, present a summary of the results obtained and possible perspectives.

1 The Keller–Segel model

Many bacteria, such as *Escherichia coli*, *Rhodobacter sphaeroides* and *Bacillus subtilus* (see [149] for a complete list), are able to respond to changes in the surrounding environment by a biased random walk. This allows cells to interact with each other by secreting a chemical substance to attract cells around them. The directed movement of cells and organisms in response to chemical gradients is called *chemotaxis*. This occurs for instance during the starvation stage of the slime mold *Dyctiostelium discoideum*. More generally, chemotaxis is widely observed in various biological fields (morphogenesis, bacterial self-organisation and inflammatory processes among others). The bacterium *Escherischia coli* is traditionally chosen for studying bacterial chemotaxis as its biochemistry as well as the dynamics of its movement are well understood.

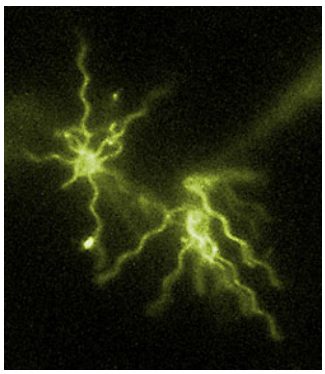

Figure 1.1: Fluorescently labeled *E. coli* . Source: Howard Berg's website[9].

Let us denote the density of bacteria and the chemoattractant concentration at position $x \in \mathbb{R}^2$ and time $t \geqslant 0$ by $\rho(t,x)$ and $S(t,x)$ respectively. Assume that cells and chemoattractant diffuse with diffusion coefficients D_ρ and D_S, and that the chemoattractant degrades with rate $\alpha \geqslant 0$ due to chemical reactions whilst it is secreted by the bacteria at rate $\beta \geqslant 0$. Then the evolution of ρ and S can be modelled by the following system known as the *Keller*[6]*–Segel*[7] *model*:

$$\begin{cases} \partial_t \rho &= D_\rho \Delta \rho - \chi \nabla \cdot (\rho \nabla S)\,, \\ \partial_t S &= D_S \Delta S - \alpha S + \beta \rho\,. \end{cases} \tag{1.1}$$

Here, $\chi > 0$ denotes the effective bacterial chemotaxis speed and is assumed to be constant. Historically, the Keller–Segel model has been the principal approach to describe bacterial motion [280, 256]. First introduced in 1970 in [196] to describe aggregation of slime mold amoebae, this model has become one of the most widely studied models in mathematical biology. It is sometimes also referred to as the Patlak[8]–Keller–Segel model as the decoupled problem has already been formulated in 1953 by Patlak [252]. A certain number of reaction-diffusion models have been developed since, mostly inspired by the pioneering work of Keller and Segel. Even if these models have helped to understand certain characteristics of bacterial chemotaxis, they also have their limits from a modelling perspective, and we will comment on some of them in this thesis.

[6] Evelyn Fox Keller (born 1936) is an American physicist, author and feminist.
[7] Lee Aaron Segel (1932-2005) was an American mathematician known for his work in the spontaneous appearance of order in convection, slime molds and chemotaxis.
[8] Clifford S. Patlak (1935-2014).
[9] www.rowland.harvard.edu/labs/bacteria/movies/index.php

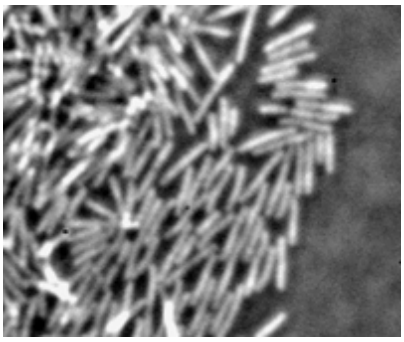

Figure 1.2: An *E. coli* swarm. Source: Howard Berg's website[10].

The reason why the Keller–Segel model (1.1) has received so much attention in the mathematical community over the last decades, see [196, 197, 243, 194, 159, 136, 41, 256], is a peculiar phenomenon: the fact that the mass of bacteria appears as a critical parameter. More precisely, let us consider (1.1) when the chemoattractant is in quasi-equilibrium ($\partial_t S = 0$), and when the time scale of observation is a lot smaller then the speed at which S degrades ($\alpha = 0$). The first assumption represents the hypothesis that $\partial_t \rho$ is very big in comparison to $\partial_t S$ and is a realistic approximation for example for very big cells which have a considerably lower displacement speed. For simplicity, let us further assume that $D_\rho = D_S = \chi_S = \beta = 1$. Under these assumptions, the second equation in (1.1) reduces to $\Delta S = -\rho$. This Poisson equation can be solved explicitly for S in terms of ρ using the fundamental solution of the Laplacian, and substituting into the evolution equation for ρ, we obtain in two space dimensions

$$\partial_t \rho = \Delta \rho + \frac{1}{2\pi} \nabla \cdot (\rho \nabla \log |x| * \rho) \ . \tag{1.2}$$

For sufficiently smooth weak solutions $\rho(t) \in L^1(\mathbb{R}^2)$ with mass $M = \int \rho \, dx$, we can calculate the dissipation of the second moment explicitly using integration by parts:

$$\begin{aligned}
\frac{d}{dt} \int_{\mathbb{R}^2} |x|^2 \rho(t,x) \, dx &= \int_{\mathbb{R}^2} |x|^2 \left(\Delta \rho + \frac{1}{2\pi} \nabla \cdot (\rho \nabla \log |x| * \rho) \right) dx \\
&= 4 \int_{\mathbb{R}^2} \rho \, dx - \frac{1}{2\pi} \int_{\mathbb{R}^2} 2x \cdot \left(\rho(x) \int_{\mathbb{R}^2} \frac{(x-y)}{|x-y|^2} \rho(y) \, dy \right) dx \\
&= 4M - \frac{1}{2\pi} \int_{\mathbb{R}^2} x \cdot \left(\rho(x) \int_{\mathbb{R}^2} \frac{(x-y)}{|x-y|^2} \rho(y) \, dy \right) dx \\
&\quad - \frac{1}{2\pi} \int_{\mathbb{R}^2} y \cdot \left(\rho(y) \int_{\mathbb{R}^2} \frac{(y-x)}{|y-x|^2} \rho(x) \, dx \right) dy \\
&= 4M - \frac{1}{2\pi} \iint\limits_{\mathbb{R}^2 \times \mathbb{R}^2} \frac{(x-y) \cdot (x-y)}{|x-y|^2} \rho(x) \rho(y) \, dx dy \\
&= \frac{M}{2\pi} (8\pi - M) \ .
\end{aligned}$$

This calculation shows how the critical mass $M_c = 8\pi$ emerges from the structure of the equation and as a result, solutions are subject to a remarkable dichotomy: they exist globally in time if $M < 8\pi$ (diffusion overcomes self-attraction), whereas blow-up occurs in finite time when $M > 8\pi$ (self-attraction overwhelms diffusion). This transition has been first formulated in [113]. Mathematical contributions are [194] for the existence part, [242] for the radial case, and [136, 41] in the full space. The critical case $M = 8\pi$ was analysed further in [40, 37, 75] in terms of stability of stationary states. In the sub-critical case $M < 8\pi$, it has been shown that solutions decay to

[10] www.rowland.harvard.edu/labs/bacteria/projects/swarming.php

self-similarity solutions exponentially fast in suitable rescaled variables [70, 71, 148]. In the super-critical case $M > 8\pi$, solutions blow-up in finite time with by now well studied blow-up profiles for close enough to critical mass, see [187, 260, 168]. In part I of this thesis, we are generalising the techniques developed in [62] where the authors show convergence to self-similarity in Wasserstein distance for (1.2) in the radial sub-critical case $M < 8\pi$.

2 Part I: Keller–Segel-type aggregation-diffusion equations

In the first and main part of this thesis, we are studying the behaviour of a family of partial differential equations of Keller-Segel-type modelling self-attracting diffusive particles at the macroscopic scale,

$$\partial_t \rho = \frac{1}{N}\Delta \rho^m + 2\chi \nabla \cdot (\rho \nabla (W * \rho)) \,, \quad t > 0 \,, \quad x \in \mathbb{R}^N \,. \tag{2.3}$$

Here, the diffusion is non-linear if $m \neq 1$, and the non-local interaction between particles is governed by the *interaction potential* W with $W : \mathbb{R}^N \to \mathbb{R}$, $W \in \mathcal{C}^1\left(\mathbb{R}^N \backslash \{0\}\right)$ and $W(-x) = W(x)$. The parameter $\chi > 0$ is measuring the *interaction strength* of the interaction term in relation to the diffusive term. Equation (2.3) exhibits three conservation laws: conservation of positivity, conservation of mass, and invariance by translation. We can therefore assume for convenience

$$\rho(t = 0, x) = \rho_0(x) \geqslant 0 \,, \quad \int_{\mathbb{R}^N} \rho_0(x)\, dx = 1 \,, \quad \int_{\mathbb{R}^N} x \rho_0(x)\, dx = 0 \,. \tag{2.4}$$

The parameter $\chi > 0$ scales with the mass of solutions ρ, and therefore, in the case where the behaviour of solutions depends on the choice of initial mass, this criticality is transferred to the parameter χ when fixing the mass. Let us point out that Part I does not address the questions of regularity, existence, or uniqueness of solutions to equation (2.3), assuming solutions are 'nice' enough in space and time for our analysis to hold.

We will now give some intuition to explain the type of behaviour that can be modelled using equation (2.3). Conceptually, the PDE (2.3) corresponds to the assumption that two main forces determine a particle's motion at the microscopic level: local non-linear diffusion on the one hand, and non-local attraction on the other hand. Diffusion can be understood as a repulsive force between particles, whereas the interaction between particles is assumed to be represented by an attractive potential, W. Here, attractive and repulsive forces compete, generating complex behviour of solutions, depending on the diffusion power m, the choice of interaction potential W, the interaction strength $\chi > 0$ and the dimensionality N.
The reason why models of the form (2.3) have attracted so much attention in recent years is not only their rich mathematical structure, but also their applicability to a wide range of physical problems ranging from collective behaviour of self-interacting individuals such as bacterial chemo-

taxis [39, 196, 252], astrophysics [108, 271, 105, 107, 106] and mean-field games [38] to phase transitions [285] and opinion dynamics [164, 165].

Before diving into the analysis of (2.3), let us investigate the dynamics of attractive and repulsive forces separately.

2.1 Non-linear diffusion

Assuming $\chi = 0$, one can interpret equation (2.3) as a non-linear heat equation, where the diffusion coefficient varies with the density of particles,

$$\partial_t \rho = \frac{1}{N}\Delta \rho^m = \nabla \cdot (D(\rho)\nabla\rho)\,, \qquad D(\rho) := \frac{m}{N}\rho^{m-1}\,, \qquad m > 0\,. \tag{2.5}$$

As above, we assume that the initial data satisfies (2.4). Diffusion can be understood as a repulsive force since 'nice' enough solutions ρ of (2.5) satisfy

$$\frac{d}{dt}\int_{\mathbb{R}^N} |x|^2 \rho(t,x)\,dx = 2\int_{\mathbb{R}^N} \rho^m(t,x)\,dx\,.$$

It follows that if $\rho(t,\cdot) \in L^1_+(\mathbb{R}^N) \cap L^m(\mathbb{R}^N)$ for any $t > 0$, then the second moment of ρ increases with time, that is, the solution is spreading out. The resulting effect is that particles get repulsed away from each other.

Equation (2.5) is one of the simplest examples of a non-linear evolution equation of parabolic type. It appears in a natural way in a number of applications across physics, chemistry, biology and engineering. The common idea is that in many diffusion processes the diffusion coefficient depends on the unknown quantities (concentration, density, temperature, etc.) of the diffusion model.
For any diffusion exponent $m > 0$, a unique mild solution exists for any initial data $\rho_0 \in L^1(\mathbb{R}^N)$, it depends continuously on the initial data, and further, the concepts of mild, weak and strong solution are equivalent [287, 25, 286]. Thanks to the form of the diffusion coefficient $D(\rho)$, the overall behaviour of solutions can be split into three cases:

- $m > 1$: Diffusion is slow in areas with few particles. This case is known as the **porous medium equation (PME)**, or slow diffusion equation. The PME owes its name to the modeling of the flow of an isentropic gas through a porous medium [216, 241]. It was introduced for the study of groundwater infiltration [51], and is used in high-temperature physics, e.g. in the context of heat radiation in plasmas [303]. Other applications have been proposed in mathematical biology, spread of viscous fluids, boundary layer theory, see [289, 287, 7, 286, 161] and the references therein.

- $m = 1$: Diffusion is linear, and we obtain the well-known **heat equation (HE)** [156].
- $0 < m < 1$: Diffusion is fast in areas with few particles. This case is known as the **fast diffusion equation (FDE)**. The FDE appears in plasma physics ($m = 1/2$ is known as the Okuda-Dawson law [246]), and when modelling the diffusion of impurities in silicon [200]. The FDE has also an important application in geometry known as the Yamabe flow ($m = (N-2)/(N+2)$, $N \geqslant 3$) [215, 288].

  Note that problems may arise when diffusion is 'too fast', i.e. when the diffusion coefficient m is very small. It is established in [186] that the range of mass conservation for the FDE is $m_* < m < 1$ with

$$m_* < m < 1\,, \qquad m_* := \begin{cases} 0\,, & \text{if } N = 1, 2\,, \\ 1 - 2/N\,, & \text{if } N \geqslant 3\,. \end{cases}$$

  This is exactly the range for which integrable solutions to (2.5) exist. Within this range, the flow associated to the fast diffusion equation is in many ways even better than the flow associated to the heat equation; see [48] and the references therein. If $m_* < m < 1$, the solutions of (2.5) with positive integrable initial data are $\mathcal{C}^\infty$ and strictly positive everywhere instantaneously, just as for the heat flow.

Equation (2.5) gives rise to a rich mathematical theory with fundamental differences in behaviour depending on these three different regimes for the diffusion exponent $m > 0$. We will see later that some of these behaviour carry over to our aggregation-diffusion equation (2.3). This illustrates how the non-linear heat equation serves as an important representative for a more general class of non-linear, formally parabolic equations that appear across the pure and applied sciences, and it has been at the heart of the development of new analytical tools that can be adapted to a range of more complicated models. We will therefore give a short overview of the main properties of the non-linear heat equation (2.5) that are relevant in the context of this thesis. For a more detailed study dealing with the problems of existence, uniqueness, stability, regularity, dynamical properties and asymptotic behaviour, we refer the reader to [289] ($m > 1$), [300] ($m = 1$), [287] ($0 < m < 1$), and the references therein.

2.1.1 Source solutions

A classical problem in the thermal propagation theory is to describe the evolution of a heat distribution after a point source release. In mathematical terms, we want to find a solution $\Phi_m(t, x)$ to (2.5) with initial data given by a Dirac Delta, $\rho_0(x) = \delta(x)$. In case of the heat equation ($m = 1$), this fundamental solution is well-known and is given by the heat kernel

$$\Phi_1(t, x) = (4\pi t)^{-\frac{N}{2}} \exp\left(-\frac{|x|^2}{4t}\right)\,.$$

It is especially useful to have source solutions given in explicit form, as they often serve as a representative example for the typical or peculiar behaviour of solutions. Further, for linear equations, they allow us to obtain the general solution by applying a convolution, $\rho = \Phi_1 * \rho_0$. Such an approach is useless in the non-linear setting, and so one needs different methods. In case of the PME ($m > 1$), source solutions are given by

$$\Phi_m(t,x) = t^{-\alpha} F_m\left(x t^{-\alpha/N}\right), \quad F_m(\xi) := \left(\beta\left(|\xi_0|^2 - |\xi|^2\right)\right)_+^{\frac{1}{m-1}}, \quad m > 1, \tag{2.6}$$

for any $\xi_0 \in \mathbb{R}^N$, $\xi_0 \neq 0$, where we define the positive part as $(s)_+ := \max\{s, 0\}$ and where

$$\alpha := \frac{N}{N(m-1)+2}, \quad \beta := \frac{\alpha(m-1)}{2Nm}. \tag{2.7}$$

Solutions Φ_m depend continuously on m and converge pointwise to the heat kernel as $m \to 1$. This class of special solutions was first obtained by Zel'dovich and Kompaneets [304] around 1950, and then studied in more detail by Barenblatt [14] and Pattle [253]. They are widely known as *Barenblatt solutions* (or, for a more complete reference, as ZKB solutions or Barenblatt-Pattle solutions). For more details on (2.6) and their derivation, see [289] and the references therein.

In fact, the same source solution (2.6) also exists for the FDE in the regime $m < 1$ as long as $\alpha > 0$, that is, $m > m_*$. The solution Φ_m is then given by the same type of expression,

$$\Phi_m(t,x) = t^{-\alpha} G_m\left(x t^{-\alpha/N}\right), \quad G_m(\xi) := \left(C + \bar{\beta}|\xi|^2\right)^{-\frac{1}{1-m}}, \quad m_* < m < 1, \tag{2.8}$$

where $\bar{\beta} := -\beta = \alpha(1-m)/(2Nm)$, and $C = C(N,m) > 0$ is a normalising constant fixed by the mass. Therefore, we obtain for the source solution of the FDE for $m_* < m < 1$:

$$\Phi_m(t,x)^{1-m} = \frac{t}{C t^{2\alpha/N} + \bar{\beta}|x|^2}.$$

In this sense, the Barenblatt self-similar solutions for $m \neq 1$, $m > m_*$ are natural generalisations of the fundamental solutions of the heat equation.

2.1.2 Support and Tails

The main difference between the source-type solution profiles in the different ranges is probably the shape at infinity, which reflects the propagation form. If $m > 1$, the profile F_m is compactly supported, supp $(F_m) = B(0, |\xi_0|)$, and it follows that the Barenblatt solution Φ_m has compact support in space for every fixed time $t > 0$. More precisely, the free boundary is the surface given by the equation

$$t = \left(\frac{|x|}{|\xi_0|}\right)^{N(m-1)+2},$$

and so the size of the support supp (Φ_m) grows with a precise finite speed (see Figure 1.3(a)). This is to be compared with the properties of the heat kernel Φ_1 in the case $m = 1$, which is supported

on the whole space at all times with exponential tails at infinity (see Figure 1.3(b)).
In the case of the FDE, $m_* < m < 1$, however, source solutions are supported on the whole space and have so-called fat tails, or overpopulated tails,

$$\Phi_m(t,x) \approx \left(t/\bar{\beta}\right)^{\frac{1}{1-m}} |x|^{-\frac{2}{1-m}}, \qquad |x| \to \infty,$$

(see Figure 1.3(c)). Moreover, for non-negative initial data ρ_0 of unit mass satisfying

$$\sup_{|x|>R} \rho_0(x)|x|^{2/(1-m)} < \infty \tag{2.9}$$

for some $R > 0$, which means that ρ_0 is decaying at infinity at least as fast as the Barenblatt solution Φ_m, the solution $\rho(t,x)$ of (2.5) with initial data ρ_0 satisfies the following remarkable bounds [74]: For any $T > 0$, there exists a constant $C = C(T) > 0$ such that

$$\frac{1}{C} \leqslant \frac{\rho(t,x)}{G_m(x)} \leqslant C, \qquad \forall t \geqslant T,\ x \in \mathbb{R}^N,$$

where G_m is the Barenblatt profile defined in (2.8). This shows 'how fast' fast diffusion really is: It spreads mass out to infinity to instantly produce fat tails.
We conclude that the Barenblatt solutions with profiles given in Figures 1.3(a) (free boundary) and 1.3(c) (polynomial decay) are natural non-linear generalisations of the Gaussian profile in Figure 1.3(b) (Gaussian decay).

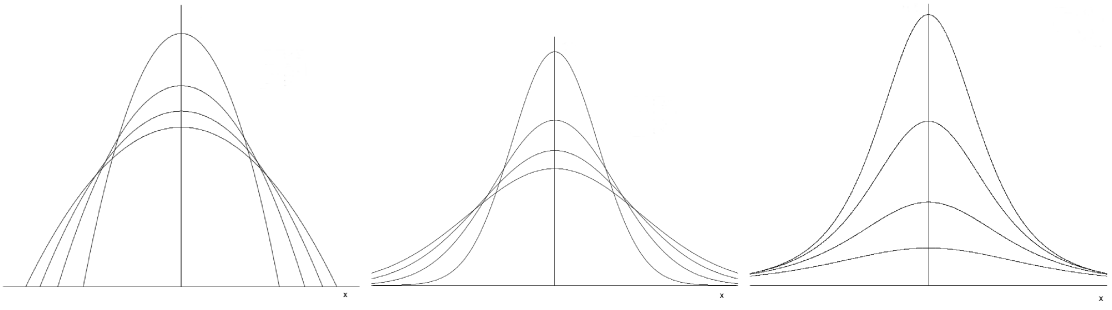

(a) (b) (c)

Figure 1.3: Source solutions $\Phi_m(t,x)$ for (a) PME ($m > 1$), (b) HE ($m = 1$) and (c) FDE ($m_* < m < 1$) at times $t = 0.5, 1, 1.5, 2$ for PME and HE, and at times $t = 1.15, 1.25, 1.4, 1.6$ for FDE. The Barenblatt solution (a) is compactly supported at each fixed $t > 0$, but has a free boundary with the support growing over time. The heat kernel (b) is supported on the whole space and its tails decay exponentially. The source solution (c) is also supported on the whole space, but has fat tails (polynomial decay). Source: [289]

2.1.3 Self-Similarity and Asymptotic Behaviour

The Barenblatt solutions can be derived using the self-similar structure of (2.5). We say that $\rho(t,x)$ satisfying (2.5) is a *self-similar solution* to the non-linear heat equation if the rescaled function

$$\rho_\lambda(t,x) = \lambda^N \rho(\lambda^{N/\alpha} t, \lambda x)$$

is also a solution of the same equation for all $\lambda > 0$ with α as given in (2.7). It is easy to see that Φ_m is indeed a self-similar solution to (2.5) for all $m > m_*$. For a detailed study of self-similarity (also known as *Renormalization Group* in theoretical physics), we refer to the classical books by G. Barenblatt, [16, 15]. For a detailed derivation of (2.6) using self-similarity, see [289].

In the case of the non-linear heat equation, there is a change of variables after which self-similar solutions to (2.5) become stationary solutions. More precisely, assume $\rho(t,x)$ is any solution to (2.5), and let

$$u(\tau,y) = e^{N\tau}\rho\left(\frac{\alpha}{N}e^{N\tau/\alpha}, e^{\tau}y\right)$$

with α given by (2.7). Then u satisfies the non-linear Fokker–Planck equation

$$\partial_\tau u = \frac{1}{N}\Delta_y u^m + \nabla_y \cdot (yu)\,, \qquad m > 0\,. \tag{2.10}$$

In Chapters 2 and 3, we use a similar scaling to find a suitable change of variables for the full aggregation-diffusion equation (2.3) that turns self-similar solutions into stationary states by adding a confinement term $\nabla_y \cdot (yu)$, see Section 3.3.1.

In the case of linear diffusion, $m = 1$, we can perform explicit estimates on the heat kernel Φ_1 to get an idea of the asymptotic behaviour of solutions. Indeed, taking $\rho(t,x)$ to be a solution of HE with initial data $\rho_0 \in L^1_+(\mathbb{R}^N)$, then

$$||\rho(t,\cdot) - \Phi_1(t,\cdot)||_1 \leqslant Ct^{-1/2}$$

for a positive constant $C > 0$ depending on the dimension only. This means that at large times, all solutions behave like the heat kernel, at least for the shape of the tails. For convergence to Φ_1 in various norms using entropy production methods, see [283]. Analogously, the Barenblatt profiles (2.6) for $m > 1$ and (2.8) for $m_* < m < 1$ are playing a key role in understanding the asymptotics of PME and FDE. For example, it is well-known that

$$\lim_{t\to\infty} ||\rho(t) - G_m||_1 = 0\,, \qquad m_* < m < 1\,, \tag{2.11}$$

$$\lim_{t\to\infty} ||\rho(t) - F_m||_1 = 0\,, \qquad m > 1\,, \tag{2.12}$$

with rate $t^{-\alpha/N}$ in the case of the PME. For the best known rates of convergence for the FDE, see [35]. If $0 < m < m_*$ and $N \geqslant 3$ such as for the Yamabe flow, then solutions to the FDE with

initial data $\rho_0 \in L^1_+(\mathbb{R}^N) \cap L^p(\mathbb{R}^N)$, $p > \frac{1-m}{2N}$, exist for sufficiently small $t > 0$, but go extinct at a given finite time $T > 0$, and in the radial case, their asymptotic behaviour as $t \to T$ is described by a uniquely determined self-similar solution [160, 255, 25]. For a detailed asymptotic analysis in the cases $m > 1$ and $m < 1$ and limitations, see [289, 287].

2.2 Non-local interaction

If we neglect the diffusive term in (2.3), the behaviour of particles is solely governed by non-local interaction,

$$\partial_t \rho = \nabla \cdot (\rho \nabla (W * \rho)) \,, \quad t > 0 \,, \quad x \in \mathbb{R}^N \tag{2.13}$$

with initial condition $\rho(t = 0) = \rho_0$. The aggregation equation (2.13) is at the core of many applications ranging from mathematical biology to granular media and economics, see [282, 237, 191, 284, 38, 154, 155] and the references therein. It can also be obtained as dissipative limits of hydrodynamic equations for collective behaviour [211]. But most importantly, equation (2.13) can be interpreted as the continuum description of an underlying particle model, a prototype example of so-called *Individual Based Models* (IBMs), see [80] and the references therein. In other words, if we consider n particles with equal masses $1/n$ located at positions $X_1, \dots, X_n \in \mathbb{R}^N$ evolving in time according to the interaction potential W, then the distribution of particles $\rho(t, x)$ solving (2.13) approximates this evolution as the number of particles n tends to infinity.

2.2.1 Assumptions on the interaction potential

The interaction potential W models the social behaviour of agents, and so $\nabla W(x - y)$ is the force that a unit-mass particle at x exerts on a unit-mass particle at y. We say that W is *attractive* at $x \in \mathbb{R}^N$ if $\nabla W(x) \cdot x \geqslant 0$, and it is *repulsive* if $\nabla W(x) \cdot x \leqslant 0$. Often, it is assumed that particles attract each other when they are far apart, and repulse each other when they are close; this reproduces the 'social', or natural, behaviour of the agents that are usually considered in applications. Some typical choices of potentials that have been studied in the literature are

1. **Power-law potentials**, see [10, 11, 29, 72, 81, 82, 83, 114, 139] and the references therein:

$$W(x) = \frac{|x|^a}{a} - \frac{|x|^b}{b} \,, \qquad b < a \,,$$

with the convention $\frac{|x|^0}{0} = \log |x|$. Because of the simpler topology, the one-dimensional case is in general better understood, see [151, 152, 79] and the references therein.

2. **Morse potentials**, see [139, 91, 95] and the references therein:

$$W(x) = -C_A e^{-|x|/l_A} + C_R e^{-|x|/l_R} \,,$$

where C_A, C_R and l_A, l_R are the strengths and the typical lengths of attraction and repulsion respectively. Biologically reasonable conditions are $C_R/C_A > 1$ and $l_R/l_A < 1$.

Most potentials that are relevant for applications have a singularity of some kind at the origin. See [87, 95, 207] for other choices of interaction potentials and a deeper discussion on the issue of biological/physical relevance.
Choosing the Dirac Delta measure as interaction potential, $W(x) = \delta(x)$, we recover the porous medium equation (2.5) with $m = 2$ as in [282].

2.2.2 Discrete aggregation equations

IBMs arise in a wide range of contexts, from swarming behaviour of animals (insects, fish, birds, ...) and collective behaviour of bacteria to the movement of robots in control engineering. They are often inspired from statistical physics and are usually formed by a set of Newton-type equations (2^{nd} order models), or by kinematic equations where inertia terms are neglected (1^{st} order models). We will here focus on a very simple 1^{st} order discrete aggregation equation derived in a phenomenological manner [238, 237, 250, 281, 282, 146]. Let us consider n particles with positions $X_1, \dots, X_n \in \mathbb{R}^N$ and equal masses $1/n$, interacting via the potential W, evolving according to the following first-order discrete aggregation equation:

$$\dot{X}_i(t) = -\frac{1}{n} \sum_{\substack{j=1,\\ j\neq i}}^{n} \nabla W(X_i(t) - X_j(t)) \,, \qquad i \in \{1, \dots, n\} \,, \, t \in (0, T) \,. \tag{2.14}$$

This model formally comes from applying Newton's second law with friction and neglecting inertia, which, in other words, means assuming that individuals can adjust to the velocity field instantaneously, an approximation valid when their speed is not too large, see [237, 139]. The scaling constant $1/n$ in front of the interaction potential ensures that the effect of the potential per particle diminishes while the associated energy is of constant order as the number of particles goes to infinity. Another reason to study the first order model (2.14) is that its stationary states have the same shape in space as flocking solutions of the second order discrete aggregation equation (see [95, 87] and the references therein)

$$\ddot{X}_i(t) = \left(a - b\left|\dot{X}_i(t)\right|^2\right) \dot{X}_i(t) - \frac{1}{n} \sum_{\substack{j=1,\\ j\neq i}}^{n} \nabla W(X_i(t) - X_j(t)) \,, \tag{2.15}$$

where $a, b \geqslant 0$ are friction parameters. Further, the stability of stationary states for (2.14) and (2.15) are related [91]. Here, we have an additional term producing a balance between self-propulsion and friction imposing an asymptotic speed for the particles (if other effects are ignored), given by $\sqrt{a/b}$.
Understanding the shape of stationary states for equations (2.14) and (2.15) when the number n

of particles is very large is of interest in statistical mechanics [267, 279], with direct implications in material science [166, 228, 229].

2.2.3 Existence and uniqueness of solutions

For the local well-posedness of solutions to equation (2.13), we refer to [30, 28, 31, 213, 80]. In particular, unique solutions for the system (2.13) were obtained in [31, Theorem 1.1]: if the initial datum $\rho_0 \in L^p(\mathbb{R}^N)$ is a probability measure with bounded second moment, and if $\nabla W \in \mathcal{W}^{1,p'}(\mathbb{R}^N)$, then there exists $T > 0$ and a unique solution $\rho \geqslant 0$ to (2.13) satisfying

$$\rho \in \mathcal{C}\left([0,T], \left(L^1 \cap L^p\right)(\mathbb{R}^N)\right) \cap \mathcal{C}^1\left([0,T], \mathcal{W}^{-1,p}(\mathbb{R}^N)\right) .$$

Existence and uniqueness at the particle level is a bit more tricky. If the potential W has no singularity at the origin, then existence of solutions to the particle system (2.14) is guaranteed thanks to the Cauchy[11]-Peano[12]-Arzelà[13] theorem. However, if one collision occurs, then uniqueness may be lost. Under suitable assumptions on the initial data $\mathbf{X}^n(0)$, one can ensure that there exists a time $T > 0$ before which no collisions between particles occur [80].

2.2.4 Mean-field limit

Studying IBMs when the number of individuals becomes large is challenging, and it is then often easier to pass to a continuous description of the system. This means going from particle descriptions to kinetic or macroscopic descriptions where the unknown is the particle density distribution. Given a solution $\mathbf{X}^n(t) := (X_1(t), \dots, X_n(t))$ to the discrete 1^{st} order aggregation equation (2.14), we define the *empirical measure* associated with $\mathbf{X}^n(t)$ as

$$\mu_{\mathbf{X}^n(t)}(x) := \frac{1}{n}\sum_{i=1}^{n} \delta_{X_i(t)}(x) \qquad x \in \mathbb{R}^N , \quad t \in [0,T) .$$

As long as two particles (or more) do not collide, and if we set $\nabla W(0) = 0$, then the empirical measure $\mu_{\mathbf{X}^n(t)}$ satisfies (2.13) in the sense of distributions. The empirical measure is the critical tool that allows to make a connection between (2.13) and (2.14).

Under suitable regularity assumptions on the initial data ρ_0 and the interaction potential W, we say that the IBM (2.14) converges to the equation (2.13) in the *mean-field sense* if the following statement holds true [80, 31, 213]: if $\mathbf{X}^n(t) := (X_1(t), \dots, X_n(t))$ is a solution to (2.14), and if

$$\mu_{\mathbf{X}^n(0)} \rightharpoonup \rho_0$$

[11] Baron Augustin-Louis Cauchy (1789 - 1857) was a French mathematician who made pioneering contributions to analysis. More concepts and theorems have been named after Cauchy than after any other mathematician.

[12] Guiseppe Peano (1858-1932) was an Italian mathematician. Peano was an accessible man, and the way he mingled with students was regarded as 'scandalous' in Turin, where he spent most of his career. He was a socialist in politics, and a tolerant universalist in all matters of life and culture.

[13] Cesare Arzelà (1847-1912) was an Italian mathematician, recognised for his contributions in the theory of functions. Arzelà came from a poor household and could therefore not start his study until the age of 24.

in the weak-$*$ sense as $n \to \infty$, then

$$\mu_{\mathbf{X}^n(t)} \rightharpoonup \rho(t)\,, \qquad \forall t \in [0,T)\,,$$

where $\rho(t)$ is a solution to (2.13) with initial data $\rho(t=0) = \rho_0$. We will not go into the details of the rigorous proof for this statement, but the fact that equation (2.13) is the good choice of model to represent the many-particle limit of (2.14) can also be understood on a more intuitive level as follows: Assume that, instead of a finite number of particles, we want to model the particle density $\rho(x,t)$. Then, according to (2.14), particles located at x at time t move with velocity

$$\bar{v}(t,x) = -\int_{\mathbb{R}^N} \nabla W(x-y)\,\rho(t,y)dy = -\nabla W * \rho\,.$$

This leads to the conservation law $\partial_t \rho + \nabla \cdot (\rho \bar{v}) = 0$, which is (2.13).

The regularity of the interaction potential W is key for the type of convergence result that can be obtained when going from (2.14) to (2.13). The classical Dobrushin strategy [131] for mean-field limits applies to (2.13) only for $\mathcal{C}^2(\mathbb{R}^N)$ smooth potentials W with at most quadratic growth at infinity [170]. In [80], the authors extended this result to more singular potentials.

In practise, one is interested in finding particle approximations $\mathbf{X}^n(0)$ to probability distributions ρ_0 such that the corresponding empirical measure converges to that distribution in a desired topology and satisfies certain constraints. This is an interesting and challenging mathematical problem that has received a lot of attention in recent years, see for example [235, 50, 204, 176] and the references therein.

2.3 Attraction vs repulsion

If the repulsion strength is very large at the origin, one can model repulsive effects by (non-linear) diffusion while attraction is considered via non-local long-range forces [240, 282]. The main goal of Part I is to understand better the behaviour of solutions when both non-linear diffusion and non-local interactions are at play. The natural question that arises when combining aggregation and diffusion terms is: which of the two forces wins, attraction or repulsion, and in which mathematical sense?

We will investigate this interplay for equation (2.3) with a rather simple yet challenging choice of potential giving rise to a rich set of behaviour patterns:

$$W_k(x) = \begin{cases} \dfrac{|x|^k}{k}\,, & \text{if} \quad k \in (-N,N)\backslash\{0\} \\ \log|x|\,, & \text{if} \quad k = 0 \end{cases}\,. \tag{2.16}$$

The conditions on k imply that the kernel W_k is locally integrable in $\mathbb{R}^N$. We need to make sure that the aggregation term in (2.3) makes sense with this choice of potential. Let us define the mean-field potential by $S_k(x) := W_k(x) * \rho(x)$. For $k > 1 - N$, the gradient $\nabla S_k := \nabla (W_k * \rho)$ is well defined. For $-N < k \leqslant 1 - N$ however, it becomes a singular integral, and we thus define it via a Cauchy principal value,

$$\begin{aligned}\nabla S_k(x) &= \lim_{\varepsilon \to 0} \int_{B^c(x,\varepsilon)} |x-y|^{k-2}(x-y)\rho(y)\,dy \\ &= \int_{\mathbb{R}^N} |x-y|^{k-2}(x-y)\left(\rho(y)-\rho(x)\right)\,dy\,,\end{aligned}$$

where $B^c(x,\varepsilon) := \mathbb{R}^N \backslash B(x,\varepsilon)$ is the complement of the ball of radius $\varepsilon > 0$ centered at $x \in \mathbb{R}^N$. Hence, the mean-field potential gradient in equation (2.3) is given by

$$\nabla S_k(x) := \begin{cases} \nabla W_k * \rho\,, & \text{if } k > 1-N\,, \\ \displaystyle\int_{\mathbb{R}^N} \nabla W_k(x-y)\left(\rho(y)-\rho(x)\right)\,dy\,, & \text{if } -N < k \leqslant 1-N\,. \end{cases} \tag{2.17}$$

For $k \in (-N, 0)$, W_k is also known as the *Riesz*[14] *potential*, and writing $k = 2s - N$ with $s \in \left(0, \frac{N}{2}\right)$, the convolution term S_k is governed by a fractional diffusion process,

$$c_{N,s}(-\Delta)^s S_k = \rho\,, \qquad c_{N,s} = (2s-N)\frac{\Gamma\left(\frac{N}{2}-2s\right)}{\pi^{N/2}4^s\Gamma(s)} = \frac{k\Gamma\left(-k-\frac{N}{2}\right)}{\pi^{N/2}2^{k+N}\Gamma\left(\frac{k+N}{2}\right)}\,.$$

In terms of regularity, this means that $S_k \in \mathcal{W}^{2s,p}_{loc}(\mathbb{R}^N)$ if $\rho \in L^1(\mathbb{R}^N) \cap L^p(\mathbb{R}^N)$, $1 < p < \infty$.

2.3.1 Energy functional and convexity properties

We make use of the special structure of equation (2.3), and its connection to the following free energy functional:

$$\mathcal{F}_{m,k}[\rho] = \int_{\mathbb{R}^N} U_m\left(\rho(x)\right)\,dx + \chi \iint_{\mathbb{R}^N\times\mathbb{R}^N} W_k(x-y)\rho(x)\rho(y)\,dxdy \tag{2.18}$$

with

$$U_m(\rho) = \begin{cases} \dfrac{1}{N(m-1)}\rho^m\,, & \text{if} \quad m \neq 1 \\ \dfrac{1}{N}\rho\log\rho\,, & \text{if} \quad m = 1 \end{cases}\,.$$

To simplify notation, we sometimes write

$$\mathcal{F}_{m,k}[\rho] := \mathcal{U}_m[\rho] + \chi\mathcal{W}_k[\rho]\,,$$

denoting by $\mathcal{U}_m$ and $\mathcal{W}_k$ the repulsive and attractive contributions respectively. For $\mathcal{F}_{m,k}$ to be finite, we require $\rho \in L^1(\mathbb{R}^N) \cap L^m(\mathbb{R}^N)$, and additionally $|x|^k\rho \in L^1(\mathbb{R}^N)$ in the case $k > 0$. Note

[14] Frigyes (Frédéric) Riesz (1880-1956) was a Hungarian mathematician who made fundamental contributions to functional analysis. He had an uncommon method of giving lectures: a docent reading passages from Riesz's handbook and an assistant inscribing the appropriate equations on the blackboard, while Riesz himself stood aside, nodding occasionally.

that $\mathcal{F}_{m,k}$ is invariant by translation, and we assume as for the aggregation-diffusion equation (2.3) that $\rho \geqslant 0$, $\int \rho\, dx = 1$ and $\int x\rho\, dx = 0$.

One of the main goals in Part I is making the connection between minimisers of the free energy functional (2.18) and stationary states of equation (2.3). Thanks to this connection, it is possible to show existence and uniqueness of stationary states to (2.3) by studying the existence and uniqueness of minimisers to the free energy functional $\mathcal{F}_{m,k}$. This is where the notion of convexity becomes important. In simple terms, if a real valued function $f : \mathbb{R}^N \to \mathbb{R}$ is strictly convex, then existence of a minimiser for f implies that it must be unique. McCann [234] discovered that there is a similar underlying convexity structure for functionals defined on absolutely continuous Borel measures, $\mathcal{E} : \mathcal{P}_{ac}(\mathbb{R}^N) \to \mathbb{R}$, using an interpolation between Borel measures following the line of optimal transportation [295]. Moreover, he used the powerful toolbox of Euclidean optimal transportation to analyse functionals like (2.18) in the case $m \geqslant 0$ and for a convex interaction kernel W_k. Here, we deal with concave homogeneous interaction kernels W_k given by (2.16) for which McCann's results [234] do not apply.

We begin by introducing some tools from optimal transport. Let $\tilde{\rho}$ and ρ be two probability densities. According to [53, 233], there exists a convex function ψ whose gradient pushes forward the measure $\tilde{\rho}(a)da$ onto $\rho(x)dx$: $\nabla\psi\#\left(\tilde{\rho}(a)da\right) = \rho(x)dx$. In other words, for any test function $\varphi \in C_b(\mathbb{R}^N)$, the following identity holds true

$$\int_{\mathbb{R}^N} \varphi(\nabla\psi(a))\tilde{\rho}(a)\, da = \int_{\mathbb{R}^N} \varphi(x)\rho(x)\, dx\,.$$

The convex map φ is known as *Brenier's map* , it is unique a.e. with respect to ρ and gives a way of interpolating measures. The interpolating curve ρ_s, $s \in [0,1]$, with $\rho_0 = \rho$ and $\rho_1 = \tilde{\rho}$ can be defined as $\rho_s(x)\, dx = (s\nabla\psi + (1-s)\mathsf{Id}_N)(x)\#\rho(x)\, dx$ where Id_N stands for the identity map in $\mathbb{R}^N$. In fact, this interpolating curve is the minimal geodesic joining the measures $\rho(x)dx$ and $\tilde{\rho}(x)dx$. The notion of convexity associated to these interpolating curves is nothing else than convexity along geodesics, introduced and called *displacement convexity* in [234]. Let us denote by $\mathcal{P}_{ac}(\mathbb{R}^N)$ the set of absolutely continuous probability measures on $\mathbb{R}^N$.

Definition 2.1 (Displacement convexity)**.** *A functional $\mathcal{E} : \mathcal{P}_{ac}(\mathbb{R}^N) \to \mathbb{R}$ is* (strictly) displacement convex *if*

$$s \mapsto \mathcal{E}\left[((1-s)\mathsf{Id}_N + s\nabla\psi)\,\#\mu\right]$$

is (strictly) convex on $[0,1]$ for any $\mu, \nu \in \mathcal{P}_{ac}$, and where ψ is the corresponding Brenier map $\nu = \nabla\psi\#\mu$.

The reason why we are interested in the displacement convexity properties of $\mathcal{F}_{m,k}$ is the following key result from [234]:

Theorem 2.2 (McCann, 1997). *If $\mathcal{E} : \mathcal{P}_{ac}(\mathbb{R}^N) \to \mathbb{R}$ is strictly displacement convex, then it has at most one minimiser up to translation.*

In other words, one recovers the property that existence of a minimiser implies uniqueness. In our case however, $\mathcal{F}_{m,k}$ is not necessarily displacement convex. The convexity of the functionals $\mathcal{U}_m$ and $\mathcal{W}_k$ can be summarised as follows [234, 85, 98]:

Theorem 2.3. *The functional $\mathcal{U}_m[\rho]$ is displacement-convex provided that $m \geqslant 1 - 1/N$. The functional $\mathcal{W}_k[\rho]$ in one dimension is displacement-concave if $k \in (-1, 1)$ and displacement-convex for $k \geqslant 1$ in any dimension.*

Therefore, the overall displacement-concavity/convexity of the energy functional $\mathcal{F}_{m,k}$ is not known since:

- if $N = 1$, then $\mathcal{U}_m[\rho]$ is displacement-convex for any $m \geqslant 0$ and $\mathcal{W}_k[\rho]$ displacement-concave since $k \in (-1, 1)$;
- if $N > 1$ and $k \in (1, N)$, then $\mathcal{W}_k[\rho]$ is displacement-convex, but we have no information about the displacement-convexity of $\mathcal{U}_m[\rho]$;
- if $N > 1$ and $k \in (-N, 1)$, then we have no information about the displacement-convexity of $\mathcal{W}_k[\rho]$.

We already observe that at least in one dimension we are dealing with the compensation between the displacement-convexity of the internal energy $\mathcal{U}_m[\rho]$ and the displacement-concavity of the interaction energy $\mathcal{W}_k[\rho]$. In Chapter 3, we will show that in certain cases, existence of a critical point for $\mathcal{F}_{m,k}$ implies its uniqueness (up to translations and dilations) in the one dimensional setting. Our main statement is that the functional (2.18) – the sum of a convex and a concave functional – behaves almost like a convex functional when attractive and repulsive forces are in balance. The bad functional contribution is somehow absorbed by the convex part for certain homogeneity relations and parameters χ.

2.3.2 Gradient flow structure

The strong connection between the functional $\mathcal{F}_{m,k}$ and the PDE (2.3) is due to the fact that the functional $\mathcal{F}_{m,k}$ is non-increasing along the trajectories of the system as it satisfies at least formally

$$\frac{d}{dt}\mathcal{F}_{m,k}[\rho(t)] = -\int_{\mathbb{R}^N} \rho(t,x) \left| \nabla \left(\frac{m}{N(m-1)} \rho(t,x)^{m-1} + 2\chi W_k(x) * \rho(t,x) \right) \right|^2 dx\,.$$

Furthermore, the system (2.3) is the formal gradient flow of the free energy functional (2.18) when the space of probability measures is endowed with the Euclidean Wasserstein metric $\mathbf{W}$.

Definition 2.4. *The Euclidean Wasserstein metric* $\boldsymbol{W}$ *between two probability measures* ρ_1 *and* ρ_2 *is defined as*

$$\boldsymbol{W}(\rho_1,\rho_2) := \left(\inf_{\gamma\in\Gamma(\rho_1,\rho_2)}\int_{\mathbb{R}^N\times\mathbb{R}^N}|x-y|^2\,d\gamma(x,y)\right)^{1/2},$$

where the set of couplings $\Gamma(\rho_1,\rho_2)$ *denotes the collection of all measures on* $\mathbb{R}^N\times\mathbb{R}^N$ *with marginals* ρ_1 *and* ρ_2 *on the first and second variable respectively.*

In other words, the family of PDEs (2.3) can be written as

$$\partial_t\rho(t) = \nabla\cdot\left(\rho(t)\,\nabla\mathcal{T}_{m,k}[\rho(t)]\right), \tag{2.19}$$

where $\mathcal{T}_{m,k}[\rho]$ denotes the first variation of the energy functional in the set of probability densities:

$$\mathcal{T}_{m,k}[\rho](x) := \frac{\delta\mathcal{F}_{m,k}}{\delta\rho}[\rho](x) = \frac{m}{N(m-1)}\rho^{m-1}(x) + 2\chi W_k(x)*\rho(x)\,. \tag{2.20}$$

The first variation can be found through explicit calculation using the identity

$$\lim_{\varepsilon\to0}\left(\frac{\mathcal{F}_{m,k}[\rho+\varepsilon\varphi]-\mathcal{F}_{m,k}[\rho]}{\varepsilon}\right) = \int_{\mathbb{R}^N} T_{m,k}[\rho](x)\varphi(x)\,dx\,,\quad \forall\varphi\in C_c^\infty(\mathbb{R}^N)\,.$$

The illuminating statement that systems of the type (2.3) can be written as the formal gradient flow of a corresponding energy functional has been clarified in the seminal paper by Otto [248] for the porous medium equation (2.5), and generalised to a large family of equations subsequently in [96, 3, 97], we refer to the books by Villani [295] and Ambrosio, Gigli and Savaré [3] for a comprehensive presentation of this theory of gradient flows in Wasserstein metric spaces, particularly in the convex case. Let us mention that such a gradient flow can be constructed as the limit of discrete in time steepest descent schemes,

$$\rho(t+\Delta t) = \operatorname*{argmin}_{\nu}\left\{\mathcal{F}_{m,k}(\nu) + \frac{1}{2\Delta t}\mathbf{W}(\rho(t),\nu)^2\right\}.$$

Performing gradient flows of a convex functional is a natural task, and suitable estimates from below on the right notion of Hessian of $\mathcal{F}_{m,k}$ translate into a rate of convergence towards equilibrium for the PDE [295, 96, 97, 3]. However, performing gradient flows of non-convex functionals is much more delicate, and one has to seek compensations. Such compensations do exist in our case, and we will observe them first of all at the level of existence of minimisers for the free energy functional $\mathcal{F}_{m,k}$ and stationary states of the family of PDEs (1.2) in particular regimes (see Chapter 2), and secondly via convergence in Wasserstein distance towards equilibrium under suitable assumptions (see Chapter 3). It is of course extremely important to understand how the convex and the concave contributions are entangled.

3 Part I: Results

3.1 The different regimes

It is important to note that this thesis is not concerned with the evolution problem of equations (2.3) and (3.29), and in all three chapters of part I, the questions of regularity/existence/uniqueness of solutions are not addressed, assuming solutions are 'nice' enough in space and time for our analysis to hold (for more details on regularity assumptions, see Chapter 3 Section 4). Whilst the required regularity may be a strong assumption to make, the necessary properties can often be obtained by regularisation, see [248, 92].

It is worth noting that the functional $\mathcal{F}_{m,k}[\rho]$ possesses remarkable homogeneity properties. Indeed, the mass-preserving dilation $\rho_\lambda(x) := \lambda^N \rho(\lambda x)$ transforms the functionals as follows:

$$\mathcal{U}_m\left[\rho_\lambda\right] = \begin{cases} \lambda^{N(m-1)}\mathcal{U}_m[\rho]\,, & \text{if} \quad m \neq 1\,, \\ \mathcal{U}_m[\rho] + \log\lambda\,, & \text{if} \quad m = 1\,, \end{cases}$$

and,

$$\mathcal{W}_k\left[\rho_\lambda\right] = \begin{cases} \lambda^{-k}\mathcal{W}_k[\rho]\,, & \text{if} \quad k \neq 0\,, \\ \mathcal{W}_k[\rho] - \log\lambda\,, & \text{if} \quad k = 0\,. \end{cases}$$

In other words, if $m \neq 1$ and $k \neq 0$, then

$$\mathcal{F}_{m,k}[\rho_\lambda] = \lambda^{N(m-1)}\mathcal{U}_m[\rho] + \lambda^{-k}\chi\mathcal{W}_k[\rho]\,.$$

Observe that $\rho_\lambda \to \delta$ in the limit $\lambda \to \infty$. A natural question arises: which of the two contributions dominates, repulsive or attractive forces?

This motivates the following classification:

Definition 3.1 (Three different regimes)**.**

$\mathbf{N(m-1)+k=0}$ *This is the* ***fair-competition*** *regime, where homogeneities of the two competing contributions exactly balance. If $k<0$, or equivalently $m>1$, then we will have a dichotomy according to χ (see Definition 3.7). Some variants of the HLS inequalities are very related to this dichotomy (see Section 3.2). This was already proven in [136, 41, 71, 148] for the Keller–Segel case with $N=2$, and in [39] for the Keller–Segel case with $N\geqslant 3$. If $k>0$, that is $m<1$, no critical χ exists as we prove in Chapter 2 Section 4.*

$\mathbf{N(m-1)+k>0}$ *This is the* ***diffusion-dominated*** *regime. Diffusion is strong, and is expected to overcome aggregation, whatever $\chi>0$ is. This domination effect means that solutions exist globally in time and are bounded uniformly in time [61, 277, 276]. Stationary states were found by minimisation of the free energy functional in two and three dimensions [273, 78, 99] in the case of attractive Newtonian potentials. Stationary states are radially symmetric if $2-N\leqslant k<0$ as proven in [89]. Moreover, in the particular case of $N=2$, $k=0$, and $m>1$ it has been proved in [89] that the asymptotic behaviour is given by compactly supported stationary solutions independently of χ.*

$\mathbf{N(m-1)+k<0}$ *This is the* ***attraction-dominated*** *regime. This regime is less understood. Self-attraction is strong, and can overcome the regularising effect of diffusion whatever $\chi>0$ is, but there also exist global in time regular solutions under some smallness assumptions, see [118, 275, 278, 109, 32, 110, 224, 65]. However, there is no complete criteria in the literature up to date distinguishing between the two behaviours. Most of the results known today deal with attractive Newtonian interactions, that is $k=2-N$, in dimension $N\geqslant 3$. For a study with linear diffusion $m=1$ and $k<0$ in one dimension, see [65]. For the Newtonian case, global existence vs blow-up of weak solutions has been investigated for the diffusion coefficients $m=1$ [118], $1<m\leqslant 2-\frac{2}{N}$ [275, 278], $m=\frac{2N}{N+2}$ [109], $\frac{2N}{N+2}<m<2-\frac{2}{N}$ [110, 224] and for the whole range $0<m\leqslant 2-\frac{2}{N}$ [32]. It was shown in [118] for linear diffusion $m=1$ that global in time weak solutions exist for initial data with small enough $L^{N/2}$-norm, whereas there are no global smooth solutions with fast decay if the second moment of the initial data is dominated by a power of the mass (with these two conditions being incompatible). For diffusion coefficient $m=\frac{2N}{N+2}$ making the free energy functional conformal invariant, there exists a family of stationary solutions characterising the transition between blow-up and global existence of radially symmetric weak solutions [109]. The case $\frac{2N}{N+2}<m<2-\frac{2}{N}$ has been studied in [110], where the authors suggest that the initial mass may not be an important quantity to classify existence vs blow-up of solutions with the behaviour depending on the free energy, the $L^{2N/(N+2)}$-norm and the second moment of the initial data. In [224], the authors proved a uniform L^∞-bound for weak solutions in the range where these stationary solutions exist given the initial data is uniformly bounded. As a consequence, uniqueness of weak solutions follows. We refer to [20] for a discussion with more general interaction potentials in the aggregation-dominated regime.*

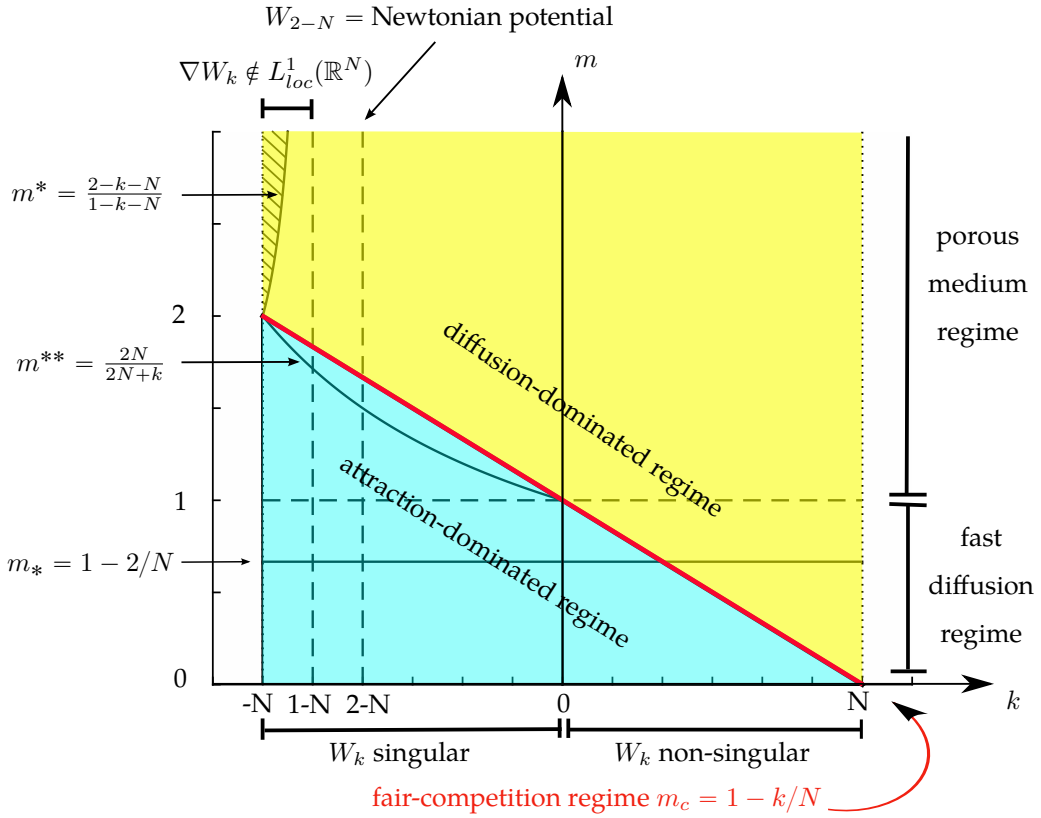

Figure 1.4: Overview of the parameter space (k, m) for $N \geqslant 3$: fair-competition regime ($m = m_c$, red line), diffusion-dominated regime ($m > m_c$, yellow region) and attraction-dominated regime ($m < m_c$, blue region). For $m = m_c$, attractive and repulsive forces are in balance (i.e., in *fair competition*). In the fast diffusion fair-competition regime ($m = m_c < 1$), self-similar profiles to equation (3.29) can only exist if diffusion is not 'too fast' with restriction $m > m_*$, see Chapter 2 Remark 4.6. Note that $m_* = 0$ for $N = 1, 2$. For $m = m^{**}$ in the aggregation-dominated regime, the free energy functional $\mathcal{F}_{m,k}$ is conformal invariant, see Chapter 3 Section 6.2. For $m_c < m < m^*$ in the diffusion-dominated regime, global minimisers of $\mathcal{F}_{m,k}$ are stationary states of (2.3), see Chapter 4 Theorem 1.1, a result which we are not able to show for $m > m^*$ (striped region).

A word of caution is in place as to how the names of these three regimes are to be understood. We introduced this terminology referring to the behaviour of the system with respect to blow-up and so they describe the dominant behaviour that is to be expected when measures concentrate onto a Dirac Delta. In light of these three regimes, we define the critical diffusion exponent as

$$m_c := 1 - \frac{k}{N}\,.$$

Chapters 2 and 3 concentrate on the fair-competition regime $m = m_c$, whereas Chapter 4 focuses on the diffusion-dominated regime $m > m_c$.

The family of non-local problems (2.3) has been intensively studied in various contexts arising in physics and biology. The two-dimensional logarithmic case $(m = 1, k = 0)$ is the so-called Keller–Segel system in its simplest formulation [196, 197, 243, 194, 136, 41, 256], see Section 1. The two- and three-dimensional configurations with Newtonian interaction $(m = 1, k = 2 - N)$ are the so-called Smoluchowski-Poisson system arising in gravitational physics [105, 107, 106]. It describes macroscopically a density of particles subject to a self-sustained gravitational field. Substituting linear diffusion by non-linear diffusion with $m > 1$ in two dimensions and higher is a way of regularising the Keller–Segel model as proved in [61, 277] where it is shown that solutions exist globally in time regardless of the value of the parameter $\chi > 0$. It corresponds to the diffusion-dominated case in two dimensions for which the existence of compactly supported stationary states and global minimisers of the free energy has only been obtained quite recently in [89]. The fair-competition case for Newtonian interaction $k = 2 - N$ was first clarified in [39], see also [276], where the authors find that there is a similar dichotomy to the two-dimensional classical Keller–Segel case $(N = 2, m = 1, k = 0)$, choosing the non-local term as the Newtonian potential, $(N \geqslant 3, m = 2-2/N, k = 2-N)$. The main difference is that the stationary states found for the critical case are compactly supported. We will see that such dichotomy also happens for $k < 0$ in our case while for $k > 0$ the system behaves totally differently.

3.2 Variations of HLS inequalities

A key ingredient for the analysis in the case $k < 0$ are certain functional inequalities which are variants of the Hardy[15]-Littlewood[16]-Sobolev[17] (HLS) inequality, also known as the weak Young's inequality [218, Theorem 4.3]:

[15] Godfrey Harold Hardy (1877-1947) was the most influential mathematician in Britain in the 20^{th} century. He wrote almost 100 papers together with Littlewood, considered to have been the most fruitful collaboration in the history of mathematics. He was also a militant atheist and liked to talk of God as his personal enemy.

[16] John Edensor Littlewood (1885-1977) is a British mathematician, best known for his achievements in analysis, number theory, and differential equations. He practised his belief that mathematicians should take a vacation of at least 21 days a year during which they should do no mathematics.

[17] Sergei Lvovich Sobolev (1908-1989) was a Soviet mathematician working in mathematical analysis and partial differential equations.

Theorem 3.2. *Given $k \in (-N, 0)$ and $p, q > 1$ satisfying*

$$\frac{1}{p} + \frac{1}{q} = 2 + \frac{k}{N}\,,$$

there exists an optimal constant $C_{HLS} = C_{HLS}(p, q, k)$ such that for all $f \in L^p(\mathbb{R}^N)$ and $g \in L^q(\mathbb{R}^N)$,

$$\left| \iint_{\mathbb{R}^N \times \mathbb{R}^N} |x - y|^k f(x) g(y)\, dxdy \right| \leqslant C_{HLS} \|f\|_p \|g\|_q\,. \tag{3.21}$$

Inequality (3.21) (not in the sharp form) was proved in [180] and [181]. Thanks to Lieb [217], the optimal constant C_{HLS} is known explicitly if $p = q = 2N/(2N + k)$ since in that case, it is possible to explicitly compute the optimisers of (3.21), i.e. functions which, when inserted into (3.21), give equality with the smallest constant. Indeed, optimisers for the sharp HLS inequality $p = q$ are non-zero multiples of translations and dilations of

$$h(x) := \left(\frac{1}{1 + |x|^2}\right)^{(2N+k)/2}\,.$$

In other words, the set of optimisers $\mathcal{O}$ to (3.21) is given by

$$\mathcal{O} := \left\{ \lambda h\left(\frac{x}{s} - x_0\right) \mid \lambda \in \mathbb{R}\backslash\{0\}\,, s \in \mathbb{R}_{>0}\,, x_0 \in \mathbb{R}^N \right\}$$

In fact, the HLS optimisers play an important role: they are stationary states of the non-linear Fokker–Planck equation (2.10) obtained from rescaling the fast diffusion (2.5) with diffusion exponent $\tilde{m}(k, N) := 1 - 2/(2N + k)$. Note that indeed $m_* < \tilde{m} < 1$ for all $k \in (-N, 0)$, and so we are in the range where the Barenblatt profile G_m (2.8) is well defined.
In the case $p \neq q$ on the other hand, optimisers to (3.21) exist, but neither the optimal constant C_{HLS} nor the optimisers are known explicitly.

As suggested by the connection between optimisers of the HLS inequality (3.21) and self-similar solutions to the fast diffusion equation (2.5), there is a rich and fruitful interplay between functional inequalities and non-linear partial differential equations [92, 125, 74, 133, 70, 132, 137] that is still in the process of being discovered. Let us illustrate the kind of connection we might want to exploit in our context with the example $k = 2-N$ in dimension $N \geqslant 3$. This is particularly interesting since $c_N|x|^{2-N}$ is the fundamental solution of the Laplacian,

$$c_N|x|^{2-N} * f = (-\Delta)^{-1} f\,, \qquad c_N := ((2 - N)\sigma_N)^{-1}\,,$$

where $\sigma_N := 2\pi^{N/2}/\Gamma(N/2)$ denotes the surface area of the N-dimensional unit ball. Therefore, choosing $p = q = 2N/(2N + k) = 2N/(N + 2)$ in (3.21), we see that the sharp HLS inequality encodes the smoothing properties of $(-\Delta)^{-1}$ on $\mathbb{R}^N$.

Let us rewrite the sharp HLS inequality (3.21) as $\mathcal{E}[f] \geqslant 0$ for $f \in L^{2N/(N+2)}(\mathbb{R}^N)$, where the so-called *HLS functional* $\mathcal{E}$ is given by

$$\mathcal{E}[f] := C_S \|f\|^2_{2N/(N+2)} - \int_{\mathbb{R}^N} f(x) \left[(-\Delta)^{-1} f\right](x)\, dx$$

with $C_S := c_N C_{HLS} = \frac{4}{N(N-2)} \sigma_{N+1}^{-2/N}$ given explicitly. Since the HLS optimisers $\mathcal{O}$ are the attracting stationary states for a fast diffusion flow (2.11) with diffusion exponent $\tilde{m} = N/(N+2)$, one might hope that the HLS functional $\mathcal{E}$ would be monotone decreasing along this flow. This is indeed the case, and was shown in [74]: Fix some $f \in L^{2N/(N+2)}(\mathbb{R}^N)$, $f \geqslant 0$, $\int f\, dx = \int G_{\tilde{m}}\, dx = 1$ satisfying (2.9) for some $R > 0$, and let $\rho(t,x)$ be a solution of the fast diffusion equation (2.5) with diffusion exponent $\tilde{m}$ and $\rho(1,x) = f(x)$. Then, for all $t > 1$, it follows that $\frac{d}{dt}\mathcal{E}[\rho(t)] \leqslant 0$. For a proof of this monotonicity relation, see [74, Theorem 2.1].
Further, using only the fast diffusion flow, rearrangement inequalities and the conformal invariance of the HLS functional $\mathcal{E}$, the authors in [74] were able to reprove the HLS inequality (3.21) for the Newtonian case $k = 2 - N$, $N \geqslant 3$. Their approach uses the fast diffusion flow to reduce the HLS inequality to a Gagliardo-Nirenberg-Sobolev (GNS) inequality, which in turn reduces to the Schwarz inequality. Note that the diffusion exponent $\tilde{m} = N/(N+2)$ corresponds to the critical exponent of the FDE related to the boundedness of the second moment of the stationary states G_m and it plays a certain role in the long-time assymptotics of the FDE, see [101, 35].

A similar role is played by the logarithmic HLS inequality, established in its sharp version in [77]:

Theorem 3.3. *Let $k = 0$, $m = 1$. For all non-negative measurable functions $f \in L^1(\mathbb{R}^N)$ such that $f \log f, f \log(1+|x|^2) \in L^1(\mathbb{R}^N)$, we have*

$$-\chi \iint_{\mathbb{R}^N \times \mathbb{R}^N} f(x) \log|x-y| f(y) dx dy \leqslant \frac{1}{N} \int_{\mathbb{R}^N} f(x) \log f(x) dx + C_0, \tag{3.22}$$

where the optimal constant $C_0 = C_0(N)$ is given by

$$C_0(N) := \frac{1}{2}\log\pi + \frac{1}{N}\log\left(\frac{\Gamma\left(\frac{N}{2}\right)}{\Gamma(N)}\right) + \frac{1}{2}\left(\psi(N) - \psi\left(\frac{N}{2}\right)\right).$$

Here ψ denotes the logarithmic derivative of the Γ-function.

Carlen and Loss, together with Beckner, have demonstrated that the logarithmic HLS inequality is also a consequence of (3.21) as $k \to 0$, see [77].
Further, the sharp logarithmic HLS inequality on $\mathbb{R}^2$ can be obtained by a similar fast diffusion flow argument as we discussed above for the HLS inequality (3.21) [74], an approach which is facilitated by the fact that the logarithmic HLS functional is invariant under scalings. It can also

be derived by optimal transport techniques in one dimension and in the two-dimensional radial setting [62], using techniques which we will adapt for our context in Chapter 2 and Chapter 3.

The above examples illustrate the intrinsic relationship between functional inequalities, their minimisers, and certain non-linear diffusion equations. We will make use of these connections in Part I when studying the stationary states to the aggregation-diffusion equations (2.3) and (3.29). We will now state the new functional inequalities derived in this thesis.

Theorem 3.4. *Let $k \in (-N, 0)$, and $m \geqslant m_c$. For $f \in L^1(\mathbb{R}^N) \cap L^m(\mathbb{R}^N)$, we have*

$$\left| \iint_{\mathbb{R}^N \times \mathbb{R}^N} |x-y|^k f(x) f(y) dx dy \right| \leqslant C_* ||f||_1^{(k+N)/N} ||f||_{m_c}^{m_c}, \tag{3.23}$$

where the optimal constant C_* is given by

$$C_*(N,k,m) := \sup_{f \neq 0} \left\{ \frac{\left| \iint_{\mathbb{R}^N \times \mathbb{R}^N} |x-y|^k f(x) f(y) dx dy \right|}{||f||_1^{(k+N)/N} ||f||_{m_c}^{m_c}},\ f \in L^1(\mathbb{R}^N) \cap L^m(\mathbb{R}^N) \right\} < \infty.$$

Proof. The inequality is a direct consequence of Theorem 3.2 by choosing $p = q = 2N/(2N+k)$, and of Hölder's inequality. More precisely, for any $f \in L^1(\mathbb{R}^N) \cap L^m(\mathbb{R}^N)$ with $m > m_c$, we have

$$\left| \iint_{\mathbb{R}^N \times \mathbb{R}^N} |x-y|^k f(x) f(y) dx dy \right| \leqslant C_{HLS} ||f||_p^2 \leqslant C_{HLS} ||f||_1^{\alpha} ||f||_m^{\beta}.$$

with

$$\alpha = 2 - \beta\,, \qquad \beta = 2\left(\frac{1-p}{p}\right)\left(\frac{m}{1-m}\right) = \left(\frac{k}{N}\right)\left(\frac{m}{1-m}\right).$$

Choosing $m = m_c$, we have $\alpha = 1 + k/N$, $\beta = m_c$, and hence (3.23) follows with $C_* = C_*(k, m, N)$ finite and bounded from above by C_{HLS}. □

Further, we will obtain as a by-product of our investigations the following one-dimensional HLS-type inequality involving a second moment term:

Theorem 3.5. *Let $k \in (-N, 0)$ and $m = m_c$. For any $0 < \chi < C_*^{-1}$, there exists an optimal constant $C = C(k, N, \chi)$ such that*

$$\chi \iint_{\mathbb{R}^N \times \mathbb{R}^N} |x-y|^k f(x) f(y)\, dx dy \leqslant C + \|f\|_{m_c}^{m_c} + \frac{(-k)}{2} \int_{\mathbb{R}^N} |x|^2 f(x)\, dx \tag{3.24}$$

for all $f \in L^1(\mathbb{R}^N) \cap L^{m_c}(\mathbb{R}^N)$ with $\|f\|_1 = 1$, $\int x f(x)\, dx = 0$ and $|x|^2 f(x) \in L^1(\mathbb{R}^N)$. If $N = 1$, then the set of optimisers is the unique self-similar solution to equation (2.3).

Moreover, we will prove the analogue version of the above functional inequality for positive $0 < k < 2/3$ in one dimension, corresponding to a reversed HLS-type inequality with a second moment term:

Theorem 3.6. *Let $N = 1$, $k \in (0, 2/3)$ and $m_c := 1 - k$. For any $\chi > 0$, there exists an optimal constant $C = C(k, \chi)$ such that*

$$\chi \iint_{\mathbb{R}\times\mathbb{R}} |x-y|^k f(x) f(y)\, dxdy + \frac{k}{2} \int_{\mathbb{R}} |x|^2 f(x)\, dx \geqslant C + \int_{\mathbb{R}} f^{m_c}(x)\, dx \tag{3.25}$$

for all $f \in L^1(\mathbb{R}) \cap L^{m_c}(\mathbb{R})$ with $\|f\|_1 = 1$, $\int x f(x)\, dx = 0$ and $\left(|x|^2 + |x|^k\right) f(x) \in L^1(\mathbb{R})$. The optimiser is given by the unique self-similar solution to equation (2.3).

Up to our knowledge, the functional inequalities (3.24) and (3.25) are not known in the literature.

The analysis of the free energy functionals $\mathcal{F}_{m,k}$ and their respective gradient flows is closely related to HLS-type inequalities [218, 163, 74, 39]. To give a flavour, we highlight the case $(m = 1, k = 0)$, called the *logarithmic case*. It is known from [136, 41] using [77, 19] that the functional $\mathcal{F}_{1,0}$ is bounded from below if and only if $0 < \chi \leqslant 1$. Moreover, $\mathcal{F}_{1,0}$ achieves its minimum if and only if $\chi = 1$ and the extremal functions are mass-preserving dilations of Cauchy's density:

$$\bar{\rho}_0(x) = \frac{1}{\pi} \left(\frac{1}{1 + |x|^2} \right) . \tag{3.26}$$

In [77], the authors have proved the uniqueness (up to dilations and translations) of this logarithmic HLS inequality based on a competing-symmetries argument. We develop in Chapter 3 an alternative argument based on some accurate use of the Jensen's inequality to extend these results to the case $N = 1$, $k \in (-1, 0)$ and $m = m_c$. This goal will be achieved for the variant of the HLS inequality (3.23) as in [39], indeed being a combination of the HLS inequality and interpolation estimates.

In Chapter 3, we develop a strategy which enables to recover directly inequalities (3.22), (3.23), (3.24) and (3.25). Our method involves two main ingredients:

- First it is required to know *a priori* that the inequality possesses some extremal function denoted *e.g.* by $\bar{\rho}(x)$ (characterised as a critical point of the energy functional). This is not an obvious task due to the intricacy of the equation satisfied by $\bar{\rho}(x)$. Without this *a priori* knowledge, the proof of the inequality remains incomplete. The situation is in fact similar to the case of convex functionals, where the existence of a critical point ensures that it is a global minimiser of the functional.

- Second we invoke convexity inequalities related to Jensen's inequality.

3.3 The fair-competition regime

In the fair-competition regime, when $m = m_c = 1 - k/N$, we denote the corresponding energy functional by $\mathcal{F}_k[\rho] = \mathcal{F}_{1-k/N,k}[\rho]$. Notice that the functional $\mathcal{F}_k$ is homogeneous in this regime, i.e. for dilations $\rho_\lambda(x) := \lambda^N \rho(\lambda x)$, we have

$$\mathcal{F}_k[\rho_\lambda] = \lambda^{-k} \mathcal{F}_k[\rho] \,. \tag{3.27}$$

In fact, using the Euler[18] theorem for homogeneous functions, we can show that for $k \in (-N, 0)$ any stationary state of the aggregation-diffusion equation (2.3) with bounded second moment has zero energy (see Chapter 2, Lemma 3.2). This argument does not apply in the logarithmic case $k = 0$ and it allows us here to make the connection between global minimisers of $\mathcal{F}_k$ and stationary states of (2.3) for $k < 0$. Indeed, for any $\rho \in \mathcal{Y}$, where

$$\mathcal{Y} := \left\{ \rho \in L^1_+\left(\mathbb{R}^N\right) \cap L^m\left(\mathbb{R}^N\right) : ||\rho||_1 = 1 \,, \int x\rho(x)\, dx = 0 \right\} \,,$$

and for any $\chi > 0$, we can rewrite the functional inequality (3.23) as follows:

$$\mathcal{F}_k[\rho] \geqslant \frac{1 - \chi C_*}{N(m-1)} ||\rho||_m^m \,,$$

where $C_* = C_*(k, N)$ is the optimal constant defined in (3.23). Since the energy of the global minimisers is always smaller or equal to the energy of the stationary states, and stationary states have zero energy as mentioned above, it follows that $\chi \geqslant 1/C_*$. We define the *critical interaction strength* by

$$\chi_c(k, N) := \frac{1}{C_*(k, N)} \,. \tag{3.28}$$

Hence, for $\chi = \chi_c$, all stationary states of equation (2.3) are global minimisers of $\mathcal{F}_k$. We can also directly see that for $0 < \chi < \chi_c$, no stationary states exist. Showing that stationary states of an equation are global minimisers of the associated energy functional is usually the more challenging implication. The converse is trivial for systems that exhibit a gradient flow structure (2.19) since global minimisers are critical points of the energy functional, i.e. the first variation of the energy functional vanishes at these points, and therefore global minimisers are automatically stationary states. It remains then to verify that global minimisers of $\mathcal{F}_k$ are regular enough to be stationary states of equation (2.3). Showing the good regularity properties can be challenging, and it is proven and explained in detail in Chapter 2.

The case $k > 0$ has been a lot less studied, and we will show in Chapter 2 that no critical interaction strength exists as there is no $\chi > 0$ for which $\mathcal{F}_k$ admits global minimisers. On the other hand, we observe certain similarities with the behaviour of the fast diffusion equation ($0 < m < 1$, $\chi = 0$) [287].

[18] Leonhard Euler (1707-1783), born in Switzerland and deceased in Russia, was one of the most influential and prolific mathematicians in history with more than 800 papers bearing his name. He was blind for the last 15 years of his life, during which time he nevertheless wrote over 300 papers.

From these observations, one can see that the analysis in the fair-competition regime depends on the sign of k. We give a short overview of the differences between the cases $k < 0$, $k = 0$, $k > 0$ in the definition below, including new insights obtained in this thesis:

Definition 3.7 (Three different cases in the fair-competition regime)**.**

k < 0 *This is the **porous medium case** with $m \in (1, 2)$, where diffusion is small in regions of small densities. The classical porous medium equation, i.e. $\chi = 0$, is very well studied, see [289] and the references therein. Here, we have a dichotomy for existence of stationary states and global minimisers of the energy functional $\mathcal{F}_k$ depending on the critical parameter χ_c defined in (3.28), and hence separate the sub-critical, the critical and the super-critical case, according to $\chi \lessgtr \chi_c$.*

k = 0 *This is the **logarithmic case**. There exists an explicit extremal density $\bar{\rho}_0$ given in (3.26) which realises the minimum of the functional $\mathcal{F}_0$ when $\chi = 1$. Moreover, the functional $\mathcal{F}_0$ is bounded below but does not achieve its infimum for $0 < \chi < 1$ while it is not bounded below for $\chi > 1$. Hence, $\chi_c = 1$ is the critical parameter in the logarithmic case whose asymptotic behaviour was analysed in [62] in one dimension and radial initial data in two dimensions. We refer to the results in [71, 148] for the two dimensional case.*

k > 0 *This is the **fast diffusion case** with $m \in (0, 1)$, where diffusion is strong in regions of small densities. For any $\chi > 0$, no radially symmetric non-increasing stationary states with bounded kth moment exist, and $\mathcal{F}_k$ has no radially symmetric non-increasing minimisers. However, we have existence of self-similar profiles independently of $\chi > 0$ as long as diffusion is not too fast, i.e. $k \leqslant 1$. Self-similar profiles can only exist if diffusion is not too strong with restriction $0 < k < 2$, that is $(N - 2)/N < m < 1$.*

3.3.1 Change of variables

As mentioned above, for certain choices of m, k and χ, there are no stationary states to (2.3), see Section 3.3.2. This is known in the case of the sub-critical classical Keller–Segel model in two dimensions [41] for instance. If there are no stationary states, the scale invariance of (2.3) motivates us to look for self-similar solutions instead. To this end, we rescale equation (2.3) to a non-linear Fokker–Planck-type equation as in explained in Section 2.1.3 in the context of the non-linear heat equation. Let us define

$$u(t, x) := \alpha^N(t)\rho\left(\beta(t), \alpha(t)x\right),$$

where $\rho(t, x)$ solves (2.3) and the functions $\alpha(t)$, $\beta(t)$ are to be determined. If we assume $u(0, x) = \rho(0, x)$, then $u(t, x)$ satisfies the rescaled aggregation-diffusion equation

$$\begin{cases} \partial_t u = \frac{1}{N}\Delta u^m + 2\chi\nabla \cdot (u\nabla S_k) + \nabla \cdot (xu)\,, \quad t > 0\,, \quad x \in \mathbb{R}^N\,, \\ u(t = 0, x) = \rho_0(x) \geqslant 0\,, \quad \int_{-\infty}^{\infty} \rho_0(x)\,dx = 1\,, \quad \int_{-\infty}^{\infty} x\rho_0(x)\,dx = 0\,, \end{cases} \tag{3.29}$$

for the choices

$$\alpha(t) = e^t, \quad \beta(t) = \begin{cases} \frac{1}{2-k}\left(e^{(2-k)t} - 1\right), & \text{if } k \neq 2, \\ t, & \text{if } k = 2, \end{cases}$$

and with ∇S_k given by (2.17) with u instead of ρ. By differentiating the centre of mass of u, we see easily that

$$\int_{\mathbb{R}^N} x u(t,x)\,dx = e^{-t}\int_{\mathbb{R}^N} x\rho_0(x)\,dx = 0\,, \qquad \forall t > 0\,,$$

and so the initial zero centre of mass is preserved for all times. Self-similar solutions to (2.3) now correspond to stationary solutions of (3.29).
From now on, we switch notation from u to ρ for simplicity, it should be clear from the context if we are in original or rescaled variables.

In rescaled variables, equation (3.29) is the formal gradient flow of the rescaled free energy functional $\mathcal{F}_{k,\mathbf{resc}}$, which is complemented with an additional quadratic confinement potential,

$$\mathcal{F}_{k,\mathbf{resc}}[\rho] = \mathcal{F}_k[\rho] + \frac{1}{2}\mathcal{V}[\rho]\,, \qquad \mathcal{V}[\rho] = \int_{\mathbb{R}^N} |x|^2\rho(x)\,dx\,.$$

Defining the sets

$$\mathcal{Y}_2 := \{\rho \in \mathcal{Y} : \mathcal{V}[\rho] < \infty\}\,, \qquad \mathcal{Y}_k := \left\{\rho \in \mathcal{Y} : \int_{\mathbb{R}^N} |x|^k\rho(x)\,dx < \infty\right\}\,,$$

we see that $\mathcal{F}_{k,\mathbf{resc}}$ is well-defined and finite on $\mathcal{Y}_2$ for $k < 0$ and on $\mathcal{Y}_{2,k} := \mathcal{Y}_2 \cap \mathcal{Y}_k$ for $k > 0$. Just like the original equation (2.3), the rescaled system (3.29) has a formal gradient flow structure in the Euclidean Wasserstein metric $\mathbf{W}$, and so we can write (3.29) as

$$\partial_t\rho = \nabla\cdot(\rho\,\nabla\mathcal{T}_{k,\mathbf{resc}}[\rho]) = -\nabla_{\mathbf{W}}\mathcal{F}_{k,\mathbf{resc}}[\rho]\,,$$

where $\mathcal{T}_{k,\mathbf{resc}}$ denotes the first variation of the rescaled energy functional,

$$\mathcal{T}_{k,\mathbf{resc}}[\rho](x) := \mathcal{T}_k[\rho](x) + \frac{|x|^2}{2}$$

with $\mathcal{T}_k$ as defined in (2.20).

3.3.2 Main results Chapter 2

In Chapter 2, we analyse the properties of the functional $\mathcal{F}_k$, its global minimisers, and its relation to stationary states of (2.3) for the fair-competition regime in any dimension $N \geqslant 1$. For the porous medium case $k < 0$, we show a similar dichotomy to [39] in the whole range $k \in (-N, 0)$ including the most singular cases $-N < k \leqslant 1 - N$. We show that stationary states exist only for a critical value of $\chi = \chi_c$ with χ_c given by (3.28) and that they are compactly supported, bounded, radially symmetric decreasing and continuous functions. Moreover, we show that they

are global minimisers of $\mathcal{F}_k$. Next, we analyse the sub-critical case $\chi < \chi_c$ in rescaled variables and we show the existence of global minimisers for the rescaled free energy functional $\mathcal{F}_{k,\mathbf{resc}}$ with the properties above leading to the existence of self-similar solutions in original variables. Let us mention that the regularity results for global minimisers of $\mathcal{F}_k$ and $\mathcal{F}_{k,\mathbf{resc}}$ need a careful treatment of the problem in radial coordinates involving non-trivial properties of hypergeometric functions, particularly in the singular regime $-N < k \leqslant 1-N$ when additional Hölder regularity $C^{0,\alpha}(\mathbb{R}^N)$ with $\alpha \in (1-k-N, 1)$ is needed for the gradient ∇S_k to be well defined. The properties of the kernel in radial coordinates are postponed to the Appendix A of Chapter 2.

In Section 4 of Chapter 2, we analyse the fast diffusion case $k > 0$. Let us mention that, to the best of our knowledge, there are no results in the literature concerning the case $k \in (0, N)$ in which $0 < m_c = 1 - k/N < 1$. There is one related result in [116] for the limiting case in one dimension taking $m = 0$, corresponding to logarithmic diffusion, and $k = 1$. In that case, there is no criticality present as solutions to (2.3) with $(m = 0, k = 1)$ are globally defined in time for all values of the parameter $\chi > 0$. We show that no radially symmetric non-increasing stationary states and no radially symmetric non-increasing global minimisers exist in original variables for all values of the critical parameter χ and for $k \in (0, N)$ while we establish the existence of stationary states for all values of the critical parameter χ in rescaled variables for $k \in (0, 1]$. In this sense, there is no criticality for $k > 0$. However, we have not analysed the minimisation problem for $\mathcal{F}_{k,\mathbf{resc}}$ directly for arbitrary dimension $N \geqslant 1$ as we did for the case $k < 0$. A full proof of non-criticality involves the analysis of the minimisation problem in rescaled variables showing that global minimisers exist in the right functional spaces for all values of the critical parameter and that they are indeed stationary states. This will be proved in one dimension in Chapter 3 by optimal transport techniques and postponed for further future investigations in general dimension. We finally illustrate these results by numerical experiments in one dimension corroborating the absence of critical behaviour for $k > 0$.

More precisely, we will prove the following main theorems in Chapter 2:

Theorem 3.8 (The Critical Porous Medium Regime)**.** *In the porous medium regime $k \in (-N, 0)$ and for critical interaction strengths $\chi = \chi_c$, there exist global minimisers of $\mathcal{F}_k$ and they are radially symmetric non-increasing, compactly supported and uniformly bounded. Furthermore, all stationary states with bounded second moment are global minimisers of the energy functional $\mathcal{F}_k$, and conversely, all global minimisers of $\mathcal{F}_k$ are stationary states of* (2.3)*.*

Theorem 3.9 (The Sub-Critical Porous Medium Regime)**.** *In the porous medium regime $k \in (-N, 0)$ and for sub-critical interaction strengths $0 < \chi < \chi_c$, no stationary states exist for equation* (2.3) *and no minimisers exist for $\mathcal{F}_k$. In rescaled variables, all stationary states are continuous and compactly sup-*

ported. There exist global minimisers of $\mathcal{F}_{k,\textbf{resc}}$ and they are radially symmetric non-increasing and uniformly bounded stationary states of equation (3.29).

Due to the homogeneity (3.27) of the functional $\mathcal{F}_k$, each global minimiser gives rise to a family of global minimisers for $\chi = \chi_c$ by dilation since they have zero energy. It is an open problem to show that there is a unique global minimiser for $\chi = \chi_c$ modulo dilations. This uniqueness was proven in the Newtonian case in [302], and for any $k \in (-1, 0)$ for the one-dimensional case in Chapter 3.

In contrast, in rescaled variables, we do not know if stationary states with bounded second moment are among global minimisers of $\mathcal{F}_{k,\textbf{resc}}$ for the sub-critical case $0 < \chi < \chi_c$ except in one dimension, see Chapter 3. It is also an open problem to show the uniqueness of radially symmetric stationary states of the rescaled equation (3.29) for $N \geqslant 2$.

Theorem 3.10 (The Fast Diffusion Regime)**.** *In the fast diffusion regime $k \in (0, N)$ equation* (2.3) *has no radially symmetric non-increasing stationary states with kth moment bounded, and there are no radially symmetric non-increasing global minimisers for the energy functional $\mathcal{F}_k$ for any $\chi > 0$. In rescaled variables, radially symmetric non-increasing stationary states can only exist if $0 < k < 2$, that is $(N - 2)/N < m_c < 1$. Similarly, global minimisers with finite energy $\mathcal{F}_{k,\textbf{resc}}$ can only exist in the range $0 < k < 2N/(2 + N)$, that is $N/(2 + N) < m_c < 1$. For $k \in (0, 1]$, there exists a continuous radially symmetric non-increasing stationary state of the rescaled equation* (3.29).

3.3.3 Main results Chapter 3

Chapter 3 focuses on the one-dimensional fair-competition regime. We will make a survey of the main results known in one dimension about the stationary states of the aggregation-diffusion equation and global minimisers of the associated energy functionals in the fair-competition regime while at the same time providing new material in one dimension with alternative proofs and information about long time asymptotics which are not known yet in higher dimensions. The novelties will be showing the functional inequalities (3.23) for $m = m_c$, (3.24) and (3.25) independently of the flow and studying the long-time asymptotics of the equations (2.3) and (3.29) by exploiting the one dimensional setting. More precisely, we will make accurate use of the expression for the dissipation of the Wasserstein distance derived in Theorem 4.1, which is only valid in one dimension. A similar identity to (**??**) can also be derived for the radial setting in higher dimension, which opens up opportunities to generalise our one-dimensional results. Let us stress that we did not develop any theory of the evolution problem as mentioned before, and in this sense, the convergence results in this chapter remain formal, assuming that solutions $\rho(t, x)$ are regular enough for our computations to hold.

In the sub-critical and critical porous medium regime, we will demonstrate convergence to equilibrium in Wasserstein distance under a certain stability condition, a restriction which is not necessary for the asymptotic behaviour in the fast diffusion regime. More precisely, the required stability condition is a uniform $\mathcal{W}^{2,\infty}(\mathbb{R})$-stability estimate on the Brenier map $\psi(t,x)$ whose gradient pushes forward a solution $\rho(t,x)$ onto a stationary state, $\rho(t,x)\,dx = \partial_x\psi(t,x)\#\bar{\rho}(x)\,dx$:

$$\partial_{xx}\psi(t,x) \in L^\infty\left(\mathbb{R}_+, L^\infty(\mathbb{R})\right) \quad \text{such that} \quad ||\partial_{xx}\psi||_{L^\infty(\mathbb{R}_+,L^\infty(\mathbb{R}))} \leqslant 1 + \frac{1}{m}\,.$$

For the sub-critical porous medium regime, and for the fast diffusion regime, we obtain exponential convergence to self-similar profiles with an explicit rate which does not depend on the interaction strength χ. This is remarkable in the sub-critical case $\chi < \chi_c$ as it means that the asymptotic behaviour does not change as χ approaches χ_c from below, whilst the behaviour at $\chi = \chi_c$ is very different with the existence of infinitely many stationary states that act as attractors for a certain class of solutions. This effect appeared in the logarithmic case ($k = 0, m = 1$) analysed in [62].

Finally, we provide numerical simulations of system (2.3) to illustrate the properties of equilibria and self-similar profiles in the different parameter regimes for the fair-competition regime. We use a Jordan-Kinderlehrer-Otto (JKO) steepest descent scheme [195, 248] which was proposed in [36] for the logarithmic case $k = 0$, and generalised to the porous-medium case $k \in (-1, 0)$ in [67]. It can easily be extended to rescaled variables and works just in the same way in the fast diffusion regime $k \in (0, 1)$.

For the logarithmic case $k = 0$, $m = 1$, we know that the critical interaction strength is given by $\chi_c = 1$ separating the blow-up regime from the regime where self-similar solutions exist [136, 41, 33]. As shown in Chapter 2, there is no critical interaction strength for the fast diffusion regime $k > 0$, however the dichotomy appears in the porous medium regime $k < 0$. It is not known how to compute the critical parameter $\chi_c(k)$ explicitly for $k < 0$, however, we can make use of the numerical scheme to compute χ_c numerically.

Figure 1.5 gives an overview of the behaviour of solutions. In the red region, we observe finite-time blow-up of solutions, whereas for a choice of (k, χ) in the green region, solutions converge exponentially fast to a unique self-similar profile. The critical regime is characterised by the black line $\chi_c(k)$ with $-1 < k \leqslant 0$, separating the grey from the white region. Note that numerically we have $\chi_c(-0.99) = 0.11$ and $\chi_c(0) = 1$. Figure 1.5 has been created by solving the rescaled equation (3.29) repeatedly for each k from -0.99 to 0 in 0.01 steps. For a given k, the numerical critical interaction strength $\chi_c(k)$ is defined to be the largest χ for which the numerical solution can be computed without blow-up until the L^2-error between two consecutive solutions is less than a specified tolerance. In Chapter 3, we describe in detail the numerical scheme and investigate the behaviour of solutions at selected points in the parameter space (k, χ).

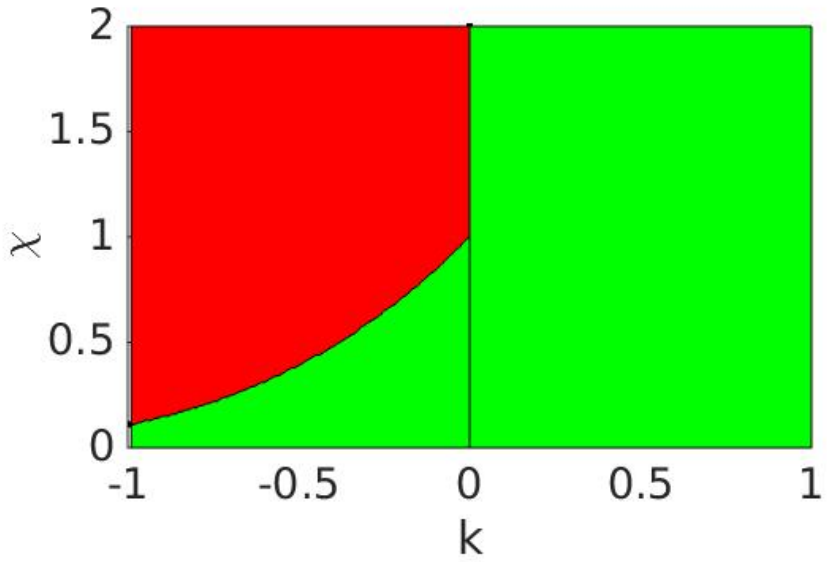

Figure 1.5: Regions of blow-up (red) and convergence to self-similarity (green) in the fair-competition regime $m_c = 1 - k/N$.

We close Chapter 3 with some investigations on the diffusion- and attraction-dominated regimes, using the numerical scheme described above to develop an intuition for the asymptotic behaviour of solutions we may expect.

For the attraction-dominated regime in any dimension $N(m-1)+k<0$, it is known that both global existence of solutions and blow-up can occur in original variables depending on the choice of initial data [118, 275, 278, 109, 32, 110, 224, 65]. In Chapter 3, we demonstrate this change of behaviour numerically in one dimension. Further, we investigate in more detail the regime $m = m^{**} := 2N/(2N+k)$ for which the free energy functional (2.18) is conformal invariant, a choice which also falls within the attraction-dominated regime $N(m-1)+k<0$. For $k<0$, we prove the existence of a critical point for the energy functional (2.18), using the fact that this choice of diffusion exponent corresponds to the case $p = q = m$ in the HLS inequality (3.21) for which the optimisers and the optimal constant are known explicitly.

Finally, we state two conjectures for the regime $m = m^{**}$. Firstly, we suggest that a similar result to [109, Theorem 2.1] holds true for general $k \in (-N, 0)$ and $m = m^{**}$ stating that global existence and blow-up in the radially symmetric setting can be characterised by a relation between the initial data and the HLS-optimisers. Numerically, we can indeed observe this behaviour for $N = 1$. Secondly, we conjecture that the unique HLS-optimiser with unit mass that is also a critical point for the energy functional (2.18) is in fact an unstable stationary state of equation (2.3). Again, we show that this can be observed numerically in one dimension.

Tables 1.1 and 1.3 provide an overview of the new results that we prove in part I of this thesis in the one dimensional fair-competition regime for the porous medium case ($k < 0$) and the fast diffusion case ($k > 0$) respectively. Table 1.2 summarises the relevant results known for the logarithmic case ($k = 0$). For an overview of the different regimes and choices of m and k discussed in this thesis, see Figure 1.4.

$\chi < \chi_c(k)$	$\chi = \chi_c(k)$	$\chi > \chi_c(k)$
Functional Inequalities: • There are no stationary states in original variables, there are no minimisers for $\mathcal{F}_k$ (Chapter 2 Theorem 2.7). • In rescaled variables, all stationary states are continuous and compactly supported (Chapter 2 Theorem 2.7). • There exists a minimiser of $\mathcal{F}_{k,\mathbf{resc}}$. Minimisers are symmetric non-increasing and uniformly bounded. Minimisers are stationary states in rescaled variables (Chapter 2 Theorem 2.7). • If $\bar{\rho}_{\mathbf{resc}}$ is a stationary state in rescaled variables, then all solutions of the rescaled equation satisfy $\mathcal{F}_{k,\mathbf{resc}}[\rho] \geqslant \mathcal{F}_{k,\mathbf{resc}}[\bar{\rho}_{\mathbf{resc}}]$ (Chapter 3 Theorem 3.6). • Stationary states in rescaled variables and minimisers of $\mathcal{F}_{k,\mathbf{resc}}$ are unique (Chapter 3 Corollary 3.9).	**Functional Inequalities:** • There exists a minimiser of $\mathcal{F}_k$. Minimisers are symmetric non-increasing, compactly supported and uniformly bounded. Minimisers are stationary states in original variables (Chapter 2 Theorem 2.6). • There are no stationary states in rescaled variables in $\mathcal{Y}_2$, and there are no minimisers of $\mathcal{F}_{k,\mathbf{resc}}$ in $\mathcal{Y}_2$ (Chapter 3 Corollary 3.11 (ii)). • If $\bar{\rho}$ is a stationary state in original variables, then all solutions satisfy $\mathcal{F}_k[\rho] \geqslant \mathcal{F}_k[\bar{\rho}] = 0$, which corresponds to a variation of the HLS inequality (Chapter 3 Theorem 3.2). • Stationary states in original variables and minimisers of $\mathcal{F}_k$ are unique up to dilations (Chapter 3 Corollary 3.5), and they coincide with the equality cases of $\mathcal{F}_k[\rho] \geqslant 0$.	**Functional Inequalities:** • There are no stationary states in original variables in $\mathcal{Y}$, and there are no minimisers of $\mathcal{F}_k$ in $\mathcal{Y}$ (Chapter 3 Corollary 3.11 (i)). • There are no stationary states in rescaled variables in $\mathcal{Y}_2$, and there are no minimisers of $\mathcal{F}_{k,\mathbf{resc}}$ in $\mathcal{Y}_2$ (Chapter 3 Corollary 3.11 (ii)).
Asymptotics: • Under a stability condition solutions converge exponentially fast in Wasserstein distance towards the unique stationary state in rescaled variables with rate 1 (Chapter 3 Proposition 4.5).	**Asymptotics:** • Under a stability condition and for solutions with second moment bounded in time, we have convergence in Wasserstein distance (without explicit rate) to a unique (up to dilation) stationary state (Chapter 3 Proposition 4.3).	**Asymptotics:** Asymptotics are not well understood yet. • If there exists a time $t_0 \geqslant 0$ such that $\mathcal{F}_k[\rho(t_0)] < 0$, then ρ blows up in finite time [275, 39]. • Numerics suggest that the energy of any solution becomes negative in finite time, but no analytical proof is known.

Table 1.1: Overview of results in one dimension for $-1 < k < 0$ and $m = m_c \in (1, 2)$.

3.4 The diffusion-dominated regime

3.4.1 Main results Chapter 4

In Chapter 4, we investigate the diffusion-dominated regime where $m > m_c = 1 - k/N$ and $k \in (-N, 0)$. In this regime diffusive forces dominate, avoiding blow-up for any choice of $\chi > 0$, and so there is no criticality for χ. Some of the techniques developed in Chapters 2 and 3 can

$\chi < 1$	$\chi = 1$	$\chi > 1$
Functional Inequalities: • There are no stationary states in original variables, but self-similar profiles [136, 41, 70, 71, 148].	**Functional Inequalities:** • If $\bar{\rho}$ is a stationary state in original variables, then all solutions satisfy $\mathcal{F}_k[\rho] \geqslant \mathcal{F}_k[\bar{\rho}]$, which corresponds to the logarithmic HLS inequality [136, 41, 62]. • Stationary states are given by dilations of Cauchy's density, $\bar{\rho}(x) = 1/(\pi(1+|x|^2))$, which coincide with the equality cases of the logarithmic HLS inequality. They all have infinite second moment [136, 41, 62].	**Functional Inequalities:** • Smooth fast-decaying solutions do not exist globally in time [242, 34, 41, 68]. • There are no stationary states in original variables and there are no minimisers of $\mathcal{F}_0$ in $\mathcal{Y}$ (Chapter 3 Remark 3.4).
Asymptotics: • Solutions converge exponentially fast in Wasserstein distance towards the unique stationary state in rescaled variables [62].	**Asymptotics:** • Solutions converge in Wasserstein distance to a dilation of Cauchy's density (without explicit rate) if the initial second moment is infinite, and to a Dirac mass otherwise [33, 40, 62, 37, 75].	**Asymptotics:** • All solutions blow up in finite time provided the second moment is initially finite [187, 260].

Table 1.2: Overview of results in one dimension for $k = 0$ and $m = m_c = 1$.

No criticality for χ
Functional Inequalities: • There are no stationary states in original variables (Chapter 3 Remark 4.9). In rescaled variables, there exists a continuous symmetric non-increasing stationary state (Chapter 2 Theorem 2.9). • There are no symmetric non-increasing global minimisers of $\mathcal{F}_k$. Global minimisers of $\mathcal{F}_{k,\mathbf{resc}}$ can only exist in the range $0 < k < \frac{2}{3}$ (Chapter 2 Theorem 2.9). • If $\bar{\rho}_{\mathbf{resc}}$ is a stationary state in rescaled variables, then all solutions of the rescaled equation satisfy $\mathcal{F}_{k,\mathbf{resc}}[\rho] \geqslant \mathcal{F}_{k,\mathbf{resc}}[\bar{\rho}_{\mathbf{resc}}]$ (Chapter 3 Theorem 3.13). Hence, for $0 < k < \frac{2}{3}$, there exists a global minimiser for $\mathcal{F}_{k,\mathbf{resc}}$. • For $0 < k < \frac{2}{3}$, stationary states in rescaled variables and global minimisers of $\mathcal{F}_{k,\mathbf{resc}}$ are unique (Chapter 3 Corollary 3.16).
Asymptotics: • Solutions converge exponentially fast in Wasserstein distance to the unique stationary state in rescaled variables with rate 1 (Chapter 3 Proposition 4.8).

Table 1.3: Overview of results in one dimension for $0 < k < 1$ and $m = m_c \in (0, 1)$.

be extended to the porous medium diffusion-dominated regime, such as the characterisation of stationary states for equation (2.3) and of global minimisers for the energy functional (2.18), which we denote by $\mathcal{F} := \mathcal{F}_{m,k}$ for simplicity. Let us define the diffusion exponent m^*,

$$m^* := \begin{cases} \frac{2-k-N}{1-k-N}\,, & \text{if} \quad N \geqslant 1 \quad \text{and} \quad -N < k < 1-N\,, \\ +\infty & \text{if} \quad N \geqslant 2 \quad \text{and} \quad 1-N \leqslant k < 0\,. \end{cases}$$

as it will play an important role for the regularity properties of global minimisers of $\mathcal{F}$.

First of all, we show in Chapter 4 that stationary states of (2.3) in $\mathcal{Y}$ are radially symmetric for all $\chi > 0$, $k \in (-N, 0)$ and $m > m_c$. This is one of the main results of [89], and is achieved under the assumption that the interaction kernel W_k is not more singular than the Newtonian potential close to the origin. The proof in [89] can be adapted to our setting as the main arguments continue to hold even for more singular W_k. Let us mention that the radiality of stationary states is crucial when making the connection to global minimisers of $\mathcal{F}$, which are also radially symmetric as the energy decreases under taking *symmetric decreasing rearrangements*[19]. In other words, this result reduces the question of uniqueness of stationary states to uniqueness of radially symmetric stationary states, allowing us to work in the radial setting instead.

Investigating the properties of global minimisers for $\mathcal{F}$, we show in Chapter 4 that they are compactly supported and uniformly bounded for all $\chi > 0$, $k \in (-N, 0)$ and $m > m_c$. Note that this result corresponds to what we find in the critical porous medium fair-competition regime, see Theorem 3.8. However here, we choose to develop a new method for the proof: instead of an iterative argument using hypergeometric functions to control global minimisers at the origin directly (see Chapter 2), we first proof an estimate for the mean-field potential $S_k = W_k * \rho$, and then argue by contradiction. The idea is that for every unbounded global minimiser one can construct a bounded competitor that decreases the energy. The difficulty in handling terms involving hypergeometric functions remains the same. Existence of global minimisers can be obtained using the concentration compactness argument by Lions [220], whereas proving Hölder regularity in the singular range $-N < k \leqslant 1 - N$ turns out to be more challenging in the diffusion-dominated case as one may have diffusion exponents m that are greater than 2, in which case one cannot transfer Hölder regularity of ρ^{m-1} to ρ directly. We obtain that global minimisers of $\mathcal{F}$ are regular enough to be stationary states of equation (2.3) under the condition that diffusion is not too fast, $m_c < m < m^*$. Moreover, bootstrapping on the obtained regularity using the Euler[18]-Lagrange[20] equation, we obtain that global minimisers of $\mathcal{F}$ in $\mathcal{Y}$ are C^∞ inside their support.

Finally, we apply the same methods as in Chapter 3 to derive an HLS-type inequality in one dimension using optimal transport techniques, establishing equivalence between global minimisers of $\mathcal{F}$ in $\mathcal{Y}$ and stationary states of equation (2.3). Additionally, this functional inequality provides uniqueness of stationary states in one dimension.

In summary, we will prove the following results in Chapter 4:

[19] The function $\rho^\#$ is said to be the symmetric decreasing rearrangement of ρ if $\rho^\#$ is radially symmetric non-increasing with the level sets of $\rho^\#$ and ρ having the same measure, i.e. $|\{x : \rho^\#(x) > c\}| = |\{x : \rho(x) > c\}|$.

[20] Joseph Louis Lagrange (1736-1813) was an Italian-French mathematician and astronomer. Lagrange was only 19 years old when he wrote to Euler announcing a new formalism to simplify Euler's method for finding a curve that satisfies an extremum condition. Using this formalism, he derived the fundamental equation of the calculus of variations, known today as *Euler-Lagrange equation*.

Theorem 3.11. *Let $N \geqslant 1$, $\chi > 0$ and $k \in (-N, 0)$. All stationary states of equation (1.2) are radially symmetric decreasing. If $m > m_c$, then there exists a global minimiser ρ of $\mathcal{F}$ on $\mathcal{Y}$. Further, all global minimisers $\rho \in \mathcal{Y}$ are radially symmetric non-increasing, compactly supported, uniformly bounded and C^∞ inside their support. Moreover, all global minimisers of $\mathcal{F}$ are stationary states of (1.2) whenever $m_c < m < m^*$. Finally, if $m_c < m < 2$, we have $\rho \in \mathcal{W}^{1,\infty}\left(\mathbb{R}^N\right)$.*

Theorem 3.12. *Let $N = 1$, $\chi > 0$ and $k \in (-1, 0)$. All stationary states of (1.2) are global minimisers of the energy functional $\mathcal{F}$ on $\mathcal{Y}$. Further, stationary states of (1.2) in $\mathcal{Y}$ are unique.*

4 Part I: Perspectives

There are many interesting open problems of varying difficulty centered around model (2.3), and I have started further investigations on some of them. In the light of Chapters 2-4, the central question is of course how to complete the picture of asymptotic behaviour in the fair-competition regime $N(m-1)+k=0$, and how to tackle the cases when attractive and repulsive forces are not in balance, namely the diffusion-dominating regime $N(m-1)+k>0$ and the aggregation-dominating regime $N(m-1)+k<0$.

4.1 The fair-competition regime $m = m_c$

The following are promising directions of work in progress or future research:

- **Uniqueness of stationary states and self-similar profiles** $k \in (-N, 0)$: Due to homogeneity, each global minimiser of $\mathcal{F}_{m,k}$ gives rise to a family of global minimisers for $\chi = \chi_c$ by dilation in the porous medium case $k \in (-N, 0)$, but it is an open problem to show that there is a unique global minimiser modulo dilations. This uniqueness was proven in the Newtonian case in [302], and in one dimension in Chapter 3. It would be interesting to explore the uniqueness modulo dilations of global minimisers in radial variables in higher dimensions, as one would then obtain the full set of stationary states with bounded second moment for model (2.3) as a by-product.

  In self-similar variables, we do not know if stationary states with second moment bounded are among global minimisers of the rescaled free energy $\mathcal{F}_{\mathbf{resc}}$ for the sub-critical regime $0 < \chi < \chi_c$ except in one dimension. For $N = 1$, we fully answered the uniqueness question in Chapter 3 using optimal transport techniques. It is also an open problem to show the uniqueness of radially symmetric self-similar profiles to (2.3) for $N > 1$.

- **Asymptotic behaviour** $k \in (-N, N)$: Formulating identity (**??**) in radial coordinates, it seems there is a natural generalisation of the methods employed in Chapter 3 to show convergence

to equilibrium in Wasserstein distance in any dimension in the radial setting. The computations are in spirit similar, but technically challenging due to the hypergeometric function terms involved. Ground states of $\mathcal{F}_{m,k}$ are the natural candidates amongst which to look for asymptotic profiles, and in this sense, Chapters 2 and 3 provide the necessary ground work for further investigations into the asymptotic behaviour of solutions.

- **Cauchy problem** $k \in (-N, N)$: The existence and uniqueness theory for the Cauchy problem of (2.3) is still an open problem. In the porous medium range $k \in (-N, 0)$, I would like to explore the possibility that a good variation of the results in [32, 39, 41] allows to tackle this question. In the fast diffusion range $k \in (0, N)$ nothing is known yet and it is not even clear which is the good functional framework to work in.

- **Very fast diffusion** $k \in (0, N)$: We showed in Chapter 2 that radially symmetric non-increasing stationary states in self-similar variables have so-called fat tails for large $|x|$. In particular, there is a critical $k_c := 2$ and respectively a critical diffusion exponent $m_c := (N-2)/N$ where a change of behaviour occurs. For $k < k_c$, mass is preserved, whereas if diffusion is too fast $k > k_c$, it is well known that mass escapes to infinity in the case of the classical fast diffusion equation ($\chi = 0$) and integrable L^∞-solutions go extinct in finite time. Extinction is an important phenomenon in the theory of non-linear diffusion, and it would be interesting to explore it for the fair-competition regime with $k > k_c$ for which – up to my knowledge – nothing is known yet. Another interesting direction would be to study smoothing effects using the techniques developed in [287] as regularisation would allow us to reduce the question of extinction to the behaviour of the tails.

- **Duality and stability estimates for related functional inequalities** $k \in (-N, 0)$: For the one-dimensional fair-competition regime we obtained the functional inequality $\mathcal{F}_{k,\mathbf{resc}}[\rho] \geqslant c$ for the sub-critical porous medium case $\chi < \chi_c$, $k \in (-1, 0)$, which contains an additional confinement potential, breaking homogeneity. We were not able to find this inequality in the literature and it certainly deserves further investigation. Rewriting the inequality as $\mathcal{G} \leqslant \mathcal{E}$ for suitable functionals $\mathcal{E}$ and $\mathcal{G}$, one can formulate the dual functional inequality

$$\mathcal{E}^* \leqslant \mathcal{G}^* \tag{4.30}$$

via Legendre[21] transforms. This dual functional inequality is by itself interesting and we are currently working on a local stability estimate for (4.30) by linearisation arguments. The optimisers of the classical HLS inequality are known explicitly, however we do not know the optimisers of $\mathcal{G} \leqslant \mathcal{E}$ due to the second moment term. To the best of our knowledge, [76] is

[21] Adrien-Marie Legendre (1752-1833) was a French mathematician. For nearly 200 years, books, paintings and articles have incorrectly shown a portrait of French politician Louis Legendre (1752-1797) representing him, until the mistake was discovered in 2005.

the only work in the literature where a stability estimate has been found without knowing the optimisers, and [111] is the first time stability has been shown for fractional powers, where the authors proved a stability estimate for the fractional HLS inequality by lifting the problem up to the sphere.

Once local stability for $\mathcal{E}^* \leqslant \mathcal{G}^*$ is established, we can hope to obtain global stability by a concentration compactness argument. Finally, it is possible to transport such a stability estimate back onto $\mathcal{G} \leqslant \mathcal{E}$ using the strategy introduced in [73]. The above argument also works in any dimension, assuming $\mathcal{G} \leqslant \mathcal{E}$ holds true for $N \geqslant 2$. Using the optimal transport approach applied in Chapter 3, it seems possible to prove the functional inequality in higher dimensions at least in the radial setting. Additionlly, this method may allow us to find an explicit expression for the critical interaction strength $\chi_c = \chi_c(k, N)$ using duality.

4.2 The diffusion-dominated regime $m > m_c$

In the diffusion-dominating regime, two main cases have been studied in the literature: the logarithmic case $k = 0$, $m > 1$ in two dimensions [78], and the Newtonian case $k = 2 - N$ with $m > 1$ [39], and $m > 2 - 2/N$ [199]. It would be interesting to see whether some techniques we used for the fair-competition regime in Chapters 2 and 3 could be applied for general $k \in (-N, N)$ and $m > m_c$, extending the results in Chapter 4. In particular, as we have only investigated the singular kernel case $k \in (-N, 0)$ so far, it would be interesting to explore the behaviour in the case $k \in (0, N)$. If $k \in (0, N)$ is large enough, one would expect that stationary states for the system (2.3) can exist. The goal here would be to first show that $\mathcal{F}_{m,k}$ is bounded below by proving a suitable version of a reversed HLS-type inequality. This allows then to tackle the question of existence of global minimisers using concentration-compactness arguments [223, 222, 221, 220].

In the case when $m_c < m < 1$, we expect global minimisers of $\mathcal{F}_{m,k}$ to be supported on the whole space, and therefore, one can use the methods developed in [35] to linearise around a minimiser – if it exists. More precisely, we expect the linearised flow to be self-adjoint in a weighted space with an appropriate norm, and a spectral gap of the linearised operator would yield an estimate for the local rate of convergence to equilibrium, which is optimal for large time. A more challenging problem is to investigate if the global rate of convergence is given by the asymptotic rate of convergence, which we do not know how to do so far without a suitable Bakry-Emery-type estimate [9].

4.3 The aggregation-dominated regime $m < m_c$

In the aggregation-dominated regime $m < m_c$ and $k \in (-N, N)$, very little is known except the work [109] by Chen, Liu and Wang where $m = 2N/(N + 2)$, and [32] by Bian and Liu where

$0 < m < 2 - 2/N$, both focusing on the Newtonian kernel case $k = 2 - N$. There, the authors classify blow-up vs global existence of radially symmetric solutions and study their long-time behaviour in terms of the non-linearity of the diffusion m and the choice of initial data. Their results rely on the special properties of the Newtonian potential and it is not at all clear how to tackle the problem for more general k and m.

5 Part II: Non-woven textiles

This part of the thesis is concerned with the development of a suitable method to show convergence to equilibrium for certain types of kinetic equations where the equilibrium state is not known a priori. We develop such a method in the context of a specific industrial application: modelling part of the production process of non-woven textiles.

5.1 Production process of non-woven textiles

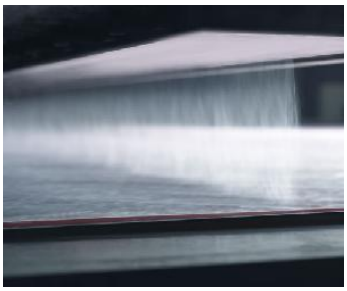

Figure 1.6: Non-woven Fabric Production Line. Source: product catalogue Zhejiang Sanlong Universal Machinery Co., Ltd[22].

Non-woven textiles are neither woven nor knitted, and have nowadays replaced traditional materials in many areas. From medical equipment such as surgical gowns and surgical masks, different types of filters for gasoline, oil and air, or coffee filters and tea bags, to diapers, tampons, mailing envelopes, pillows, cushions and mattress cores – non-woven textiles have become part of our everyday lives. They are now also being used as geotextiles for roadway underlayment, erosion control, canal construction, drainage systems, frost protection and agricultural mulch. They have the advantage that the production process does not require to convert fibres to yarn, and one can use recycled fabrics and oil-based materials to produce non-woven textiles. Depending on the application, these textiles are required to possess specific properties such as absorbency, liquid repellence, resilience, stretch, softness, strength, flame retardancy, washability, cushioning, thermal insulation, acoustic insulation, filtration, or act as a bacterial barrier. It is desirable to be able to control these properties during the production process. In particular, one would like to create a homogeneous material with the same set of properties at each point. Modelling the production process as an evolution equation, this corresponds to finding a stationary state of the system. Because of the equation's particular structure, mathematically, it is an interesting question to understand in which way the system converges to this stationary state and how to find an explicit rate of convergence in terms of the model parameters.

Let us now describe in more detail how non-woven textiles are produced using melt-spinning operations. A melted polymer is extruded through nozzles placed densely and equidistantly in a row at a spinning beam, creating hundreds of individual endless fibres. The visco-elastic, slender and in-extensible fibres lay down on a moving conveyor belt to form a web, where they solidify

[22] sinotongyong.en.made-in-china.com/product/nXuJrewvhxcM/China%2DSMMS%2DFour%2DBeams%2DNonwoven%2DFabric%2DProduction%2DLine.html

due to cooling air streams. Before touching the conveyor belt, the fibres become entangled and form loops due to highly turbulent air flow.

5.2 The fibre lay-down model

Figure 1.7: Compound for non-woven fabric production line. Source: product catalogue Zhejiang Sanlong Universal Machinery Co., Ltd[23].

The mathematical description of non-woven textile production has received a lot of interest in recent years with the development of several models [230, 231, 172, 203, 205, 134, 206]. We will now describe the context and the derivation of the model analysed in Chapter 5.

5.2.1 Stochastic description

In [230] a general mathematical model for the fibre dynamics is presented which enables the full simulation of the process. Due to the huge amount of physical details, these simulations of the production process usually require an extremely large computational effort and high memory storage, see [231]. Thus, a simplified two-dimensional stochastic model is introduced in [172], where the production of the fibres at the spinning beam and their entanglement due to air turbulence are not included, focusing instead on the way in which the fibres distribute onto the conveyor belt, called *fibre lay-down*. Generalisations of the two-dimensional stochastic model [172] to three dimensions have been developed by Klar et al. in [203] and to any dimension $N \geqslant 2$ by Grothaus et al. in [177].

We now describe the model we are interested in, developed in [172]. We track the position $x(t) \in \mathbb{R}^2$ and the angle $\alpha(t) \in \mathbb{S}^1$ of the fibre at the lay-down point where it touches the conveyor belt, see Figure 1.8. Interactions of neighbouring fibres are neglected. If $x_0(t)$ is the lay-down point in the coordinate system following the conveyor belt, then the tangent vector of the fibre is denoted by $\tau(\alpha(t))$ with $\tau(\alpha) = (\cos\alpha, \sin\alpha)$. Since the extrusion of fibres happens at a constant speed, and the fibres are in-extensible, the lay-down process can be assumed to happen at constant normalised speed $\|x_0'(t)\| = 1$. If the conveyor belt moves with constant normalised speed κ in direction $e_1 = (1, 0)$, then

$$\frac{\mathrm{d}x}{\mathrm{d}t} = \tau(\alpha) + \kappa e_1.$$

[23] sinotongyong.en.made-in-china.com/productimage/HbjmKkDMGOWw-2f1j00kjgTKfpCgYov/China-SMMS-Spunbond-and-Melt-Blown-Compound-Non-Woven-Fabric-Production-Line-Ty-S-Series.html

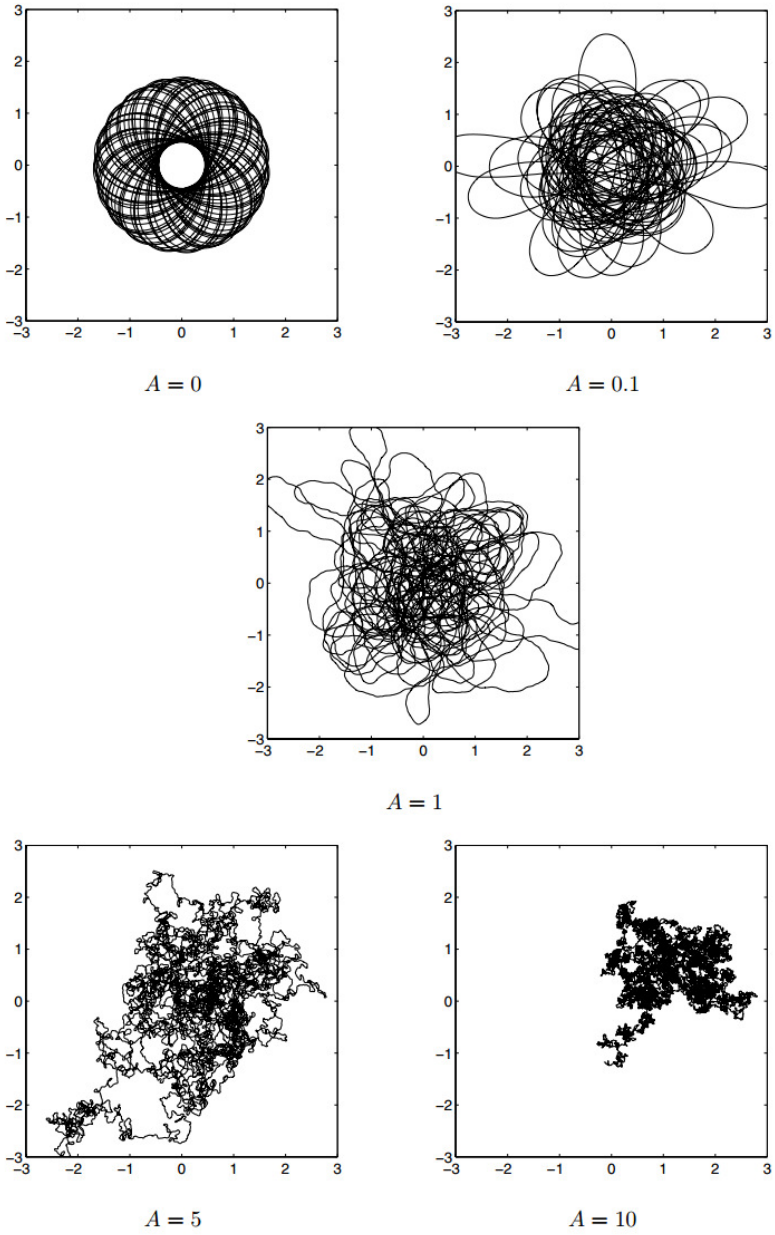

Figure 1.9: Representative path behaviours for solutions $X_t = (x_t, \alpha_t)$ to model (5.31) with a stationary conveyor belt ($\kappa = 0$), potential $V(x) = |x|$, for balanced ($A = 1$) as well as deterministic ($A < 1$) and stochastic ($A > 1$) dominated scenarios. Source: [172].

Note that the speed of the conveyor belt cannot exceed the lay-down speed: $0 \leqslant \kappa \leqslant 1$. The fibre is produced at a point above the origin, and so the coiling properties of the fibre push the lay-down point back to $x = 0$. The fibre dynamics in the deposition region close to the conveyor belt are dominated by the turbulent air flow. Applying this concept, the dynamics of the angle $\alpha(t)$ can be described by a deterministic force moving the lay-down point towards the origin and by a Brownian motion modelling the effect of the turbulent air flow. We obtain the following stochastic

differential equation for the random variable $X_t = (x_t, \alpha_t)$ on $\mathbb{R}^2 \times \mathbb{S}^1$,

$$\begin{cases} \mathrm{d}x_t &= (\tau(\alpha_t) + \kappa e_1)\,\mathrm{d}t, \\ \mathrm{d}\alpha_t &= \left[-\tau^\perp(\alpha_t) \cdot \nabla_x V(x_t)\right]\,\mathrm{d}t + A\,\mathrm{d}W_t\,, \end{cases} \tag{5.31}$$

where W_t denotes a one-dimensional Wiener[24] process, $A > 0$ measures its strength relative to the deterministic forcing, $\tau^\perp(\alpha) = (-\sin\alpha, \cos\alpha)$, and $V : \mathbb{R}^2 \to \mathbb{R}$ is an external potential carrying information on the coiling properties of the fibre. More precisely, since a curved fibre tends back to its starting point, the change of the angle α is assumed to be proportional to $\tau^\perp(\alpha) \cdot \nabla_x V(x)$. See Figure 1.9 for representative path behaviour of the system (5.31) with stationary conveyor belt ($\kappa = 0$) and for the choice of potential $V(x) = |x|$ with different noise intensities A describing the strength of the air turbulence.

It is shown in [206] that under suitable assumptions on the external potential V, the fibre lay down process (5.31) has a unique invariant distribution and is geometrically ergodic. More precisely, in [206] the authors assume that the potential satisfies

$$\lim_{|x|\to\infty} \frac{|\nabla_x V(x)|}{V(x)} = 0, \qquad \lim_{|x|\to\infty} \frac{|\nabla_x^2 V(x)|}{|\nabla_x V(x)|} = 0, \qquad \lim_{|x|\to\infty} |\nabla_x V(x)| = \infty. \tag{5.32}$$

Conceptually, these conditions ensure that the potential V is driving the process back inside a compact set where the noise can be controlled. Under assumptions (5.32), there exists an invariant distribution ν to the fibre lay-down process (5.31), and some constants $C(x_0) > 0$, $\lambda > 0$ such that

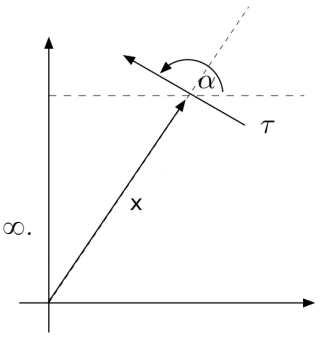

Figure 1.8: Position $x(t) \in \mathbb{R}^2$ and angle $\alpha(t) \in \mathbb{S}^1$ of the fibre where it is touching the conveyor belt.

$$\|\mathcal{P}_{x_0,\alpha_0}(X_t \in \cdot) - \nu\|_{TV} \leqslant C(x_0)e^{-\lambda t}\,,$$

where $\mathcal{P}_{x_0,\alpha_0}$ is the law of X_t starting at $X_0 = (x_0, \alpha_0)$, and $\|\cdot\|_{TV}$ denotes the total variation norm. The stochastic Lyapunov technique applied in [206] however does not give any information on how the constant $C(x_0)$ depends on the initial position x_0, or how the rate of convergence λ depends on the conveyor belt speed κ, the potential V and the noise strength A. We will show in Chapter 5 that a stronger result can be obtained with a functional analysis approach. Our framework is more general than conditions (5.32) in some aspects (including bounded potential gradient) and more restrictive in others (assuming a Poincaré inequality). Using hypocoercivity techniques and adapting the Lyapunov function argument presented in [206] to control the effect of the perturba-

[24] Norbert Wiener (1894-1964), an American mathematician and philosopher, was awarded his Ph.D. when just 18 years old. Wiener was a non-conformist, scientifically and mathematically, but also socially, culturally, politically, and philosophically. A *Wiener process* is a one-dimensional Brownian motion, named after the Scottish botanist Robert Brown (1773-1858).

tion $\kappa\partial_{x_1}$, we prove convergence in a weighted L^2-norm and derive an explicit rate of convergence in terms of κ, D and V.

5.2.2 Kinetic description

As we are not interested in the behaviour of the lay-down point of an individual fibre, but rather in the distribution of fibres on the belt as the number of fibres is large, we adopt a continuum description of the stochastic model (5.31). Let us denote by $f(t,x,\alpha)$ the density of the law of $X_t = (x_t, \alpha_t)$ in $\mathbb{R}^2 \times \mathbb{S}^1$. Then by Itô's Lemma[25] [266], $f(t,x,\alpha)$ is governed by the linear Fokker–Planck equation

$$\partial_t f + (\tau + \kappa e_1) \cdot \nabla_x f - \partial_\alpha \left(\tau^\perp \cdot \nabla_x V f\right) = D\partial_{\alpha\alpha} f \tag{5.33}$$

with diffusivity $D = A^2/2$. In other words, $f(t,x,\alpha)$ is the probability density distribution of fibres touching the belt at point $x \in \mathbb{R}^2$ at angle $\alpha \in \mathbb{S}^1$ at time $t \geqslant 0$.
In Chapter 5, we study the asymptotic behaviour of the kinetic model (5.33) using hypocoercivity techniques, a framework which we explain in more detail in the next section.

6 Part II: Hypocoercivity

Hypocoercivity is a method to show convergence to equilibrium for dissipative evolution equations involving a degenerate dissipative operator, and a first order operator generating a time-reversible conservative equation. Typically, the dissipative part is not coercive, in the sense that it does not admit a spectral gap. Additionally, its kernel is not stable under the action of the conservative part. A strategy to show convergence to equilibrium for this type of equation has been developed by several groups in the 2000s, see for instance [185, 178, 225, 129**?**], and a theoretical framework was adopted by Villani in [298]. The term *hypocoercivity*[26] has been introduced by Villani by analogy with problems encountered in the theory of *hypoellipticity*, a concept introduced by Hörmander in 1967 [193] and in which one is concerned with regularity issues instead of convergence to equilibrium. For many important equations, hypoellipticity has been established around the same time as hypocoercivity through the works of Hérau and Nier [185, 184], Eckmann and Hairer [141], Helffer and Nier [182]. However, hypocoercivity and hypoellipticity are independent concepts, despite the fact that they occur together in a number of models. More precisely, hypoellipticity can be localised as a property, whereas hypocoercivity cannot as it is always a global property of the operator.

[25] Itô's lemma is occasionally referred to as the Itô–Doeblin Theorem in recognition of posthumously discovered work of Wolfgang Doeblin.
[26] *Hypo* is an ancient Greek preposition, which translates as *under*, whereas *hyper* means *over* or *beyond*. The term *hypocoercivity* makes allusion to the fact that the operator is 'less than coercive'.

As described by Villani himself, the motivation for developing the general hypocoercivity theory as presented in [298] was 1) to simplify and unify the approach for the results obtained in [129, 130] for the Fokker–Planck equation and the Boltzmann equation, and 2) to find general methods that apply to various models sharing similar features. Villani derives in [298] results for exponential convergence to equilibrium for rather general operators in an abstract Hörmander form and under some commutator assumptions. With this new framework, Villani was able to prove an abstract and more general version of the non-linear results previously obtained in [129, 130].

Since the publication of [298], the hypocoercivity approach has been applied in a variety of contexts, from micro-magnetism and fluid mechanics (stability of Oseen vortices [162]) to statistical mechanics (models for propagation of heat [296, 226]). The advantage of the method is that one can find an explicit rate of convergence to equilibrium. However, this rate is most likely not optimal, and it remains to see if it is quantitatively relevant in the context of the model.

6.1 Abstract hypocoercivity approach: an example

Let us begin with a concrete and simple yet important example to give an idea of the general and rather abstract hypocoercivity approach. Consider the kinetic Fokker–Planck equation

$$\partial_t f + v \cdot \nabla_x f = \Delta_v f + \nabla_v \cdot (vf) \qquad x \in \mathbb{T}^N \,,\, v \in \mathbb{R}^N \,,$$

which has normalised stationary state $M(v) := (2\pi)^{-N/2} e^{-\frac{|v|^2}{2}}$. Since we have omitted the presence of a confining potential, we work on the torus $\mathbb{T}^N$ to keep the space variable confined. It is convenient to formulate the equation for the normalised solution $h := f/M$:

$$\partial_t h + v \cdot \nabla_x h = \Delta_v h - v \cdot \nabla_v h \tag{6.34}$$

with stationary state $h_\infty = 1$. Working in the Hilbert space $L^2(M(v)\,\mathrm{d}x\mathrm{d}v)$, we denote by $\langle \cdot \,,\, \cdot \rangle$ and $||\cdot||$ the corresponding inner product and norm. Hoping that the operator

$$\mathsf{L} := v \cdot \nabla_x h - \Delta_v h + v \cdot \nabla_v h$$

may be coercive on $\mathcal{H}^1$, one would like to show decay to the equilibrium h_∞ in the $\mathcal{H}^1$-norm $||h||^2_{\mathcal{H}^1} := ||h||^2 + ||\nabla_x h||^2 + ||\nabla_v h||^2$. This however is not possible. Taking for example a density $h = h(x) \in L^2(M(v)\,\mathrm{d}x\mathrm{d}v)$ that is independent of velocities, we find

$$\begin{aligned} \frac{1}{2}\frac{\mathrm{d}}{\mathrm{d}t}||h||^2_{\mathcal{H}^1} &= \iint\limits_{\mathbb{T}^N \times \mathbb{R}^N} v \cdot \nabla_x h \Delta_x h M \,\mathrm{d}x\mathrm{d}v - \iint\limits_{\mathbb{T}^N \times \mathbb{R}^N} h v \cdot \nabla_x h M \,\mathrm{d}x\mathrm{d}v \\ &= - \iint\limits_{\mathbb{T}^N \times \mathbb{R}^N} (\Delta_x h - h) \nabla_x \cdot \nabla_v M \,\mathrm{d}x\mathrm{d}v = 0 \,, \end{aligned}$$

and so decay cannot be guaranteed once the evolution reaches the set of velocity-independent densities. Since the null space of the dissipative part $-\Delta_v + v\cdot\nabla_v$ is not stable under the transport part $v\cdot\nabla_x$ of the operator, the set of velocity-independent densities is strictly larger than $\mathrm{Ker}\,\mathsf{L}$ and the evolution may not have reached equilibrium yet. The core idea of the hypocoercivity strategy is to add a mixed term $\langle \nabla_x h\,,\,\nabla_v h\rangle$ that can recover the missing decay. Let us define the modified entropy

$$\mathsf{G}[h] := ||h||^2 + a||\nabla_v h||^2 + 2b\langle \nabla_x h\,,\,\nabla_v h\rangle + c||\nabla_x h||^2 \tag{6.35}$$

with suitable constants $c \ll b \ll a \ll 1$. Then $\mathsf{G}[\cdot]$ is norm-equivalent to $||\cdot||_{\mathcal{H}^1}$ as long as $b^2 < ac$. However, these two norms are quite different since L is coercive with respect to G, whereas it is not with respect to $||\cdot||_{\mathcal{H}^1}$. The reason is the fact that the mixed term $\langle \nabla_x h\,,\,\nabla_v h\rangle$ is able to pick up the influence of the anti-symmetric part $\mathsf{B} := v\cdot\nabla_x$ of L to recover the derivative in the space variable:

$$\begin{aligned}\langle \nabla_x \mathsf{B}h\,,\,\nabla_v h\rangle + \langle \nabla_x h\,,\,\nabla_v \mathsf{B}h\rangle &= \langle \mathsf{B}\nabla_x h\,,\,\nabla_v h\rangle + \langle \nabla_x h\,,\,\nabla_v \mathsf{B}h\rangle\\ &= \langle \nabla_x h\,,\,\mathsf{B}^*\nabla_v h\rangle + \langle \nabla_x h\,,\,\nabla_v \mathsf{B}h\rangle\\ &= -\langle \nabla_x h\,,\,\mathsf{B}\nabla_v h\rangle + \langle \nabla_x h\,,\,\nabla_v \mathsf{B}h\rangle\\ &= \langle \nabla_x h, [\nabla_v\,,\,\mathsf{B}]h\rangle = ||\nabla_x h||^2\,.\end{aligned}$$

Here, we used that ∇_x and B commute, anti-symmetry of B, and the fact that $[\nabla_v\,,\,\mathsf{B}] = \nabla_x$. This shows why it may be useful to work with a Hörmander commutator notation similar to Hörmander's hypoellipticity theorem [193]. Let us give the main ideas of a simplified (i.e. only one commutator instead of several iterated commutators) hypocoercivity statement without going too much into detail. Following the hypocoercivity formalism established in [298], we write

$$\partial_t f + \mathsf{L}f = 0\,,\quad \mathsf{L} := \mathsf{A}^*\mathsf{A} + \mathsf{B}\,.$$

In the example (6.34), we have $\mathsf{A} := (0_N, \nabla_v)$ and $\mathsf{B} := (v, 0_N)\cdot\nabla_{x,v}$. Then $\mathsf{A}^* = (0_N, -\nabla_v - v)$, and so L can be written in Hörmander form of second type[27]: $\mathsf{L} = -\sum_j \mathsf{A}_j^2 + (\mathsf{B} + \sum_j c_j\mathsf{A}_j)$ with $c := (0_N, v)$. Let us define the commutator $\mathsf{C} := [\mathsf{A},\mathsf{B}] = \mathsf{AB} - (\mathsf{B}\otimes \mathrm{Id}_{2N})\mathsf{A} = (0_N, \nabla_x)$. [298, Theorem 18][28] states

Theorem 6.1. *If* B *is anti-symmetric, and there exist constants* α, β *such that*

(i) A *and* A^* *commute with* C; A *commutes with* A *(i.e.* A_i *commutes with* A_j *for all* $i,j\in\{1,\dots,2N\}$*);*

(ii) $[\mathsf{A},\mathsf{A}^*]$ *is* α*-bounded relatively to* $\mathrm{Id}_{2N} + \mathsf{A}$*;*

[27] In short, this means the operator can be written as sum of squares of derivations, plus a derivation, see [185, 141, 182].
[28] For a detailed description of the commutator notation used here and relative boundedness of operators, see [298].

(iii) $[\mathsf{B},\mathsf{C}]$ *is* β*-bounded relatively to* $\mathsf{A}, \mathsf{A}^2, \mathsf{C}$ *and* AC*;*

then there exists a scalar product $\langle\langle \cdot\,,\cdot \rangle\rangle$ *on* $\mathcal{H}^1/\mathcal{K}$*, where* $\mathcal{K} := Ker\,\mathsf{L}$*, that is norm-equivalent to* $||\cdot||_{\mathcal{H}^1}$ *such that*

$$\langle\langle h\,,\,\mathsf{L}h\rangle\rangle \geqslant K_1\left(||\mathsf{A}h||^2 + ||\mathsf{C}h||^2\right)$$

for some constant $K_1 > 0$*, only depending on* α *and* β*. If, in addition,* $\mathsf{A}^*\mathsf{A} + \mathsf{C}^*\mathsf{C}$ *is* K_2*-coercive for some* $K_2 > 0$*, then there is a constant* $\lambda = \lambda(\alpha,\beta,K_2) > 0$*, such that*

$$\forall h \in \mathcal{H}^1/\mathcal{K}\,, \qquad \langle\langle h\,,\,\mathsf{L}h\rangle\rangle \geqslant \lambda\langle\langle h\,,\,h\rangle\rangle\,.$$

It follows that L is hypocoercive on fluctuations $\mathcal{H}^1/\mathcal{K}$. It is easy to see that our example (6.34) satisfies all assumptions of the above theorem. Here, $\mathcal{H}^1/\mathcal{K} = \left\{h \in \mathcal{H}^1 \mid \iint_{\mathbb{T}^N\times\mathbb{R}^N} hM(v)\,\mathrm{d}x\mathrm{d}v = 0\right\}$ is the orthogonal of all constant functions $\langle h_\infty\rangle$ in $\langle\,\cdot\,,\,\cdot\,\rangle$, and $\mathsf{C} = \nabla_x$. Conditions (i)-(iii) are trivially satisfied since (i) A only acts on velocities, whereas C only acts on space, (ii) $[\mathsf{A},\mathsf{A}^*] = \mathsf{Id}_{2N}$ and (iii) $[\mathsf{B},\mathsf{C}] = 0$. Thanks to the Poincaré[29] inequality

$$\forall h \in \mathcal{H}^1 \quad \text{s.t.} \quad \iint\limits_{\mathbb{T}^N\times\mathbb{R}^N} hM(v)\,\mathrm{d}x\mathrm{d}v = 0\ : \qquad ||\nabla_x h||^2 + ||\nabla_v h||^2 \geqslant K_2||h||^2\,,$$

the operator $\mathsf{A}^*\mathsf{A} + \mathsf{C}^*\mathsf{C}$ is coercive on $\mathcal{H}^1/\mathcal{K}$. Further, $\langle\langle h\,,\,h\rangle\rangle = \mathsf{G}[h]$, and so Theorem 6.1 tells us that there exists a constant $\lambda > 0$ such that

$$\frac{\mathrm{d}}{\mathrm{d}t}\mathsf{G}[h] \leqslant -2\lambda\mathsf{G}[h]\,. \tag{6.36}$$

Generally, it is not possible to show $||h(t)||_{\mathcal{H}^1} \leqslant ||h(0)||_{\mathcal{H}^1}e^{-\lambda t}$ as explained above. However, it follows from norm-equivalence between $\mathsf{G}[\cdot]$ and $||\cdot||^2_{\mathcal{H}^1}$ and from (6.36) that

$$||h(t)||_{\mathcal{H}^1} \leqslant c_0||h(0)||_{\mathcal{H}^1}e^{-\lambda t}$$

on $\mathcal{H}^1/\mathcal{K}$ for some $\lambda > 0$ and $c_0 > 1$. This is exactly what we mean by saying that L is hypocoercive on $\mathcal{H}^1/\mathcal{K}$.

6.2 Framework for linear kinetic equations

In Chapter 5, we focus on a specific example of a linear kinetic equation conserving mass, a class of equations for which the general hypocoercivity theory simplifies greatly [135]. For a detailed account of the general method, see [298, 296] and the references therein. Consider the abstract ODE

$$\frac{\mathrm{d}}{\mathrm{d}t}f + \mathsf{T}f = \mathsf{Q}f \tag{6.37}$$

[29] Jules Henri Poincaré (1854-1912) was a French mathematician, theoretical physicist, engineer, and philosopher of science, and often described as a 'polymath'. He was proponent of the view, known as conventionalism, that it is not an objective question which model of geometry best fits physical space, but is rather a matter of which model we find most convenient.

governing the evolution of a density $f(t,x,v)$, where x and v denote the space and velocity variables respectively, and $f(t,\cdot) \in \mathcal{H}$ for all $t \geqslant 0$ for some Hilbert space $\mathcal{H}$. Here, T denotes a skew-symmetric transport operator and Q is a collision operator that is assumed to be negative semi-definite. Both operators are possibly unbounded. Further, let us assume that we have existence of a unique equilibrium distribution $F \in \mathcal{H}$ of unit mass satisfying $\mathsf{T}F = \mathsf{Q}F$. The goal is to show convergence to F in the norm $\|\cdot\|$ corresponding to the Hilbert space $\mathcal{H}$ for initial data $f_{in} \in \mathcal{H}$ of unit mass.

Hypocoercivity as a method has been developed for equations where the collision part of the operator only acts on the velocity variable. In particular, denoting by Π the projection onto velocity-independent densities, $\Pi f := \rho_f F/\rho_F$ with $\rho_f := \int f \mathrm{d}v$, we have $\Pi\mathsf{Q} = \mathsf{Q}\Pi = 0$. Since the mixing only occurs in the velocity variable, it is not directly obvious why one would expect to observe convergence to equilibrium both in space and in velocity. However, with the good assumptions on T, the mixing in v can be transferred to x via transport effects.

Under the assumptions that T is skew-symmetric and Q is negative semi-definite, one obtains the H-theorem

$$\frac{\mathrm{d}}{\mathrm{d}t}\|f\|^2 = \langle \mathsf{Q}f, f\rangle \leqslant 0\,, \tag{6.38}$$

In other words, $\|\cdot\|^2$ is a Lyapunov functional for equation (6.37). However, this does not give us any information about the kernel of T. Further, since Q is only negative semi-definite and not coercive, we cannot directly derive convergence to equilibrium from identity (6.38) as the decay in $\|\cdot\|^2$ pauses as soon as the solution $f(t)$ reaches the kernel of Q without necessarily being in the kernel of T. As described in the previous section, this can be remedied by adding a suitable mixed term as an equivalent norm, for which the operator is coercive. In this section, we describe how to formulate the framework of Theorem 6.1 for linear kinetic equations conserving mass without recourse to commutators, following the functional setting in [135]. The main difference of the approach taken in [135] compared to [298] is to work in an L^2-framework instead of $\mathcal{H}^1$, giving important physical information on the behaviour of solutions. For example, one can obtain exponential decay even if the initial datum f_{in} oscillates wildly, meaning that the hypocoercivity method is not sensitive to the regularity of f_{in}. Even though hypoellipticity may provide $\mathcal{H}^1$-regularity, there are two advantages to showing convergence in L^2: firstly, the approach in [135] also applies to equations that are not hypoelliptic, and secondly, an L^2-framework is preferable if one is interested in physical applications and dependence on the initial data. We also point out that $\mathcal{H}^1$-regularisation with global estimates in weighted norms has not been done yet for equation (6.37). In order to work in L^2, definition (6.35) is replaced with a different generalised entropy using a suitable auxiliary operator.

6.2.1 Generalised entropy

The main idea of the convergence proof for hypocoercive operators is to find a Lyapunov functional, a *generalised entropy*, that is better than the 'natural' entropy $\|\cdot\|^2$, by adding carefully chosen lower-order terms. This approach is motivated by [184] in the context of commutator theory for hypoelliptic operators, see Section 6.1. In the case of a linear kinetic equation of type (6.37), a suitable generalised entropy $\mathsf{G} : \mathcal{H} \to \mathbb{R}_+$ is given by

$$\mathsf{G}[f] := \frac{1}{2}\|f\|^2 + \varepsilon\langle \mathsf{A}f, f\rangle, \qquad \varepsilon > 0$$

with

$$\mathsf{A} := (1 + (\mathsf{T}\Pi)^*\mathsf{T}\Pi)^{-1}(\mathsf{T}\Pi)^*. \tag{6.39}$$

The *-notation refers to the adjoint in the inner product $\langle\cdot,\cdot\rangle$ corresponding to $\mathcal{H}$. Note that $(\mathsf{T}\Pi)^*\mathsf{T}\Pi$ is an elliptic operator. The operator A is bounded and regularises the solution to (6.37) in the space variable (and it is not the same as the operator A in Section 6.1). The idea of choosing this generalised entropy is due to [135] and allows to use the projection Π instead of having to deal with ∇_v. Here, $(\mathsf{T}\Pi)^*$ plays the role of the mixed term $\langle \nabla_x h\,,\, \nabla_v h\rangle$ in (6.35), and choosing $\mathsf{A} = (\mathsf{T}\Pi)^*$ would be enough to build a hypocoercivity theory along the lines of Theorem 6.1. The main idea of choosing A as in (6.39) is borrowed from Hérau [184]: replacing the $\mathcal{H}^1$-norm plus a mixed term with a mixed term only, but which is divided by a second order operator to obtain an operator of order zero (i.e. no derivatives). Here, the operator A is of order -1, but allows to show that solutions to (6.37) decay exponentially fast in L^2, i.e. the aim is to find an explicit $\lambda > 0$ such that $\frac{\mathrm{d}}{\mathrm{d}t}\mathsf{G} \leqslant -\lambda\mathsf{G}$ and show that G is norm-equivalent to $||\cdot||^2$.

6.2.2 Microscopic and macroscopic coercivity

Let us differentiate G along trajectories of the system,

$$\frac{\mathrm{d}}{\mathrm{d}t}\mathsf{G}[f] = \langle \mathsf{Q}f, f\rangle - \varepsilon\langle \mathsf{AT}\Pi f, f\rangle - \varepsilon\langle \mathsf{AT}(1-\Pi)f, f\rangle + \varepsilon\langle \mathsf{TA}f, f\rangle + \varepsilon\langle \mathsf{AQ}f, f\rangle, \tag{6.40}$$

using the fact that T is skew-symmetric, and so $\langle \mathsf{T}f, f\rangle = 0$, as well as $\mathsf{QA} = 0$ which follows since $g := \mathsf{A}f$ satisfies $g = -\Pi\mathsf{T}f + \Pi\mathsf{T}^2\Pi g$ and so it is in the kernel of Q. The first term can be conrolled by the following *microscopic coercivity* assumption: there exists $\lambda_m > 0$ such that

$$-\langle \mathsf{Q}f, f\rangle \geqslant \lambda_m\|(1-\Pi)f\|^2. \tag{6.41}$$

In other words, this means that we require the collision operator Q to be coercive on the complement of its kernel. In order to control the second term in (6.40), we need that the elliptic operator $\mathsf{AT}\Pi$ satisfies a Poincaré inequality, which corresponds to a spectral gap on the macroscopic level. This can be formulated as the following *macroscopic coercivity* assumption: there exists $\lambda_M > 0$

such that

$$\|\mathsf{T}\Pi f\|^2 \geqslant \lambda_M \|\Pi f\|^2 \Longrightarrow \langle \mathsf{A}\mathsf{T}\Pi f, f\rangle \geqslant \frac{\lambda_M}{1+\lambda_M}\|\Pi f\|^2 . \tag{6.42}$$

In other words, the restriction of T to $\operatorname{Ker}\mathsf{Q}$ is coercive.

6.2.3 Diffusive macroscopic limit

Take a change of variables $(t,x,v) \mapsto (t/\varepsilon^2, x/\varepsilon, v)$ in equation (6.37) depending on $0 < \varepsilon \ll 1$ such that the rescaled density $f^\varepsilon(t,x,v) = f\left(t/\varepsilon^2, x/\varepsilon, v\right)$ satisfies

$$\varepsilon^2 \frac{\mathrm{d}}{\mathrm{d}t} f^\varepsilon + \varepsilon \mathsf{T} f^\varepsilon = \mathsf{Q} f^\varepsilon . \tag{6.43}$$

Consider fluctuations around the set of velocity-independent densities, that is $f^\varepsilon = \Pi f^\varepsilon + \varepsilon R^\varepsilon$ for some $R^\varepsilon \in \mathcal{H}$. Substituting this ansatz into (6.43) and projecting onto the kernel of Q, we obtain the conservation law

$$\varepsilon \frac{\mathrm{d}}{\mathrm{d}t}(\Pi f^\varepsilon) + \Pi\mathsf{T}\Pi f^\varepsilon + \varepsilon \Pi \mathsf{T} R^\varepsilon = 0 , \tag{6.44}$$

since $\Pi^2 = \Pi$, $\Pi R^\varepsilon = \Pi(1-\Pi)f^\varepsilon/\varepsilon = 0$ and $\Pi\mathsf{Q} = 0$. Assuming that $f^\varepsilon \to f^0$ and $R^\varepsilon \to R^0$ in the limit $\varepsilon \to 0$, we obtain the identity

$$\Pi\mathsf{T}\Pi = 0 . \tag{6.45}$$

It follows from (6.43) that $\mathsf{Q} f^0 = 0$, and since f^0 is in $\operatorname{Ker}\mathsf{Q}$, we conclude that $f^0 = \Pi f^0$. Further, dividing (6.43) by ε and using that $\mathsf{Q}\Pi = 0$, we have

$$\varepsilon \frac{\mathrm{d}}{\mathrm{d}t} f^\varepsilon + \mathsf{T} f^\varepsilon = \mathsf{Q} f^\varepsilon/\varepsilon = \mathsf{Q}(1-\Pi) f^\varepsilon/\varepsilon = \mathsf{Q} R^\varepsilon .$$

Therefore, we obtain in the limit that $\mathsf{T} f^0 = \mathsf{Q} R^0$. Recalling that $f^0 = \Pi f^0$, we have

$$R^0 = \hat{\mathsf{Q}}^{-1}\mathsf{T} f^0 = \hat{\mathsf{Q}}^{-1}\mathsf{T}\Pi f^0 , \qquad \hat{\mathsf{Q}} := \mathsf{Q}|_{(1-\Pi)\mathcal{H}} .$$

Finally, dividing (6.44) by ε and using (6.45), we obtain in the limit $\varepsilon \to 0$ the macroscopic equation

$$\partial_t \Pi f^0 - (\mathsf{T}\Pi)^* \hat{\mathsf{Q}}^{-1}\mathsf{T}\Pi f^0 = 0 ,$$

where we used that T is skew-symmetric $\mathsf{T}^* = -\mathsf{T}$, and $\Pi^* = \Pi$. In other words, assuming $\Pi\mathsf{T}\Pi = 0$ corresponds to a diffusive macroscopic limit of equation (6.37).

6.2.4 Exponential convergence

The price to pay by using the generalised entropy G is that one needs to be able to control the last three terms in (6.40) also. The assumption $\Pi\mathsf{T}\Pi = 0$ yields [135, Lemma 1]

$$\|\mathsf{A} f\| \leqslant \frac{1}{2}\|(1-\Pi)f\| , \qquad \|\mathsf{T}\mathsf{A} f\| \leqslant \|(1-\Pi)f\| .$$

It follows from the first estimate that G is norm-equivalent to the Hilbert space norm $\|\cdot\|^2$ if $\varepsilon < 1$. Finally, it remains to show that the following auxiliary operators are bounded:

$$\big\langle \mathsf{AT}(1-\Pi)f, f\big\rangle + \big\langle \mathsf{AQ}f, f\big\rangle \leqslant C_M \|(1-\Pi)f\|^2 \tag{6.46}$$

for some constant $C_M > 0$. Putting all the bounds together, we obtain exponential decay of $\|f(t)\|$, i.e. *hypocoercivity*, with an explicitly computable rate depending on λ_m, λ_M, C_M, assuming that (6.41), (6.42), (6.46) and $\Pi\mathsf{T}\Pi = 0$ hold. For the detailed proof of this statement, see [135].

Applications of the hypocoercivity approach in the linear kinetic setting include equations containing confinement terms and different types of collision operators with mass conservation, such as the Fokker–Planck equation, scattering models and the linearised BGK equations, see [135] and the references therein. Further recent applications include the fibre-lay down process (5.33) for a stationary conveyor belt [134], a velocity-jump model for bacterial chemotaxis [69], and particles interacting with a vibrating medium [1].

7 Part II: Results

In Chapter 5, we apply the hypocoercivity method described above to the linear kinetic equation modelling the fibre lay-down in the production process of non-woven textiles as formulated in (5.33). The full hypocoercivity analysis of the long-time behaviour of solutions to this kinetic model in the case of a stationary conveyor belt $\kappa = 0$ is completed in [134]. In the case $\kappa = 0$, there exists a unique global normalised equilibrium distribution

$$F_0(x) = \frac{e^{-V(x)}}{\int_{\mathbb{R}^2} e^{V(x)}\mathrm{d}x}\,.$$

For technical applications in the production process of non-wovens, one is interested in a model including the movement of the conveyor belt, and in Chapter 5, we extend the results in [134] to the case $\kappa > 0$. This is not a trivial task for several reasons. First of all, for a moving conveyor belt, we are not able to find a stationary state for equation (5.33) explicitly. The hypocoercivity method however is used to find estimates about rates of convergence *after* the existence and uniqueness of a steady state have been established.
Secondly, adding the movement of the belt breaks the symmetry of the problem, and the operator assumptions required for the hypocoercivity strategy to work do not hold in the 'natural' functional framework. However, the hypocoercivity theory is based on a priori estimates [135], and is therefore stable under perturbation. We will show in Chapter 5 how the hypocoercivity technique can be adapted to this context under the assumption that the conveyor belt moves slow enough.

7.1 Functional framework

To set up a suitable functional framework for the fibre lay-down process, we rewrite the Fokker–Planck equation (5.33) as an abstract ODE

$$\partial_t f = \mathsf{L}_\kappa f = (\mathsf{Q} - \mathsf{T})\, f + \mathsf{P}_\kappa f, \tag{7.47}$$

where $\mathsf{Q} := D\partial_{\alpha\alpha}$ represents collisions, P_κ is the perturbation introduced by the moving belt,

$$\mathsf{P}_\kappa f := -\kappa e_1 \cdot \nabla_x f,$$

and the transport operator T is given by

$$\mathsf{T} f := \tau \cdot \nabla_x f - \partial_\alpha \left(\tau^\perp \cdot \nabla_x V f\right).$$

The main idea here is to introduce a weight function g that allows the control of the perturbative term in the case when the potential gradient $\nabla_x V$ is unbounded:

$$g(x,\alpha) = \exp\left(\beta V(x) + |\nabla_x V(x)|\Gamma\left(\tau(\alpha)\cdot\frac{\nabla_x V(x)}{|\nabla_x V(x)|}\right)\right)$$

if $|\nabla_x V| \to \infty$ as $|x| \to \infty$, and $g \equiv 0$ otherwise. For a detailed definition of $\beta > 1$ and $\Gamma \in C^1([-1,1]), \Gamma > 0$, see Chapter 5 Section 3. We consider solutions to (7.47) in the space $L^2(\mathrm{d}\mu_\kappa) := L^2(\mathbb{R}^2 \times \mathbb{S}^1, \mathrm{d}\mu_\kappa)$ with measure

$$\mathrm{d}\mu_\kappa(x,\alpha) = \left(e^{V(x)} + \zeta\kappa g(x,\alpha)\right)\frac{\mathrm{d}x\,\mathrm{d}\alpha}{2\pi}.$$

We denote by $\langle\cdot,\cdot\rangle_\kappa$ the corresponding scalar product and by $\|\cdot\|_\kappa$ the associated norm. Here, $\zeta > 0$ is a free parameter that needs to be chosen big enough depending on the relative speed of the conveyor belt κ in order to guarantee convergence to equilibrium.

In this functional setting, the operators T, Q and P_κ have several nice properties that allow us to apply the general hypocoercivity theory for linear kinetic equations conserving mass as outlined in [135]. First of all, if $\kappa = 0$, then Q and T are closed operators on $L^2(\mathrm{d}\mu_0)$ such that $\mathsf{Q} - \mathsf{T}$ generates the $\mathcal{C}_0$-semigroup $e^{(\mathsf{Q}-\mathsf{T})t}$ on $L^2(\mathrm{d}\mu_0)$ [134]. Adding the movement of the belt ($\kappa > 0$), we use the additional weight function $g > 0$ to control the perturbative term P_κ in the case of unbounded potential gradients. This allows us to construct a $\mathcal{C}_0$-semigroup for $\mathsf{L}_\kappa = \mathsf{Q} - \mathsf{T} + \mathsf{P}_\kappa$ also for $\kappa > 0$ (Theorem 4.1 in Chapter 5). Note that L_κ is closable in $L^2(\mathrm{d}\mu_\kappa)$ and its operator core is given by $\mathcal{C} := C_c^\infty\left(\mathbb{R}^2 \times \mathbb{S}^1\right)$. Unless otherwise specified, all computations are performed on $\mathcal{C}$, and can be extended to $L^2(\mathrm{d}\mu_\kappa)$ by density arguments.

The orthogonal projection Π on the set of local equilibria $\operatorname{Ker}\mathsf{Q}$ is $\Pi f := \frac{1}{2\pi}\int_{\mathbb{S}^1} f\,\mathrm{d}\alpha$, and we define the *mass* of a given distribution $f \in L^2(\mathrm{d}\mu_\kappa)$ by $M_f = \int_{\mathbb{R}^2} \Pi f\,\mathrm{d}x$. Integrating (7.47) over $\mathbb{R}^2 \times \mathbb{S}^1$, we see that the mass of any solution of (7.47) is conserved over time. Moreover, any solution of

(7.47) remains non-negative as soon as the initial datum is non-negative.

In the case of a stationary conveyor belt $\kappa = 0$, it was shown in [134] that the fibre lay-down model (7.47) fits into the hypocoercivity theory of linear kinetic equations conserving mass described in Section 6.2. Indeed, the collision operator Q is symmetric and negative semi-definite on $\mathcal{C}$,

$$\langle \mathsf{Q}f, f\rangle_0 = -D\,\|\partial_\alpha f\|_0^2 \leqslant 0\,,$$

i.e. Q is dissipative in $L^2(\mathrm{d}\mu_0)$. Further, we have $\mathsf{T}\Pi f = e^{-V}\tau\cdot\nabla_x u_f$ for $f\in\mathcal{C}$ with $u_f := e^V\Pi f$, which implies $\Pi\mathsf{T}\Pi = 0$ on $\mathcal{C}$. Our approach for tackling the problem of exponential convergence if $\kappa > 0$ is to treat the system as a small perturbation of the case $\kappa = 0$ for which microscopic and macroscopic coercivity are satisfied for sufficiently 'nice' potentials V.

In order to ensure that the operators Q and T satisfy microscopic and macroscopic coercivity respectively, we need to impose certain assumptions on the external potential V. Further, in order to recover convergence to equilibrium for the perturbed equation $\kappa > 0$, we need to make sure that the perturbation P_κ can be controlled in a suitable way. Therefore, we make the following assumptions on the external potential V:

(H1) *Regularity and symmetry*: $V\in C^2(\mathbb{R}^2)$ and V is spherically symmetric outside some ball $B(0,R_V)$.

(H2) *Normalisation*: $\int_{\mathbb{R}^2} e^{-V(x)}\,\mathrm{d}x = 1$.

(H3) *Spectral gap condition*: there exists a positive constant Λ such that for any $u\in H^1(e^{-V}\mathrm{d}x)$ with $\int_{\mathbb{R}^2} ue^{-V}\mathrm{d}x = 0$, we have the Poincaré inequality

$$\int_{\mathbb{R}^2} |\nabla_x u|^2\, e^{-V}\,\mathrm{d}x \geqslant \Lambda\int_{\mathbb{R}^2} u^2 e^{-V}\,\mathrm{d}x.$$

(H4) *Pointwise condition*: there exists $c_1 > 0$ such that for any $x\in\mathbb{R}^2$,

$$|\nabla_x^2 V(x)| \leqslant c_1(1+|\nabla_x V(x)|),$$

where $\nabla_x^2 V$ denotes the Hessian of $V(x)$.

(H5) *Behaviour at infinity*:

$$\lim_{|x|\to\infty}\frac{|\nabla_x V(x)|}{V(x)} = 0, \qquad \lim_{|x|\to\infty}\frac{|\nabla_x^2 V(x)|}{|\nabla_x V(x)|} = 0\,.$$

Assumptions **(H2-3-4)** are as stated in [134]. Assumption **(H1)** assumes regularity of the potential that is stronger and included in that discussed in [134] since **(H1)** implies $V\in W^{2,\infty}_{\mathrm{loc}}(\mathbb{R}^2)$. Roughly speaking, **(H2)** and **(H3)** require a sufficiently strong growth of $V(x)$ at infinity, whereas **(H4)** puts

a limitation on the growth behaviour. This leaves room, however, for a large class of confining potentials including $V(x) = (1 + |x|^2)^{s/2}$, $s \geqslant 1$. Assumption **(H5)** is only necessary if the potential gradient $|\nabla_x V|$ is unbounded. Both bounded and unbounded potential gradients may appear depending on the physical context.

Thanks to the spectral gap condition **(H3)**, microscopic and macroscopic coercivity follow:

- **Microscopic coercivity**: The operator Q is symmetric and the Poincaré inequality on $\mathbb{S}^1$,
$$\frac{1}{2\pi}\int_{\mathbb{S}^1} |\partial_\alpha f|^2 \,\mathrm{d}\alpha \geqslant \frac{1}{2\pi}\int_{\mathbb{S}^1} \left(f - \frac{1}{2\pi}\int_{\mathbb{S}^1} f \,\mathrm{d}\alpha\right)^2 \mathrm{d}\alpha,$$
yields that for all f in the operator domain $\mathcal{D}(\mathsf{Q})$,
$$-\langle \mathsf{Q}f, f\rangle_0 \geqslant D\,\|(1-\Pi)f\|_0^2\,.$$

- **Macroscopic coercivity**: The operator T is skew-symmetric and for any $h \in L^2(\mathrm{d}\mu)$ such that $u_h = e^V \Pi h \in \mathcal{H}^1(e^{-V}\mathrm{d}x)$ and $\iint_{\mathbb{R}^2\times\mathbb{S}^1} h \,\mathrm{d}\mu = 0$, we have
$$\begin{aligned}\|\mathsf{T}\Pi h\|_0^2 &= \frac{1}{4\pi}\iint_{\mathbb{R}^2\times\mathbb{S}^1} e^{-V}|\nabla_x u_h|^2 \,\mathrm{d}x\,\mathrm{d}\alpha \\ &\geqslant \frac{\Lambda}{4\pi}\iint_{\mathbb{R}^2\times\mathbb{S}^1} e^{-V} u_h^2 \,\mathrm{d}x\,\mathrm{d}\alpha = \frac{\Lambda}{2}\,\|\Pi h\|_0^2\end{aligned}$$
by the spectral gap condition **(H3)**.

Inspired by [135], we define the *hypocoercivity functional*
$$\mathsf{G}[f] := \frac{1}{2}\|f\|_\kappa^2 + \varepsilon_1\langle \mathsf{A}f, f\rangle_0\,,$$
with the auxiliary operator A as given in (6.39), and for some suitably chosen $\varepsilon_1 \in (0,1)$ to be determined later. It follows from [135] that $\mathsf{G}[\cdot]$ is equivalent to $\|\cdot\|_\kappa^2$ on $L^2(\mathrm{d}\mu_\kappa)$,
$$\left(\frac{1-\varepsilon_1}{2}\right)\|f\|_\kappa^2 \leqslant \mathsf{G}[f] \leqslant \left(\frac{1+\varepsilon_1}{2}\right)\|f\|_\kappa^2\,,$$

7.2 Hypocoercivity estimate and convergence

In Chapter 5, we prove a hypocoercivity estimate on the dissipation of the generalised entropy G that allows us to deduce both existence and uniqueness of an equilibrium distribution F_κ to equation (7.47) in the case of a moving conveyor belt $\kappa > 0$. Let us emphasize that a specific contribution of this work is to introduce *two* (and not one as in [135, 134]) modifications of the entropy: 1) we first modify the *space itself* with the coercivity weight g, then 2) we change the norm with an auxiliary operator following the hypocoercivity approach. As opposed to [134], where the authors estimate $\mathrm{d}\mathsf{G}/\mathrm{d}t$ on fluctuations around the equilibrium F_0 for $\kappa = 0$, we derive a more general estimate for any $f \in L^2(\mathrm{d}\mu_\kappa)$, involving an additional mass term:

Proposition 7.1. *Assume that hypothesis* ***(H1-2-3-4-5)*** *hold and that* $0 < \kappa < 1$ *is small enough (with a quantitative estimate). Let* $f_{\text{in}} \in L^2(\mathrm{d}\mu_\kappa)$ *and* $f = f(t, x, \alpha)$ *be a solution of* (5.33) *in* $L^2(\mathrm{d}\mu_\kappa)$ *subject to the initial condition* $f(t = 0) = f_{\text{in}}$*. Then* f *satisfies the following Grönwall type estimate:*

$$\frac{\mathrm{d}}{\mathrm{d}t}\mathsf{G}[f(t,\cdot)] \leqslant -\gamma_1 \mathsf{G}[f(t,\cdot)] + \gamma_2 M_f^2, \tag{7.48}$$

where $\gamma_1 > 0, \gamma_2 > 0$ *are explicit constants only depending on* κ*,* D *and* V*.*

Estimate (7.48) allows us to establish existence of solutions to (7.47) using semigroup theory (Theorem 4.1 in Chapter 5). More importantly, the above hypocoercivity estimate is the key ingredient that ensures existence and uniqueness of an equilibrium distribution $F_k \in L^2(\mathrm{d}\mu_\kappa)$ for equation (7.47). The main idea of the existence proof is to seek a stationary state in the bounded set

$$\mathcal{B} := \left\{ f \in L^2(\mathrm{d}\mu_\kappa) \,:\, \mathsf{G}[f] \leqslant \frac{\gamma_2}{\gamma_1},\, f \geqslant 0,\, M_f = 1 \right\}$$

using a contraction argument. More precisely, we show in Chapter 5 Section 4.2 that the set $\mathcal{B}$ is preserved under the action of the semi-group: $S_t(\mathcal{B}) \subset \mathcal{B}$ for all $t \geqslant 0$. Together with the hypocoercivity estimate (7.48) and Banach's fixed point theorem, this allows us to find $u^t \in \mathcal{B}$ such that $S_t(u^t) = u^t$ for all $t \geqslant 0$. Further, proving that $\mathcal{B}$ is sequentially compact and repeatedly applying the semi-group property of S_t, we show that there exists $u \in \mathcal{B}$ independent of t such that $S_t(u) = u$ for all $t \geqslant 0$. This concludes the existence of a stationary state F_k of unit mass for equation (7.47). Moreover, when applied to the difference of two solutions with the same mass, the hypocoercivity estimate (7.48) gives an estimate on the exponential decay rate towards equilibrium, and so uniqueness follows.

Our results in Chapter 5 can be summarised by the following theorem:

Theorem 7.2. *Let* $f_{\text{in}} \in L^2(\mathrm{d}\mu_\kappa)$ *and let* ***(H1-2-3-4-5)*** *hold. For* $0 < \kappa < 1$ *small enough (with a quantitative estimate) and* $\zeta > 0$ *large enough (with a quantitative estimate), there exists a unique non-negative stationary state* $F_\kappa \in L^2(\mathrm{d}\mu_\kappa)$ *with unit mass* $M_{F_\kappa} = 1$*. In addition, for any solution* f *of* (5.33) *in* $L^2(\mathrm{d}\mu_\kappa)$ *with mass* M_f *and subject to the initial condition* $f(t = 0) = f_{\text{in}}$*, we have*

$$\|f(t,\cdot) - M_f F_\kappa\|_\kappa \leqslant C \|f_{\text{in}} - M_f F_\kappa\|_\kappa \, e^{-\lambda_\kappa t},$$

where the rate of convergence $\lambda_\kappa > 0$ *depends only on* κ*,* D *and* V*, and the constant* $C > 0$ *depends only on* D *and* V*.*

In the case of a stationary conveyor belt $\kappa = 0$ considered in [134], the stationary state is characterised by the eigenpair (Λ_0, F_0) with $\Lambda_0 = 0$, $F_0 = e^{-V}$, and so $\mathrm{Ker}\, \mathsf{L}_0 = \langle F_0 \rangle$. This means that there is an isolated eigenvalue $\Lambda_0 = 0$ and a spectral gap of size at least $[-\lambda_0, 0]$ with the rest of the spectrum $\Sigma(\mathsf{L}_0)$ to the left of $-\lambda_0$ in the complex plane. Adding the movement of the conveyor belt, Theorem 7.2 shows that $\mathrm{Ker}\, \mathsf{L}_\kappa = \langle F_\kappa \rangle$ and the exponential decay to equilibrium with rate λ_κ corresponds to a spectral gap of size at least $[-\lambda_\kappa, 0]$. Further, it allows to recover an explicit expression for the rate of convergence λ_0 for $\kappa = 0$. In general, we are not able to compute the stationary state F_κ for $\kappa > 0$ explicitly, but F_κ converges to $F_0 = e^{-V}$ weakly as $\kappa \to 0$.

Remark 7.3. *Let us compare our assumptions* ***(H1-2-3-4-5)*** *with the conditions the authors require in [206] to show a stochastic convergence result in the case of a perturbed process ($\kappa > 0$). Our framework* ***(H1-2-3-4-5)*** *is more general than conditions (1.4) in some aspects (including bounded potential gradient) and more restrictive in others (assuming a Poincaré inequality). The proof in [206] relies on the strong Feller property which can be translated in some cases into a spectral gap; it also uses hypoellipticity to deduce the existence of a transition density, and concludes via an explicit Lyapunov function argument. With our framework* ***(H1-2-3-4-5)****, and adapting the Lyapunov function argument presented in [206] to control the effect of $\kappa \partial_{x_1}$, we derive an explicit rate of convergence in terms of κ, D and V.*

7.3 Perspectives

Working in $L^2(\mathrm{d}\mu_\kappa) \subset L^2(\mathrm{d}\mu_0)$ we are treating the operator L_κ as a small perturbation of the case $\kappa = 0$ with stationary conveyor belt. The natural space to investigate the convergence to F_κ in the case $\kappa > 0$ however is $L^2\left(F_\kappa^{-1}\, \mathrm{d}x\, \mathrm{d}\alpha\right)$. In this L^2-space the transport operator $\mathsf{T} - \mathsf{P}_\kappa$ is not skew-symmetric and the collision operator Q is not self-adjoint, so the hypocoercivity method [135] cannot be applied. To get around this, one can split the operator L_κ differently into a transport and a collision part following the approach in [69]. More precisely, we can write $\mathsf{L}_\kappa = \tilde{\mathsf{Q}} - \tilde{\mathsf{T}}$ where

$$\begin{cases} \tilde{\mathsf{Q}} f = \partial_\alpha \left(D \partial_\alpha f - \frac{\partial_\alpha F_\kappa}{F_\kappa} f \right), \\ \tilde{\mathsf{T}} f = (\tau + \kappa e_1) \cdot \nabla_x f - \partial_\alpha \left[\left(\tau^\perp \cdot \nabla_x V + \frac{\partial_\alpha F_\kappa}{F_\kappa} \right) f \right]. \end{cases}$$

Then in $L^2\left(F_\kappa^{-1}\, \mathrm{d}x\, \mathrm{d}\alpha\right)$ the operator $\tilde{\mathsf{Q}}$ is symmetric and negative semi-definite, and the operator $\tilde{\mathsf{T}}$ is skew-symmetric. Furthermore, the stationary state F_κ lies in the intersection of the kernels of the collision and transport operators, i.e. $F_\kappa \in \mathrm{Ker}\, \tilde{\mathsf{Q}} \cap \mathrm{Ker}\, \tilde{\mathsf{T}}$. The hypocoercivity approach requires microscopic and macroscopic coercivity of $\tilde{\mathsf{Q}}$ and $\tilde{\mathsf{T}}$. To this end, we need to be able to control the behaviour of the stationary state at infinity as in [69], i.e. for large enough $|x|$,

$$\forall\, \alpha \in \mathbb{S}^1, \quad e^{-\sigma_1 V(x)} \leqslant F_\kappa(x, \alpha) \leqslant e^{-\sigma_2 V(x)}$$

for some constants $\sigma_1, \sigma_2 > 0$. If true, this would be an important physical information on the stationary state, but we still do not know how to prove it. Even with this information at hand,

this approach requires that the existence of the stationary state be known a priori. The rate of convergence one obtains in this case may be different from the rate obtained here, and it is not clear which method yields the better rate as both are most likely not optimal.

There are several ways in which one could seek to improve the results in Chapter 5. For example, one could try to push the convergence result to larger values of κ using bifurcation techniques. More precisely, for a path $p : \kappa \mapsto F_k$ mapping κ to the stationary state F_κ of equation (5.33), Theorem (7.2) guarantees that p is defined on a small interval $[0, \kappa_0)$ for some $0 < \kappa_0 \ll 1$. It may be possible to extend this interval by showing that the implicit equation $P(\kappa, F_\kappa) = 0$ defining the stationary state F_κ is non-degenerate, i.e. that $\partial_2 P(\kappa, F_\kappa) \neq 0$.
Another future avenue would be to apply the techniques developed here to other models where the global equilibrium is not known a priori.

8 Part III: From micro to macro

The 6^{th} problem asked by Hilbert[30] in 1900 is concerned with the axiomatisation of physics. More than 100 years later it is still unresolved, and might never be considered completed as the problem statement is rather broad. Precisely, the original German text *Mathematische Probleme* states:

> Durch die Untersuchungen über die Grundlagen der Geometrie wird uns die Aufgabe nahegelegt, nach diesem Vorbilde diejenigen physikalischen Disciplinen axiomatisch zu behandeln, in denen schon heute die Mathematik eine hervorragende Rolle spielt; dies sind in erster Linie die Wahrscheinlichkeitsrechnung und die Mechanik.
> Was die Axiome der Wahrscheinlichkeitsrechnung[31] angeht, so scheint es mir wünschenswert, daß mit der logischen Untersuchung derselben zugleich eine strenge und befriedigende Entwickelung der Methode der mittleren Werte in der mathematischen Physik, speziell in der kinetischen Gastheorie Hand in Hand gehe.
> Ueber die Grundlagen der Mechanik liegen von physikalischer Seite bedeutende Untersuchungen vor; ich weise hin auf die Schriften von Mach[32], Hertz[33], Boltzmann[34] und Volkmann[35]; es ist daher sehr wünschenswert, wenn auch von den Mathematikern die Erörterung der Grundlagen der Mechanik aufgenommen würde. So regt uns beispielsweise das Boltzmannsche Buch über die Principe der Mechanik an, die dort angedeuteten Grenzprocesse, die von der atomistischen Auffassung zu den Gesetzen über die Bewegung der Continua führen, streng mathematisch zu begründen und durchzuführen. Umgekehrt könnte man die Bewegung über die Gesetze starrer Körper durch Grenzprocesse aus einem System von Axiomen abzuleiten suchen, die auf der Vorstellung von stetig veränderlichen, durch Parameter zu definirenden Zuständen eines den ganzen Raum stetig erfüllenden Stoffes beruhen - ist doch die Frage nach der Gleichberechtigung verschiedener Axiomensysteme stets von hohem principiellen Interesse.

The problem, suggested by Boltzmann's work on the principles of mechanics [45], is therefore to develop "mathematically the limiting processes [...] which lead from the atomistic view to the laws of motion of continua", namely to obtain a unified description of gases, including all levels

[30] David Hilbert (1862-1943) was a German mathematician and is recognised as one of the most influential and universal mathematicians of the 19^{th} and early 20^{th} centuries. He was invited to address the 2^{nd} International Congress of Mathematicians in Paris in 1900, where he proposed 23 problems that are known today as *Hilbert's problems*.
[31] Vgl. Bohlmann, Ueber Versicherungsmathematik 2te Vorlesung aus Klein und Riecke, Ueber angewandte Mathematik und Physik, Leipzig und Berlin 1900
[32] Die Mechanik in ihrer Entwickelung, Leipzig, zweite Auflage. Leipzig 1889
[33] Die Principien der Mechanik, Leipzig 1894
[34] Vorlesungen über die Principien der Mechanik, Leipzig 1897
[35] Einführung in das Studium der theoretischen Physik, Leipzig 1900

of description. In other words, the challenging question is whether macroscopic concepts can be understood microscopically.
The set of methods for making the connection between microscopic and macroscopic models are called *multiscale analysis* or s*caling process* or *limiting process*. The idea of multiscale analysis is to mathematically derive one particular model describing macroscopic phenomena in the observable physical world, from a microscopic model that is based on interactions between atoms, particles, or agents. Typically, the microscopic model (depending on space, time and velocity) contains more information than the macroscopic one (depending only on space and time). One can make the connection between these two regimes by averaging over the velocities and rescaling the time and space variables. Mathematically, this corresponds to 'zooming out', and so we are exchanging the loss of information on the kinetics with the ability to capture emerging dynamics of the bulk of particles that were only implicit in the kinetic equation. The choice of rescaling influences which phenomena we are able to observe on the macroscopic scale and has to be chosen in a sensible way to match the physical context: if we speed up time too much with respect to the scaling in space, the particles may escape to infinity and we see nothing; if we do not speed up time fast enough, no change will occur on the macroscopic level and so no interesting phenomena arise. Since certain information are lost in the scaling process, it is possible that different kinetic models lead to the same macroscopic equation. Examples of limiting processes for kinetic equations can be found in the classical references [263, 103, 294]. Let us mention that the terms 'microscopic', 'macroscopic' and 'mesoscopic' are sometimes used ambiguously in the literature. In this thesis, we will use 'microscopic' in the sense of 'kinetic' as opposed to a regime describing individual particle dynamics.

Building on the ideas of Maxwell in [232], in 1872, Boltzmann published his famous work [46] on what can be considered the master equation of kinetic theory

$$\partial_t f + v \cdot \nabla_x f = \mathsf{Q}(f, f)\,, \tag{8.49}$$

where $x \in \mathbb{R}^N$ represents position and $v \in \mathbb{R}^N$ velocity, for the probability density $f(t, x, v)$. The bilinear collision operator Q may differ depending on the type of microscopic interactions at play. Equation (8.49) is known as the *Boltzmann equation* and was derived for a monoatomic rarefied gas by merging mechanical concepts and statistical considerations [232, 46]. It describes gas particles undergoing free transport and collisions. In the modern literature, the term Boltzmann equation is often used in a more general sense, referring to any kinetic equation that describes the change of some quantity such as energy, charge or particle number in a thermodynamic system.

Chapter 6 is centred around the idea of understanding the relationship between different kinetic and macroscopic models using multiscale analysis. Diffusion approximations to kinetic

equations have been studied in various works, see for example [293, 13, 26, 121, 210, 258] and the references therein. In this section, we discuss two particular scaling approaches that play a role in Chapter 6, grazing collision limits and parabolic diffusion limits, exemplified by the Boltzmann equation (8.49) for different choices of collision kernels Q. The latter shows how a limiting process can be used to derive the classical Keller–Segel model (1.1) from a kinetic description for bacterial motion.

8.1 The Boltzmann equation: grazing collisions

The Boltzmann equation (8.49) has generated over the past century (and is still generating) a vast volume of literature, see [294] and the references therein. The Boltzmann collision kernel Q is given in its general form by

$$\mathsf{Q}(f,f) = \int_{\mathbb{R}^3}\int_{\mathbb{S}^2} B(v-v_*,\theta)(f'f'_* - ff_*)\,d\sigma dv_*\,,$$

where v and v_* are the pre-collisional velocities that determine the post-collisional velocities v' and v'_* respecting conservation of energy and momentum, parametrised by the unit vector σ:

$$v' = \frac{v+v_*}{2} + \frac{|v-v_*|}{2}\sigma\,,$$
$$v'_* = \frac{v+v_*}{2} - \frac{|v-v_*|}{2}\sigma\,.$$

For brevity, we write $f'_* = f(t,x,v'_*)$ etc. The deflection angle $\theta \in [0,\pi/2]$ is such that $\cos\theta = (v-v_*)\cdot\sigma/|v-v_*|$. The kernel B is determined depending on the nature of interaction between particles. We will here only concentrate on one particular type of particle interaction that is relevant for the analysis in Chapter 6: If we assume that particles interact through a $1/r^s$ force law, where r is the distance between interacting particles, then the kernel B has a non-integrable singularity at $\theta = 0$ which corresponds to grazing collisions. *Grazing collisions* are collisions that do not deviate the particles too much. In many studies, the singularity issue is avoided by replacing B with a locally integrable collision kernel, which is usually referred to as *cut-off process* [175]. But what happens if there are more and more collisions, but these collisions generate smaller and smaller deviations? This limit process is known as *grazing collision limit*.

It is known that in the limit and under certain assumptions, solutions of the Boltzmann equation (8.49) converge to solutions of the Fokker-Planck-Landau (FPL) equation [158, 157]. The FPL equation describes the binary collisions between charged particles occurring in a plasma [128, 219] and was introduced as an approximation of the Boltzmann equation (8.49) in the case of Coulomb interactions [208]. In fact, the Boltzmann operator $\mathsf{Q}(f,f)$ is meaningless in the case of a Coulomb interaction as the effect of grazing collisions prevails over the effect of other collisions in that case. In the early 90's, Degond and Lucquin-Desreux [122] and Desvillettes [127] showed the convergence

of the Boltzmann operator Q to the FPL operator (not to be confused with convergence of the solutions). For further results clarifying the connection between the Boltzmann equation and the FPL equation, see [291, 158]. For more details on the grazing collision limit, see [8, 122, 127, 291, 292] and the references therein. In Chapter 6, we will use a grazing collision limit to derive a Vlasov-type flocking equation from a kinetic model for collective animal behaviour. The kinetic model is of Boltzmann-type in the sense that the collision kernel describing the interaction between two colliding gas particles is replaced with an interaction kernel describing the communication mechanism between individuals. Albeit very different applications, the general structures of these equations are similar. Applying a grazing limit to this Boltzmann-type equation, we obtain a flocking model that has been previously derived from individual-based models (Vicsek or Cucker-Smale models), see Chapter 6 Section 3.2.

8.2 Bacterial chemotaxis: a kinetic description

Boltzmann's idea for modelling the dynamics of a rarefied monoatomic gas can be transferred to a wide range of applications using kinetic equations of a similar structure. In the context of this thesis, it is noteworthy that a non-linear generalisation of the classical Keller–Segel model (1.1) can, in fact, be derived from a kinetic Boltzmann-type equation via multiscale analysis. Or, to be more precise, by making the connection to the underlying microscopic dynamics that drive the emerging patterns on the macroscopic level, we can understand better why certain limitations of the classical Keller–Segel model arise. In fact, the classical Keller–Segel model does not take the microscopic scale into account and it is an oversimplified description of the real dynamics as can be seen by the dramatic blow-up in the two dimensional case [136]. Starting with a microscopic description of the movement of a single cell in response to chemical gradients, one can use a diffusive limiting process to derive a macroscopic model for bacterial chemotaxis. We will here explain this scaling in more detail since it provides the mathematical tools for performing the multiscale analysis of a two-dimensional kinetic models for social interactions studied in Chapter 6.

Let us consider a model for bacterial chemotaxis, where the first equation in (1.1) (macroscopic evolution of the cell density) is replaced by a kinetic equation, whilst the chemoattractant concentration $S(t,x)$ is still governed by the macroscopic diffusion equation

$$\partial_t S = D_S \Delta S - \alpha S + \beta \rho \,. \tag{8.50}$$

where $\rho(t,x) = \int_{v\epsilon V} f(t,x,v)dv$ denotes the macroscopic cell density. Here, $\alpha \geqslant 0$ and $\beta \geqslant 0$ are the degradation and production rates of the chemoattractant respectively.

The motion of a single bacterium combines so-called *run* and *tumbling* phases. During a *run* phase a bacterium swims at a constant speed c in a given direction, while during a *tumble* event it changes direction in a way that is almost uniformly random, see Figure 1.10. Therefore, the evolution of the microscopic density of cells $f(t,x,v)$ can be described by the following Boltzmann-type equation, proposed in the pioneering works of Othmer, Dunbar and Alt [247, 2, 274, 150, 301]:

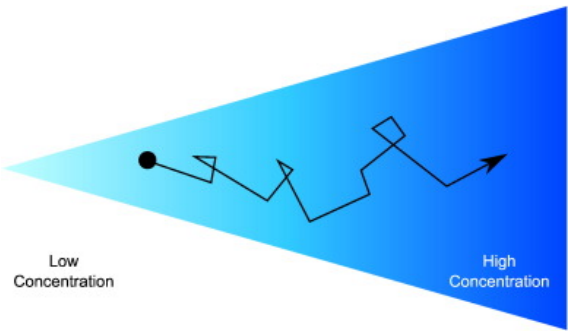

Figure 1.10: Run and tumble swimming pattern of *E. coli* . Source: [142].

$$\underbrace{\partial_t f + v\cdot\nabla_x f}_{run} = \underbrace{\int_{v'\in V} \mathbf{T}[S](v',v)f(t,x,v')\,dv' - \boldsymbol{\lambda}[S]f(t,x,v)}_{tumble}\,. \tag{8.51}$$

Here, the set V of all possible velocities is bounded and symmetric in general. The tumbling kernel $\boldsymbol{T}[S](v,v')$ describes the frequency of changing velocity from v to v' as a function of the chemoattractant S, and the tumbling rate is given by $\boldsymbol{\lambda}[S] = \int_{v'\in V}\mathbf{T}[S](v,v')\,dv'$. In absence of any external stimulus, *E. coli* perform a random walk, and so $\boldsymbol{T}[0]$ is a positive constant. *E. coli* have receptors on their outer membrane that allow them to sense changes in chemical concentration in their environment, which in turn introduces a bias into their tumbling frequency, and so it is reasonable to assume that *E. coli* react instantaneously to a variation of S along their trajectories,

$$\mathbf{T}[S](v,v') = \psi\left(\frac{DS}{Dt}\right) = \psi\left(\partial_t S + v\cdot\nabla_x S\right)\,,$$

where $\frac{DS}{Dt} = \partial_t S + v\cdot\nabla_x S$ denotes the material derivative of S. The tumbling kernel $\boldsymbol{T}$ is defined in analogy with the Boltzmann collision kernel B. However, $\boldsymbol{T}$ is not bilinear as it depends on the macroscopic cell density ρ via the dynamics of S (8.50). Further, notice that the tumbling kernel does not depend on the posterior speed v' as cells can be considered to choose a new direction uniformly random during a tumble. Finally, the function $\psi:\mathbb{R}\to\mathbb{R}_{>0}$ is decreasing, expressing that a cell is less likely to tumble when the external chemical signal increases along the cell's trajectory.

8.3 Parabolic scaling

When the bias (that is, the amplitude of the variation of ψ) is small compared to a cell's unbiased movement, we expect the limiting macroscopic equations to be of diffusion or drift-diffusion type, see for instance [104] for a rigorous proof. Therefore, a parabolic diffusion limit is well adapted to capture the macroscopic dynamics of (8.51). We will here explain the limiting process performed

in [265] that allows to recover the classical Keller–Segel model for the fully coupled system.

The key assumption allowing to pass to a macroscopic description is that the turning probability $\mathbf{T}[S](v,v')$ is a small perturbation of a random turning process,

$$\mathbf{T}[S](v,v') = \psi_0 + \varepsilon\psi_0\phi[S](v)\,, \quad \varepsilon \ll 1\,,$$

where the signal response function ϕ is to be chosen according to the reaction of cells to the stimulus S. Rescaling the kinetic equation to its non-dimensional form, and changing variables $(t,x,v) \mapsto (t/\varepsilon^2, x/\varepsilon, v)$, we obtain the following equation for the rescaled density $f^\varepsilon(t,x,v)$ in the new variables:

$$\begin{aligned}\varepsilon\partial_t f^\varepsilon + v\cdot\nabla_x f = \frac{\mu}{\varepsilon}\Big(\rho^\varepsilon(t,x) - |V| f^\varepsilon(t,x,v)\Big) + \\ \mu\left[\int_{v'\epsilon V}\phi[S^\varepsilon](v') f^\varepsilon(t,x,v')dv' - |V|\phi[S^\varepsilon](v) f^\varepsilon(t,x,v)\right],\end{aligned} \tag{8.52}$$

where $\rho^\varepsilon(t,x) = \int_{v\epsilon V} f^\varepsilon(t,x,v)dv$ denotes the macroscopic cell density, and μ is a non-dimensional coefficient of order 1. Taking the limit $\varepsilon \to 0$, and assuming that $f^\varepsilon, \rho^\varepsilon, S^\varepsilon$ converge to f^0, ρ^0, S^0 respectively, the dominant term is a relaxation towards a uniform distribution in velocity at each position: $f^0(t,x,v) = \rho^0(t,x)/|V|$. Integrating (8.52) over V, we obtain

$$\partial_t\rho^\varepsilon + \nabla\,.\,j^\varepsilon = 0, \qquad j^\varepsilon := \frac{1}{\varepsilon}\int_{v\epsilon V} v f^\varepsilon(t,x,v)dv. \tag{8.53}$$

In order to determine the bacterial flow $j^\varepsilon \in \mathbb{R}^N$, we integrate (8.52) against $v \in V$,

$$\begin{aligned}\varepsilon\partial_t\left(\int_{v\epsilon V} v f^\varepsilon(t,x,v)\,dv\right) + \nabla_x\cdot\left(\int_{v\epsilon V} v\otimes v f^\varepsilon(t,x,v)\,dv\right) \\ = -\mu|V| j^\varepsilon - \mu|V|\int_{v\epsilon V} v\phi[S^\varepsilon](v) f^\varepsilon(t,x,v)\,dv\,,\end{aligned}$$

which becomes formally in the limit $\varepsilon \to 0$:

$$j^0 = -\nabla_x\Big(\rho^0(t,x)\frac{1}{\mu N|V|^2}\int_{v\epsilon V}|v|^2\,dv\Big) - \rho^0(t,x)\frac{1}{|V|}\int_{v\epsilon V} v\phi[S^0](v)\,dv\,.$$

Hence, by (8.53), the cell density ρ^0 solves the macroscopic drift-diffusion equation

$$\partial_t\rho^0 = D_\rho\Delta\rho^0 - \nabla\cdot(\rho^0\mathbf{u}[S^0])\,, \tag{8.54}$$

where the macroscopic bacterial diffusion coefficient D_ρ and the chemotactic flux $\mathbf{u}[S^0]$ are derived from the microscopic parameters μ, the velocity set V and the signal response function ϕ:

$$D_\rho = \frac{1}{\mu N|V|^2}\int_{v\epsilon V}|v|^2\,dv\,, \qquad \mathbf{u}[S^0] = \frac{1}{|V|}\int_{v\epsilon V} v\phi(v\cdot\nabla S^0)\,dv\,.$$

The only unknown of the model remains the response function ϕ which indicates how a cell reacts to chemical variations in its environment. In the most general description, it is only assumed

to be odd and decreasing in order to be consistent with the biological context. Linearising (8.54) by assuming that the chemotactic flux is of the form $\mathbf{u}[S] = \chi \nabla S$, we obtain exactly the classical Keller–Segel model (1.1). In other words, the macroscopic model (1.1) describes sufficiently well the observed behaviour as long as the non-linear terms of the chemotactic flux are not predominant, which holds true for small enough chemical gradients.

9 Part III: Collective animal behaviour

Migrating herds of ungulates, zigzagging flocks of birds, stationary aggregations formed by resting animals, moving bands of bacteria or milling schools of fish are just some of the many patters that we observe in animal communities. In many instances, these (temporarily) stable macroscopic patterns are of surprising complexity but appear with remarkable regularity. How do these patterns arise? Can we reproduce them mathematically? And if yes, which are the driving factors for the dynamics? In Chapter 6, we try to answer some of these questions focusing on collective behaviour in absence of a leader, which is why we call it *self-organised* behaviour. If each individual can only communicate with neighbours within a certain range, which is the case for starlings and certain types of bats for example, how is it possible that we observe beautiful coordination on a macroscopic level, as if the group is moving with one body and one mind?

(a) (b) (c)

Figure 1.11: Murmurations by photographer and artist Alain Delorme[36]. Source: Delorme's website[37].

Over the past 10-20 years a multitude of kinetic and macroscopic models have been introduced to investigate the formation and movement of various biological aggregations: from cells [22, 5] and bacteria [257] to flocks of birds, schools of fish and even human aggregations (see, for example, [290, 124, 147, 146, 153, 86] and the references therein). Generally, these models assume that individuals, particles, or cells can organise themselves in the absence of a leader as a results of various social forces: repulsion from nearby neighbours, attraction to far-away neighbours (or to

[36] Did you think you are looking at birds? This art project tricks the eye by making trash bags look like flocks of starlings. For more details, see www.wired.com/2014/05/alain-delorme-murmurations/.

[37] www.alaindelorme.com/works-murmurations

roosting areas [93]) and alignment/orientation with neighbours positioned at intermediate distances.

9.1 Overview of models and scalings

In Chapter 6, we consider two families of nonlocal kinetic models proposed in [147, 146, 153], one being one-dimensional, and the other two-dimensional, and make the connection to several macroscopic models using multiscale analysis (parabolic limits/grazing collision limits), see Figure 1.12. In this section, we give an overview of the models and scaling approaches presented in Chapter 6, summarising the obtained results.

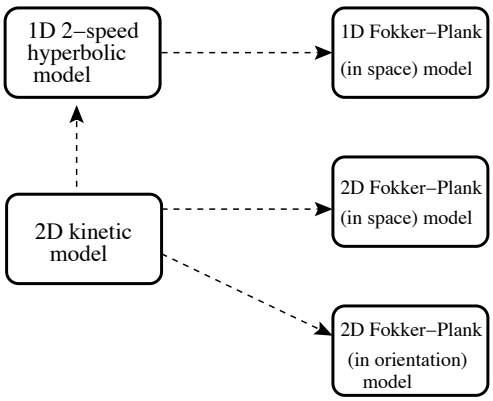

Figure 1.12: Scaling approaches taken in Chapter 6.

The following one-dimensional model was introduced in [147, 146] to describe the densities of left-moving (u^-) and right-moving (u^+) individuals that interact with conspecifics via social interactions:

$$\partial_t u^+ + \gamma \partial_x u^+ = -\lambda^+ u^+ + \lambda^- u^- \,, \tag{9.55a}$$

$$\partial_t u^- - \gamma \partial_x u^- = \lambda^+ u^+ - \lambda^- u^- \,. \tag{9.55b}$$

Here, individuals travel at constant speed γ and $\lambda^+ = \lambda^+[u^+, u^-]$ denotes the rate at which right-moving individuals turn left (vice versa for $\lambda^- = \lambda^-[u^+, u^-]$). In Chapter 6, we generalise the turning rates in [147, 146, 144] and assume that

$$\lambda^\pm[u^+, u^-] = \lambda_1 + \lambda_2 f(y_N) + \lambda_3 f(y_D^\pm) \,, \tag{9.56}$$

where $y_N = y_N[u^+, u^-]$ and $y_D^\pm = y_D^\pm[u^+, u^-]$ denote the non-directed and directed turning mechanisms respectively. The turning function $f(\cdot)$ is a non-negative, increasing, bounded functional of the interactions with neighbours, and $\lambda_1, \lambda_2, \lambda_3$ denote constant turning rates. In Chapter 6, we focus on two particular choices of $\lambda^\pm$ corresponding to models M2 and M4 in [146]. We focus on these two particular choices because: (i) model M2 with $\lambda_1 = 0$ has been generalised to 2D in [153]; (ii) model M4 with $\lambda_2 = 0$ has been investigated analytically and numerically, and it was shown that it can exhibit Hopf bifurcations (even without alignment forces) giving rise to spatio-temporal patterns such as rotating waves and modulated rotating waves [56]. In contrast, model M2 with $\lambda_2 = 0$ does not seem to exhibit rotating waves in the absence of alignment, see [146].

We perform a parabolic scaling of the kinetic model (9.55) via $(t,x) \mapsto (t/\varepsilon^2, x/\varepsilon)$, using two different scaling assumptions. Firstly, let us assume that individuals have a reduced perception of their surroundings for small values of ε [143], that is, in rescaled variables

$$f_\varepsilon\Big(y_D^\pm[u,v]\Big) = \varepsilon f\Big(y_D^\pm[u, \int_{x/\varepsilon} \varepsilon\partial_t u]\Big)\,, \quad f_\varepsilon\Big(y_N[u]\Big) = \varepsilon f\Big(y_N[u]\Big)\,,$$

where $u := u^+ + u^-$ and $v := \gamma(u^+ - v^-)$. We obtain formally in the limit $\varepsilon \to 0$,

$$\partial_t u = D_0 \partial_{xx} u - \partial_x\Big(S_0\, u\, V(u)\Big)\,,$$

with diffusion rate $D_0 = \gamma^2/(2\lambda_1)$ and drift rate $S_0 = \lambda_3\gamma/(2\lambda_1)$ explicitly given in terms of the microscopic parameters. The expression for the velocity $V(u)$ differs for M2 or M4.
Secondly, if instead we assume f to be a linear function with a very weak directed turning behaviour, we can write

$$\lambda^\pm = \lambda_1 + \lambda_2\, K^N * u + \varepsilon\, \lambda_3 y_D^\pm[u] \tag{9.57}$$

with $y_N[u] = K^N * u$ for a social interaction kernel K^N given in terms of attraction, repulsion and alignment terms. By taking the limit $\varepsilon \to 0$ in (9.55) with scaling assumption (9.57), we obtain in Chapter 6 a parabolic equation with density-dependent coefficients,

$$\partial_t u = \partial_x\left(D[u]\partial_x u\right) - \partial_x\Big(S[u]u\big(y_D^-[u] - y_D^+[u]\big)\Big), \tag{9.58a}$$

$$D[u] = \frac{\gamma^2}{2(\lambda_1 + \lambda_2 K^N * u)} \quad \text{and} \quad S[u] = \frac{\lambda_3\gamma}{2(\lambda_1 + \lambda_2 K^N * u)}. \tag{9.58b}$$

A specific case of the 1D kinetic model (9.55) has been generalised to a 2D kinetic Boltzmann-type equation in [153]:

$$\partial_t u + \gamma \mathbf{e}_\phi \cdot \nabla_{\mathbf{x}} u = \int_{-\pi}^{\pi} T(\mathbf{x},\phi',\phi) u(\mathbf{x},\phi',t) d\phi' - \lambda(\mathbf{x},\phi) u(\mathbf{x},\phi,t)\,. \tag{9.59}$$

Here, $u(\mathbf{x},\phi,t)$ is the total population density of individuals located at $\mathbf{x} = (x,y) \in \mathbb{R}^2$, moving at a constant speed $\gamma > 0$ in direction $\phi \in [0, 2\pi)$. The term $\mathbf{e}_\phi = (\cos\phi, \sin\phi)$ gives the movement direction of individuals. The re-orientation terms, $\lambda(\mathbf{x},\phi)$ and $T(\mathbf{x},\phi',\phi)$ depend on the non-local interactions with neighbours, which can be positioned in the repulsive, attractive, and alignment ranges depicted in Fig. 1.13. Thus, these terms have three components each, corresponding to the three social interactions, $T(\mathbf{x},\phi',\phi) = T_{al}(\mathbf{x},\phi',\phi) + T_a(\mathbf{x},\phi',\phi) + T_r(\mathbf{x},\phi',\phi)$, and we define $\lambda = \sum_j \lambda_j$ with

$$\lambda_j(\mathbf{x},\phi') = \int_{-\pi}^{\pi} T_j(\mathbf{x},\phi',\phi) \mathrm{d}\phi, \quad j = r,a,al\,.$$

For a detailed description of the turning mechanism, see Chapter 6 Section 3. In Chapter 6, we generalise the turning mechanisms $\bar{T}_j$, $j = \{al, a, r\}$, from [153] by adding a constant turning rate,

$T_j := \eta_j/(2\pi) + \lambda_3 \bar{T}_j$ for constants $\lambda_1 := \eta_r + \eta_{al} + \eta_a$ and $\lambda_3 \geqslant 0$ chosen according to the biological context.

Fetecau [153] showed that by imposing the turning angle to have only two possible values $\phi = \pm\pi$, the 2D model (9.59) can be reduced to the 1D model (9.55) for a specific choice of turning rates $\lambda^{\pm}$. In Chapter 6, we perform a similar reduction making the connection to the 1D model (9.55) for $\lambda_1, \lambda_3 \geqslant 0$, $\lambda_2 = 0$ and a linear turning function $f(z) = z$. The model we obtain is similar to M2 in [146].

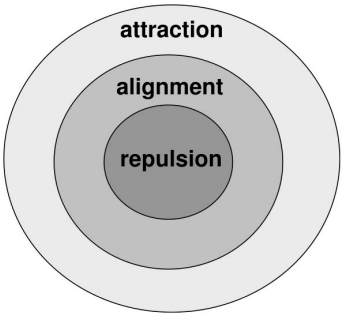

Figure 1.13: Interaction ranges.

Further, in Chapter 6, we consider the parabolic limit for the change of variables $t = t^*/\varepsilon^2$, $\mathbf{x} = \mathbf{x}^*/\varepsilon$ of model (9.59) with density-dependent turning rates[38]. The diffusion limit of a transport model similar to (9.59), but with constant turning rates λ was discussed in [189, 190]. Since the velocity in the new variables is of order $1/\varepsilon$, we make the scaling assumption that an individual's turning behaviour is only influenced slightly by the presence of neighbours:

$$T[u](\mathbf{x}, \phi', \phi) = \frac{\lambda_1}{2\pi} + \frac{\lambda_2}{2\pi} K^d * \rho(\mathbf{x}, t) + \varepsilon\, \lambda_3\, B[u](\mathbf{x}, \phi', \phi),$$

where $\rho(\mathbf{x}, t) = \int_{-\pi}^{\pi} u(\mathbf{x}, \phi, t)\, \mathrm{d}\phi$ is the macroscopic density of individuals, $K^d(\mathbf{x}) = \sum_j K_j^d(\mathbf{x})$ is a *social distance kernel* given in terms of attraction, repulsion and alignment terms and we call $B[u]$ the *social response function*. For explicit expressions, see Chapter 6. Note that the turning rate $\lambda(\mathbf{x}, \phi)$ then corresponds to the 1D turning rates (9.57) with the choice $y_D[u] = \int_{-\pi}^{\pi} B[u](\mathbf{x}, \phi', \phi)\mathrm{d}\phi'$. Further, note that the set-up of this limiting process is very similar to the one discussed in Section 8.3, especially for $\lambda_2 = 0$. With the good scaling of K^d and $B[u]$, and matching orders of ε for the Hilbert expansion $u = u_0 + \varepsilon u_1 + \varepsilon^2 u_2 + \ldots$, we obtain at leading order a relaxation towards a uniform angular distribution at each position:

$$u_0(\mathbf{x}, \phi, t) = \rho_0(\mathbf{x}, t) F(\phi)\,, \qquad F(\phi) := \frac{1}{2\pi} \mathbb{1}_{\phi \in (-\pi, \pi]}.$$

Under the assumptions that (i) individuals can process information in a similar manner for all three types of social interactions, and (ii) individuals can process information equally well from

[38] This parabolic scaling was already completed in my master thesis for the case $\eta_j = 0$, $j = \{al, a, r\}$.

left and right (symmetric perception), we obtain formally in the limit $\varepsilon \to 0$

$$\partial_t \rho = \nabla_{\mathbf{x}} \cdot (D_0[\rho] \nabla_{\mathbf{x}} \rho) - \nabla_{\mathbf{x}} \cdot (\rho\, \mathbf{k}[\rho]) \,, \tag{9.60a}$$

$$D_0[\rho] = \frac{\gamma^2}{2(\lambda_1 + \lambda_2\, K^d * \rho)} \,, \tag{9.60b}$$

$$\mathbf{k}[\rho](\mathbf{x}, t) = \frac{\lambda_2 \pi \gamma}{\lambda_1 + \lambda_2\, K^d * \rho} \left(q_r\, K_r^d(\mathbf{x})\, \frac{\mathbf{x}}{|\mathbf{x}|} - q_a\, K_a^d(\mathbf{x})\, \frac{\mathbf{x}}{|\mathbf{x}|} \right) * \rho \,, \tag{9.60c}$$

where q_r and q_a denote the strength of repulsive and attractive forces respectively. For notational convenience, we dropped the zero in ρ_0. Note that this equation is similar to the 1D drift-diffusion equation (9.58) obtained via the parabolic limit for linear social interactions. Indeed, the above diffusive limit of the 2D model (9.59) reduces to a special case of the parabolic scaling of the 1D model, which includes a λ_2 term for non-directed turning.

Remark 9.1. *For some particular choices of distance kernels K^d, the limiting parabolic model (9.60) can be reduced to a particular case of the Keller–Segel type model (2.3) discussed in part I of this thesis. Let us assume, for example, that the distance kernels are constant on the whole domain,*

$$K_j^d(\mathbf{x}) = 1, \quad j = al, a, r. \tag{9.61}$$

This assumption corresponds to a setting in which individuals interact equally well with all other individuals present in the entire domain. This is true locally for example if many individuals are packed in little space. Under assumption (9.61) together with $\lambda_1 = 0$ and in the case when attractive and repulsive interactions are not exactly equally strong $q_r \neq q_a$ (as they would cancel out otherwise), model (9.60) simplifies to the aggregation-diffusion equation

$$\partial_t \rho = D \Delta \rho + \chi \nabla \cdot (\rho\, (\nabla W * \rho)) \,, \tag{9.62}$$

with $W(\mathbf{x}) = |\mathbf{x}|$ and $D > 0$, $\chi > 0$ only depending on the parameters of the model and the total mass $\int \rho \, d\mathbf{x}$. Even for more general distance kernels K_j^d, the social flux can be written in the form $\mathbf{k}[\rho] = \nabla W * \rho$ with the interaction potential W behaving like $|\mathbf{x}|$ close to zero and decaying exponentially fast as $|\mathbf{x}| \longrightarrow \infty$ (e.g. Morse potentials). Equation (9.62) models the behaviour of particles interacting through a pairwise potential while diffusing with Brownian motion and is part of the family of aggregation-diffusion equations analysed in Part I with linear diffusion ($m = 1$) and a non-singular interaction kernel ($k = 1$).

Finally, we consider the case where individuals turn only a small angle upon interactions with neighbours, quantified by the parameter $\varepsilon \ll 1$. This is biologically realistic as, for example, many migratory birds follow favourable winds or magnetic fields [244] and social interactions with neighbours might not have a considerable impact on directional changes of individuals. Following the discussion in Section 8.1, a grazing collision limit is well adapted when collisions with

small deviation dominate. In Chapter 6, we show that the Boltzmann-type equation (9.59) can be reduced via a grazing collision limit to the following Fokker-Planck equation with non-local advective and diffusive terms in the orientation space.

$$\partial_t u + \gamma \mathbf{e}_\phi \cdot \nabla_{\mathbf{x}} u = \lambda_1 \left(\frac{1}{2\pi} \rho(\mathbf{x}, t) - u(\mathbf{x}, \phi, t) \right) + \partial_\phi \Big[- u C^\varepsilon[u, \mathbf{x}, \phi] + \partial_\phi (u D^\varepsilon[u, \mathbf{x}, \phi]) \Big], \tag{9.63}$$

We omit here the details of $C^\varepsilon[u, \mathbf{x}, \phi]$ and $D^\varepsilon[u, \mathbf{x}, \phi]$ for brevity. While non-local 2D Fokker-Planck models have been introduced in the past years in connection with self-organised aggregations, the majority of these models consider local diffusion [123, 12]. If we neglect second order terms in ε (i.e. $D^\varepsilon \approx 0$) and assume $\lambda_1 = 0$, equation (9.63) reduces to a Vlasov-type flocking equation:

$$\partial_t u + \gamma e_\phi \cdot \nabla_x u + \partial_\phi \Big[u C^\varepsilon[u, x, \phi] \Big] = 0.$$

These type of models have been previously derived from individual-based models (Vicsek or Cucker-Smale models) with or without noise [123, 179, 87].

9.2 Asymptotic preserving numerical methods

Finally, we investigate how two types of patterns (travelling and stationary aggregations) displayed by the 1D kinetic models, are preserved in the limit to macroscopic parabolic models. To this end, we first analyse the local stability of spatially homogeneous patterns characterised by individuals spread evenly over the domain, and show that local Hopf bifurcations are lost in the parabolic limit. These Hopf bifurcations give rise to travelling aggregations (i.e. rotating waves). We then test this observation numerically with the help of asymptotic preserving (AP) methods, analysing changes in the patterns as the scaling coefficient ϵ is varied from $\epsilon = 1$ (for kinetic models) to $\epsilon = 0$ (for the limiting parabolic models). Understanding these transitions is important when investigating biological phenomena that occur on multiple scales, since it allows to make decisions regarding the models that are most suitable to reproduce the observed dynamics. While AP schemes have been derived since the late 1990's to investigate the asymptotic dynamics of various transport models [201, 202, 88], they have only recently been applied to investigate multiscale aspects of biological aggregations [102]. In Chapter 6, we show that some patterns (describing stationary aggregations) are preserved in the limit $\epsilon \to 0$, while others (describing moving aggregations) are lost. To understand the loss of these patterns, we construct bifurcation diagrams. Numerical and analytical investigation is still difficult for 2D non-local models, see [153].

9.3 Conclusions and perspectives

The scaling approaches taken in Chapter 6 allow to simplify the kinetic models that incorporate microscopic-level interactions (such as individuals' speed and turning rates) to obtain parabolic models described in terms of average speed and average turning behaviour. While for the kinetic models the non-local interactions influence the turning rates, for the limit parabolic models the non-local interactions influence the dispersion and the drift of the aggregations. In particular, the assumption that individuals can turn randomly following the non-directional perception of neighbours around them leads, in the macroscopic scaling, to density-dependent diffusion. Moreover, this diffusion decreases with increasing population density. Biologically, this means that larger animal groups are less likely to spread out. This phenomenon has been observed for various species. For example, studies have shown that aggregations of locusts [55] or ants [21] can persist only if the number of individuals is above a certain threshold.

The introduction in (9.56) of the term y_N describing random non-directional turning (which generalises the turning rates in [147]) is required in order to compare the parabolic limit models in 1D and 2D. This suggests that even if the 2D model (9.59) can be reduced to a special case of the 1D model (9.55) (as shown in [153]) there are more subtle differences between these non-local 1D and 2D models. These differences can impact the types of patterns displayed by the 2D models – an aspect that would be interesting to study in the future.

In Chapter 6, we use asymptotic preserving numerical methods to investigate the preservation of patterns via the 1D parabolic limit, but similar investigations could be performed for the grazing collision limit. Moreover, as shown previously [146], model (9.55) can display many more types of complex spatio-temporal patterns than the two types of patterns investigated here. We choose to focus on travelling and stationary aggregations since our aim is not to investigate how all possible patterns are preserved by all these different scaling approaches. Rather, we want to show that by taking these asymptotic limits, some patterns could be lost. Therefore, even if the macroscopic models are simpler to investigate, they might not exhibit the same patterns as the kinetic models. Our analysis aims at highlighting the usefulness of AP schemes to understand the bifurcation of the solutions as one investigates the transition from microscopic-level to macroscopic-level aggregation dynamics.

Part I

Keller-Segel-Type Aggregation-Diffusion Equations

ἀνδρῶν γὰρ ἐπιφανῶν πᾶσα γῆ τάφος,
καὶ οὐ στηλῶν μόνον ἐν τῇ οἰκείᾳ σημαίνει ἐπιγραφή,
ἀλλὰ καὶ ἐν τῇ μὴ προσηκούσῃ ἄγραφος μνήμη παρ᾽ ἑκάστῳ
τῆς γνώμης μᾶλλον ἢ τοῦ ἔργου ἐνδιαιτᾶται.[39]

What you leave behind
is not what is engraved
in stone monuments,
but what is woven
into the lives of others[40].

Pericles

[39] as quoted in Thucydides' *History of the Peloponnesian War*, II.43.3 (5th century BC) from Pericles' funeral oration. Literal translation by Steven Lattimore: "The whole earth is the tomb of famous men, and not only inscriptions set up in their own country mark it but even in foreign lands an unwritten memorial, present not in monument but in mind, abides within each man." [212, page 98]

[40] modern paraphrasing of the above as quoted in [249, page 118].

Chapter 2

Ground States in the Fair-Competition Regime

This chapter follows in most parts the article "Equilibria of homogeneous functionals in the fair-competition regime" written in collaboration with Vincent Calvez[1] and José A. Carrillo[2], and published in the special issue "Advances in Reaction-Cross-Diffusion Systems" of *Nonlinear Analysis TMA*.

Chapter Summary

We consider macroscopic descriptions of particles where repulsion is modelled by non-linear power-law diffusion and attraction by a homogeneous singular/non-singular kernel leading to variants of the Keller–Segel model of chemotaxis. We analyse the regime in which both homogeneities scale the same with respect to dilations, that we coin as fair-competition. In the singular kernel case, we show that existence of global equilibria can only happen at a certain critical value and they are characterised as optimisers of a variant of HLS inequalities. We also study the existence of self-similar solutions for the sub-critical case, or equivalently of optimisers of rescaled free energies. These optimisers are shown to be compactly supported radially symmetric and non-increasing stationary solutions of the non-linear Keller–Segel equation. On the other hand, we show that no radially symmetric non-increasing stationary solutions exist in the non-singular kernel case, implying that there is no criticality. However, we show the existence of positive self-similar solutions for all values of the parameter under the condition that diffusion is not too fast. We finally illustrate some of the open problems in the non-singular kernel case by numerical experiments.

[1]Unité de Mathématiques Pures et Appliquées, CNRS UMR 5669 and équipe-projet INRIA NUMED, École Normale Supérieure de Lyon, Lyon, France.

[2]Department of Mathematics, Imperial College London, South Kensington Campus, London SW7 2AZ, UK.

Chapter Content

Haba na haba hujaza kibaba.

Little by little fills up the measure.

Kiswahili proverb

1 Introduction

The goal of this chapter is to investigate properties of the following class of homogeneous functionals, defined for centred probability densities $\rho(x)$, belonging to suitable L^p-spaces, and some interaction strength coefficient $\chi > 0$ and diffusion power $m > 0$:

$$\begin{aligned}\mathcal{F}_{m,k}[\rho] &= \int_{\mathbb{R}^N} U_m\left(\rho(x)\right)\, dx + \chi \iint\limits_{\mathbb{R}^N\times\mathbb{R}^N} \rho(x) W_k(x-y)\rho(y)\, dxdy \\ &:= \mathcal{U}_m[\rho] + \chi \mathcal{W}_k[\rho]\,, \\ \rho(x) &\geqslant 0\,, \quad \int_{\mathbb{R}^N} \rho(x)\, dx = 1\,, \quad \int_{\mathbb{R}^N} x\rho(x)\, dx = 0\,,\end{aligned} \tag{1.1}$$

with

$$U_m(\rho) = \begin{cases} \dfrac{1}{N(m-1)}\rho^m\,, & \text{if} \quad m \neq 1 \\ \dfrac{1}{N}\rho\log\rho\,, & \text{if} \quad m = 1 \end{cases},$$

and

$$W_k(x) = \begin{cases} \dfrac{|x|^k}{k}\,, & \text{if} \quad k \in (-N, N)\backslash\{0\} \\ \log|x|\,, & \text{if} \quad k = 0 \end{cases}.$$

The conditions on k imply that the kernel $W_k(x)$ is locally integrable in $\mathbb{R}^N$. The centre of mass is assumed to be zero since the free energy functional is invariant by translation.

There exists a strong link between the aforementioned functional (1.1) and the following family of partial differential equations modelling self-attracting diffusive particles at the macroscopic scale,

$$\begin{cases} \partial_t\rho = \dfrac{1}{N}\Delta\rho^m + 2\chi\nabla\cdot(\rho\nabla S_k)\,, \quad t > 0\,, \quad x \in \mathbb{R}^N\,, \\ \rho(t=0,x) = \rho_0(x) \geqslant 0\,, \quad \displaystyle\int_{\mathbb{R}^N} \rho_0(x)\, dx = 1\,, \quad \int_{\mathbb{R}^N} x\rho_0(x)\, dx = 0\,, \end{cases} \tag{1.2}$$

where we define the mean-field potential $S_k(x) := W_k(x) * \rho(x)$. For $k > 1-N$, the gradient $\nabla S_k := \nabla\left(W_k * \rho\right)$ is well defined. For $-N < k \leqslant 1-N$ however, it becomes a singular integral, and we thus define it via a Cauchy principal value. Hence, the mean-field potential gradient in equation (1.2) is given by

$$\nabla S_k(x) := \begin{cases} \nabla W_k * \rho\,, & \text{if } k > 1-N\,, \\ \displaystyle\int_{\mathbb{R}^N} \nabla W_k(x-y)\left(\rho(y)-\rho(x)\right)\, dy\,, & \text{if } -N < k \leqslant 1-N\,. \end{cases} \tag{1.3}$$

The noticeable characteristic of the class of PDEs (1.2) and the functional $\mathcal{F}_{m,k}$ consists in the competition between the diffusion (possibly non-linear), and the non-local, quadratic non-linearity which is due to the self-attraction of the particles through the mean-field potential S_k. The parameter $\chi > 0$ measures the strength of the interaction and scales with the mass of solution densities.

The strong connection between the functional $\mathcal{F}_{m,k}$ and the PDE (1.2) is due to the fact that the functional $\mathcal{F}_{m,k}$ is non-increasing along the trajectories of the system. Namely $\mathcal{F}_{m,k}$ is the free energy of the system and it satisfies at least formally

$$\frac{d}{dt}\mathcal{F}_{m,k}[\rho(t)] = -\int_{\mathbb{R}^N} \rho(t,x)\left|\nabla\left(\frac{m}{N(m-1)}\rho(t,x)^{m-1} + 2\chi W_k(x) * \rho(t,x)\right)\right|^2 dx\,.$$

Furthermore, the system (1.2) is the formal gradient flow of the free energy functional (1.1) when the space of probability measures is endowed with the Euclidean Wasserstein metric $\mathbf{W}$. This means that the family of PDEs (1.2) can be written as

$$\partial_t\rho(t) = \nabla\cdot(\rho(t)\,\nabla\mathcal{T}_{m,k}[\rho(t)]) = -\nabla_{\mathbf{W}}\mathcal{F}_{m,k}[\rho(t)]\,,$$

where $\mathcal{T}_{m,k}[\rho]$ denotes the first variation of the energy functional in the set of probability densities:

$$\mathcal{T}_{m,k}[\rho](x) := \frac{\delta\mathcal{F}_{m,k}}{\delta\rho}[\rho](x) = \frac{m}{N(m-1)}\rho^{m-1}(x) + 2\chi W_k(x) * \rho(x)\,. \tag{1.4}$$

This illuminating statement has been clarified in the seminal paper by Otto [248] for the porous medium equation, and generalised to a large family of equations subsequently in [96, 3, 97], we refer to [295, 3] for a comprehensive presentation of this theory of gradient flows in Wasserstein metric spaces, particularly in the convex case. Let us mention that such a gradient flow can be constructed as the limit of discrete in time steepest descent schemes. Performing gradient flows of a convex functional is a natural task, and suitable estimates from below on the right notion of Hessian of $\mathcal{F}_{m,k}$ translate into a rate of convergence towards equilibrium for the PDE [295, 96, 3]. However, performing gradient flows of non-convex functionals is much more delicate, and one has to seek compensations. Such compensations do exist in our case, and we will observe them at the level of existence of minimisers for the free energy functional $\mathcal{F}_{m,k}$ and stationary states of the family of PDEs (1.2) in particular regimes.

The family of non-local problems (1.2) has been intensively studied in various contexts arising in physics and biology. The two-dimensional logarithmic case $(m = 1, k = 0)$ is the so-called Keller–Segel system in its simplest formulation [196, 197, 243, 194, 136, 41, 256]. It has been proposed as a model for chemotaxis in cell populations. Cells may interact with each other by secreting a chemical substance to attract cells around them. This occurs for instance during the starvation stage of the slime mould *Dictyostelium discoideum*. More generally, chemotaxis is widely observed in various biological fields (morphogenesis, bacterial self-organisation, inflammatory processes among others). The two- and three-dimensional configurations with Newtonian interaction $(m = 1, k = 2 - N)$ are the so-called Smoluchowski-Poisson system arising in gravitational physics. It describes macroscopically a density of particles subject to a self-sustained gravitational field [106, 107].

Let us describe in more detail the two-dimensional Keller–Segel system as the analysis of its peculiar structure will serve as a guideline to understand the other cases. In fact, the functional (1.1) $(m = 1, k = 0)$ is bounded from below if and only if $\chi = 1$. The gradient flow is also subject to a remarkable dichotomy, well described mathematically. The density exists globally in time if $\chi < 1$ (diffusion overcomes self-attraction), whereas blow-up occurs in finite time when $\chi > 1$ (self-attraction overwhelms diffusion). This transition has been first formulated in [113]. Mathematical contributions are [194] for the existence part, [242] for the radial case, and [136, 41] in the full space. The critical case $\chi = 1$ was analysed further in [40, 37, 75] in terms of stability of stationary states.

The effect of substituting linear diffusion by non-linear diffusion with $m > 1$ in two dimensions and higher was described in [61, 277] where it is shown that solutions exist globally in time for all values of the parameter $\chi > 0$. The role of both non-linear diffusion and non-local aggregation terms was clarified in [39], see also [276], where the authors find that there is a similar dichotomy to the two-dimensional classical Keller–Segel case $(N = 2, m = 1, k = 0)$, for a whole range of parameters, choosing the non-local term as the Newtonian potential, $(N \geqslant 3, m = 2 - 2/N, k = 2 - N)$. The main difference is that the stationary states found for the critical case are compactly supported. Choosing the non-local term as the Newtonian potential, this range of parameters can be understood as fixing the non-linear diffusion such that both terms in the functional $\mathcal{F}_{m,k}$ scale equally for mass-preserving dilations. This mass-preserving dilation homogeneity of the functional $\mathcal{F}_{m,k}$ is shared by the range of parameters (m, k) with $N(m-1)+k = 0$ for all dimensions, $m > 0$ and $k \in (-N, N)$. We call this range of parameters the fair-competition regime, since both terms are competing each other at equal foot.

In this chapter, we will analyse the properties of the functional $\mathcal{F}_{m.k}$ in relation to global minimisers and its relation to stationary states of (1.2). We will first define properly the notion of stationary states to (1.2) and analyse their basic properties in Section 2. We will also state and explain the main results of this chapter once the different regimes have been introduced. We postpone further discussion of the related literature to Section 2. Section 3 is devoted to the fair-competition regime with $k < 0$ for which we show a similar dichotomy to [39] in the whole range $k \in (-N, 0)$ including the most singular cases. We show that stationary states exist only for a critical value of χ and that they are compactly supported, bounded, radially symmetric decreasing and continuous functions. Moreover, we show that they are global minimisers of $\mathcal{F}_{m.k}$. The sub-critical case is also analysed in scaled variables and we show the existence of global minimisers with the properties above leading to the existence of self-similar solutions in original variables. The critical parameter is characterised by a variant of HLS inequalities as in [39]. Let us mention that the regularity results need a careful treatment of the problem in radial coordinates involving non-trivial properties

of hypergeometric functions. The properties of the kernel in radial coordinates are postponed to the Appendix A.

In Section 4, we analyse the case $k > 0$. Let us mention that there are no results in the literature to our knowledge concerning the case $k \in (0, N)$ in which $0 < m = 1 - k/N < 1$. There is one related result in [116] for the limiting case in one dimension taking $m = 0$, corresponding to logarithmic diffusion, and $k = 1$. They showed that no criticality is present in that case as solutions to (1.2) with $(m = 0, k = 1)$ are globally defined in time for all values of the parameter $\chi > 0$. We show that no radially symmetric non-increasing stationary states and no radially symmetric non-increasing global minimisers exist in original variables for all values of the critical parameter χ and for $k \in (0, N)$ while we show the existence of stationary states for all values of the critical parameter χ in scaled variables for $k \in (0, 1]$. In this sense, we show that there is no criticality for $k > 0$. A full proof of non-criticality involves the analysis of the minimisation problem in scaled variables as for $k < 0$ showing that global minimisers exist in the right functional spaces for all values of the critical parameter and that they are indeed stationary states. This is proven in one dimension in Chapter 3 by optimal transport techniques and postponed for further future investigations in general dimension. We finally illustrate these results by numerical experiments in one dimension corroborating the absence of critical behaviour for $k > 0$.

2 Stationary states & main results

2.1 Stationary states: definition & basic properties

Let us define precisely the notion of stationary states to the aggregation equation (1.2).

Definition 2.1. *Given $\bar{\rho} \in L^1_+(\mathbb{R}^N) \cap L^\infty(\mathbb{R}^N)$ with $||\bar{\rho}||_1 = 1$, it is a **stationary state** for the evolution equation (1.2) if $\bar{\rho}^m \in \mathcal{W}^{1,2}_{loc}(\mathbb{R}^N)$, $\nabla \bar{S}_k \in L^1_{loc}(\mathbb{R}^N)$, and it satisfies*

$$\frac{1}{N}\nabla \bar{\rho}^m = -2\chi\, \bar{\rho}\nabla \bar{S}_k \tag{2.5}$$

in the sense of distributions in $\mathbb{R}^N$. If $-N < k \leqslant 1 - N$, we further require $\bar{\rho} \in C^{0,\alpha}(\mathbb{R}^N)$ with $\alpha \in (1 - k - N, 1)$.

We start by showing that the function S_k and its gradient defined in (1.3) satisfy even more than the regularity $\nabla S_k \in L^1_{loc}(\mathbb{R}^N)$ required in Definition 2.1.

Lemma 2.2. *Let $\rho \in L^1_+(\mathbb{R}^N) \cap L^\infty(\mathbb{R}^N)$ with $||\rho||_1 = 1$. If $0 < k < N$, we additionally assume $|x|^k \rho \in L^1(\mathbb{R}^N)$. Then the following regularity properties hold:*

i) $S_k \in L^\infty_{loc}(\mathbb{R}^N)$ for $0 < k < N$ and $S_k \in L^\infty(\mathbb{R}^N)$ for $-N < k < 0$.

ii) $\nabla S_k \in L^\infty_{loc}\left(\mathbb{R}^N\right)$ *for* $1 < k < N$ *and* $\nabla S_k \in L^\infty\left(\mathbb{R}^N\right)$ *for* $-N < k < 0$ *and* $0 < k \leqslant 1$, *assuming additionally* $\rho \in C^{0,\alpha}\left(\mathbb{R}^N\right)$ *with* $\alpha \in (1-k-N, 1)$ *in the range* $-N < k \leqslant 1-N$.

Proof. A direct decomposition in near- and far-field sets $\mathcal{A} := \{y : |x-y| \leqslant 1\}$ and $\mathcal{B} := \mathbb{R}^N - \mathcal{A}$ yields for $-N < k < 0$ and $x \in \mathbb{R}^N$,

$$\begin{aligned} |S_k(x)| &\leqslant \int_{\mathbb{R}^N} |W_k(x-y)|\rho(y)\,dy \leqslant \frac{1}{|k|}\int_{\mathcal{A}} |x-y|^k \rho(y)\,dy + \frac{1}{|k|}\int_{\mathcal{B}} \rho(y)\,dy \\ &\leqslant \frac{1}{|k|}\left(\frac{\sigma_N}{k+N}||\rho||_\infty + 1\right) < \infty\,, \end{aligned}$$

where $\sigma_N = 2\pi^{(N/2)}/\Gamma(N/2)$ denotes the surface area of the N-dimensional unit ball. Locally, boundedness extends to the fast diffusion regime $0 < k < N$ by using the inequality

$$|x-y|^k \leqslant \eta\left(|x|^k + |y|^k\right)\,, \qquad \eta = \max\{1, 2^{k-1}\}\,. \tag{2.6}$$

This inequality follows directly from splitting into cases $k < 1$ and $k > 1$. The inequality $|x-y|^k \leqslant |x|^k + |y|^k$ is true for any $k \in (0,1]$ with $x, y \in \mathbb{R}^N$ by direct inspection. For $N > 1$ and $k \in (1, N)$, we have by convexity $|x-y|^k \leqslant 2^{k-1}\left(|x|^k + |y|^k\right)$, for any $x, y \in \mathbb{R}^N$, and so (2.6) holds true.

Similarly, in order to prove ii) for $1-N < k \leqslant 1$ and $x \in \mathbb{R}^N$, we estimate ∇S_k as

$$\begin{aligned} |\nabla S_k(x)| &\leqslant \int_{\mathbb{R}^N} |\nabla W_k(x-y)|\rho(y)\,dy \leqslant \int_{\mathcal{A}} |x-y|^{k-1}\rho(y)\,dy + \int_{\mathcal{B}} \rho(y)\,dy \\ &\leqslant \left(\frac{\sigma_N}{k+N-1}||\rho||_\infty + 1\right) < \infty\,. \end{aligned}$$

In the Cauchy integral range $-N < k \leqslant 1-N$, we additionally require a certain Hölder regularity, yielding

$$\begin{aligned} |\nabla S_k(x)| &= \left|\int_{\mathcal{A}} \nabla W_k(x-y)\left(\rho(y)-\rho(x)\right)\,dy + \int_{\mathcal{B}} \nabla W_k(x-y)\left(\rho(y)-\rho(x)\right)\,dy\right| \\ &\leqslant \int_{\mathcal{A}} |\nabla W_k(x-y)|\,|\rho(y)-\rho(x)|\,dy + \int_{\mathcal{B}} |\nabla W_k(x-y)|\rho(y)\,dy \\ &\leqslant [\rho]_{C^{0,\alpha}}\int_{\mathcal{A}} |x-y|^{k-1}|x-y|^\alpha\,dy + \int_{\mathcal{B}} \rho(y)\,dy < \infty\,, \end{aligned}$$

where $[\rho]_{C^{0,\alpha}}$ denotes the α-Hölder semi-norm of ρ, and where the term $\int_{\mathcal{B}} \nabla W_k(x-y)\,dy$ vanishes by anti-symmetry. For $1 < k < N$ and x in some compact set, we have

$$\begin{aligned} |\nabla S_k(x)| &\leqslant \int_{\mathcal{A}} |x-y|^{k-1}\rho(y)\,dy + \int_{\mathcal{B}} |x-y|^{k-1}\rho(y)\,dy \\ &\leqslant \frac{\sigma_N}{k+N-1}||\rho||_\infty + \int_{\mathcal{B}} |x-y|^k\rho(y)\,dy \end{aligned}$$

which concludes $\nabla S_k \in L^\infty_{loc}\left(\mathbb{R}^N\right)$ using (2.6) and the fact that the kth moment of ρ is bounded. □

We will prove that for certain cases there are no stationary states to (1.2) in the sense of Definition 2.1, for instance for the sub-critical classical Keller–Segel model in two dimensions [41].

However, the scale invariance of (1.2) motivates us to look for self-similar solutions instead. To this end, we rescale equation (1.2) to a non-linear Fokker–Planck type equation as in [100]. Let us define

$$u(t,x) := \alpha^N(t)\rho\left(\beta(t), \alpha(t)x\right),$$

where $\rho(t,x)$ solves (1.2) and the functions $\alpha(t)$, $\beta(t)$ are to be determined. If we assume $u(0,x) = \rho(0,x)$, then $u(t,x)$ satisfies the rescaled drift-diffusion equation

$$\begin{cases} \partial_t u = \frac{1}{N}\Delta u^m + 2\chi\nabla\cdot(u\nabla S_k) + \nabla\cdot(xu)\,, \quad t>0\,, \quad x\in\mathbb{R}^N\,, \\ u(t=0,x) = \rho_0(x) \geqslant 0\,, \quad \int_{-\infty}^{\infty}\rho_0(x)\,dx = 1\,, \quad \int_{-\infty}^{\infty} x\rho_0(x)\,dx = 0\,, \end{cases} \tag{2.7}$$

for the choices

$$\alpha(t) = e^t, \quad \beta(t) = \begin{cases} \frac{1}{2-k}\left(e^{(2-k)t}-1\right), & \text{if } k\neq 2, \\ t, & \text{if } k = 2, \end{cases}$$

and with ∇S_k given by (1.3) with u instead of ρ. By differentiating the centre of mass of u, we see easily that

$$\int_{\mathbb{R}^N} xu(t,x)\,dx = e^{-t}\int_{\mathbb{R}^N} x\rho_0(x)\,dx = 0\,, \qquad \forall t>0\,,$$

and so the initial zero centre of mass is preserved for all times. Self-similar solutions to (1.2) now correspond to stationary solutions of (2.7). Similar to Definition 2.1, we state what we exactly mean by stationary states to the aggregation equation (2.7).

Definition 2.3. *Given $\bar{u}\in L^1_+\left(\mathbb{R}^N\right)\cap L^\infty\left(\mathbb{R}^N\right)$ with $||\bar{u}||_1 = 1$, it is a **stationary state** for the evolution equation (2.7) if $\bar{u}^m\in\mathcal{W}^{1,2}_{loc}\left(\mathbb{R}^N\right)$, $\nabla\bar{S}_k\in L^1_{loc}\left(\mathbb{R}^N\right)$, and it satisfies*

$$\frac{1}{N}\nabla\bar{u}^m = -2\chi\,\bar{u}\nabla\bar{S}_k - x\,\bar{u} \tag{2.8}$$

in the sense of distributions in $\mathbb{R}^N$. If $-N < k \leqslant 1-N$, we further require $\bar{u}\in C^{0,\alpha}\left(\mathbb{R}^N\right)$ with $\alpha\in(1-k-N,1)$.

From now on, we switch notation from u to ρ for simplicity, it should be clear from the context if we are in original or rescaled variables. In fact, stationary states as defined above have even more regularity:

Lemma 2.4. *Let $k\in(-N,N)\backslash\{0\}$ and $\chi>0$.*

(i) If $\bar{\rho}$ is a stationary state of equation (1.2) with $|x|^k\bar{\rho}\in L^1\left(\mathbb{R}^N\right)$ in the case $0<k<N$, then $\bar{\rho}$ is continuous on $\mathbb{R}^N$.

(ii) If $\bar{\rho}_{resc}$ is a stationary state of equation (2.7) with $|x|^k\bar{\rho}_{resc}\in L^1\left(\mathbb{R}^N\right)$ in the case $0<k<N$, then $\bar{\rho}_{resc}$ is continuous on $\mathbb{R}^N$.

Proof. (i) First, note that $\nabla \bar{S}_k \in L^\infty_{loc}\left(\mathbb{R}^N\right)$ by Lemma 2.2, and therefore, $\bar{\rho}\nabla\bar{S}_k \in L^1_{loc}\left(\mathbb{R}^N\right) \cap L^\infty_{loc}\left(\mathbb{R}^N\right)$. Hence, we get by interpolation that $\nabla\cdot\left(\bar{\rho}\nabla\bar{S}_k\right) \in \mathcal{W}^{-1,p}_{loc}\left(\mathbb{R}^N\right)$ for all $1 < p < \infty$. Recall from Definition 2.1 that $\bar{\rho}^m$ is a weak $\mathcal{W}^{1,2}_{loc}\left(\mathbb{R}^N\right)$ solution of

$$\frac{1}{N}\Delta\bar{\rho}^m = -2\chi\,\nabla\cdot\left(\bar{\rho}\nabla\bar{S}_k\right)$$

in $\mathbb{R}^N$, and so $\bar{\rho}^m$ is in fact a weak solution in $\mathcal{W}^{1,p}_{loc}\left(\mathbb{R}^N\right)$ for all $1 < p < \infty$ by classic elliptic regularity. Using Morrey's inequality, we deduce that $\bar{\rho}^m$ belongs to the Hölder space $C^{0,\alpha}_{loc}\left(\mathbb{R}^N\right)$ with $\alpha = (p-N)/N$ for any $N < p < \infty$, and thus $\bar{\rho}^m \in C\left(\mathbb{R}^N\right)$. Hence, $\bar{\rho}$ itself is continuous as claimed.

(ii) Since $x\bar{\rho}_{\mathbf{resc}} \in L^1_{loc}\left(\mathbb{R}^N\right) \cap L^\infty_{loc}\left(\mathbb{R}^N\right)$, we obtain again by interpolation $\nabla\cdot(x\bar{\rho}_{\mathbf{resc}}) \in \mathcal{W}^{-1,p}_{loc}\left(\mathbb{R}^N\right)$ for all $1 < p < \infty$. By Definition 2.3, $\bar{\rho}^m_{\mathbf{resc}}$ is a weak $\mathcal{W}^{1,2}_{loc}\left(\mathbb{R}^N\right)$ solution of

$$\frac{1}{N}\Delta\bar{\rho}^m_{\mathbf{resc}} = -2\chi\,\nabla\cdot\left(\bar{\rho}_{\mathbf{resc}}\nabla\bar{S}_k\right) - \nabla\cdot\left(x\bar{\rho}_{\mathbf{resc}}\right)$$

in $\mathbb{R}^N$, and so $\bar{\rho}^m_{\mathbf{resc}}$ is again a weak solution in $\mathcal{W}^{1,p}_{loc}\left(\mathbb{R}^N\right)$ for all $1 < p < \infty$ by classic elliptic regularity. We conclude as in original variables.

□

In the case $k < 0$, we furthermore have a non-linear algebraic equation for stationary states:

Corollary 2.5 (Necessary Condition for Stationary States)**.** *Let $k \in (-N, 0)$ and $\chi > 0$.*

(i) If $\bar{\rho}$ is a stationary state of equation (1.2), then $\bar{\rho} \in \mathcal{W}^{1,\infty}\left(\mathbb{R}^N\right)$ and it satisfies

$$\bar{\rho}(x)^{m-1} = \frac{N(m-1)}{m}\left(C_k[\bar{\rho}](x) - 2\chi\,\bar{S}_k(x)\right)_+\,, \qquad \forall\, x \in \mathbb{R}^N\,, \tag{2.9}$$

where $C_k[\bar{\rho}](x)$ is constant on each connected component of supp $(\bar{\rho})$.

(ii) If $\bar{\rho}_{\mathbf{resc}}$ is a stationary state of equation (2.7), then $\bar{\rho}_{\mathbf{resc}} \in \mathcal{W}^{1,\infty}_{loc}\left(\mathbb{R}^N\right)$ and it satisfies

$$\bar{\rho}_{\mathbf{resc}}(x)^{m-1} = \frac{N(m-1)}{m}\left(C_{k,\mathbf{resc}}[\bar{\rho}](x) - 2\chi\,\bar{S}_k(x) - \frac{|x|^2}{2}\right)_+\,, \qquad \forall\, x \in \mathbb{R}^N\,, \tag{2.10}$$

where $C_{k,\mathbf{resc}}[\bar{\rho}](x)$ is constant on each connected component of supp $(\bar{\rho}_{\mathbf{resc}})$.

Proof. (i) For a stationary state $\bar{\rho}$ of equation (1.2), let us define the set

$$\Omega = \left\{x \in \mathbb{R}^N : \bar{\rho}(x) > 0\right\}\,.$$

Since $\bar{\rho}$ is continuous by Lemma 2.4, Ω is an open set with countably many open, possibly unbounded connected components. Let us take any bounded smooth connected open subset $\mathcal{U}$ such that $\overline{\mathcal{U}} \subset \Omega$. By continuity, $\bar{\rho}$ is bounded away from zero in $\mathcal{U}$, and thus $\nabla\bar{\rho}^{m-1} =$

$\frac{m-1}{m\bar\rho}\nabla\bar\rho^m$ holds in the distributional sense in $\mathcal{U}$. From (2.5) in the definition of stationary states, we conclude that

$$\nabla\left(\frac{m}{N(m-1)}\bar\rho^{m-1}+2\chi\,\bar S_k\right)=0\,, \tag{2.11}$$

in the sense of distributions in Ω. Hence, the function $C_k[\bar\rho](x):=\frac{m}{N(m-1)}\bar\rho^{m-1}(x)+2\chi\,\bar S_k(x)$ is constant in each connected component of Ω, and so (2.9) follows. Additionally, it follows from (2.11) that for any $x\in\mathbb{R}^N$

$$\left|\nabla\bar\rho^{m-1}(x)\right|=\frac{2\chi N(m-1)}{m}\left|\nabla\bar S_k(x)\right|\leqslant c$$

for some constant $c>0$ since $\bar S_k\in\mathcal{W}^{1,\infty}\left(\mathbb{R}^N\right)$ by Lemma 2.2. Since $m\in(1,2)$, we conclude $\bar\rho\in\mathcal{W}^{1,\infty}\left(\mathbb{R}^N\right)$.

(ii) We follow the same argument for a stationary state $\bar\rho_{\mathbf{resc}}$ of the rescaled equation (2.7) and using (2.8) in Definition 2.3, we obtain

$$\nabla\left(\frac{m}{N(m-1)}\bar\rho_{\mathbf{resc}}^{m-1}+2\chi\,\bar S_k+\frac{|x|^2}{2}\right)=0\,,$$

in the sense of distributions in Ω. Here, the function $C_{k,\mathbf{resc}}[\bar\rho_{\mathbf{resc}}](x):=\frac{m}{N(m-1)}\bar\rho_{\mathbf{resc}}^{m-1}(x)+2\chi\,\bar S_k(x)+\frac{|x|^2}{2}$ is again constant in each connected component of $\operatorname{supp}(\bar\rho_{\mathbf{resc}})$. Similarly, it follows from Lemma 2.2 that for any $\omega>0$ and $x\in B(0,\omega)$,

$$\left|\nabla\bar\rho_{\mathbf{resc}}^{m-1}(x)\right|=\frac{N(m-1)}{m}\left(2\chi\left|\nabla\bar S_k(x)\right|+|x|\right)\leqslant c$$

for some constant $c>0$, and so $\bar\rho_{\mathbf{resc}}\in\mathcal{W}^{1,\infty}_{loc}\left(\mathbb{R}^N\right)$.

□

2.2 Fair-competition regime: main results

It is worth noting that the functional $\mathcal{F}_{m,k}[\rho]$ possesses remarkable homogeneity properties, see Chapter 1 Section 3.1. We will here only concentrate on the fair-competition regime $N(m-1)+k=0$, and denote the corresponding energy functional by $\mathcal{F}_k[\rho]=\mathcal{F}_{1-k/N,k}[\rho]$. For a definition of the different regimes and detailed explanations and references, see Chapter 1 Definition 3.1. An overview of the parameter space (k,m) and the different regimes is given in Chapter 1 Figure 1.4. Notice that the functional $\mathcal{F}_k$ is homogeneous in this regime, i.e.,

$$\mathcal{F}_k[\rho_\lambda]=\lambda^{-k}\mathcal{F}_k[\rho]\,. \tag{2.12}$$

The analysis in the fair-competition regime depends on the sign of k, see Chapter 1 Definition 3.7, and we therefore split our investigations into the porous medium case ($k<0$), and the fast diffusion case ($k>0$). More information on the logarithmic case ($k=0$) can be found in [62]. When

dealing with the energy functional $\mathcal{F}_k$, we work in the set of non-negative normalised densities,

$$\mathcal{Y} := \left\{ \rho \in L^1_+\left(\mathbb{R}^N\right) \cap L^m\left(\mathbb{R}^N\right) : ||\rho||_1 = 1\,,\ \int x\rho(x)\,dx = 0 \right\}.$$

In rescaled variables, equation (2.7) is the formal gradient flow of the rescaled free energy functional $\mathcal{F}_{k,\mathbf{resc}}$, which is complemented with an additional quadratic confinement potential,

$$\mathcal{F}_{k,\mathbf{resc}}[\rho] = \mathcal{F}_k[\rho] + \frac{1}{2}\mathcal{V}[\rho]\,, \qquad \mathcal{V}[\rho] = \int_{\mathbb{R}^N} |x|^2\rho(x)\,dx\,.$$

Defining the sets

$$\mathcal{Y}_2 := \{\rho \in \mathcal{Y} : \mathcal{V}[\rho] < \infty\}\,, \qquad \mathcal{Y}_k := \left\{ \rho \in \mathcal{Y} : \int_{\mathbb{R}^N} |x|^k\rho(x)\,dx < \infty \right\}\,,$$

we see that $\mathcal{F}_{k,\mathbf{resc}}$ is well-defined and finite on $\mathcal{Y}_2$ for $k < 0$ and on $\mathcal{Y}_{2,k} := \mathcal{Y}_2 \cap \mathcal{Y}_k$ for $k > 0$. Thanks to the formal gradient flow structure in the Euclidean Wasserstein metric $\mathbf{W}$, we can write the rescaled equation (2.7) as

$$\partial_t\rho = \nabla\cdot(\rho\,\nabla\mathcal{T}_{k,\mathbf{resc}}[\rho]) = -\nabla_{\mathbf{W}}\mathcal{F}_{k,\mathbf{resc}}[\rho]\,,$$

where $\mathcal{T}_{k,\mathbf{resc}}$ denotes the first variation of the rescaled energy functional,

$$\mathcal{T}_{k,\mathbf{resc}}[\rho](x) := \mathcal{T}_k[\rho](x) + \frac{|x|^2}{2} \tag{2.13}$$

with $\mathcal{T}_k$ as defined in (1.4). In this chapter, we prove the following results:

Theorem 2.6 (The Critical Porous Medium Regime)**.** *In the porous medium regime $k \in (-N, 0)$ and for critical interaction strengths $\chi = \chi_c$, there exist global minimisers of $\mathcal{F}_k$ and they are radially symmetric non-increasing, compactly supported and uniformly bounded. Furthermore, all stationary states with bounded second moment are global minimisers of the energy functional $\mathcal{F}_k$, and conversely, all global minimisers of $\mathcal{F}_k$ are stationary states of* (1.2)*.*

Theorem 2.7 (The Sub-Critical Porous Medium Regime)**.** *In the porous medium regime $k \in (-N, 0)$ and for sub-critical interaction strengths $0 < \chi < \chi_c$, no stationary states exist for equation* (1.2) *and no minimisers exist for $\mathcal{F}_k$. In rescaled variables, all stationary states are continuous and compactly supported. There exist global minimisers of $\mathcal{F}_{k,resc}$ and they are radially symmetric non-increasing and uniformly bounded stationary states of equation* (2.7)*.*

Remark 2.8. *Due to the homogeneity* (2.12) *of the functional $\mathcal{F}_k$, each global minimiser gives rise to a family of global minimisers for $\chi = \chi_c$ by dilation since they have zero energy, see* (3.19)*. It is an open problem to show that there is a unique global minimiser for $\chi = \chi_c$ modulo dilations. This uniqueness was proven in the Newtonian case in [302], but is still an open problem in the general. Notice that from uniqueness one obtains the full set of stationary states with bounded second moment for* (1.2) *as a by-product.*

In contrast, in rescaled variables, we do not know if stationary states with second moment bounded are among global minimisers of $\mathcal{F}_{k,\mathbf{resc}}$ for the sub-critical case $0 < \chi < \chi_c$ except in one dimension, see Chapter 3. It is also an open problem to show the uniqueness of radially symmetric stationary states of the rescaled equation (2.7) for $N \geqslant 2$.

Theorem 2.9 (The Fast Diffusion Regime). *In the fast diffusion regime $k \in (0, N)$ equation (1.2) has no radially symmetric non-increasing stationary states with kth moment bounded, and there are no radially symmetric non-increasing global minimisers for the energy functional $\mathcal{F}_k$ for any $\chi > 0$. In rescaled variables, radially symmetric non-increasing stationary states can only exist if $0 < k < 2$, that is $(N-2)/N < m < 1$. Similarly, global minimisers with finite energy $\mathcal{F}_{k,\mathbf{resc}}$ can only exist in the range $0 < k < 2N/(2+N)$, that is $N/(2+N) < m < 1$. For $k \in (0, 1]$, there exists a continuous radially symmetric non-increasing stationary state of the rescaled equation (2.7).*

3 Porous medium case $k < 0$

In the porous medium case, we have $-N < k < 0$ and hence $1 < m < 2$. Our aim in this section is to make a connection between global minimisers of the functionals $\mathcal{F}_k$ and $\mathcal{F}_{k,\mathbf{resc}}$ and stationary states of equations (1.2) and (2.7) respectively. We will show that in the critical case $\chi = \chi_c$, global minimisers and stationary states are equivalent for original variables. In the sub-critical case $0 < \chi < \chi_c$, all minimisers of $\mathcal{F}_{k,\mathbf{resc}}$ will turn out to be stationary states of the rescaled equation (2.7).

3.1 Global minimisers

A key ingredient for the analysis in the porous medium case are certain functional inequalities which are variants of the Hardy-Littlewood-Sobolev (HLS) inequality, also known as the weak Young's inequality [218, Theorem 4.3]:

$$\iint\limits_{\mathbb{R}^N\times\mathbb{R}^N} f(x)|x-y|^k f(y)\,dxdy \leqslant C_{HLS}(p,q,k)\|f\|_p\|f\|_q\,, \tag{3.14}$$
$$\frac{1}{p}+\frac{1}{q} = 2+\frac{k}{N}\,, \quad p,q>1\,, \quad k\in(-N,0)\,.$$

Theorem 3.1 (Variation of HLS). *Let $k \in (-N, 0)$. For $f \in L^1\left(\mathbb{R}^N\right) \cap L^m\left(\mathbb{R}^N\right)$, we have*

$$\left|\iint\limits_{\mathbb{R}^N\times\mathbb{R}^N} f(x)|x-y|^k f(y)dxdy\right| \leqslant C_*||f||_1^{\frac{N+k}{N}}||f||_m^m, \tag{3.15}$$

where $C_*(k, N)$ is defined as the best constant.

Proof. The inequality is a direct consequence of the standard HLS inequality (3.14) by choosing $p = q = \frac{2N}{2N+k}$, and of Hölder's inequality. For $k \in (-N, 0)$ and for any $f \in L^1\left(\mathbb{R}^N\right) \cap L^m\left(\mathbb{R}^N\right)$,

we have

$$\left| \iint_{\mathbb{R}\times\mathbb{R}} f(x)|x-y|^k f(y)dxdy \right| \leqslant C_{HLS}||f||_p^2 \leqslant C_{HLS}||f||_1^{\frac{N+k}{N}}||f||_m^m.$$

Consequently, C_* is finite and bounded from above by C_{HLS}. □

Now, let us compute explicitly the energy of stationary states:

Lemma 3.2. *For any $-N < k < 0$ and $\chi > 0$, all stationary states $\bar\rho$ of (1.2) with $|x|^2\bar\rho \in L^1\left(\mathbb{R}^N\right)$ satisfy $\mathcal{F}_k\left[\bar\rho\right] = 0$.*

Proof. Integrating (2.5) against x, we obtain for $1 - N < k < 0$:

$$\begin{aligned}
\frac{1}{N}\int_{\mathbb{R}^N} x\cdot\nabla\bar\rho^m &= -2\chi \iint_{\mathbb{R}^N\times\mathbb{R}^N} x\cdot(x-y)|x-y|^{k-2}\bar\rho(x)\bar\rho(y)\,dxdy\\
-\int_{\mathbb{R}^N}\bar\rho^m &= -\chi \iint_{\mathbb{R}^N\times\mathbb{R}^N} (x-y)\cdot(x-y)|x-y|^{k-2}\bar\rho(x)\bar\rho(y)\,dxdy\\
\frac{1}{N(m-1)}\int_{\mathbb{R}^N}\bar\rho^m &= -\chi \iint_{\mathbb{R}^N\times\mathbb{R}^N} \frac{|x-y|^k}{k}\bar\rho(x)\bar\rho(y)\,dxdy\,,
\end{aligned} \tag{3.16}$$

and the result immediately follows. For $-N < k \leqslant 1-N$, the term $\nabla\bar S_k$ is a singular integral, and thus writes

$$\begin{aligned}
\nabla\bar S_k(x) &= \lim_{\varepsilon\to 0}\int_{B^c(x,\varepsilon)} |x-y|^{k-2}(x-y)\bar\rho_k(y)\,dy\\
&= \int_{\mathbb{R}} |x-y|^{k-2}(x-y)\left(\bar\rho_k(y)-\bar\rho_k(x)\right)\,dy\,.
\end{aligned}$$

The singularity disappears when integrating against x,

$$\int_{\mathbb{R}^N} x\cdot\nabla\bar S_k(x)\bar\rho_k(x)\,dx = \frac{1}{2}\iint_{\mathbb{R}^N\times\mathbb{R}^N} |x-y|^k\bar\rho_k(x)\bar\rho_k(y)\,dxdy\,. \tag{3.17}$$

In order to prove (3.17), let us define

$$f_\varepsilon(x) := \int_{B^c(x,\varepsilon)} x\cdot\nabla_x W_k(x-y)\bar\rho_k(y)\,dy.$$

Then by definition of the Cauchy Principle Value, $f_\varepsilon(x) \to x\cdot\nabla\bar S_k(x)$ pointwise for almost every $x\in\mathbb{R}^N$ as $\varepsilon\to 0$. Further, we have for $0<\varepsilon<1$,

$$\begin{aligned}
|f_\varepsilon(x)| &\leqslant |x|\left|\int_{B^c(x,\varepsilon)\cap B(x,1)}\nabla_x W_k(x-y)\bar\rho_k(y)\,dy + \int_{B^c(x,\varepsilon)\cap B^c(x,1)}\nabla_x W_k(x-y)\bar\rho_k(y)\,dy\right|\\
&\leqslant |x|\left(\left|\int_{B^c(x,\varepsilon)\cap B(x,1)}\nabla_x W_k(x-y)\bar\rho_k(y)\,dy\right| + \int_{|x-y|\geqslant 1}|x-y|^{k-1}\bar\rho_k(y)\,dy\right)\\
&\leqslant |x|\left(\left|\int_{B^c(x,\varepsilon)\cap B(x,1)}\nabla_x W_k(x-y)\bar\rho_k(y)\,dy\right| + 1\right)
\end{aligned}$$

Since ∇W_k is anti-symmetric, the term $\int_{B^c(x,\varepsilon)\cap B(x,1)} \nabla_x W_k(x-y)\,dy$ vanishes and we are thus free to subtract it. Using the fact that $\bar\rho_k \in C^{0,\alpha}(\mathbb{R}^N)$ for some $\alpha \in (1-k-N, 1)$, we have

$$\begin{aligned}\left|\int_{B^c(x,\varepsilon)\cap B(x,1)} \nabla_x W_k(x-y)\bar\rho_k(y)\,dy\right| &= \left|\int_{B^c(x,\varepsilon)\cap B(x,1)} \nabla_x W_k(x-y)\left[\bar\rho_k(y)-\bar\rho_k(x)\right]\,dy\right| \\ &\leqslant \int_{B^c(x,\varepsilon)\cap B(x,1)} |x-y|^{k-1}\left|\bar\rho_k(y)-\bar\rho_k(x)\right|\,dy \\ &\leqslant \int_{B^c(x,\varepsilon)\cap B(x,1)} |x-y|^{k+\alpha-1}\,dy \\ &= \frac{\sigma_N}{k+N-1+\alpha}\left(1-\varepsilon^{k+N-1+\alpha}\right) \\ &\leqslant \frac{\sigma_N}{k+N-1+\alpha}\,.\end{aligned}$$

We conclude that $|f_\varepsilon(x)| \leqslant \left(\frac{\sigma_N+k+N-1+\alpha}{k+N-1+\alpha}\right)|x|$ for all $0<\varepsilon<1$, and therefore by Lebesgue's dominated convergence theorem,

$$\begin{aligned}\int_{\mathbb{R}^N} x\cdot\nabla\bar S_k(x)\bar\rho_k(x)\,dx &= \int_{\mathbb{R}} \lim_{\varepsilon\to 0} f_\varepsilon(x)\bar\rho_k(x)\,dx = \lim_{\varepsilon\to 0}\int_{\mathbb{R}} f_\varepsilon(x)\bar\rho_k(x)\,dx \\ &= \lim_{\varepsilon\to 0}\iint\limits_{|x-y|\geqslant\varepsilon} x\cdot(x-y)|x-y|^{k-2}\bar\rho_k(x)\bar\rho_k(y)\,dxdy \\ &= \frac{1}{2}\lim_{\varepsilon\to 0}\iint\limits_{|x-y|\geqslant\varepsilon} |x-y|^{k}\bar\rho_k(x)\bar\rho_k(y)\,dxdy \\ &= \frac{1}{2}\iint\limits_{\mathbb{R}^N\times\mathbb{R}^N} |x-y|^{k}\bar\rho_k(x)\bar\rho_k(y)\,dxdy\,.\end{aligned}$$

This concludes the proof of (3.17). Therefore, it follows that (3.16) holds true for any $-N<k<0$. We remark that a bounded second moment is necessary to allow for the use of $|x|^2/2$ as a test function by a standard approximation argument using suitable truncations. □

Let us point out that the the previous computation is possible due to the homogeneity of the functional $\mathcal{F}_k$. In fact, a formal use of the Euler theorem for homogeneous functions leads to this statement. This argument does not apply in the logarithmic case $k=0$. Here, it allows to connect stationary states and minimisers of $\mathcal{F}_k$.

It follows directly from Theorem 3.1, that for all $\rho\in\mathcal{Y}$ and for any $\chi>0$,

$$\mathcal{F}_k[\rho] \geqslant \frac{1-\chi C_*}{N(m-1)}||\rho||_m^m\,,$$

where $C_* = C_*(k,N)$ is the optimal constant defined in (3.15). Since global minimisers have always smaller or equal energy than stationary states, and stationary states have zero energy by Lemma 3.2, it follows that $\chi \geqslant 1/C_*$. We define the *critical interaction strength* by

$$\chi_c(k,N) := \frac{1}{C_*(k,N)}\,, \tag{3.18}$$

and so for $\chi = \chi_c$, all stationary states of equation (1.2) are global minimisers of $\mathcal{F}_k$. We can also directly see that for $0 < \chi < \chi_c$, no stationary states exist. These observations can be summarised in the following theorem:

Theorem 3.3 (Stationary States in Original Variables)**.** *Let $-N < k < 0$. For critical interaction strength $\chi = \chi_c$, all stationary states $\bar{\rho}$ of equation (1.2) with $|x|^2\bar{\rho} \in L^1\left(\mathbb{R}^N\right)$ are global minimisers of $\mathcal{F}_k$. For sub-critical interaction strengths $0 < \chi < \chi_c$, no stationary states with $|x|^2\bar{\rho} \in L^1\left(\mathbb{R}^N\right)$ exist for equation (1.2).*

We now turn to the study of global minimisers of $\mathcal{F}_k$ and $\mathcal{F}_{k,\mathbf{resc}}$ with the aim of proving the converse implication to Theorem 3.3. Firstly, we have the following existence result:

Proposition 3.4 (Existence of Global Minimisers)**.** *Let $k \in (-N, 0)$.*

(i) If $\chi = \chi_c$, then there exists a radially symmetric and non-increasing function $\tilde{\rho} \in \mathcal{Y}$ satisfying $\mathcal{F}_k[\tilde{\rho}] = 0$.

(ii) If $\chi < \chi_c$, then $\mathcal{F}_k$ does not admit global minimisers, but there exists a global minimiser $\tilde{\rho}$ of $\mathcal{F}_{k,\mathbf{resc}}$ in $\mathcal{Y}_2$.

(iii) If $\chi > \chi_c$, then both $\mathcal{F}_k$ and $\mathcal{F}_{k,\mathbf{resc}}$ are not bounded below.

Proof. Generalising the argument in [39, Proposition 3.4], we obtain the following result for the behaviour of the free energy functional $\mathcal{F}_k$: Let $\chi > 0$. For $k \in (-N, 0)$, we have

$$I_k(\chi) := \inf_{\rho\in\mathcal{Y}} \mathcal{F}_k[\rho] = \begin{cases} 0 & \text{if} \quad \chi \in (0, \chi_c], \\ -\infty & \text{if} \quad \chi > \chi_c\,, \end{cases} \tag{3.19}$$

and the infimum $I_k(\chi)$ is only achieved if $\chi = \chi_c$. This implies statements (ii) and (iii) for $\mathcal{F}_k$. Case (iii) directly follows also in rescaled variables as in [39, Proposition 5.1]. The argument in the sub-critical case (ii) for $\mathcal{F}_{k,\mathbf{resc}}$ is a bit more subtle than in the critical case (i) since we need to make sure that the second moment of our global minimiser is bounded. We will here only prove (ii) for rescaled variables, as (i) and (ii) in original variables are straightforward generalisations from [39, Lemma 3.3] and [39, Proposition 3.4] respectively.

Inequality (3.15) implies that the rescaled free energy is bounded on $\mathcal{Y}_2$ by

$$-\frac{C_*}{k}\left(\chi_c + \chi\right)||\rho||_m^m + \frac{1}{2}\mathcal{V}[\rho] \geqslant \mathcal{F}_{k,\mathbf{resc}}[\rho] \geqslant -\frac{C_*}{k}\left(\chi_c - \chi\right)||\rho||_m^m + \frac{1}{2}\mathcal{V}[\rho], \tag{3.20}$$

and it follows that the infimum of $\mathcal{F}_{k,\mathbf{resc}}$ over $\mathcal{Y}_2$ in the sub-critical case is non negative. Hence, there exists a minimising sequence $(p_j) \in \mathcal{Y}_2$,

$$\mathcal{F}_{k,\mathbf{resc}}[p_j] \to \mu := \inf_{\rho\in\mathcal{Y}_2} \mathcal{F}_{k,\mathbf{resc}}[\rho].$$

Note that $||p_j||_m$ and $\mathcal{V}[p_j]$ are uniformly bounded, $||p_j||_m + \mathcal{V}[p_j] \leqslant C_0$ say, since from (3.20)

$$0 < -\frac{C_*}{k}\left(\chi_c - \chi\right)||p_j||_m^m + \frac{1}{2}\mathcal{V}[p_j] \leqslant \mathcal{F}_{k,\mathbf{resc}}[p_j] \leqslant \mathcal{F}_{k,\mathbf{resc}}[p_0].$$

Further, the radially symmetric decreasing rearrangement (p_j^*) of (p_j) satisfies

$$||p_j^*||_m = ||p_j||_m, \quad \mathcal{V}[p_j^*] \leqslant \mathcal{V}[p_j], \quad \mathcal{W}_k[p_j^*] \leqslant \mathcal{W}_k[p_j]$$

by the reversed Hardy-Littlewood-Sobolev inequality [198] and Riesz rearrangement inequality [218]. In other words, $\mathcal{F}_{k,\mathbf{resc}}[p_j^*] \leqslant \mathcal{F}_{k,\mathbf{resc}}[p_j]$ and so (p_j^*) is also a minimising sequence.

To show that the infimum is achieved, we start by showing that (p_j^*) is uniformly bounded at a point. For any choice of $R > 0$, we have

$$\begin{aligned} 1 = ||p_j^*||_1 &= \sigma_N \int_0^\infty p_j^*(r) r^{N-1}\, dr \\ &\geqslant \sigma_N \int_0^R p_j^*(r) r^{N-1}\, dr \geqslant \sigma_N \frac{R^N}{N} p_j^*(R)\,. \end{aligned}$$

Similarly, since $||p_j^*||_m$ is uniformly bounded,

$$\begin{aligned} C_0 \geqslant ||p_j^*||_m^m &= \sigma_N \int_0^\infty r^{N-1} p_j^*(r)^m\, dr \\ &\geqslant \sigma_N \int_0^R r^{N-1} p_j^*(r)^m\, dr \geqslant \sigma_N \frac{R^N}{N} p_j^*(R)^m\,. \end{aligned}$$

We conclude that

$$0 \leqslant p_j(R) \leqslant b(R) := C_1 \inf\left\{R^{-N}, R^{-\frac{N}{m}}\right\}, \qquad \forall R > 0 \tag{3.21}$$

for a positive constant C_1 only depending on N, m and C_0. Then by Helly's[3] Selection Theorem there exists a subsequence $(p_{j_n}^*)$ and a non-negative function $\tilde{\rho} : \mathbb{R}^N \to \mathbb{R}$ such that $p_{j_n}^* \to \tilde{\rho}$ pointwise almost everywhere. In addition, a direct calculation shows that $x \mapsto b(|x|) \in L^{\frac{2N}{2N+k}}\left(\mathbb{R}^N\right)$, and hence, using (3.14) for $p = q = 2N/(2N+k)$, we obtain

$$(x,y) \mapsto |x-y|^k b(|x|)b(|y|) \in L^1(\mathbb{R}^N \times \mathbb{R}^N).$$

Together with (3.21) and the pointwise convergence of $(p_{j_n}^*)$, we conclude

$$\mathcal{W}_k(p_{j_n}^*) \to \mathcal{W}_k(\tilde{\rho}) < \infty$$

by Lebesgue's[4] dominated convergence theorem. In fact, since $||p_{j_n}^*||_m$ and $\mathcal{V}[p_{j_n}^*]$ are uniformly bounded and $||p_{j_n}^*||_1 = 1$, we have the existence of a subsequence $(p_{j_l}^*)$ and a limit

[3] Eduard Helly (1884-1943) was an Austrian mathematician. After being enlisted in the Austrian army during World War I, he was shot in 1915, and spent the rest of the war as a prisoner of the Russians. He continued organising mathematical seminars and writing important contributions to functional analysis while in Siberian prison camps.

[4] Henri Léon Lebesgue (1875-1941) was a French mathematician. Even though a very good lecturer, he never taught his own theory of integration, saying "Réduites à des thóries générales, les mathématiques seraient une belle forme sans contenu".

$P \in L^1\left(\mathbb{R}^N\right)$ such that $p^*_{j_l} \to P$ weakly in $L^1\left(\mathbb{R}^N\right)$ by the Dunford–Pettis[5] Theorem. Using a variant of Vitali's[6] Lemma [262], we see that the sequence $(p^*_{j_l})$ actually converges strongly to $\tilde{\rho}$ in $L^1\left(\mathbb{R}^N\right)$ on all finite balls in $\mathbb{R}^N$. In other words, $P = \tilde{\rho}$ almost everywhere. Furthermore, $\tilde{\rho}$ has finite second moment by Fatou's Lemma,

$$\mathcal{V}[\tilde{\rho}] \leqslant \liminf_{l\to\infty} \mathcal{V}[p^*_{j_l}] \leqslant C_0,$$

and by convexity of $|.|^m$ for $m \in (1,2)$, we have lower semi-continuity,

$$\int \tilde{\rho}^m \leqslant \liminf_{l\to\infty} \int \left(p^*_{j_l}\right)^m \leqslant C_0.$$

We conclude that $\tilde{\rho} \in \mathcal{Y}_2$ and

$$\mathcal{F}_{k,\mathbf{resc}}[\tilde{\rho}] \leqslant \lim_{l\to\infty} \mathcal{F}_{k,\mathbf{resc}}[p^*_{j_l}] = \mu.$$

Hence, $\tilde{\rho}$ is a global minimiser of $\mathcal{F}_{k,\mathbf{resc}}$.

□

Remark 3.5. *The existence result in original variables also provides optimisers for the variation of the HLS inequality (3.15), and so the supremum in the definition of $C_*(N,k)$ is in fact attained.*

The following necessary condition is a generalisation of results in [39], but using a different argument inspired by [78].

Proposition 3.6 (Necessary Condition for Global Minimisers)**.** *Let $k \in (-N, 0)$.*

(i) If $\chi = \chi_c$ and $\rho \in \mathcal{Y}$ is a global minimiser of $\mathcal{F}_k$, then ρ is radially symmetric non-increasing, satisfying

$$\rho^{m-1}(x) = \frac{N(m-1)}{m}\left(-2\chi(W_k * \rho)(x) + D_k[\rho]\right)_+ \quad \text{a.e. in } \mathbb{R}^N. \tag{3.22}$$

Here, we denote

$$D_k[\rho] := 2\mathcal{F}_k[\rho] + \frac{m-2}{N(m-1)}||\rho||_m^m.$$

(ii) If $0 < \chi < \chi_c$ and $\rho \in \mathcal{Y}_2$ is a global minimiser of $\mathcal{F}_{k,resc}$, then ρ is radially symmetric non-increasing, satisfying

$$\rho^{m-1}(x) = \frac{N(m-1)}{m}\left(-2\chi(W_k * \rho)(x) - \frac{|x|^2}{2} + D_{k,resc}[\rho]\right)_+ \quad \text{a.e. in } \mathbb{R}^N. \tag{3.23}$$

Here, we denote

$$D_{k,resc}[\rho] := 2\mathcal{F}_{k,resc}[\rho] - \frac{1}{2}\mathcal{V}[\rho] + \frac{m-2}{N(m-1)}||\rho||_m^m.$$

[5] Nelson James Dunford (1906-1986) and Billy James Pettis (1913-1979) were American mathematicians, known for their contributions to functional analysis.

[6] Giuseppe Vitali (1875-1932) was an Italian mathematician. From 1926, Vitali developed a serious illness, suffered a paralysed arm and could no longer write. Despite this about half his research papers were written in the last four years of his life.

Proof. (i) Let us write as in (1.1)

$$\mathcal{F}_k[\rho] = \mathcal{U}_{1-k/N}[\rho] + \chi\mathcal{W}_k[\rho], \qquad \mathcal{U}_m[\rho] = \frac{1}{N(m-1)}||\rho||_m^m, \quad \text{and}$$

$$\mathcal{W}_k[\rho] = \iint\limits_{\mathbb{R}^N\times\mathbb{R}^N} \frac{|x-y|^k}{k}\rho(x)\rho(y)\,dxdy.$$

We will first show that all global minimisers of $\mathcal{F}_k$ are radially symmetric non-increasing. Indeed, let ρ be a global minimiser of $\mathcal{F}_k$ in $\mathcal{Y}$, then for the symmetric decreasing rearrangement $\rho^\#$ of ρ, we have $\mathcal{U}_m[\rho^\#] = \mathcal{U}_m[\rho]$ and by the Riesz rearrangement inequality [77, Lemma 2], $\mathcal{W}[\rho^\#] \leqslant \mathcal{W}[\rho]$. So $\mathcal{F}_k[\rho^\#] \leqslant \mathcal{F}_k[\rho]$ and since ρ is a global minimiser this implies $\mathcal{W}_k[\rho^\#] = \mathcal{W}_k[\rho]$. By Riesz rearrangement properties [77, Lemma 2], there exists $x_0 \in \mathbb{R}^N$ such that $\rho(x) = \rho^\#(x - x_0)$ for all $x \in \mathbb{R}^N$. Moreover, we have

$$\int_{\mathbb{R}^N} x\rho(x)\,dx = x_0 + \int_{\mathbb{R}^N} x\rho^\#(x)\,dx = x_0,$$

and thus the zero centre-of-mass condition holds if and only if $x_0 = 0$, giving $\rho = \rho^\#$. For any test function $\psi \in C_c^\infty\left(\mathbb{R}^N\right)$ such that $\psi(-x) = \psi(x)$, we define

$$\varphi(x) = \rho(x)\left(\psi(x) - \int_{\mathbb{R}^N}\psi(x)\rho(x)\,dx\right).$$

We fix $0 < \varepsilon < \varepsilon_0 := (2||\psi||_\infty)^{-1}$. Then

$$\rho + \varepsilon\varphi = \rho\left(1 + \varepsilon\left(\psi - \int_{\mathbb{R}^N}\psi\rho\right)\right) \geqslant \rho\left(1 - 2||\psi||_\infty\varepsilon\right) \geqslant 0,$$

and so $\rho + \varepsilon\varphi \in L^1_+\left(\mathbb{R}^N\right) \cap L^m\left(\mathbb{R}^N\right)$. Further, $\int\varphi(x)\,dx = \int x\varphi(x)\,dx = 0$, and hence $\rho + \varepsilon\varphi \in \mathcal{Y}$. Note also that supp $(\varphi) \subseteq \bar{\Omega} :=$ supp (ρ). To calculate the first variation $\mathcal{T}_k$ of the functional $\mathcal{F}_k$, we need to be careful about regularity issues. Denoting by Ω the interior of $\bar{\Omega}$, we write

$$\begin{aligned}\frac{\mathcal{F}_k[\rho+\varepsilon\varphi] - \mathcal{F}_k[\rho]}{\varepsilon} &= \frac{1}{N(m-1)}\int_\Omega \frac{(\rho+\varepsilon\varphi)^m - \rho^m}{\varepsilon}\,dx \\ &\quad + 2\chi\int_{\mathbb{R}^N}\left(W_k * \rho\right)(x)\varphi(x)\,dx + \varepsilon\mathcal{W}_k[\varphi] \\ &= \frac{m}{N(m-1)}\int_0^1 \mathcal{G}_\varepsilon(t)\,dt \\ &\quad + 2\chi\int_{\mathbb{R}^N}\left(W_k * \rho\right)(x)\varphi(x)\,dx + \varepsilon\mathcal{W}_k[\varphi],\end{aligned}$$

where $\mathcal{G}_\varepsilon(t) := \int_\Omega |\rho + t\varepsilon\varphi|^{m-2}(\rho + t\varepsilon\varphi)\varphi\,dx$. Then by Hölder's inequality,

$$|\mathcal{G}_\varepsilon(t)| \leqslant \left(||\rho||_m + \varepsilon_0||\varphi||_m\right)^{m-1}||\varphi||_m$$

for all $t \in [0,1]$ and $\varepsilon \in (0,\varepsilon_0)$. Lebesgue's dominated convergence theorem yields

$$\int_0^1 \mathcal{G}_\varepsilon(t)\,dt \to \int_\Omega \rho^{m-1}(x)\varphi(x)\,dx$$

as $\varepsilon \to 0$. In addition, one can verify that $\mathcal{W}_k[\varphi] \leqslant 4||\psi||_\infty^2 \mathcal{W}_k[\rho] < \infty$. Hence,

$$\begin{aligned}\lim_{\varepsilon\to 0}\left(\frac{\mathcal{F}_k[\rho+\varepsilon\varphi]-\mathcal{F}_k[\rho]}{\varepsilon}\right) &= \frac{m}{N(m-1)}\int_\Omega \rho^{m-1}(x)\varphi(x)\,dx \\ &\quad + 2\chi\int_{\mathbb{R}^N}(W_k*\rho)(x)\varphi(x)\,dx \\ &= \int_{\mathbb{R}^N}\mathcal{T}_k[\rho](x)\varphi(x)\,dx\,,\end{aligned}$$

proving (1.4). Since ρ is a global minimiser, $\mathcal{F}_k[\rho+\varepsilon\varphi] \geqslant \mathcal{F}_k[\rho]$ and hence $\int \mathcal{T}_k[\rho](x)\varphi(x)\,dx \geqslant 0$. Taking $-\psi$ instead of ψ, we obtain by the same argument $\int \mathcal{T}_k[\rho](x)\varphi(x)\,dx \leqslant 0$, and so

$$\int_{\mathbb{R}^N}\mathcal{T}_k[\rho](x)\varphi(x)\,dx = 0.$$

Owing to the choice of φ,

$$\begin{aligned}0 &= \int_{\mathbb{R}^N}\mathcal{T}_k[\rho](x)\varphi(x)\,dx \\ &= \int_{\mathbb{R}^N}\mathcal{T}_k[\rho](x)\rho(x)\psi(x)\,dx - \left(\int_{\mathbb{R}^N}\psi\rho\right)\left(2\mathcal{F}_k[\rho]+\frac{m-2}{N(m-1)}||\rho||_m^m\right) \\ &= \int_{\mathbb{R}^N}\rho(x)\psi(x)\left(\mathcal{T}_k[\rho](x)-D_k[\rho]\right)\,dx\end{aligned}$$

for any symmetric test function $\psi \in C_c^\infty\left(\mathbb{R}^N\right)$. Hence $\mathcal{T}_k[\rho](x) = D_k[\rho]$ a.e. in $\bar{\Omega}$, i.e.

$$\rho^{m-1}(x) = \frac{N(m-1)}{m}\left(-2\chi\,(W_k*\rho)(x)+D_k[\rho]\right) \quad \text{a.e. in } \bar{\Omega}. \tag{3.24}$$

Now, we turn to conditions over ρ on the whole space. Let $\psi \in C_c^\infty\left(\mathbb{R}^N\right)$, $\psi(-x) = \psi(x)$, $\psi \geqslant 0$, and define

$$\varphi(x) := \psi(x) - \rho(x)\int_{\mathbb{R}^N}\psi(x)\,dx \quad \in L^1\left(\mathbb{R}^N\right)\cap L^m\left(\mathbb{R}^N\right).$$

Then for $0 < \varepsilon < \varepsilon_0 := (||\psi||_\infty|\text{supp }(\psi)|)^{-1}$, we have

$$\rho+\varepsilon\varphi \geqslant \rho\left(1-\varepsilon\int_{\mathbb{R}^N}\psi\right) \geqslant \rho\left(1-\varepsilon||\psi||_\infty|\text{supp }(\psi)|\right).$$

So $\rho+\varepsilon\varphi \geqslant 0$ in $\bar{\Omega}$, and also outside $\bar{\Omega}$ since $\psi \geqslant 0$, hence $\rho+\varepsilon\varphi \in \mathcal{Y}$. Repeating the previous argument, we obtain

$$\int_{\mathbb{R}^N}\mathcal{T}_k[\rho](x)\varphi(x)\,dx \geqslant 0.$$

Using the expression of φ, we have

$$\begin{aligned}0 &\leqslant \int_{\mathbb{R}^N}\mathcal{T}_k[\rho](x)\varphi(x)\,dx \\ &= \int_{\mathbb{R}^N}\mathcal{T}_k[\rho](x)\psi(x)\,dx - \left(\int_{\mathbb{R}^N}\psi\right)\left(2\mathcal{F}_k[\rho]+\frac{m-2}{N(m-1)}||\rho||_m^m\right) \\ &= \int_{\mathbb{R}^N}\psi(x)\left(\mathcal{T}_k[\rho](x)-D_k[\rho]\right)\,dx\,.\end{aligned}$$

Hence $\mathcal{T}_k[\rho](x) \geqslant D_k[\rho]$ a.e. in $\mathbb{R}^N$, and so

$$\rho^{m-1}(x) \geqslant \frac{N(m-1)}{m}\left(-2\chi\left(W_k * \rho\right)(x) + D_k[\rho]\right) \quad \text{a.e. in } \mathbb{R}^N. \tag{3.25}$$

Note that (3.25) means that the support $\bar{\Omega}$ coincides with the set

$$\left\{x \in \mathbb{R}^N \mid -2\chi\left(W_k * \rho\right)(x) + D_k[\rho] > 0\right\}.$$

Combining (3.24) and (3.25) completes the proof of (3.22).

(ii) First, note that if $\rho \in \mathcal{Y}_2$ and $\rho^\#$ denotes the symmetric decreasing rearrangement of ρ, then it follows from the reversed Hardy-Littlewood-Sobolev inequality [198] that $\mathcal{V}[\rho^\#] \leqslant \mathcal{V}[\rho]$. Since $\mathcal{U}_m[\rho^\#] = \mathcal{U}_m[\rho]$ and $\mathcal{W}[\rho^\#] \leqslant \mathcal{W}[\rho]$, we conclude $\mathcal{F}_{k,\mathbf{resc}}[\rho^\#] \leqslant \mathcal{F}_{k,\mathbf{resc}}[\rho]$. For a global minimiser $\rho \in \mathcal{Y}_2$, we have $\mathcal{F}_{k,\mathbf{resc}}[\rho^\#] = \mathcal{F}_{k,\mathbf{resc}}[\rho]$ and hence $\mathcal{W}[\rho^\#] = \mathcal{W}[\rho]$ and $\mathcal{V}[\rho^\#] = \mathcal{V}[\rho]$. The former implies that there exists $x_0 \in \mathbb{R}^N$ such that $\rho(x) = \rho^\#(x - x_0)$ for all $x \in \mathbb{R}^N$ by Riesz rearrangement properties [77, Lemma 2], and so the equality in second moment gives $\rho = \rho^\#$.

Next, we will derive equation (3.23). We define for any test function $\psi \in C_c^\infty\left(\mathbb{R}^N\right)$ the function $\varphi(x) = \rho(x)\left(\psi(x) - \int_{\mathbb{R}^N}\psi(x)\rho(x)\,dx\right)$, and by the same argument as in (i), we obtain

$$0 = \int_{\mathbb{R}^N} \mathcal{T}_{k,\mathbf{resc}}[\rho](x)\varphi(x)\,dx = \int_{\mathbb{R}^N} \rho(x)\psi(x)\left(\mathcal{T}_{k,\mathbf{resc}}[\rho](x) - D_{k,\mathbf{resc}}[\rho]\right)\,dx\,,$$

with $\mathcal{T}_{k,\mathbf{resc}}$ as given in (2.13). Hence $\mathcal{T}_{k,\mathbf{resc}}[\rho](x) = D_{k,\mathbf{resc}}[\rho]$ a.e. in $\bar{\Omega} := \operatorname{supp}(\rho)$. Following the same argument as in (i), we further conclude $\mathcal{T}_{k,\mathbf{resc}}[\rho](x) \geqslant D_{k,\mathbf{resc}}[\rho]$ a.e. in $\mathbb{R}^N$. Together with the equality on $\bar{\Omega}$, this completes the proof of (3.23).

□

Remark 3.7. *For critical interaction strength $\chi = \chi_c$, if $\bar{\rho}$ is a stationary state of equation (1.2) with bounded second moment, then it is a global minimiser of $\mathcal{F}_k$ by Theorem 3.3. In that case, we can identify the constant $C_k[\bar{\rho}]$ in (2.9) with $D_k[\bar{\rho}]$ in (3.22), which is the same on all connected components of $\operatorname{supp}(\bar{\rho})$.*

3.2 Regularity properties of global minimisers

Proposition 3.6 allows us to conclude the following useful corollary, adapting some arguments developed in [39].

Corollary 3.8 (Compactly Supported Global Minimisers)**.** *If $\chi = \chi_c$, then all global minimisers of $\mathcal{F}_k$ in $\mathcal{Y}$ are compactly supported. If $0 < \chi < \chi_c$, then global minimisers of $\mathcal{F}_{k,\mathbf{resc}}$ are compactly supported.*

Proof. Let $\rho \in \mathcal{Y}$ be a global minimiser of $\mathcal{F}_k$. Then ρ is radially symmetric and non-increasing by Proposition 3.6 (i) and has zero energy by (3.19). Using the expression of the constant $D_k[\rho]$ given by Proposition 3.6 (i), we obtain

$$D_k[\rho] = \frac{m-2}{N(m-1)}||\rho||_m^m < 0\,.$$

Let us assume that ρ is supported on $\mathbb{R}^N$. We will arrive at a contradiction by showing that ρ^{m-1} and $W_k * \rho$ are in $L^{m/(m-1)}\left(\mathbb{R}^N\right)$. Since

$$D_k[\rho] = \frac{m}{N(m-1)}\rho(x)^{m-1} + 2\chi\left(W_k * \rho\right)(x)$$

a.e. in $\mathbb{R}^N$ by (3.22), this would mean that the constant $D_k[\rho] < 0$ is in $L^{m/(m-1)}$ and decays at infinity, which is obviously false.

It remains to show that $W_k * \rho$ is in $L^{m/(m-1)}\left(\mathbb{R}^N\right)$ since $\rho \in L^m\left(\mathbb{R}^N\right)$ by assumption. From $\rho \in L^1\left(\mathbb{R}^N\right) \cap L^m\left(\mathbb{R}^N\right)$ we have $\rho \in L^r\left(\mathbb{R}^N\right)$ for all $r \in (1, m]$ by interpolation, and hence $W_k * \rho \in L^s\left(\mathbb{R}^N\right)$ for all $s \in (-N/k, Nm/(k(1-m))]$ by [218, Theorem 4.2]. Finally, we conclude that $W_k * \rho$ is in $L^{m/(m-1)}\left(\mathbb{R}^N\right)$ since $-N/k < m/(m-1) < Nm/(k(1-m))$.

In the sub-critical case for the rescaled functional $\mathcal{F}_{k,\mathbf{resc}}$, we argue as above to conclude that for any global minimiser ρ in $\mathcal{Y}_2$ we have ρ^{m-1} and $W_k * \rho$ in $L^{m/(m-1)}\left(\mathbb{R}^N\right)$. If ρ were supported on the whole space, it followed from the Euler-Lagrange condition for the rescaled equation (3.23) that $|x|^2 + C \in L^{m/(m-1)}\left(\mathbb{R}^N\right)$ for some constant C. This is obviously false. □

The same argument works for stationary states by using the necessary conditions (2.9) and (2.10).

Corollary 3.9 (Compactly Supported Stationary States)**.** *If $\chi = \chi_c$, then all stationary states of equation (1.2) are compactly supported. If $0 < \chi < \chi_c$, then all stationary states of the rescaled equation (2.7) are compactly supported.*

Lemma 3.10. *Let ρ be either a global minimiser of $\mathcal{F}_k$ over $\mathcal{Y}$ or a global minimiser of $\mathcal{F}_{k,\mathbf{resc}}$ over $\mathcal{Y}_2$. If there exists $p \in (-N, 0]$ such that*

$$\rho(r) \lesssim 1 + r^p \qquad \text{for all } r \in (0,1)\,, \tag{3.26}$$

then for $r \in (0,1)$,

$$\rho(r) \lesssim \begin{cases} 1 + r^{g(p)} & \text{if } p \neq -N-k\,, \\ 1 + |\log(r)|^{\frac{1}{m-1}} & \text{if } p = -N-k\,, \end{cases} \tag{3.27}$$

where

$$g(p) = \frac{p+N+k}{m-1}\,. \tag{3.28}$$

Proof. Since global minimisers are radially symmetric non-increasing, we can bound $\rho(r)$ by $\rho(1)$ for all $r \geqslant 1$, and hence the bound (3.26) holds true for all $r > 0$. Further, we know from Corollary 3.8 that all global minimisers are compactly supported. Let us denote $\operatorname{supp}(\rho) = B(0,R)$, $0 < R < \infty$. We split our analysis in four cases: (1) the regime $1 - N < k < 0$ with $k \neq 2 - N$ and $N \geqslant 2$, where we can use hypergeometric functions in our estimates, (2) the Newtonian case

$k = 2 - N$, $N \geqslant 3$, (3) the one dimensional regime $-1 < k < 0$ where we need a Cauchy principle value to deal with the singular integral in the mean-field potential gradient, but everything can be computed explicitly, and finally (4) the regime $-N < k \leqslant 1 - N$ and $N \geqslant 2$, where again singular integrals are needed to deal with the singularities of the hypergeometric functions.

Case 1: $1 - N < k < 0$, $k \neq 2 - N$, $N \geqslant 2$

We would like to make use of the Euler-Lagrange condition (3.22), and hence we need to understand the behaviour of $W_k * \rho$. It turns out that it is advantageous to estimate the derivative instead, writing

$$-\left(W_k * \rho\right)(r) = -\left(W_k * \rho\right)(1) + \int_r^1 \partial_r \left(W_k * \rho\right)(s)\, ds\,. \tag{3.29}$$

The first term on the right-hand side can be estimated explicitly, and we claim that for any $x \in \mathbb{R}^N$, we have

$$-\left(W_k * \rho\right)(x) < \infty\,. \tag{3.30}$$

To see this, let us denote $\gamma := |x|$, and let us fix $\bar{R} \geqslant R$ such that $0 < \gamma < \bar{R}$. If $\gamma/2 \leqslant R$, then

$$\begin{aligned}
-\left(W_k * \rho\right)(\gamma) =& \left(-\frac{1}{k}\right) \int_{B(0,R)\setminus B(0,\gamma/2)} |x-y|^k \rho(y)\, dy + \left(-\frac{1}{k}\right) \int_{B(0,\gamma/2)} |x-y|^k \rho(y)\, dy \\
\leqslant& \left(-\frac{1}{k}\right) \rho\left(\frac{\gamma}{2}\right) \int_{B(0,R)\setminus B(0,\gamma/2)} |x-y|^k\, dy \\
&+ \left(-\frac{\sigma_N}{k}\right) \int_0^{\gamma/2} |\gamma - r|^k \rho(r) r^{N-1}\, dr \\
\lesssim& \gamma^{-N} \int_{B(0,\bar{R})\setminus B(0,\gamma/2)} |x-y|^k\, dy + \int_0^{\gamma/2} |\gamma - r|^k \rho(r) r^{N-1}\, dr \\
\lesssim& \gamma^{-N} \int_{B(x,\bar{R}+\gamma)} |x-y|^k\, dy + \left(\frac{\gamma}{2}\right)^k ||\rho||_1 \\
=& \gamma^{-N} \sigma_N \int_0^{\bar{R}+\gamma} r^{k+N-1}\, dr + \left(\frac{\gamma}{2}\right)^k < \infty\,,
\end{aligned}$$

where we used in the third line the fact that ρ is radially symmetric non-increasing, and so

$$1 \geqslant \int_{B(0,\gamma/2)} \rho(x)\, dx \geqslant \rho\left(\frac{\gamma}{2}\right) \int_{B(0,\gamma/2)} dx = \rho\left(\frac{\gamma}{2}\right) \left(\frac{\sigma_N}{N}\right) \left(\frac{\gamma}{2}\right)^N .$$

If $\gamma/2 > R$ on the other hand, we simply have similar to above

$$-\left(W_k * \rho\right)(\gamma) \leqslant \left(-\frac{1}{k}\right) \int_{B(0,\gamma/2)} |x-y|^k \rho(y)\, dy \lesssim \left(\frac{\gamma}{2}\right)^k < \infty\,,$$

which concludes the proof of (3.30).

In order to control the second term in (3.29), we use the formulation (A.56) from Appendix A,

$$\partial_r \left(W_k * \rho\right)(r) = r^{k-1} \int_0^\infty \psi_k\left(\frac{\eta}{r}\right) \rho(\eta) \eta^{N-1}\, d\eta\,, \tag{3.31}$$

where ψ_k is given by (A.57) and can be written in terms of Gauss hypergeometric functions, see (A.60).

Sub-Newtonian Regime $1 - N < k < 2 - N$

Note that $\psi_k(s) < 0$ for $s > 1$ in the sub-Newtonian regime $1 - N < k < 2 - N$ (see Appendix A Lemma A.3 and Figure 2.3(a)). Together with the induction assumption (3.26) and using the fact that ρ is compactly supported, we have for any $r \in (0, R)$

$$\begin{aligned}
\partial_r \left(W_k * \rho\right)(r) &= r^{k-1} \int_0^r \psi_k\left(\frac{\eta}{r}\right) \rho(\eta) \eta^{N-1} \, d\eta + r^{k-1} \int_r^R \psi_k\left(\frac{\eta}{r}\right) \rho(\eta) \eta^{N-1} \, d\eta \\
&= r^{k+N-1} \int_0^1 \psi_k\left(s\right) \rho(rs) s^{N-1} \, ds + r^{k+N-1} \int_1^{R/r} \psi_k\left(s\right) \rho(rs) s^{N-1} \, ds \\
&\leqslant r^{k+N-1} \int_0^1 \psi_k\left(s\right) \rho(rs) s^{N-1} \, ds \\
&\lesssim r^{k+N-1} \left(\int_0^1 \psi_k\left(s\right) s^{N-1} \, ds \right) + r^{p+k+N-1} \left(\int_0^1 \psi_k\left(s\right) s^{p+N-1} \, ds \right) \\
&= C_1 r^{k+N-1} + C_2 r^{p+k+N-1} \,, \qquad (3.32)
\end{aligned}$$

where we defined

$$C_1 := \int_0^1 \psi_k\left(s\right) s^{N-1} \, ds \,, \qquad C_2 := \int_0^1 \psi_k\left(s\right) s^{p+N-1} \, ds \,.$$

In the case when $r \in [R, \infty)$, we use the fact that $\psi_k(s) > 0$ for $s \in (0, 1)$ by Lemma A.3 and so we obtain by the same argument

$$\begin{aligned}
\partial_r \left(W_k * \rho\right)(r) &= r^{k-1} \int_0^R \psi_k\left(\frac{\eta}{r}\right) \rho(\eta) \eta^{N-1} \, d\eta \lesssim r^{k-1} \int_0^R \psi_k\left(\frac{\eta}{r}\right) \left(1 + \eta^p\right) \eta^{N-1} \, d\eta \\
&= r^{k+N-1} \left(\int_0^{R/r} \psi_k\left(s\right) s^{N-1} \, ds \right) + r^{p+k+N-1} \left(\int_0^{R/r} \psi_k\left(s\right) s^{p+N-1} \, ds \right) \\
&\leqslant C_1 r^{k+N-1} + C_2 r^{p+k+N-1} \,, \qquad (3.33)
\end{aligned}$$

with constants C_1, C_2 as given above. It is easy to see that C_1 and C_2 are indeed finite. From (A.61) it follows that $\psi_k\left(s\right) s^{N-1}$ and $\psi_k\left(s\right) s^{p+N-1}$ are integrable at zero since $-N < p$ and ψ_k is continuous on $[0, 1)$. Similarly, both expressions are integrable at one using (A.63) in Lemma A.4. Hence, we conclude from (3.32) and (3.33) that for any $r \in (0, 1)$,

$$\partial_r \left(W_k * \rho\right)(r) \lesssim r^{k+N-1} + r^{p+k+N-1} \,.$$

Substituting into the right-hand side of (3.29) and using (3.30) yields

$$-\left(W_k * \rho\right)(r) \lesssim 1 + \int_r^1 \left(s^{k+N-1} + s^{p+k+N-1}\right) ds$$

for any $r \in (0, 1)$. It follows that for $p \neq -k - N$,

$$-\left(W_k * \rho\right)(r) \lesssim 1 + \frac{1 - r^{k+N}}{k+N} + \frac{1 - r^{p+k+N}}{p+k+N} \lesssim 1 + r^{p+k+N} \,.$$

If $p = -k - N$, we have instead

$$-\left(W_k * \rho\right)(r) \lesssim 1 + \frac{1 - r^{k+N}}{k+N} - \log(r) \lesssim 1 + |\log(r)| .$$

If ρ is a global minimiser of $\mathcal{F}_k$, then it satisfies the Euler-Lagrange condition (3.22). Hence, we obtain (3.27) with the function $g(p)$ as defined in (3.28). If ρ is a global minimiser of the rescaled functional $\mathcal{F}_{k,\mathbf{resc}}$, then it satisfied condition (3.23) instead, and we arrive at the same result.

Super-Newtonian Regime $\mathbf{k > 2 - N}$

In this regime, $\psi_k(s)$ is continuous, positive and strictly decreasing for $s > 0$ (see Appendix A Lemma A.3 and Figure 2.3(b)) and hence integrable on $(0, s)$ for any $s > 0$. Under the induction assumption (3.26) and using the fact that ρ is compactly supported and radially symmetric non-increasing, we have for any $r \in (0, R)$

$$\begin{aligned}
\partial_r \left(W_k * \rho\right)(r) &= r^{k-1} \int_0^R \psi_k\left(\frac{\eta}{r}\right) \rho(\eta) \eta^{N-1} \, d\eta = r^{N+k-1} \int_0^{R/r} \psi_k(s) \, \rho(rs) s^{N-1} \, d\eta \\
&\lesssim r^{k+N-1} \left(\int_0^{R/r} \psi_k(s) \, s^{N-1} \, ds \right) + r^{p+k+N-1} \left(\int_0^{R/r} \psi_k(s) \, s^{p+N-1} \, ds \right) \\
&= C_1(r) r^{k+N-1} + C_2(r) r^{p+k+N-1} ,
\end{aligned}$$

where we defined

$$C_1(r) := \int_0^{R/r} \psi_k(s) \, s^{N-1} \, ds , \qquad C_2(r) := \int_0^{R/r} \psi_k(s) \, s^{p+N-1} \, ds .$$

Next, let us verify that $C_1(\cdot)$ and $C_2(\cdot)$ are indeed bounded above. From (A.61) it follows again that $\psi_k(s) \, s^{N-1}$ and $\psi_k(s) \, s^{p+N-1}$ are integrable at zero since $-N < p$. In order to deal with the upper limit, we make use of property (A.62), which implies that there exist constants $L > 1$ and $C_L > 0$ such that for all $s \geqslant L$, we have

$$\psi_k(s) \leqslant C_L s^{k-2} .$$

It then follows that for $r < R/L$,

$$\int_L^{R/r} \psi_k(s) \, s^{N-1} \, ds \leqslant \frac{C_L}{N+k-2} \left(\left(\frac{R}{r}\right)^{N+k-2} - L^{N+k-2} \right) ,$$

and hence we obtain

$$C_1(r) = \int_0^L \psi_k(s) \, s^{N-1} \, ds + \int_L^{R/r} \psi_k(s) \, s^{N-1} \, ds \lesssim 1 + r^{-N-k+2} .$$

Similarly,

$$C_2(r) = \int_0^L \psi_k(s) \, s^{p+N-1} \, ds + \int_L^{R/r} \psi_k(s) \, s^{p+N-1} \, ds \lesssim 1 + r^{-p-N-k+2} .$$

We conclude

$$\begin{aligned}\partial_r \left(W_k * \rho\right)(r) \lesssim & \left(1 + r^{-N-k+2}\right) r^{k+N-1} + \left(1 + r^{-p-N-k+2}\right) r^{p+k+N-1} \\ \lesssim & 1 + r^{k+N-1} + r^{p+k+N-1} \,. \end{aligned} \tag{3.34}$$

For $R/L \leqslant r < R$ on the other hand we can do an even simpler bound:

$$C_1(r) + C_2(r) \leqslant \int_0^L \psi_k(s)\, s^{N-1}\, ds + \int_0^L \psi_k(s)\, s^{p+N-1}\, ds \lesssim 1\,,$$

and so we can conclude for (3.34) directly. In the case when $r \in [R, \infty)$, we obtain by the same argument

$$\begin{aligned}\partial_r \left(W_k * \rho\right)(r) \lesssim & r^{k+N-1} \left(\int_0^{R/r} \psi_k(s)\, s^{N-1}\, ds \right) + r^{p+k+N-1} \left(\int_0^{R/r} \psi_k(s)\, s^{p+N-1}\, ds \right) \\ \leqslant & C_1(R) r^{k+N-1} + C_2(R) r^{p+k+N-1}\,, \end{aligned}$$

with constants $C_1(\cdot)$, $C_2(\cdot)$ as given above, and so we conclude that the estimate (3.34) holds true for any $r > 0$. Substituting (3.34) into (3.29), we obtain for $r \in (0,1)$

$$-\left(W_k * \rho\right)(r) \lesssim 1 + \int_r^1 \left(s^{k+N-1} + s^{p+k+N-1}\right) ds$$

and so we conclude as in the sub-Newtonian regime.

Case 2: $k = 2 - N$, $N \geqslant 3$ **Newtonian Regime**

In the Newtonian case, we can make use of known explicit expressions. We write as above

$$-\left(W_k * \rho\right)(r) = -\left(\frac{r^{2-N}}{(2-N)} * \rho \right)(1) + \int_r^1 \partial_r \left(\frac{r^{2-N}}{(2-N)} * \rho \right)(s)\, ds\,, \tag{3.35}$$

where $-\left(\frac{r^{2-N}}{(2-N)} * \rho \right)(1)$ is bounded using (3.30). To control $\int_r^1 \partial_r \left(\frac{r^{2-N}}{(2-N)} * \rho \right)(s)\, ds$, we use Newton's Shell Theorem implying

$$\partial_r \left(\frac{r^{2-N}}{(2-N)} * \rho \right)(s) = \frac{\sigma_N M(s)}{|\partial B(0,s)|} = M(s) s^{1-N}\,,$$

where we denote by $M(s) = \sigma_N \int_0^s \rho(t) t^{N-1}\, dt$ the mass of ρ in $B(0,s)$. Note that this is precisely expression (3.31) we obtained in the previous case, choosing $\psi_k(s) = 1$ for $s < 1$ and $\psi_k = 0$ for $s > 1$ with a jump singularity at $s = 1$ (see also (A.54) in Appendix A). By our induction assumption (3.26), we have

$$M(s) \lesssim \sigma_N \int_0^s (1 + t^p) t^{N-1}\, dt = \sigma_N \left(\frac{s^N}{N} + \frac{s^{N+p}}{N+p} \right)\,, \qquad s \in (0,1)\,,$$

and hence if $p \neq -2$, then

$$\int_r^1 \partial_r \left(\frac{r^{2-N}}{(2-N)} * \rho \right)(s)\, ds \lesssim \frac{1}{2N}\left(1-r^2\right) + \frac{1}{(N+p)(p+2)}\left(1-r^{p+2}\right).$$

If $p = -2$, we obtain instead

$$\int_r^1 \partial_r \left(\frac{r^{2-N}}{(2-N)} * \rho \right)(s)\, ds \lesssim \frac{1}{2N}\left(1-r^2\right) - \frac{1}{(N+p)}\log(r).$$

Substituting into the right-hand side of (3.35) yields for all $r \in (0,1)$

$$-\left(W_k * \rho\right)(r) \lesssim \begin{cases} 1 + r^{p+2} & \text{if } p \neq -2, \\ 1 + |\log(r)| & \text{if } p = -2. \end{cases}$$

Thanks again to the Euler-Lagrange condition (3.22) if ρ is a global minimiser of $\mathcal{F}_k$, or thanks to condition (3.23) if ρ is a global minimiser of $\mathcal{F}_{k,\mathbf{resc}}$ instead, we arrive in both cases at (3.27).

Case 3: $-1 < k < 0$, $N = 1$

In one dimension, we can calculate everything explicitly. Since the mean-field potential gradient is a singular integral, we have

$$\begin{aligned} \partial_x S_k(x) &= \int_{\mathbb{R}} \frac{x-y}{|x-y|^{2-k}} \left(\rho(y) - \rho(x)\right)\, dy \\ &= \lim_{\delta \to 0} \int_{|x-y|>\delta} \frac{x-y}{|x-y|^{2-k}} \rho(y)\, dy = \frac{x}{r} \partial_r S_k(r) \end{aligned}$$

with the radial component for $r \in (0,R)$ given by

$$\begin{aligned} \partial_r S_k(r) &= \int_0^\infty \left(\frac{r-\eta}{|r-\eta|^{2-k}} + \frac{r+\eta}{|r+\eta|^{2-k}} \right) \left(\rho(\eta) - \rho(r)\right)\, d\eta \\ &= \int_0^\infty \frac{r+\eta}{|r+\eta|^{2-k}} \rho(\eta)\, d\eta + \lim_{\delta \to 0} \int_{|r-\eta|>\delta} \frac{r-\eta}{|r-\eta|^{2-k}} \rho(\eta)\, d\eta \\ &= r^{k-1} \int_0^\infty \psi_1\left(\frac{\eta}{r}\right) \rho(\eta)\, d\eta + r^{k-1} \lim_{\delta \to 0} \int_{|r-\eta|>\delta} \psi_2\left(\frac{\eta}{r}\right) \rho(\eta)\, d\eta \\ &= r^{k-1} \int_0^R \psi_1\left(\frac{\eta}{r}\right) \rho(\eta)\, d\eta + r^{k-1} \lim_{\delta \to 0} \left(\int_0^{r-\delta} + \int_{r+\delta}^R \right) \psi_2\left(\frac{\eta}{r}\right) \rho(\eta)\, d\eta \end{aligned}$$

where

$$\psi_1(s) := \frac{1+s}{|1+s|^{2-k}} = (1+s)^{k-1}, \qquad \psi_2(s) := \frac{1-s}{|1-s|^{2-k}} = \begin{cases} (1-s)^{k-1} & \text{if } 0 \leqslant s < 1, \\ -(s-1)^{k-1} & \text{if } s > 1 \end{cases}$$

are well defined on $[0,1) \cup (1,\infty)$. Define $\gamma := \min\{1, R/2\}$. Since $\psi_2(s) < 0$ for $s > 1$ and ρ radially symmetric decreasing, we can estimate the last term for any $r \in (0,\gamma)$ and small $\delta > 0$ by

$$\begin{aligned} & r^{k-1}\left(\int_0^{r-\delta} + \int_{r+\delta}^{R}\right)\psi_2\left(\frac{\eta}{r}\right)\rho(\eta)\,d\eta \\ & \leqslant r^{k-1}\int_0^{r-\delta}\psi_2\left(\frac{\eta}{r}\right)\rho(\eta)\,d\eta + r^{k-1}\rho(2r)\int_{r+\delta}^{2r}\psi_2\left(\frac{\eta}{r}\right)\,d\eta \\ & = r^k\int_0^{1-\delta/r}\psi_2\left(s\right)\rho(rs)\,ds + r^k\rho(2r)\int_{1+\delta/r}^{2}\psi_2\left(s\right)\,ds\,. \end{aligned}$$

Under assumption (3.26), we can bound the above expression by

$$\begin{aligned} \partial_r S_k(r) \lesssim\ & r^k\int_0^{R/r}\psi_1(s)\,ds + r^{k+p}\int_0^{R/r}\psi_1(s)s^p\,ds \\ & + r^k\lim_{\delta\to 0}\left[\int_0^{1-\delta/r}\psi_2(s)\,ds + r^p\int_0^{1-\delta/r}\psi_2(s)s^p\,ds + (1+r^p)\int_{1+\delta/r}^{2}\psi_2\left(s\right)\,ds\right] \\ & = r^k\lim_{\delta\to 0}C_1(r,\delta) + r^{k+p}\lim_{\delta\to 0}C_2(r,\delta)\,, \end{aligned}$$

where we defined

$$\begin{aligned} C_1(r,\delta) &:= \int_0^{R/r}\psi_1(s)\,ds + \int_0^{1-\delta/r}\psi_2(s)\,ds + \int_{1+\delta/r}^{2}\psi_2\left(s\right)\,ds\,, \\ C_2(r,\delta) &:= \int_0^{R/r}\psi_1(s)s^p\,ds + \int_0^{1-\delta/r}\psi_2(s)s^p\,ds + \int_{1+\delta/r}^{2}\psi_2\left(s\right)\,ds\,. \end{aligned}$$

Next, let us show that the functions $\lim_{\delta\to 0} C_1(r,\delta)$ and $\lim_{\delta\to 0} C_2(r,\delta)$ can be controlled in terms of r. The function ψ_2 has a non-integrable singularity at $s = 1$, however, we can seek compensations from below and above the singularity. One can compute directly that

$$\begin{aligned} C_1(r,\delta) =& \frac{1}{k}\left[\left(\frac{R}{r}+1\right)^k - 1\right] + \frac{1}{k}\left[1 - \left(\frac{\delta}{r}\right)^k\right] + \frac{1}{k}\left[\left(\frac{\delta}{r}\right)^k - 1\right] \\ =& \frac{1}{k}\left(\left(\frac{R}{r}+1\right)^k - 1\right) \leqslant -\frac{1}{k}\,, \\ C_2(r,\delta) =& \left[\left(\frac{R}{r}+1\right)^{k-1}\left(\frac{R}{r}\right)^{p+1}\right] - \frac{1}{k}\left[\left(\frac{\delta}{r}\right)^k\right] + \frac{1}{k}\left[\left(\frac{\delta}{r}\right)^k - 1\right] \\ =& \left(\frac{R}{r}+1\right)^{k-1}\left(\frac{R}{r}\right)^{p+1} - \frac{1}{k} \leqslant \left(\frac{R}{r}\right)^{k-1}\left(\frac{R}{r}\right)^{p+1} - \frac{1}{k} = R^{k+p}r^{-k-p} - \frac{1}{k}\,, \end{aligned}$$

so that we obtain the estimate

$$\partial_r S_k(r) \lesssim 1 + r^k + r^{k+p}\,.$$

Finally, we have for all $r \in (0,\gamma)$:

$$-\left(W_k * \rho\right)(r) = -\left(W_k * \rho\right)(\gamma) + \int_r^{\gamma}\partial_r S_k(s)\,ds \lesssim 1 + \int_r^{\gamma}\left(s^k + s^{p+k}\right)\,ds\,,$$

where we made again use of estimate (3.30). If $p \neq -k-1$, we have

$$-\left(W_k * \rho\right)(r) \lesssim 1 + \frac{\gamma^{k+1} - r^{k+1}}{k+1} + \frac{\gamma^{p+k+1} - r^{p+k+1}}{p+k+1} \lesssim 1 + r^{p+k+1}\,.$$

If $p = -k-1$ however, we obtain

$$-\left(W_k * \rho\right)(r) \lesssim 1 + \frac{\gamma^{k+1} - r^{k+1}}{k+1} + \log(\gamma) - \log(r) \lesssim 1 + |\log(r)|\,.$$

Using again the Euler-Lagrange condition (3.22) for a global minimiser of $\mathcal{F}_k$ or (3.23) for a global minimiser of $\mathcal{F}_{k,\mathbf{resc}}$ respectively, we obtain (3.27) in the one dimensional case.

Case 4: $-N < k \leqslant 1-N$, $N \geqslant 2$

In this case, we can again use hypogeometric functions, but here the mean-field potential gradient is a singular integral due to the singularity properties of hypogeometric functions. It writes as

$$\nabla S_k(x) = \lim_{\delta \to 0} \int_{|x-y|>\delta} \frac{x-y}{|x-y|^{2-k}} \rho(y)\, dy = \frac{x}{r} \partial_r S_k(r)$$

with the radial component given by

$$\begin{aligned}\partial_r S_k(r) =& r^{k-1} \lim_{\delta \to 0} \int_{|r-\eta|>\delta} \psi_k\left(\frac{\eta}{r}\right) \rho(\eta) \eta^{N-1}\, d\eta \\ =& r^{k-1} \lim_{\delta \to 0} \left(\int_0^{r-\delta} + \int_{r+\delta}^{R} \right) \psi_k\left(\frac{\eta}{r}\right) \rho(\eta) \eta^{N-1}\, ds\,,\end{aligned}$$

where ψ_k is given by (A.60) on $[0,1) \cup (1,\infty)$, and we used the fact that ρ is compactly supported. In this regime, the singularity at $s=1$ is non-integrable and has to be handled with care. Define $\gamma := \min\{1, R/2\}$. Since $\psi_2(s) < 0$ for $s > 1$ (see Appendix A Lemma A.3) and since ρ is radially symmetric non-increasing, we can estimate the second integral above for any $r \in (0,\gamma)$ and small $\delta > 0$ by

$$\begin{aligned}r^{k-1} \int_{r+\delta}^{R} \psi_k\left(\frac{\eta}{r}\right) \rho(\eta) \eta^{N-1}\, d\eta \leqslant& r^{k-1} \rho(2r) \int_{r+\delta}^{2r} \psi_k\left(\frac{\eta}{r}\right) \eta^{N-1}\, d\eta \\ =& r^{N+k-1} \rho(2r) \int_{1+\delta/r}^{2} \psi_k\left(s\right) s^{N-1}\, ds\,.\end{aligned}$$

Under assumption (3.26), we can then bound the above expression by

$$\begin{aligned}\partial_r \left(W_k * \rho\right)(r) \lesssim& r^{N+k-1} \lim_{\delta \to 0} \left[\int_0^{1-\delta/r} \psi_k(s) s^{N-1}\, ds + r^p \int_0^{1-\delta/r} \psi_k(s) s^{p+N-1}\, ds \right. \\ & \left. + \left(1 + r^p\right) \int_{1+\delta/r}^{2} \psi_k\left(s\right) s^{N-1}\, ds \right] \\ =& r^{N+k-1} \lim_{\delta \to 0} C_1(r,\delta) + r^{p+N+k-1} \lim_{\delta \to 0} C_2(r,\delta)\,,\end{aligned}$$

where

$$C_1(r,\delta) := \int_0^{1-\delta/r} \psi_k(s) s^{N-1}\, ds + \int_{1+\delta/r}^{2} \psi_k\left(s\right) s^{N-1}\, ds\,,$$
$$C_2(r,\delta) := \int_0^{1-\delta/r} \psi_k(s) s^{p+N-1}\, ds + \int_{1+\delta/r}^{2} \psi_k\left(s\right) s^{N-1}\, ds\,.$$

The crucial step is again to show that $\lim_{\delta\to 0} C_1(r,\delta)$ and $\lim_{\delta\to 0} C_2(r,\delta)$ are well-defined and can be controlled in terms of r, seeking compensations from above and below the singularity at $s = 1$. Recalling that $\psi_k(s)s^{N-1}$ and $\psi_k(s)s^{p+N-1}$ are integrable at zero by Lemma A.1 and at any finite value above $s = 1$ by continuity, we see that the lower bound 0 and upper bound 2 in the integrals only contribute constants, independent of r and δ. The essential step is therefore to check integrability close to the singularity $s = 1$. From (A.63) and (A.64) in Appendix A Lemma A.4(2), we have for any $\alpha \in \mathbb{R}$ and s close to 1:

$$s<1: \qquad \psi_k\left(s\right) s^{\alpha} = K_1 \left(1-s\right)^{N+k-2} + O\left(\left(1-s\right)^{N+k-1}\right)\,,$$
$$s>1: \qquad \psi_k\left(s\right) s^{\alpha} = -K_1 \left(s-1\right)^{N+k-2} + O\left(\left(s-1\right)^{N+k-1}\right)\,,$$

where the constant K_1 is given by (A.65)–(A.66). Hence, for $-N < k < 1-N$ we obtain

$$\begin{aligned} C_1(r,\delta) &\lesssim 1 - \frac{K_1}{N+k-1}\left(\frac{\delta}{r}\right)^{N+k-1} + \frac{K_1}{N+k-1}\left(\frac{\delta}{r}\right)^{N+k-1} + O\left(\left(\frac{\delta}{r}\right)^{N+k}\right) \\ &= 1 + O\left(\left(\frac{\delta}{r}\right)^{N+k}\right) \end{aligned}$$

with exactly the same estimate for $C_2(r,\delta)$. Taking the limit $\delta \to 0$, we see that both terms are bounded by a constant. For $k = 1-N$, we obtain similarly that both $C_1(r,\delta)$ and $C_2(r,\delta)$ are bounded by

$$1 - K_1 \log\left(\frac{\delta}{r}\right) + K_1 \log\left(\frac{\delta}{r}\right) + O\left(\left(\frac{\delta}{r}\right)\right) = 1 + O\left(\left(\frac{\delta}{r}\right)\right)$$

multiplied by some constant. In other words, for any $r \in (0,\gamma)$ and $-N < k \leqslant 1-N$ we have

$$\partial_r \left(W_k * \rho\right)(r) \lesssim r^{N+k-1} + r^{p+N+k-1}\,.$$

Now, we are ready to estimate the behaviour of ρ around the origin using again the Euler-Lagrange condition. To estimate the mean-field potential, we use again (3.30) and write

$$-\left(W_k * \rho\right)(r) = -\left(W_k * \rho\right)(\gamma) + \int_r^{\gamma} \partial_r \left(W_k * \rho\right)(s)\, ds \lesssim 1 + \int_r^{\gamma} \left(s^{k+N-1} + s^{p+k+N-1}\right)\, ds$$

for any $r \in (0,\gamma)$. It follows that for $p \neq -k-N$,

$$-\left(W_k * \rho\right)(r) \lesssim 1 + \frac{\gamma^{k+N} - r^{k+N}}{k+N} + \frac{\gamma^{p+k+N} - r^{p+k+N}}{p+k+N} \lesssim 1 + r^{p+k+N}\,.$$

If $p = -k - N$, we have instead

$$-(W_k * \rho)(r) \lesssim 1 + \frac{\gamma^{k+N} - r^{k+N}}{k+N} + \log(\gamma) - \log(r) \lesssim 1 + |\log(r)|\,.$$

This concludes the proof of Lemma 3.10 using again Euler-Lagrange condition (3.22) if ρ is a minimiser of $\mathcal{F}_k$, or condition (3.23) if ρ is a minimiser of $\mathcal{F}_{k,\mathbf{resc}}$, to obtain (3.27). □

Corollary 3.11 (Boundedness). *If $\chi = \chi_c$ and ρ is a global minimiser of $\mathcal{F}_k$ over $\mathcal{Y}$, then $\rho \in L^\infty(\mathbb{R}^N)$. If $0 < \chi < \chi_c$ and ρ is a global minimiser of $\mathcal{F}_{k,\mathbf{resc}}$ over $\mathcal{Y}_2$, then $\rho \in L^\infty(\mathbb{R}^N)$.*

Proof. Let ρ be a global minimiser of either $\mathcal{F}_k$ over $\mathcal{Y}$, or of $\mathcal{F}_{k,\mathbf{resc}}$ over $\mathcal{Y}_2$. Since ρ is radially symmetric non-increasing by Proposition 3.6, it is enough to show that $\rho(0) < \infty$. Following the argument in [89], we use induction to show that there exists some $\alpha > 0$ such that for all $r \in (0,1)$ we have

$$\rho(r) \lesssim 1 + r^\alpha\,. \tag{3.36}$$

Note that $g(p)$ as defined in (3.28) is a linear function of p with positive slope, and let us denote $g^{(n)}(p) = (g \circ g \cdots \circ g)(p)$. Computing explicitly, we have for all $n \in \mathbb{N}$

$$g^{(n)}(p) = \frac{N+k}{m-2} + \frac{p(m-2) - N - k}{(m-2)(m-1)^n} = -N + \frac{p+N}{(m-1)^n}\,,$$

so that

$$\lim_{n\to\infty} g^{(n)}(p) = +\infty \quad \text{for any } p > -N\,.$$

Since $\rho(r)^m |B(0,r)| \leqslant ||\rho||_m^m < \infty$ we obtain the estimate

$$\rho(r) \leqslant C(N,m,||\rho||_m) r^{-N/m} \quad \text{for all } r > 0\,.$$

It follows that ρ satisfies the induction requirement (3.26) with choice $p_0 := -N/m$. Since $p_0 > -N$ there exists $n_0 \in \mathbb{N}$ such that $g^{(n_0)}(p_0) > 0$ and so we can apply Lemma 3.10 n_0 times. This concludes the proof with $\alpha = g^{(n_0)}(p_0)$. We point out that $p_0 < -N-k$ and so there is a possibility that $g^{(n)}(p_0) = -N - k$ might occur for some $0 < n \leqslant n_0$: if this happens, the logarithmic case occurs and by the second bound in (3.27), we obtain

$$\rho(r) \lesssim 1 + |\log(r)|^{\frac{1}{m-1}} \leqslant 1 + r^{-1}\,,$$

hence applying the first bound in (3.27) for $p = -1$ yields (3.36) with $\alpha = 1/(m-1)$. □

Corollary 3.12 (Regularity). *If $\chi = \chi_c$, then all global minimisers $\rho \in \mathcal{Y}$ of $\mathcal{F}_k$ satisfy $S_k \in \mathcal{W}^{1,\infty}(\mathbb{R}^N)$ and $\rho^{m-1} \in \mathcal{W}^{1,\infty}(\mathbb{R}^N)$. If $0 < \chi < \chi_c$, then all minimisers $\rho \in \mathcal{Y}_2$ of $\mathcal{F}_{k,\mathbf{resc}}$ satisfy $S_k \in \mathcal{W}^{1,\infty}(\mathbb{R}^N)$ and $\rho^{m-1} \in \mathcal{W}^{1,\infty}(\mathbb{R}^N)$. In the singular range $-N < k \leqslant 1-N$, we further obtain $\rho \in C^{0,\alpha}(\mathbb{R}^N)$ with $\alpha \in (1-k-N, 1)$ in both original and rescaled variables.*

Proof. Let ρ be a global minimiser either of $\mathcal{F}_k$ over $\mathcal{Y}$, or of $\mathcal{F}_{k,\mathbf{resc}}$ over $\mathcal{Y}_2$. Then $\rho \in L^\infty\left(\mathbb{R}^N\right)$ by Corollary 3.11. Let us start by considering the singular regime $-N < k \leqslant 1-N$, $N \geqslant 2$ or $-1 < k < 0$ for $N = 1$. Since $\rho \in L^1\left(\mathbb{R}^N\right) \cap L^\infty\left(\mathbb{R}^N\right)$, we have $\rho \in L^p\left(\mathbb{R}^N\right)$ for any $1 < p < \infty$.

Using the fact that $\rho = (-\Delta)^s S_k$ with fractional exponent $s = (N+k)/2 \in (0, 1/2)$, we gain $2s$ derivatives implying $S_k \in \mathcal{W}^{2s,p}\left(\mathbb{R}^N\right)$ for $p \geqslant 2$ if $N \geqslant 2$ or for $p > -1/k$ if $N = 1$ by using the HLS inequality for Riesz kernels, see [272, Chapter V]. More precisely, by definition of the Bessel potential space $\mathcal{L}^{2s,p}(\mathbb{R}^N)$, if $u, (-\Delta)^s u \in L^p(\mathbb{R}^N)$, then $u \in \mathcal{L}^{2s,p}(\mathbb{R}^N)$. Since $\mathcal{L}^{2s,p}(\mathbb{R}^N) \subset \mathcal{W}^{2s,p}(\mathbb{R}^N)$ for any $p \geqslant 2$ and $s \in (0, 1/2)$ [272, p.155, Theorem 5(A)], we have $u \in \mathcal{W}^{2s,p}(\mathbb{R}^N)$. Next, we use classical Sobolev embedding, $\mathcal{W}^{2s,p}\left(\mathbb{R}^N\right) \subset C^{0,\beta}\left(\mathbb{R}^N\right)$ with $\beta = 2s - N/p$ for $p > \frac{N}{2s} > 2$ if $N \geqslant 2$ or for $p > \max\{\frac{1}{k+1}, -\frac{1}{k}\}$ if $N = 1$, which yields $\rho \in C^{0,\beta}\left(\mathbb{R}^N\right)$. If $N \geqslant 2$ and $s = 1/2$, we use instead that $S_k \in \mathcal{L}^{1,p}(\mathbb{R}^N)$ for all $p \geqslant 2$ implies $S_k \in \mathcal{L}^{2r,p}(\mathbb{R}^N)$ for all $p \geqslant 2$ and $r \in (0, 1/2)$ [272, p.135], and then reason as above using any $r \in (0, 1/2)$ instead of $s = 1/2$.
In the case $1/2 - N < k \leqslant 1 - N$, we can ensure $\beta > 1 - k - N$ for large enough p, obtaining the required Hölder regularity. For $k \leqslant 1/2 - N$ on the other hand, we need to bootstrap a bit further. Let us fix $n \in \mathbb{N}$, $n \geqslant 2$ such that

$$\frac{1}{n+1} - N < k \leqslant \frac{1}{n} - N$$

and let us define $\beta_n := \beta + (n-1)2s = n2s - N/p$. Note that $S_k \in L^\infty\left(\mathbb{R}^N\right)$ by Lemma 2.2, and $\beta_{n-1} + 2s < 1$. This allows us to repeatedly apply [270, Proposition 2.8] stating that $\rho \in C^{0,\gamma}\left(\mathbb{R}^N\right)$ implies $S_k \in C^{0,\gamma+2s}\left(\mathbb{R}^N\right)$ for any $\gamma \in (0, 1]$ such that $\gamma + 2s < 1$. It then follows that $\rho^{m-1} \in C^{0,\gamma+2s}\left(\mathbb{R}^N\right)$ using the Euler-Lagrange conditions (3.22) and (3.23) respectively and Corollary 3.8. Since $m \in (1, 2)$, we conclude $\rho \in C^{0,\gamma+2s}\left(\mathbb{R}^N\right)$. Iterating this argument $(n-1)$ times starting with $\gamma = \beta$, we obtain $\rho \in C^{0,\beta_n}\left(\mathbb{R}^N\right)$ and choosing p large enough, we have indeed

$$\beta_n > 1 - k - N\,.$$

For any $-N < k < 0$, we then have $S_k \in \mathcal{W}^{1,\infty}\left(\mathbb{R}^N\right)$ by Lemma 2.2. It also immediately follows that $\rho^{m-1} \in \mathcal{W}^{1,\infty}\left(\mathbb{R}^N\right)$ using the Euler-Lagrange conditions (3.22) and (3.23) respectively, Corollary 3.8 and Lemma 2.2. Since $m \in (1, 2)$, we also conclude $\rho \in \mathcal{W}^{1,\infty}\left(\mathbb{R}^N\right)$. □

Remark 3.13. *For proving sufficient Hölder regularity in the singular regime $-N < k \leqslant 1-N$, one may choose to bootstrap on the fractional Sobolev space $\mathcal{W}^{2s,p}\left(\mathbb{R}^N\right)$ directly, making use of the Euler-Lagrange conditions (3.22) and (3.23) respectively to show that $\rho \in \mathcal{W}^{r,p}\left(\mathbb{R}^N\right) \Rightarrow S_k \in \mathcal{W}^{r+2s,p}\left(\mathbb{R}^N\right)$ with $r > 0$ for p large enough depending only on N. Here, we need that $\mathcal{W}^{r,p}\left(\mathbb{R}^N\right)$ is preserved under taking positive parts of a function for $0 < r \leqslant 1$ and compositions with Lipschitz functions since we take the $1/(m-1)$ power of ρ, see [268, Section 3.1].*

Theorem 3.14 (Global Minimisers as Stationary States). *If $\chi = \chi_c$, then all global minimisers of $\mathcal{F}_k$ are stationary states of equation (1.2). If $0 < \chi < \chi_c$, then all global minimisers of $\mathcal{F}_{k,\textbf{resc}}$ are stationary states of the rescaled equation (2.7).*

Proof. For $\chi = \chi_c$, let $\rho \in \mathcal{Y}$ be a global minimiser of $\mathcal{F}_k$. The regularity properties provided by Corollary 3.12 imply that $\nabla \rho^m = \frac{m}{m-1}\rho \nabla \rho^{m-1}$ and that ρ is indeed a distributional solution of (2.5) using (3.22). As a consequence, ρ is a stationary state of equation (1.2) according to Definition 2.1. A similar argument holds true in the rescaled case for sub-critical χ. □

Remark 3.15. *As a matter of fact, the recent result of radial symmetry of stationary states [89] applies to the critical case $\chi = \chi_c$ in the range $k \in [2-N, 0)$. Together, Theorem 3.3 and Proposition 3.6 show that all stationary states are radially symmetric for the full range $k \in (-N, 0)$. In other words, the homogeneity of the energy functional $\mathcal{F}_k$ allows us to extend the result in [89] to $k \in (-N, 2-N)$ and to find a simple alternative proof in the less singular than Newtonian range.*

4 Fast diffusion case $k > 0$

We investigate in this section the case $k \in (0, N)$ and hence $m \in (0, 1)$ where the diffusion is fast in regions where the density of particles is low. The main difficulty is that it seems there is no HLS-type inequality in this range which would provide a lower bound on the free energy, and so a different approach is needed than in the porous medium regime. We concentrate here on the radial setting. Let us define $\mathcal{X}$ to be the set

$$\mathcal{X} := \left\{ \rho \in L^1_+\left(\mathbb{R}^N\right) : ||\rho||_1 = 1\,,\ \int x\rho(x)\,dx = 0 \right\}.$$

The following Lemma will be a key ingredient for studying the behaviour in the fast diffusion case.

Lemma 4.1. *For $k \in (0, N)$, any radially symmetric non-increasing $\rho \in \mathcal{X}$ with $|x|^k \rho \in L^1\left(\mathbb{R}^N\right)$ satisfies*

$$I_k[\rho] \leqslant (W_k * \rho)(x) \leqslant \eta\left(\frac{|x|^k}{k} + I_k[\rho]\right), \qquad \forall\ x \in \mathbb{R}^N \tag{4.37}$$

with

$$I_k[\rho] := \int_{\mathbb{R}^N} \frac{|x|^k}{k}\rho(x)\,dx, \qquad \eta = \max\{1, 2^{k-1}\}.$$

Proof. The bound from above was proven in (2.6). To prove the lower bound in one dimension, we use the symmetry and monotonicity assumption to obtain

$$\partial_x\left(W_k * \rho\right) = \frac{1}{k}\int_{y>0}\left(|x-y|^k - |x+y|^k\right)\partial_y\rho\,dy \quad \geqslant 0\,, \qquad \forall\ x \geqslant 0$$

since $|x-y|^k - |x+y|^k \leqslant 0$ for $x, y \geqslant 0$. By symmetry of $W_k * \rho$ it follows that $\partial_x\left(W_k * \rho\right)(x) \leqslant 0$ for all $x \leqslant 0$ and hence (4.37) holds true in one dimension for the bound from below.

For $N \geqslant 2$, note that since both W_k and ρ are radial functions, so is the convolution $W_k * \rho$. By slight abuse of notation, we write $(W_k * \rho)(r)$. For $r > 0$, we have

$$\int_{B(0,r)} \Delta_x \left(W_k * \rho\right) dx = \int_{\partial B(0,r)} \nabla_x \left(W_k * \rho\right) \cdot \overline{n}\, dS$$
$$= |\partial B(0,r)|\, \partial_r \left(W_k * \rho\right) = r^{N-1} \sigma_N\, \partial_r \left(W_k * \rho\right).$$

From $\Delta_x W_k(x) = (N + k - 2)\,|x|^{k-2} > 0$, it then follows that $\partial_r \left(W_k * \rho\right)(r) > 0$ for all $r > 0$. This implies the lower bound in higher dimensions. □

4.1 Results in original variables

Theorem 4.2 (Non-Existence of Stationary States)**.** *Let $k \in (0, N)$. For any $\chi > 0$, there are no radially symmetric non-increasing stationary states in $\mathcal{X}$ for equation (1.2) with kth moment bounded.*

Proof. Assume $\bar{\rho} \in \mathcal{X}$ is a radially symmetric non-increasing stationary state for equation (1.2) such that $|x|^k \bar{\rho} \in L^1\left(\mathbb{R}^N\right)$. Then $\bar{\rho}$ is continuous by Lemma 2.4. We claim that $\bar{\rho}$ is supported on $\mathbb{R}^N$ and satisfies

$$\bar{\rho}(x) = \left(A W_k * \bar{\rho}(x) + C[\bar{\rho}]\right)^{-N/k}, \quad a.e.\ x \in \mathbb{R}^N, \tag{4.38}$$

with $A := 2\chi N k/(N-k) > 0$ and some suitably chosen constant $C[\bar{\rho}]$. Indeed, by radiality and monotonicity, $\operatorname{supp}(\bar{\rho}) = B(0,R)$ for some $R \in (0,\infty]$ and by the same arguments as in Corollary 2.5 leading to (2.11), we obtain

$$\bar{\rho}(x)^{-k/N} = A W_k * \bar{\rho}(x) + C[\bar{\rho}], \quad a.e.\ x \in B(0,R).$$

Assume $\bar{\rho}$ has compact support, $R < \infty$. It then follows from Lemma 4.1 that the left-hand side is bounded above,

$$\bar{\rho}(x)^{-k/N} \leqslant \eta A I_k[\bar{\rho}] + \frac{\eta A R^k}{k} + C[\bar{\rho}], \quad a.e.\ x \in B(0,R).$$

By continuity, $\rho(x) \to 0$ as $|x| \to R$, but then $\rho(x)^{-k/N}$ diverges, contradicting the bound from above. We must therefore have $R = \infty$, which concludes the proof of (4.38).
Next, taking the limit $x \to 0$ in (4.38) yields

$$A I_k[\bar{\rho}] + C[\bar{\rho}] > 0.$$

We then have from Lemma 4.1 for a.e. $x \in \mathbb{R}^N$,

$$0 \leqslant \left(A\,\eta \left(\frac{|x|^k}{k} + I_k[\bar{\rho}]\right) + C[\bar{\rho}]\right)^{-N/k} \leqslant \bar{\rho}(x).$$

However, the lower bound in the estimate above is not integrable on $\mathbb{R}^N$, and hence $\bar{\rho} \notin L^1\left(\mathbb{R}^N\right)$. This contradicts $\bar{\rho} \in \mathcal{X}$. □

In the fast diffusion regime, we do not have a suitable HLS-type inequality to show boundedness of the energy functional $\mathcal{F}_k$. Although we do not know whether $\mathcal{F}_k$ is bounded below or not, we can show that the infimum is not achieved in the radial setting.

Theorem 4.3 (Non-Existence of Global Minimisers). *Let $k \in (0, N)$. For any $\chi > 0$, there are no radially symmetric non-increasing global minimisers of $\mathcal{F}_k$ over $\mathcal{Y}_k$.*

Proof. Let ρ be a global minimiser of $\mathcal{F}_k$ over $\mathcal{Y}_k$. Following the same argument as in Proposition 3.6, we obtain

$$\rho(x)^{-k/N} = A(W_k * \rho)(x) + D_k[\rho] \quad \text{a.e. in supp}\,(\rho)\,, \tag{4.39}$$

$$\rho(x)^{-k/N} \geqslant A(W_k * \rho)(x) + D_k[\rho] \quad \text{a.e. in}\,\mathbb{R}^N\,. \tag{4.40}$$

where

$$D_k[\rho] := -\frac{2Nk}{(N-k)}\mathcal{F}_k[\rho] - \left(\frac{N+k}{N-k}\right)\int_{\mathbb{R}^N} \bar{\rho}^m(x)\,dx\,.$$

Since W_k is continuous and $\rho \in L^1\left(\mathbb{R}^N\right)$, it follows from (4.39) that ρ is continuous inside its support, being a continuous function of W_k convolved with ρ. If ρ is radially symmetric non-increasing, then supp $(\rho) = B(0, R)$ for some $R \in (0, \infty]$. By continuity of ρ at the origin, we can take the limit $|x| \to 0$ in (4.39) to obtain $AI_k[\rho] + D_k[\rho] > 0$. It then follows from (4.40) and (4.37) that in fact $\rho(x)^{-k/N} > 0$ for a.e. $x \in \mathbb{R}^N$. Hence, we conclude that supp $(\rho) = \mathbb{R}^N$. The Euler-Lagrange condition (4.39) and estimate (4.37) yield

$$\rho(x) = \left(A\,(W_k * \rho)(x) + D_k[\rho]\right)^{-N/k} \geqslant \left(A\,\eta\,\left(\frac{|x|^k}{k} + I_k[\rho]\right) + D_k[\rho]\right)^{-N/k}$$

a.e. on $\mathbb{R}^N$. Again, the right-hand side is not integrable for any $k \in (0, N)$ and hence $\rho \notin \mathcal{Y}_k$. □

4.2 Results in rescaled variables

Corollary 4.4 (Necessary Condition for Stationary States). *Let $k \in (0, N)$, $\chi > 0$ and $\bar{\rho} \in \mathcal{X}$. If $\bar{\rho}$ is a radially symmetric non-increasing stationary state of the rescaled equation (2.7) with bounded kth moment, then $\bar{\rho}$ is continuous, supported on $\mathbb{R}^N$ and satisfies*

$$\bar{\rho}(x) = \left(A(W_k * \bar{\rho})(x) + B|x|^2 + C[\bar{\rho}]\right)^{-N/k}, \quad a.e.\ x \in \mathbb{R}^N\,. \tag{4.41}$$

Here, the constant $C[\bar{\rho}]$ is chosen such that $\bar{\rho}$ integrates to one and

$$A := 2\chi\frac{Nk}{(N-k)} > 0, \quad B := \frac{Nk}{2(N-k)} > 0. \tag{4.42}$$

Proof. Continuity follows from Lemma 2.4, and we can show supp $(\bar{\rho}) = \mathbb{R}^N$ and (4.41) by a similar argument as for (4.38). □

From the above analysis, if diffusion is too fast, then there are no stationary states to the rescaled equation (2.7):

Theorem 4.5 (Non-Existence of Stationary States)**.** *Let $\chi > 0$, $N \geqslant 3$ and $k \in [2, N)$, then there are no radially symmetric non-increasing stationary states in $\mathcal{X}$ with kth moment bounded to the rescaled equation (2.7).*

Proof. Assume $\bar{\rho} \in \mathcal{X}$ is a radially symmetric non-increasing stationary state such that $|x|^k \bar{\rho} \in L^1\left(\mathbb{R}^N\right)$. It follows from (4.41) and (4.37) that

$$\bar{\rho}(x) \geqslant \left(A\,\eta\left(\frac{|x|^k}{k} + I_k[\bar{\rho}]\right) + B|x|^2 + C[\bar{\rho}]\right)^{-N/k}.$$

However, the lower bound is not integrable on $\mathbb{R}^N$ for $k \geqslant 2$, contradicting $\bar{\rho} \in L^1\left(\mathbb{R}^N\right)$. □

Remark 4.6. *Condition (4.41) tells us that radially symmetric non-increasing stationary states have so-called fat tails for large $r = |x|$. More precisely, Lemma 4.1 shows they behave at least like r^{-N} for large r if $k \geqslant 2$, whereas $\bar{\rho}(r) \sim r^{-2N/k}$ for large $r > 0$ and for $k < 2$. This means there is a critical $k_* := 2$ and respectively a critical diffusion exponent $m_* := 1 - 2/N$ where a change of behaviour occurs.*

For $k < k_*$, radially symmetric non-increasing stationary states, if they exist, are integrable and mass is preserved. This restriction on k corresponds exactly to the well-known classical fast diffusion regime $m > m_*$ in the case $\chi = 0$ [287], where mass escapes to the far field but is still preserved. In our case, the behaviour of the tails is dominated by the non-linear diffusion effects even for $\chi > 0$ as for the classical fast-diffusion equation when $m > m_*$.

If diffusion is 'too fast', i.e. $k > k_*$ and $m < m_*$, then no radially symmetric non-increasing stationary states of the rescaled equation (2.7) exist as stated in Theorem 4.5. It is well known that mass escapes to infinity in the case of the classical fast diffusion equation ($\chi = 0$) and integrable L^∞-solutions go extinct in finite time (for a detailed explanation of this phenomenon, see [287, Chapter 5.5]). It would be interesting to explore this in our case.

Remark 4.7. *If $N \geqslant 2$ and $k \in [K, 2)$ with*

$$K(N) := -\frac{N}{2} + \sqrt{\frac{N^2}{4} + 2N} \quad \in [1, 2)\,, \tag{4.43}$$

then radially symmetric non-increasing solutions $\bar{\rho} \in \mathcal{X}$ to equation (4.41) have unbounded kth moment. Indeed, assuming for a contradiction that $|x|^k \bar{\rho} \in L^1\left(\mathbb{R}^N\right)$. It then follows from (4.41) and (4.37) that

$$|x|^k \bar{\rho}(x) \geqslant |x|^k \left(A\,\eta\left(\frac{|x|^k}{k} + I_k[\bar{\rho}]\right) + B|x|^2 + C[\bar{\rho}]\right)^{-N/k}$$

a.e. on $\mathbb{R}^N$, and the right-hand side is integrable only in the region $k^2 + Nk - 2N < 0$. This condition yields (4.43).

Proposition 4.8 (Necessary Condition for Global Minimisers). *For $k \in (0, N)$, let ρ be a global minimiser of $\mathcal{F}_{k,\textbf{resc}}$ in $\mathcal{Y}_{2,k}$. Then for any $\chi > 0$, ρ is continuous inside its support and satisfies*

$$\rho(x)^{-k/N} = A(W_k * \rho)(x) + B|x|^2 + D_{k,\textbf{resc}}[\rho] \quad \text{a.e. in supp } (\rho)\,, \tag{4.44}$$

$$\rho(x)^{-k/N} \geqslant A(W_k * \rho)(x) + B|x|^2 + D_{k,\textbf{resc}}[\rho] \quad \text{a.e. in } \mathbb{R}^N\,. \tag{4.45}$$

Here, constants A, B are given by (4.42) and

$$D_{k,\textbf{resc}}[\rho] := -4B\mathcal{F}_{k,\textbf{resc}}[\rho] + B\mathcal{V}[\rho] - \left(\frac{N+k}{N-k}\right)\int_{\mathbb{R}^N} \bar{\rho}^m(x)\,dx\,.$$

Moreover, radially symmetric non-increasing global minimisers in $\mathcal{Y}_{2,k}$ are supported on the whole space, and so in that case (4.44) holds true in $\mathbb{R}^N$.

Proof. The proof of (4.44) and (4.45) follows analogously to Proposition 3.6. Further, since W_k is continuous and $\rho \in L^1\left(\mathbb{R}^N\right)$, it follows from (4.44) that ρ is continuous inside its support being a continuous function of the convolution between W_k and ρ. Now, if ρ is radially symmetric non-increasing, we argue as for Theorem 4.3 to conclude that supp $(\rho) = \mathbb{R}^N$. □

Remark 4.9. *Just like (4.41), condition (4.44) provides the behaviour of the tails for radially symmetric non-increasing global minimisers of $\mathcal{F}_{k,\textbf{resc}}$ using the bounds in Lemma 4.1. In particular, they have unbounded kth moment for any $\chi > 0$ if $k \geqslant K$ with K given by (4.43), and they are not integrable for $k > k_* := 2$. Further, their second moment is bounded and $\rho^m \in L^1\left(\mathbb{R}^N\right)$ if and only if $k < 2N/(2+N)$. Note that*

$$\frac{2N}{2+N} < K(N) < k_*\,.$$

Hence, radially symmetric non-increasing global minimisers with finite energy $\mathcal{F}_{k,\textbf{resc}}[\rho] < \infty$ can only exist in the range $0 < k < 2N/(2+N)$. For $k \geqslant \frac{2N}{2+N}$, one may have to work with relative entropies instead.

Apart from the Euler-Lagrange condition above, we have very little information about global minimisers of $\mathcal{F}_{k,\textbf{resc}}$ in general, and it is not known in general if solutions to (4.44)-(4.45) exist. Thus, we use a different approach here than in the porous medium regime, showing existence of stationary states to (2.7) directly by a compactness argument. Let us define the set

$$\bar{\mathcal{X}} := \left\{\rho \in C(\mathbb{R}^N) \cap \mathcal{X} : \int |x|^k \rho(x)\,dx < \infty\,,\ \rho^{\#} = \rho\,,\ \lim_{r\to\infty} \rho(r) = 0\right\}\,,$$

where $\rho^{\#}$ denotes the symmetric decreasing rearrangement of ρ.

Theorem 4.10 (Existence of Stationary States). *Let $\chi > 0$ and $k \in (0, 1] \cap (0, N)$. Then there exists a stationary state $\bar{\rho} \in \bar{\mathcal{X}}$ for the rescaled system (2.7).*

Here, decay at infinity of the equilibrium distribution is a property we gain automatically thanks to the properties of the equation, but we choose to include it here a priori.

Proof. Corollary 4.4 suggests that we are looking for a fixed point of the operator $T : \mathcal{X} \to \mathcal{X}$,

$$T\rho(x) := \left(A(W_k * \rho)(x) + B|x|^2 + C\right)^{-N/k} .$$

For this operator to be well-defined, we need to be able to choose a constant $C = C[\rho]$ such that $\int_{\mathbb{R}} T\rho(x)\,dx = 1$. To show that this is indeed the case, let us define for any $\alpha > 0$,

$$w(\alpha) := \int_{\mathbb{R}^N} \left(\alpha + A\frac{|x|^k}{k} + B|x|^2\right)^{-N/k} dx\,, \qquad W(\alpha) := \int_{\mathbb{R}^N} \left(\alpha + B|x|^2\right)^{-N/k} dx\,.$$

Note that w and W are finite and well-defined since $k < 2$. Furthermore, both w and W are continuous, strictly decreasing to zero as α increases, and blow-up at $\alpha = 0$. Hence, we can take inverses $\underline{\delta} := w^{-1}(1) > 0$ and $\overline{\delta} := W^{-1}(1) > 0$. Here is where we use the condition $k \leqslant 1$ as this means $\eta = 1$ in Lemma 4.1 (see also Remark 4.11). Fixing some $\rho \in \bar{\mathcal{X}}$ and denoting by $M(\rho, C)$ the mass of $T\rho$, we obtain from Lemma 4.1,

$$M\left(\rho, \underline{\delta} - AI_k[\rho]\right) \geqslant 1\,, \qquad M\left(\rho, \overline{\delta} - AI_k[\rho]\right) \leqslant 1\,.$$

Since $M(\rho, \cdot)$ is continuous and strictly decreasing on the interval $\left[\underline{\delta} - AI_k[\rho], \overline{\delta} - AI_k[\rho]\right]$, we conclude that there exists $C[\rho]$ with $\underline{\delta} - AI_k[\rho] \leqslant C[\rho] \leqslant \overline{\delta} - AI_k[\rho]$ and $M(\rho, C[\rho]) = 1$. From Lemma 4.1, we obtain for all $x \in \mathbb{R}^N$,

$$\left(AI_k[\rho] + C[\rho] + A\frac{|x|^k}{k} + B|x|^2\right)^{-N/k} \leqslant T\rho(x) \leqslant \left(AI_k[\rho] + C[\rho] + B|x|^2\right)^{-N/k},$$

and integrating over $\mathbb{R}^N$,

$$w\left(AI_k[\rho] + C[\rho]\right) \leqslant 1 \leqslant W\left(AI_k[\rho] + C[\rho]\right)\,, \tag{4.46}$$

implying

$$0 < \underline{\delta} \leqslant AI_k[\rho] + C[\rho] \leqslant \overline{\delta} < \infty. \tag{4.47}$$

As a consequence, we have a pointwise estimate for $T\rho$,

$$m(x) \leqslant T\rho(x) \leqslant M(x), \tag{4.48}$$

where we define

$$m(x) := \left(\overline{\delta} + A\frac{|x|^k}{k} + B|x|^2\right)^{-N/k}, \qquad M(x) := \left(\underline{\delta} + B|x|^2\right)^{-N/k}. \tag{4.49}$$

We are now ready to look for a fixed point of T. Applying T to $\bar{\mathcal{X}}$, we are able to make use of a variant of the Arzéla-Ascoli Theorem to obtain compactness. The key ingredients are the bounds in Lemma 4.1 and the uniform estimate (4.47) since they allow us to derive the pointwise estimate (4.48), which gives decay at infinity and uniform boundedness of $T\rho$:

$$T\rho(x) \leqslant \left(\underline{\delta} + B|x|^2\right)^{-N/k} \leqslant \min\left\{B^{-N/k}\,|x|^{-2N/k},\, \underline{\delta}^{-N/k}\right\}. \tag{4.50}$$

Further, we claim $T\rho$ is k-Hölder continuous on compact balls $K_R := \overline{B(0,R)} \subset \mathbb{R}^N$, $R > 0$,

$$|T\rho(x_1) - T\rho(x_2)| \leqslant C_{R,N,k}\,|x_1 - x_2|^k, \tag{4.51}$$

with k-Hölder semi-norm

$$C_{R,N,k} := [T\rho(\cdot)]_{C^{0,k}} = \frac{N}{k}\,\underline{\delta}^{-(1+N/k)}\left(\frac{A}{k} + 3BR^{2-k}\right) > 0\,. \tag{4.52}$$

To see this, let $G(x) := A(W_k * \rho)(x) + B|x|^2 + C[\rho]$ and $u(G) := G^{-N/k}$ so that we can write

$$\begin{aligned}|T\rho(x_1) - T\rho(x_2)| = |G(x_1)^{-N/k} - G(x_2)^{-N/k}| &\leqslant \mathrm{Lip}\,(u)\,|G(x_1) - G(x_2)| \\ &\leqslant \mathrm{Lip}\,(u)\left(A\,[W_k * \rho]_{C^{0,k}} + B\left[|\cdot|^2\right]_{C^{0,k}}\right)|x_1 - x_2|^k,\end{aligned}$$

where $\mathrm{Lip}(\cdot)$ denotes the Lipschitz constant on a suitable domain specified below. Indeed, $G(x)$ satisfies the inequality $0 < \underline{\delta} \leqslant G(x) \leqslant A\frac{|x|^k}{k} + B|x|^2 + \overline{\delta}$ for all $x \in \mathbb{R}^N$ by (4.37) and (4.47). Moreover, G is k-Hölder continuous:

$$\begin{aligned}|(W_k * \rho)(x_1) - (W_k * \rho)(x_2)| &= \frac{1}{k}\int_{\mathbb{R}^N} \left||x_1 - y|^k - |x_2 - y|^k\right| \rho(y)\,dy \\ &\leqslant \frac{|x_1 - x_2|^k}{k}\,2^{k-1} \leqslant \frac{|x_1 - x_2|^k}{k}\end{aligned}$$

and hence $[W_k * \rho]_{C^{0,k}} \leqslant 1/k$ uniformly. Further, the k-Hölder semi-norm of $|x|^2$ is bounded by $3R^{2-k}$ on K_R: for $x, y \in K_R$, $x \neq y$ and $z := x - y$, we have for $|z| \leqslant R$,

$$\frac{\left||x|^2 - |y|^2\right|}{|x - y|^k} \leqslant \frac{|z|^2 + 2|z|\min\{|x|, |y|\}}{|z|^k} \leqslant 3R|z|^{1-k} \leqslant 3R^{2-k},$$

and similarly for $|z| \geqslant R$,

$$\frac{\left||x|^2 - |y|^2\right|}{|x - y|^k} \leqslant \frac{2R^2}{R^k} = 2R^{2-k},$$

and so $\left[|\cdot|^2\right]_{C^{0,k}} \leqslant 3R^{2-k}$. We are left to estimate the Lipschitz coefficient $\mathrm{Lip}\,(u)$ for $G \in [\underline{\delta}, \infty)$. Indeed, we can calculate it explicitly using the mean value theorem,

$$|u(G_1) - u(G_2)| \leqslant \left(\max_{\xi \in [\underline{\delta}, \infty)} |u'(\xi)|\right)|G_1 - G_2|,$$

and so we have

$$\mathrm{Lip}\,(u) \leqslant \max_{\xi \in [\underline{\delta}, \infty)} |u'(\xi)| = \frac{N}{k}\underline{\delta}^{-(1+N/k)}.$$

This concludes the proof of Hölder continuity of $T\rho$ on K_R, (4.51)-(4.52). Since $\int_{\mathbb{R}^N} |x|^k M(x)\,dx < \infty$ if $k \in (0, 1]$, it follows from (4.48) that $T\rho$ has bounded kth moment. Together with the estimate of the tails (4.50), we have indeed $T\bar{\mathcal{X}} \subset \bar{\mathcal{X}}$, and so T is well-defined. We conclude that the operator $T : \bar{\mathcal{X}} \to \bar{\mathcal{X}}$ is compact by a variant of the Arzéla-Ascoli Theorem using uniform decay at infinity and uniform boundedness (4.50) together with equi-Hölder-continuity (4.51). Continuity of the map $T : \bar{\mathcal{X}} \to \bar{\mathcal{X}}$ can be analogously checked since the convolution with

W_k is a continuous map from $\bar{\mathcal{X}}$ to $C(\mathbb{R}^N)$ together with a similar argument as before for the Hölder continuity of $T\rho$. Additionally, we use that $C[\rho]$ is continuous in terms of ρ as $M(\rho, C)$, the mass of $T\rho$, is a continuous function in terms of both ρ and C and strictly decreasing in terms of C, and hence $C[\rho] = M^{-1}(\rho, 1)$ is continuous in terms of ρ. Here, $M^{-1}(\rho, \cdot)$ denotes the inverse of $M(\rho, \cdot)$.

Finally, by Schauder's fixed point theorem there exists $\bar{\rho} \in \bar{\mathcal{X}}$ such that $T\bar{\rho} = \bar{\rho}$. In other words, $\bar{\rho}$ satisfies relation (4.41) on $\mathbb{R}^N$. By continuity and radial monotonicity, we further have $\bar{\rho} \in L^\infty(\mathbb{R}^N)$ from which we deduce the required regularity properties using $\operatorname{supp}(\bar{\rho}) = \mathbb{R}^N$ and Lemma 2.2. We conclude that $\bar{\rho}$ is a stationary state of the rescaled equation according to Definition 2.3. □

Remark 4.11. *Note that the restriction $k \leqslant 1$ in the statement of Theorem 4.10 arises from Lemma 4.1 as we need the upper and lower bounds in (4.37) to scale with the same factor ($\eta = 1$). By Corollary 4.4, this restriction on k also means that we are in the range where stationary states have bounded kth moment since $((0,1] \cap (0,N)) \subset (0,K)$. To see why this is the case, let us take any $k \in (0,K)$ and so $\eta \geqslant 1$. Applying Lemma 4.1 to $T\rho(x)$ and integrating over $\mathbb{R}^N$ then gives*

$$w_\eta\left(\eta A I_k[\rho] + C[\rho]\right) \leqslant 1 \leqslant W\left(A I_k[\rho] + C[\rho]\right)$$

instead of (4.46), with

$$w_\eta(\alpha) := \int_{\mathbb{R}^N} \left(\alpha + \eta A \frac{|x|^k}{k} + B|x|^2\right)^{-N/k} dx\,.$$

Taking inverses, we conclude

$$\underline{\delta}_\eta \leqslant \eta A I_k[\rho] + C[\rho]\,, \qquad A I_k[\rho] + C[\rho] \leqslant \overline{\delta} \tag{4.53}$$

for $\underline{\delta}_\eta := w_\eta^{-1}(1)$ and for $\eta \geqslant 1$. This is where $\eta = 1$ becomes necessary in order to conclude for the pointwise estimate (4.48).

If the constant $C[\rho]$ is non-negative however, we can go a bit further and remove the condition $k \leqslant 1$ whilst still recovering a pointwise estimate on $T\rho$. More precisely, if $C[\rho] \geqslant 0$, then we obtain from (4.53) for any $k \in (0,K)$

$$0 < \frac{\underline{\delta}_\eta}{\eta} \leqslant A I_k[\rho] + C[\rho] \leqslant \overline{\delta}\,.$$

Instead of (4.48), we get

$$m_\eta(x) \leqslant T\rho(x) \leqslant M_\eta(x)$$

with

$$m_\eta(x) := \left(\eta\overline{\delta} + A\frac{|x|^k}{k} + B|x|^2\right)^{-N/k}, \qquad M_\eta(x) := \left(\frac{\underline{\delta}_\eta}{\eta} + B|x|^2\right)^{-N/k}.$$

However, firstly, the sign of $C[\rho]$ depends on the kth moment $I_k[\rho]$, and secondly, knowing a priori that $C[\rho] \geqslant 0$ implies $C[T\rho] \geqslant 0$ for all $\rho \in \bar{\mathcal{X}}$ is complicated, see Remark 4.12.

Remark 4.12. *Both $C[\rho] < 0$ and $C[\rho] \geqslant 0$ are possible for $\rho \in \bar{\mathcal{X}}$ and $k \in (0, K)$, depending on the kth moment of ρ. More precisely, $C[\rho]$ is defined as the value in the interval $\left[\underline{\delta}_\eta - \eta A I_k[\rho], \overline{\delta} - A I_k[\rho]\right]$ such that $M(\rho, C[\rho]) = 1$. Hence, we have*

$$I_k[\rho] \leqslant \underline{\delta}_\eta/(\eta A) \quad \Longrightarrow \quad C[\rho] \geqslant 0\,,$$
$$I_k[\rho] > \overline{\delta}/A \quad \Longrightarrow \quad C[\rho] < 0\,.$$

Remark 4.13. *Having established existence of radially symmetric stationary states to the rescaled equation (2.7), it is a natural question to ask whether these stationary states correspond to minimisers of the rescaled free energy functional $\mathcal{F}_{k,\mathit{resc}}$. For a stationary state $\bar{\rho}$ to have finite energy, we require in addition $\mathcal{V}[\bar{\rho}] < \infty$, $\bar{\rho}^m \in L^1\left(\mathbb{R}^N\right)$ and $|x|^k \bar{\rho} \in L^1\left(\mathbb{R}^N\right)$, in which case $\bar{\rho} \in \mathcal{Y}_{2,k}$. As noted in Remark 4.9, this is true if and only if $0 < k < \frac{2N}{2+N}$. This restriction corresponds to $\frac{N}{2+N} < m < 1$ and coincides with the regime of the fast diffusion equation ($\chi = 0$) where the Barenblatt profile has second moment bounded and its mth power is integrable [47].*

Remark 4.14. *In particular, the non-existence result in original variables Theorem 4.3 means that there is no interaction strengths χ for which the energy functional $\mathcal{F}_k$ admits radially symmetric non-increasing global minimisers. In this sense, there is no critical χ_c for $k > 0$ as it is the case in the porous medium regime. Existence of global minimisers for the rescaled free energy functional $\mathcal{F}_{k,\mathit{resc}}$ for all $\chi > 0$ would provide a full proof of non-criticality in the fast diffusion range and is still an open problem for arbitrary dimensions N. We suspect that $\mathcal{F}_{k,\mathit{resc}}$ is bounded below. In one dimension, one can establish equivalence between stationary states of the rescaled equation (2.7) and global minimisers of $\mathcal{F}_{k,\mathit{resc}}$ by completely different methods, proving a type of reversed HLS inequality, see Chapter 3. The non-existence of a critical parameter χ is a very interesting phenomenon, which has already been observed in [116] for the one-dimensional limit case $k = 1$, $m = 0$.*

4.3 Numerical simulations in one dimension

To illustrate our analysis of the fast diffusion regime, we present numerical simulations in one dimension. We use a Jordan–Kinderlehrer–Otto (JKO) steepest descent scheme [195, 248] which was proposed in [36] for the logarithmic case $k = 0$, and generalised to the porous-medium case $k \in (-1, 0)$ in [67]. It corresponds to a standard implicit Euler method for the pseudoinverse of the cumulative distribution function, where the solution at each time step of the non-linear system of equations is obtained by an iterative Newton-Raphson procedure. It can easily be extended to rescaled variables and works just in the same way in the fast diffusion regime $k \in (0, 1)$.

Our simulations show that solutions in scaled variables for $k \in (0, 1)$ converge always to a stationary state suggesting the existence of stationary states as discussed in the previous subsection.

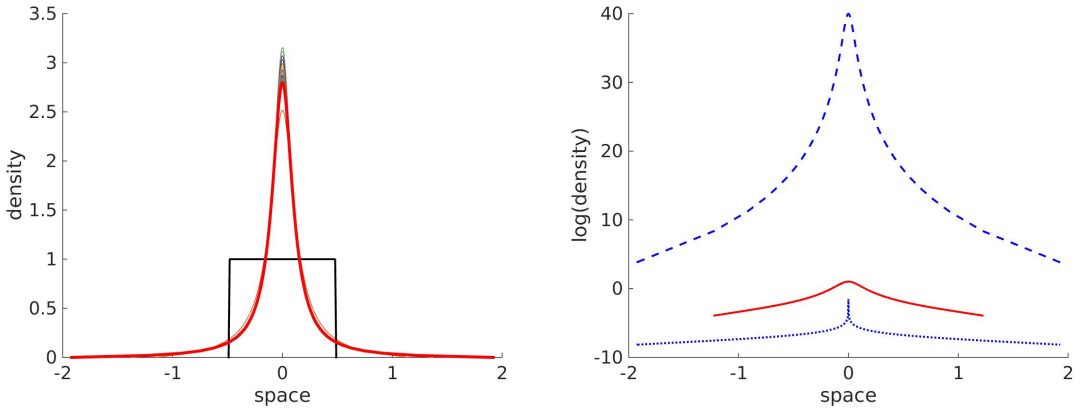

(a) (b)

Figure 2.1: Parameter choices: $\chi = 1.2$, $k = 0.2$. (a) Density distribution in rescaled variables: As initial data (black) we chose a characteristic supported on the centred ball of radius $1/2$, which can be seen to converge to the stationary state $\bar{\rho}$ (red); (b) Logplot of the density including bounds $m(x)$ (dotted blue) and $M(x)$ (dashed blue) as given in (4.48).

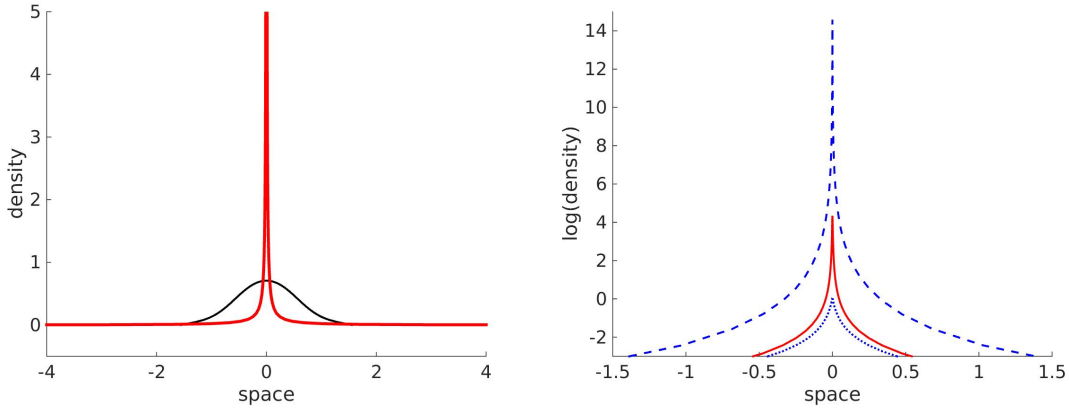

(a) (b)

Figure 2.2: Parameter choices: $\chi = 0.8$, $k = 0.95$. (a) Density distribution in rescaled variables: As initial data (black) we chose a centred Gaussian distribution, which can be seen to converge to the stationary state $\bar{\rho}$ (red) - here, $\bar{\rho}$ is more peaked as k is closer to 1 and so we only display the lower part of the density plot ($\max_{x\in\mathbb{R}} \bar{\rho}(x) = 75.7474$); (b) Logplot of the density including bounds $m(x)$ (dotted blue) and $M(x)$ (dashed blue) as given in (4.48).

Using the numerical scheme, we can do a quality check of the upper and lower bounds derived in (4.48) for stationary states in $\bar{\mathcal{X}}$:

$$m(x) \leqslant \bar{\rho}(x) \leqslant M(x)$$

with $m(x)$ and $M(x)$ given by (4.49). Figures 2.1 and 2.2 show numerical results at two different points in the (k, χ)-parameter space. For a more detailed description of the numerical scheme and a comprehensive list of numerical results, see Chapter 3.

A Appendix: Properties of ψ_k

We are here investigating in more detail the properties of the mean-field potential gradient for global minimisers in the porous medium regime. In more than one dimension, it can be expressed in terms of hypergeometric functions. Their properties are well understood and allow us to analyse the regularity properties of global minimisers. Since global minimisers of $\mathcal{F}_k$ and $\mathcal{F}_{k,\mathbf{resc}}$ are radially symmetric by Proposition 3.6, the aim is here to find the radial formulation of ∇S_k defined in (1.3). In one dimension, explicit expressions are available, and so we are assuming from now on that $N \geqslant 2$. There are three different cases: (1) The Newtonian case $k = 2-N$ with $N \geqslant 3$, (2) the range $1-N < k < 0$, $k \neq 2-N$ where $\nabla(W_k * \rho)$ is well defined, and (3) the singular range $-N < k \leqslant 1-N$ where the force field is given by a Cauchy principle value.

(1) In the Newtonian case $k = 2-N$, we have an explicit formula for the radial derivative of the force field using Newton's Shell Theorem,

$$\partial_r \left(W_{2-N} * \rho\right)(r) = M(r) r^{1-N}\,,$$

where $M(r) = \sigma_N \int_0^r \rho(s) s^{N-1}\, ds$ is the mass of ρ in a ball of radius r. Hence, we can write

$$\partial_r (W_{2-N} * \rho)(r) = r^{1-N} \int_0^\infty \psi_{2-N}\left(\frac{\eta}{r}\right) \rho(\eta) \eta^{N-1}\, \mathrm{d}\eta$$

where ψ_{2-N} is defined to have a jump singularity at $s = 1$,

$$\psi_{2-N}(s) := \begin{cases} 1 & \text{if} \quad 0 \leqslant s < 1\,, \\ 0 & \text{if} \quad s > 1\,. \end{cases} \tag{A.54}$$

(2) In the range $1-N < k < 0$ and $k \neq 2-N$, the mean-field potential gradient is given by

$$\begin{aligned} \nabla S_k(x) := \nabla(W_k * \rho)(x) &= \int_{\mathbb{R}^N} \nabla W(x-y)\rho(y)\, \mathrm{d}y \\ &= \frac{1}{\sigma_N} \int_0^\infty \int_{\partial B(0,|y|)} \nabla W(x-y)\, \mathrm{d}\sigma(y) \rho(|y|)\, \mathrm{d}|y|\,. \end{aligned}$$

Denoting $|y| = \eta$, we can write for $x = re_1$,

$$\begin{aligned} \frac{1}{\sigma_N} \int_{\partial B(0,|y|)} \nabla W(x-y)\, \mathrm{d}\sigma(y) &= \frac{1}{\sigma_N} \int_{\partial B(0,|y|)} (x-y)|x-y|^{k-2}\, \mathrm{d}\sigma(y) \\ &= \left(\frac{1}{\sigma_N} \int_{\partial B(0,\eta)} e_1 \cdot (re_1 - y)|re_1 - y|^{k-2}\, \mathrm{d}\sigma(y)\right) \frac{x}{r} \\ &= \eta^{N-1} \left(\frac{1}{\sigma_N} \int_{\partial B(0,1)} (r - \eta e_1.z)|re_1 - \eta z|^{k-2}\, \mathrm{d}\sigma(z)\right) \frac{x}{r} \\ &= \eta^{N-1} r^{k-1} \psi_k\left(\frac{\eta}{r}\right) \frac{x}{r}\,, \end{aligned}$$

where

$$\psi_k(s) = \frac{1}{\sigma_N} \int_{\partial B(0,1)} (1 - se_1.z)|e_1 - sz|^{k-2} \, \mathrm{d}\sigma(z) \,, \qquad s \in [0,1) \cup (1,\infty) \,. \tag{A.55}$$

By radial symmetry,

$$\nabla(W_k * \rho)(x) = r^{k-1} \left(\int_0^\infty \psi_k\left(\frac{\eta}{r}\right) \rho(\eta) \eta^{N-1} \, \mathrm{d}\eta \right) \frac{x}{r} = \partial_r (W_k * \rho)(r) \frac{x}{r}$$

with

$$\partial_r (W_k * \rho)(r) = r^{k-1} \int_0^\infty \psi_k\left(\frac{\eta}{r}\right) \rho(\eta) \eta^{N-1} \, \mathrm{d}\eta \,. \tag{A.56}$$

(3) In the regime $-N < k \leqslant 1-N$ however, the derivative of the convolution with the interaction kernel is a singular integral, and in this case the force field is defined as

$$\begin{aligned} \nabla S_k &:= \int_{\mathbb{R}} \frac{x-y}{|x-y|^{2-k}} \left(\rho(y) - \rho(x)\right) \, dy \\ &= \lim_{\delta \to 0} \int_{|x-y|>\delta} \frac{x-y}{|x-y|^{2-k}} \rho(y) \, dy = \frac{x}{r} \partial_r S_k(r) \end{aligned}$$

with the radial component given by

$$\begin{aligned} \partial_r S_k(r) =& r^{k-1} \int_0^\infty \psi_k\left(\frac{\eta}{r}\right) \left(\rho(\eta) - \rho(r)\right) \eta^{N-1} \, d\eta \\ =& r^{k-1} \lim_{\delta \to 0} \int_{|r-\eta|>\delta} \psi_k\left(\frac{\eta}{r}\right) \rho(\eta) \eta^{N-1} \, d\eta \,, \end{aligned}$$

and ψ_k is given by (A.55) on $[0,1) \cup (1,\infty)$.

For any $-N < k < 0$ with $k \neq 2-N$, we can rewrite (A.55) as

$$\psi_k(s) = \frac{\sigma_{N-1}}{\sigma_N} \int_0^\pi (1 - s\cos(\theta)) \sin^{N-2}(\theta) A(s,\theta)^{k-2} \, d\theta \,, \qquad s \in [0,1) \cup (1,\infty) \tag{A.57}$$

with

$$A(s,\theta) = \left(1 + s^2 - 2s\cos(\theta)\right)^{1/2} \,.$$

It is useful to express ψ_k in terms of Gauss Hypergeometric Functions. The hypergeometric function $F(a,b;c;z)$ is defined as the power series

$$F(a,b;c;z) = \sum_{n=0}^{\infty} \frac{(a)_n (b)_n}{(c)_n} \frac{z^n}{n!} \tag{A.58}$$

for $|z| < 1$ and $a, b \in \mathbb{C}$, $c \in \mathbb{C} \backslash \{\mathbb{Z}^- \cup \{0\}\}$, see [4], where $(q)_n$ is the Pochhammer symbol defined for any $q > 0$, $n \in \mathbb{N}$ by

$$(q)_0 = 1, \qquad (q)_n = \frac{(n+q-1)!}{(q-1)!} \,.$$

We will here make use of its well known integral representation [4]

$$F(a,b;c;z) = \frac{\Gamma(c)}{\Gamma(b)\Gamma(c-b)} \int_0^1 t^{b-1} (1-t)^{c-b-1} (1-tz)^{-a} \, dt$$

for $c > b > 0$, $a > 0$ and $|z| < 1$. Moreover, if $c - a - b > 0$, then F is well defined at $z = 1$ and satisfies

$$F(a, b; c; 1) = \frac{\Gamma(c)\Gamma(c-a-b)}{\Gamma(c-a)\Gamma(c-b)}\,.$$

Otherwise, we have the limiting case discussed in [4]:

$$\lim_{z\to 1^-} \frac{F(a, b; c; z)}{(1-z)^{c-a-b}} = \frac{\Gamma(c)\Gamma(a+b-c)}{\Gamma(a)\Gamma(b)}\,, \qquad \text{if} \quad c-a-b<0\,. \tag{A.59}$$

Let us define

$$H(a, b; c; z) := \frac{\Gamma(b)\Gamma(c-b)}{\Gamma(c)} F(a, b; c; z)\,.$$

To express ψ_k as a combination of hypergeometric functions, we write

$$\begin{aligned}
\psi_k(s) =& \frac{\sigma_{N-1}}{\sigma_N} \int_0^\pi (1 - s\cos(\theta)) \left(1 + s^2 - 2s\cos(\theta)\right)^{\frac{k-2}{2}} \sin^{N-2}(\theta)\, d\theta \\
=& \frac{\sigma_{N-1}}{\sigma_N} (1+s)^{k-2} \int_0^\pi (1 - s\cos(\theta)) \left(1 - \frac{4s}{(1+s)^2}\cos^2\left(\frac{\theta}{2}\right)\right)^{\frac{k-2}{2}} \sin^{N-2}(\theta)\, d\theta \\
=& \frac{\sigma_{N-1}}{\sigma_N} (1+s)^{k-2} \int_0^\pi \left(1 - \frac{4s}{(1+s)^2}\cos^2\left(\frac{\theta}{2}\right)\right)^{\frac{k-2}{2}} \sin^{N-2}(\theta)\, d\theta \\
& - \frac{\sigma_{N-1}}{\sigma_N} (1+s)^{k-2}\, s \int_0^\pi \cos(\theta) \left(1 - \frac{4s}{(1+s)^2}\cos^2\left(\frac{\theta}{2}\right)\right)^{\frac{k-2}{2}} \sin^{N-2}(\theta)\, d\theta \\
=:& f_1(s) - f_2(s)\,.
\end{aligned}$$

Now, we use the change of variable $t = \cos^2(\theta/2)$ to get

$$\begin{aligned}
f_1(s) =& \frac{\sigma_{N-1}}{\sigma_N} (1+s)^{k-2} \int_0^\pi \left(1 - \frac{4s}{(1+s)^2}\cos^2\left(\frac{\theta}{2}\right)\right)^{\frac{k-2}{2}} \sin^{N-2}(\theta)\, d\theta \\
=& \frac{\sigma_{N-1}}{\sigma_N} (1+s)^{k-2}\, 2^{N-2} \int_0^1 \left(1 - \frac{4s}{(1+s)^2} t\right)^{\frac{k-2}{2}} t^{\frac{N-3}{2}} (1-t)^{\frac{N-3}{2}}\, dt \\
=& \frac{\sigma_{N-1}}{\sigma_N} (1+s)^{k-2}\, 2^{N-2} H\left(a, b_1; c_1; z\right)
\end{aligned}$$

with

$$a := 1 - \frac{k}{2}, \quad b_1 := \frac{N-1}{2}, \quad c_1 := N-1, \quad z := \frac{4s}{(1+s)^2}\,.$$

Let us define $h_1(s) := f_1(s)$, and

$$h_2(s) := \frac{\sigma_{N-1}}{\sigma_N} (1+s)^{k-2}\, 2^{N-2} H\left(a, b_2; c_2; z\right)$$

with

$$a := 1 - \frac{k}{2}, \quad b_2 := \frac{N-1}{2}, \quad c_2 := N-1, \quad z := \frac{4s}{(1+s)^2}\,.$$

Then

$$\begin{aligned}
f_2(s) =& \frac{\sigma_{N-1}}{\sigma_N} (1+s)^{k-2}\, s \int_0^\pi \cos(\theta) \left(1 - \frac{4s}{(1+s)^2}\cos^2\left(\frac{\theta}{2}\right)\right)^{\frac{k-2}{2}} \sin^{N-2}(\theta)\, d\theta \\
=& - s h_1(s) + 2 s h_2(s)
\end{aligned}$$

by the same change of variable. We conclude

$$\psi_k(s) = (1+s)h_1(s) - 2sh_2(s)\,, \qquad s \in [0,1) \cap (1,\infty)\,. \tag{A.60}$$

Let us now study the behaviour of ψ_k in more detail for $k \neq 2-N$. For any fixed $s \in [0,1) \cap (1,\infty)$,

$$|\psi_k(s)| \leqslant \frac{1}{\sigma_N} \int_{\partial B(0,1)} |e_1 - sx|^{k-1}\, d\sigma(x) < \infty$$

and by the dominated convergence theorem, it is easy to see that ψ_k is continuous on $s \in [0,1) \cap (1,\infty)$ for any $-N < k < 2-N$ and $2-N < k < 0$. A singularity occurs at $s = 1$ if $k < 2-N$, however this singularity is integrable in the range $1-N < k < 2-N$.

In order to handle the expression of the mean-field potential gradient, it is important to understand the behaviour of ψ_k at the limits of the integral 0 and ∞ as well as at the singularity $s = 1$.

Lemma A.1 (Behaviour at 0)**.** *For $\alpha > -1$, $-N < k < 0$ and small $s > 0$,*

$$\psi_k(s)s^\alpha = s^\alpha + O\left(s^{\alpha+1}\right)\,. \tag{A.61}$$

Proof. Following the same argument as in [138, Lemma 4.4], we obtain $\psi_k(0) = 1$ for any $-N < k < 0$, and so (A.61) follows. □

Similarly, extending the argument in [138, Lemma 4.4] to $-N < k < 0$, we have

Lemma A.2 (Behaviour at ∞)**.** *For $-N < k < 0$,*

$$\lim_{s\to\infty} s^{2-k}\psi_k(s) = \frac{N+k-2}{N}\,. \tag{A.62}$$

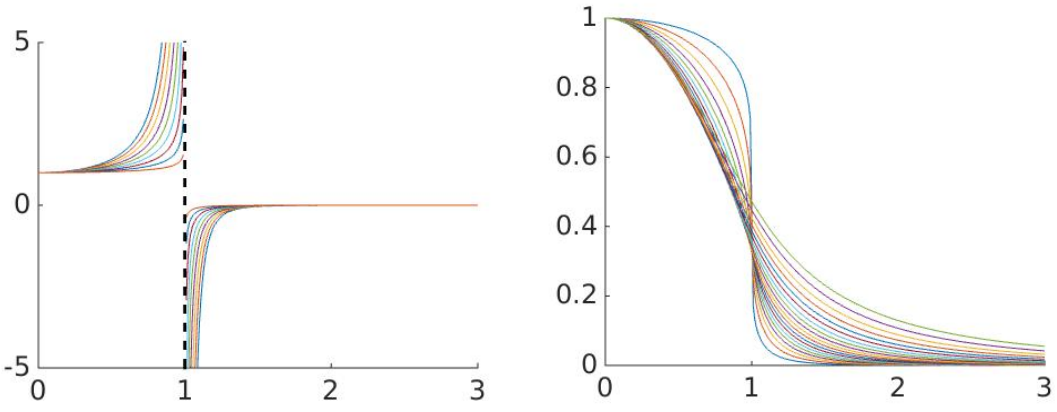

(a) (b)

Figure 2.3: ψ_k for different values of k with $N = 6$, increasing k by 0.2 for each plot: (a) $-N < k < 2-N$, (b) $2-N < k < 0$.

Further, it is obvious from (A.57) that $\psi_k(s) > 0$ for $s \in (0,1)$. From [138],

$$\psi_k'(s) = \left(\frac{\sigma_{N-1}}{\sigma_N}\right)\frac{(k-2)(N+k-2)}{(N-1)} s \int_0^\pi \sin^N(\theta) A(s,\theta)^{k-4}\, d\theta\,, \qquad s \in [0,1) \cap (1,\infty)$$

and hence ψ_k is strictly decreasing for $k > 2-N$ and strictly increasing for $k < 2-N$. It then follows from (A.62) that in the super-Newtonian regime $k > 2-N$, ψ_k converges to zero as $s \to \infty$, is finite and continuous at $s = 1$, and strictly positive on $[0,\infty)$ (Figure 2.3(b)). In the sub-Newtonian regime $-N < k < 2-N$ on the other hand, the monotonicity of ψ_k and the fact that ψ_k converges to 0 as $s \to \infty$ imply that

$$\lim_{s\to 1^-} \psi_k(s) = +\infty\,, \qquad \lim_{s\to 1^+} \psi_k(s) = -\infty\,,$$

and so we conclude that $\psi_k < 0$ on $(1,\infty)$ if $-N < k < 2-N$ (Figure 2.3(a)). We summarise these observations in the following lemma:

Lemma A.3 (Overall Behaviour). *Let ψ_k be as defined in (A.55).*

(i) If $2-N < k < 0$, then ψ_k is continuous, positive and strictly decreasing on $[0,\infty)$.

(ii) If $-N < k < 2-N$, then ψ_k is continuous, positive and strictly increasing on $[0,1)$, and it is continuous, negative and strictly increasing on $(1,\infty)$. Further, it has a singularity at $s = 1$ which is integrable for $1-N < k < 2-N$.

Using the hypergeometric function representation of ψ_k, we can characterise its behaviour near the singularity.

Lemma A.4 (Behaviour at 1). *For $\alpha \in \mathbb{R}$ and $\varepsilon > 0$ small, we have*

(1) in the super-Newtonian regime $2-N < k < 0$ and for $s = 1 \pm \varepsilon$:

$$\psi_k(s) s^\alpha = \psi_k(1) + O(\varepsilon)\,,$$

(2) in the sub-Newtonian regime $-N < k < 2-N$ and

(i) for $s = 1-\varepsilon$:

$$\psi_k(s)\, s^\alpha = K_1 \varepsilon^{N+k-2} + K_2 \varepsilon^{N+k-1} + O\left(\varepsilon^{N+k}\right)\,, \tag{A.63}$$

(ii) for $s = 1+\varepsilon$:

$$\psi_k(s)\, s^\alpha = -K_1 \varepsilon^{N+k-2} + K_3 \varepsilon^{N+k-1} + O\left(\varepsilon^{N+k}\right)\,, \tag{A.64}$$

where

$$K_1 = \left(\frac{\sigma_{N-1}}{\sigma_N}\right)\frac{\gamma}{2} > 0\,, \qquad K_2[\alpha] = -\left(\frac{\sigma_{N-1}}{\sigma_N}\right)\left(\frac{B_1+\gamma(1-N+2\alpha)}{4}\right), \tag{A.65}$$
$$K_3[\alpha] = -\left(\frac{\sigma_{N-1}}{\sigma_N}\right)\left(\frac{B_1+\gamma(2k+N-5+2\alpha)}{4}\right)$$

and

$$\gamma = \frac{\Gamma(c_2-b_2)\Gamma(a+b_2-c_2)}{\Gamma(a)} > 0\,. \tag{A.66}$$

Proof. (1) follows directly from the fact that ψ_k is continuous at $s=1$ [138, Lemma 4.4]. In order to prove (2), we make use of expression (A.60) for ψ_k in terms of hypergeometric functions and known expansions around the point of singularity. Denoting $\delta := \varepsilon/|2-\varepsilon| > 0$, we have for any $\beta > 0$,

$$\delta^\beta = \left(\frac{\varepsilon}{2}\right)^\beta + \beta\left(\frac{\varepsilon}{2}\right)^{\beta+1} + O\left(\varepsilon^{\beta+2}\right). \tag{A.67}$$

From (A.60) we can write

$$\psi_k(s) = (1+s)h_1(s) - 2sh_2(s) = (1+s)\left(h_1(s)-h_2(s)\right) + (1-s)h_2(s)\,,$$

and hence, denoting $z = 1-\delta^2$, we obtain for $s = 1-\varepsilon$:

$$\begin{aligned} 2^{2-N}\frac{\sigma_N}{\sigma_{N-1}}\psi_k(1-\varepsilon) &= (2-\varepsilon)^{k-1}\left(H\left(a,b_1;c_1;z\right) - H\left(a,b_2;c_2;z\right)\right) \\ &\quad + \varepsilon\,(2-\varepsilon)^{k-2}\,H\left(a,b_2;c_2;z\right) \\ &= (2-\varepsilon)^{k-1}\,\delta^{N+k-3}\left(\frac{H\left(a,b_1;c_1;z\right)}{(1-z)^{c_1-a-b_1}} - \frac{H\left(a,b_2;c_2;z\right)}{(1-z)^{c_2-a-b_2}}\right) \\ &\quad + \varepsilon\,(2-\varepsilon)^{k-2}\,\delta^{N+k-3}\left(\frac{H\left(a,b_2;c_2;z\right)}{(1-z)^{c_2-a-b_2}}\right). \end{aligned} \tag{A.68}$$

Similarly, above the singularity point at $s = 1+\varepsilon$, we obtain:

$$\begin{aligned} 2^{2-N}\frac{\sigma_N}{\sigma_{N-1}}\psi_k(1+\varepsilon) &= (2+\varepsilon)^{k-1}\,\delta^{N+k-3}\left(\frac{H\left(a,b_1;c_1;z\right)}{(1-z)^{c_1-a-b_1}} - \frac{H\left(a,b_2;c_2;z\right)}{(1-z)^{c_2-a-b_2}}\right) \\ &\quad - \varepsilon\,(2+\varepsilon)^{k-2}\,\delta^{N+k-3}\left(\frac{H\left(a,b_2;c_2;z\right)}{(1-z)^{c_2-a-b_2}}\right). \end{aligned} \tag{A.69}$$

Using the power series expression (A.58) for hypergeometric functions, we can write

$$\left(\frac{H\left(a,b_1;c_1;z\right)}{(1-z)^{c_1-a-b_1}} - \frac{H\left(a,b_2;c_2;z\right)}{(1-z)^{c_2-a-b_2}}\right) = \sum_{n=0}^{\infty} A_n\frac{z^n}{n!} = \sum_{m=0}^{\infty}\frac{(-1)^m B_m}{m!}\,\delta^{2m}\,,$$
$$B_m := \sum_{n=m}^{\infty}\frac{A_n}{(n-m)!}\,,$$
$$A_n := \left(\frac{(c_1-a)_n(c_1-b_1)_n}{(c_1)_n} - b_1\frac{(c_2-a)_n(c_2-b_2)_n}{(c_2)_n}\right)\frac{\Gamma(b_1)\Gamma(c_1-b_1)}{\Gamma(a)}\,.$$

In the singularity regime $-N < k < 2-N$, we have

$$c_1 - a - b_1 = c_2 - a - b_2 = \frac{N+k-3}{2} < 0\,,$$

and so we can make use of (A.59) to show that the leading order term vanishes:

$$\begin{aligned} B_0 &= \lim_{\delta\to 0}\sum_{m=0}^{\infty}\frac{(-1)^m B_m}{m!}\,\delta^{2m} = \lim_{z\to 1^-}\left(\frac{H\left(a,b_1;c_1;z\right)}{(1-z)^{c_1-a-b_1}} - \frac{H\left(a,b_2;c_2;z\right)}{(1-z)^{c_2-a-b_2}}\right) \\ &= \frac{\Gamma(c_1-b_1)\Gamma(a+b_1-c_1)}{\Gamma(a)} - \frac{\Gamma(c_2-b_2)\Gamma(a+b_2-c_2)}{\Gamma(a)} = 0\,. \end{aligned}$$

Hence

$$\begin{aligned} &\frac{H\left(a,b_1;c_1;z\right)}{(1-z)^{c_1-a-b_1}} - \frac{H\left(a,b_2;c_2;z\right)}{(1-z)^{c_2-a-b_2}} = -B_1\delta^2 + O(\delta^4)\,, \\ &\frac{H\left(a,b_2;c_2;z\right)}{(1-z)^{c_2-a-b_2}} = \frac{\Gamma(c_2-b_2)\Gamma(a+b_2-c_2)}{\Gamma(a)} + O\left(\delta^2\right) := \gamma + O\left(\delta^2\right)\,. \end{aligned}$$

Substituting these estimates and making use of (A.67), (A.68) becomes

$$\begin{aligned} 2^{2-N}\frac{\sigma_N}{\sigma_{N-1}}\psi_k(1-\varepsilon) =& \,\varepsilon\left(2-\varepsilon\right)^{k-2}\left(\gamma\delta^{N+k-3} + O\left(\delta^{N+k-1}\right)\right)\,, \\ &+ \left(2-\varepsilon\right)^{k-1}\left(-B_1\delta^{N+k-1} + O\left(\delta^{N+k+1}\right)\right) \\ =& \,\varepsilon\left[2^{k-2} - \varepsilon(k-2)2^{k-3} + O\left(\varepsilon^2\right)\right] \\ &\times\left[\gamma\left(\frac{\varepsilon}{2}\right)^{N+k-3} + \gamma\left(N+k-3\right)\left(\frac{\varepsilon}{2}\right)^{N+k-2} + O\left(\varepsilon^{N+k-1}\right)\right] \\ &+ \left[2^{k-1} + O\left(\varepsilon\right)\right]\left[-B_1\left(\frac{\varepsilon}{2}\right)^{N+k-1} + O\left(\varepsilon^{N+k}\right)\right] \\ =& \,\gamma 2^{-N+1}\varepsilon^{N+k-2} + \gamma 2^{-N}\left[(N+k-3) + (2-k)\right]\varepsilon^{N+k-1} \\ &- B_1 2^{-N}\varepsilon^{N+k-1} + O\left(\varepsilon^{N+k}\right) \\ =& \,\gamma 2^{-N+1}\varepsilon^{N+k-2} + 2^{-N}\left[\gamma\left(N-1\right) - B_1\right]\varepsilon^{N+k-1} + O\left(\varepsilon^{N+k}\right)\,. \end{aligned}$$

Similarly, (A.69) has expansion

$$\begin{aligned} 2^{2-N}\frac{\sigma_N}{\sigma_{N-1}}\psi_k(1+\varepsilon) =& -\varepsilon\left(2+\varepsilon\right)^{k-2}\left(\gamma\delta^{N+k-3} + O\left(\delta^{N+k-1}\right)\right)\,, \\ &+ \left(2+\varepsilon\right)^{k-1}\left(-B_1\delta^{N+k-1} + O\left(\delta^{N+k+1}\right)\right) \\ =& -\varepsilon\left[2^{k-2} + \varepsilon(k-2)2^{k-3} + O\left(\varepsilon^2\right)\right] \\ &\times\left[\gamma\left(\frac{\varepsilon}{2}\right)^{N+k-3} + \gamma\left(N+k-3\right)\left(\frac{\varepsilon}{2}\right)^{N+k-2} + O\left(\varepsilon^{N+k-1}\right)\right] \\ &+ \left[2^{k-1} + O\left(\varepsilon\right)\right]\left[-B_1\left(\frac{\varepsilon}{2}\right)^{N+k-1} + O\left(\varepsilon^{N+k}\right)\right] \\ =& -\gamma 2^{-N+1}\varepsilon^{N+k-2} + \gamma 2^{-N}\left[-\left(N+k-3\right) + (2-k)\right]\varepsilon^{N+k-1} \\ &- B_1 2^{-N}\varepsilon^{N+k-1} + O\left(\varepsilon^{N+k}\right) \\ =& -\gamma 2^{-N+1}\varepsilon^{N+k-2} + 2^{-N}\left[\gamma\left(5-N-2k\right) - B_1\right]\varepsilon^{N+k-1} + O\left(\varepsilon^{N+k}\right)\,. \end{aligned}$$

We conclude

$$\psi_k(1-\varepsilon) = \left(\frac{\sigma_{N-1}}{\sigma_N}\right)\left(\frac{\gamma}{2}\right)\varepsilon^{N+k-2} + \left(\frac{\sigma_{N-1}}{\sigma_N}\right)\left(\frac{\gamma\,(N-1)-B_1}{4}\right)\varepsilon^{N+k-1} + O\left(\varepsilon^{N+k}\right),$$

$$\psi_k(1+\varepsilon) = -\left(\frac{\sigma_{N-1}}{\sigma_N}\right)\left(\frac{\gamma}{2}\right)\varepsilon^{N+k-2} + \left(\frac{\sigma_{N-1}}{\sigma_N}\right)\left(\frac{\gamma\,(5-N-2k)-B_1}{4}\right)\varepsilon^{N+k-1} + O\left(\varepsilon^{N+k}\right),$$

and so (2)(i)-(ii) directly follow. □

Chapter 3

Asymptotics in the One-Dimensional Fair-Competition Regime

This chapter follows in most parts the article "The geometry of diffusing and self-attracting particles in a one-dimensional fair-competition regime" written in collaboration with Vincent Calvez[1] and José A. Carrillo[2], and to appear in "Nonlocal and Nonlinear Diffusions and Interactions: New Methods and Directions", volume 2186 of *Lecture Notes in Math.*, Springer.

Chapter Summary

We consider an aggregation-diffusion equation modelling particle interaction with nonlinear diffusion and non-local attractive interaction using a homogeneous kernel (singular and non-singular) leading to variants of the Keller–Segel model of chemotaxis. We analyse the *fair-competition regime* in which both homogeneities scale the same with respect to dilations. Our analysis here deals with the one-dimensional case, building on the work in Chapter 2, and provides an almost complete classification. In the singular kernel case and for critical interaction strength, we prove uniqueness of stationary states via a variant of the Hardy-Littlewood-Sobolev inequality. Using the same methods, we show uniqueness of self-similar profiles in the sub-critical case by proving a new type of functional inequality. Surprisingly, the same results hold true for any interaction strength in the non-singular kernel case. Further, we investigate the asymptotic behaviour of solutions, proving convergence to equilibrium in Wasserstein distance in the critical singular kernel case, and convergence to self-similarity for sub-critical interaction strength, both under a uniform stability condition. Moreover, solutions converge to a unique self-similar profile in the non-singular kernel case. Finally, we provide a numerical overview for the asymptotic behaviour of solutions in the full parameter space demonstrating the above results. We also discuss a number of phenomena appearing in the numerical explorations for the diffusion-dominated and attraction-dominated regimes.

[1]Unité de Mathématiques Pures et Appliquées, CNRS UMR 5669 and équipe-projet INRIA NUMED, École Normale Supérieure de Lyon, Lyon, France.

[2]Department of Mathematics, Imperial College London, South Kensington Campus, London SW7 2AZ, UK.

Chapter Content

Ati deka metua xo o.

One stick cannot build a house[3].

Ghanaian proverb (Ewe)

[3] In unity is strength, therefore, one should learn to work together with others.

1 Introduction

Mean field macroscopic models for interacting particle systems have been derived in the literature [245, 240] with the objective of explaining the large time behaviour, the qualitative properties and the stabilisation of systems composed by a large number of particles with competing effects such as repulsion and attraction between particles. They find natural applications in mathematical biology, gravitational collapse, granular media and self-assembly of nanoparticles, see [105, 196, 96, 282, 191, 207] and the references therein. These basic models start from particle dynamics in which their interaction is modelled via pairwise potentials. By assuming the right scaling between the typical interaction length and the number of particles per unit area one can obtain different mean field equations, see for instance [43]. In the mean-field scaling they lead to non-local equations with velocity fields obtained as an average force from a macroscopic density encoding both repulsion and attraction, see [39, 10] and the references therein. However, if the repulsion strength is very large at the origin, one can model repulsive effects by (non-linear) diffusion while attraction is considered via non-local long-range forces [240, 282].

In this chapter, we concentrate on this last approximation: repulsion is modelled by diffusion and attraction by non-local forces. We will make a survey of the main results in this topic exemplifying them in the one dimensional setting while at the same time we will provide new material in one dimension with alternative proofs and information about long time asymptotics which are not known yet in higher dimensions. In order to understand the interplay between repulsion via non-linear diffusion and attraction via non-local forces, we concentrate on the simplest possible situation in which both the diffusion and the non-local attractive potential are homogeneous functions. We will focus on models with a variational structure that dissipate the free energy of the system.

The plan for this chapter is twofold. In a first part we shall investigate some properties of the following class of homogeneous functionals, defined for centered probability densities $\rho(x)$, belonging to suitable weighted L^p-spaces, and some interaction strength coefficient $\chi > 0$ and diffusion power $m > 0$:

$$\mathcal{F}_{m,k}[\rho] = \int_{\mathbb{R}} U_m\left(\rho(x)\right)\, dx + \chi \iint\limits_{\mathbb{R}\times\mathbb{R}} \rho(x) W_k(x-y)\rho(y)\, dxdy := \mathcal{U}_m[\rho] + \chi \mathcal{W}_k[\rho]\,, \tag{1.1}$$

$$\rho(x) \geqslant 0\,, \quad \int_{\mathbb{R}} \rho(x)\, dx = 1\,, \quad \int_{\mathbb{R}} x\rho(x)\, dx = 0\,,$$

with

$$U_m(\rho) = \begin{cases} \dfrac{1}{m-1}\,\rho^m\,, & \text{if} \quad m \neq 1 \\ \rho\log\rho\,, & \text{if} \quad m = 1 \end{cases}\,,$$

and

$$W_k(x) = \begin{cases} \dfrac{|x|^k}{k}, & \text{if} \quad k \in (-1,1)\backslash\{0\} \\ \log|x|, & \text{if} \quad k = 0 \end{cases} . \tag{1.2}$$

The center of mass of the density ρ is assumed to be zero since the free energy functional is invariant by translation. Taking mass preserving dilations, one can see that $\mathcal{U}_m[\cdot]$ scales with a power $m-1$, whilst $\mathcal{W}_k[\cdot]$ scales with power $-k$, indicating that the relation between the parameters k and m plays a crucial role here. And indeed, one observes different types of behaviour depending on which of the two forces dominates, non-linear diffusion or non-local attraction. This motivates the definition of three different regimes: the *diffusion-dominated regime* ($m-1 > -k$), the *fair-competition regime* ($m-1 = -k$), and the *attraction-dominated regime* ($m-1 < -k$). We will here concentrate mostly on the fair-competition regime.

This chapter can be viewed as a continuation of the seminal paper by McCann [234] in a non-convex setting. Indeed, McCann used the very powerful toolbox of Euclidean optimal transportation to analyse functionals like (1.1) in the case $m \geqslant 0$ and for a convex interaction kernel W_k. He discovered that such functionals are equipped with an underlying convexity structure, for which the interpolant $[\rho_0, \rho_1]_t$ follows the line of optimal transportation [295]. This provides many interesting features among which a natural framework to show uniqueness of the ground state as soon as it exists. In this chapter we deal with concave homogeneous interaction kernels W_k given by (1.2) for which McCann's results [234] do not apply. Actually, the conditions on k imply that the interaction kernel W_k is locally integrable on $\mathbb{R}$ and concave on $\mathbb{R}_+$, which means that $\mathcal{W}_k[\cdot]$ is displacement concave as shown in [85]. We explain in this chapter how some ideas from [234] can be extended to some convex-concave competing effects. Our main statement is that the functional (1.1) – the sum of a convex and a concave functional – behaves almost like a convex functional in some good cases detailed below. In particular, existence of a critical point implies uniqueness (up to translations and dilations). The bad functional contribution is somehow absorbed by the convex part for certain homogeneity relations and parameters χ.

The analysis of these free energy functionals and their respective gradient flows is closely related to some functional inequalities of Hardy-Littlewood-Sobolev (HLS) type [218, 163, 74, 39]. To give a flavour, we highlight the case $(m = 1, k = 0)$, called the *logarithmic case*. It is known from [136, 41] using [77, 19] that the functional $\mathcal{F}_{1,0}$ is bounded from below if and only if $0 < \chi \leqslant 1$. Moreover, $\mathcal{F}_{1,0}$ achieves its minimum if and only if $\chi = 1$ and the extremal functions are mass-preserving dilations of Cauchy's density:

$$\bar{\rho}_0(x) = \frac{1}{\pi}\left(\frac{1}{1+|x|^2}\right) . \tag{1.3}$$

In [77] authors have proved the uniqueness (up to dilations and translations) of this logarithmic HLS inequality based on a competing-symmetries argument. We develop in this chapter an alternative argument based on some accurate use of the Jensen's inequality to get similar results in the porous medium case $-1 < k < 0$. This goal will be achieved for some variant of the HLS inequality as in [39], indeed being a combination of the HLS inequality and interpolation estimates, see Theorem 3.1. The case $0 < k < 1$ has been a lot less studied, and we will show here that no critical interaction strength exists as there is no $\chi > 0$ for which $\mathcal{F}_{m,k}$ admits global minimisers. On the other hand, we observe certain similarities with the behaviour of the fast diffusion equation ($0 < m < 1$, $\chi = 0$) [287]. The mass-preserving dilation homogeneity of the functional $\mathcal{F}_{m,k}$ is shared by the range of parameters (m, k) with $N(m-1) + k = 0$ for all dimensions, $m > 0$ and $k \in (-N, N)$. This general fair-competition regime is analysed in Chapter 2.

In a second stage, here we also tackle the behaviour of the following family of partial differential equations modelling self-attracting diffusive particles at the macroscopic scale,

$$\begin{cases} \partial_t \rho = \partial_{xx} \left(\rho^m\right) + 2\chi \partial_x \left(\rho\, \partial_x S_k\right) , \quad t > 0 , \quad x \in \mathbb{R} , \\ \rho(t=0,x) = \rho_0(x) . \end{cases} \tag{1.4}$$

where we define the mean-field potential $S_k(x) := W_k(x) * \rho(x)$. For $k > 0$, the gradient $\partial_x S_k := \partial_x \left(W_k * \rho\right)$ is well defined. For $k < 0$ however, it becomes a singular integral, and we thus define it via a Cauchy principal value. Hence, the mean-field potential gradient in equation (1.4) is given by

$$\partial_x S_k(x) := \begin{cases} \partial_x W_k * \rho , & \text{if } 0 < k < 1 , \\ \displaystyle\int_{\mathbb{R}} \partial_x W_k(x-y) \left(\rho(y) - \rho(x)\right) dy , & \text{if } -1 < k < 0 . \end{cases} \tag{1.5}$$

Further, it is straightforward to check that equation (1.4) formally preserves positivity, mass and centre of mass, and so we can choose to impose

$$\rho_0(x) \geqslant 0 , \quad \int \rho_0(x)\, dx = 1 , \quad \int x \rho_0(x)\, dx = 0 .$$

This class of PDEs are one of the prime examples for competition between the diffusion (possibly non-linear), and the non-local, quadratic non-linearity which is due to the self-attraction of the particles through the mean-field potential $S_k(x)$. The parameter $\chi > 0$ measures the strength of the interaction. We would like to point out that we are here not concerned with the regularity of solutions or existence/uniqueness results for equation (1.4), allowing ourselves to assume solutions are 'nice' enough in space and time for our analysis to hold (for more details on regularity assumptions, see Section 4).

There exists a strong link between the PDE (1.4) and the functional (1.1). Not only is $\mathcal{F}_{m,k}$ decreasing along the trajectories of the system, but more importantly, system (1.4) is the formal gradient flow of the free energy functional (1.1) when the space of probability measures is endowed with the Euclidean Wasserstein metric **W**:

$$\partial_t \rho(t) = -\nabla_{\mathbf{W}} \mathcal{F}_{m,k}[\rho(t)]\,. \tag{1.6}$$

This illuminating statement has been clarified in the seminal paper by Otto [248]. We also refer to the books by Villani [295] and Ambrosio, Gigli and Savaré [3] for a comprehensive presentation of this theory of gradient flows in Wasserstein metric spaces, particularly in the convex case. Performing gradient flows of a convex functional is a natural task, and suitable estimates from below on the Hessian of $\mathcal{F}_{m,k}$ in (1.1) translate into a rate of convergence towards equilibrium for the PDE [96, 295, 97]. However, performing gradient flow of functionals with convex and concave contributions is more delicate, and one has to seek compensations. Such compensations do exist in our case, and one can prove convergence in Wasserstein distance towards some stationary state under suitable assumptions, in some cases with an explicit rate of convergence. It is of course extremely important to understand how the convex and the concave contributions are entangled.

The results obtained in the fully convex case generally consider each contribution separately, resp. internal energy, potential confinement energy or interaction energy, see [96, 295, 3, 97]. It happens however that adding two contributions provides better convexity estimates. In [96] for instance the authors prove exponential speed of convergence towards equilibrium when a degenerate convex potential W_k is coupled with strong enough diffusion, see [44] for improvements.

The family of non-local PDEs (1.4) has been intensively studied in various contexts arising in physics and biology. The two-dimensional logarithmic case $(m = 1, k = 0)$ is the so-called Keller–Segel system in its simplest formulation [196, 197, 243, 194, 41, 256]. It has been proposed as a model for chemotaxis in cell populations. The three-dimensional configuration $(m = 1, k = -1)$ is the so-called Smoluchowski-Poisson system arising in gravitational physics [105, 107, 106]. It describes macroscopically a density of particles subject to a self-sustained gravitational field.

Let us describe in more details the two-dimensional Keller–Segel system, as the analysis of its peculiar structure will serve as a guideline to understand other cases. The corresponding gradient flow is subject to a remarkable dichotomy, see [113, 194, 242, 159, 136, 41] . The density exists globally in time if $\chi < 1$ (diffusion overcomes self-attraction), whereas blow-up occurs in finite time when $\chi > 1$ (self-attraction overwhelms diffusion). In the sub-critical case, it has been proved that solutions decay to self-similarity solutions exponentially fast in suitable rescaled variables [70, 71, 148]. In the super-critical case, solutions blow-up in finite time with by now well studied blow-up profiles for close enough to critical cases, see [187, 260].

Substituting linear diffusion by non-linear diffusion with $m > 1$ in two dimensions and higher is a way of regularising the Keller–Segel model as proved in [61, 277] where it is shown that solutions exist globally in time regardless of the value of the parameter $\chi > 0$. It corresponds to the diffusion-dominated case in two dimensions for which the existence of compactly supported stationary states and global minimisers of the free energy has only been obtained quite recently in [89]. The fair-competition case for Newtonian interaction $k = 2 - N$ was first clarified in [39], see also [276], where the authors find that there is a similar dichotomy to the two-dimensional classical Keller–Segel case $(N = 2, m = 1, k = 0)$, choosing the non-local term as the Newtonian potential, $(N \geqslant 3, m = 2-2/N, k = 2-N)$. The main difference is that the stationary states found for the critical case are compactly supported. We will see that such dichotomy also happens for $k < 0$ in our case while for $k > 0$ the system behaves totally differently. In fact, exponential convergence towards equilibrium seems to be the generic behaviour in rescaled variables as observed in Figure 3.1.

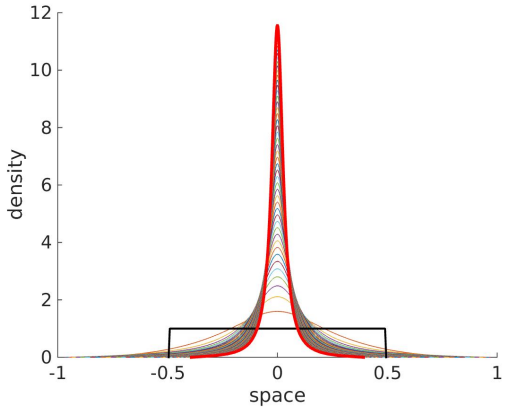

Figure 3.1: Density evolution for parameter choices $\chi = 0.7$, $k = -0.2$, $m = 1.2$ following the PDE (1.4) in rescaled variables from a characteristic supported on $B(0, 1/2)$ (black) converging to a unique stationary state (red). For more details, see Figure 3.6 and the explanations in Section 5.

The chapter is structured as follows: in Section 2, we give an analytic framework with all necessary definitions and assumptions. In cases where no stationary states exist for the aggreg-ation-diffusion equation (1.4), we look for self-similar profiles instead. Self-similar profiles can be studied by changing variables in (1.4) so that stationary states of the rescaled equation correspond to self-similar profiles of the original system. Further, we give some main results of optimal transportation needed for the analysis of Sections 3 and 4. In Section 3, we establish several functional inequalities of HLS type that allow us to make a connection between minimisers of $\mathcal{F}_{m,k}$ and stationary states of (1.4), with similar results for the rescaled system. Section 4 investigates the long-time asymptotics where we demonstrate convergence to equilibrium in Wasserstein distance under certain conditions, in some cases with an explicit rate. Finally, in Section 5, we provide

numerical simulations of system (1.4) to illustrate the properties of equilibria and self-similar profiles in the different parameter regimes for the fair-competition regime. In Section 6, we use the numerical scheme to explore the asymptotic behaviour of solutions in the diffusion- and attraction-dominated regimes.

2 Preliminaries

2.1 Stationary states: definition & basic properties

Let us define precisely the notion of stationary states to the aggregation-diffusion equation (1.4).

Definition 2.1. *Given $\bar{\rho} \in L^1_+(\mathbb{R}) \cap L^\infty(\mathbb{R})$ with $||\bar{\rho}||_1 = 1$, it is a **stationary state** for the evolution equation (1.4) if $\bar{\rho}^m \in \mathcal{W}^{1,2}_{loc}(\mathbb{R})$, $\partial_x \bar{S}_k \in L^1_{loc}(\mathbb{R})$, and it satisfies*

$$\partial_x \bar{\rho}^m = -2\chi\, \bar{\rho} \partial_x \bar{S}_k$$

in the sense of distributions in $\mathbb{R}$. If $k \in (-1, 0)$, we further require $\bar{\rho} \in C^{0,\alpha}(\mathbb{R})$ with $\alpha \in (-k, 1)$.

In fact, the function S_k and its gradient defined in (1.5) satisfy even more than the regularity $\partial_x S_k \in L^1_{loc}(\mathbb{R})$ required in Definition 2.1. We have from Chapter 2 Lemma 2.2:

Lemma 2.2. *Let $\rho \in L^1_+(\mathbb{R}) \cap L^\infty(\mathbb{R})$ with $||\rho||_1 = 1$. If $k \in (0, 1)$, we additionally assume $|x|^k \rho \in L^1(\mathbb{R})$. Then the following regularity properties hold:*

i) $S_k \in L^\infty_{loc}(\mathbb{R})$ for $0 < k < 1$ and $S_k \in L^\infty(\mathbb{R})$ for $-1 < k < 0$.

ii) $\partial_x S_k \in L^\infty(\mathbb{R})$ for $k \in (-1, 1)\backslash\{0\}$, assuming additionally $\rho \in C^{0,\alpha}(\mathbb{R})$ with $\alpha \in (-k, 1)$ in the range $-1 < k < 0$.

Furthermore, for certain cases, see Chapter 2, there are no stationary states to (1.4) in the sense of Definition 2.1 (for a dynamical proof of this fact, see Remark 4.6 in Section 4.1.2), and so the scale invariance of (1.4) motivates us to look for self-similar solutions instead. To this end, we rescale equation (1.4) to a non-linear Fokker–Planck type equation as in [100]. Let us define

$$u(t, x) := \alpha(t)\rho\left(\beta(t), \alpha(t)x\right),$$

where $\rho(t, x)$ solves (1.4) and the functions $\alpha(t)$, $\beta(t)$ are to be determined. If we assume $u(0, x) = \rho(0, x)$, then $u(t, x)$ satisfies the rescaled drift-diffusion equation

$$\begin{cases} \partial_t u = \partial_{xx} u^m + 2\chi \partial_x \left(u\, \partial_x S_k\right) + \partial_x (xu)\,, \quad t > 0\,, \quad x \in \mathbb{R}\,, \\ u(t = 0, x) = \rho_0(x) \geqslant 0\,, \quad \displaystyle\int_{-\infty}^{\infty} \rho_0(x)\, dx = 1\,, \quad \int_{-\infty}^{\infty} x\rho_0(x)\, dx = 0\,, \end{cases} \tag{2.7}$$

for the choices

$$\alpha(t) = e^t, \quad \beta(t) = \begin{cases} \frac{1}{2-k}\left(e^{(2-k)t} - 1\right), & \text{if } k \neq 2\,, \\ t, & \text{if } k = 2\,, \end{cases} \tag{2.8}$$

and with $\partial_x S_k$ given by (1.5) with u instead of ρ. By differentiating the centre of mass of u, we see easily that

$$\int_{\mathbb{R}} xu(t,x)\,dx = e^{-t}\int_{\mathbb{R}} x\rho_0(x)\,dx = 0\,, \qquad \forall t > 0\,,$$

and so the initial zero centre of mass is preserved for all times. Self-similar solutions to (1.4) now correspond to stationary solutions of (2.7). Similar to Definition 2.1, we state what we exactly mean by stationary states to the aggregation-diffusion equation (2.7).

Definition 2.3. *Given $\bar{u} \in L^1_+(\mathbb{R}) \cap L^\infty(\mathbb{R})$ with $||\bar{u}||_1 = 1$, it is a **stationary state** for the evolution equation (2.7) if $\bar{u}^m \in \mathcal{W}^{1,2}_{loc}(\mathbb{R})$, $\partial_x \bar{S}_k \in L^1_{loc}(\mathbb{R})$, and it satisfies*

$$\partial_x \bar{u}^m = -2\chi\,\bar{u}\partial_x \bar{S}_k - x\,\bar{u}$$

in the sense of distributions in $\mathbb{R}$. If $-1 < k < 0$, we further require $\bar{u} \in C^{0,\alpha}(\mathbb{R})$ with $\alpha \in (-k, 1)$.

From now on, we switch notation from u to ρ for simplicity, it should be clear from the context if we are in original or rescaled variables. In fact, stationary states as defined above have even more regularity:

Lemma 2.4. *Let $k \in (-1,1)\backslash\{0\}$ and $\chi > 0$.*

(i) If $\bar{\rho}$ is a stationary state of equation (1.4) with $|x|^k\bar{\rho} \in L^1(\mathbb{R})$ in the case $0 < k < 1$, then $\bar{\rho}$ is continuous on $\mathbb{R}$.

(ii) If $\bar{\rho}_{resc}$ is a stationary state of equation (2.7) with $|x|^k\bar{\rho}_{resc} \in L^1(\mathbb{R})$ in the case $0 < k < 1$, then $\bar{\rho}_{resc}$ is continuous on $\mathbb{R}$.

In the case $k < 0$, we furthermore have a non-linear algebraic equation for stationary states as shown in Chapter 2 Corollary 2.5:

Corollary 2.5 (Necessary Condition for Stationary States)**.** *Let $k \in (-1,0)$ and $\chi > 0$.*

(i) If $\bar{\rho}$ is a stationary state of equation (1.4), then $\bar{\rho} \in \mathcal{W}^{1,\infty}(\mathbb{R})$ and it satisfies

$$\bar{\rho}(x)^{m-1} = \frac{(m-1)}{m}\left(C_k[\bar{\rho}](x) - 2\chi\,\bar{S}_k(x)\right)_+\,, \qquad \forall\, x \in \mathbb{R}\,,$$

where $C_k[\bar{\rho}](x)$ is constant on each connected component of supp $(\bar{\rho})$.

(ii) If $\bar{\rho}_{resc}$ is a stationary state of equation (2.7), then $\bar{\rho}_{resc} \in \mathcal{W}^{1,\infty}_{loc}(\mathbb{R})$ and it satisfies

$$\bar{\rho}_{resc}(x)^{m-1} = \frac{(m-1)}{m}\left(C_{k,resc}[\bar{\rho}](x) - 2\chi\,\bar{S}_k(x) - \frac{|x|^2}{2}\right)_+\,, \qquad \forall\, x \in \mathbb{R}\,,$$

where $C_{k,resc}[\bar{\rho}](x)$ is constant on each connected component of supp $(\bar{\rho}_{resc})$.

2.2 Overview of results in the fair-competition regime

It is worth noting that the functional $\mathcal{F}_{m,k}[\rho]$ possesses remarkable homogeneity properties, see Chapter 1 Section 3.1. We will here only concentrate on the one-dimensional fair-competition regime $m + k = 1$, and denote the corresponding energy functional by $\mathcal{F}_k[\rho] = \mathcal{F}_{1-k,k}[\rho]$. For a definition of the different regimes and detailed explanations and references, see Chapter 1 Definition 3.1. An overview of the parameter space (k, m) and the different regimes is given in Chapter 1 Figure 1.4. Notice that the functional $\mathcal{F}_k$ is homogeneous in the fair-competition regime, i.e.,

$$\mathcal{F}_k[\rho_\lambda] = \lambda^{-k}\mathcal{F}_k[\rho]\,.$$

In this chapter, we wil first do a review of the main results known in one dimension about the stationary states and minimisers of the aggregation-diffusion equation in the fair-competition case. The novelties will be showing the functional inequalities independently of the flow and studying the long-time asymptotics of the equations (1.4) and (2.7) by exploiting the one dimensional setting. The analysis in the fair-competition regime depends on the sign of k, see Chapter 1 Definition 3.7, and we therefore split our investigations into the porous medium case ($k < 0$), and the fast diffusion case ($k > 0$). More information on the logarithmic case ($k = 0$) can be found in [62]. When dealing with the energy functional $\mathcal{F}_k$, we work in the set of non-negative normalised densities,

$$\mathcal{Y} := \left\{\rho \in L^1_+(\mathbb{R}) \cap L^m(\mathbb{R}) : ||\rho||_1 = 1\,,\ \int x\rho(x)\,dx = 0\right\}.$$

In rescaled variables, equation (2.7) is the formal gradient flow of the rescaled free energy functional $\mathcal{F}_{k,\mathbf{resc}}$, which is complemented with an additional quadratic confinement potential,

$$\mathcal{F}_{k,\mathbf{resc}}[\rho] = \mathcal{F}_k[\rho] + \frac{1}{2}\mathcal{V}[\rho]\,, \qquad \mathcal{V}[\rho] = \int_{\mathbb{R}} |x|^2\rho(x)\,dx\,.$$

Defining the set $\mathcal{Y}_2 := \{\rho \in \mathcal{Y} : \mathcal{V}[\rho] < \infty\}$, we see that $\mathcal{F}_{k,\mathbf{resc}}$ is well-defined and finite on $\mathcal{Y}_2$. Thanks to the formal gradient flow structure in the Euclidean Wasserstein metric $\mathbf{W}$, we can write the rescaled equation (2.7) as

$$\partial_t\rho = -\nabla_{\mathbf{W}}\mathcal{F}_{k,\mathbf{resc}}[\rho]\,.$$

In what follows, we will make use of a different characterisation of stationary states based on some integral reformulation of the necessary condition stated in Corollary 2.5. This characterisation was also the key idea in [62] to improve on the knowledge of the asymptotic stability of steady states and the functional inequalities behind.

Lemma 2.6 (Characterisation of stationary states). *Let $k \in (-1, 1)\backslash\{0\}$, $m = 1 - k$ and $\chi > 0$.*

(i) Any stationary state $\bar\rho_k \in \mathcal{Y}$ of system (1.4) can be written in the form

$$\bar\rho_k(p)^m = \chi \int_{\mathbb{R}}\int_0^1 |q|^{1-m}\bar\rho_k(p - sq)\bar\rho_k(p - sq + q)\,dsdq\,. \tag{2.9}$$

Moreover, if such a stationary state exists, it satisfies $\mathcal{F}_k[\bar\rho_k] = 0$.

(ii) Any stationary state $\bar\rho_{k,\textit{resc}} \in \mathcal{Y}_2$ of system (2.7) can be written in the form

$$\bar\rho_{k,\textit{resc}}(p)^m = \int_{\mathbb{R}}\int_0^1 \left(\chi|q|^{1-m} + \frac{|q|^2}{2}\right)\bar\rho_{k,\textit{resc}}(p-sq)\bar\rho_{k,\textit{resc}}(p-sq+q)\,dsdq\,. \tag{2.10}$$

Moreover, it satisfies

$$\mathcal{F}_{k,\textit{resc}}[\bar\rho_{k,\textit{resc}}] = \frac{m+1}{2(m-1)}\,\mathcal{V}[\bar\rho_{k,\textit{resc}}] = \left(\frac12 - \frac1k\right)\mathcal{V}[\bar\rho_{k,\textit{resc}}]\,. \tag{2.11}$$

Proof. We can apply the same methodology as for the logarithmic case (Lemma 2.3, [62]). We will only prove (2.9), identity (2.10) can be deduced in a similar manner. We can see directly from the equation that all stationary states of (1.4) in $\mathcal{Y}$ satisfy

$$\partial_x\left(\bar\rho_k^m\right) + 2\chi\bar\rho_k\partial_x\bar S_k = 0\,.$$

Hence, if $k\in(0,1)$, we can write for any test function $\varphi\in C_c^\infty(\mathbb{R})$

$$\begin{aligned}0 &= -\int_{\mathbb{R}}\varphi'(p)\bar\rho_k^m(p)\,dp + 2\chi\iint_{\mathbb{R}\times\mathbb{R}}\varphi(x)|x-y|^{k-2}(x-y)\bar\rho_k(x)\bar\rho_k(y)\,dxdy\\ &= -\int_{\mathbb{R}}\varphi'(p)\bar\rho_k^m(p)\,dp + \chi\iint_{\mathbb{R}\times\mathbb{R}}\left(\frac{\varphi(x)-\varphi(y)}{x-y}\right)|x-y|^k\bar\rho_k(x)\bar\rho_k(y)\,dxdy\,.\end{aligned}$$

For $k\in(-1,0)$, the term $\partial_x\bar S_k$ is a singular integral, and thus writes

$$\begin{aligned}\partial_x\bar S_k(x) &= \lim_{\varepsilon\to0}\int_{B^c(x,\varepsilon)}|x-y|^{k-2}(x-y)\bar\rho_k(y)\,dy\\ &= \int_{\mathbb{R}}|x-y|^{k-2}(x-y)\left(\bar\rho_k(y)-\bar\rho_k(x)\right)\,dy\,.\end{aligned}$$

The singularity disappears when integrating against a test function $\varphi\in C_c^\infty(\mathbb{R})$,

$$\int_{\mathbb{R}}\varphi(x)\partial_x\bar S_k(x)\bar\rho_k(x)\,dx = \frac12\iint_{\mathbb{R}\times\mathbb{R}}\left(\frac{\varphi(x)-\varphi(y)}{x-y}\right)|x-y|^k\bar\rho_k(x)\bar\rho_k(y)\,dxdy\,. \tag{2.12}$$

In order to prove (2.12), let us define

$$f_\varepsilon(x) := \varphi(x)\int_{B^c(x,\varepsilon)}\partial_x W_k(x-y)\bar\rho_k(y)\,dy.$$

Then by definition of the Cauchy Principle Value, $f_\varepsilon(x)\to\varphi(x)\partial_x\bar S_k(x)$ pointwise for almost every $x\in\mathbb{R}$ as $\varepsilon\to0$. Further, we have for $0<\varepsilon<1$,

$$\begin{aligned}|f_\varepsilon(x)| &= |\varphi(x)|\left|\int_{B^c(x,\varepsilon)\cap B(x,1)}\partial_x W_k(x-y)\bar\rho_k(y)\,dy + \int_{B^c(x,\varepsilon)\cap B^c(x,1)}\partial_x W_k(x-y)\bar\rho_k(y)\,dy\right|\\ &\leqslant |\varphi(x)|\left(\left|\int_{B^c(x,\varepsilon)\cap B(x,1)}\partial_x W_k(x-y)\bar\rho_k(y)\,dy\right| + \int_{|x-y|\geqslant1}|x-y|^{k-1}\bar\rho_k(y)\,dy\right)\\ &\leqslant |\varphi(x)|\left(\left|\int_{B^c(x,\varepsilon)\cap B(x,1)}\partial_x W_k(x-y)\bar\rho_k(y)\,dy\right| + 1\right)\end{aligned}$$

Since $\partial_x W_k$ is anti-symmetric, the term $\int_{B^c(x,\varepsilon)\cap B(x,1)} \partial_x W_k(x-y)\,dy$ vanishes and we are thus free to subtract it. Using the fact that $\bar\rho_k \in C^{0,\alpha}(\mathbb{R})$ for some $\alpha \in (-k,1)$, we have

$$\begin{aligned}\left|\int_{B^c(x,\varepsilon)\cap B(x,1)} \partial_x W_k(x-y)\bar\rho_k(y)\,dy\right| &= \left|\int_{B^c(x,\varepsilon)\cap B(x,1)} \partial_x W_k(x-y)\left[\bar\rho_k(y)-\bar\rho_k(x)\right]\,dy\right| \\ &\leqslant \int_{B^c(x,\varepsilon)\cap B(x,1)} |x-y|^{k-1}\left|\bar\rho_k(y)-\bar\rho_k(x)\right|\,dy \\ &\leqslant \int_{B^c(x,\varepsilon)\cap B(x,1)} |x-y|^{k+\alpha-1}\,dy \\ &= \frac{2}{k+\alpha}\left(1-\varepsilon^{k+\alpha}\right) \leqslant \frac{2}{k+\alpha}\,.\end{aligned}$$

We conclude that $|f_\varepsilon(x)| \leqslant \left(\frac{2+k+\alpha}{k+\alpha}\right)|\varphi(x)|$ for all $0<\varepsilon<1$, and therefore by Lebesgue's dominated convergence theorem,

$$\begin{aligned}\int_{\mathbb{R}} \varphi(x)\partial_x \bar S_k(x)\bar\rho_k(x)\,dx &= \int_{\mathbb{R}} \lim_{\varepsilon\to 0} f_\varepsilon(x)\bar\rho_k(x)\,dx = \lim_{\varepsilon\to 0}\int_{\mathbb{R}} f_\varepsilon(x)\bar\rho_k(x)\,dx \\ &= \lim_{\varepsilon\to 0}\iint\limits_{|x-y|\geqslant\varepsilon} \varphi(x)|x-y|^{k-2}(x-y)\bar\rho_k(x)\bar\rho_k(y)\,dxdy \\ &= \frac{1}{2}\lim_{\varepsilon\to 0}\iint\limits_{|x-y|\geqslant\varepsilon}\left(\frac{\varphi(x)-\varphi(y)}{x-y}\right)|x-y|^k\bar\rho_k(x)\bar\rho_k(y)\,dxdy \\ &= \frac{1}{2}\iint\limits_{\mathbb{R}\times\mathbb{R}}\left(\frac{\varphi(x)-\varphi(y)}{x-y}\right)|x-y|^k\bar\rho_k(x)\bar\rho_k(y)\,dxdy\,.\end{aligned}$$

This concludes the proof of (2.12). Hence, we obtain for any $k\in(-1,1)\backslash\{0\}$,

$$\begin{aligned}0 &= -\int_{\mathbb{R}}\varphi'(p)\bar\rho_k^m(p)\,dp + \chi\iint\limits_{\mathbb{R}\times\mathbb{R}}\left(\frac{\varphi(x)-\varphi(y)}{x-y}\right)|x-y|^k\bar\rho_k(x)\bar\rho_k(y)\,dxdy \\ &= -\int_{\mathbb{R}}\varphi'(p)\bar\rho_k^m(p)\,dp + \chi\iint\limits_{\mathbb{R}\times\mathbb{R}}\int_0^1\varphi'\left((1-s)x+sy\right)|x-y|^k\bar\rho_k(x)\bar\rho_k(y)\,dsdxdy \\ &= -\int_{\mathbb{R}}\varphi'(p)\bar\rho_k^m(p)\,dp + \chi\int_{\mathbb{R}}\varphi'(p)\left\{\int_{\mathbb{R}}\int_0^1|q|^k\bar\rho_k(p-sq)\bar\rho_k(p-sq+q)\,dsdq\right\}dp\end{aligned}$$

and so (2.9) follows up to a constant. Since both sides of (2.9) have mass one, the constant is zero. To see that $\mathcal{F}_k[\bar\rho_k]=0$, we substitute (2.9) into (1.1) and use the same change of variables as above.

Finally, identity (2.11) is a consequence of various homogeneities. For every stationary state $\bar\rho_{k,\mathbf{resc}}$ of (2.7), the first variation $\frac{\delta\mathcal{F}_{k,\mathbf{resc}}}{\delta\rho}[\bar\rho_{k,\mathbf{resc}}] = m/(m-1)\bar\rho_{k,\mathbf{resc}}^{m-1}+2\chi W_k*\bar\rho_{k,\mathbf{resc}}+|x|^2/2$ vanishes on the support of $\bar\rho_{k,\mathbf{resc}}$ and hence it follows that for dilations $\bar\rho_\lambda(x) := \lambda\bar\rho_{k,\mathbf{resc}}(\lambda x)$ of the stationary state $\bar\rho_{k,\mathbf{resc}}$:

$$\begin{aligned}-k\mathcal{F}_{k,\mathbf{resc}}[\bar\rho_{k,\mathbf{resc}}] + \left(\frac{k}{2}-1\right)\mathcal{V}[\bar\rho_{k,\mathbf{resc}}] &= \frac{d}{d\lambda}\mathcal{F}_{k,\mathbf{resc}}[\bar\rho_\lambda]\Big|_{\lambda=1} \\ &= \int_{\mathbb{R}}\left(\frac{\delta\mathcal{F}_{k,\mathbf{resc}}}{\delta\rho}[\bar\rho_\lambda](x)\,\frac{d\bar\rho_\lambda}{d\lambda}(x)\right)dx\Big|_{\lambda=1} = 0\,.\end{aligned}$$

In the fair-competition regime, attractive and repulsive forces are in balance $m + k = 1$, and so (2.11) follows. □

2.3 Optimal transport tools

This sub-section summarises the main results of optimal transportation we will need. They were already used for the case of logarithmic HLS inequalities and the classical Keller–Segel model in 1D and radial 2D, see [62], where we refer for detailed proofs.

Let $\tilde{\rho}$ and ρ be two density probabilities. According to [53, 233], there exists a convex function ψ whose gradient pushes forward the measure $\tilde{\rho}(a)da$ onto $\rho(x)dx$: $\psi' \# (\tilde{\rho}(a)da) = \rho(x)dx$. This convex function satisfies the Monge-Ampère equation in the weak sense: for any test function $\varphi \in C_b(\mathbb{R})$, the following identity holds true

$$\int_{\mathbb{R}} \varphi(\psi'(a))\tilde{\rho}(a)\, da = \int_{\mathbb{R}} \varphi(x)\rho(x)\, dx\,. \tag{2.13}$$

The convex map is unique a.e. with respect to ρ and it gives a way of interpolating measures. In fact, the interpolating curve ρ_s, $s \in [0,1]$, with $\rho_0 = \rho$ and $\rho_1 = \tilde{\rho}$ can be defined as $\rho_s(x)\, dx = (s\psi' + (1-s)\mathsf{Id})(x)\#\rho(x)\, dx$ where Id stands for the identity map in $\mathbb{R}$. This interpolating curve is actually the minimal geodesic joining the measures $\rho(x)dx$ and $\tilde{\rho}(x)dx$. The notion of convexity associated to these interpolating curves is nothing else than convexity along geodesics, introduced and called displacement convexity in [234]. In one dimension, the displacement convexity/concavity of functionals is easier to check as seen in [85, 98]. The convexity of the functionals involved can be summarised as follows [234, 85]:

Theorem 2.7. *The functional $\mathcal{U}_m[\rho]$ is displacement-convex provided that $m \geqslant 0$. The functional $\mathcal{W}_k[\rho]$ is displacement-concave if $k \in (-1, 1)$.*

This means we have to deal with convex-concave compensations. On the other hand, regularity of the transport map is a complicated matter. Here, as it was already done in [62], we will only use the fact that the Hessian measure $\det_H D^2\psi(a)da$ can be decomposed in an absolute continuous part $\det_A D^2\psi(a)da$ and a positive singular measure (Chapter 4, [295]). Moreover, it is known that a convex function ψ has Aleksandrov second derivative $D^2_A\psi(a)$ almost everywhere and that $\det_A D^2\psi(a) = \det D^2_A\psi(a)$. In particular we have $\det_H D^2\psi(a) \geqslant \det_A D^2\psi(a)$. The formula for the change of variables will be important when dealing with the internal energy contribution. For any measurable function U, bounded below such that $U(0) = 0$ we have [234]

$$\int_{\mathbb{R}} U(\tilde{\rho}(x))\, dx = \int_{\mathbb{R}} U\left(\frac{\rho(a)}{\det_A D^2\psi(a)}\right) \det_A D^2\psi(a)\, da\,. \tag{2.14}$$

Luckily, the complexity of Brenier's transport problem dramatically reduces in one dimension. More precisely, the transport map ψ' is a non-decreasing function, therefore it is differentiable a.e.

and it has a countable number of jump singularities. The singular part of the positive measure $\psi''(x)\,dx$ corresponds to having holes in the support of the density ρ. Also, the Aleksandrov second derivative of ψ coincides with the absolutely continuous part of the positive measure $\psi''(x)\,dx$ that will be denoted by $\psi''_{\rm ac}(x)\,dx$. Moreover, the a.e. representative ψ' can be chosen to be the distribution function of the measure $\psi''(x)\,dx$ and it is of bounded variation locally, with lateral derivatives existing at all points and therefore, we can always write for all $a < b$

$$\psi'(b) - \psi'(a) = \int_{(a,b]} \psi''(x)\,dx \geqslant \int_a^b \psi''_{\rm ac}(x)\,dx$$

for a well chosen representative of ψ'.

The following Lemma proved in [62] will be used to estimate the interaction contribution in the free energy, and in the evolution of the Wasserstein distance.

Lemma 2.8. *Let $\mathcal{K} : (0,\infty) \to \mathbb{R}$ be an increasing and strictly concave function. Then, for any (a,b)*

$$\mathcal{K}\left(\frac{\psi'(b)-\psi'(a)}{b-a}\right) \geqslant \int_0^1 \mathcal{K}\left(\psi''_{\rm ac}([a,b]_s)\right)\,ds\,, \tag{2.15}$$

where the convex combination of a and b is given by $[a,b]_s = (1-s)a + sb$. Equality is achieved in (2.15) if and only if the distributional derivative of the transport map ψ'' is a constant function.

Optimal transport is a powerful tool for reducing functional inequalities onto pointwise inequalities (*e.g.* matrix inequalities). In other words, to pass from microscopic inequalities between particle locations to macroscopic inequalities involving densities. We highlight for example the seminal paper by McCann [234] where the displacement convexity issue for some energy functional is reduced to the concavity of the determinant. We also refer to the works of Barthe [17, 18] and Cordero-Erausquin *et al.* [117]. The previous lemma will allow us to connect microscopic to macroscopic inequalities by simple variations of the classical Jensen inequality.

3 Functional inequalities

The first part of analysing the aggregation-diffusion equations (1.4) and (2.7) is devoted to the derivation of functional inequalities which are all variants of the Hardy-Littlewood-Sobolev (HLS) inequality also known as the weak Young's inequality [218, Theorem 4.3]:

$$\iint_{\mathbb{R}\times\mathbb{R}} f(x)|x-y|^k f(y)\,dxdy \leqslant C_{HLS}(p,q,\lambda)\|f\|_{L^p}\|f\|_{L^q}\,, \tag{3.16}$$
$$\frac{1}{p}+\frac{1}{q} = 2+k\,, \quad p,q>1\,, \quad k\in(-1,0)\,.$$

Theorem 3.1 (Variation of HLS). *Let $k \in (-1,0)$ and $m = 1-k$. For $f \in L^1(\mathbb{R}) \cap L^m(\mathbb{R})$, we have*

$$\left| \iint_{\mathbb{R}\times\mathbb{R}} f(x)|x-y|^k f(y)dxdy \right| \leqslant C_*||f||_1^{1+k}||f||_m^m, \tag{3.17}$$

where $C_* = C_*(k)$ is the best constant.

Proof. The inequality is a direct consequence of the standard HLS inequality (3.16) by choosing $p = q = \frac{2}{2+k}$, and of Hölder's inequality. For $k \in (-1,0)$ and for any $f \in L^1(\mathbb{R}) \cap L^m(\mathbb{R})$, we have

$$\left| \iint_{\mathbb{R}\times\mathbb{R}} f(x)|x-y|^k f(y)dxdy \right| \leqslant C_{HLS}||f||_p^2 \leqslant C_{HLS}||f||_1^{1+k}||f||_m^m.$$

Consequently, C_* is finite and bounded from above by C_{HLS}. □

For instance inequality (3.17) is a consequence of interpolation between L^1 and L^m. We develop in this section another strategy which enables to recover inequality (3.17), as well as further variations which contain an additional quadratic confinement potential. This method involves two main ingredients:

- First it is required to know *a priori* that the inequality possesses some extremal function denoted *e.g.* by $\bar{\rho}(x)$ (characterised as a critical point of the energy functional). This is not an obvious task due to the intricacy of the equation satisfied by $\bar{\rho}(x)$. Without this *a priori* knowledge, the proof of the inequality remains incomplete. The situation is in fact similar to the case of convex functionals, where the existence of a critical point ensures that it is a global minimiser of the functional. The existence of optimisers was shown in Chapter 2.
- Second we invoke some simple lemma at the microscopic level. It is nothing but the Jensen's inequality for the case of inequality (3.17) (which is somehow degenerated). It is a variation of Jensen's inequality in the rescaled case.

3.1 Porous medium case $k < 0$

In the porous medium case, we have $k \in (-1,0)$ and hence $m \in (1,2)$. For $\chi = 0$, this corresponds to the well-studied porous medium equation (see [289] and references therein). It follows directly from Theorem 3.1, that for all $\rho \in \mathcal{Y}$ and for any $\chi > 0$,

$$\mathcal{F}_k[\rho] \geqslant \frac{1-\chi C_*}{m-1}||\rho||_m^m,$$

where $C_* = C_*(k)$ is the optimal constant defined in (3.17). Since global minimisers have always smaller or equal energy than stationary states, and stationary states have zero energy by Lemma 2.6, it follows that $\chi \geqslant 1/C_*$. We define the *critical interaction strength* by

$$\chi_c(k) := \frac{1}{C_*(k)}, \tag{3.18}$$

and so for $\chi = \chi_c(k)$, all stationary states of equation (1.4) are global minimisers of $\mathcal{F}_k$. From Theorem 2.6 in Chapter 2, we further know that there exist global minimisers of $\mathcal{F}_k$ only for critical interaction strength $\chi = \chi_c(k)$ and they are radially symmetric non-increasing, compactly supported and uniformly bounded. Further, all minimisers of $\mathcal{F}_k$ are stationary states of equation (1.4).

From the above, we can also directly see that for $0 < \chi < \chi_c(k)$, no stationary states exist for equation (1.4). Further, there are no minimisers of $\mathcal{F}_k$. However, there exist global minimisers of the rescaled free energy $\mathcal{F}_{k,\mathbf{resc}}$ and they are radially symmetric non-increasing and uniformly bounded stationary states of the rescaled equation (2.7) (Chapter 2 Theorem 2.7).

Theorem 3.2. *Let $k \in (-1, 0)$ and $m = 1 - k$. If (1.4) admits a stationary density $\bar{\rho}_k$ in $\mathcal{Y}$, then for any $\chi > 0$*

$$\mathcal{F}_k[\rho] \geqslant 0, \quad \forall \rho \in \mathcal{Y}$$

with the equality cases given dilations of $\bar{\rho}_k$. In other words, for critical interaction strength $\chi = \chi_c(k)$, inequality (3.17) holds true for all $f \in L^1(\mathbb{R}) \cap L^m(\mathbb{R})$.

Proof. For a given stationary state $\bar{\rho}_k \in \mathcal{Y}$ and solution $\rho \in \mathcal{Y}$ of (1.4), we denote by ψ the convex function whose gradient pushes forward the measure $\bar{\rho}_k(a)da$ onto $\rho(x)dx$: $\psi' \# (\bar{\rho}_k(a)da) = \rho(x)dx$. Using (2.14), the functional $\mathcal{F}_k[\rho]$ rewrites as follows:

$$\begin{aligned}
\mathcal{F}_k[\rho] &= \frac{1}{m-1}\int_{\mathbb{R}} \left(\frac{\bar{\rho}_k(a)}{\psi''_{ac}(a)}\right)^{m-1} \bar{\rho}_k(a)\, da \\
&\quad + \frac{\chi}{k}\iint_{\mathbb{R}\times\mathbb{R}} \left(\frac{\psi'(a)-\psi'(b)}{a-b}\right)^{k} |a-b|^k \bar{\rho}_k(a)\bar{\rho}_k(b)\, dadb \\
&= \frac{1}{m-1}\int_{\mathbb{R}} \left(\psi''_{ac}(a)\right)^{1-m} \bar{\rho}_k(a)^m\, da \\
&\quad + \frac{\chi}{1-m}\iint_{\mathbb{R}\times\mathbb{R}} \left(\frac{\psi'(a)-\psi'(b)}{a-b}\right)^{1-m} |a-b|^{1-m} \bar{\rho}_k(a)\bar{\rho}_k(b)\, dadb\,,
\end{aligned}$$

where ψ' non-decreasing. By Lemma 2.6 (i), we can write for any $\gamma \in \mathbb{R}$,

$$\int_{\mathbb{R}} (\psi''_{ac}(a))^{-\gamma} \bar{\rho}_k(a)^m\, da = \chi \iint_{\mathbb{R}\times\mathbb{R}} \left\langle \psi''_{ac}([a,b])^{-\gamma} \right\rangle |a-b|^{1-m} \bar{\rho}_k(a)\bar{\rho}_k(b)\, dadb\,,$$

where

$$\left\langle u([a,b]) \right\rangle = \int_0^1 u([a,b]_s)\, ds$$

and $[a,b]_s = (1-s)a + sb$ for any $a, b \in \mathbb{R}$ and $u : \mathbb{R} \to \mathbb{R}_+$. Hence, choosing $\gamma = m - 1$,

$$\mathcal{F}_k[\rho] = \frac{\chi}{m-1}\iint_{\mathbb{R}\times\mathbb{R}} \left\{ \left\langle \psi''_{ac}([a,b])^{1-m} \right\rangle - \left(\frac{\psi'(a)-\psi'(b)}{a-b}\right)^{1-m} \right\} |a-b|^{1-m} \bar{\rho}_k(a)\bar{\rho}_k(b)\, dadb\,.$$

Using the strict concavity and increasing character of the power function $-(\cdot)^{1-m}$ and Lemma 2.8, we deduce $\mathcal{F}_k[\rho] \geqslant 0$. Equality arises if and only if the derivative of the transport map ψ'' is a constant function, i.e. when ρ is a dilation of $\bar{\rho}_k$.
We conclude that if (1.4) admits a stationary state $\bar{\rho}_k \in \mathcal{Y}$, then $\mathcal{F}_k(\rho) \geqslant 0$ for any $\rho \in \mathcal{Y}$. This functional inequality is equivalent to (3.17) if we choose $\chi = \chi_c(k)$. □

Remark 3.3 (Comments on the Inequality Proof). *In the case of critical interaction strength $\chi = \chi_c(k)$, Theorem 3.2 provides an alternative proof for the variant of the HLS inequality Theorem 3.1 assuming the existence of a stationary density for (1.4). More precisely, the inequalities $\mathcal{F}_k[\rho] \geqslant 0$ and (3.17) are equivalent if $\chi = \chi_c(k)$. However, the existence proof Proposition 3.4 in Chapter 2 crucially uses the HLS type inequality (3.17). If we were able to show the existence of a stationary density by alternative methods, e.g. fixed point arguments, we would obtain a full alternative proof of inequality (3.17).*

Remark 3.4 (Logarithmic Case). *There are no global minimisers of $\mathcal{F}_0$ in the logarithmic case $k = 0$, $m = 1$ except for critical interaction strength $\chi = 1$. To see this, note that the characterisation of stationary states [62, Lemma 2.3] which corresponds to Lemma 2.6(i) for the case $k \neq 0$, holds true for any $\chi > 0$. Similarly, the result that the existence of a stationary state $\bar{\rho}$ implies the inequality $\mathcal{F}_0[\rho] > \mathcal{F}_0[\bar{\rho}]$ [62, Theorem 1.1] holds true for any $\chi > 0$, and corresponds to Theorem 3.2 in the case $k \neq 0$. Taking dilations of Cauchy's density (1.3), $\rho_\lambda(x) = \lambda\bar{\rho}_0(\lambda x)$, we have $\mathcal{F}_0[\rho_\lambda] = (1-\chi)\log\lambda + \mathcal{F}_0[\bar{\rho}_0]$, and letting $\lambda \to \infty$ for super-critical interaction strengths $\chi > 1$, we see that $\mathcal{F}_0$ is not bounded below. Similarly, for sub-critical interaction strengths $0 < \chi < 1$, we take the limit $\lambda \to 0$ to see that $\mathcal{F}_0$ is not bounded below. Hence, there are no global minimisers of $\mathcal{F}_0$ and also no stationary states (by equivalence of the two) except if $\chi = 1$.*

Further, we obtain the following uniqueness result:

Corollary 3.5 (Uniqueness in the Critical Case). *Let $k \in (-1, 0)$ and $m = 1 - k$. If $\chi = \chi_c(k)$, then there exists a unique stationary state (up to dilations) to equation (1.4), with second moment bounded, and a unique minimiser (up to dilations) for $\mathcal{F}_k$ in $\mathcal{Y}$.*

Proof. By Theorem 2.6 in Chapter 2, there exists a minimiser of $\mathcal{F}_k$ in $\mathcal{Y}$, which is a stationary state of equation (1.4). Assume (1.4) admits two stationary states $\bar{\rho}_1$ and $\bar{\rho}_2$. By Lemma 2.6, $\mathcal{F}_k[\bar{\rho}_1] = \mathcal{F}_k[\bar{\rho}_2] = 0$. It follows from Theorem 3.2 that $\bar{\rho}_1$ and $\bar{\rho}_2$ are dilations of each other. □

A functional inequality similar to (3.17) holds true for sub-critical interaction strengths in rescaled variables:

Theorem 3.6 (Rescaled Variation of HLS). *For any $\chi > 0$, let $k \in (-1, 0)$ and $m = 1-k$. If $\bar{\rho}_{k,\textit{resc}} \in \mathcal{Y}_2$ is a stationary state of (2.7), then we have for any solution $\rho \in \mathcal{Y}_2$,*

$$\mathcal{F}_{k,\textit{resc}}[\rho] \geqslant \mathcal{F}_{k,\textit{resc}}[\bar{\rho}_{k,\textit{resc}}]$$

with the equality cases given by $\rho = \bar{\rho}_{k,\textit{resc}}$.

The proof is based on two lemmatas: the characterisation of steady states Lemma 2.6 and a microscopic inequality. The difference with the critical case lies in the nature of this microscopic inequality: Jensen's inequality needs to be replaced here as homogeneity has been broken. To simplify the notation, we denote by $u_{ac}(s) := \psi''_{ac}([a,b]_s)$ as above with $[a,b]_s := (1-s)a + sb$ for any $a, b \in \mathbb{R}$. We also introduce the notation

$$\langle u \rangle := \frac{\psi'(a) - \psi'(b)}{a-b} = \int_0^1 \psi''([a,b]_s)\, ds$$

with $u(s) := \psi''([a,b]_s)$. Both notations coincide when ψ'' has no singular part. Note there is a little abuse of notation since ψ'' is a measure and not a function, but this notation allows us for simpler computations below.

Lemma 3.7. *Let $\alpha, \beta > 0$ and $m > 1$. For any $a, b \in \mathbb{R}$ and any convex function $\psi : \mathbb{R} \to \mathbb{R}$:*

$$\alpha \langle \psi''([a,b]) \rangle^{1-m} + \beta(1-m) \langle \psi''([a,b]) \rangle^2 \leqslant (\alpha + 2\beta) \langle \left(\psi''_{ac}([a,b])\right)^{1-m} \rangle - \beta(m+1)\,, \tag{3.19}$$

where equality arises if and only if $\psi'' \equiv 1$ a.e.

Proof. We have again by Lemma 2.8,

$$(\alpha + 2\beta) \langle u \rangle^{1-m} \leqslant (\alpha + 2\beta) \langle u_{ac}^{1-m} \rangle\,,$$

thus

$$\alpha \langle u \rangle^{1-m} + \beta(1-m) \langle u \rangle^2 \leqslant (\alpha + 2\beta) \langle u_{ac}^{1-m} \rangle - \beta \left[2 \langle u \rangle^{1-m} + (m-1) \langle u \rangle^2 \right].$$

We conclude since the quantity in square brackets verifies

$$\forall X > 0 : \; 2X^{1-m} + (m-1)X^2 \geqslant m+1\,.$$

Equality arises if and only if u is almost everywhere constant and $\langle u \rangle = 1$. □

Proof of Theorem 3.6. We denote by $\bar\rho = \bar\rho_{k,\mathbf{resc}} \in \mathcal{Y}_2$ a stationary state of (2.7) for the sake of clarity. Then for any solution $\rho \in \mathcal{Y}_2$ of (2.7), there exists a convex function ψ whose gradient pushes forward the measure $\bar\rho(a)da$ onto $\rho(x)dx$,

$$\psi' \# \left(\bar\rho(a)da\right) = \rho(x)dx.$$

Similarly to the proof of Theorem 3.2, the functional $\mathcal{F}_{k,\mathbf{resc}}[\rho]$ rewrites as follows:

$$\begin{aligned}
\mathcal{F}_{k,\mathbf{resc}}[\rho] = {} & \frac{1}{m-1} \int_{\mathbb{R}} (\psi''_{ac}(a))^{1-m} \bar\rho(a)^m\, da \\
& + \frac{\chi}{k} \iint_{\mathbb{R}\times\mathbb{R}} \left(\frac{\psi'(a) - \psi'(b)}{a-b} \right)^k |a-b|^k \bar\rho(a)\bar\rho(b)\, dadb \\
& + \frac{1}{4} \iint_{\mathbb{R}\times\mathbb{R}} \left(\frac{\psi'(a) - \psi'(b)}{a-b} \right)^2 |a-b|^2 \bar\rho(a)\bar\rho(b)\, dadb\,.
\end{aligned}$$

From the characterisation of steady states Lemma 2.6 (ii), we know that for all $\gamma \in \mathbb{R}$:

$$\int_{\mathbb{R}} (\psi''_{ac}(a))^{-\gamma} \bar{\rho}(a)^m \, da = \iint\limits_{\mathbb{R}\times\mathbb{R}} \left\langle \psi''_{ac}([a,b])^{-\gamma} \right\rangle \left(\chi|a-b|^{1-m} + \frac{|a-b|^2}{2} \right) \bar{\rho}(a)\bar{\rho}(b) \, dadb \,.$$

Choosing $\gamma = m-1$, we can rewrite the energy functional as

$$\begin{aligned}
(m-1)\mathcal{F}_{k,\textbf{resc}}[\rho] = &\iint\limits_{\mathbb{R}\times\mathbb{R}} \left\langle \psi''_{ac}([a,b])^{1-m} \right\rangle \left(\chi|a-b|^{1-m} + \frac{|a-b|^2}{2} \right) \bar{\rho}(a)\bar{\rho}(b) \, dadb \\
&- \iint\limits_{\mathbb{R}\times\mathbb{R}} \Big(\big\langle \psi''([a,b]) \big\rangle^{1-m} \chi|a-b|^{1-m} \\
&\qquad + \big\langle \psi''([a,b]) \big\rangle^{2} (1-m) \frac{|a-b|^2}{4} \Big) \bar{\rho}(a)\bar{\rho}(b) \, dadb \\
&\geqslant (m+1) \iint\limits_{\mathbb{R}\times\mathbb{R}} \frac{|a-b|^2}{4} \bar{\rho}(a)\bar{\rho}(b) \, dadb \\
&= \frac{m+1}{2} \int_{\mathbb{R}} |a|^2 \bar{\rho}(a) \, da = (m-1)\mathcal{F}_{k,\textbf{resc}}[\bar{\rho}] \,.
\end{aligned}$$

Here, we use the variant of Jensen's inequality (3.19) and for the final step, identity (2.11). Again equality holds true if and only if ψ'' is identically one. □

Remark 3.8 (New Inequality)**.** *Up to our knowledge, the functional inequality in Theorem 3.2 is not known in the literature. Theorem 3.6 makes a connection between equation (2.7) and this new general functional inequality by showing that stationary states of the rescaled equation (2.7) correspond to global minimisers of the free energy functional $\mathcal{F}_{k,\textbf{resc}}$. The converse was shown in Theorem 2.7 in Chapter 2.*

As a direct consequence of Theorem 3.6 and the scaling given by (2.8), we obtain the following corollaries:

Corollary 3.9 (Uniqueness in the Sub-Critical Case)**.** *Let $k \in (-1,0)$ and $m = 1-k$. If $0 < \chi < \chi_c(k)$, then there exists a unique stationary state with second moment bounded to the rescaled equation (2.7), and a unique minimiser for $\mathcal{F}_{k,\textbf{resc}}$ in $\mathcal{Y}_2$.*

Proof. By Theorem 2.7 in Chapter 2, there exists a minimiser of $\mathcal{F}_{k,\textbf{resc}}$ in $\mathcal{Y}_2$ for sub-critical interaction strengths $0 < \chi < \chi_c(k)$, which is a stationary state of equation (2.7). Assume (2.7) admits two stationary states $\bar{\rho}_1$ and $\bar{\rho}_2$. By Theorem 3.6, $\mathcal{F}_{k,\textbf{resc}}[\bar{\rho}_1] = \mathcal{F}_{k,\textbf{resc}}[\bar{\rho}_2]$ and it follows that $\bar{\rho}_1$ and $\bar{\rho}_2$ are dilations of each other. □

Corollary 3.10 (Self-Similar Profiles)**.** *For $0 < \chi < \chi_c(k)$, let $k \in (-1,0)$ and $m = 1-k$. There exists a unique (up to dilations) self-similar solution ρ to (1.4) given by*

$$\rho(t,x) = ((2-k)t+1)^{\frac{1}{k-2}} \; u\left(((2-k)t+1)^{\frac{1}{k-2}} \, x \right) \,,$$

where u is the unique minimiser of $\mathcal{F}_{k,\textbf{resc}}$ in $\mathcal{Y}_2$.

Corollary 3.11 (Non-Existence Super-Critical and Critical Case). *(i) If $\chi > \chi_c(k)$, there are no stationary states of equation (1.4) in $\mathcal{Y}$, and the free energy functional $\mathcal{F}_k$ does not admit minimisers in $\mathcal{Y}$.*

(ii) If $\chi \geqslant \chi_c(k)$, there are no stationary states of the rescaled equation (2.7) in $\mathcal{Y}_2$, and the rescaled free energy functional $\mathcal{F}_{k,\mathbf{resc}}$ does not admit minimisers in $\mathcal{Y}_2$.

Proof. For critical $\chi_c(k)$, there exists a minimiser $\bar{\rho} \in \mathcal{Y}$ of $\mathcal{F}_k$ by Theorem 2.6 in Chapter 2, which is a stationary state of equation (1.4) by Theorem 3.14 in Chapter 2. For $\chi > \chi_c(k)$, we have

$$\mathcal{F}_k[\bar{\rho}] = \mathcal{U}_m[\bar{\rho}] + \chi \mathcal{W}_k[\bar{\rho}] < \mathcal{U}_m[\bar{\rho}] + \chi_c(k)\mathcal{W}_k[\bar{\rho}] = 0$$

since stationary states have zero energy by Lemma 2.6 (i). However, by Theorem 3.2, if there exists a stationary state for $\chi > \chi_c(k)$, then all $\rho \in \mathcal{Y}$ satisfy $\mathcal{F}_k[\rho] \geqslant 0$, which contradicts the above. Therefore, the assumptions of the theorem cannot hold and so there are no stationary states in original variables. Further, taking dilations $\rho_\lambda(x) = \lambda\bar{\rho}(\lambda x)$, we have $\mathcal{F}_k[\rho_\lambda] = \lambda^{-k}\mathcal{F}_k[\bar{\rho}] < 0$, and letting $\lambda \to \infty$, we see that $\inf_{\rho\in\mathcal{Y}} \mathcal{F}_k[\rho] = -\infty$, and so (i) follows.

In order to prove (ii), observe that the minimiser $\bar{\rho} \in \mathcal{Y}$ of $\mathcal{F}_k$ for critical $\chi = \chi_c(k)$ is in $\mathcal{Y}_2$ as it is compactly supported (Corollary 3.8 in Chapter 2). We obtain for the rescaled free energy of its dilations

$$\mathcal{F}_{k,\mathbf{resc}}[\rho_\lambda] = \lambda^{-k}\mathcal{F}_k[\bar{\rho}] + \frac{\lambda^{-2}}{2}\mathcal{V}[\bar{\rho}] \to -\infty\,, \qquad \text{as } \lambda \to \infty\,.$$

Hence, $\mathcal{F}_{k,\mathbf{resc}}$ is not bounded below in $\mathcal{Y}_2$. Similarly, for $\chi = \chi_c(k)$,

$$\mathcal{F}_{k,\mathbf{resc}}[\rho_\lambda] = \frac{\lambda^{-2}}{2}\mathcal{V}[\bar{\rho}] \to 0\,, \qquad \text{as } \lambda \to \infty\,,$$

and so for a minimiser $\tilde{\rho} \in \mathcal{Y}_2$ to exist, it should satisfy $\mathcal{F}_{k,\mathbf{resc}}[\tilde{\rho}] \leqslant 0$. However, it follows from Theorem 3.1 that $\mathcal{F}_{k,\mathbf{resc}}[\rho] \geqslant \frac{1}{2}\mathcal{V}[\rho] > 0$ for any $\rho \in \mathcal{Y}_2$, and therefore, $\mathcal{F}_{k,\mathbf{resc}}$ does not admit minimisers in $\mathcal{Y}_2$ for $\chi = \chi_c(k)$.
Further, if equation (2.7) admitted stationary states in $\mathcal{Y}_2$ for any $\chi \geqslant \chi_c(k)$, then they would be minimisers of $\mathcal{F}_{k,\mathbf{resc}}$ by Theorem 3.6, which contradicts the non-existence of minimisers. □

Remark 3.12 (Linearisation around the stationary density). *We linearise the functional $\mathcal{F}_k$ around the stationary distribution $\bar{\rho}_k$ of equation (1.4). For the perturbed measure $\mu_\varepsilon = (\mathsf{Id} + \varepsilon\eta')\#\bar{\mu}_k$, with $d\bar{\mu}_k(x) = \bar{\rho}_k(x)\,dx$ and $d\mu_\varepsilon(x) = \rho_\varepsilon(x)\,dx$, we have*

$$\begin{aligned}\mathcal{F}_k[\rho_\varepsilon] &= \frac{\varepsilon^2}{2} m \left[\int_{\mathbb{R}} \eta''(a)^2 \bar{\rho}_k(a)^m \, da - \chi_c(k) \iint_{\mathbb{R}\times\mathbb{R}} \left(\frac{\eta'(a) - \eta'(b)}{a-b} \right)^2 |a-b|^{1-m} \bar{\rho}_k(a)\bar{\rho}_k(b)\, dadb \right] \\ &\quad + o(\varepsilon^2) \\ &= \frac{\varepsilon^2}{2} m\chi_c(k) \iint_{\mathbb{R}\times\mathbb{R}} \left\{ \langle \eta''([a,b])^2 \rangle - \langle \eta''([a,b]) \rangle^2 \right\} |a-b|^{1-m} \bar{\rho}_k(a)\bar{\rho}_k(b)\, dadb + o(\varepsilon^2)\,.\end{aligned}$$

We define the local oscillations (in L^2) of functions over intervals as

$$osc\ _{(a,b)}(v) := \int_{t=0}^{1} \left\{ v([a,b]_t) - \big\langle v([a,b]) \big\rangle \right\}^2 \, dt \geqslant 0 \, .$$

The Hessian of the functional $\mathcal{F}_k$ evaluated at the stationary density $\bar{\rho}_k$ then reads

$$D^2\mathcal{F}_k[\bar{\rho}_k](\eta,\eta) = m\chi_c(k) \iint\limits_{\mathbb{R}\times\mathbb{R}} osc\ _{(a,b)}(\eta'')|a-b|^{1-m}\bar{\rho}_k(a)\bar{\rho}_k(b)\,dadb \geqslant 0.$$

Similarly, we obtain for the rescaled free energy

$$\begin{aligned}
\mathcal{F}_{k,\textit{resc}}[\rho_\varepsilon] &= \mathcal{F}_{k,\textit{resc}}[\bar{\rho}_k] + \frac{\varepsilon^2}{2} m \int_{\mathbb{R}} \eta''(a)^2 \bar{\rho}_k(a)^m \, da \\
&\quad - \frac{\varepsilon^2}{2} m\chi \iint\limits_{\mathbb{R}\times\mathbb{R}} \left(\frac{\eta'(a)-\eta'(b)}{a-b} \right)^2 |a-b|^{1-m} \bar{\rho}_k(a)\bar{\rho}_k(b)\,dadb \\
&\quad + \frac{\varepsilon^2}{4} \iint\limits_{\mathbb{R}\times\mathbb{R}} \left(\frac{\eta'(a)-\eta'(b)}{a-b} \right)^2 |a-b|^{2} \bar{\rho}_k(a)\bar{\rho}_k(b)\,dadb + o(\varepsilon^2) \\
&= \mathcal{F}_{k,\textit{resc}}[\bar{\rho}_k] \\
&\quad + \frac{\varepsilon^2}{2} \left[m\chi \iint\limits_{\mathbb{R}\times\mathbb{R}} \left\{ \big\langle \eta''([a,b])^2 \big\rangle - \big\langle \eta''([a,b]) \big\rangle^2 \right\} |a-b|^{1-m} \bar{\rho}_k(a)\bar{\rho}_k(b)\,dadb \right. \\
&\quad \left. + \iint\limits_{\mathbb{R}\times\mathbb{R}} \left\{ \frac{m}{2} \big\langle \eta''([a,b])^2 \big\rangle + \frac{1}{2} \big\langle \eta''([a,b]) \big\rangle^2 \right\} |a-b|^{2} \bar{\rho}_k(a)\bar{\rho}_k(b)\,dadb \right] + o(\varepsilon^2)
\end{aligned}$$

to finally conclude

$$\begin{aligned}
\mathcal{F}_{k,\textit{resc}}[\rho_\varepsilon] &= \mathcal{F}_{k,\textit{resc}}[\bar{\rho}_k] \\
&\quad + \frac{\varepsilon^2}{2} \left[\iint\limits_{\mathbb{R}\times\mathbb{R}} osc\ _{(a,b)}(\eta'') \left(m\chi|a-b|^{1-m} + \frac{m}{2}|a-b|^2 \right) \bar{\rho}_k(a)\bar{\rho}_k(b)\,dadb \right. \\
&\quad \left. + \frac{m+1}{2} \iint\limits_{\mathbb{R}\times\mathbb{R}} \big(\eta'(a)-\eta'(b)\big)^2 \bar{\rho}_k(a)\bar{\rho}_k(b)\,dadb \right] + o(\varepsilon^2) \, ,
\end{aligned}$$

and hence, the Hessian evaluated at the stationary state $\bar{\rho}_k$ of (2.7) is given by the expression

$$\begin{aligned}
D^2\mathcal{F}_{k,\textit{resc}}[\bar{\rho}_k](\eta,\eta) &= \iint\limits_{\mathbb{R}\times\mathbb{R}} osc\ _{(a,b)}(\eta'') \left(m\chi|a-b|^{1-m} + \frac{m}{2}|a-b|^2 \right) \bar{\rho}_k(a)\bar{\rho}_k(b)\,dadb \\
&\quad + (m+1) \int_{\mathbb{R}} \eta'(a)^2 \bar{\rho}_k(a)\,da \geqslant 0 \, .
\end{aligned}$$

We have naturally that the functional $\mathcal{F}_{k,\textit{resc}}$ is locally uniformly convex, with the coercivity constant $m+1$. However, the local variations of $\mathcal{F}_{k,\textit{resc}}$ can be large in the directions where the Brenier's map η is large in the $\mathcal{C}^3$-norm. Interestingly enough the coercivity constant does not depend on χ, even in the limit $\chi \nearrow \chi_c(k)$.

3.2 Fast diffusion case $k > 0$

Not very much is known about the fast diffusion case where $k \in (0,1)$ and hence $m = 1-k \in (0,1)$, that is diffusion is fast in regions where the density of particles is low. In Chapter 2, we showed that equation (1.4) has no radially symmetric non-increasing stationary states with kth moment bounded, and there are no radially symmetric non-increasing global minimisers for the energy functional $\mathcal{F}_k$ for any $\chi > 0$. By Theorem 2.9 in Chapter 2, there exists a continuous radially symmetric non-increasing stationary state of the rescaled equation (2.7) for all $\chi > 0$. In this sense, there is no criticality for the parameter χ. We provide here a full proof of non-criticality by optimal transport techniques involving the analysis of the minimisation problem in rescaled variables, showing that global minimisers exist in the right functional spaces for all values of the critical parameter and that they are indeed stationary states - as long as diffusion is not too fast. More precisely, we showed in Chapter 2 that global minimisers with finite energy $\mathcal{F}_{k,\mathbf{resc}}$ can only exist in the range $0 < k < \frac{2}{3}$, that is $\frac{1}{3} < m < 1$. This restriction is exactly what we would expect looking at the behaviour of the fast diffusion equation ($\chi = 0$) [287]. In particular, for $k \in (0,1)$ and $m = 1-k \in (0,1)$, radially symmetric non-increasing stationary states, if they exist, are integrable and have bounded kth moment (Chapter 2 Remarks 4.6 and 4.9). By Remarks 4.13 in Chapter 2 however, their second moment is bounded and $\rho^m \in L^1(\mathbb{R})$ if and only if $k < 2/3$, in which case they belong to $\mathcal{Y}_2$ and their rescaled free energy is finite. This restriction corresponds to $\frac{1}{3} < m < 1$ and coincides with the regime of the one-dimensional fast diffusion equation ($\chi = 0$) where the Barenblatt profile has second moment bounded and its mth power is integrable [47]. Intuitively, adding attractive interaction to the dynamics helps to counteract the escape of mass to infinity. However, the quadratic confinement due to the rescaling of the fast-diffusion equation is already stronger than the additional attractive force since $k < 2$ and hence, we expect that the behaviour of the tails is dominated by the non-linear diffusion effects even for $\chi > 0$ as for the classical fast-diffusion equation.

Using completely different methods, the non-criticality of χ has also been observed in [116, 115] for the limiting case in one dimension taking $m = 0$, corresponding to logarithmic diffusion, and $k = 1$. The authors showed that solutions to (1.4) with $(m = 0, k = 1)$ are globally defined in time for all values of the parameter $\chi > 0$.

In order to establish equivalence between global minimisers and stationary states in one dimension, we prove a type of reversed HLS inequality providing a bound on $\int \rho^m$ in terms of the interaction term $\int (W_k * \rho)\rho$. The inequality gives a lower bound on the rescaled energy $\mathcal{F}_{k,\mathbf{resc}}$:

Theorem 3.13. *Let $k \in (0,1)$, $m = 1-k$ and $\chi > 0$. Then $\bar{\rho} \in \mathcal{Y}_{2,k}$ is a stationary state of (2.7) if and only if for any solution $\rho \in \mathcal{Y}_{2,k}$ we have the inequality*

$$\mathcal{F}_{k,\textit{resc}}[\rho] \geqslant \mathcal{F}_{k,\textit{resc}}[\bar{\rho}]$$

with the equality cases given by $\rho = \bar{\rho}$.

The above theorem implies that stationary states in $\mathcal{Y}_{2,k}$ of the rescaled equation (2.7) are mimimisers of the rescaled free energy $\mathcal{F}_{k,\mathbf{resc}}$. Since the converse is true by Theorem 2.9 in Chapter 2, it allows us to establish equivalence between stationary states of (2.7) and minimisers of $\mathcal{F}_{k,\mathbf{resc}}$. To prove Theorem 3.13, we need a result similar to Lemma 3.7:

Lemma 3.14. *Let $\alpha, \beta > 0$ and $m \in (0,1)$. For any $a, b \in \mathbb{R}$ and any convex function $\psi : \mathbb{R} \to \mathbb{R}$:*

$$(\alpha+\beta)\left\langle \left(\psi''_{ac}([a,b])\right)^{1-m} \right\rangle \leqslant \alpha\left\langle \psi''([a,b])\right\rangle^{1-m} + \frac{\beta(1-m)}{2}\left\langle \psi''([a,b])\right\rangle^{2} + \frac{\beta(m+1)}{2}, \quad (3.20)$$

where equality arises if and only if $\psi'' \equiv 1$ a.e.

Proof. Denote $u(s) := \psi''\left([a,b]_s\right)$ with $[a,b]_s := (1-s)a + sb$ and we write u_{ac} for the absolutely continuous part of u. We have by Lemma 2.8,

$$(\alpha+\beta)\left\langle u_{ac}^{1-m}\right\rangle \leqslant (\alpha+\beta)\left\langle u\right\rangle^{1-m}.$$

Further by direct inspection,

$$\forall X > 0: \ \frac{1}{m-1}X^{1-m} + \frac{1}{2}X^2 \geqslant \frac{m+1}{2(m-1)},$$

thus

$$(\alpha+\beta)\left\langle u_{ac}\right\rangle^{1-m} \leqslant \alpha\left\langle u\right\rangle^{1-m} + \frac{\beta(1-m)}{2}\left\langle u\right\rangle^{2} + \frac{\beta(m+1)}{2}$$

and equality arises if and only if u is almost everywhere constant and $\left\langle u\right\rangle = 1$. □

Proof of Theorem 3.13. For a stationary state $\bar{\rho} \in \mathcal{Y}_{2,k}$ and any solution $\rho \in \mathcal{Y}_{2,k}$ of (2.7), there exists a convex function ψ whose gradient pushes forward the measure $\bar{\rho}(a)da$ onto $\rho(x)dx$

$$\psi' \# \left(\bar{\rho}(a)da\right) = \rho(x)dx.$$

From characterisation (2.10) we have for any $\gamma \in \mathbb{R}$,

$$\int_{\mathbb{R}} \left(\psi''_{ac}(t,a)\right)^{-\gamma} \bar{\rho}_k(a)^m \, da = \iint\limits_{\mathbb{R}\times\mathbb{R}} \left(\chi|a-b|^{1-m} + \frac{|a-b|^2}{2}\right)\left\langle \psi''_{ac}(t,(a,b))^{-\gamma}\right\rangle \bar{\rho}_k(a)\bar{\rho}_k(b)\, dadb\,.$$

Choosing $\gamma = m - 1$, the functional $\mathcal{F}_{k,\mathbf{resc}}[\rho]$ rewrites similarly to the proof of Theorem 3.6:

$$\begin{aligned}
\mathcal{F}_{k,\mathbf{resc}}[\rho] &= \frac{1}{m-1}\int_{\mathbb{R}} (\psi''_{ac}(a))^{1-m}\bar{\rho}(a)^m\,da \\
&\quad + \frac{\chi}{1-m}\iint_{\mathbb{R}\times\mathbb{R}} \left(\frac{\psi'(a)-\psi'(b)}{a-b}\right)^{1-m} |a-b|^{1-m}\bar{\rho}(a)\bar{\rho}(b)\,dadb \\
&\quad + \frac{1}{4}\iint_{\mathbb{R}\times\mathbb{R}} \left(\frac{\psi'(a)-\psi'(b)}{a-b}\right)^{2} |a-b|^{2}\bar{\rho}(a)\bar{\rho}(b)\,dadb \\
&= \frac{1}{m-1}\iint_{\mathbb{R}\times\mathbb{R}} \left\langle \psi''_{ac}([a,b])^{1-m}\right\rangle \left(\chi|a-b|^{1-m} + \frac{|a-b|^2}{2}\right)\bar{\rho}(a)\bar{\rho}(b)\,dadb \\
&\quad - \frac{1}{m-1}\iint_{\mathbb{R}\times\mathbb{R}} \Big(\left\langle \psi''([a,b])\right\rangle^{1-m}\chi|a-b|^{1-m} \\
&\qquad\qquad + \left\langle \psi''([a,b])\right\rangle^{2}(1-m)\frac{|a-b|^2}{4}\Big)\bar{\rho}(a)\bar{\rho}(b)\,dadb
\end{aligned}$$

Now, using the variant of Jensen's inequality (3.20) of Lemma 3.14, this simplifies to

$$\mathcal{F}_{k,\mathbf{resc}}[\rho] \geqslant \frac{m+1}{m-1}\iint_{\mathbb{R}\times\mathbb{R}} \frac{|a-b|^2}{4}\bar{\rho}(a)\bar{\rho}(b)\,dadb = \frac{m+1}{2(m-1)}\int_{\mathbb{R}} |a|^2\bar{\rho}(a)\,da = \mathcal{F}_{k,\mathbf{resc}}[\bar{\rho}]\,.$$

Here, we used identity (2.11) for the final step. Again equality holds true if and only if ψ'' is identically one. □

Remark 3.15 (Sign of the Rescaled Free Energy). *In fact, $\mathcal{F}_{k,resc}[\bar{\rho}] \leqslant 0$. Choosing $\rho_\lambda(x) = \lambda\bar{\rho}(\lambda x)$ a dilation of the stationary state, we obtain thanks to the homogeneity properties of the energy functional,*

$$\lambda^{-k}\mathcal{U}_m[\bar{\rho}] + \lambda^{-k}\mathcal{W}_k[\bar{\rho}] + \lambda^{-2}\mathcal{V}[\bar{\rho}] = \mathcal{F}_{k,resc}[\rho_\lambda] \geqslant \mathcal{F}_{k,resc}[\bar{\rho}],$$

and so we conclude that $\mathcal{F}_{k,resc}[\bar{\rho}]$ must be non-positive for any stationary state $\bar{\rho} \in \mathcal{Y}_2$ by taking the limit $\lambda \to \infty$.

Corollary 3.16 (Uniqueness). *Let $k \in \left(0, \frac{2}{3}\right)$ and $m = 1 - k$. For any $\chi > 0$, there exists a unique stationary state with second and kth moment bounded to equation (2.7), and a unique minimiser for $\mathcal{F}_{k,resc}$ in $\mathcal{Y}_{2,k}$.*

Proof. By Theorem 2.9 in Chapter 2 there exists a minimiser of $\mathcal{F}_{k,\mathbf{resc}}$ in $\mathcal{Y}_{2,k}$, which is a stationary state of equation (2.7). Assume (2.7) admits two stationary states $\bar{\rho}_1$ and $\bar{\rho}_2$ in $\mathcal{Y}_{2,k}$. By Theorem 3.13, $\mathcal{F}_{k,\mathbf{resc}}[\bar{\rho}_1] = \mathcal{F}_{k,\mathbf{resc}}[\bar{\rho}_2]$ and so $\bar{\rho}_1 = \bar{\rho}_2$. □

Corollary 3.17 (Self-Similar Profiles). *Let $k \in (0,1)$ and $m = 1 - k$. For any $\chi > 0$, if u is a symmetric stationary state of the rescaled equation (2.7), then there exists a self-similar solution to (1.4) given by*

$$\rho(t,x) = ((2-k)t+1)^{\frac{1}{k-2}}\; u\left(((2-k)t+1)^{\frac{1}{k-2}}\,x\right).$$

4 Long-time asymptotics

This part is devoted to the asymptotic behaviour of solutions, adapting the above computations, ensuring *e.g.* uniqueness of the functional ground state, at the level of the gradient flow dynamics. We will demonstrate convergence towards these ground states in Wasserstein distance under certain conditions, in some cases with an explicit rate. Our results rely on the fact that there is a simple expression for the Wasserstein distance in one dimension. Therefore, our methodology cannot be extended to dimension two or more so far except possibly under radial symmetry assumptions.

We assume here that solutions are smooth enough so that the operations in this section are well-defined. Firstly, we require the mean-field potential gradient $\partial_x S_k(t,x)$ to be well-defined for all $t > 0$ which is guaranteed if $\rho(t,x)$ has at least the same regularity at each time $t > 0$ as provided by Definition 2.1 for stationary states. From now on, we assume that solutions of (1.4) satisfy $\rho(t,x) \in C\left([0,T], C^{0,\alpha}_{loc}(\mathbb{R}) \cap \mathcal{Y} \cap L^\infty(\mathbb{R})\right)$ with $\alpha \in (-k, 1)$.
Secondly, certain computations in this section remain formal unless the convex Brenier map ψ satisfying $\rho(t,x)dx = \partial_x\psi(t,x)\#\bar{\rho}_k(x)dx$ is regular enough. As shown in Chapter 2 for the fast diffusion regime $k > 0$, stationary states are everywhere positive, and thus ψ'' is absolutely continuous. However, in the porous medium regime $k < 0$, stationary states are compactly supported, and therefore, the following computations remain formal depending on the regularity and properties of the solutions of the evolution problem. From now on, we assume that ψ'' is absolutely continuous whenever we talk about solutions of the evolution problems (1.4) or (2.7).

In order to analyse the asymptotic behaviour of solutions, we make use of the fact that one can find an upper bound on the disspation of the Wasserstein-2 distance $\mathbf{W}$ in terms of the push-forward between two absolutely continuous probability measures.

Theorem 4.1. *Let $\bar{\rho}(x)$ be a stationary state to equation (1.4). For any solution $\rho(t,x)$ of (1.4), let $\phi(t,x)$ denote the convex Brenier map that pushes forward $\bar{\rho}(x)$ onto $\rho(t,x)$:*

$$\bar{\rho}(x)\,dx = \partial_x\phi(t,x)\#\rho(t,x)\,dx\,.$$

Then

$$\frac{d}{dt}\mathbf{W}(\rho(t),\bar{\rho})^2 \leqslant \int_{\mathbb{R}^N} \big\langle (\partial_x\phi(t,x) - x)\ ,\ \partial_x\mathcal{T}_{m,k}[\rho](t,x)\big\rangle \rho(t,x)\,dx \tag{4.21}$$

with the first variation $\mathcal{T}_{m,k}$ given by (2.20) in Chapter 1. Identity (4.21) also holds true with equality under the additional assumption that the velocity field $\nabla\mathcal{T}_{m,k}[\rho](t,\cdot)$ is locally Lipschitz.

For a detailed proof, see [297, Theorem 23.9]. A similar identity can be obtained for the rescaled equation (2.7).

4.1 Porous medium asymptotics

4.1.1 The critical case $\chi = \chi_c(k)$

In the critical case, the set of global minimisers coincides with the set of stationary states of equation (1.4) (Chapter 2 Theorem 2.6), but as we will see, it is not clear whether this set is a global attractor in the Wasserstein sense or not. We will prove here a convergence result under some conditions, which provides a dynamical proof of uniqueness up to dilations. Recall that in the fair-competition regime, we have $\mathcal{F}_k[\rho_\lambda] = \lambda^{-k}\mathcal{F}_k[\rho]$ for any dilation $\rho_\lambda(x) = \lambda\rho(\lambda x)$, $\lambda \in \mathbb{R}$ of a density $\rho \in \mathcal{Y}$, and so every stationary state provides in fact a family of stationary states by scale invariance. Given a density $\rho \in \mathcal{Y}$, $|x|^2\rho(x) \in L^1_+(\mathbb{R})$, we define the rescaling ρ_1 by

$$\rho_1(x) := \sigma\rho(\sigma x)\,, \quad \sigma^2 = \mathcal{V}[\rho] = \int_{\mathbb{R}} |x|^2\rho(x)\,dx\,, \tag{4.22}$$

and so any stationary state $\bar\rho_k$ with finite second moment has a dilation $\bar\rho_{k,1}$ with normalised second moment $\mathcal{V}[\bar\rho_{k,1}] = 1$. In particular, $\bar\rho_{k,1}$ provides a convenient representative for the family of stationary states formed by dilations of $\bar\rho_k$. Our aim here is to show that although uniqueness is degenerate due to homogeneity, we have a unique representative $\bar\rho_{k,1}$ with second moment equal to one. We will present here a discussion of partial results and open questions around the long-time behaviour of solutions in the critical case.

We first recall the logarithmic case ($m = 1, k = 0$), where the ground state is explicitly given by Cauchy's density $\bar\rho_0$ (1.3). The second momentum is thus infinite, and the Wasserstein distance to some ground state cannot be finite if the initial datum has finite second momentum. For a $\rho(t)$ satisfying (1.4), we have the estimate [62]

$$\frac{d}{dt}\mathbf{W}(\rho(t), \bar\rho_0)^2 \leqslant 0\,,$$

where equality holds if and only if $\rho(t)$ is a dilation of $\bar\rho_0$. This makes sense only if $\rho(0)$ has infinite second momentum, and is at finite distance from one of the equilibrium configurations. Notice that possible ground states (dilations of Cauchy's density) are all infinitely far from each other with respect to the Wasserstein distance,

$$\mathbf{W}\left(\rho_{\lambda_1}, \rho_{\lambda_2}\right)^2 = \frac{\left(\lambda_1 - \lambda_2\right)^2}{\lambda_1\lambda_2}\mathcal{V}[\bar\rho_0] = \infty.$$

Dynamics have been described in [40] when the initial datum has finite second momentum: the solution converges to a Dirac mass as time goes to $+\infty$. However, this does not hold true in the porous medium case $k \in (-1, 0)$, $m = 1 - k$, since stationary states are compactly supported by Corollary 3.9 in Chapter 2. The case where the initial data is at a finite distance from some dilation of a thick-tail stationary state has been investigated in [37] in two dimensions.

Proposition 4.2. *For $\chi = \chi_c(k)$, let $\rho(t)$ satisfy (1.4) in the porous medium case $k \in (-1,0)$ and $m = 1-k$. If $\bar\rho_k$ is a stationary state of (1.4), then the evolution of the Wasserstein distance to equilibrium can be estimated by*

$$\frac{d}{dt}\mathbf{W}(\rho(t),\bar\rho_k)^2 \leqslant (m-1)\mathcal{F}_k[\rho(t)]\,, \tag{4.23}$$

where equality holds if and only if $\rho(t)$ is a dilation of $\bar\rho_k$.

Proof. Let ϕ be the convex Brenier map such that $\bar\rho_k(x)dx = \partial_x\phi(t,x)\#\rho(t,x)dx$ and denote by $\partial_x\psi(t,x)$ the reverse transport map, $\partial_x\phi(t,\partial_x\psi(t,a)) = a$. By (4.21), following [62, 295] and using the regularity of $\rho(t,x)$ together with the argument as in the proof of Lemma 2.6 that allows for the singularity of the mean-field potential gradient to disappear, we have

$$\begin{aligned}
\frac12\frac{d}{dt}\mathbf{W}(\rho(t),\bar\rho_k)^2 &\leqslant \int_{\mathbb{R}}(\phi'(t,x)-x)\left(\frac{\partial}{\partial x}\left(\frac{m}{m-1}\rho(t,x)^{m-1}\right)+2\chi_c(k)\partial_x S_k(t,x)\right)\rho(t,x)\,dx\\
&= -\int_{\mathbb{R}}\phi''(t,x)\rho(t,x)^m\,dx\\
&\quad+\chi_c(k)\iint_{\mathbb{R}\times\mathbb{R}}\left(\frac{\phi'(t,x)-\phi'(t,y)}{x-y}\right)|x-y|^k\rho(t,x)\rho(t,y)\,dxdy\\
&\quad+(m-1)\mathcal{F}_k[\rho(t)]\\
&= -\int_{\mathbb{R}}\big(\psi''(t,a)\big)^{-1}\big(\psi''(t,a)\big)^{1-m}\bar\rho_k(a)^m\,da\\
&\quad+\chi_c(k)\iint_{\mathbb{R}\times\mathbb{R}}\left(\frac{\psi'(t,a)-\psi'(t,b)}{a-b}\right)^{k-1}|a-b|^k\bar\rho_k(a)\bar\rho_k(b)\,dadb\\
&\quad+(m-1)\mathcal{F}_k[\rho(t)]
\end{aligned}$$

to finally conclude that

$$\begin{aligned}
\frac12\frac{d}{dt}\mathbf{W}(\rho(t),\bar\rho_k)^2 &\leqslant -\int_{\mathbb{R}}\big(\psi''(t,a)\big)^{-m}\bar\rho_k(a)^m\,da\\
&\quad+\chi_c(k)\iint_{\mathbb{R}\times\mathbb{R}}\int_{s=0}^1\big(\psi''(t,[a,b]_s)\big)^{-m}|a-b|^k\bar\rho_k(a)\bar\rho_k(b)\,dsdadb\\
&\quad+(m-1)\mathcal{F}_k[\rho(t)]\,,
\end{aligned}$$

where we have crucially used the convexity of $(\cdot)^{-m}$ in the last step. We conclude as for the proof of Theorem 3.2 thanks to the characterisation (2.9). □

By definition of the critical value $\chi_c(k)$, the functional $\mathcal{F}_k$ is everywhere non-negative. It vanishes if and only if ρ is a dilation of some critical density. Therefore we cannot deduce from (4.23) that the density $\rho(t)$ converges to some dilation of $\bar\rho_k$. However, we can show convergence in Wasserstein distance if we assume a rather restrictive uniform $W^{2,\infty}(\mathbb{R})$-stability estimate on the Brenier map ψ connecting the solution density to the stationary state:

$$\psi''(t,x)\in L^\infty\left(\mathbb{R}_+,L^\infty(\mathbb{R})\right)\quad\text{such that}\quad ||\psi''||_{L^\infty(\mathbb{R}_+,L^\infty(\mathbb{R}))}\leqslant 1+\frac1m\,. \tag{4.24}$$

This condition is equivalent to

$$\forall t>0 \quad \big\langle \psi''(t,(x,y))\big\rangle := \int_0^1 \psi''(t,[x,y]_s)\,ds \in \left(0, 1+\frac{1}{m}\right], \quad \text{for a.e. } x,y\in\mathbb{R}\,, \quad \forall t>0\,. \tag{4.25}$$

where $[x,y]_s := (1-s)x + sy$. If we want to show convergence of a solution $\rho(t)$ to a stationary state $\bar\rho_k$ in Wasserstein distance, we need to investigate quantities that are comparable.

Proposition 4.3. *For $\chi = \chi_c(k)$, let $\bar\rho_k$ be a stationary state of (1.4) in the porous medium case $k\in(-1,0)$, $m = 1-k$. Let $\rho(t)$ be a solution such that*

$$\mathcal{V}_\infty := \lim_{t\to\infty} \mathcal{V}[\rho(t)] < \infty\,,$$

and we denote by ψ the transport map from $\bar\rho_k$ onto the solution,

$$\rho(t,x)dx = \partial_x\psi(t,x)\#\bar\rho_k(x)dx\,.$$

If ψ satisfies the uniform stability estimate (4.24), then

$$\frac{d}{dt}\mathbf{W}(\rho(t),\bar\rho_k)^2 \leqslant 0\,,$$

where equality holds if and only if $\rho(t)$ is a dilation of $\bar\rho_k$.

Proof. Note that $\mathcal{V}[\bar\rho_k] < \infty$ since $\bar\rho_k$ is compactly supported (Chapter 2 Corollary 3.9). We compute the evolution of the Wasserstein distance along the gradient flow, denoting by ϕ the inverse transport map, $\partial_x\phi(t,x) = \partial_x\psi(t,x)^{-1}$, we proceed as in Proposition 4.2:

$$\begin{aligned}
&\frac12\frac{d}{dt}\mathbf{W}(\rho(t),\bar\rho_k)^2\\
&\quad\leqslant -\int_{\mathbb{R}} \phi''(t,x)\rho(t,x)^m\,dx + \chi_c(k)\iint_{\mathbb{R}\times\mathbb{R}}\left(\frac{\phi'(t,x)-\phi'(t,y)}{x-y}\right)|x-y|^k\rho(t,x)\rho(t,y)\,dxdy\\
&\qquad+\int_{\mathbb{R}}\rho(t,x)^m\,dx - \chi_c(k)\iint_{\mathbb{R}\times\mathbb{R}}|x-y|^k\rho(t,x)\rho(t,y)\,dxdy\,,
\end{aligned}$$

which we can rewrite in terms of the transport map ψ' as

$$\begin{aligned}
&\frac12\frac{d}{dt}\mathbf{W}(\rho(t),\bar\rho_k)^2\\
&\quad\leqslant -\int_{\mathbb{R}}\big(\psi''(t,a)\big)^{-m}\bar\rho_k(a)^m\,da + \chi_c(k)\iint_{\mathbb{R}\times\mathbb{R}}\big\langle\psi''(t,(a,b))\big\rangle^{-m}|a-b|^{1-m}\bar\rho_k(a)\bar\rho_k(b)\,dadb\\
&\qquad+\int_{\mathbb{R}}\big(\psi''(t,a)\big)^{1-m}\bar\rho_k(a)^m\,da - \chi_c(k)\iint_{\mathbb{R}\times\mathbb{R}}\big\langle\psi''(t,(a,b))\big\rangle^{1-m}|a-b|^{1-m}\bar\rho_k(a)\bar\rho_k(b)\,dadb\,.
\end{aligned}$$

Using the characterisation (2.9), we obtain for any $\gamma\in\mathbb{R}$,

$$\int_{\mathbb{R}}\big(\psi''(t,a)\big)^{-\gamma}\bar\rho_k(a)^m\,da = \chi_c(k)\iint_{\mathbb{R}\times\mathbb{R}}\big\langle\psi''(t,(a,b))^{-\gamma}\big\rangle|a-b|^{1-m}\bar\rho_k(a)\bar\rho_k(b)\,dadb\,.$$

Hence, the dissipation of the distance to equilibrium can be written as

$$\frac{1}{2}\frac{d}{dt}\mathbf{W}(\rho(t),\bar\rho_k)^2 \leqslant \chi_c(k)\iint\limits_{\mathbb{R}\times\mathbb{R}} |a-b|^k\Big(-\big\langle \psi''(t,(a,b))^{-m}\big\rangle + \big\langle \psi''(t,(a,b))^{1-m}\big\rangle \\ + \big\langle \psi''(t,(a,b))\big\rangle^{-m} - \big\langle \psi''(t,(a,b))\big\rangle^{1-m}\Big)\bar\rho_k(a)\bar\rho_k(b)\,dadb\,.$$

We now investigate the sign of the microscopic functional $J_m[u]$ defined for non-negative functions $u:(0,1)\to\mathbb{R}_+$ by

$$J_m[u] := -\big\langle u^{-m}\big\rangle + \big\langle u^{1-m}\big\rangle + \big\langle u\big\rangle^{-m} - \big\langle u\big\rangle^{1-m}\,.$$

The first two terms can be written as

$$-\big\langle u^{-m}\big\rangle + \big\langle u^{1-m}\big\rangle = -\alpha\big\langle u\big\rangle^{-m} + \beta\big\langle u\big\rangle^{1-m}\,,$$

where $\alpha = \big\langle u\big\rangle^{m}\big\langle u^{-m}\big\rangle$ and $\beta = \big\langle u\big\rangle^{m-1}\big\langle u^{1-m}\big\rangle$. By Jensen's inequality we have $\alpha\geqslant 1$, $\beta\geqslant 1$, and by interpolation we have $\beta\leqslant\alpha^{m/(m+1)}$. Therefore,

$$J_m[u]\leqslant j_m(\langle u\rangle) = \max_{\alpha\geqslant 1}\Big\{-\alpha\big\langle u\big\rangle^{-m} + \alpha^{m/(m+1)}\big\langle u\big\rangle^{1-m}\Big\} + \big\langle u\big\rangle^{-m} - \big\langle u\big\rangle^{1-m}\,.$$

We can compute explicitly the maximal value in the above expression. The first order condition gives

$$\alpha_{max} := \left(\frac{m}{m+1}\big\langle u\big\rangle\right)^{m+1}\,.$$

Since the function

$$g(\alpha) := -\alpha\big\langle u\big\rangle^{-m} + \alpha^{m/(m+1)}\big\langle u\big\rangle^{1-m}$$

achieves its maximum at $\alpha_{max}\leqslant 1$ for $\big\langle u\big\rangle\leqslant 1+1/m$ and is strictly decreasing for $\alpha>\alpha_{max}$, we have

$$\max_{\alpha\geqslant 1} g(\alpha) = g(1), \qquad \text{for } \big\langle u\big\rangle\leqslant 1+1/m$$

and so we conclude $j_m(\langle u\rangle)=0$ for $\big\langle u\big\rangle\leqslant 1+1/m$. Therefore

$$\begin{aligned}\frac{1}{2}\frac{d}{dt}\mathbf{W}(\rho(t),\bar\rho_k)^2 &\leqslant \chi_c(k)\iint\limits_{\mathbb{R}\times\mathbb{R}} |a-b|^k J_m[\psi''(t,(a,b))]\bar\rho_k(a)\bar\rho_k(b)\,dadb\\ &\leqslant \chi_c(k)\iint\limits_{\mathbb{R}\times\mathbb{R}} |a-b|^k j_m[\big\langle\psi''(t,(a,b))\big\rangle]\bar\rho_k(a)\bar\rho_k(b)\,dadb = 0\end{aligned}$$

thanks to the stability estimate (4.25). To investigate the equality cases, note that $\beta=\alpha^{m/(m+1)}$ if and only if $u\equiv 1$ (looking at the equality cases in Hölder's inequality). Moreover, $\langle u\rangle\in(0,1+1/m]$ implies

$$J_m[u]\leqslant -\alpha\big\langle u\big\rangle^{-m} + \alpha^{m/(m+1)}\big\langle u\big\rangle^{1-m} + \big\langle u\big\rangle^{-m} - \big\langle u\big\rangle^{1-m}\leqslant 0\,,$$

using $\alpha\geqslant 1$. Hence, if $J_m[u]=0$, then we must have $\beta=\alpha^{m/(m+1)}$, and so $u\equiv 1$. The converse is trivial by substituting into the expression for $J_m[u]$. Taking u to be the Brenier map ψ'', we conclude that $\frac{d}{dt}\mathbf{W}(\rho(t),\bar\rho_k)^2=0$ if and only if $\rho=\bar\rho_k$. □

The utility of the previous result for understanding the asymptotic behaviour of solutions depends of course on the set of initial data for which solutions satisfy the stability estimate (4.24) at all times. This set is rather difficult to characterise, and we do not know its size.

Let us now explore what we can say about the long-time behaviour of solutions in the general case. The first insight consists in calculating the evolution of the second moment. It follows from homogeneity that

$$\frac{d}{dt}\mathcal{V}[\rho(t)] = 2(m-1)\mathcal{F}_k[\rho(t)]\,. \tag{4.26}$$

Identity (4.26) implies that the second moment is non-decreasing, and it converges to some value $\mathcal{V}_\infty \in \mathbb{R}_+ \cup \{+\infty\}$. Following [39] we discuss the dichotomy of $\mathcal{V}_\infty < +\infty$ and $\mathcal{V}_\infty = +\infty$. Let $\rho(t) \in \mathcal{Y}$ be a solution of (1.4) such that $|x|^2\rho(t) \in L^1_+(\mathbb{R})$ for all $t > 0$. Let $\bar\rho_k$ be a stationary state of (1.4) according to Definition 2.1. Note that $\mathcal{V}[\bar\rho_k] < \infty$ since $\bar\rho_k$ is compactly supported by Corollary 3.9 in Chapter 2.

Case 1: $\mathcal{V}_\infty < +\infty$ If the second moment $\mathcal{V}[\rho(t)]$ converges to $\mathcal{V}_\infty < +\infty$, then we deduce from (4.26) that the energy functional $\mathcal{F}_k[\rho(t)]$ converges to $\mathcal{F}_k[\bar\rho_k] = 0$ since $\mathcal{F}_k$ is non-increasing along trajectories. This is however not enough to conclude convergence of $\rho(t)$ to $\bar\rho_k$ and the question remains open. Note further that in order to have convergence, we need to choose a dilation of $\bar\rho_k$ with second moment equal to $\mathcal{V}_\infty$. For any dilation $\bar\rho_k^\lambda$ of $\bar\rho_k$, we have $\mathcal{V}[\bar\rho_k^\lambda] = \mathcal{V}[\bar\rho_k]/\lambda^2$, and so there exists a unique λ_* such that $\mathcal{V}[\bar\rho_k^{\lambda_*}] = \mathcal{V}_\infty$. This would be the natural candidate for the asymptotic behaviour of the solution $\rho(t)$.

Case 2: $\mathcal{V}_\infty = +\infty$ If the second moment $\mathcal{V}[\rho(t)]$ diverges to $\mathcal{V}_\infty = +\infty$ however, the discussion is more subtle and we can give some further intuition. First of all, let us remark that one has to seek a convergence other than in Wasserstein distance since $\infty = \mathcal{V}_\infty \neq \mathcal{V}[\bar\rho_k] < \infty$. We can not exclude this case a priori however since a convergence in another sense may be possible in principle. We use the homogeneity properties of the flow to derive refined inequalities. To do this, we renormalise the density as in (4.22), but now with a time dependency in σ:

$$\hat\rho(t,y) = \sigma(t)\rho(t,\sigma(t)y)\,, \quad \sigma(t)^2 = \mathcal{V}[\rho(t)] = \int_{\mathbb{R}} |x|^2\rho(t,x)\,dx\,. \tag{4.27}$$

Then $\hat\rho$ satisfies the equation

$$\begin{aligned}\partial_t\hat\rho(t,y) =& \sigma(t)\partial_t\rho(t,x) + \dot\sigma(t)\left(\rho(t,x) + x\cdot\partial_x\rho(t,x)\right)\\ =& \sigma(t)\left\{\sigma(t)^{-2-m}\partial_{yy}\hat\rho(t,y)^m + 2\chi_c(k)\sigma(t)^{-3+k}\partial_y\left(\hat\rho(t,y)\partial_y(W_k(y)*\hat\rho(t,y))\right)\right\}\\ &+ \frac{\dot\sigma(t)}{\sigma(t)}\left(\hat\rho(t,y) + y\cdot\partial_y\hat\rho(t,y)\right)\,.\end{aligned}$$

By homogeneity of $\mathcal{F}_k$, we have

$$\mathcal{F}_k[\rho(t)] = \sigma(t)^{1-m}\mathcal{F}_k[\hat{\rho}(t)]\,, \tag{4.28}$$

and so it follows from (4.26) that $2\sigma(t)\dot{\sigma}(t) = 2(m-1)\mathcal{F}_k[\rho(t)] = 2(m-1)\sigma(t)^{1-m}\mathcal{F}_k[\hat{\rho}(t)]$. We deduce

$$\begin{aligned}\partial_t\hat{\rho}(t,y) =&\sigma(t)^{-1-m}\left\{\partial_{yy}\hat{\rho}(t,y)^m + 2\chi_c(k)\partial_y\left(\hat{\rho}(t,y)\partial_y(W_k(y)*\hat{\rho}(t,y))\right)\right\}\\ &+\sigma(t)^{-1-m}(m-1)\mathcal{F}_k[\hat{\rho}(t)]\left(\hat{\rho}(t,y)+y\cdot\partial_y\hat{\rho}(t,y)\right)\,.\end{aligned}$$

Alternatively, we get

$$\begin{aligned}\frac{d}{dt}\mathcal{F}_k[\hat{\rho}(t)] &= \frac{d}{dt}\left\{\sigma(t)^{m-1}\mathcal{F}_k[\rho(t)]\right\}\\ &= -\sigma(t)^{m-1}\int_{\mathbb{R}}\rho(t,x)\left|\partial_x\left(\frac{m}{m-1}\rho(t,x)^{m-1}+2\chi_c(k)W_k(x)*\rho(t,x)\right)\right|^2\,dx\\ &\quad+(m-1)^2\sigma(t)^{m-2}\sigma(t)^{-m}\mathcal{F}_k[\hat{\rho}(t)]\mathcal{F}_k[\rho(t)]\\ &= \sigma(t)^{-1-m}\mathcal{G}[\hat{\rho}]\,,\end{aligned} \tag{4.29}$$

where

$$\mathcal{G}[\hat{\rho}] := -\int_{\mathbb{R}}\left|\partial_y\left(\frac{m}{m-1}\hat{\rho}(y)^{m-1}+2\chi_c(k)W_k(y)*\hat{\rho}(y)\right)\right|^2\hat{\rho}(y)\,dy + (m-1)^2\mathcal{F}_k[\hat{\rho}]^2\,.$$

Proposition 4.4. *The functional $\mathcal{H}$ defined by $\mathcal{H}[\rho] := \mathcal{G}[\hat{\rho}]$ on $\mathcal{Y}_2$ is zero-homogeneous, and everywhere non-positive. Moreover, $\mathcal{H}[\rho] = 0$ if and only if ρ is a stationary state of equation (1.4).*

Proof. Homogeneity follows from the very definition of $\mathcal{H}$. Non-positivity is a consequence of the Cauchy-Schwarz inequality:

$$\begin{aligned}|(m-1)\mathcal{F}_k[\hat{\rho}]|^2 &= \left|-\int_{\mathbb{R}} y\cdot\partial_y\left(\frac{m}{m-1}\hat{\rho}(y)^{m-1}+2\chi_c(k)W_k(y)*\hat{\rho}(y)\right)\hat{\rho}(y)\,dy\right|^2\\ &\leqslant\left(\int_{\mathbb{R}}|y|^2\hat{\rho}(y)\,dy\right)\left(\int_{\mathbb{R}}\left|\partial_y\left(\frac{m}{m-1}\hat{\rho}(y)^{m-1}+2\chi_c(k)W_k(y)*\hat{\rho}(y)\right)\right|^2\hat{\rho}(y)\,dy\right)\,.\end{aligned} \tag{4.30}$$

If ρ is a stationary state of equation (1.4), so is $\hat{\rho}$ and it follows from (4.29) that $\mathcal{G}[\hat{\rho}] = 0$. Conversely, if $\mathcal{G}[\hat{\rho}] = 0$, then we can achieve equality in the Cauchy-Schwarz inequality (4.30) above, and so the two functions y and

$$\partial_y\left(\frac{m}{m-1}\hat{\rho}(y)^{m-1}+2\chi_c(k)W_k(y)*\hat{\rho}(y)\right)$$

are proportional to each other. In other words, there exists a constant $\hat{\pi}$ such that for all $y\in\mathbb{R}$,

$$\partial_y\left(\frac{m}{m-1}\hat{\rho}(y)^{m-1}+2\chi_c(k)W_k(y)*\hat{\rho}(y)\right)+\hat{\pi}y = 0\,. \tag{4.31}$$

This equation is the Euler-Langrange condition of the gradient flow given by the energy functional $\mathcal{F}_k + \hat{\pi}\mathcal{V}$:

$$\partial_t u = \partial_y \left(u \, \partial_y \left(\frac{\delta}{\delta u} \left(\mathcal{F}_k + \hat{\pi}\mathcal{V} \right)[u] \right) \right) , \tag{4.32}$$

and since $\hat{\rho}$ satisfies (4.31), it is a stationary state of equation (4.32). Testing this equation against $y\hat{\rho}(y)$, we obtain

$$\hat{\pi} = (m-1)\mathcal{F}_k[\hat{\rho}] \geqslant 0 .$$

Non-negativity of $\hat{\pi}$ follows from the variant of the HLS inequality Theorem 3.1 since $\mathcal{F}_k[\rho] \geqslant 0$ for any $\rho \in \mathcal{Y}$ if $\chi = \chi_c(k)$. We will show $\hat{\pi} = 0$ by contradiction. Assume $\hat{\pi} > 0$. Applying Theorem 3.6 for $\mathcal{F}_k[\cdot] + \hat{\pi}\mathcal{V}[\cdot]$ instead of $\mathcal{F}_k[\cdot] + \frac{1}{2}\mathcal{V}[\cdot]$, we deduce that $\hat{\rho}$ is a minimiser of the rescaled energy $\mathcal{F}_k[\cdot] + \hat{\pi}\mathcal{V}[\cdot]$. In particular, this means that we have for any $u \in \mathcal{Y}_2$,

$$\mathcal{F}_k[u] + \hat{\pi}\mathcal{V}[u] \geqslant \mathcal{F}_k[\hat{\rho}] + \hat{\pi}\mathcal{V}[\hat{\rho}] = \hat{\pi}/(m-1) + \hat{\pi} > \hat{\pi} .$$

However, Proposition 3.4(i) and Corollary 3.8 in Chapter 2 provide a global minimiser $\bar{\rho}_{k,1} \in \mathcal{Y}_2$ with unit second moment for $\mathcal{F}_k$, which is also a stationary state by Theorem 3.14 in Chapter 2. Then choosing $u = \bar{\rho}_{k,1}$ in the above inequality yields $\mathcal{F}_k[\bar{\rho}_{k,1}] + \hat{\pi}\mathcal{V}[\bar{\rho}_{k,1}] = 0 + \hat{\pi}$, a contradiction. Therefore we necessarily have $\hat{\pi} = 0$ and so $\mathcal{F}_k[\hat{\rho}] = 0$. By (4.28), $\mathcal{F}_k[\rho] = 0$ and this implies that ρ is a global minimiser of $\mathcal{F}_k$ by Theorem 3.1, and consequently it is a stationary state of (1.4) by Theorem 2.6 in Chapter 2. □

It would be desirable to be able to show that $\mathcal{H}[\rho(t)] \to \mathcal{H}[\bar{\rho}_{k,1}]$ as $t \to \infty$ to make appropriate use of the new energy functional $\mathcal{H}$. But even then, similar to the first case, we are lacking a stability result for $\mathcal{H}$ to prove that in fact $\hat{\rho}(t)$ converges to $\bar{\rho}_{k,1}$. Here, in addition, we do not know at which rate the second moment goes to $+\infty$.

We conjecture that only the first case $\mathcal{V}_\infty < +\infty$ is admissible. The motivation for this claim is the following: $\mathcal{F}$ and $\mathcal{H}$ have both constant signs, and vanish only when $\hat{\rho} = \bar{\rho}_{k,1}$. If the stability inequality

$$\eta\mathcal{F}_k[\hat{\rho}] \leqslant -\mathcal{H}[\rho], \quad \forall \rho \tag{4.33}$$

were satisfied for some $\eta > 0$, then we would be able to prove that $\mathcal{V}_\infty < +\infty$. To see this, we derive a second-order differential inequality for $\omega(t) := \sigma(t)^{m+1}$. We have

$$\dot{\omega}(t) = (m+1)\sigma(t)^m \dot{\sigma}(t) = (m+1)(m-1)\mathcal{F}_k[\hat{\rho}(t)] \geqslant 0 ,$$

and so by (4.29),

$$\ddot{\omega}(t) = (m+1)(m-1)\omega(t)^{-1}\mathcal{H}[\rho(t)] \leqslant 0 .$$

Here, non-positivity of $\ddot{\omega}(t)$ follows from Proposition 4.4. Therefore, the stability estimate (4.33), if true, would imply that $\ddot{\omega}(t) \leqslant -\eta\omega(t)^{-1}\dot{\omega}(t)$, hence

$$\dot{\omega}(t) \leqslant C - \eta \log \omega(t).$$

Consequently, $\omega(t)$ would be bounded, and so we arrive at a contradiction with the assumption $\mathcal{V}_\infty = +\infty$.

4.1.2 The sub-critical case $\chi < \chi_c$

We know that in the logarithmic case ($m = 1, k = 0$), solutions to (1.4) converge exponentially fast towards a unique self-similar profile as $t \to \infty$, provided that the parameter χ is sub-critical ($\chi < 1$) [62]. A similar argument works in the porous medium regime $k \in (-1, 0)$ under certain regularity assumptions as we will show below. Surprisingly enough, convergence is uniform as the rate of convergence does not depend on the parameter χ. In particular, it was shown in [62] for $k = 0$ that we have uniform convergence in Wasserstein distance of any solution $\rho(t)$ for the rescaled system (2.7) to the equilibrium distribution $\bar{\rho}_0$ of (2.7),

$$\frac{d}{dt}\mathbf{W}(\rho(t), \bar{\rho}_0)^2 \leqslant -2\mathbf{W}(\rho(t), \bar{\rho}_0)^2 .$$

A similar result has been obtained in two dimension in [71].

Studying the long-time behaviour of the system in the porous medium case $k < 0$ is more subtle than the logarithmic case and we cannot deduce exponentially fast convergence from our calculations without assuming a uniform stability estimate, which coincides with (4.25). But as in the critical case, we do not know how many initial data actually satisfy this condition. Note also that due to the additional confining potential, homogeneity has been broken, and so we cannot renormalise the second moment of minimisers as we did in the critical case. As in the critical case, stationary states of the rescaled equation (2.7) are compactly supported by Corollary 3.9 in Chapter 2.

Proposition 4.5. *For sub-critical interaction strength $0 < \chi < \chi_c(k)$, let $\rho(t)$ be a solution to (2.7) in the porous medium case $k \in (-1, 0)$, $m = 1 - k$ and $\bar{\rho}_k$ a stationary state of (2.7). If the transport map ψ given by $\rho(t, x)dx = \partial_x\psi(t, x)\#\bar{\rho}_k(x)dx$ satisfies the uniform stability estimate (4.24), then*

$$\frac{d}{dt}\mathbf{W}(\rho(t), \bar{\rho}_k)^2 \leqslant -2\mathbf{W}(\rho(t), \bar{\rho}_k)^2 ,$$

where equality holds if and only if $\rho(t)$ is a dilation of $\bar{\rho}_k$. It follows that

$$\lim_{t\to\infty} \mathcal{V}[\rho(t)] = \mathcal{V}[\bar{\rho}_k] .$$

Proof. We compute the evolution of the Wasserstein distance along the gradient flow similar to the proof of Proposition 4.3, denoting by ϕ the inverse transport map, $\partial_x \phi(t,x) = \partial_x \psi(t,x)^{-1}$,

$$\begin{aligned}
&\frac{1}{2}\frac{d}{dt}\mathbf{W}(\rho(t),\bar\rho_k)^2 \\
&\leqslant -\int_{\mathbb{R}} \phi''(t,x)\rho(t,x)^m\,dx + \chi \iint_{\mathbb{R}\times\mathbb{R}} \left(\frac{\phi'(t,x)-\phi'(t,y)}{x-y}\right)|x-y|^k\rho(t,x)\rho(t,y)\,dxdy \\
&\quad + \int_{\mathbb{R}} \rho(t,x)^m\,dx - \chi \iint_{\mathbb{R}\times\mathbb{R}} |x-y|^k\rho(t,x)\rho(t,y)\,dxdy \\
&\quad + \frac{1}{2}\iint_{\mathbb{R}\times\mathbb{R}} (\phi'(t,x)-\phi'(t,y))(x-y)\rho(t,x)\rho(t,y)\,dxdy - \int_{\mathbb{R}} |x|^2\rho(t,x)\,dx\,,
\end{aligned}$$

where we have used the fact that the centre of mass is zero at all times to double the variables:

$$\int_{\mathbb{R}} \phi'(t,x)x\rho(t,x)\,dx = \frac{1}{2}\iint_{\mathbb{R}\times\mathbb{R}} (\phi'(t,x)-\phi'(t,y))(x-y)\rho(t,x)\rho(t,y)\,dxdy\,.$$

This rewrites as follows in terms of the transport map ψ':

$$\begin{aligned}
&\frac{1}{2}\frac{d}{dt}\mathbf{W}(\rho(t),\bar\rho_k)^2 \\
&\leqslant -\int_{\mathbb{R}} \big(\psi''(t,a)\big)^{-m}\bar\rho_k(a)^m\,da + \chi\iint_{\mathbb{R}\times\mathbb{R}} \big\langle\psi''(t,(a,b))\big\rangle^{-m}|a-b|^{1-m}\bar\rho(a)\bar\rho_k(b)\,dadb \\
&\quad + \int_{\mathbb{R}} \big(\psi''(t,a)\big)^{1-m}\bar\rho_k(a)^m\,da - \chi\iint_{\mathbb{R}\times\mathbb{R}} \big\langle\psi''(t,(a,b))\big\rangle^{1-m}|a-b|^{1-m}\bar\rho_k(a)\bar\rho_k(b)\,dadb \\
&\quad + \frac{1}{2}\iint_{\mathbb{R}\times\mathbb{R}} \big\langle\psi''(t,(a,b))\big\rangle|a-b|^2\bar\rho_k(a)\bar\rho_k(b)\,dadb \\
&\quad - \frac{1}{2}\iint_{\mathbb{R}\times\mathbb{R}} \big\langle\psi''(t,(a,b))\big\rangle^2|a-b|^2\bar\rho_k(a)\bar\rho_k(b)\,dadb\,.
\end{aligned}$$

Using the characterisation (2.10), we obtain for any $\gamma\in\mathbb{R}$,

$$\begin{aligned}
&\int_{\mathbb{R}} \big(\psi''(t,a)\big)^{-\gamma}\bar\rho_k(a)^m\,da \\
&\qquad = \iint_{\mathbb{R}\times\mathbb{R}} \left(\chi|a-b|^{1-m} + \frac{|a-b|^2}{2}\right)\big\langle\psi''(t,(a,b))^{-\gamma}\big\rangle\bar\rho_k(a)\bar\rho_k(b)\,dadb\,.
\end{aligned}$$

Hence, the dissipation of the distance to equilibrium can be written as

$$\begin{aligned}
&\frac{1}{2}\frac{d}{dt}\mathbf{W}(\rho(t),\bar\rho_k)^2 \\
&\quad\leqslant \chi\iint_{\mathbb{R}\times\mathbb{R}} |a-b|^k\Big\{-\big\langle\psi''(t,(a,b))^{-m}\big\rangle + \big\langle\psi''(t,(a,b))^{1-m}\big\rangle \\
&\qquad\qquad + \big\langle\psi''(t,(a,b))\big\rangle^{-m} - \big\langle\psi''(t,(a,b))\big\rangle^{1-m}\Big\}\bar\rho_k(a)\bar\rho_k(b)\,dadb \\
&\quad + \frac{1}{2}\iint_{\mathbb{R}\times\mathbb{R}} |a-b|^2\Big\{-\big\langle\psi''(t,(a,b))^{-m}\big\rangle + \big\langle\psi''(t,(a,b))^{1-m}\big\rangle \\
&\qquad\qquad + \big\langle\psi''(t,(a,b))\big\rangle - \big\langle\psi''(t,(a,b))\big\rangle^2\Big\}\bar\rho_k(a)\bar\rho_k(b)\,dadb\,.
\end{aligned}$$

We now examinate the signs of the microscopic functionals $J_m[u]$ and $J_{m,2}[u]$ defined as follows for non-negative functions $u : (0,1) \to \mathbb{R}_+$,

$$J_m[u] := -\langle u^{-m} \rangle + \langle u^{1-m} \rangle + \langle u \rangle^{-m} - \langle u \rangle^{1-m}, \tag{4.34}$$

$$J_{m,2}[u] := -\langle u^{-m} \rangle + \langle u^{1-m} \rangle + \langle u \rangle - \langle u \rangle^{2}. \tag{4.35}$$

The first two terms in the functionals J_m and $J_{m,2}$ are common. We can rewrite them as

$$-\langle u^{-m} \rangle + \langle u^{1-m} \rangle = -\alpha \langle u \rangle^{-m} + \beta \langle u \rangle^{1-m},$$

where $\alpha = \langle u \rangle^{m} \langle u^{-m} \rangle$ and $\beta = \langle u \rangle^{m-1} \langle u^{1-m} \rangle$. By Jensen's inequality we have $\alpha \geqslant 1$, $\beta \geqslant 1$, and by interpolation we have $\beta \leqslant \alpha^{m/(m+1)}$. Therefore,

$$J_m[u] \leqslant j_m(\langle u \rangle) := \max_{\alpha \geqslant 1} g(\alpha) + \langle u \rangle^{-m} - \langle u \rangle^{1-m},$$

$$J_{m,2}[u] \leqslant j_{m,2}(\langle u \rangle) := \max_{\alpha \geqslant 1} g(\alpha) + \langle u \rangle - \langle u \rangle^{2},$$

where

$$g(\alpha) := -\alpha \langle u \rangle^{-m} + \alpha^{m/(m+1)} \langle u \rangle^{1-m}.$$

We can compute explicitly the maximal value of g, and as before the first order condition gives

$$\alpha_{max} = \left(\frac{m}{m+1} \langle u \rangle \right)^{m+1}.$$

It is straight forward to see that

$$\max_{\alpha \geqslant 1} g(\alpha) = g(1) \qquad \text{for } \langle u \rangle \leqslant 1 + 1/m,$$

and hence we obtain

$$j_m(\langle u \rangle) = \begin{cases} 0, & \text{if} \quad \langle u \rangle \leqslant 1 + \dfrac{1}{m} \\ \left(\dfrac{m}{m+1} \right)^{m} \dfrac{1}{m+1} \langle u \rangle + \langle u \rangle^{-m} - \langle u \rangle^{1-m}, & \text{if} \quad \langle u \rangle \geqslant 1 + \dfrac{1}{m} \end{cases}, \tag{4.36}$$

$$j_{m,2}(\langle u \rangle) = \begin{cases} -\langle u \rangle^{-m} + \langle u \rangle^{1-m} + \langle u \rangle - \langle u \rangle^{2}, & \text{if} \quad \langle u \rangle \leqslant 1 + \dfrac{1}{m} \\ \left(\dfrac{m}{m+1} \right)^{m} \dfrac{1}{m+1} \langle u \rangle + \langle u \rangle - \langle u \rangle^{2}, & \text{if} \quad \langle u \rangle \geqslant 1 + \dfrac{1}{m} \end{cases}. \tag{4.37}$$

We have $\lim_{+\infty} j_m = +\infty$, and $\lim_{+\infty} j_{m,2} = -\infty$. In addition, the function $j_{2,m}$ is non-positive and uniformly strictly concave:

$$\forall \langle u \rangle \in \left(0, 1 + \frac{1}{m}\right] \quad j''_{m,2}(\langle u \rangle) = m \langle u \rangle^{-m-2} \left(-(m+1) + (m-1) \langle u \rangle \right) - 2$$
$$\leqslant -(m+1) \langle u \rangle^{-m-2} - 2.$$

Thus, $\forall \langle u \rangle \in \mathbb{R}_+$, $j''_{m,2}(\langle u \rangle) \leqslant -2$ and so the following coercivity estimate holds true:

$$\forall \langle u \rangle \in \left(0, 1 + \frac{1}{m}\right], \quad j_{m,2}(\langle u \rangle) \leqslant -\left(\langle u \rangle - 1\right)^2 . \tag{4.38}$$

Furthermore, the function j_m is everywhere non-negative. The above analysis allows us to rewrite the dissipation in Wasserstein distance as

$$\begin{aligned}
\frac{1}{2}\frac{d}{dt}\mathbf{W}(\rho(t), \bar{\rho}_k)^2 &\leqslant \iint_{\mathbb{R}\times\mathbb{R}} \chi|a-b|^k J_m[\psi''(t,(a,b))]\bar{\rho}_k(a)\bar{\rho}_k(b)\,dadb \\
&\quad + \frac{1}{2}\iint_{\mathbb{R}\times\mathbb{R}} |a-b|^2 J_{m,2}[\psi''(t,(a,b))]\bar{\rho}_k(a)\bar{\rho}_k(b)\,dadb \\
&\leqslant \iint_{\mathbb{R}\times\mathbb{R}} \chi|a-b|^k j_m[\langle\psi''(t,(a,b))\rangle]\bar{\rho}_k(a)\bar{\rho}_k(b)\,dadb \\
&\quad + \frac{1}{2}\iint_{\mathbb{R}\times\mathbb{R}} |a-b|^2 j_{m,2}[\langle\psi''(t,(a,b))\rangle]\bar{\rho}_k(a)\bar{\rho}_k(b)\,dadb
\end{aligned}$$

to finally conclude that

$$\frac{1}{2}\frac{d}{dt}\mathbf{W}(\rho(t), \bar{\rho}_k)^2 \leqslant -\frac{1}{2}\iint_{\mathbb{R}\times\mathbb{R}} |a-b|^2 \left(\langle\psi''(t,(a,b))\rangle - 1\right)^2 \bar{\rho}_k(a)\bar{\rho}_k(b)\,dadb,$$

where the last inequality follows from (4.36) and the coercivity property (4.38) thanks to the stability estimate (4.25). This concludes the proof,

$$\begin{aligned}
\frac{d}{dt}\mathbf{W}(\rho(t), \bar{\rho}_k)^2 &\leqslant -\iint_{\mathbb{R}\times\mathbb{R}} |a-b|^2 \left(\langle\psi''(t,(a,b))\rangle - 1\right)^2 \bar{\rho}_k(a)\bar{\rho}_k(b)\,dadb \\
&= -\iint_{\mathbb{R}\times\mathbb{R}} \left(\psi'(a) - a - \left(\psi'(b) - b\right)\right)^2 \bar{\rho}_k(a)\bar{\rho}_k(b)\,dadb, \\
&= -2\int_{\mathbb{R}} \left(\psi'(a) - a\right)^2 \bar{\rho}_k(a)\,da, = -2\,\mathbf{W}(\rho(t), \bar{\rho}_k)^2,
\end{aligned}$$

using the fact that $\rho(t)$ and $\bar{\rho}_k$ both have zero centre of mass. □

Remark 4.6 (Non-Existence of Stationary States)**.** *Proposition 4.5 motivates the rescaling in the sub-critical case since it means that there are no stationary states in original variables. Indeed, assume $\bar{u}$ is a stationary states of equation (1.4), then its rescaling $\rho(t,x) = e^t\bar{u}(e^t x)$ is a solution to (2.7) and converges to δ_0 as $t \to \infty$. Proposition 3.4(ii) and Theorem 3.14 in Chapter 2 on the other hand provide a stationary state $\bar{\rho}_k$, and the transport map $\partial_x\psi(t,x)$ pushing forward $\bar{\rho}_k$ onto $\rho(t,x)$ can be written as $\psi(t,x) = e^{-t}\phi(x)$ for some convex function ϕ. Hence, for large enough $t > 0$, $\psi(t,x)$ satisfies the stability estimate (4.24) and so eventually $\rho(t,x)$ converges to $\bar{\rho}_k$ by Proposition 4.5 which is not possible.*

4.1.3 The super-critical case $\chi > \chi_c$

Here, we investigate the possible blow-up dynamics of the solution in the super-critical case. In contrast to the logarithmic case $(m = 1, k = 0)$, for which all solutions blow-up when $\chi > \chi_c$,

provided the second momentum is initially finite, see [41], the picture is not so clear in the fair-competition regime with negative homogeneity $k < 0$. There, the key identity is (4.26), which states in particular that the second momentum is a concave function.

It has been observed in [39] that if the free energy is negative for some time t_0, $\mathcal{F}_k[\rho(t_0)] < 0$, then the second momentum is a decreasing concave function for $t > t_0$. So, it cannot remain non-negative for all time. Necessarily, the solution blows up in finite time. Whether or not the free energy could remain non-negative for all time was left open. In [302], the author proved that solutions blow-up without condition on the sign of the free energy at initial time, but for the special case of the Newtonian potential, for which comparison principles are at hand.
In [67], a continuous time, finite dimensional, Lagrangian numerical scheme of [36] was analysed. This scheme preserves the gradient flow structure of the equation. It was proven that, except for a finite number of values of χ, the free energy necessarily becomes negative after finite time. Thus, blow-up seems to be a generic feature of (1.4) in the super-critical case. However, we could not extend the proof of [67] to the continuous case for two reasons: firstly, we lack compactness estimates, secondly, the set of values of χ to be excluded gets dense as the number of particles in the Lagrangian discretisation goes to ∞.

Below, we transpose the analysis of [67] to the continuous level. We highlight the missing pieces. Let us define the renormalised density $\hat{\rho}$ as in (4.27). The following statement is the analogue of Proposition 4.4 in the super-critical case.

Proposition 4.7. *The functional $\mathcal{H}$ defined by $\mathcal{H}[\rho] := \mathcal{G}[\hat{\rho}]$ on $\mathcal{Y}_2$ is zero-homogeneous, and everywhere non-positive. Moreover, it cannot vanish in the cone of non-negative energy:*

$$(\mathcal{F}[\rho] \geqslant 0) \Longrightarrow (\mathcal{H}[\rho] < 0)\ . \tag{4.39}$$

Proof. We proceed as in the proof of Proposition 4.4. Zero-homogeneity follows from the definition of $\mathcal{H}$, and non-positivity is a direct consequence of the Cauchy-Schwarz inequality. It remains to show (4.39). Assume that ρ is such that $\mathcal{F}[\rho] \geqslant 0$ and $\mathcal{H}[\rho] = 0$. The latter condition ensures that there exists a constant $\hat{\pi}$ such that $\hat{\rho}$ is a critical point of the energy functional $\mathcal{F} + \hat{\pi}\mathcal{V}$:

$$\partial_y \left(\frac{m}{m-1} \hat{\rho}(y)^{m-1} + 2\chi W_k(y) * \hat{\rho}(y) \right) + \hat{\pi} y = 0\,.$$

Testing this equation against $y\hat{\rho}(y)$, we obtain

$$\hat{\pi} = (m-1)\mathcal{F}_k[\hat{\rho}] = (m-1)\sigma(t)^{m-1}\mathcal{F}_k[\rho] \geqslant 0\,.$$

Applying as in the proof of Proposition 4.4 a variant of Theorem 3.6, we obtain that $\hat{\rho}$ is a global minimiser of the energy functional $\mathcal{F} + \hat{\pi}\mathcal{V}$. Here, the amplitude of the confinement potential $\hat{\pi}$

plays no role, but the sign $\hat{\pi} \geqslant 0$ is crucial. By Theorem 2.6 in Chapter 2, there exists a stationary state $\bar{\rho} \in \mathcal{Y}_2$ for critical interaction strength $\chi = \chi_c(k)$. If $\chi > \chi_c(k)$, we have

$$\mathcal{F}_k[\bar{\rho}] = \mathcal{U}_m[\bar{\rho}] + \chi \mathcal{W}_k[\bar{\rho}] < \mathcal{U}_m[\bar{\rho}] + \chi_c(k)\mathcal{W}_k[\bar{\rho}] = 0\,.$$

Taking mass-preserving dilations of $\bar{\rho}$, we see immediately that the functional $\mathcal{F} + \hat{\pi}\mathcal{V}$ is not bounded below in the super-critical case. This is a contradiction with $\hat{\rho}$ being a minimiser. Hence, $\mathcal{H}[\rho] < 0$ and (4.39) holds true. □

As in Section 4.1.1, the following non-linear function of the second momentum,

$$\omega(t) = \sigma(t)^{m+1} = \left(\int_{\mathbb{R}} |x|^2 \rho(t,x)\, dx \right)^{\frac{m+1}{2}}\,,$$

satisfies the second order differential inequality,

$$\ddot{\omega}(t) = (m^2-1)\omega(t)^{-1}\mathcal{H}[\rho(t)] \leqslant 0\,. \tag{4.40}$$

In view of the property (4.39) of the zero-homogeneous functional $\mathcal{H}$, it seems natural to ask whether there exists a positive constant $\delta > 0$, such that

$$(\mathcal{F}[\rho] \geqslant 0) \Longrightarrow (\mathcal{H}[\rho] < -\delta)\,. \tag{4.41}$$

If this would be the case, then (4.40) could be processed as follows: assume that $\dot{\omega}(t) \geqslant 0$ for all t. This is equivalent to say that the free energy remains non-negative for all $t \geqslant 0$ using (4.26). Hence, assuming (4.41) holds, (4.40) becomes

$$\ddot{\omega}(t) < -\delta(m^2-1)\omega(t)^{-1} < 0. \tag{4.42}$$

Multiplying by $\dot{\omega}(t) \geqslant 0$, and integrating between 0 and T, we would get

$$\frac{1}{2}\dot{\omega}(T)^2 + \delta(m^2-1)\log\left(\omega(T)\right) \leqslant \frac{1}{2}\dot{\omega}(0)^2 + \delta(m^2-1)\log\left(\omega(0)\right)\,.$$

Hence, for any $t > 0$,

$$\omega(t) \leqslant \omega(0)\exp\left(\frac{\dot{\omega}(0)^2}{2\delta(m^2-1)}\right)\,.$$

Back to estimate (4.42), we would conclude that ω is uniformly concave,

$$\ddot{\omega}(t) \leqslant -\left(\frac{\delta(m^2-1)}{\omega(0)}\right)\exp\left(-\frac{\dot{\omega}(0)^2}{2\delta(m^2-1)}\right) < 0\,.$$

Therefore, $\frac{d}{dt}\mathcal{V}[\rho(t)]$ would become negative in finite time. This would be a contradiction with the everywhere non-negativity of the free energy by (4.26). As a conclusion, the existence of positive $\delta > 0$ as in (4.41) implies unconditional blow-up. In [67], existence of such δ is proven for a finite dimensional Lagrangian discretisation of $\mathcal{F}_k$, and accordingly $\mathcal{H}$, except for a finite set of values for χ. Numerical simulations using the numerical scheme proposed in [36] clearly show that the energy has the tendency to become negative, even for positive initial data. Proving (4.41) remains an open problem.

4.2 Fast diffusion asymptotics

In the fast diffusion case $k > 0$, we are able to show a much stronger result: every stationary state of (2.7) is in fact a global attractor for any choice of interaction strength $\chi > 0$. Investigating the evolution of the Wasserstein distance to equilibrium yields exponential convergence with an explicit rate which is independent of the interaction strength $\chi > 0$. In contrast to the porous medium case, where we required a stability estimate on Brenier's map, we do not need such an estimate here. As a consequence, we obtain an alternative proof of uniqueness of stationary states by a dynamical argument.

Proposition 4.8 (Long-time asymptotics)**.** *For $k \in (0,1)$ and $m = 1-k$, if $\rho(t)$ has zero centre of mass initially and satisfies (2.7), then the evolution of the Wasserstein distance to the stationary states $\bar\rho_k$ of (2.7) can be estimated by*

$$\frac{d}{dt}\boldsymbol{W}(\rho(t),\bar\rho_k)^2 \leqslant -2\boldsymbol{W}(\rho(t),\bar\rho_k)^2 \tag{4.43}$$

for any interaction strength $\chi > 0$. As a consequence, stationary states are unique if they exist.

Proof. We compute the evolution of the Wasserstein distance along the gradient flow, denoting by ϕ the inverse transport map, $\partial_x\phi(t,x) = \partial_x\psi(t,x)^{-1}$. Proceeding as in the proof of Proposition 4.5, we can write the dissipation of the distance to equilibrium as

$$\begin{aligned}\frac{1}{2}\frac{d}{dt}\boldsymbol{W}(\rho(t),\bar\rho_k)^2 \leqslant \chi \iint_{\mathbb{R}\times\mathbb{R}} |a-b|^k \Big\{ &-\big\langle \psi''(t,(a,b))^{-m}\big\rangle + \big\langle \psi''(t,(a,b))^{1-m}\big\rangle \\ &+\big\langle \psi''(t,(a,b))\big\rangle^{-m} - \big\langle \psi''(t,(a,b))\big\rangle^{1-m}\Big\}\bar\rho_k(a)\bar\rho_k(b)\,dadb \\ + \frac{1}{2}\iint_{\mathbb{R}\times\mathbb{R}} |a-b|^2 \Big\{ &-\big\langle \psi''(t,(a,b))^{-m}\big\rangle + \big\langle \psi''(t,(a,b))^{1-m}\big\rangle \\ &+\big\langle \psi''(t,(a,b))\big\rangle - \big\langle \psi''(t,(a,b))\big\rangle^{2}\Big\}\bar\rho_k(a)\bar\rho_k(b)\,dadb\,.\end{aligned}$$

We now examine the signs of the microscopic functionals $J_m[u]$ and $J_{m,2}[u]$ defined as in (4.34) and (4.35) for non-negative functions $u : (0,1) \to \mathbb{R}_+$ by

$$\begin{aligned}J_m[u] &:= -\big\langle u^{-m}\big\rangle + \big\langle u^{1-m}\big\rangle + \big\langle u\big\rangle^{-m} - \big\langle u\big\rangle^{1-m}\,,\\ J_{m,2}[u] &:= -\big\langle u^{-m}\big\rangle + \big\langle u^{1-m}\big\rangle + \big\langle u\big\rangle - \big\langle u\big\rangle^{2}\,.\end{aligned}$$

However, since $m < 1$ we now have by convexity $\big\langle u\big\rangle^{-m} - \big\langle u^{-m}\big\rangle \leqslant 0$ and $\big\langle u^{1-m}\big\rangle - \big\langle u\big\rangle^{1-m} \leqslant 0$, hence

$$J_m[u] \leqslant 0, \quad m \in (0,1). \tag{4.44}$$

For the functional $J_{m,2}$, the first two terms can be written as

$$-\big\langle u^{-m}\big\rangle + \big\langle u^{1-m}\big\rangle = -\alpha\big\langle u\big\rangle^{-m} + \beta\big\langle u\big\rangle^{1-m}\,,$$

where $\alpha = \langle u \rangle^m \langle u^{-m} \rangle$ and $\beta = \langle u \rangle^{m-1} \langle u^{1-m} \rangle$. As opposed to the proof of Proposition 4.5, we now have $\beta \leqslant 1 \leqslant \alpha$ by Jensen's inequality since $m < 1$, and therefore,

$$\forall \langle u \rangle \in \mathbb{R}_+, \quad J_{m,2}[u] \leqslant j_{m,2}(\langle u \rangle) := -\langle u \rangle^{-m} + \langle u \rangle^{1-m} + \langle u \rangle - \langle u \rangle^2 .$$

Note that $\lim_{+\infty} j_{m,2} = -\infty$. In addition, the function $j_{2,m}$ is non-positive and uniformly strictly concave:

$$\forall \langle u \rangle \in \mathbb{R}_+, \quad j''_{m,2}(\langle u \rangle) = -m(1+m)\langle u \rangle^{-m-2} - m(1-m)\langle u \rangle^{-m-1} - 2 \leqslant -2 ,$$

and hence

$$\forall \langle u \rangle \in \mathbb{R}_+, \quad j_{m,2}(\langle u \rangle) \leqslant -(\langle u \rangle - 1)^2 . \tag{4.45}$$

From these estimates, we can deduce the exponential speed of convergence for the stationary state $\bar\rho_k$ by rewriting the dissipation to equilibrium as

$$\begin{aligned}
\frac{1}{2}\frac{d}{dt}\mathbf{W}(\rho(t),\bar\rho_k)^2 &\leqslant \iint_{\mathbb{R}\times\mathbb{R}} \chi|a-b|^k J_m[\psi''(t,(a,b))]\bar\rho_k(a)\bar\rho_k(b)\,dadb \\
&\quad + \iint_{\mathbb{R}\times\mathbb{R}} \frac{1}{2}|a-b|^2 J_{m,2}[\psi''(t,(a,b))]\bar\rho_k(a)\bar\rho_k(b)\,dadb \\
&\leqslant \iint_{\mathbb{R}\times\mathbb{R}} \frac{1}{2}|a-b|^2 j_{m,2}[\langle\psi''(t,(a,b))\rangle]\bar\rho_k(a)\bar\rho_k(b)\,dadb \\
&\leqslant -\frac{1}{2}\iint_{\mathbb{R}\times\mathbb{R}} |a-b|^2 \left(\langle\psi''(t,(a,b))\rangle - 1\right)^2 \bar\rho_k(a)\bar\rho_k(b)\,dadb,
\end{aligned}$$

where the last inequality follows from (4.44) and (4.45). This concludes the proof,

$$\begin{aligned}
\frac{d}{dt}\mathbf{W}(\rho(t),\bar\rho_k)^2 &\leqslant -\iint_{\mathbb{R}\times\mathbb{R}} |a-b|^2 \left(\langle\psi''(t,(a,b))\rangle - 1\right)^2 \bar\rho_k(a)\bar\rho_k(b)\,dadb \\
&= -\iint_{\mathbb{R}\times\mathbb{R}} \left(\psi'(a) - a - \left(\psi'(b) - b\right)\right)^2 \bar\rho_k(a)\bar\rho_k(b)\,dadb, \\
&= -2\int_{\mathbb{R}} \left(\psi'(a) - a\right)^2 \bar\rho_k(a)\,da, = -2\,\mathbf{W}(\rho(t),\bar\rho_k)^2,
\end{aligned}$$

using the fact that $\rho(t)$ and $\bar\rho_k$ both have zero centre of mass. □

Remark 4.9 (Non-Existence of Stationary States)**.** *This result also provides a dynamical proof for the non-existence of stationary states for $k \in (0, 2/3)$ in original variables. Indeed, if $\bar u$ were a stationary state of equation (1.4), then its rescaled density $\rho(t,x)$ would converge to δ_0 for large times. This contradicts the existence of a stationary state in rescaled variables (Chapter 2 Theorem 4.10) for $k \in (0, 2/3)$ together with exponential convergence to equilibrium Proposition 4.8.*

5 Numerical simulations

There exists an illuminating way to rewrite the energy functional $\mathcal{F}_k[\rho]$ due to the particular form of the transport map. We use the Lagrangian transformation $\rho \mapsto X$, where $X : (0,1) \to \mathbb{R}$ denotes the pseudo-inverse of the cumulative distribution function (cdf) associated with ρ [295, 171, 36, 62],

$$X(\eta) = F^{-1}(\eta) := \inf\{x \,:\, F(x) \geqslant \eta\}\,, \quad F(x) := \int_{-\infty}^{x} \rho(y)\,dy\,.$$

We introduce the parameter $r \in \{0,1\}$ as we are interested in both original ($r = 0$) and rescaled ($r = 1$) variables. Integrating equations (1.4) and (2.7) over $(-\infty, X(t,\eta))$ with respect to the space variable yields

$$\partial_t \int_{-\infty}^{X(t,\eta)} \rho(t,y)\,dy = \left[\partial_x \rho^m + 2\chi\rho\partial_x\left(W_k * \rho\right) + rx\rho\right]\big|_{x=X(t,\eta)}\,. \tag{5.46}$$

Differentiating the identity $F(t, X(t,\eta)) = \eta$ with respect to η twice yields

$$\rho(t, X(t,\eta)) = \left(\partial_\eta X(t,\eta)\right)^{-1} \qquad \text{and} \qquad \partial_x \rho(t, X(t,\eta)) = -\partial_{\eta\eta} X(t,\eta)/\left(\partial_\eta X(t,\eta)\right)^3\,.$$

Differentiating with respect to time, we obtain $\partial_t F(t, X(t,\eta)) = -\partial_t X(t,\eta)/\partial_\eta X(t,\eta)$. This allows us to simplify (5.46),

$$\partial_t X(t,\eta) = -\partial\eta\left(\left(\partial_\eta X(t,\eta)\right)^{-m}\right) - 2\chi\int_0^1 |X(t,\eta) - X(t,\tilde\eta)|^{k-2}\left(X(t,\eta) - X(t,\tilde\eta)\right)\,d\tilde\eta - rX(t,\eta)\,.$$

Similarly, the functionals $\mathcal{G}_{k,0} := \mathcal{F}_k$ and $\mathcal{G}_{k,1} := \mathcal{F}_{k,\mathbf{resc}}$ read equivalently

$$\mathcal{G}_{k,r}[X] = \frac{1}{m-1}\int_0^1 \left(\partial_\eta X(\eta)\right)^{1-m} d\eta + \chi\int_0^1\int_0^1 \frac{|X(\eta) - X(\tilde\eta)|^k}{k}\,d\eta d\tilde\eta + \frac{r}{2}\int_0^1 |X(\eta)|^2\,d\eta\,.$$

for $k \in (-1,1)\backslash\{0\}$, and

$$\mathcal{G}_{0,r}[X] = -\int_0^1 \log\left(\frac{dX}{d\eta}(\eta)\right)\,d\eta + \chi\int_0^1\int_0^1 \log|X(\eta) - X(\tilde\eta)|\,d\eta d\tilde\eta + \frac{r}{2}\int_0^1 |X(\eta)|^2\,d\eta\,.$$

in the logarithmic case $k = 0$. Intuitively, X encodes the position of particles with respect to the partial mass $\eta \in (0,1)$, and the same homogeneity is preserved: $\mathcal{G}_{k,0}[\lambda X] = \lambda^k \mathcal{G}_{k,0}[X]$.

In Section 3, we showed uniqueness of minimisers of the rescaled energy functional $\mathcal{F}_{k,\mathbf{resc}}[\rho]$ for $0 < k < 2/3$ and any $\chi > 0$ (Corollary 3.16) and also for the sub-critical porous medium case $-1 < k < 0$, $\chi < \chi_c(k)$ (Corollary 3.9). One may take these results as an indication that $\mathcal{F}_{k,\mathbf{resc}}[\rho]$ could in fact be displacement convex. As discussed in Section 2.3, $\mathcal{F}_{k,\mathbf{resc}}[\rho]$ is a sum of displacement convex and concave contributions and we do not know its overall convexity properties. We recall that the functionals related to the classical Keller–Segel models in two dimensions are displacement convex once restricted to bounded densities [94]. We will give some heuristics for the power-law potential case. If $\mathcal{G}_{k,1}[X]$ were convex, then $\mathcal{F}_{k,\mathbf{resc}}[\rho]$ would be displacement convex [295, 98] and uniqueness of minimisers directly follows [234]. Taylor expanding $\mathcal{G}_{k,1}$ around

X yields for any test function $\varphi \in C_c^\infty([0,1])$,

$$\mathcal{G}_{k,1}[X+\epsilon\varphi] = \mathcal{G}_{k,1}[X] + \epsilon D_\varphi \mathcal{G}_{k,1}[X] + \frac{\epsilon^2}{2} D_\varphi^2 \mathcal{G}_{k,1}[X] + O(\epsilon^3),$$

where $D_\varphi \mathcal{G}_{k,1}[X] = \int_0^1 \delta\mathcal{G}_{k,1}[X](\eta)\,\varphi(\eta)\,d\eta$ with the first variation $\frac{\delta \mathcal{G}_{k,1}}{\delta X}[X](\eta)$ given by

$$\frac{\delta \mathcal{G}_{k,1}}{\delta X}[X](\eta) = \partial_\eta \left((\partial_\eta X)^{-m} \right) + 2\chi \int_0^1 |X(\eta) - X(\tilde{\eta})|^{k-2} \left(X(\eta) - X(\tilde{\eta}) \right) d\tilde{\eta} + X(\eta)$$

for $k \in (-1,1)/\{0\}$. However, the Hessian

$$\begin{aligned} D_\varphi^2 \mathcal{G}_{k,1}[X] =& m \int_0^1 \left(\partial_\eta \varphi(\eta)\right)^2 \left(\partial_\eta X(\eta)\right)^{-(m+1)} d\eta \\ &+ \chi(k-1) \int_0^1 \int_0^1 |X(\eta) - X(\tilde{\eta})|^{k-2} \left(\varphi(\eta) - \varphi(\tilde{\eta})\right)^2 d\eta d\tilde{\eta} + \int_0^1 \varphi(\eta)^2 \, d\eta \end{aligned}$$

does not have a sign. In other words, we cannot use this strategy to conclude overall convexity/concavity properties of the rescaled energy functional $\mathcal{F}_{k,\mathbf{resc}}$. It is an interesting problem to explore convexity properties of $\mathcal{G}_{k,r}$ in a restricted set of densities such as bounded densities as in [94, 119].

5.1 Numerical scheme

To simulate the dynamics of X we use a numerical scheme which was proposed in [36, 67] for the logarithmic case, and generalised to the one-dimensional fair-competition regime for the porous medium case $k \in (-1,0)$ in [66]. It can easily be extended to rescaled variables adding a confining potential, and works just in the same way in the fast diffusion case $k \in (0,1)$. We discretise the energy functional via a finite difference approximation of $X(\eta)$ on a regular grid. If $(X_i)_{1 \leqslant i \leqslant n}$ are the positions of n ordered particles sharing equal mass $\Delta\eta = 1/n$ such that $X_1 < X_2 < \cdots < X_n$, then we define the discretised energy functional by

$$\mathcal{G}_{k,r}^n\left[(X_i)\right] = \frac{(\Delta\eta)^m}{m-1} \sum_{i=1}^{n-1} \left(X_{i+1} - X_i\right)^{1-m} + \chi\,(\Delta\eta)^2 \sum_{1 \leqslant i \neq j \leqslant n} \frac{|X_j - X_i|^k}{k} + r\frac{\Delta\eta}{2} \sum_{i=1}^n |X_i|^2$$

for $k \in (-1,1)\backslash\{0\}$, and by

$$\mathcal{G}_{0,r}^n\left[(X_i)\right] = -\Delta\eta \sum_{i=1}^{n-1} \log\left(\frac{X_{i+1} - X_i}{\Delta\eta}\right) + \chi\,(\Delta\eta)^2 \sum_{1 \leqslant i \neq j \leqslant n} \log|X_j - X_i| + r\frac{\Delta\eta}{2} \sum_{i=1}^n |X_i|^2$$

in the logarithmic case $k = 0$. The Euclidean gradient flow of $\mathcal{G}_{k,r}^n$ writes for $1 < i < n$

$$\begin{aligned} \dot{X}_i =& -(\Delta\eta)^{m-1} \left(\left(X_{i+1} - X_i\right)^{-m} - \left(X_i - X_{i-1}\right)^{-m} \right) \\ &- 2\chi\Delta\eta \sum_{1 \leqslant j \neq i \leqslant n} \mathrm{sign}(i-j)\,|X_i - X_j|^{k-1} - rX_i\,, \end{aligned} \tag{5.47}$$

complemented with the dynamics of the extremal points

$$\dot{X}_1 = -(\Delta\eta)^{m-1}\left(X_2 - X_1\right)^{-m} + 2\chi\Delta\eta \sum_{j\neq 1} |X_j - X_1|^{k-1} - rX_1\,, \tag{5.48}$$

$$\dot{X}_n = (\Delta\eta)^{m-1}\left(X_n - X_{n-1}\right)^{-m} - 2\chi\Delta\eta \sum_{j\neq n} |X_j - X_n|^{k-1} - rX_n\,. \tag{5.49}$$

Equations (5.48)-(5.49) follow from imposing $X_0 = -\infty$ and $X_{n+1} = +\infty$ so that the initial centre of mass $\sum_{i=1}^n X_i = 0$ is conserved. Working with the pseudo-inverse of the cummulative distribution function of ρ also has the advantage that we can express the Wasserstein distance between two densities ρ and $\tilde{\rho}$ in a more tractable way. More precisely, if ψ' is the optimal map which transports $\tilde{\rho}$ onto ρ, then the Monge-Ampére equation (2.13) is an increasing rearrangement. Let F and $\tilde{F}$ be the cummulative distribution function of ρ and $\tilde{\rho}$ respectively, with pseudo-inverses X and $\tilde{X}$. Then we have

$$\tilde{F}(x) = \int_{-\infty}^{x} \tilde{\rho}(y)\,dy = \int_{-\infty}^{\psi'(x)} \rho(y)\,dy = F\circ\psi'(x)\,.$$

Hence the transport map is given explicitly by $\psi' = F^{-1}\circ\tilde{F}$, and we have for the Wasserstein distance

$$\mathbf{W}(\rho,\tilde{\rho})^2 = \int_0^1 \left|\tilde{F}^{-1}(\eta) - F^{-1}(\eta)\right|^2 d\eta = \int_0^1 \left|\tilde{X}(\eta) - X(\eta)\right|^2 d\eta = ||\tilde{X} - X||_2^2\,. \tag{5.50}$$

This means that this numerical scheme can be viewed formally as the time discretisation of the abstract gradient flow equation (1.6) in the Wasserstein-2 metric space, which corresponds to a gradient flow in $L^2\left((0,1)\right)$ for the pseudo-inverse X,

$$\dot{X}(t) = -\nabla_{L^2}\mathcal{G}_{k,r}[X(t)]\,.$$

Discretising (5.47)-(5.48)-(5.49) by an implicit in time Euler scheme, this numerical scheme then coincides with a Jordan-Kinderlehrer-Otto (JKO) steepest descent scheme (see [248, 36] and references therein). The solution at each time step of the non-linear system of equations is obtained by an iterative Newton-Raphson procedure.

5.2 Results

For the logarithmic case $k = 0$, $m = 1$, we know that the critical interaction strength is given by $\chi_c = 1$ separating the blow-up regime from the regime where self-similar solutions exist [136, 41, 33]. As shown in Chapter 2, there is no critical interaction strength for the fast diffusion regime $k > 0$, however the dichotomy appears in the porous medium regime $k < 0$ (see Chapter 2 and [39]). It is not known how to compute the critical parameter $\chi_c(k)$ explicitly for $k < 0$, however, we can make use of the numerical scheme described in Section 5.1 to compute $\chi_c(k)$ numerically.

Figure 3.2 gives an overview of the behaviour of solutions. In the grey region, we observe finite-time blow-up of solutions, whereas for a choice of (k,χ) in the white region, solutions converge

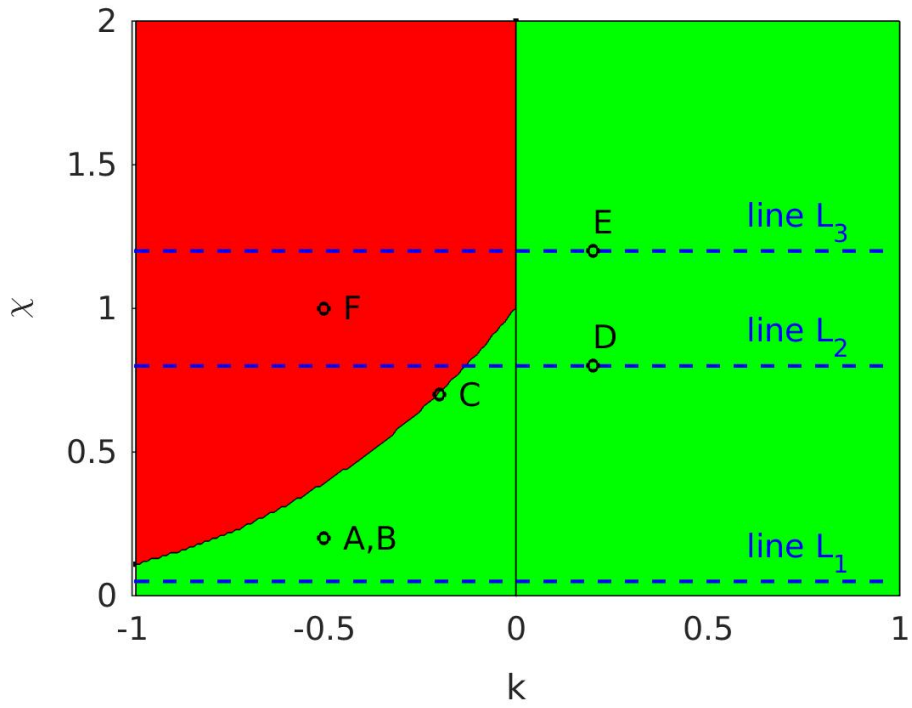

Figure 3.2: **Regions of blow-up (grey) and convergence to self-similarity (white).** The notation refers to subsequent figures as follows: Lines L_1, L_2 and L_3 show the asymptotic profiles over the range $k \in (-1, 1)$ for $\chi = 0.05$, $\chi = 0.8$ and $\chi = 1.2$ respectively (Figure 3.3). Point A shows the density evolution at $(k, \chi) = (-0.5, 0.2)$ in original variables (Figure 3.4), and Point B for the same choice of parameters $(k, \chi) = (-0.5, 0.2)$ in rescaled variables (Figure 3.5). Points C, D and E correspond to simulations at $(-0.2, 0.7)$ (Figure 3.6), $(0.2, 0.8)$ (Figure 3.7) and $(0.2, 1.2)$ (Figure 3.8) respectively in the parameter space (k, χ), all in rescaled variables. Point F corresponds to simulations at $(k, \chi) = (-0.5, 1.0)$ in original variables (Figure 3.9).

exponentially fast to a unique self-similar profile. The critical regime is characterised by the black line $\chi_c(k)$, $-1 < k \leqslant 0$, separating the grey from the white region. Note that numerically we have $\chi_c(-0.99) = 0.11$ and $\chi_c(0) = 1$. Figure 3.2 has been created by solving the rescaled equation (2.7) using the numerical scheme described above with particles equally spaced at a distance $\Delta\eta = 10^{-2}$. For all choices of $k \in (-1, 0)$ and $\chi \in (0, 1.5)$, we choose as initial condition a centered normalised Gaussian with variance $\sigma^2 = 0.32$, from where we let the solution evolve with time steps of size $\Delta t = 10^{-3}$. We terminate the time evolution of the density distribution if one of the following two conditions is fullfilled: either the L^2-error between two consecutive solutions is less than a certain tolerance (i.e. we consider that the solution converged to a stationary state), or the Newton-Raphson procedure does not converge for $\rho(t, x)$ at some time $t < t_{max}$ because the mass is too concentrated (i.e. the solution sufficiently approached a Dirac Delta to assume blow-up). We choose t_{max} large enough, and $\Delta\eta$ and Δt small enough so that one of the two cases occurs. For Figure 3.2, we set the maximal time to $t_{max} = 10$ and the tolerance to 10^{-5}. For a fixed k, we

start with $\chi = 0.01$ and increase the interaction strength by 0.01 each run until $\chi = 1.5$. This is repeated for each k from -0.99 to 0 in 0.01 steps. For a given k, the numerical critical interaction strength $\chi_c(k)$ is defined to be the largest χ for which the numerical solution can be computed without blow-up until the L^2-error between two consecutive solutions is less than the specified tolerance. In what follows, we investigate the behaviour of solutions in more detail for chosen points in the parameter space Figure 3.2.

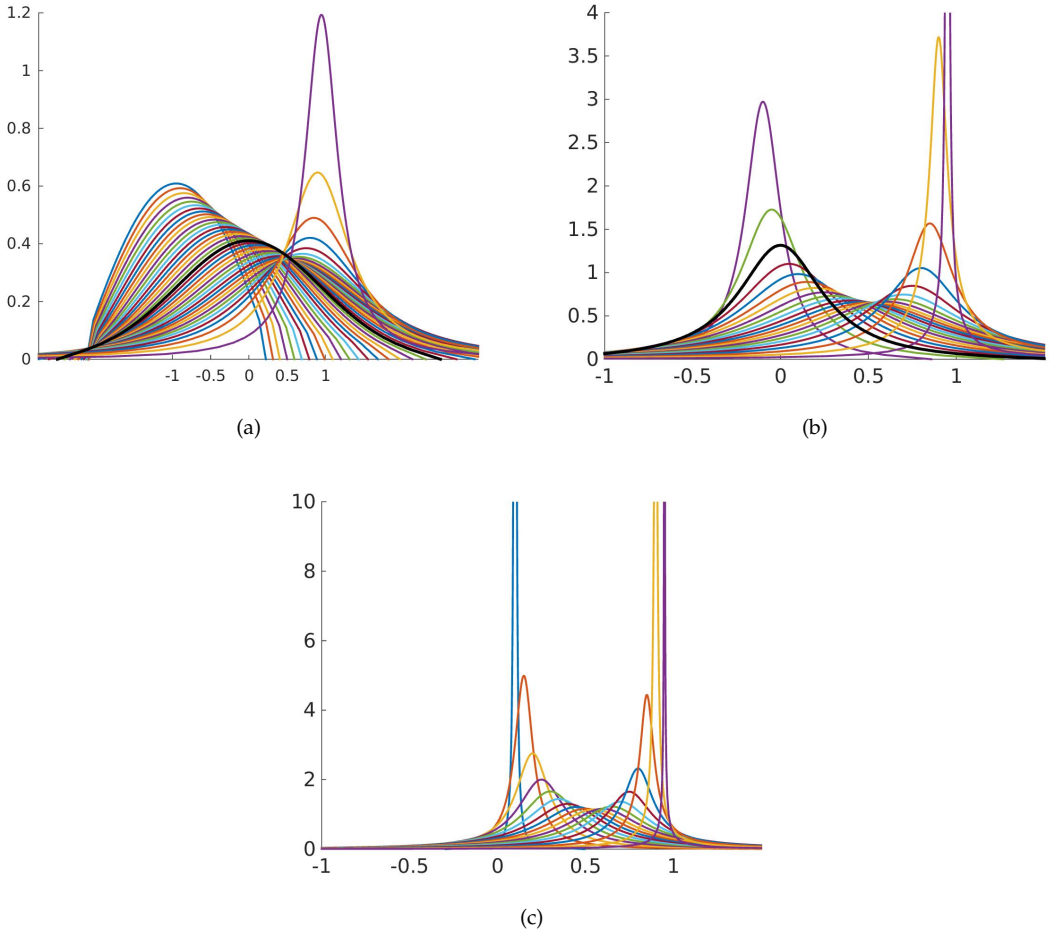

Figure 3.3: Profiles of stationary states in rescaled variables ($r = 1$) corresponding to lines L_1, L_2 and L_3 in Figure 3.2 for (a) $\chi = 0.05$, (b) $\chi = 0.8$ and (c) $\chi = 1.2$ with k ranging from 0.95 to (a) -0.95, (b) -0.1 and (c) 0.1 in 0.05 steps respectively. All stationary states are centered at zero, but are here displayed shifted so that they are centered at their corresponding value of k. The black curve indicates the stationary state for $k = 0$.

5.2.1 Lines L_1, L_2 and L_3

Apart from points $A - F$ shown in Figure 3.2, it is also interesting to observe how the asymptotic profile changes more globally as we move through the parameter space. To this purpose, we

choose three different values of χ and investigate how the stationary profile in rescaled variables changes with k. Three representative choices of interaction strengths are given by lines L_1, L_2 and L_3 as indicated in Figure 3.2, where L_1 corresponds to $\chi = 0.05$ and lies entirely in the self-similarity region (white), L_2 corresponds to $\chi = 0.8$ and captures part of the sub-critical region in the porous medium regime $k < 0$ (white), as well as some of the blow-up regime (grey), and finally line L_3 which corresponds to $\chi = 1.2$ and therefore captures the jump from the self-similarity (white) to the blow-up region (grey) at $k = 0$. Note also that points D and E are chosen to lie on lines L_2 and L_3 respectively as to give a more detailed view of the behaviour on these two lines for the same k-value. The asymptotic profiles over the range $k \in (-1, 1)$ for lines L_1, L_2 and L_3 are shown in Figure 3.3, all with the same choice of parameters using time step size $\Delta t = 10^{-3}$ and equally spaced particles at distance $\Delta\eta = 10^{-2}$.

For each choice of interaction strength χ, we start with $k = 0.95$ and decrease k in 0.05 steps for each simulation either until $k = -0.95$ is reached, or until blow-up occurs and (k, χ) lies within the grey region. For each simulation, we choose as initial condition the stationary state of the previous k-value (starting with a centered normalised Gaussian distribution with variance $\sigma^2 = 0.32$ for $k = 0.95$). As for Figure 3.2, we terminate the time evolution of the density distribution for a given choice of k and χ if either the L^2-error between two consecutive solutions is less than the tolerance 10^{-5}, or the Newton-Raphson procedure does not converge. All stationary states are centered at zero. To better display how the profile changes for different choices of k, we shift each stationary state in Figure 3.3 so that it is centered at the corresponding value of k. The black curve indicates the stationary profile for $k = 0$.

In Figure 3.3(a), we observe corners close to the edge of the support of the stationary profiles for $k < 0$. This could be avoided by taking $\Delta\eta$ and Δt smaller, which we chose not to do here, firstly to be consistent with Figure 3.2 and secondly to avoid excessive computation times. For interaction strength $\chi = 0.8$, the smallest k for which the solution converges numerically to a stationary state is $k = -0.1$ (see Figure 3.3(b)). This fits with what is predicted by the critical curve $\chi_c(k)$ in Figure 3.2 (line L_2).

In Figures 3.3(b) and 3.3(c), we see that the stationary profiles become more and more concentrated for k approaching the critical parameter $k = k^*$ with $\chi = \chi_c(k^*)$, which is to be expected as we know that the stationary state $\bar{\rho}_k$ converges to a Dirac Delta as k approaches the blow-up region. In fact, for $\chi = 1.2$ the numerical scheme stops converging for $k = 0.05$ already since the mass is too concentrated, and so we only display profiles up to $k = 0.1$ in Figure 3.3(c). Further, in all three cases $\chi = 0.05$, $\chi = 0.8$ and $\chi = 1.2$ we observe that the stationary profiles become more and more concentrated as $k \to 1$. This reflects the fact that attractive forces dominate as the diffusivity m converges to zero. Finally, note that we have chosen here to show only a part of the full picture for Figures 3.3(b) and 3.3(c), cutting the upper part. More precisely, the maximum of

the stationary state for $k = 0.95$ and $\chi = 0.8$ in Figure 3.3(b) lies at 75.7474, whereas it is at $3, 216.8$ for parameter choices $k = 0.95$ and $\chi = 1.2$ shown in Figure 3.3(c).

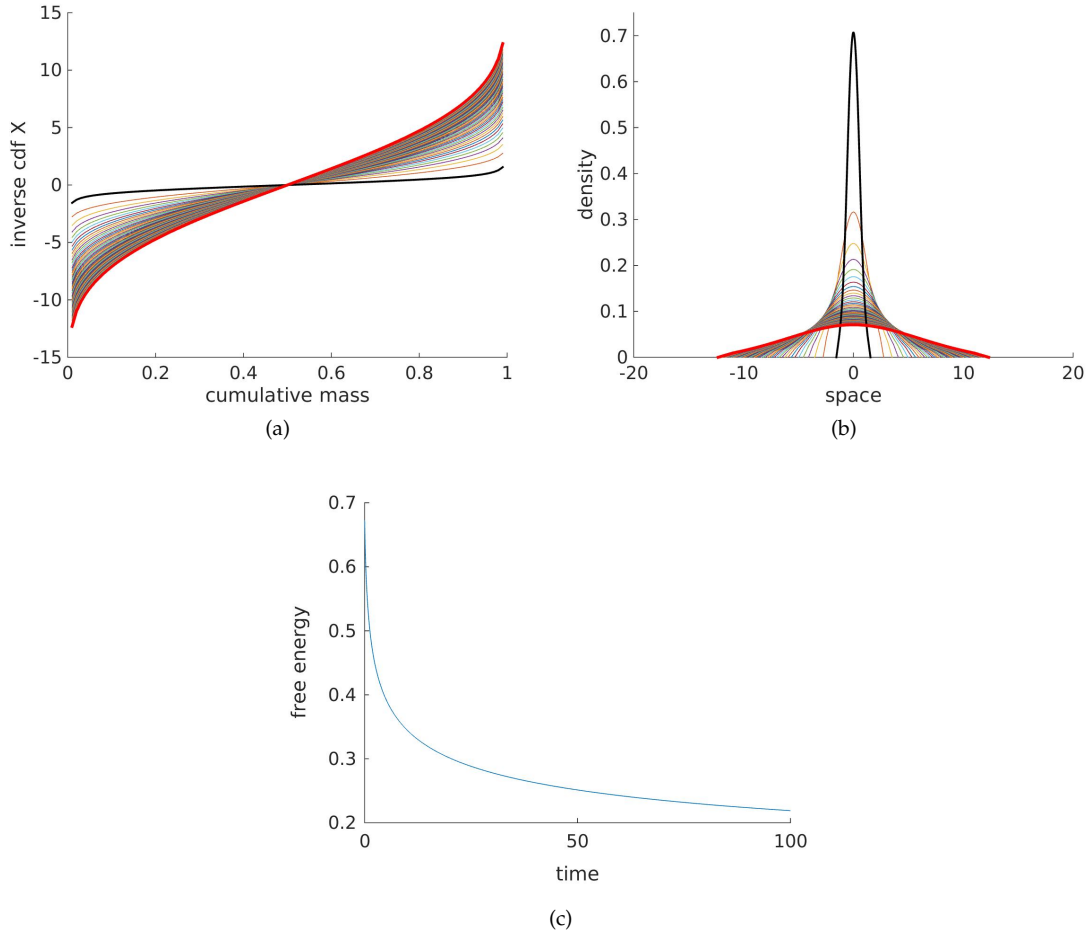

Figure 3.4: Point A: $\chi = 0.2$, $k = -0.5$, $r = 0$.
(a) Inverse cumulative distribution function, (b) solution density, (c) free energy.

5.2.2 Points A-F

Let us now investigate in more detail the time-evolution behaviour at the points A–F in Figure 3.2. For $k = -0.5$ in the porous medium regime and sub-critical $\chi = 0.2$ (point A in Figure 3.2), the diffusion dominates and the density goes pointwise to zero as $t \to \infty$ in original variables. Figure 3.4(a) and 3.4(b) show the inverse cumulative distribution function and the density profile for $(k, \chi) = (-0.5, 0.2)$ respectively, from time $t = 0$ (black) to time $t = 100$ (red) in time steps of size $\Delta t = 10^{-3}$ and with $\Delta\eta = 10^{-2}$. We choose a centered normalised Gaussian with variance $\sigma^2 = 0.32$ as initial condition. Figure 3.4(c) shows the evolution of the free energy (1.1) over time, which continues to decay as expected.

For exactly the same choice of parameters $(k, \chi) = (-0.5, 0.2)$ and the same initial condition we then investigate the evolution in rescaled variables (point B in Figure 3.2), and as predicted by Proposition 4.5, the solution converges to a stationary state. See Figures 3.5(a) and 3.5(b) for the evolution of the inverse cumulative distribution function and the density distribution with $\Delta t =$

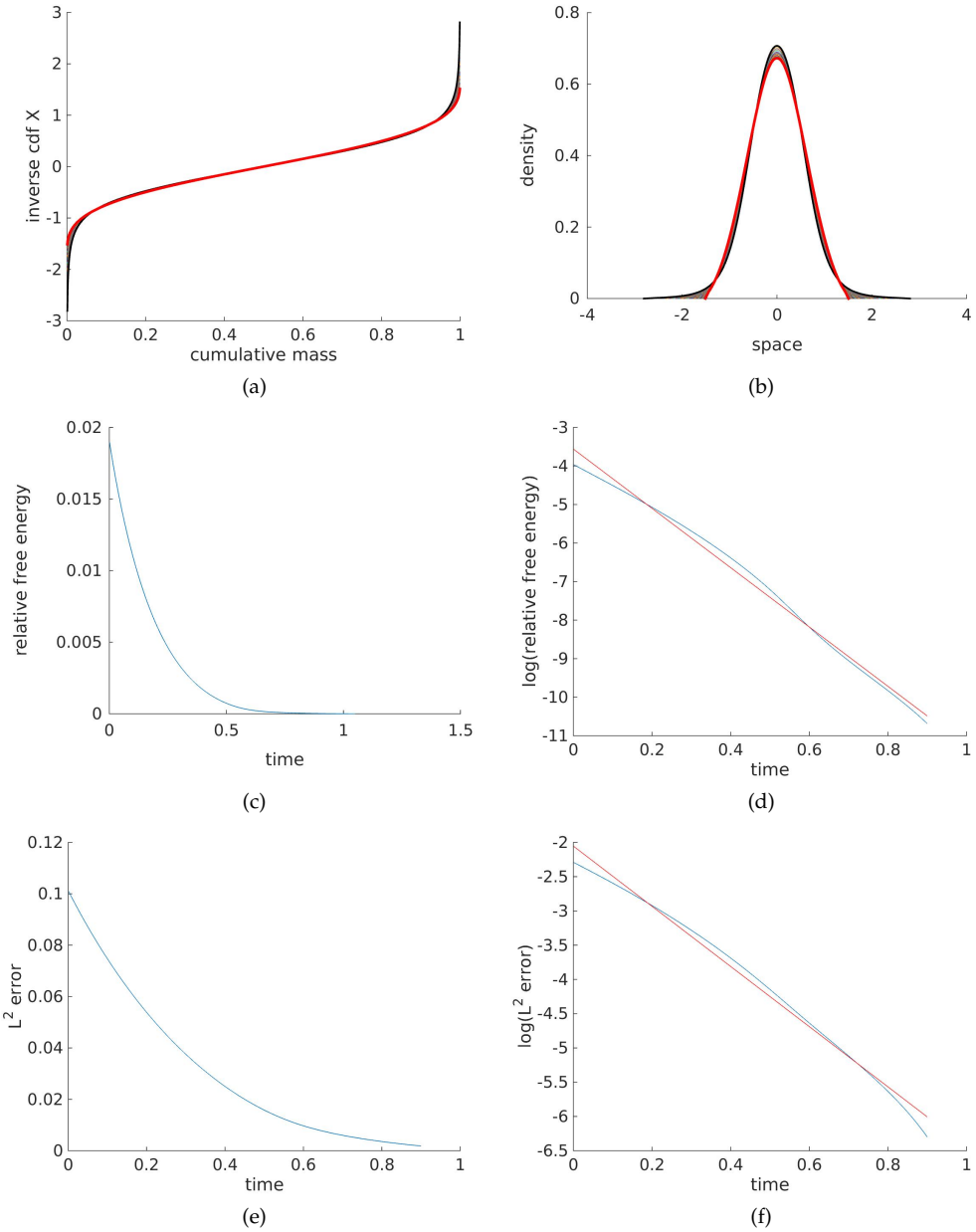

Figure 3.5: Point B: $\chi = 0.2$, $k = -0.5$, $r = 1$.
(a) Inverse cumulative distribution function from initial condition (black) to the profile at the last time step (red), (b) solution density from initial condition (black) to the profile at the last time step (red), (c) relative free energy, (d) log(relative free energy) and fitted line between times 0 and 0.9 with slope -7.6965 (red), (e) L^2-error between the solutions at time t and at the last time step, (f) log(L^2-error) and fitted line with slope -4.392 (red).

10^{-3} and $\Delta\eta = 10^{-3}$ from $t = 0$ (black) to the stationary state $\bar{\rho}$ (red). Again, we terminate the evolution as soon as the L^2-distance between the numerical solution at two consecutive time steps is less than a certain tolerance, chosen at 10^{-5}. We see that the solution converges very quickly both in relative energy $|\mathcal{F}_k[\rho(t)] - \mathcal{F}_k[\bar{\rho}]|$ (Figure 3.5(c)) and in terms of the Wasserstein distance to the solution at the last time step $\mathbf{W}(\rho(t), \bar{\rho})$ (Figure 3.5(e)). To check that the convergence is indeed

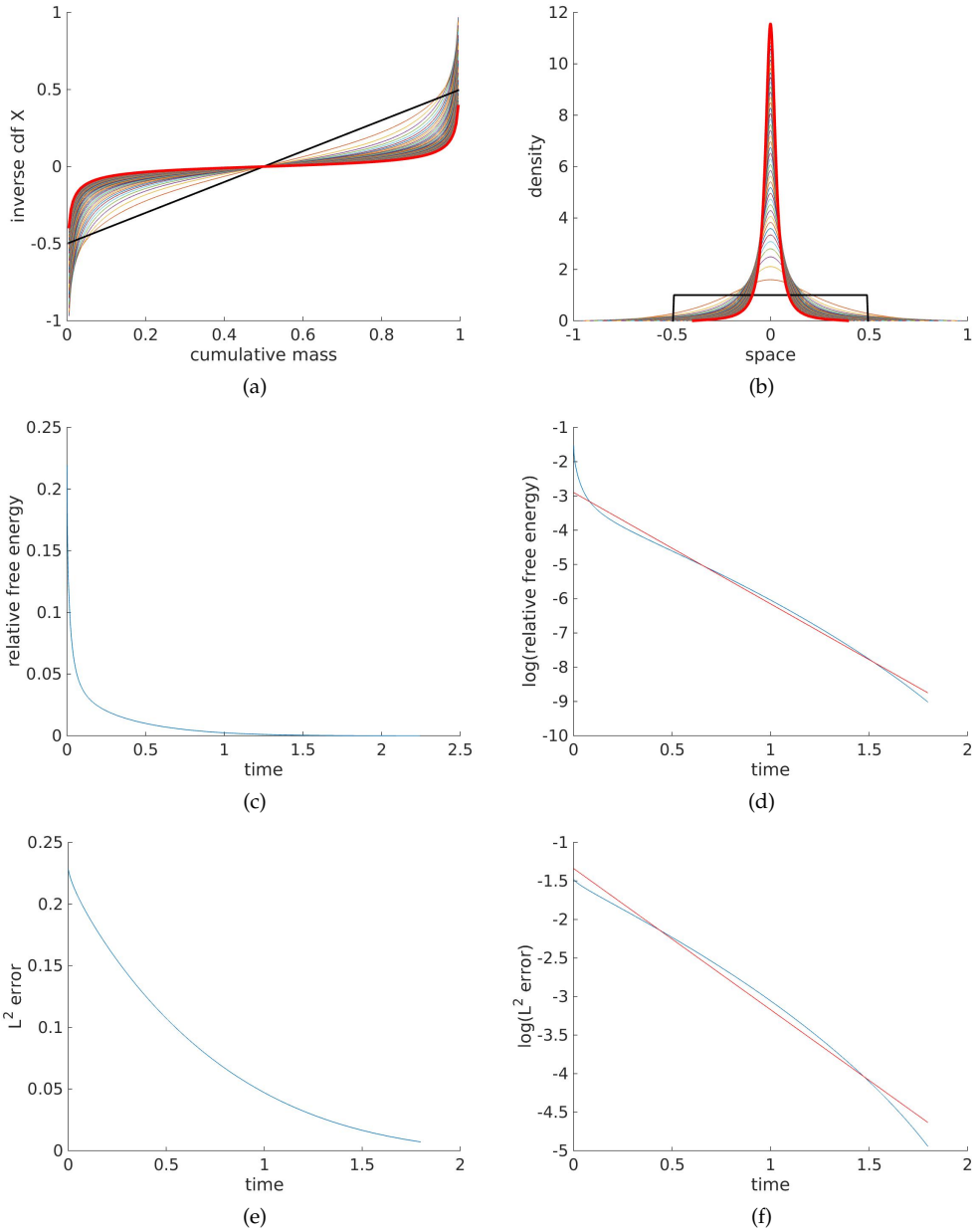

Figure 3.6: Point C: $\chi = 0.7$, $k = -0.2$, $r = 1$.
(a) Inverse cumulative distribution function from initial condition (black) to the profile at the last time step (red), (b) solution density from initial condition (black) to the profile at the last time step (red), (c) relative free energy, (d) log(relative free energy) and fitted line between times 0 and 1.8 with slope -3.2522 (red), (e) L^2-error between the solutions at time t and at the last time step, (f) log(L^2-error) and fitted line with slope -1.8325 (red).

exponential as predicted by Proposition 4.5, we fit a line to the logplot of both the relative free energy (between times $t = 0$ and $t = 0.9$), see Figure 3.5(d), and to the logplot of the Wasserstein distance to equilibrium, see Figure 3.5(f). In both cases, we obtain a fitted line $y = -a * t + b$ with some constant b and rate $a = 7.6965$ for the relative free energy and rate $a = 4.392$ for the

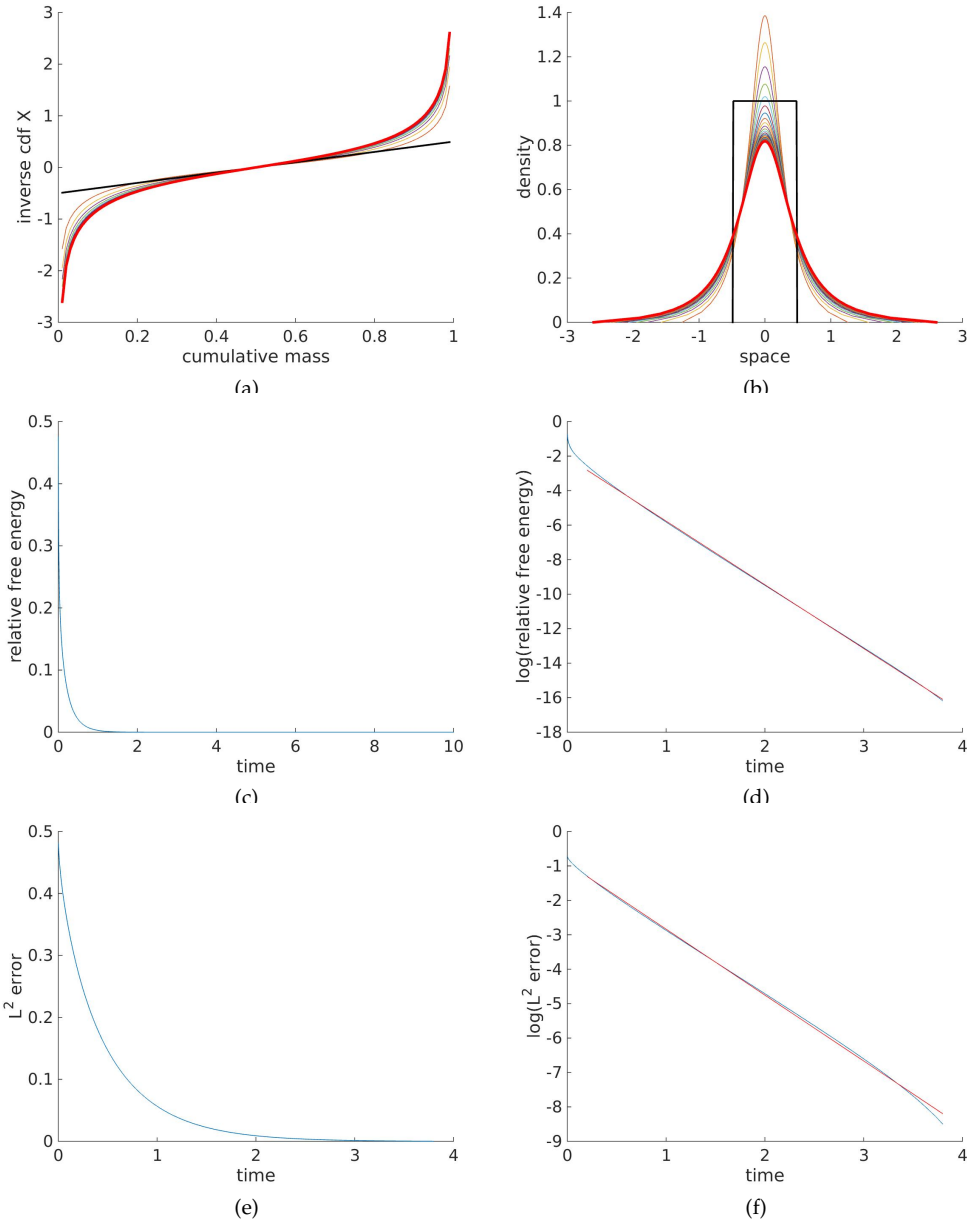

Figure 3.7: Point D: $\chi = 0.8$, $k = 0.2$, $r = 1$.
(a) Inverse cumulative distribution function from initial condition (black) to the profile at the last time step (red), (b) solution density from initial condition (black) to the profile at the last time step (red), (c) relative free energy, (d) log(relative free energy) and fitted line between times 0.2 and 3.8 with slope -3.6904 (red), (e) L^2-error between the solutions at time t and at the last time step, (f) log(L^2-error) and fitted line between times 0.2 and 3.8 with slope -1.9148 (red).

Wasserstein distance to equilibrium. Recall that the L^2-error between two solutions $X(\eta)$ and $\tilde{X}(\eta)$ is equal to the Wasserstein distance between the corresponding densities $\rho(x)$ and $\tilde{\rho}(x)$ as described in (5.50). We observe a rate of convergence that is in agreement with [62, 71, 148] for the logarithmic case $k = 0$.

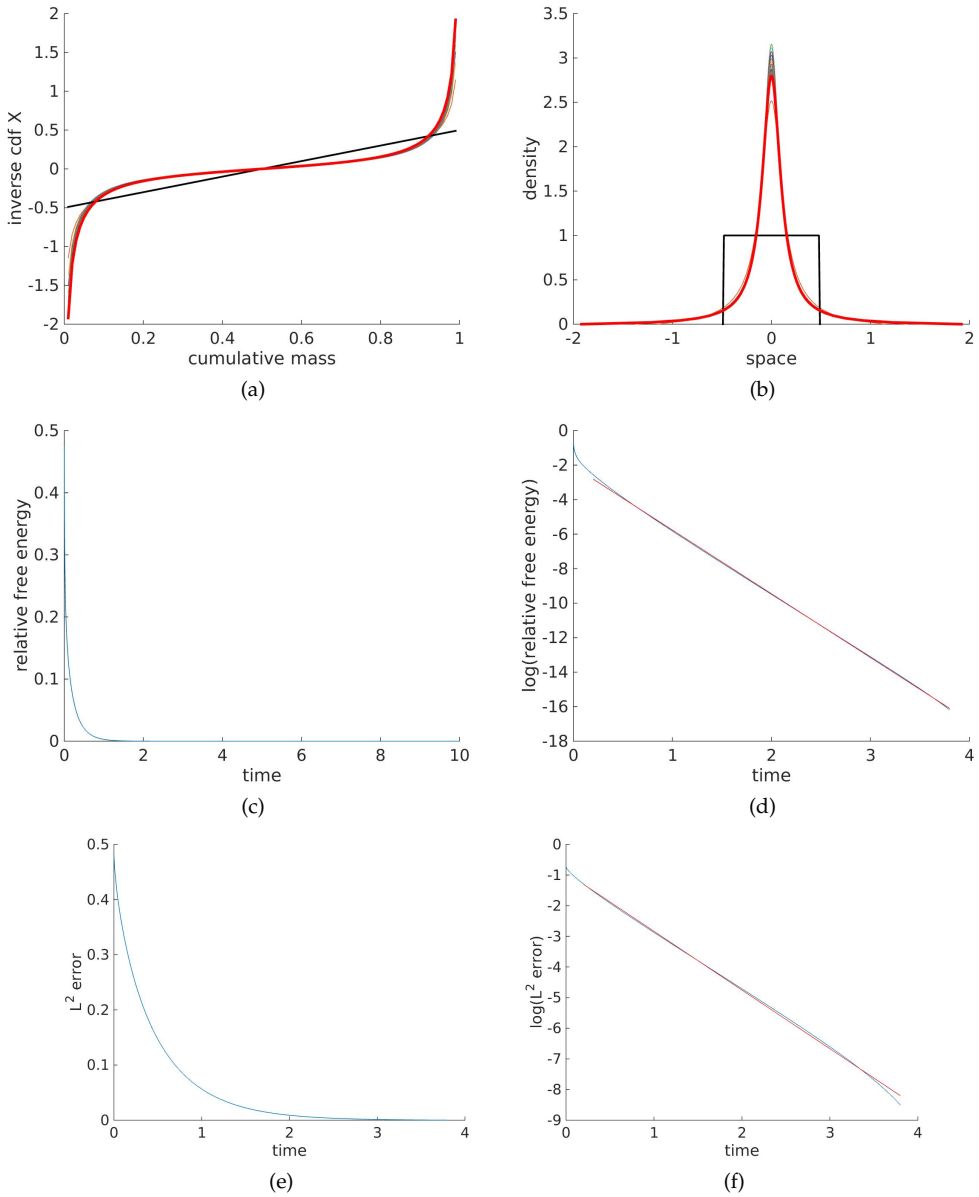

Figure 3.8: Point E: $\chi = 1.2$, $k = 0.2$, $r = 1$.
(a) Inverse cumulative distribution function from initial condition (black) to the profile at the last time step (red), (b) solution density from initial condition (black) to the profile at the last time step (red), (c) relative free energy, (d) log(relative free energy) and fitted line between times 0.3 and 3.5 with slope -3.6898 (red), (e) L^2-error between the solutions at time t and at the last time step, (f) log(L^2-error) and fitted line between times 0.3 and 3.5 with slope -1.9593 (red).

For parameter choices $k = -0.2$ and $\chi = 0.7$ (point C in Figure 3.2), we are again in the subcritical regime where solutions converge to a stationary state in rescaled variables according to Proposition 4.5, see Figures 3.6(a) and 3.6(b). However, point C is closer to the critical interaction strength $\chi_c(k)$ than point B (numerically, we have $\chi_c(-0.2) = 0.71$), and as a result we can observe that the stationary density $\bar{\rho}$ in Figure 3.6(b) (red) is more concentrated than in Figure 3.5(b). Here, we choose as initial condition a characteristic function supported on the ball centered at zero with radius $1/2$ (black, Figure 3.6(b)), and fix $\Delta t = 10^{-3}$, $\Delta\eta = 5 * 10^{-3}$ with tolerance 10^{-5}. We observe that the solution converges very quickly to a stationary state both in relative free energy $|\mathcal{F}_k[\rho(t)] - \mathcal{F}_k[\bar{\rho}]|$ (Figure 3.6(c)) and in terms of the Wasserstein distance to equilibrium $\mathbf{W}(\rho(t), \bar{\rho})$ (Figure 3.6(e)). To investigate the exponential rate of convergence, we fit again a line to the logplot of both the relative free energy (here between times $t = 0$ and $t = 1.8$) see Figure 3.6(d), and the Wasserstein distance to equilibrium, see Figure 3.6(f). We obtain fitted lines $y = -a * t + b$ with some constant b and rate $a = 3.2407$ for the relative free energy, whereas the rate is $a = 1.8325$ for the Wasserstein distance to equilibrium.

Next, we are looking at point D in Figure 3.2, which corresponds to the choice $(k, \chi) = (0.2, 0.8)$ and is part of line L_2 (see Figure 3.3(b)). Since point D lies in the fast diffusion regime $k > 0$, no critical interaction strength exists as shown in Chapter 2, and so we look at convergence to self-similarity. Figures 3.7(a) and 3.7(b) display the evolution of the inverse cumulative distribution function and the density distribution from $t = 0$ (black) to the stationary state $\bar{\rho}$ (red) in rescaled variables including the solutions at 50 intermediate time steps. We start with a characteristic function supported on a centered ball of radius $1/2$. Choosing $\Delta t = 10^{-3}$ and $\Delta\eta = 10^{-2}$ is enough. The density seems to become instantaneously supported on the whole space for any $t > 0$, which cannot be fully represented numerically since the tails are cut by numerical approximation, see Figure 3.7(a)-(b). Again, we observe very fast convergence both in relative energy (Figure 3.7(c)-(d)) and in Wasserstein distance to equilibrium (Figure 3.7(e)-(f)) as predicted by Proposition 4.8. A logplot of the relative free energy (Figure 3.7(d)) and the Wasserstein distance to equilibrium (Figure 3.7(f)) show exponential rates of convergence with rates $a = 3.6904$ and $a = 1.9148$ respectively for the fitted line $y = -a * t + b$ with some constant b and for times $0.2 \leqslant t \leqslant 3.8$.

For the same choice of $k = 0.2$ in the fast diffusion regime, but with higher interaction strength $\chi = 1.2$ (point E in Figure 3.2, which is part of line L_3, see Figure 3.3(c)), we obtain a similar behaviour. Figures 3.8(a) and 3.8(b) show the inverse cumulative distribution function and the density distribution, both for the initial data (black), a characteristic supported on the centered ball of radius $1/2$, and for the stationary state $\bar{\rho}$ (red). Here we choose as before $\Delta t = 10^{-3}$ and $\Delta\eta = 10^{-2}$. We observe that the stationary state for $\chi = 1.2$ (Figure 3.8(b)) is more concentrated than for $\chi = 0.8$ (Figure 3.7(b)), which is exactly what we would expect for decreasing k as $\bar{\rho}$ approaches a Dirac Delta for $k \to 0$ if $\chi = 1.2$, whereas it becomes compactly supported if $\chi = 0.8$

as k crosses the χ-axis (see Chapter 2 Corollary 3.9). Again, we observe very fast convergence both in relative energy (Figure 3.8(c)-(d)) and in Wasserstein distance to equilibrium (Figure 3.8(e)-(f)) as predicted by Proposition 4.8. A logplot of the relative free energy (Figure 3.8(d)) and the Wasserstein distance to equilibrium (Figure 3.8(f)) show exponential rates of convergence with rates $a = 3.6898$ and $a = 1.9593$ respectively for the fitted lines $y = -a * t + b$ and some constant b between times $0.3 \leqslant t \leqslant 3.5$.

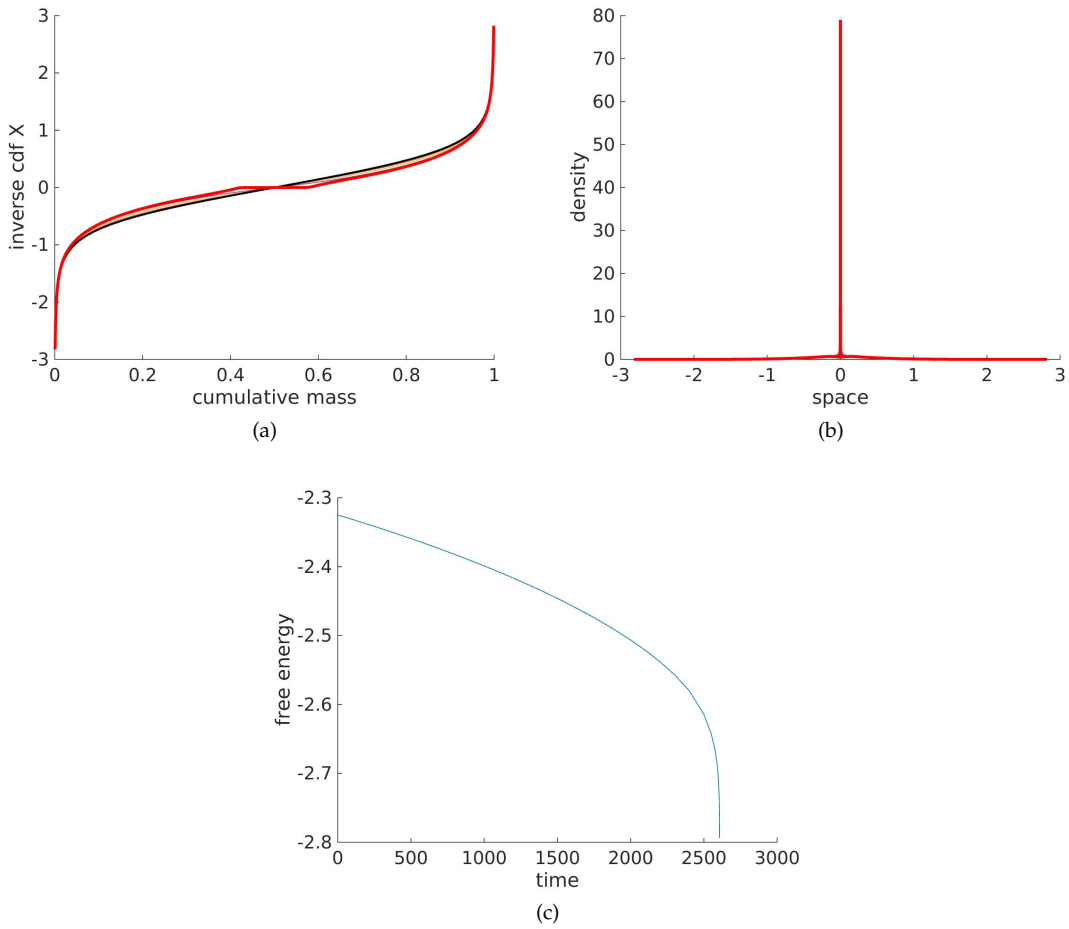

Figure 3.9: Point F: $\chi = 1$, $k = -0.5$, $r = 0$.
(a) Inverse cumulative distribution function from initial condition (black) to the profile at the last time step (red), (b) solution density from initial condition (black) to the profile at the last time step (red), (c) free energy.

Finally, let us investigate the behaviour for $(k, \chi) = (-0.5, 1)$ in original variables (point F in Figure 3.2). Point F lies in the porous medium regime and we expect blow-up as $\chi_c(-0.5) < 1$, see Section 4.1.3. If the mass becomes too concentrated, the Newton-Raphson procedure does not converge and the simulation stops. We have therefore adapted the numerical scheme to better capture the blow-up. We fix $\Delta t = 10^{-3}$ and $\Delta\eta = 10^{-3}$ and take a centered normalised Gaussian with variance $\sigma^2 = 0.32$ as initial data. When the simulation stops, we divide the time step size Δt

by two and repeat the simulation, taking as initial condition the last density profile before blow-up. This process can be repeated any number of times, each time improving the approximation of an emerging Dirac Delta. The formation of a Dirac Delta in Figure 3.9(b) corresponds to the formation of a plateaux in 3.9(a). As expected from the analysis in Section 4.1.3, the free energy diverges to $-\infty$ (Figure 3.9(c)).

6 Explorations in other regimes

6.1 Diffusion-dominated regime in one dimension

The numerical scheme described here gives us a tool to explore the asymptotic behaviour of solutions for parameter choices that are less understood. For example, choosing $\chi = 0.3$, $k = -0.5$ and $m = 1.6$ in original variables ($r = 0$), we observe convergence to a compactly supported stationary state, see Figure 3.10. This choice of parameters is within the diffusion-dominated regime since $m + k > 1$ (see Definition 3.1 in Chapter 1). We choose as initial condition a normalised characteristic function supported on $B(0, 15)$ from where we let the solution evolve with time steps of size $\Delta t = 10^{-2}$ and particles spaced at $\Delta\eta = 10^{-2}$. We let the density solution evolve until the L^2-error between two consecutive solutions is less than 10^{-7}. Note that here $m + k = 1.1$ is close to the fair-competition regime, for which $\chi_c(-0.5) = 0.39$ (see Figure 3.2).

6.2 Attraction-dominated regime in any dimension

In the attraction-dominated regime $N(m-1)+k < 0$ (corresponding to Definition 3.1 in Chapter 1) both global existence of solutions and blow-up can occur in original variables in dimension $N \geqslant 1$ depending on the choice of initial data [118, 275, 278, 109, 32, 110, 224, 65]. Using the numerical scheme introduced in Section 5, we can demonstrate this change of behaviour numerically in one dimension, see Figures 3.11 (dispersion) and 3.12 (blow-up).

We will now investigate in more detail a special parameter choice (m, k) that belongs to the attraction-dominated regime. Instead of fixing m and k such that attractive and repulsive forces are in balance ($N(m-1)+k = 0$), one may choose instead to investigate the regime $m = m^{**}$ where the free energy functional (1.1) is conformal invariant,

$$m^{**} := \frac{2N}{2N+k}\,.$$

For $k < 0$, this corresponds to the case $p = q = m$ in the HLS inequality (3.16) for which the optimisers ρ_{HLS} and the optimal constant C_{HLS} are known explicitly [217]. We have the following existence result:

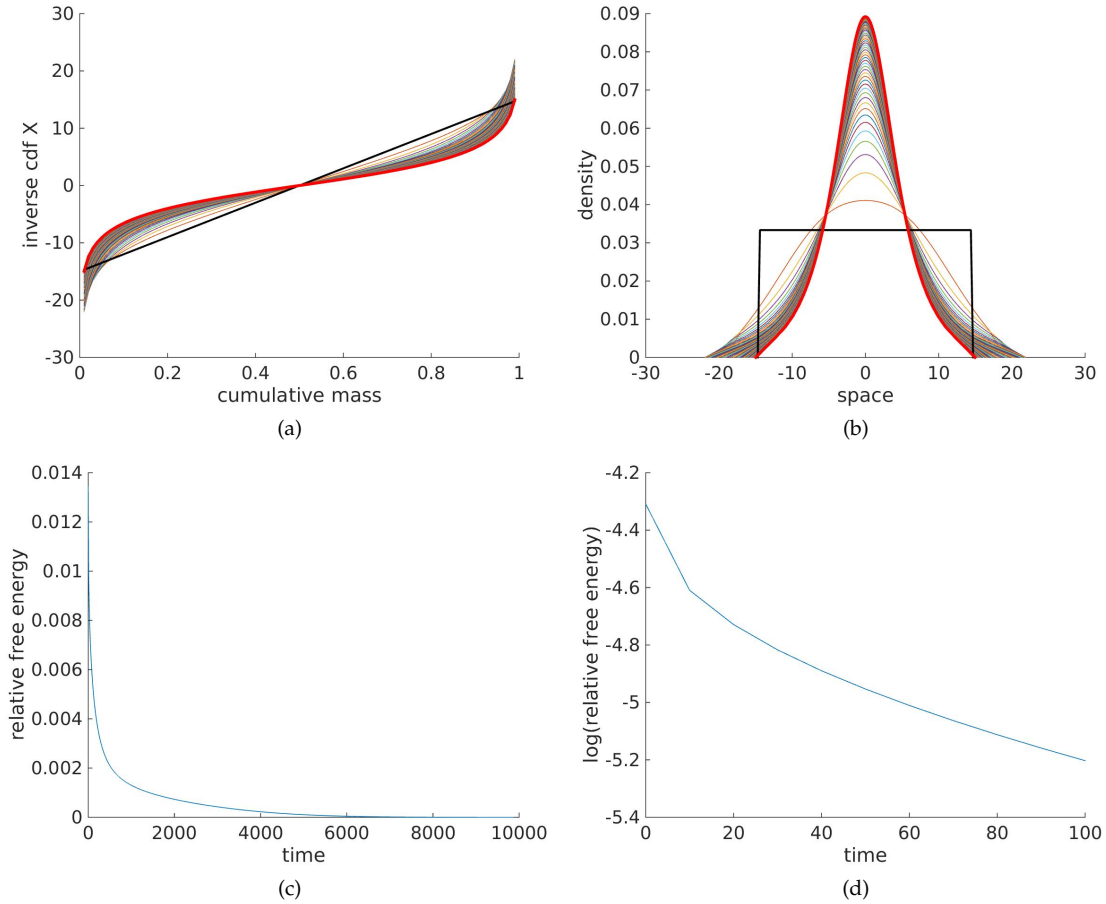

Figure 3.10: Diffusion-dominated regime: $\chi = 0.3$, $k = -0.5$, $m = 1.6$, $r = 0$.
(a) Inverse cumulative distribution function from initial condition (black) to the profile at the last time step (red), (b) solution density from initial condition (black) to the profile at the last time step (red), (c) relative free energy, (d) log(relative free energy).

Theorem 6.1. *Let $\chi > 0$, $k \in (-N, 0)$ and $m = m^{**} \in (1, 2)$. Then the free energy functional $\mathcal{F}_k$ admits a critical point in $\mathcal{Y}$.*

Proof. Following the approach in [109], we rewrite the free energy functional (1.1) as a sum of two functionals

$$\mathcal{F}_k[\rho] = \mathcal{F}_k^1[\rho] + \mathcal{F}_k^2[\rho]\,,$$

where

$$\begin{aligned}\mathcal{F}_k^1[\rho] :=& \frac{1}{N(m-1)}||\rho||_m^m \left(1 - \chi C_{HLS}\frac{N(m-1)}{(-k)}||\rho||_m^{2-m}\right)\\ =& \frac{2N+k}{N(-k)}||\rho||_m^m \left(1 - \chi C_{HLS}\frac{N}{2N+k}||\rho||_m^{2-m}\right)\,,\end{aligned} \tag{6.51}$$

and

$$\mathcal{F}_k^2[\rho] := \frac{\chi}{(-k)} \left(C_{HLS} ||\rho||_m^2 - \iint\limits_{\mathbb{R}^N \times \mathbb{R}^N} |x-y|^k \rho(x)\rho(y)\, dxdy \right). \tag{6.52}$$

By the HLS inequality (3.16), the second functional (6.52) is bounded below for any $\chi > 0$,

$$\mathcal{F}_k^2[\rho] \geqslant 0\,, \quad \forall \rho \in \mathcal{Y}\,,$$

and by [217, Theorem 3.1], there exists a family of optimisers $\rho_{HLS,\lambda,c}$,

$$\rho_{HLS,\lambda,c}(x) = c \left(\frac{\lambda}{\lambda^2 + |x|^2} \right)^{N/m}, \quad \lambda > 0, c > 0 \tag{6.53}$$

satisfying $\mathcal{F}_k^2 [\rho_{HLS,\lambda,c}] = 0$ with the optimal constant C_{HLS} given by

$$C_{HLS} := \pi^{-k/2} \left(\frac{\Gamma\left(\frac{N+k}{2}\right)}{\Gamma\left(N + \frac{k}{2}\right)} \right) \left(\frac{\Gamma\left(\frac{N}{2}\right)}{\Gamma\left(N\right)} \right)^{-(N+k)/N}.$$

The parameter $\lambda > 0$ in (6.53) corresponds to the scaling that leaves the L^m-norm of $\rho_{HLS,\lambda,c}$ invariant. Since the first variation of the functional $\mathcal{F}_k^1$ defined in (6.51) is given by

$$\frac{\delta \mathcal{F}_k^1}{\delta \rho}[\rho](x) = \frac{2}{(-k)} \left(1 - \chi C_{HLS} ||\rho||_m^{2-m}\right) \rho^{m-1}(x)$$

and since the L^m-norm of the optimiser can be calculated explicitly,

$$||\rho_{HLS,\lambda,c}||_m = c \left(\frac{2^{1-N} \pi^{\frac{N+1}{2}}}{\Gamma\left(\frac{N+1}{2}\right)} \right)^{1/m},$$

there exists a unique choice of $(\lambda, c) = (\lambda^*, c^*)$ for each $\chi > 0$ such that

$$\frac{\delta \mathcal{F}_k^1}{\delta \rho}[\rho_{HLS,\lambda^*,c^*}](x) = 0 \quad \text{and} \quad \int_{\mathbb{R}^N} \rho_{HLS,\lambda^*,c^*}(x)\, dx = 1$$

given by

$$c^*(\chi) := \left(\frac{2^{1-N} \pi^{\frac{N+1}{2}}}{\Gamma\left(\frac{N+1}{2}\right)} \right)^{-1/m} (\chi C_{HLS})^{1/(m-2)}, \quad \lambda^*(\chi) := \left(\int_{\mathbb{R}^N} \rho_{HLS,1,c^*(\chi)}(x)\, dx \right)^{2/k}. \tag{6.54}$$

Hence ρ_{HLS,λ^*,c^*} is a critical point of $\mathcal{F}_k$ in $\mathcal{Y}$. □

We can choose to leave $\lambda > 0$ as a free parameter in (6.53), only fixing $c = c^*(\chi)$ so that ρ_{HLS,λ,c^*} is a critical point of $\mathcal{F}_k$ with arbitrary mass. We conjecture that a similar result to [109, Theorem 2.1] holds true for general $k \in (-N, 0)$ and $m = m^{**}$ for radially symmetric initial data:

Conjecture 1 (Global Existence vs Blow-up). *Let $\chi > 0$, $k \in (-N, 0)$ and $m = m^{**}$ in dimension $N \geqslant 1$. Assume the initial datum $\rho_0 \in \mathcal{Y}$ is radially symmetric.*

(i) If there exists $\lambda_0 > 0$ such that

$$\rho_0(r) < \rho_{HLS,\lambda_0,c^*}(r)\,, \quad \forall\, r \geqslant 0,,$$

then any radially symmetric solution $\rho(t,r)$ of (1.4) with initial datum $\rho(0,r) = \rho_0(r)$ is vanishing in $L^1_{loc}\left(\mathbb{R}^N\right)$ as $t \to \infty$.

(ii) If there exists $\lambda_0 > 0$ such that

$$\rho_0(r) > \rho_{HLS,\lambda_0,c^*}(r)\,, \quad \forall\, r \geqslant 0\,,$$

then any radially symmetric solution $\rho(t,r)$ of (1.4) with initial datum $\rho(0,r) = \rho_0(r)$ must blow-up at a finite time T^* or has a mass concentration at $r = 0$ as time goes to infinity in the sense that there exist $R(t) \to 0$ as $t \to \infty$ and a positive constant $C > 0$ such that

$$\int_{B(0,R(t))} \rho(t,x)\,dx \geqslant C\,.$$

Further, we expect the following to be true analogous to [109]:

Conjecture 2 (Unstable Stationary State). *For any $\chi > 0$, the density $\rho_{HLS,\lambda^*,c^*} \in \mathcal{Y}$ with (λ^*, c^*) given by (6.54) is an unstable stationary state of equation (1.4).*

Numerically, we indeed observe the behaviour predicted in Conjecture 1 for $N = 1$. Using the scheme introduced in Section 5, we choose as initial data the density ρ_{HLS,λ_0,c_0} given by the optimisers of the HLS inequality (6.53). For any choice of $c_0 > 0$, we fix $\lambda_0 > 0$ such that ρ_{HLS,λ_0,c_0} has unit mass and is therefore in $\mathcal{Y}$. Note that ρ_{HLS,λ_0,c_0} is not a critical point of $\mathcal{F}_k$ unless $c_0 = c^*$. Comparing with the stationary state ρ_{HLS,λ_0,c^*}, we have

$$\text{sign}\,(c^* - c_0) = \text{sign}\left(\rho_{HLS,\lambda_0,c^*}(x) - \rho_{HLS,\lambda_0,c_0}(x)\right)\,, \qquad \forall x \in \mathbb{R}\,.$$

Note that the mass of the stationary state ρ_{HLS,λ_0,c^*} is given by

$$\int_{\mathbb{R}^N} \rho_{HLS,\lambda_0,c^*(\chi)}(x)\,dx = \lambda_0^{-k/2} \int_{\mathbb{R}^N} \rho_{HLS,1,c^*(\chi)}(x)\,dx\,,$$

which is equal to one if and only if $\lambda_0 = \lambda^*$, that is $c_0 = c^*$. If we choose $c_0 < c^*$, then $\rho_0 := \rho_{HLS,\lambda_0,c_0} < \rho_{HLS,\lambda_0,c^*}$ and according to Conjecture 1(i), we would expect the solution $\rho(t,r)$ to vanish in $L^1_{loc}(\mathbb{R})$. This is exactly what can be observed in Figure 3.11 for the choice of parameters $\chi = 0.35$, $k = -1/2$, $m = 4/3$ in original variables ($r = 0$) and with $c_0 = 0.4\,c^*$. Here,

we chose time steps of size $\Delta t = 10^{-2}$ and particles spaced at $\Delta\eta = 10^{-2}$. We let the density solution evolve until the L^2-error between two consecutive solutions is less than 10^{-4} (plotting every 1000 iterations).

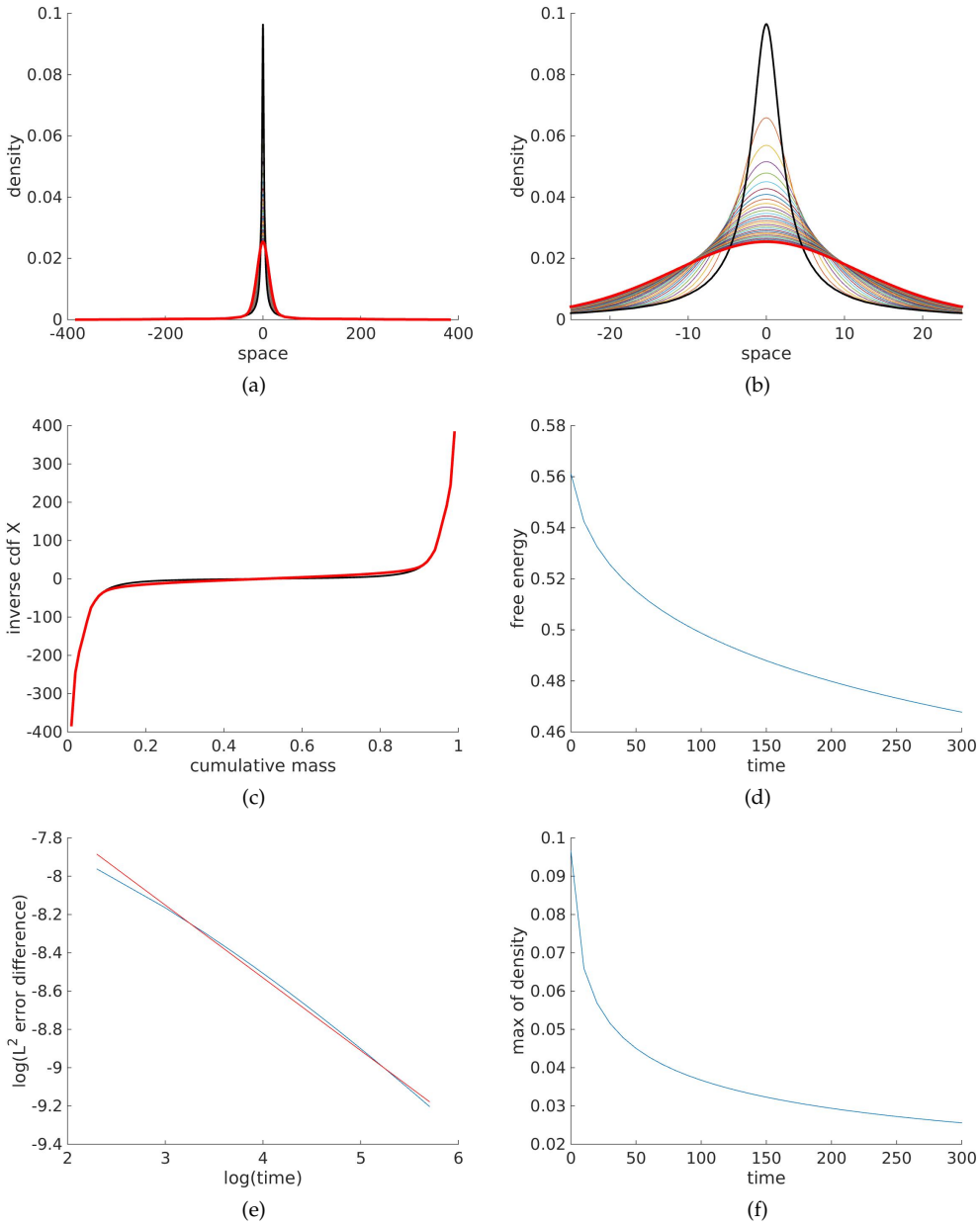

Figure 3.11: Attraction-dominated regime: $\chi = 0.35$, $k = -1/2$, $m = 4/3$, $r = 0$ with initial data $\rho(t = 0, x) = \rho_{HLS,\lambda_0,c_0}(x) < \rho_{HLS,\lambda_0,c*}(x)$ for all $x \in \mathbb{R}$ with $c_0 = 0.4c^*$.
(a) Solution density from initial condition (black) to the profile at the last time step (red), (b) zoom of Figure (a), (c) inverse cumulative distribution function from initial condition (black) to the profile at the last time step (red), (d) free energy, (e) log-log plot of the L^2-error difference between two consecutive solutions and fitted line with slope -0.37987, (f) time evolution of $\max_x \rho(t, x)$.

For the same choice of initial data, but with $c_0 = 1.1\,c^* > c^*$ we observe numerically that the solution density concentrates at $x = 0$ as predicted by Conjecture 1(ii), see Figure 3.12. The Newton-Raphson procedure stops converging once the mass it too concentrated. Here, we chose time steps of size $\Delta t = 10^{-3}$ and particles spaced at $\Delta\eta = 2 * 10^{-3}$.

One may also take as initial condition exactly the steady state $\rho_0 = \rho_{HLS,\lambda*,c*}$, see Figure 3.13. However, the numerical approximation of the initial data is only accurate up to $\Delta\eta = 10^{-2}$ and we observe indeed pointwise convergence to zero, in accordance with the statement of Conjecture 2 that the stationary state $\rho_{HLS,\lambda*,c*}$ is unstable. Again, we let the Newton-Raphson procedure evolve with time steps of size $\Delta t = 10^{-2}$ until the L^2-error between two consecutive solutions is less than the tolerance 10^{-4}.

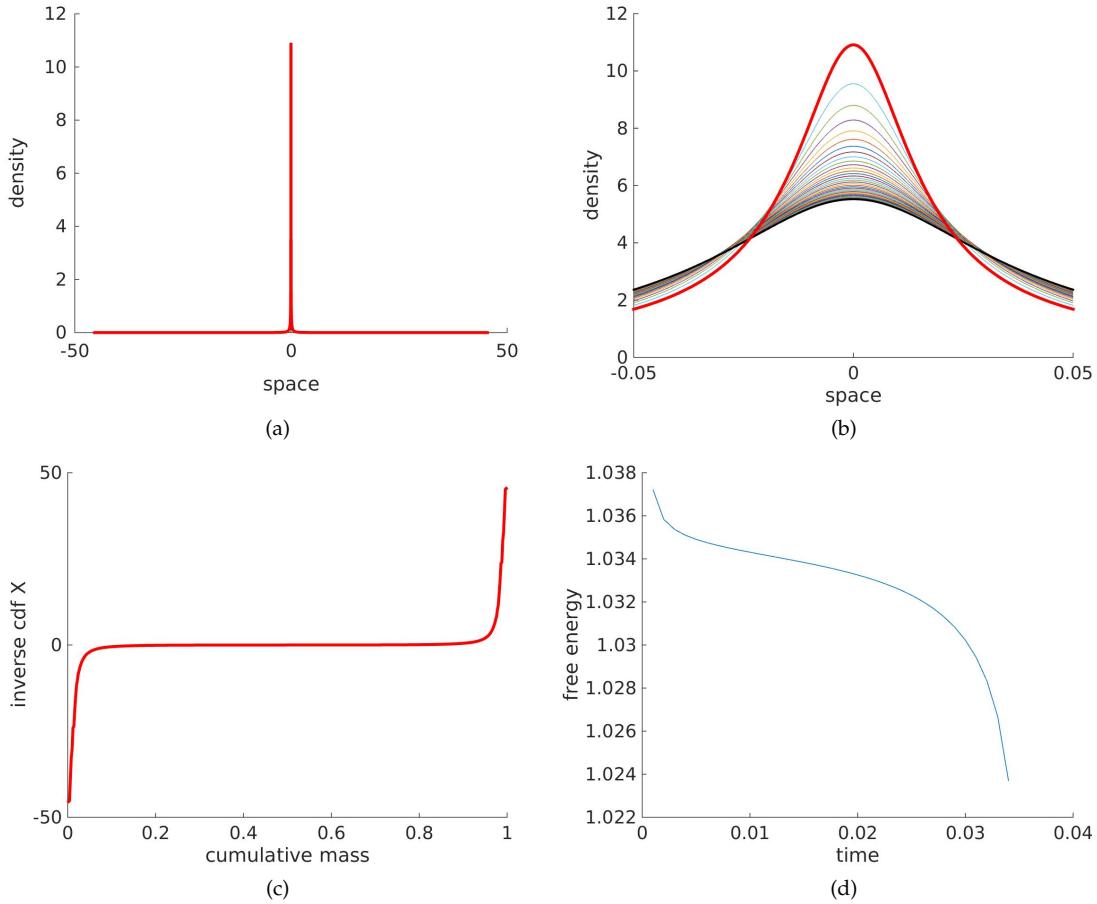

Figure 3.12: Attraction-dominated regime: $\chi = 0.35$, $k = -1/2$, $m = 4/3$, $r = 0$ with initial data $\rho(t = 0, x) = \rho_{HLS,\lambda_0,c_0}(x) > \rho_{HLS,\lambda_0,c*}(x)$ for all $x \in \mathbb{R}$ with $c_0 = 1.1c^*$.
(a) Solution density from initial condition (black) to the profile at the last time step (red), (b) zoom of Figure (a), (c) inverse cumulative distribution function from initial condition (black) to the profile at the last time step (red), (d) free energy.

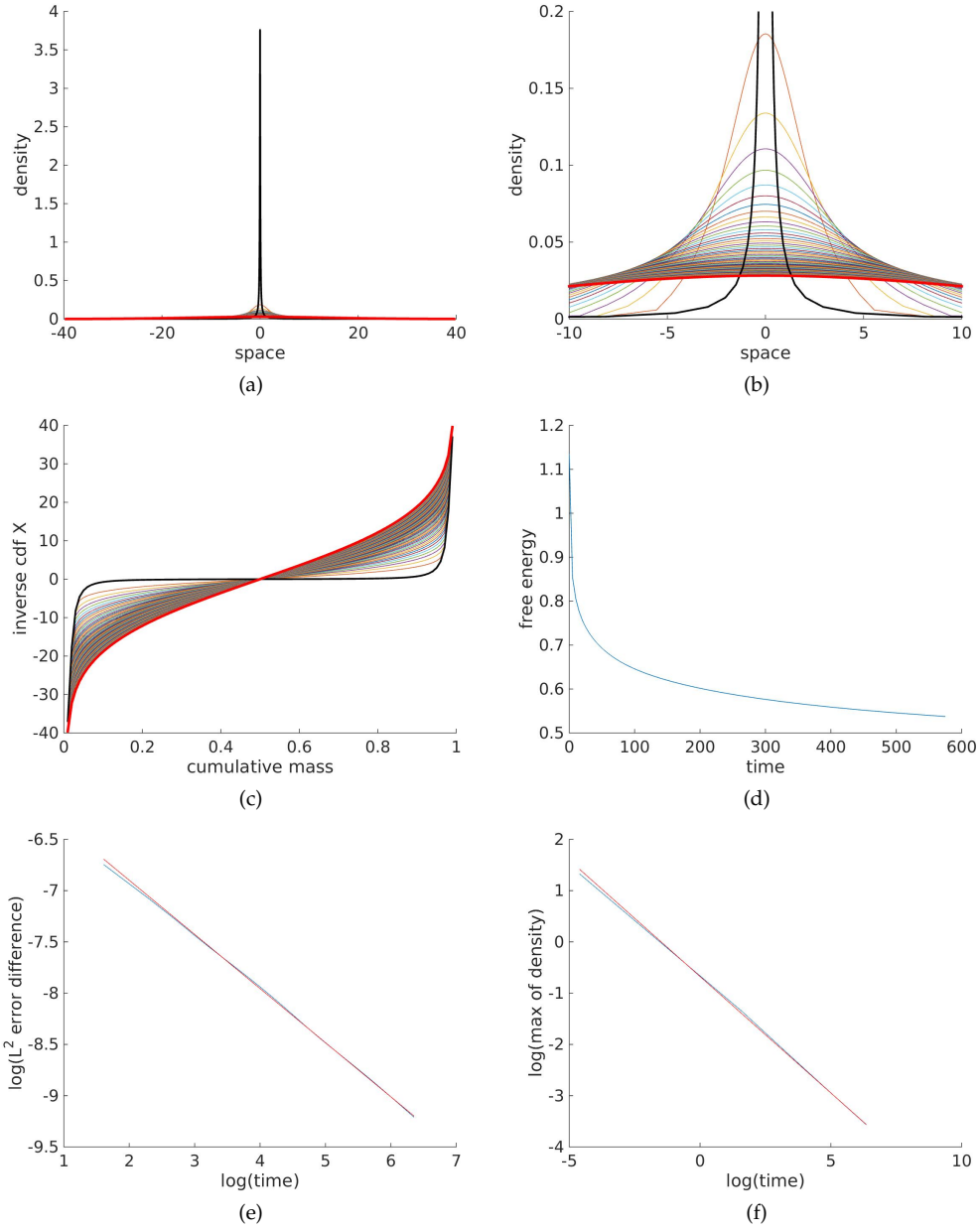

Figure 3.13: Attraction-dominated regime: $\chi = 0.35$, $k = -1/2$, $m = 4/3$, $r = 0$ with initial data $\rho(t = 0, x) = \rho_{HLS,\lambda*,c*}(x)$ given in (6.53).
(a) Solution density from initial condition (black) to the profile at the last time step (red), (b) zoom of Figure (a), (c) inverse cumulative distribution function from initial condition (black) to the profile at the last time step (red), (d) free energy, (e) log-log plot of the L^2-error difference between two consecutive solutions and fitted line with slope -0.52817, (f) log-log plot of $\max_x \rho(t, x)$ and fitted line with slope -0.45431 .

Chapter 4

Ground States in the Diffusion-Dominated Regime

This chapter follows in most parts the article "Ground states in the diffusion-dominated regime" written in collaboration with José A. Carrillo[1], Edoardo Mainini[2] and Bruno Volzone[3], and submitted for publication. The radiality proof in Section 2.1 of Chapter 4 was contributed by José A. Carrillo and Bruno Volzone.

Chapter Summary

We consider macroscopic descriptions of particles where repulsion is modelled by nonlinear power-law diffusion and attraction by a homogeneous singular kernel leading to variants of the Keller–Segel model of chemotaxis. We analyse the regime in which diffusive forces are stronger than attraction between particles, known as the diffusion-dominated regime, and show that all stationary states of the system are radially symmetric decreasing and compactly supported. The model can be formulated as a gradient flow of a free energy functional for which the overall convexity properties are not known. We show that global minimisers of the free energy always exist. Further, they are radially symmetric, compactly supported, uniformly bounded and C^∞ inside their support. Global minimisers enjoy certain regularity properties if the diffusion is not too slow, and in this case, provide stationary states of the system. In one dimension, stationary states are characterised as optimisers of a functional inequality which establishes equivalence between global minimisers and stationary states, and allows to deduce uniqueness.

[1]Department of Mathematics, Imperial College London, South Kensington Campus, London SW7 2AZ, UK.
[2]Dipartimento di Ingegneria Meccanica, Università degli Studi di Genova, Genova, Italia
[3]Dipartimento di Ingegneria, Università degli Studi di Napoli "Parthenope", Napoli, Italia

Chapter Content

Man begreift nur,
was man selbst machen kann,
und man faßt nur,
was man selbst hervorbringen kann[4].

Johann Wolfgang von Goethe

[4] quoted from a letter from Johann Wolfgang von Goethe to Carl Friedrich Zelter, 28th March 1804 [299].

1 Introduction

As in Chapters 2 and 3, we are interested in the aggregation-diffusion equation

$$\partial_t \rho = \frac{1}{N}\Delta \rho^m + 2\chi \nabla \cdot (\rho \nabla S_k) \tag{1.1}$$

for a density $\rho(t,x)$ of unit mass defined on $\mathbb{R}_+ \times \mathbb{R}^N$, and where we denote the mean-field potential by $S_k(x) := W_k(x) * \rho(x)$ with the interaction kernel W_k given by the Riesz potential,

$$W_k(x) := \frac{|x|^k}{k}, \quad k \in (-N, 0).$$

For an extensive survey of applications and literature around equation (1.1), see Chapters 1, 2 and 3. In this chapter, we focus on the case when diffusion is non-linear and of porous medium type $m > 1$ whilst W_k has a singularity at the origin $k < 0$. The lower bound on k ensures that the kernel W_k is locally integrable in $\mathbb{R}^N$. As the Riesz potential W_k is the fundamental solution of the fractional Laplacian $(-\Delta)^s$ with $k = 2s - N$, we sometimes use the notation $s \in (0, N/2)$ instead of $k \in (-N, 0)$. More precisely, the convolution term S_k is governed by a fractional diffusion process,

$$c_{N,s}(-\Delta)^s S_k = \rho\,, \qquad c_{N,s} := (2s-N)\frac{\Gamma\left(\frac{N}{2}-s\right)}{\pi^{N/2} 4^s \Gamma(s)}\,.$$

For $k > 1 - N$, the gradient $\nabla S_k := \nabla\,(W_k * \rho)$ is well defined locally. For $k \in (-N, 1-N]$ however, it becomes a singular integral, and we thus define it via a Cauchy principal value,

$$\nabla S_k(x) := \begin{cases} \nabla\,(W_k * \rho)\,(x)\,, & \text{if } 1 - N < k < 0\,, \\ \displaystyle\int_{\mathbb{R}^N} \nabla W_k(x-y)\,(\rho(y) - \rho(x))\,dy\,, & \text{if } -N < k \leqslant 1 - N\,. \end{cases} \tag{1.2}$$

The parameter $\chi > 0$ denotes the interaction strength and scales with the mass of solutions. Since (1.1) conserves mass, is positivity preserving and invariant by translation, we work with solutions ρ in the set

$$\mathcal{Y} := \left\{ \rho \in L^1_+(\mathbb{R}^N) \cap L^m(\mathbb{R}^N)\,,\ ||\rho||_1 = 1\,,\ \int_{\mathbb{R}^N} x\rho(x)\,dx = 0 \right\}\,.$$

The associated free energy functional to the evolution equation (1.1) is given by

$$\mathcal{F}_{m,k}[\rho] := \mathcal{H}_m[\rho] + \chi \mathcal{W}_k[\rho]$$

with

$$\mathcal{H}_m[\rho] := \frac{1}{N(m-1)}\int_{\mathbb{R}^N} \rho^m(x)\,dx\,, \qquad \mathcal{W}_k[\rho] := \iint\limits_{\mathbb{R}^N \times \mathbb{R}^N} \frac{|x-y|^k}{k}\rho(x)\rho(y)\,dxdy$$

Note that $\mathcal{F}_{m,k} < \infty$ on $\mathcal{Y}$. The noticeable characteristic of the class of PDEs (1.1) and the functional $\mathcal{F}_{m,k}$ consists in the competition between non-linear diffusion and a non-local quadratic interaction term which is due to the self-attraction of the particles through the mean-field potential S_k. The free energy functional $\mathcal{F}_{m,k}$ is not only non-increasing along the trajectories of the system,

equation (1.1) is also the formal gradient flow of $\mathcal{F}_{m,k}$ when the space of probability measures is endowed with the Euclidean Wasserstein metric $\mathbf{W}$, see Chapter 1 Section 2.3.2. This means that the family of PDEs (1.1) can be written as

$$\partial_t \rho(t) = -\nabla_{\mathbf{W}} \mathcal{F}_{m,k}[\rho(t)] \,.$$

Performing gradient flows of a convex functional is a natural task, and suitable estimates from below on the right notion of Hessian of $\mathcal{F}_{m,k}$ translate into a rate of convergence towards equilibrium for the PDE [295, 96, 3]. However, in our case, the overall convexity properties of the free energy functional $\mathcal{F}_{m,k}$ are not known, see Chapter 1 Section 2.3. Performing gradient flows of functionals with convex and concave contributions is much more delicate, and one has to seek compensations. Such compensations do exist in our case, and we will observe them at the level of existence of minimisers for the free energy functional $\mathcal{F}_{m,k}$ and stationary states of the family of PDEs (1.1) for certain ranges of the diffusion exponent $m > 1$.

The functional $\mathcal{F}_{m,k}$ possesses remarkable homogeneity properties that motivate the definition of the *fair-competition regime* $N(m-1)+k=0$, the *diffusion-dominated regime* $N(m-1)+k>0$ and the *attraction-dominated regime* $N(m-1)+k<0$, see Chapter 1 Definition 3.1. An overview of the parameter space (k,m) and the different regimes is given in Chapter 1 Figure 1.4. More precisely, taking mass-preserving dilations $\rho^\lambda(x) := \lambda^N \rho(\lambda x)$ for $\lambda > 0$ of a density $\rho \in \mathcal{Y}$, we obtain

$$\mathcal{F}_{m,k}[\rho^\lambda] = \lambda^{N(m-1)} \mathcal{H}_m[\rho] + \lambda^{-k} \chi \mathcal{W}_k[\rho] \,.$$

In other words, the diffusion and aggregation forces are in balance if $N(m-1) = -k$. This is the case for choosing the critical diffusion exponent

$$m_c := 1 - \frac{k}{N} \,. \tag{1.3}$$

In this chapter, we deal with the diffusion-dominated regime $m > m_c$, i.e. diffusion is expected to overcome aggregation as $\lambda \to \infty$, for any choice of $\chi > 0$. This domination effect means that solutions exist globally in time and are bounded uniformly in time [61, 277, 276]. Stationary states were found by minimisation of the free energy functional in two and three dimensions [273, 78, 99] in the case of attractive Newtonian potentials $k = 2 - N$. Stationary states are radially symmetric if $2 - N \leqslant k < 0$ as proven in [89]. Moreover, in the particular case of $N = 2$, $k = 0$, and $m > 1$ it has been shown in [89] that the asymptotic behaviour is given by compactly supported stationary solutions independently of χ. For a detailed review of known results, see Chapter 1 Section 3. Our goal is to generalise these results to the full range $k \in (-N, 0)$ and $m > m_c$. Stationary states of the system (1.1) provide natural candidates for asymptotic profiles of the evolution problem, and we focus therefore on understanding the stationary problem first, making the connection to

minimisers of the energy functional $\mathcal{F}_{m,k}$. In what follows, we denote $\mathcal{F} := \mathcal{F}_{m,k}$ for simplicity. Further, we define the diffusion exponent m^* that will play an important role for the regularity properties of global minimisers of $\mathcal{F}$:

$$m^* := \begin{cases} \frac{2-k-N}{1-k-N}\,, & \text{if} \quad N \geqslant 1 \quad \text{and} \quad -N < k < 1-N\,, \\ +\infty & \text{if} \quad N \geqslant 2 \quad \text{and} \quad 1-N \leqslant k < 0\,. \end{cases} \tag{1.4}$$

In this chapter, we will prove the following main results:

Theorem 1.1. *Let $N \geqslant 1$, $\chi > 0$ and $k \in (-N, 0)$. All stationary states of equation (1.1) are radially symmetric decreasing. If $m > m_c$, then there exists a global minimiser ρ of $\mathcal{F}$ on $\mathcal{Y}$. Further, all global minimisers $\rho \in \mathcal{Y}$ are radially symmetric non-increasing, compactly supported, uniformly bounded and C^∞ inside their support. Moreover, all global minimisers of $\mathcal{F}$ are stationary states of (1.1) whenever $m_c < m < m^*$. Finally, if $m_c < m \leqslant 2$, we have $\rho \in \mathcal{W}^{1,\infty}\left(\mathbb{R}^N\right)$.*

Theorem 1.2. *Let $N = 1$, $\chi > 0$ and $k \in (-1, 0)$. All stationary states of (1.1) are global minimisers of the energy functional $\mathcal{F}$ on $\mathcal{Y}$. Further, stationary states of (1.1) in $\mathcal{Y}$ are unique.*

2 Stationary states

Let us begin by defining precisely the notion of stationary states to the aggregation-diffusion equation (1.1).

Definition 2.1. *Given $\bar{\rho} \in L^1_+\left(\mathbb{R}^N\right) \cap L^\infty\left(\mathbb{R}^N\right)$ with $||\bar{\rho}||_1 = 1$, and letting $\bar{S}_k = W_k * \bar{\rho}$, we say that $\bar{\rho}$ is a **stationary state** for the evolution equation (1.1) if $\bar{\rho}^m \in \mathcal{W}^{1,2}_{loc}\left(\mathbb{R}^N\right)$, $\nabla \bar{S}_k \in L^1_{loc}\left(\mathbb{R}^N\right)$, and it satisfies*

$$\frac{1}{N}\nabla \bar{\rho}^m = -2\chi\, \bar{\rho} \nabla \bar{S}_k$$

in the sense of distributions in $\mathbb{R}^N$. If $-N < k \leqslant 1-N$, we further require $\bar{\rho} \in C^{0,\alpha}\left(\mathbb{R}^N\right)$ for some $\alpha \in (1-k-N, 1)$.

In fact, as shown in Chapter 2, the function S_k and its gradient defined in (1.2) satisfy even more than the regularity $\nabla S_k \in L^1_{loc}\left(\mathbb{R}^N\right)$ required in Definition 2.1:

Lemma 2.2. *Let $\rho \in L^1_+\left(\mathbb{R}^N\right) \cap L^\infty\left(\mathbb{R}^N\right)$ with $||\rho||_1 = 1$ and $k \in (-N, 0)$. Then the following regularity properties hold:*

(i) $S_k \in L^\infty\left(\mathbb{R}^N\right)$.

(ii) $\nabla S_k \in L^\infty\left(\mathbb{R}^N\right)$, *assuming additionally* $\rho \in C^{0,\alpha}\left(\mathbb{R}^N\right)$ *with* $\alpha \in (1-k-N, 1)$ *in the range* $k \in (-N, 1-N]$.

Using the same techniques as in Chapter 2, we can show that Lemma 2.2 implies further regularity properties for stationary states of (1.1).

Proposition 2.3. *Let $k \in (-N, 0)$ and $m > m_c$. If $\bar\rho$ is a stationary state of equation (1.1) and $\bar S_k = W_k * \bar\rho$, then $\bar\rho$ is continuous on $\mathbb{R}^N$, $\bar\rho^{m-1} \in \mathcal{W}^{1,\infty}\left(\mathbb{R}^N\right)$, and it satisfies*

$$\bar\rho(x)^{m-1} = \frac{N(m-1)}{m}\left(C[\bar\rho](x) - 2\chi \bar S_k(x)\right)_+ , \qquad \forall\, x \in \mathbb{R}^N ,$$

where $C[\bar\rho](x)$ is constant on each connected component of supp $(\bar\rho)$.

It follows from Proposition 2.3 that any stationary state $\bar\rho$ of equation (1.1) enjoys $\mathcal{W}^{1,\infty}$-regularity in the case $m_c < m \leqslant 2$.

2.1 Radial symmetry of stationary states

The aim of this section is to prove that stationary states of (1.1) are radially symmetric. This is one of the main results of [89], and is achieved there under the assumption that the interaction kernel is not more singular than the Newtonian potential close to the origin. As we will briefly describe in the proof of the next result, the main arguments continue to hold even for the more singular Riesz kernels W_k.

Theorem 2.4 (Radiality of stationary states)**.** *Let $\chi > 0$ and $m > m_c$. If $\bar\rho \in L^1_+(\mathbb{R}^N) \cap L^\infty(\mathbb{R}^N)$ with $\|\bar\rho\|_1 = 1$ is a stationary state of (1.1) in the sense of Definition 2.1, then $\bar\rho$ is radially symmetric non-increasing up to a translation.*

Proof. The proof is based on a contradiction argument, being an adaptation of that in [89, Theorem 2.2], to which we address the reader the more technical details. Assume that $\bar\rho$ is *not* radially decreasing up to *any* translation. By Proposition 2.3, we have

$$\left|\nabla \bar\rho^{m-1}(x)\right| \leqslant c \tag{2.5}$$

for some positive constant c in supp$(\bar\rho)$. Let us now introduce the *continuous Steiner symmetrisation* $S^\tau\bar\rho$ in direction $e_1 = (1, 0, \cdots, 0)$ of $\bar\rho$ as follows. For any $x_1 \in \mathbb{R}, x' \in \mathbb{R}^{N-1}, h > 0$, let

$$S^\tau\bar\rho(x_1, x') := \int_0^\infty \mathbb{1}_{M^\tau(U^h_{x'})}(x_1)dh,$$

where

$$U^h_{x'} = \{x_1 \in \mathbb{R} : \bar\rho(x_1, x') > h\}$$

and $M^\tau(U^h_{x'})$ is the continuous Steiner symmetrisation of the $U^h_{x'}$ (see [89] for the precise definitions and all the related properties). As in [89], our aim is to show that there exist a continuous

family of functions $\mu(\tau, x)$ such that $\mu(0, \cdot) = \bar{\rho}$ and some positive constants $C_1 > 0$, $c_0 > 0$ and a small $\delta_0 > 0$ such that the following estimates hold for all $\tau \in [0, \delta_0]$:

$$\mathcal{F}[\mu[\tau]] - \mathcal{F}[\bar{\rho}] \leqslant -c_0\tau \tag{2.6}$$

$$|\mu(\tau, x) - \bar{\rho}(x)| \leqslant C_1\bar{\rho}(x)\tau \qquad \text{for all } x \in \mathbb{R}^N \tag{2.7}$$

$$\int_{\Omega_i} [\mu(\tau, x) - \bar{\rho}(x)]\, dx = 0 \qquad \text{for any connected component } \Omega_i \text{ of } \operatorname{supp}(\bar{\rho}). \tag{2.8}$$

Following the arguments of the proof in [89, Proposition 2.7], if we want to construct a continuous family $\mu(\tau, \cdot)$ for (2.7) to hold, it is convenient to modify suitably the continuous Steiner symmetrisation $S^\tau\bar{\rho}$ in order to have a better control of the speed in which the level sets $U^h_{x'}$ are moving. More precisely, we define $\mu(\tau, \cdot) = \tilde{S}^\tau\bar{\rho}$ as

$$\tilde{S}^\tau\bar{\rho}_0(x_1, x') := \int_0^\infty \mathbb{1}_{M^{v(h)\tau}(U^h_{x'})}(x_1)dh$$

with $v(h)$ defined as

$$v(h) := \begin{cases} 1 & h > h_0\,, \\ 0 & 0 < h \leqslant h_0\,, \end{cases}$$

for some sufficiently small constant $h_0 > 0$ to be determined. Note that this choice of the velocity is different to the one in [89, Proposition 2.7] since we are actually keeping the level sets of $\tilde{S}^\tau\bar{\rho}(\cdot, x')$ frozen below the layer at height h_0. Next, we note that inequality (2.5) and the Lipschitz regularity of $\bar{S}_k$ (Lemma 2.2) are the only basic ingredients used in the proof of [89, Proposition 2.7] to show that the family $\mu(\tau, \cdot)$ satisfies (2.7) and (2.8). Therefore, it remains to prove (2.6). Since different level sets of $\tilde{S}^\tau\bar{\rho}(\cdot, x')$ are moving at different speeds $v(h)$, we do not have $M^{v(h_1)\tau}(U^{h_1}_{x'}) \subset M^{v(h_2)\tau}(U^{h_2}_{x'})$ for all $h_1 > h_2$, but it is still possible to prove that (see [89, Proposition 2.7])

$$\mathcal{H}_m[\tilde{S}^\tau\bar{\rho}] \leqslant \mathcal{H}_m[\bar{\rho}] \text{ for all } \tau \geqslant 0.$$

Then, in order to establish (2.6), it is enough to show

$$\mathcal{W}_k[\tilde{S}^\tau\bar{\rho}] \leqslant \mathcal{W}_k[\bar{\rho}] - 2\chi c_0\tau \quad \text{for all } \tau \in [0, \delta_0], \text{ for some } c_0 > 0 \text{ and } \delta_0 > 0. \tag{2.9}$$

As in the proof of [89, Proposition 2.7], proving (2.9) reduces to show that for sufficiently small $h_0 > 0$ one has

$$\left|\mathcal{W}_k[\tilde{S}^\tau\bar{\rho}] - \mathcal{W}_k[S^\tau\bar{\rho}]\right| \leqslant c\chi\tau \quad \text{for all } \tau. \tag{2.10}$$

To this aim, we write

$$S^\tau\bar{\rho}(x_1, x') = \int_{h_0}^\infty \mathbb{1}_{M^\tau(U^h_{x'})}(x_1)dh + \int_0^{h_0} \mathbb{1}_{M^\tau(U^h_{x'})}(x_1)dh =: f_1(\tau, x) + f_2(\tau, x)$$

and we split $\tilde{S}^\tau\bar{\rho}$ similarly, taking into account that $v(h) = 1$ for all $h > h_0$:

$$\tilde{S}^\tau\bar{\rho}(x_1, x') = f_1(\tau, x) + \int_0^{h_0} \mathbb{1}_{M^{v(h)\tau}(U^h_{x'})}(x_1)dh =: f_1(\tau, x) + \tilde{f}_2(\tau, x).$$

Note that

$$f_2 = S^\tau(\mathcal{T}^{h_0}\bar{\rho}),$$

where $\mathcal{T}^{h_0}\bar{\rho}$ is the truncation at height h_0 of $\bar{\rho}$. Since $v(h) = 0$ for $h \leqslant h_0$, we have

$$\tilde{f}_2 = \mathcal{T}^{h_0}\bar{\rho}.$$

If we are in the singular range $k \in (-N, 1-N]$, we have $\bar{\rho} \in C^{0,\alpha}\left(\mathbb{R}^N\right)$ for some $\alpha \in (1-k-N, 1)$. Since the continuous Steiner symmetrisation decreases the modulus of continuity (see [54, Theorem 3.3] and [54, Corollary 3.1]), we also have $S^\tau\bar{\rho},\ f_2,\ \tilde{f}_2 \in C^{0,\alpha}\left(\mathbb{R}^N\right)$. Further, Lemma 2.2 guarantees that the expressions

$$A_1(\tau) := \left|\int f_2(W_k * f_1) - \tilde{f}_2(W_k * f_1)dx\right| \quad \text{and} \quad A_2(\tau) := \left|\int f_2(W_k * f_2) - \tilde{f}_2(W_k * \tilde{f}_2)dx\right|$$

can be controlled by $||\bar{\rho}||_\infty$ and the α-Hölder seminorm of $\bar{\rho}$. Hence, we can apply the argument in [89, Proposition 2.7] to conclude for the estimate (2.10). Now it is possible to proceed exactly as in the proof of [89, Theorem 2.2] to show that for some positive constant C_2, we have the quadratic estimate

$$|\mathcal{F}[\mu[\tau]] - \mathcal{F}[\bar{\rho}]| \leqslant C_2\tau^2,$$

which is a contradiction with (2.6) for small τ. □

2.2 Stationary states are compactly supported

In this section, we will prove that all stationary states of equation (1.1) have compact support, which agrees with the properties shown in [199, 78, 89]. We begin by stating a useful asymptotic estimate on the Riesz potential inspired by [269, §4]. For the proof of Proposition 2.5, see Appendix A.

Proposition 2.5 (Riesz potential estimates). *Let $k \in (-N, 0)$ and let $\rho \in \mathcal{Y}$ be radially symmetric.*

(i) If $1 - N < k < 0$, then $|x|^k * \rho(x) \leqslant C_1|x|^k$ on $\mathbb{R}^N$.

(ii) If $-N < k \leqslant 1 - N$ and if ρ is supported on a ball B_R for some $R < \infty$, then

$$|x|^k * \rho(x) \leqslant C_2 T_k(|x|, R)\,|x|^k, \qquad \forall\ |x| > R,$$

where

$$T_k(|x|, R) := \begin{cases} \left(\frac{|x|+R}{|x|-R}\right)^{1-k-N} & \text{if } k \in (-N, 1-N), \\ \left(1 + \log\left(\frac{|x|+R}{|x|-R}\right)\right) & \text{if } k = 1-N \end{cases} \tag{2.11}$$

Here, $C_1 > 0$ and $C_2 > 0$ are explicit constants depending only on k and N.

From the above estimate, we can derive the expected asymptotic behaviour at infinity.

Corollary 2.6. *Let $\rho \in \mathcal{Y}$ be radially non-increasing. Then $W_k * \rho$ vanishes at infinity, with decay not faster than that of $|x|^k$.*

Proof. Notice that Proposition 2.5(i) entails the decay of the Riesz potential at infinity for $1 - N < k < 0$. Instead, let $-N < k \leqslant 1 - N$. Let $r \in (1 - k - N, 1)$ and notice that $|y|^k \leqslant |y|^{k+r}$ if $|y| \geqslant 1$, so that if B_1 is the unit ball centered at the origin we have

$$\begin{aligned} |x|^k * \rho(x) &\leqslant \int_{B_1} \rho(x-y)|y|^k \, dy + \int_{B_1^C} \rho(x-y)|y|^{k+r} \, dy \\ &\leqslant \left(\sup_{y \in B_1} \rho(x-y) \right) \int_{B_1} |y|^k \, dy + (W_{k+r} * \rho)(x). \end{aligned}$$

The first term in the right hand side vanishes as $|x| \to \infty$, since $y \mapsto |y|^k$ is integrable at the origin, and since ρ is radially non-increasing and vanishing at infinity as well. The second term goes to zero at infinity thanks to Proposition 2.5(i), since the choice of r yields $k + r > 1 - N$.

On the other hand, the decay at infinity of the Riesz potential can not be faster than that of $|x|^k$. To see this, notice that there holds

$$|x|^k * \rho(x) \geqslant \int_{B_1} \rho(y)|x-y|^k \, dy \geqslant (|x|+1)^k \int_{B_1} \rho(y) \, dy$$

with $\int_{B_1} \rho > 0$ since $\rho \in \mathcal{Y}$ is radially non-increasing. □

As a rather simple consequence of Corollary 2.6, we obtain:

Corollary 2.7. *Let $\bar{\rho}$ be a stationary state of (1.1). Then $\bar{\rho}$ is compactly supported.*

Proof. By Theorem 2.4 we have that $\bar{\rho}$ is radially non-increasing up to a translation. Since the translation of a stationary state is itself a stationary state, we may assume that $\bar{\rho}$ is radially symmetric with respect to the origin. Suppose by contradiction that $\bar{\rho}$ is supported on the whole of $\mathbb{R}^N$, so that equation (2.9) holds on the whole $\mathbb{R}^N$, with $C_k[\bar{\rho}](x)$ replaced by a unique constant C. Then we necessarily have $C = 0$. Indeed, $\bar{\rho}^{m-1}$ vanishes at infinity since it is radially decreasing and integrable, and by Corollary 2.6 we have that $\bar{S}_k = W_k * \bar{\rho}$ vanishes at infinity as well. Therefore

$$\bar{\rho} = \left(2\chi \frac{N(m-1)}{m} \bar{S}_k \right)^{1/(m-1)}.$$

But Corollary 2.6 shows that $W_k * \rho$ decays at infinity not faster than $|x|^k$ and this would entail, since $m > m_c$, a decay at infinity of ρ not faster than that of $|x|^{-N}$, contradicting the integrability of ρ. □

3 Global minimisers

3.1 Existence of global minimisers

Theorem 3.1 (Existence of Global Minimisers). *For all $\chi > 0$ and $k \in (-N, 0)$, there exists a global minimiser ρ of $\mathcal{F}$ in $\mathcal{Y}$. Moreover, all global minimisers of $\mathcal{F}$ in $\mathcal{Y}$ are radially non-increasing.*

We follow the concentration compactness argument as applied in Appendix A.1 of [199]. Our proof is based on [220, Theorem II.1, Corollary II.1]. Let us denote by $\mathcal{M}^p(\mathbb{R}^N)$ the Marcinkiewicz space or weak L^p space.

Theorem 3.2. *(see [220, Theorem II.1]) Suppose $W \in \mathcal{M}^p(\mathbb{R}^N)$, $1 < p < \infty$, and consider the problem*

$$I_M = \inf_{\rho \in \mathcal{Y}_{q,M}} \left\{ \frac{1}{N(m-1)} \int_{\mathbb{R}^N} \rho^m dx + \chi \int_{\mathbb{R}^N} \rho(\rho * W) dx \right\} .$$

where

$$\mathcal{Y}_{q,M} = \left\{ \rho \in L^q(\mathbb{R}^N) \cap L^1(\mathbb{R}^N) \, , \, \rho \geqslant 0 \ a.e., \int_{\mathbb{R}^N} \rho(x)\, dx = M \right\} , \qquad q = \frac{p+1}{p} < m \, .$$

Then there exists a minimiser of problem (I_M) if the following holds:

$$I_{M_0} < I_M + I_{M_0 - M} \qquad \text{for all } M \in (0, M_0) \, . \tag{3.12}$$

Proposition 3.3. *(see [220, Corollary II.1]) Suppose there exists some $\lambda \in (0, N)$ such that*

$$W(tx) \geqslant t^{-\lambda} W(x)$$

for all $t \geqslant 1$. Then (3.12) holds if and only if

$$I_M < 0 \qquad \text{for all } M > 0 \, . \tag{3.13}$$

Proof of Theorem 3.1. First of all, notice that our choice of potential $W_k(x) = |x|^k/k$ is indeed in $\mathcal{M}^p(\mathbb{R}^N)$ with $p = -N/k$. Further, it can easily be verified that Proposition 3.3 applies with $\lambda = -k$. Hence we are left to show that there exists a choice of $\rho \in \mathcal{Y}_{q,M}$ such that $\mathcal{F}[\rho] < 0$. Let us fix $R > 0$ and define

$$\rho_*(x) := \frac{MN}{\sigma_N R^N} \mathbb{1}_{B_R}(x) \, ,$$

where B_R denotes the ball centered at zero and of radius $R > 0$, and where $\sigma_N = 2\pi^{(N/2)}/\Gamma(N/2)$ denotes the surface area of the N-dimensional unit ball. Then

$$\begin{aligned}
\mathcal{H}_m[\rho_*] &= \frac{1}{N(m-1)} \int_{\mathbb{R}^N} \rho_*^m dx = \frac{(MN)^m \sigma_N^{1-m}}{N^2(m-1)} R^{N(1-m)} \, , \\
\mathcal{W}_k[\rho_*] &= \iint_{\mathbb{R}^N \times \mathbb{R}^N} W_k(x-y) \rho_*(x) \rho_*(y)\, dxdy \\
&= \frac{(MN)^2}{k\sigma_N^2 R^{2N}} \iint_{\mathbb{R}^N \times \mathbb{R}^N} |x-y|^k \mathbb{1}_{B_R}(x) \mathbb{1}_{B_R}(y)\, dxdy \\
&\leqslant \frac{(MN)^2}{k\sigma_N^2 R^{2N}} (2R)^k \frac{\sigma_N^2}{N^2} R^{2N} = 2^k M^2 \frac{R^k}{k} < 0 \, .
\end{aligned}$$

We conclude that

$$\mathcal{F}[\rho_*] = \mathcal{H}_m[\rho_*] + \chi \mathcal{W}_k[\rho_*] \leqslant \frac{M^m N^{m-2} \sigma_N^{1-m}}{(m-1)} R^{N(1-m)} + 2^k M^2 \chi \frac{R^k}{k} .$$

Since we are in the diffusion-dominated regime $N(1-m) < k < 0$, we can choose $R > 0$ large enough such that $\mathcal{F}[\rho_*] < 0$, and hence condition (3.13) is satisfied. We conclude by Proposition 3.3 and Theorem 3.2 that there exists a minimiser $\bar{\rho}$ of $\mathcal{F}$ in $\mathcal{Y}_{q,M}$ with $q = (p+1)/p = (N-k)/N$.

It can easily be seen that in fact $\bar{\rho} \in L^m(\mathbb{R}^N)$ using the HLS inequality (3.21) in Chapter 1:

$$-\mathcal{W}_k[\rho] = \iint\limits_{\mathbb{R}^N \times \mathbb{R}^N} \frac{|x-y|^k}{(-k)} \rho(x)\rho(y)\, dxdy \leqslant \frac{C_{HLS}}{(-k)} ||\rho||_r^2 ,$$

where $r = 2N/(2N+k) = 2p/(2p-1)$. Using Hölder's inequality, we find

$$-\mathcal{W}_k[\rho] \leqslant \frac{C_{HLS}}{(-k)} ||\rho||_q^q ||\rho||_1^{2-q} .$$

Hence, since $\mathcal{F}[\bar{\rho}] < 0$,

$$||\bar{\rho}||_m^m \leqslant -\chi N(m-1)\mathcal{W}_k[\bar{\rho}] \leqslant \chi N(m-1) \left(\frac{M^{2-q} C_{HLS}}{(-k)} \right) ||\bar{\rho}||_q^q < \infty .$$

Translating $\bar{\rho}$ so that its centre of mass is at zero and choosing $M = 1$, we obtain a minimiser $\bar{\rho}$ of $\mathcal{F}$ in $\mathcal{Y}$. Moreover, by Riesz's rearrangement inequality [218, Theorem 3.7], we have

$$\mathcal{W}_k[\rho^\#] \leqslant \mathcal{W}_k[\rho] , \qquad \forall \rho \in \mathcal{Y}, ,$$

where $\rho^\#$ is the symmetric decreasing rearrangement of ρ. Thus, if $\bar{\rho}$ is a global minimiser of $\mathcal{F}$ in $\mathcal{Y}$, then so is $\bar{\rho}^\#$, and it follows that

$$\mathcal{W}_k[\bar{\rho}^\#] = \mathcal{W}_k[\bar{\rho}] .$$

We conclude from [218, Theorem 3.7] that $\bar{\rho} = \bar{\rho}^\#$, and so all global minimisers of $\mathcal{F}$ in $\mathcal{Y}$ are radially symmetric non-increasing. □

Global minimisers of $\mathcal{F}$ satisfy a corresponding Euler-Lagrange condition. The proof can be directly adapted from [78, Theorem 3.1] or Chapter 2 Proposition 3.6, and we omit it here.

Proposition 3.4. *Let $k \in (-N, 0)$ and $m > m_c$. If ρ is a global minimiser of the free energy functional $\mathcal{F}$ in $\mathcal{Y}$, then ρ is radially symmetric and non-increasing, satisfying*

$$\rho^{m-1}(x) = \frac{N(m-1)}{m} \left(D[\rho] - 2\chi W_k * \rho(x) \right)_+ \quad \text{a.e. in } \mathbb{R}^N. \tag{3.14}$$

Here, we denote

$$D[\rho] := 2\mathcal{F}[\rho] + \frac{m-2}{N(m-1)} ||\rho||_m^m, \qquad \rho \in \mathcal{Y} .$$

3.2 Boundedness of global minimisers

This section is devoted to showing that all global minimisers of $\mathcal{F}$ in $\mathcal{Y}$ are uniformly bounded. In the following, for a radial function $\rho \in L^1(\mathbb{R}^N)$ we denote by $M_\rho(R) := \int_{B_R} \rho\, dx$ the corresponding mass function, where B_R is a ball of radius R, centered at the origin. We start with the following technical lemma:

Lemma 3.5. *Let $\chi > 0$, $-N < k < 0$, $m > 1$ and $0 \leqslant q < m/N$. Assume $\rho \in \mathcal{Y}$ is radially decrasing. For a fixed $H > 0$, the level set $\{\rho \geqslant H\}$ is a ball centered at the origin whose radius we denote by A_H. Then we have the following cross-range interaction estimate: There exists $H_0 > 1$, depending only on $q, N, m, \|\rho\|_m$, such that, for any $H > H_0$,*

$$\int_{B^C_{A_H}} \int_{B_{A_H}} |x-y|^k \rho(x)\rho(y)\, dx\, dy \leqslant C_{k,N}\, M_\rho(A_H)\, \mathcal{K}_{k,q,N}(H),$$

where

$$\mathcal{K}_{k,q,N}(H) := \begin{cases} H^{1-q(k+N)} + H^{-kq} & \text{if } k \in (-N, 0),\ k \neq 1-N, \\ H^{1-q}(2 + \log(1+H^q)) + H^{q(N-1)} & \text{if } k = 1-N \end{cases}$$

and $C_{k,N}$ is a constant depending only on k and N.

Proof. Notice that the result is trivial if ρ is bounded. The interesting case here is ρ unbounded, implying that $A_H > 0$ for any $H > 0$.

First of all, since $\rho \in L^m(\mathbb{R}^N)$ and $\rho \geqslant H$ on B_{A_H}, the estimate

$$\frac{\sigma_N A_H^N}{N} H^m = \int_{B_{A_H}} H^m \leqslant \int_{B_{A_H}} \rho^m \leqslant ||\rho||_m^m$$

implies that $H^q A_H$ is vanishing as $H \to +\infty$ as soon as $q < m/N$, and in particular that we can find $H_0 > 1$, depending only on $q, m, N, ||\rho||_m$, such that

$$H^{-q} \geqslant 2A_H \quad \text{for any } H > H_0.$$

We fix $q \in [0, m/N)$ and $H > H_0$ as above from here on.

Let us make use of Proposition 2.5, which we apply to the compactly supported function $\rho_H := \rho \mathbb{1}_{\{\rho \geqslant H\}} / M_\rho(A_H)$.

Case $1 - N < k < 0$ Proposition 2.5(i) applied to ρ_H gives the estimate

$$\int_{B_{A_H}} |x-y|^k \rho(y)\, dy \leqslant C_1 M_\rho(A_H)\, |x|^k, \qquad \forall x \in \mathbb{R}^N,$$

and hence, integrating against ρ on $B^C_{A_H}$ and using $\rho \leqslant H$ on $B^C_{A_H}$,

$$\begin{aligned}
&\int_{B^C_{A_H}} \int_{B_{A_H}} |x-y|^k \rho(x)\rho(y)\,dx\,dy \leqslant C_1 M_\rho(A_H) \int_{B^C_{A_H}} |x|^k \rho(x)\,dx \\
&\quad = C_1 M_\rho(A_H) \left(\int_{B^C_{A_H}\cap B_{H^{-q}}} |x|^k \rho(x)\,dx + \int_{B^C_{A_H}\setminus B_{H^{-q}}} |x|^k \rho(x)\,dx \right) \\
&\quad \leqslant C_1 M_\rho(A_H) \left(H \int_{B^C_{A_H}\cap B_{H^{-q}}} |x|^k\,dx + H^{-kq} \int_{B^C_{A_H}\setminus B_{H^{-q}}} \rho(x)\,dx \right) \\
&\quad \leqslant C_1 M_\rho(A_H) \left(H\sigma_N \int_{A_H}^{H^{-q}} r^{k+N-1}\,dr + H^{-kq} \right) \\
&\quad \leqslant C_1 M_\rho(A_H) \left(\frac{\sigma_N}{k+N} H^{1-q(k+N)} + H^{-kq} \right),
\end{aligned}$$

which conludes the proof in that case.

Case $-N < k \leqslant 1-N$ In this case, we obtain from Proposition 2.5(ii) applied to ρ_H the estimate

$$\int_{B_{A_H}} |x-y|^k \rho(y)\,dy \leqslant C_2 M_\rho(A_H)\, T_k(|x|, A_H)|x|^k, \qquad \forall x \in B^C_{A_H},$$

and integrating against $\rho(x)$ over $B^C_{A_H}$, we have

$$\int_{B^C_{A_H}} \int_{B_{A_H}} |x-y|^k \rho(x)\rho(y)\,dx\,dy \leqslant C_2 M_\rho(A_H) \int_{B^C_{A_H}} T_k(|x|, A_H)|x|^k \rho(x)\,dx. \tag{3.15}$$

We split the integral in the right hand side as $I_1 + I_2$, where

$$I_1 := \int_{B^C_{A_H}\cap B_{H^{-q}}} T_k(|x|, A_H)|x|^k \rho(x)\,dx, \quad I_2 := \int_{B^C_{A_H}\setminus B_{H^{-q}}} T_k(|x|, A_H)|x|^k \rho(x)\,dx.$$

Let us first consider I_2, where we have $|x| \geqslant H^{-q} \geqslant 2A_H$ on the integration domain. Since the map $|x| \mapsto \frac{|x|+A_H}{|x|-A_H}$ is monotonically decreasing to 1 in $(A_H, +\infty)$, it is bounded above by 3 on $(2A_H, +\infty)$. We conclude from (2.11) that $T_k(|x|, A_H) \leqslant 3$ for $|x| \in (H^{-q}, +\infty)$. This entails

$$I_2 \leqslant 3 \int_{B^C_{A_H}\setminus B_{H^{-q}}} |x|^k \rho(x)\,dx \leqslant 3\, H^{-kq}, \tag{3.16}$$

where we used once again $|x| \geqslant H^{-q}$, recalling that $k < 0$.

Concerning I_1, we have $\rho \leqslant H$ on $B^C_{A_H}$ which entails

$$I_1 \leqslant H \int_{B^C_{A_H}\cap B_{H^{-q}}} T_k(|x|, A_H)|x|^k\,dx = \sigma_N H \int_{A_H}^{H^{-q}} T_k(r, A_H) r^{k+N-1}\,dr. \tag{3.17}$$

If $-N < k < 1-N$, we use (2.11) and $(r+2A_H)/(r+A_H) < 2$ for $r \in (0, +\infty)$, so that

$$\int_{A_H}^{H^{-q}} T_k(r, A_H) r^{k+N-1}\,dr \leqslant \int_0^{H^{-q}} \left(\frac{r+2A_H}{r+A_H} \right)^{1-k-N} r^{k+N-1}\,dr \leqslant \frac{2^{1-k-N}}{k+N} H^{-q(k+N)}. \tag{3.18}$$

If $k = 1 - N$ we have from (2.11), since $2A_H \leqslant H^{-q} < 1$,

$$\begin{aligned}\int_{A_H}^{H^{-q}} T_k(r, A_H) r^{k+N-1}\, dr &= \int_{A_H}^{H^{-q}} \left(1 + \log\left(\frac{r + A_H}{r - A_H}\right)\right) dr \\ &\leqslant \int_0^{H^{-q}} \left(1 + \log\left(\frac{r+1}{r}\right)\right) dr \\ &= H^{-q} + H^{-q}\log(1 + H^q) + \log(1 + H^{-q}) \\ &\leqslant H^{-q}(2 + \log(1 + H^q)).\end{aligned} \tag{3.19}$$

Combining (3.17), (3.18), (3.19) we conclude $I_1 \leqslant \frac{\sigma_N 2^{1-k+N}}{k+N} H^{1-q(k+N)}$ if $-N < k < 1 - N$, and $I_1 \leqslant \sigma_N H^{1-q}(2 + \log(1 + H^q))$ if $k = 1 - N$. These information together with the estimate (3.16) can be inserted into (3.15) to conclude. □

We are now in a position to prove that any global minimiser of $\mathcal{F}$ is uniformly bounded.

Proposition 3.6. *Let $\chi > 0$, $k \in (-N, 0)$ and $m > m_c$. Then any global minimiser of $\mathcal{F}$ over $\mathcal{Y}$ is uniformly bounded and compactly supported.*

Proof. Since ρ is radially symmetric decreasing by Proposition 3.4, it is enough to show $\rho(0) < \infty$. Let us reason by contradiction and assume that ρ is unbounded at the origin. We will show that $\mathcal{F}[\rho] - \mathcal{F}[\tilde{\rho}] > 0$ for a suitably chosen competitor $\tilde{\rho}$,

$$\tilde{\rho}(x) = \tilde{\rho}_{H,r}(x) := \frac{NM_\rho(A_H)}{\sigma_N r^N} \mathbb{1}_{D_r}(x) + \rho(x)\mathbb{1}_{B^C_{A_H}}(x)\,,$$

where B_{A_H} and q are defined as in Lemma 3.5, $B^C_{A_H}$ denotes the complement of B_{A_H} and $\mathbb{1}_{D_r}$ is the characteristic function of a ball $D_r := B_r(x_0)$ of radius $r > 0$, centered at some $x_0 \neq 0$ and such that $D_r \cap B_{A_H} = \varnothing$. Note that $A_H \leqslant H^{-q}/2 < H_0^{-q}/2 < 1/2$. Hence, wlog, we can take $r > 1$ and D_r centered at the point $x_0 = (2r, 0, \dots, 0) \in \mathbb{R}^N$. Notice in particular that since ρ is unbounded, for any $H > 0$ we have that B_{A_H} has non-empty interior. On the other hand, B_{A_H} shrinks to the origin as $H \to \infty$ since ρ is integrable. As $D_r \subset B^C_{A_H}$ and $\rho = \tilde{\rho}$ on $B^C_{A_H} \backslash D_r$, we obtain

$$\begin{aligned}N(m-1)\left(\mathcal{H}_m[\rho] - \mathcal{H}_m[\tilde{\rho}]\right) &= \int_{B_{A_H}} \rho^m + \int_{B^C_{A_H}} \rho^m - \int_{B^C_{A_H}} \left(\rho + \frac{NM_\rho(A_H)}{\sigma_N r^N}\mathbb{1}_{D_r}\right)^m \\ &= \int_{B_{A_H}} \rho^m + \int_{D_r} \left[\rho^m - \left(\rho + \frac{NM_\rho(A_H)}{\sigma_N r^N}\right)^m\right].\end{aligned}$$

We bound

$$\varepsilon_r := \int_{D_r} \left[\rho^m - \left(\rho + \frac{NM_\rho(A_H)}{\sigma_N r^N} \right)^m \right] \leqslant M_\rho(A_H)^m \left(\frac{\sigma_N}{N} \right)^{1-m} r^{N(1-m)},$$

where we use the convexity identity $(a+b)^m \geqslant |a^m - b^m|$ for $a, b > 0$. Hence, ε_r goes to 0 as $r \to \infty$. Summarising we have for any $r > 1$,

$$N(m-1)\left(\mathcal{H}_m[\rho] - \mathcal{H}_m[\tilde{\rho}]\right) = \int_{B_{A_H}} \rho^m + \varepsilon_r, \tag{3.20}$$

with ε_r vanishing as $r \to \infty$.

To estimate the interaction term, we split the double integral into three parts:

$$\begin{aligned} k\left(\mathcal{W}_k[\rho] - \mathcal{W}_k[\tilde{\rho}]\right) &= \iint\limits_{\mathbb{R}^N \times \mathbb{R}^N} |x-y|^k \left(\rho(x)\rho(y) - \tilde{\rho}(x)\tilde{\rho}(y)\right) dxdy \\ &= \iint\limits_{B_{A_H} \times B_{A_H}} |x-y|^k \rho(x)\rho(y)\, dxdy \\ &\quad + 2 \iint\limits_{B_{A_H} \times B^C_{A_H}} |x-y|^k \rho(x)\rho(y)\, dxdy \\ &\quad + \iint\limits_{B^C_{A_H} \times B^C_{A_H}} |x-y|^k \left(\rho(x)\rho(y) - \tilde{\rho}(x)\tilde{\rho}(y)\right) dxdy \\ &=: I_1 + I_2 + I_3(r). \end{aligned} \tag{3.21}$$

Let us start with I_3. By noticing once again that $\rho = \tilde{\rho}$ on $B^C_{A_H} \backslash D_r$ for any $r > 0$, we have

$$\begin{aligned} I_3(r) &= \int\int_{D_r \times D_r} |x-y|^k \left(\rho(x)\rho(y) - \tilde{\rho}(x)\tilde{\rho}(y)\right) \\ &\quad + 2 \int\int_{D_r \times (B^C_{A_H} \backslash D_r)} |x-y|^k \left(\rho(x)\rho(y) - \tilde{\rho}(x)\tilde{\rho}(y)\right) \\ &=: I_{31}(r) + I_{32}(r). \end{aligned}$$

Since $\tilde{\rho} = \rho + \frac{NM_\rho(A_H)}{\sigma_N r^N}$ on D_r, we have

$$I_{32}(r) = -2\frac{NM_\rho(A_H)}{\sigma_N r^N} \int\int_{D_r \times (B^C_{A_H} \backslash D_r)} |x-y|^k \rho(y)\, dxdy.$$

By the HLS inequality (3.21) in Chapter 1, we have

$$\begin{aligned} |I_{32}(r)| &\leqslant 2\frac{NM_\rho(A_H)}{\sigma_N r^N} \int\int_{D_r \times \mathbb{R}^N} |x-y|^k \rho(y)\, dxdy \\ &\leqslant 2C_{HLS} \frac{NM_\rho(A_H)}{\sigma_N r^N} \|\mathbb{1}_{D_r}\|_a \|\rho\|_b \end{aligned}$$

if $a > 1, b > 1$ and $1/a + 1/b - k/N = 2$. We can choose $b \in (1, \min\{m,\, N/(k+N)\})$, which is possible as $-N < k < 0, m > 1$, and then we get $a > 1$, $\rho \in L^b(\mathbb{R}^N)$ as $1 < b < m$, and

$$|I_{32}(r)| \leqslant 2C_{HLS} ||\rho||_b M_\rho(A_H) \left(\frac{\sigma_N r^N}{N} \right)^{\frac{1}{a}-1},$$

and the latter vanishes as $r \to \infty$. For the term I_{31}, we have

$$\begin{aligned} I_{31}(r) = &- 2\frac{NM_\rho(A_H)}{\sigma_N r^N} \int\int_{D_r \times D_r} |x-y|^k \rho(y)\, dxdy \\ &- \left(\frac{NM_\rho(A_H)}{\sigma_N r^N}\right)^2 \int\int_{D_r \times D_r} |x-y|^k \, dxdy\,. \end{aligned}$$

With the same choice of a, b as above, the HLS inequality implies

$$\begin{aligned} |I_{31}(r)| \leqslant & 2\frac{NM_\rho(A_H)}{\sigma_N r^N} \int\int_{D_r \times \mathbb{R}^N} |x-y|^k \rho(y)\, dxdy \\ &+ \left(\frac{NM_\rho(A_H)}{\sigma_N r^N}\right)^2 \int\int_{D_r \times D_r} |x-y|^k \, dxdy \\ \leqslant & C_{HLS} M_\rho(A_H) \left(2||\rho||_b \left(\frac{\sigma_N r^N}{N}\right)^{\frac{1}{a}-1} + M_\rho(A_H) \left(\frac{\sigma_N r^N}{N}\right)^{\frac{1}{a}+\frac{1}{b}-2} \right), \end{aligned}$$

which vanishes as $r \to \infty$ since $a > 1$ and $b > 1$. We conclude that $I_3(r) \to 0$ as $r \to \infty$.

The integral I_1 can be estimated using Theorem 3.4 in Chapter 1, and the fact that $\rho \geqslant H > 1$ on B_{A_H} together with $m > m_c$,

$$\begin{aligned} I_1 = \iint\limits_{B_{A_H} \times B_{A_H}} |x-y|^k \rho(x)\rho(y)\, dxdy &\leqslant C_* M_\rho(A_H)^{1+k/N} \int_{B_{A_H}} \rho^{m_c}(x)\, dx \\ &\leqslant C_* M_\rho(A_H)^{1+k/N} \int_{B_{A_H}} \rho^{m}(x)\, dx\,. \end{aligned} \tag{3.22}$$

On the other hand, the HLS inequalities (3.21) and (3.23) in Chapter 1 do not seem to give a sharp enough estimate for the cross-term I_2, for which we instead invoke Lemma 3.5, yielding

$$I_2 \leqslant 2C_{k,N}\, M_\rho(A_H)\, \mathcal{K}_{k,q,N}(H), \tag{3.23}$$

for given $q \in [0, m/N)$ and large enough H as specified in Lemma 3.5.

In order to conclude, we join together (3.20), (3.21), (3.22) and (3.23) to obtain for any $r > 1$ and any large enough H,

$$\begin{aligned} \mathcal{F}[\rho] - \mathcal{F}[\tilde{\rho}] &= \mathcal{H}_m[\rho] - \mathcal{H}_m[\tilde{\rho}] + \chi\left(\mathcal{W}_k[\rho] - \mathcal{W}_k[\tilde{\rho}]\right) \\ &\geqslant \left(\frac{1}{N(m-1)} + \chi\frac{C_*}{k} M_\rho(A_H)^{1+k/N}\right) \int_{B_{A_H}} \rho^m + 2\chi\, \frac{C_{k,N}}{k}\, M_\rho(A_H)\, \mathcal{K}_{s,q,N}(H) \\ &\quad + \frac{\varepsilon_r}{N(m-1)} + \frac{\chi}{k} I_3(r)\,. \end{aligned} \tag{3.24}$$

Now we choose q. On the one hand, notice that for a choice $\eta > 0$ small enough such that $m > m_c + \eta$, we have

$$\frac{2-m+\eta}{k+N} < \frac{m-1-\eta}{(-k)}\,. \tag{3.25}$$

On the other hand, $-N < k < 0$ implies $1 - k/N > 2N/(2N+k)$. Since $m > m_c$, this gives the inequality $m > 2N/(2N+k)$. Hence, for small enough $\eta > 0$ such that $m > N(2+\eta)/(2N+k)$, we have

$$\frac{2-m+\eta}{k+N} < \frac{m}{N}. \tag{3.26}$$

Thanks to (3.25) and (3.26) we see that we can fix a non-negative q such that

$$\frac{2-m+\eta}{k+N} < q < \min\left\{\frac{m}{N}\,,\ \frac{(m-1-\eta)}{(-k)}\right\}. \tag{3.27}$$

Since q satisfies (3.27), it follows that $-kq < m-1-\eta$ and at the same time $1-q(k+N) < m-1-\eta$, showing that $\mathcal{K}_{k,q,N}(H)$ from Lemma 3.5 grows slower than $H^{m-1-\eta}$ as $H \to \infty$ for $k \neq 1-N$. If $k = 1-N$, we have that for any $C > 0$ there exists $H > H_0$ large enough such that $CH^{1-q}\log(1+H^q) < H^{m-1-\eta}$ since $q > 2-m+\eta$, and so the same result follows. Hence, for any large enough H we have

$$C_{k,N}\, M_\rho(A_H)\, \mathcal{K}_{k,q,N}(H) < C_{k,N} H^{m-1-\eta}\, M_\rho(A_H) \leqslant C_{k,N} H^{-\eta} \int_{B_{A_H}} \rho^m$$

since $\rho \geqslant H$ on B_{A_H}. Inserting the last two estimates in (3.24) we get for some $\eta > 0$

$$\begin{aligned}\mathcal{F}[\rho] - \mathcal{F}[\tilde{\rho}] \geqslant \left(\frac{1}{N(m-1)} + \chi\frac{C_*}{k} M_\rho(A_H)^{1+k/N} + 2\chi\,\frac{C_{k,N}H^{-\eta}}{k}\right)\int_{B_{A_H}} \rho^m \\ + \frac{\varepsilon_r}{N(m-1)} + \frac{\chi}{k} I_3(r)\,.\end{aligned}$$

for any $r > 1$ and any large enough H. First of all, notice that $\int_{B_{A_H}} \rho^m$ is strictly positive since we are assuming that ρ is unbounded. We can therefore fix H large enough such that the constant in front of $\int_{B_{A_H}} \rho^m$ is strictly positive. Secondly, we have already proven that ε_r and $I_3(r)$ vanish as $r \to \infty$, so we can choose r large enough such that

$$\mathcal{F}[\rho] - \mathcal{F}[\tilde{\rho}] > 0\,,$$

contradicting the minimality of ρ. We conclude that global minimisers of $\mathcal{F}$ are bounded. Finally, we can just use the Euler-Lagrange equation (3.14) and the same argument as for Corollary 2.7 to prove that ρ is compactly supported. □

3.3 Regularity properties of global minimisers

This section is devoted to the regularity properties of global minimisers. With enough regularity, global minimisers satisfy the conditions of Definition 2.1, and are therefore stationary states of equation (1.1). This will allow us to complete the proof of Theorem 1.1.

We begin by introducing some notation and preliminary results. As we will make use of the Hölder regularising properties of the fractional Laplacian, see [261, 270], the notation

$$c_{N,s}(-\Delta)^s S_k = \rho\,, \quad s \in (0, N/2)$$

is better adapted to the arguments that follow, fixing $s = (k+N)/2$, and we will therefore state the results in this section in terms of s.

One fractional regularity result that we will use repeatedly in this section follows directly from the HLS inequality (3.21) in Chapter 1 applied with $k = 2r - N$ for any $r \in (0, N/2)$:

$$(-\Delta)^r f \in L^p\left(\mathbb{R}^N\right) \;\Rightarrow\; f \in L^q\left(\mathbb{R}^N\right), \quad q = \frac{Np}{N-2rp}, \qquad 1 < p < \frac{N}{2r}, \quad r \in (0, N/2). \tag{3.28}$$

For $1 \leqslant p < \infty$ and $s \geqslant 0$, we define the *Bessel potential space* $\mathcal{L}^{2s,p}(\mathbb{R}^N)$ as made by all functions $f \in L^p(\mathbb{R}^N)$ such that $(I-\Delta)^s f \in L^p(\mathbb{R}^N)$, meaning that f is the Bessel potential of an $L^p(\mathbb{R}^N)$ function (see [272, pag. 135]). Since we are working with the operator $(-\Delta)^s$ instead of $(I-\Delta)^s$, we make use of a characterisation of the space $\mathcal{L}^{2s,p}(\mathbb{R}^N)$ in terms of Riesz potentials. For $1 < p < \infty$ and $0 < s < 1$ we have

$$\mathcal{L}^{2s,p}(\mathbb{R}^N) = \left\{ f \in L^p(\mathbb{R}^N) : f = g * W_{2s-N},\ g \in L^p(\mathbb{R}^N) \right\}, \tag{3.29}$$

see [264, Theorem 26.8, Theorem 27.3], see also exercise 6.10 in Stein's book [272, pag. 161]. Moreover, for $1 \leqslant p < \infty$ and $0 < s < 1/2$ we define the *fractional Sobolev* space $\mathcal{W}^{2s,p}(\mathbb{R}^N)$ by

$$\mathcal{W}^{2s,p}\left(\mathbb{R}^N\right) := \left\{ f \in L^p(\mathbb{R}^N) : \iint\limits_{\mathbb{R}^N \times \mathbb{R}^N} \frac{|f(x) - f(y)|^p}{|x-y|^{N+2sp}} dx\, dy < \infty \right\}.$$

We have the embeddings

$$\mathcal{L}^{2s,p}(\mathbb{R}^N) \subset W^{2s,p}(\mathbb{R}^N) \quad \text{for} \quad p \geqslant 2, \quad s \in (0, 1/2), \tag{3.30}$$

$$\mathcal{W}^{2s,p}\left(\mathbb{R}^N\right) \subset C^{0,\beta}\left(\mathbb{R}^N\right) \quad \text{for} \quad \beta = 2s - N/p, \quad p > N/2s, \quad s \in (0,1/2), \tag{3.31}$$

see [272, pag. 155] and [126, Theorem 4.4.7] respectively.

Letting $s \in (0,1)$ and $\alpha > 0$ such that $\alpha + 2s$ is not an integer, since $c_{N,s}(-\Delta)^s S_k = \rho$ holds in $\mathbb{R}^N$, then we have from [261, Theorem 1.1, Corollary 3.5] (see also [60, Proposition 5.2] that

$$\|S_k\|_{C^{0,\alpha+2s}(\overline{B_{1/2}(0)})} \leqslant c\left(\|S_k\|_{L^\infty(\mathbb{R}^N)} + \|\rho\|_{C^{0,\alpha}(\overline{B_1(0)})} \right), \tag{3.32}$$

with the convention that if $\alpha \geqslant 1$ for any open set U in $\mathbb{R}^N$, $C^{0,\alpha}(\overline{U}) := C^{\alpha',\alpha''}(\overline{U})$, where $\alpha' + \alpha'' = \alpha$, $\alpha'' \in (0,1)$ and α' is the greatest integer less than α. With this notation, we have $C^{1,0}(\mathbb{R}^N) = C^{0,1}(\mathbb{R}^N) = \mathcal{W}^{1,\infty}(\mathbb{R}^N)$. In particular, using (3.32) it follows that for $\alpha > 0$, $s \in (0,1)$ and $\alpha + 2s$ not an integer,

$$\|S_k\|_{C^{0,\alpha+2s}(\mathbb{R}^N)} \leqslant c\left(\|S_k\|_{L^\infty(\mathbb{R}^N)} + \|\rho\|_{C^{0,\alpha}(\mathbb{R}^N)} \right). \tag{3.33}$$

Moreover, rescaling inequality (3.32) in any ball $B_R(x_0)$ where $R \neq 1$, we have the estimate

$$\begin{aligned} &\sum_{\ell=0}^{\alpha_2} R^\ell \|D^\ell S_k\|_{L^\infty(B_{R/2}(x_0))} + R^{\alpha+2s}[D^{\alpha_1} S_k]_{C^{0,\alpha+2s-\alpha_2}(B_{R/2}(x_0))} \\ &\leqslant C\left[\|S_k\|_{L^\infty(\mathbb{R}^N)} + \sum_{\ell=0}^{\alpha_1} R^{2s+\ell} \|D^\ell \rho\|_{L^\infty(B_R(x_0))} + R^{\alpha+2s}[D^{\alpha_1}\rho]_{C^{0,\alpha-\alpha_1}(B_R(x_0))} \right] \end{aligned} \tag{3.34}$$

where α_1, α_2 are the greatest integers less than α and $\alpha + 2s$ respectively. In (3.34) the quantities $\|D^\ell S_k\|_{L^\infty}$ and $[D^\ell \rho]_{C^{0,\alpha}}$ denote the sum of the L^∞-norms and the α-Hölder semi-norms of the derivatives $D^{(\beta)} S_k$ of order ℓ (that is $|\beta| = \ell$).

Finally, we recall the definition of m_c and m^* in (1.3)-(1.4):

$$m_c := 2 - \frac{2s}{N},$$

$$m^* := \begin{cases} \dfrac{2-2s}{1-2s} & \text{if} \quad N \geqslant 1 \quad \text{and} \quad s \in (0, 1/2), \\ +\infty & \text{if} \quad N \geqslant 2 \quad \text{and} \quad s \in [1/2, N/2). \end{cases}$$

Let us begin by showing that global minimisers of $\mathcal{F}$ enjoy the good Hölder regularity in the most singular range, as long as diffusion is not too slow.

Theorem 3.7. *Let $\chi > 0$ and $s \in (0, N/2)$. If $m_c < m < m^*$, then any global minimiser $\rho \in \mathcal{Y}$ of $\mathcal{F}$ satisfies $S_k = W_k * \rho \in \mathcal{W}^{1,\infty}(\mathbb{R}^N)$, $\rho^{m-1} \in \mathcal{W}^{1,\infty}(\mathbb{R}^N)$ and $\rho \in C^{0,\alpha}(\mathbb{R}^N)$ with $\alpha = \min\{1, \frac{1}{m-1}\}$.*

Proof. Recall that the global minimiser $\rho \in \mathcal{Y}$ of $\mathcal{F}$ is radially symmetric non-increasing and compactly supported by Theorem 3.1 and Proposition 3.6. Since $\rho \in L^1(\mathbb{R}^N) \cap L^\infty(\mathbb{R}^N)$ by Proposition 3.6, we have $\rho \in L^p(\mathbb{R}^N)$ for any $1 < p < \infty$. Since $\rho = c_{N,s}(-\Delta)^s S_k$, it follows from (3.28) that $S_k \in L^q(\mathbb{R}^N)$, $q = \frac{Np}{N-2sp}$ for all $1 < p < \frac{N}{2s}$, that is $S_k \in L^p(\mathbb{R}^N)$ for all $p \in (\frac{N}{N-2s}, \infty)$. If $s \in (0,1)$, by the definition (3.29) of the Bessel potential space, we conclude that $S_k \in \mathcal{L}^{2s,p}(\mathbb{R}^N)$ for all $p > \frac{N}{N-2s}$. Let us first consider $s < 1/2$, as the cases $s > 1/2$ and $s = 1/2$ will follow as a corollary.

$\boxed{0 < s < 1/2}$ In this case, we have the embedding (3.30) and so $S_k \in \mathcal{W}^{2s,p}(\mathbb{R}^N)$ for all $p \geqslant 2 > \frac{N}{N-2s}$ if $N \geqslant 2$ and for all $p > \max\{2, \frac{1}{1-2s}\}$ if $N = 1$. Using (3.31), we conclude that $S_k \in C^{0,\beta}(\mathbb{R}^N)$ with

$$\beta := 2s - N/p,$$

for any $p > \frac{N}{2s} > 2$ if $N \geqslant 2$ and for any $p > \max\{\frac{1}{2s}, \frac{1}{1-2s}\}$ if $N = 1$. Hence $\rho^{m-1} \in C^{0,\beta}(\mathbb{R}^N)$ for the same choice of β using the Euler-Lagrange condition (3.14) since ρ^{m-1} is the truncation of a function which is S_k up to a constant.

Note that $m_c \in (1,2)$ and $m^* > 2$, and in what follows we split our analysis into the cases $m_c < m \leqslant 2$ and $2 < m < m^*$, still assuming $s < 1/2$. If $m \leqslant 2$, the argument follows along the lines of Chapter 2 Corollary 3.12 since $\rho^{m-1} \in C^{0,\alpha}(\mathbb{R}^N)$ implies that ρ is in the same Hölder space for any $\alpha \in (0,1)$. Indeed, in such case we bootstrap in the following way. Let us fix $n \in \mathbb{N}$ such that

$$\frac{1}{n+1} < 2s \leqslant \frac{1}{n} \tag{3.35}$$

and let us define

$$\beta_n := \beta + (n-1)2s = 2ns - N/p. \tag{3.36}$$

Form (3.35) and (3.36) we see that by choosing large enough p there hold $1-2s < \beta_n < 1$. Note that $S_k \in L^\infty\left(\mathbb{R}^N\right)$ by Lemma 2.2, and if $\rho \in C^{0,\gamma}\left(\mathbb{R}^N\right)$ for some $\gamma \in (0,1)$ such that $\gamma + 2s < 1$, then $S_k \in C^{0,\gamma+2s}\left(\mathbb{R}^N\right)$ by (3.33), implying $\rho^{m-1} \in C^{0,\gamma+2s}\left(\mathbb{R}^N\right)$ using the Euler-Lagrange conditions (3.14), therefore $\rho \in C^{0,\gamma+2s}\left(\mathbb{R}^N\right)$ since $m \in (m_c, 2]$. Iterating this argument $(n-1)$ times starting with $\gamma = \beta$ gives $\rho \in C^{0,\beta_n}\left(\mathbb{R}^N\right)$. Since $\beta_n < 1$ and $\beta_n + 2s > 1$, a last application of (3.33) yields $S_k \in \mathcal{W}^{1,\infty}(\mathbb{R}^N)$, so that $\rho^{m-1} \in \mathcal{W}^{1,\infty}(\mathbb{R}^N)$, thus $\rho \in \mathcal{W}^{1,\infty}(\mathbb{R}^N)$. This concludes the proof in the case $m \leqslant 2$.

Now, let us assume $2 < m < m^*$ and $s < 1/2$. Recall that $\rho^{m-1} \in C^{0,\gamma}\left(\mathbb{R}^N\right)$ for any $\gamma < 2s$, and so $\rho \in C^{0,\gamma}\left(\mathbb{R}^N\right)$ for any $\gamma < \frac{2s}{m-1}$. By (3.33) we get $S_k \in C^{0,\gamma}\left(\mathbb{R}^N\right)$ for any $\gamma < \frac{2s}{m-1} + 2s$, and the same for ρ^{m-1} by the Euler Lagrange equation (3.14). Once more with a bootstrap argument, we obtain improved Hölder regularity for ρ^{m-1}. Indeed, since

$$\sum_{j=0}^{+\infty} \frac{2s}{(m-1)^j} = \frac{2s(m-1)}{m-2} \tag{3.37}$$

and since $m < m^*$ means $\frac{2s(m-1)}{m-2} > 1$, after taking a suitably large number of iterations we get $S_k \in \mathcal{W}^{1,\infty}(\mathbb{R}^N)$ and $\rho^{m-1} \in \mathcal{W}^{1,\infty}(\mathbb{R}^N)$. Hence, $\rho \in C^{0,1/(m-1)}\left(\mathbb{R}^N\right)$.

$\boxed{N \geqslant 2,\ 1/2 \leqslant s < N/2}$ We start with the case $s = 1/2$. We have $S_k \in L^p(\mathbb{R}^N)$ for any $p > \frac{N}{N-1}$ as shown at the beginning of the proof. By (3.29) we get $S_k \in \mathcal{L}^{1,p}\left(\mathbb{R}^N\right)$ for all $p > \frac{N}{N-1}$. Then we also have $S_k \in \mathcal{L}^{2r,p}(\mathbb{R}^N)$ for all $p > \frac{N}{N-1}$ and for all $r \in (0,1/2)$ by the embeddings between Bessel potential spaces, see [272, pag. 135]. Noting that $2 \geqslant \frac{N}{N-1}$ for $N \geqslant 2$, by (3.30) and (3.31) we get $S_k \in C^{0,2r-N/p}(\mathbb{R}^N)$ for any $r \in (0,1/2)$ and any $p > \frac{N}{2r}$. That is, $S_k \in C^{0,\gamma}(\mathbb{R}^N)$ for any $\gamma \in (0,1)$. Since $m < m^*$ we may choose γ close enough to 1 such that $\frac{\gamma}{1\wedge(m-1)} + 2s > 1$. Therefore (3.33) implies $S_k \in \mathcal{W}^{1,\infty}(\mathbb{R}^N)$. By the Euler-Lagrange equation (3.14), we obtain again $\rho^{m-1} \in \mathcal{W}^{1,\infty}(\mathbb{R}^N)$.

If $1/2 < s < N/2$ on the other hand, we obtain directly that $S_k \in \mathcal{W}^{1,\infty}(\mathbb{R}^N)$ by Lemma 2.2, and so $\rho^{m-1} \in \mathcal{W}^{1,\infty}(\mathbb{R}^N)$.

We conclude that $\rho \in C^{0,\alpha}(\mathbb{R}^N)$ with $\alpha = \min\{1, \frac{1}{m-1}\}$ for any $1/2 \leqslant s < N/2$. □

Remark 3.8. *If $m \geqslant m^*$ and $s < 1/2$, we recover some Hölder regularity, but it is not enough to show that global minimisers of $\mathcal{F}$ are stationary states of (1.1). More precisely, $m \geqslant m^*$ means $\frac{2s(m-1)}{m-2} \leqslant 1$, and so it follows from (3.37) that $\rho \in C^{0,\gamma}\left(\mathbb{R}^N\right)$ for any $\gamma < \frac{2s}{m-2}$. Note that $m \geqslant m^*$ also implies $\frac{2s}{m-2} \leqslant 1-2s$, and we are therefore not able to go above the desired Hölder exponent $1-2s$.*

Remark 3.9. *In the proof of Theorem 3.7 one may choose to bootstrap on the fractional Sobolev space $\mathcal{W}^{2s,p}\left(\mathbb{R}^N\right)$ directly, making use of the Euler-Lagrange condition (3.14) to show that $\rho \in \mathcal{W}^{r,p}\left(\mathbb{R}^N\right) \Rightarrow$*

$S_k \in \mathcal{W}^{r+2s,p}(\mathbb{R}^N)$ with $r \in (0,1)$ for p large enough depending only on N. This is possible since $\rho \in L^1 \cap L^\infty(\mathbb{R}^N)$, so we can use the regularity properties of the Riesz potential see [272, Chapter V]. Further, for $m_c < m \leqslant 2$, we have that ρ has the same Sobolev regularity as ρ^{m-1}. If $m > 2$ on the other hand, we can make use of the fact that $\rho^{m-1} \in \mathcal{W}^{2s,p}$ implies $\rho \in \mathcal{W}^{\frac{2s}{m-1},p(m-1)}$ as suggested by Mironescu in [236]. Indeed, let $\alpha < 1$ and $u \in \mathcal{W}^{2s,p}$, where $0 < s < 1/2$ and $p \in [1,\infty)$. By the algebraic inequality $||a|^\alpha - |b|^\alpha| \leqslant C|a-b|^\alpha$ we have

$$\iint \frac{||u(x)|^\alpha - |u(y)|^\alpha|^{p/\alpha}}{|x-y|^{N+\alpha 2s(p/\alpha)}} dx\, dy \leqslant C \iint \frac{|u(x)-u(y)|^p}{|x-y|^{N+2sp}} dx\, dy$$

thus $|u|^\alpha \in \mathcal{W}^{\alpha s,p/\alpha}$. This property is also valid for Sobolev spaces with integer order, see [236].

We are now ready to show that global minimisers possess the good regularity properties to be stationary states of equation (1.1) according to Definition 2.1.

Theorem 3.10. *Let $\chi > 0$, $s \in (0, N/2)$ and $m_c < m < m^*$. Then all global minimisers of $\mathcal{F}$ in $\mathcal{Y}$ are stationary states of equation (1.1) according to Definition 2.1.*

Proof. Note that $m < m^*$ means $1 - 2s < 1/(m-1)$, and so thanks to Theorem 3.7, S_k and ρ satisfy the regularity conditions of Definition 2.1. Further, since $\rho^{m-1} \in \mathcal{W}^{1,\infty}(\mathbb{R}^N)$, we can take gradients on both sides of the Euler-Lagrange condition (3.14). Multiplying by ρ and writing $\rho\nabla\rho^{m-1} = \frac{m-1}{m}\nabla\rho^m$, we conclude that global minimisers of $\mathcal{F}$ in $\mathcal{Y}$ satisfy relation (2.1) for stationary states of equation (1.1). □

In fact, we can show that global minimisers have even more regularity inside their support.

Theorem 3.11. *Let $\chi > 0$, $m_c < m$ and $s \in (0, N/2)$. If $\rho \in \mathcal{Y}$ is a global minimiser of $\mathcal{F}$, then ρ is C^∞ in the interior of its support.*

Proof. By Theorem 3.7 and Remark 3.8, we have $\rho \in C^{0,\alpha}(\mathbb{R}^N)$ for some $\alpha \in (0,1)$. Since ρ is radially symmetric non-increasing, the interior of supp (ρ) is a ball centered at the origin, which we denote by B. Note also that $\rho \in L^1(\mathbb{R}^N) \cap L^\infty(\mathbb{R}^N)$ by Proposition 3.6, and so $S_k \in L^\infty(\mathbb{R}^N)$ by Lemma 2.2.

Assume first that $s \in (0,1) \cap (0, N/2)$. Applying (3.34) with B_R centered at a point within B and such that $B_R \subset\subset B$, we obtain $S_k \in C^{0,\gamma}(B_{R/2})$ for any $\gamma < \alpha + 2s$. It follows from the Euler-Langrange condition (3.14) that ρ^{m-1} has the same regularity as S_k on $B_{R/2}$, and since ρ is bounded away from zero on $B_{R/2}$, we conclude $\rho \in C^{0,\gamma}(B_{R/2})$ for any $\gamma < \alpha + 2s$. Repeating the previous step now on $B_{R/2}$, we get the improved regularity $S_k \in C^{0,\gamma}(B_{R/4})$ for any $\gamma < \alpha + 4s$ by (3.34), which we can again transfer onto ρ using (3.14), obtaining $\rho \in C^{0,\gamma}(B_{R/4})$ for any $\gamma < \alpha + 4s$. Iterating, any order ℓ of differentiability for S_k (and then for ρ) can be reached in a neighbourhood of the center of B_R. We notice that the argument can be applied starting from any point $x_0 \in B$,

and hence $\rho \in C^\infty(B)$.

When $N \geqslant 3$ and $s \in [1, N/2)$, we take numbers $s_1, \dots, s_l$ such that $s_i \in (0,1)$ for any $i = 1, \dots, l$ and such that $\sum_{i=1}^l s_i = s$. We also let

$$S_k^{l+1} := S_k\,, \quad S_k^j := \Pi_{i=j}^l (-\Delta)^{s_j} S_k\,, \qquad \forall\, j \in \{1, \dots, l\}\,.$$

Then $S_k^1 = \rho$. Note that Lemma 2.2(i) can be restated as saying that $\rho \in \mathcal{Y} \cap L^\infty(\mathbb{R}^N)$ implies $(-\Delta)^{-\delta}\rho \in L^\infty(\mathbb{R}^N)$ for all $\delta \in (0, N/2)$. Taking $\delta = s - r$ for any $r \in (0, s)$, we have $(-\Delta)^r S_k = (-\Delta)^{r-s}\rho \in L^\infty$. In particular, this means $S_k^j \in L^\infty(\mathbb{R}^N)$ for any $j = 1, \dots, l+1$. Moreover, there holds

$$(-\Delta)^{s_j} S_k^{j+1} = S_k^j\,, \qquad \forall\, j \in \{1, \dots, l\}\,.$$

Therefore we may recursively apply (3.34), starting from $S_k^1 = \rho \in C^{0,\alpha}(B_R)$, where the ball B_R is centered at a point within B such that $B_R \subset\subset B$, and using the iteration rule

$$\begin{aligned} &S_k^j \in C^{0,\gamma}(B_\sigma) \;\Rightarrow\; S_k^{j+1} \in C^{0,\gamma+2s_j}\left(B_{\sigma/2}\right) \\ &\forall\, j \in \{1, \dots, l\}\,, \quad \forall\, \gamma > 0 \text{ s.t. } \gamma + 2s_j \text{ is not an integer}, \quad \forall\, B_\sigma \subset\subset B. \end{aligned}$$

We obtain $S_k^{l+1} = S_k \in C^{0,\gamma}(B_{R/(2^l)})$ for any $\gamma < \alpha + 2s$, and as before, the Euler-Lagrange equation (3.14) implies that $\rho \in C^{0,\gamma}(B_{R/(2^l)})$ for any $\gamma < \alpha + 2s$. If we repeat the argument, we gain $2s$ in Hölder regularity for ρ each time we divide the radius R by 2^l. In this way, we can reach any differentiability exponent for ρ around any point of B, and thus $\rho \in C^\infty(B)$. □

The main result Theorem 1.1 follows from Theorem 2.4, Corollary 2.7, Theorem 3.1, Proposition 3.4, Proposition 3.6, Theorem 3.14 and Theorem 3.11.

4 Uniqueness in one dimension

4.1 Optimal transport tools

Optimal transport is a powerful tool for reducing functional inequalities onto pointwise inequalities. In other words, to pass from microscopic inequalities between particle locations to macroscopic inequalities involving densities. This sub-section summarises the main results of optimal transportation we will need in the one-dimensional setting. They were already used in [62] and in Chapter 3, where we refer for detailed proofs.

Let $\tilde\rho$ and ρ be two probability densities. According to [53, 233], there exists a convex function ψ whose gradient pushes forward the measure $\tilde\rho(a)da$ onto $\rho(x)dx$: $\psi' \# (\tilde\rho(a)da) = \rho(x)dx$. This convex function satisfies the Monge-Ampère equation in the weak sense: for any test function

$\varphi \in C_b(\mathbb{R})$, the following identity holds true

$$\int_{\mathbb{R}} \varphi(\psi'(a))\tilde{\rho}(a)\, da = \int_{\mathbb{R}} \varphi(x)\rho(x)\, dx\,.$$

The convex map is unique a.e. with respect to ρ and it gives a way of interpolating measures using displacement convexity [234]. The convexity of the functionals involved can be summarised as follows [234, 85]:

Theorem 4.1. *Let $N = 1$. The functional $\mathcal{H}_m[\rho]$ is displacement-convex provided that $m \geqslant 0$. The functional $\mathcal{W}_k[\rho]$ is displacement-concave if $k \in (-1, 1)$.*

This means we have to deal with convex-concave compensations. On the other hand, regularity of the transport map is a complicated matter. Here, as it was already done in [62], we will only use the fact that $\psi''(a)da$ can be decomposed in an absolute continuous part $\psi''_{ac}(a)da$ and a positive singular measure [295, Chapter 4]. In one dimension, the transport map ψ' is a non-decreasing function, therefore it is differentiable a.e. and it has a countable number of jump singularities. The singular part of the positive measure $\psi''(a)\, da$ corresponds to having holes in the support of the density ρ. For any measurable function U, bounded below such that $U(0) = 0$ we have [234]

$$\int_{\mathbb{R}} U(\tilde{\rho}(x))\, dx = \int_{\mathbb{R}} U\left(\frac{\rho(a)}{\psi''_{ac}(a)}\right)\psi''_{ac}(a)\, da\,. \tag{4.38}$$

The following Lemma proved in [62] will be used to estimate the interaction contribution in the free energy.

Lemma 4.2. *Let $\mathcal{K} : (0, \infty) \to \mathbb{R}$ be an increasing and strictly concave function. Then, for any $a, b \in \mathbb{R}$*

$$\mathcal{K}\left(\frac{\psi'(b) - \psi'(a)}{b - a}\right) \geqslant \int_0^1 \mathcal{K}\left(\psi''_{\mathrm{ac}}([a, b]_s)\right)\, ds\,, \tag{4.39}$$

where the convex combination of a and b is given by $[a, b]_s = (1 - s)a + sb$. Equality is achieved in (4.39) if and only if the distributional derivative of the transport map ψ'' is a constant function.

4.2 Functional inequality in one dimension

In what follows, we will make use of a characterisation of stationary states based on some integral reformulation of the necessary condition stated in Proposition 3.4. This characterisation was also the key idea in [62] and in Chapter 3 to analyse the asymptotic stability of steady states and the functional inequalities behind.

Lemma 4.3 (Characterisation of stationary states)**.** *Let $N = 1$, $\chi > 0$ and $k \in (-1, 0)$. If $m > m_c$ with $m_c = 1 - k$, then any stationary state $\bar{\rho} \in \mathcal{Y}$ of system (1.1) can be written in the form*

$$\bar{\rho}(p)^m = \chi \int_{\mathbb{R}} \int_0^1 |q|^k \bar{\rho}(p - sq)\bar{\rho}(p - sq + q)\, dsdq\,. \tag{4.40}$$

The proof follows the same methodology as for the fair-competition regime (see Chapter 3 Lemma 2.8) and we omit it here. If $m = m_c$, then it follows from Lemma 4.3 that any stationary state $\bar{\rho} \in \mathcal{Y}$ satisfies $\mathcal{F}[\bar{\rho}] = 0$ by simple substitution.

Theorem 4.4. *Let $N = 1$, $\chi > 0$, $k \in (-1, 0)$ and $m > m_c$. If (1.1) admits a stationary density $\bar{\rho}$ in $\mathcal{Y}$, then*

$$\mathcal{F}[\rho] \geqslant \mathcal{F}[\bar{\rho}], \quad \forall \rho \in \mathcal{Y}$$

with equality if and only if $\rho = \bar{\rho}$.

Proof. For a given stationary state $\bar{\rho} \in \mathcal{Y}$ and solution $\rho \in \mathcal{Y}$ of (1.1), we denote by ψ the convex function whose gradient pushes forward the measure $\bar{\rho}(a)da$ onto $\rho(x)dx$: $\psi' \# (\bar{\rho}(a)da) = \rho(x)dx$. Using (4.38), the functional $\mathcal{F}[\rho]$ rewrites as follows:

$$\begin{aligned}
\mathcal{F}[\rho] &= \frac{1}{m-1} \int_{\mathbb{R}} \left(\frac{\bar{\rho}(a)}{\psi''_{ac}(a)} \right)^{m-1} \bar{\rho}(a)\, da \\
&\quad + \frac{\chi}{k} \iint\limits_{\mathbb{R}\times\mathbb{R}} \left| \frac{\psi'(a) - \psi'(b)}{a-b} \right|^k |a-b|^k \bar{\rho}(a)\bar{\rho}(b)\, dadb \\
&= \frac{1}{m-1} \int_{\mathbb{R}} \left(\psi''_{ac}(a)\right)^{1-m} \bar{\rho}(a)^m\, da \\
&\quad + \frac{\chi}{k} \iint\limits_{\mathbb{R}\times\mathbb{R}} \left\langle \psi''([a,b]) \right\rangle^k |a-b|^k \bar{\rho}(a)\bar{\rho}(b)\, dadb\,,
\end{aligned}$$

where $\langle u([a,b]) \rangle = \int_0^1 u([a,b]_s)\, ds$ and $[a,b]_s = (1-s)a + bs$ for any $a, b \in \mathbb{R}$ and $u : \mathbb{R} \to \mathbb{R}_+$. By Lemma 4.3, we can write for any $a \in \mathbb{R}$,

$$(\psi''_{ac}(a))^{1-m} \bar{\rho}(a)^m = \chi \int_{\mathbb{R}} \left\langle \psi''_{ac}([a,b])^{1-m} \right\rangle |a-b|^k \bar{\rho}(a)\bar{\rho}(b)\, db\,,$$

and hence

$$\mathcal{F}[\rho] = \chi \iint\limits_{\mathbb{R}\times\mathbb{R}} \left\{ \frac{1}{(m-1)} \left\langle \psi''_{ac}([a,b])^{1-m} \right\rangle + \frac{1}{k} \left\langle \psi''([a,b]) \right\rangle^k \right\} |a-b|^k \bar{\rho}(a)\bar{\rho}(b)\, dadb\,.$$

Using the concavity of the power function $(\cdot)^{1-m}$ and and Lemma 4.2, we deduce

$$\mathcal{F}[\rho] \geqslant \chi \iint\limits_{\mathbb{R}\times\mathbb{R}} \left\{ \frac{1}{(m-1)} \left\langle \psi''([a,b]) \right\rangle^{1-m} + \frac{1}{k} \left\langle \psi''([a,b]) \right\rangle^k \right\} |a-b|^k \bar{\rho}(a)\bar{\rho}(b)\, dadb\,.$$

Applying characterisation (4.40) to the energy of the stationary state $\bar{\rho}$, we obtain

$$\mathcal{F}[\bar{\rho}] = \chi \iint\limits_{\mathbb{R}\times\mathbb{R}} \left(\frac{1}{(m-1)} + \frac{1}{k} \right) |a-b|^k \bar{\rho}(a)\bar{\rho}(b)\, dadb\,.$$

Since

$$\frac{z^{1-m}}{m-1} + \frac{z^k}{k} \geqslant \frac{1}{m-1} + \frac{1}{k} \tag{4.41}$$

for any real $z > 0$ and for $m > m_c = 1 - k$, we conclude $\mathcal{F}[\rho] \geqslant \mathcal{F}[\bar{\rho}]$. Equality in the convexity inequality (4.39) arises if and only if the derivative of the transport map ψ'' is a constant function, i.e. when ρ is a dilation of $\bar{\rho}$. In agreement with this, equality in (4.41) is realised if and only if $z = 1$. □

In fact, the result in Theorem 4.4 implies that all critical points of $\mathcal{F}$ in $\mathcal{Y}$ are global minimisers. Further, we obtain the following uniqueness result:

Corollary 4.5 (Uniqueness). *Let $\chi > 0$ and $k \in (-1, 0)$. If $m_c < m$, then there exists at most one stationary state in $\mathcal{Y}$ to equation (1.1). If $m_c < m < m^*$, then there exists a unique global minimiser for $\mathcal{F}$ in $\mathcal{Y}$.*

Proof. Assume there are two stationary states to equation (1.1), $\bar{\rho}_1, \bar{\rho}_2 \in \mathcal{Y}$. Then Theorem 4.4 implies that $\mathcal{F}[\bar{\rho}_1] = \mathcal{F}[\bar{\rho}_2]$, and so $\bar{\rho}_1 = \bar{\rho}_2$.
By Theorem 3.1, there exists a global minimiser of $\mathcal{F}$ in $\mathcal{Y}$, which is a stationary state of equation (1.1) if $m_c < m < m^*$ by Theorem 3.10, and so uniqueness follows. □

Theorem 4.4 and Corollary 4.5 complete the proof of the main result Theorem 1.2.

A Appendix: Properties of the Riesz potential

The estimates in Proposition 2.5 are mainly based on the fact that the Riesz potential of a radial function can be expressed in terms of the hypergeometric function

$$F(a, b; c; z) := \frac{\Gamma(c)}{\Gamma(b)\Gamma(c-b)} \int_0^1 (1 - zt)^{-a} (1 - t)^{c-b-1} t^{b-1} \, dt,$$

which we define for $z \in (-1, 1)$, with the parameters a, b, c being positive. Notice that $F(a, b, c, 0) = 1$ and F is increasing with respect to $z \in (-1, 1)$. Moreover, if $c > 1$, $b > 1$ and $c > a + b$, the limit as $z \uparrow 1$ is finite and it takes the value

$$\frac{\Gamma(c)\Gamma(c - a - b)}{\Gamma(c - a)\Gamma(c - b)}, \tag{A.42}$$

see [214, §9.3]. We will also make use of some elementary relations. Let $c > a \vee b > 0$, then there holds

$$F(a, b; c; z) = (1 - z)^{c-a-b} F(c - a, c - b; c; z), \tag{A.43}$$

see [214, §9.5], and it is easily seen that

$$\frac{d}{dz} F(a, b; c; z) = \frac{ab}{c} F(a + 1, b + 1; c + 1; z).$$

Inserting (A.43) we find

$$\frac{d}{dz} F(a, b; c; z) = \frac{ab}{c} (1 - z)^{c-a-b-1} F(c - a, c - b; c + 1; z). \tag{A.44}$$

To simplify notation, let us define

$$H(a,b;c;z) := \frac{\Gamma(b)\Gamma(c-b)}{\Gamma(c)} F(a,b;c;z) = \int_0^1 (1-zt)^{-a}(1-t)^{c-b-1}t^{b-1}\,dt\,. \tag{A.45}$$

Proof of Proposition 2.5. For a given radial function $\rho \in \mathcal{Y}$ we use polar coordinates, still denoting by ρ the radial profile of ρ, and compute as in [269, Theorem 5], see also [10], [138] or [140, §1.3],

$$|x|^k * \rho(x) = \sigma_{N-1} \int_0^\infty \left(\int_0^\pi \left(|x|^2 + \eta^2 - 2|x|\eta\cos\theta \right)^{k/2} \sin^{N-2}\theta\,d\theta \right) \rho(\eta)\eta^{N-1}\,d\eta\,. \tag{A.46}$$

Then we need to estimate the integral

$$\Theta_k(r,\eta) := \sigma_{N-1} \int_0^\pi \left(r^2 + \eta^2 - 2r\eta\cos(\theta) \right)^{k/2} \sin^{N-2}(\theta)\,d\theta = \begin{cases} r^k \vartheta_k\left(\eta/r\right), & \eta < r\,, \\ \eta^k \vartheta_k\left(r/\eta\right), & r < \eta\,, \end{cases} \tag{A.47}$$

with

$$\begin{aligned} \vartheta_k(s) &:= \sigma_{N-1} \int_0^\pi \left(1 + s^2 - 2s\cos(\theta) \right)^{k/2} \sin^{N-2}(\theta)\,d\theta \\ &= \sigma_{N-1}\,(1+s)^k \int_0^\pi \left(1 - 4\frac{s}{(1+s)^2}\cos^2\left(\frac{\theta}{2}\right) \right)^{k/2} \sin^{N-2}(\theta)\,d\theta\,. \end{aligned}$$

Using the change of variables $t = \cos^2\left(\frac{\theta}{2}\right)$, we get from the integral formulation (A.45),

$$\begin{aligned} \vartheta_k(s) &= 2^{N-2}\sigma_{N-1}\,(1+s)^k \int_0^1 \left(1 - 4\frac{s}{(1+s)^2}t \right)^{k/2} t^{\frac{N-3}{2}}\,(1-t)^{\frac{N-3}{2}}\,dt \\ &= 2^{N-2}\sigma_{N-1}\,(1+s)^k\,H\left(a,b;c;z\right) \end{aligned} \tag{A.48}$$

with

$$a = -\frac{k}{2}\,, \qquad b = \frac{N-1}{2}\,, \qquad c = N-1\,, \qquad z = \frac{4s}{(1+s)^2}\,.$$

The function $F(a,b;c;z)$ is increasing in z and then for any $z \in (0,1)$ there holds

$$F(a,b;c;z) \leqslant \lim_{z\uparrow 1} F(a,b;c;z). \tag{A.49}$$

Note that $c-a-b = (k+N-1)/2$ changes sign at $k = 1-N$, and the estimate of Θ_k depends on the sign of $c-a-b$:

Case $k > 1-N$ The limit (A.49) is finite if $c-a-b > 0$ and it is given by the expression $\Gamma(c)\Gamma(c-a-b)/[\Gamma(c-a)\Gamma(c-b)]$, thanks to (A.42). Therefore we get from (A.47)-(A.48) and (A.45)

$$\Theta_k(|x|,\eta) \leqslant C_1(|x|+\eta)^k \leqslant C_1|x|^k \qquad \text{if } 1-N < k < 0$$

with $C_1 := 2^{N-2}\sigma_{N-1}\Gamma(b)\Gamma(c-a-b)/\Gamma(c-a)$. Inserting this into (A.46) concludes the proof of (i).

Case $k < 1 - N$ If $c - a - b < 0$ we use (A.43),

$$F(a, b; c; z) = (1 - z)^{c-a-b} F(c - a, c - b; c; z),$$

where now the right hand side, using (A.49) and (A.42), can be bounded from above by $(1 - z)^{c-a-b}\Gamma(c)\Gamma(a + b - c)/[\Gamma(a)\Gamma(b)]$ for $z \in (0, 1)$. This yields from (A.47)-(A.48) and (A.45) the estimate

$$\Theta_k(|x|, \eta) \leqslant C_2 |x|^k \left(\frac{|x| + \eta}{|x| - \eta} \right)^{1-k-N} \qquad \text{if } k < 1 - N \tag{A.50}$$

with $C_2 := 2^{N-2}\sigma_{N-1}\Gamma(c - b)\Gamma(a + b - c)/\Gamma(a)$.

Case $k = 1 - N$ If on the other hand $c - a - b = 0$, we use (A.44) with $c = 2a = 2b = N - 1$, integrating it and obtaining, since $F = 1$ for $z = 0$,

$$F(a, b; c; z) = 1 + \frac{N - 1}{4} \int_0^z \frac{F(c - a, c - b; c + 1; t)}{1 - t}\, dt,$$

and the latter right hand side is bounded above, thanks to (A.49) and (A.42), by

$$1 + \frac{(N - 1)\Gamma(N)}{4(\Gamma(N/2 + 1/2))^2} \log\left(\frac{1}{1 - z} \right)$$

for $z \in (0, 1)$. This leads from (A.47)-(A.48) to the new estimate

$$\Theta_k(|x|, \eta) \leqslant C_2 |x|^k \left(1 + \log\left(\frac{|x| + \eta}{|x| - \eta} \right) \right) \qquad \text{if } k = 1 - N\,, \tag{A.51}$$

with $C_2 := 2^{N-2}\sigma_{N-1} \frac{\Gamma(N/2-1/2)^2}{\Gamma(N-1)} \max\left\{1, \frac{(N-1)\Gamma(N)}{2\Gamma((N+1)/2)^2}\right\}$.

Now, if ρ is supported on a ball B_R, the radial representation (A.46) reduces to

$$|x|^k * \rho(x) = \int_0^R \Theta_k(|x|, \eta)\rho(\eta)\eta^{N-1}\, d\eta, \quad x \in \mathbb{R}^N. \tag{A.52}$$

If $|x| > R$, we have $(|x| + \eta)(|x| - \eta)^{-1} \leqslant (|x| + R)(|x| - R)^{-1}$ for any $\eta \in (0, R)$, therefore we can put R in place of η in the right hand side of (A.50) and (A.51), insert into (A.52) and conclude. □

Part II

Hypocoercivity Techniques

Ein Tag mit dem Zigeunergelehrten
(One Day with the Gipsy Scholar)

Stöckel tragend Gestalten hinken,
verwischte Schminken,
glitzernde Roben
mit Matsch betrogen,
verrutschte Fliegen,
oh wie die Bäuche wiegen,
so voll mit Kamel am Stil,
oder auch mit Krokodil,
betrunken mit Glück und Wunderlichkeit,
eine Nacht der Unvergesslichkeit.

Die Sonne geht über den Baumwipfeln auf,
unberührt nimmt der Tag seinen Lauf
als die Blitze des tüchtigen Hoffotografen
die singende Masse der Überlebenden trafen.

Was kann es besseres geben
als nach einer St John's May Ball Nacht
Herz und Geist zu beleben
inmitten reiner natürlicher Pracht.

Ahoi Matrosen!
Wie die großen
Seeentdecker,
Freiheitsschmecker,
Selbstentzwecker
stechen wir in Fluss.
Oh, Genuss!

Alsbald die Türme
    von Cambridge entschwinden,
zwischen Wiesen und Weiden
    wir uns befinden,
Vögel zwitschern, Reiher stacksen,
Libellen flattern, Rebhühner gacksen,
lieblich leise die Wellen schlagen,
wie mühelos sie den Kutter tragen!

Drinnen hört man es rappern und klappern,
sausen und brausen,
denn bald gibt's zu schmausen,
gebackene Bohnen, Schinken und Eier,
was für eine Frühstücksfeier,
Orangensaft
gibt neue Kraft,
und das wichtigste, ich seh'
ist der gute englische Tee.

Für die Verdauungspause
geht's auf's Dach vom Hause.
Fröhlich keck die Noten entschwinden
in den rauen Morgenwinden.

Die Schifffahrtsleute staunten sehr,
Wo kommen diese Klänge her?
Näher und näher kommt unser Kahn
und als sie sah'n
erst die Flöte,
dann die Tröte,
und den fröhlichen Gesang,
der vom Deck des Kutters erklang,
da schmunzelten und lachten sie sehr,
und winkten und grüßten mehr und mehr.

Oh, Happy Day!
What can I say?
Das Zigeunerleben ist komplett
mit improvisiertem Jazzquartett.

Nach einem May Ball, das muss sein,
die Seelen waschen wir uns rein.
Dafür nehmen wir Station
um nach alter Tradition
Eiseskälte zu inhalieren
und die Cam zu schamponieren.
Stop!
Und Hop!

Die Geister erweckt geht's weiter voran
auf der geschlungenen silbernen Bahn.
Jeder wird mal angeheuert.
Ach, so wird also ein Kahn gesteuert!
Gar nicht so hart.
Was für eine Fahrt!
Völlig außer Rand und Band,
gehen wir in Ely an Land.

Kapitäns Judge, wir danken sehr
für Haus und Schmaus und vieles mehr,
denn die beste Glückseligkeit
ist voll genossene Lebenszeit.

for the Captains Judge (Junior and Senior)
by Franca Hoffmann
Kortrijk, 21. Juli 2014

Chapter 5

A fibre lay-down model for non-woven textile production

This chapter follows in most parts the article "Exponential decay to equilibrium for a fibre lay-down process on a moving conveyor belt" written in collaboration with Emeric Bouin[1] and Clément Mouhot[2], and accepted for publication in *SIAM Journal on Mathematical Analysis*.

Chapter Summary

We show existence and uniqueness of a stationary state for a kinetic Fokker-Planck equation modelling the fibre lay-down process in the production of non-woven textiles. Following a micro-macro decomposition, we use hypocoercivity techniques to show exponential convergence to equilibrium with an explicit rate assuming the conveyor belt moves slow enough. This chapter is an extension of [134], where the authors consider the case of a stationary conveyor belt. Adding the movement of the belt, the global Gibbs state is not known explicitly. We thus derive a more general hypocoercivity estimate from which existence, uniqueness and exponential convergence can be derived. To treat the same class of potentials as in [134] we make use of an additional weight function following the Lyapunov functional approach in [206].

[1]CEREMADE - Université Paris-Dauphine, UMR CNRS 7534, Paris, France
[2]DPMMS, Centre for Mathematical Sciences, University of Cambridge, Wilberforce Road, Cambridge CB3 0WA, UK.

Chapter Content

When will it stop moving,
When will it stop changing,
Never,
For we are forever moving along.

Ileana N. Kraus-Nikitakis

1 Introduction

The mathematical analysis of the fibre lay-down process in the production of non-woven textiles has seen a lot of interest in recent years [230, 231, 172, 203, 205, 134, 206]. Non-woven materials are produced in melt-spinning operations: hundreds of individual endless fibres are obtained by continuous extrusion through nozzles of a melted polymer. The nozzles are densely and equidistantly placed in a row at a spinning beam. The visco-elastic, slender and in-extensible fibres lay down on a moving conveyor belt to form a web, where they solidify due to cooling air streams. Before touching the conveyor belt, the fibres become entangled and form loops due to highly turbulent air flow. In [230] a general mathematical model for the fibre dynamics is presented which enables the full simulation of the process. Due to the huge amount of physical details, these simulations of the fibre spinning and lay-down usually require an extremely large computational effort and high memory storage, see [231]. Thus, a simplified two-dimensional stochastic model for the fibre lay-down process, together with its kinetic limit, is introduced in [172]. Generalisations of the two-dimensional stochastic model [172] to three dimensions have been developed by Klar et al. in [203] and to any dimension $d \geqslant 2$ by Grothaus et al. in [177].

We now describe the model we are interested in, which comes from [172]. We track the position $x(t) \in \mathbb{R}^2$ and the angle $\alpha(t) \in \mathbb{S}^1$ of the fibre at the lay-down point where it touches the conveyor belt. Interactions of neighbouring fibres are neglected. If $x_0(t)$ is the lay-down point in the coordinate system following the conveyor belt, then the tangent vector of the fibre is denoted by $\tau(\alpha(t))$ with $\tau(\alpha) = (\cos\alpha, \sin\alpha)$. Since the extrusion of fibres happens at a constant speed, and the fibres are in-extensible, the lay-down process can be assumed to happen at constant normalised speed $\|x_0'(t)\| = 1$. If the conveyor belt moves with constant speed κ in direction $e_1 = (1, 0)$, then

$$\frac{\mathrm{d}x}{\mathrm{d}t} = \tau(\alpha) + \kappa e_1.$$

Note that the speed of the conveyor belt cannot exceed the lay-down speed: $0 \leqslant \kappa \leqslant 1$. The fibre dynamics in the deposition region close to the conveyor belt are dominated by the turbulent air flow. Applying this concept, the dynamics of the angle $\alpha(t)$ can be described by a deterministic force moving the lay-down point towards the equilibrium $x = 0$ and by a Brownian motion modelling the effect of the turbulent air flow. We obtain the following stochastic differential equation for the random variable $X_t = (x_t, \alpha_t)$ on $\mathbb{R}^2 \times \mathbb{S}^1$,

$$\begin{cases} \mathrm{d}x_t &= (\tau(\alpha_t) + \kappa e_1)\,\mathrm{d}t, \\ \mathrm{d}\alpha_t &= \left[-\tau^\perp(\alpha_t) \cdot \nabla_x V(x_t)\right]\,\mathrm{d}t + A\,\mathrm{d}W_t\,, \end{cases} \tag{1.1}$$

where W_t denotes a one-dimensional Wiener process, $A > 0$ measures its strength relative to the deterministic forcing, $\tau^\perp(\alpha) = (-\sin\alpha, \cos\alpha)$, and $V : \mathbb{R}^2 \to \mathbb{R}$ is an external potential carrying

information on the coiling properties of the fibre. More precisely, since a curved fibre tends back to its starting point, the change of the angle α is assumed to be proportional to $\tau^{\perp}(\alpha) \cdot \nabla_x V(x)$. It has been shown in [206] that under suitable assumptions on the external potential V, the fibre lay down process (1.1) has a unique invariant distribution and is even geometrically ergodic (see Remark 1.2). The stochastic approach yields exponential convergence in total variation norm, however without explicit rate. We will show here that a stronger result can be obtained with a functional analysis approach. Our argument uses crucially the construction of an additional weight functional for the fibre lay-down process in the case of unbounded potential gradients inspired by [206, Proposition 3.7].

The probability density function $f(t, x, \alpha)$ corresponding to the stochastic process (1.1) is governed by the Fokker-Planck equation

$$\partial_t f + (\tau + \kappa e_1) \cdot \nabla_x f - \partial_\alpha \left(\tau^{\perp} \cdot \nabla_x V f\right) = D \partial_{\alpha\alpha} f \tag{1.2}$$

with diffusivity $D = A^2/2$. We state below assumptions on the external potential V that will be used regularly throughout the chapter:

(H1) *Regularity and symmetry*: $V \in C^2(\mathbb{R}^2)$ and V is spherically symmetric outside some ball $B(0, R_V)$.

(H2) *Normalisation*: $\int_{\mathbb{R}^2} e^{-V(x)}\,\mathrm{d}x = 1$.

(H3) *Spectral gap condition* (Poincaré inequality): there exists a positive constant Λ such that for any $u \in H^1(e^{-V}\mathrm{d}x)$ with $\int_{\mathbb{R}^2} u e^{-V}\mathrm{d}x = 0$,

$$\int_{\mathbb{R}^2} |\nabla_x u|^2 \, e^{-V}\,\mathrm{d}x \geqslant \Lambda \int_{\mathbb{R}^2} u^2 e^{-V}\,\mathrm{d}x.$$

(H4) *Pointwise regularity condition on the potential*: there exists $c_1 > 0$ such that for any $x \in \mathbb{R}^2$, the Hessian $\nabla_x^2 V$ of $V(x)$ satisfies

$$|\nabla_x^2 V(x)| \leqslant c_1(1 + |\nabla_x V(x)|).$$

(H5) *Behaviour at infinity*:

$$\lim_{|x|\to\infty} \frac{|\nabla_x V(x)|}{V(x)} = 0, \qquad \lim_{|x|\to\infty} \frac{|\nabla_x^2 V(x)|}{|\nabla_x V(x)|} = 0\,.$$

Remark 1.1. *Assumptions **(H2-3-4)** are as stated in [134]. Assumption **(H1)** assumes regularity of the potential that is stronger and included in that discussed in [134] since **(H1)** implies $V \in W^{2,\infty}_{loc}(\mathbb{R}^2)$. Assumption **(H5)** is only necessary if the potential gradient $|\nabla_x V|$ is unbounded. Both bounded and unbounded potential gradients may appear depending on the physical context, and we will treat these two cases separately where necessary. A typical example for an external potential satisfying assumptions **(H1-2-3-4-5)** is given by*

$$V(x) = K\left(1 + |x|^2\right)^{s/2} \tag{1.3}$$

*for some constants $K > 0$ and $s \geqslant 1$ [135, 206]. The potential (1.3) satisfies **(H3)** since*

$$\liminf_{|x|\to\infty} \left(|\nabla_x V|^2 - 2\Delta_x V\right) > 0\,,$$

see for instance [298, A.19. Some criteria for Poincaré inequalities, page 135]. The other assumptions are trivially satisfied as can be checked by direct inspection. In this family of potentials, the gradient $\nabla_x V$ is bounded for $s = 1$ and unbounded for $s > 1$.

Remark 1.2. *The proof of ergodicity in [206] assumes that the potential satisfies*

$$\lim_{|x|\to\infty} \frac{|\nabla_x V(x)|}{V(x)} = 0\,, \qquad \lim_{|x|\to\infty} \frac{|\nabla_x^2 V(x)|}{|\nabla_x V(x)|} = 0\,, \qquad \lim_{|x|\to\infty} |\nabla_x V(x)| = \infty\,. \tag{1.4}$$

Under these assumptions, there exists an invariant distribution ν to the fibre lay-down process (1.1), and some constants $C(x_0) > 0$, $\lambda > 0$ such that

$$\left\|\mathcal{P}_{x_0,\alpha_0}\left(X_t \in \cdot\right) - \nu\right\|_{TV} \leqslant C(x_0)e^{-\lambda t}\,,$$

*where $\mathcal{P}_{x_0,\alpha_0}$ is the law of X_t starting at $X_0 = (x_0, \alpha)$, and where $\|\cdot\|_{TV}$ denotes the total variation norm. The stochastic Lyapunov technique applied in [206] however does not give any information on how the constant $C(x_0)$ depends on the initial position x_0, or how the rate of convergence λ depends on the conveyor belt speed κ, the potential V and the noise strength A. This can be achieved using hypocoercivity techniques, proving convergence in a weighted L^2-norm, which is slightly stronger than the convergence in total variation norm shown in [206]. Conceptually, the conditions (1.4) ensure that the potential V is driving the process back inside a compact set where the noise can be controlled. Our framework **(H1-2-3-4-5)** is more general than conditions (1.4) in some aspects (including bounded potential gradient) and more restrictive in others (assuming a Poincaré inequality). The proof in [206] relies on the strong Feller property which can be translated in some cases into a spectral gap; it also uses hypoellipticity to deduce the existence of a transition density, and concludes via an explicit Lyapunov function argument. With our framework **(H1-2-3-4-5)**, and adapting the Lyapunov function argument presented in [206] to control the effect of $\kappa\partial_{x_1}$, we derive an explicit rate of convergence in terms of κ, D and V.*

To set up a functional framework, rewrite (1.2) as

$$\partial_t f = \mathsf{L}_\kappa f = (\mathsf{Q} - \mathsf{T})\, f + \mathsf{P}_\kappa f\,, \tag{1.5}$$

where the collision operator $\mathsf{Q} := D\partial_{\alpha\alpha}$ acts as a multiplicator in the space variable x, P_κ is the perturbation introduced by the moving belt with respect to [134]:

$$\mathsf{P}_\kappa f := -\kappa e_1 \cdot \nabla_x f\,,$$

and the transport operator T is given by

$$\mathsf{T} f := \tau \cdot \nabla_x f - \partial_\alpha \left(\tau^\perp \cdot \nabla_x V f\right).$$

We consider solutions to (1.5) in the space $L^2(\mathrm{d}\mu_\kappa) := L^2(\mathbb{R}^2 \times \mathbb{S}^1, \mathrm{d}\mu_\kappa)$ with measure

$$\mathrm{d}\mu_\kappa(x,\alpha) = \left(e^{V(x)} + \zeta\kappa g(x,\alpha)\right)\frac{\mathrm{d}x\,\mathrm{d}\alpha}{2\pi}\,.$$

We denote by $\langle\cdot,\cdot\rangle_\kappa$ the corresponding scalar product and by $\|\cdot\|_\kappa$ the associated norm. Here, $\zeta > 0$ is a free parameter to be chosen later. The construction of the weight g depends on the boundedness of $\nabla_x V$. When it is bounded, no additional weight is needed to control the perturbation, and so we simply set $g \equiv 0$ in that case. When the gradient is unbounded, the weight is constructed thanks to the following proposition:

Proposition 1.3. *Assume that V satisfies **(H1)** and **(H5)** and that*

$$\lim_{|x|\to\infty} |\nabla_x V| = +\infty.$$

If $\kappa < 1/3$ holds true, then there exists a function $g(x,\alpha)$, a constant $c = c(\kappa, D) > 0$ and a finite radius $R = R(k, D, V) > 0$ such that

$$\forall\, |x| > R,\ \forall\, \alpha \in \mathbb{S}^1, \quad \mathcal{L}_\kappa(g)(x,\alpha) \leqslant -c\,|\nabla_x V(x)| g(x,\alpha)\,, \tag{1.6}$$

where $\mathcal{L}_\kappa$ is defined by

$$\mathcal{L}_\kappa(h) := D\partial_{\alpha\alpha} h + (\tau + \kappa e_1)\cdot\nabla_x h - \left(\tau^\perp\cdot\nabla_x V\right)\partial_\alpha h - (\tau\cdot\nabla_x V)\,h\,. \tag{1.7}$$

The weight g is of the form

$$g(x,\alpha) := \exp\left(\beta V(x) + |\nabla_x V(x)|\Gamma\left(\tau(\alpha)\cdot\frac{\nabla_x V(x)}{|\nabla_x V(x)|}\right)\right)\,,$$

where the parameter $\beta > 1$ and the function $\Gamma \in C^1([-1,1])$, $\Gamma > 0$ are determined along the proof and only depend on κ.

We show in Section 3 the existence of such a weight function g under appropriate conditions following ideas from [206].

We denote $\mathcal{C} := C_c^\infty\left(\mathbb{R}^2 \times \mathbb{S}^1\right)$, and define the orthogonal projection Π on the set of local equilibria $\mathrm{Ker}\,\mathsf{Q}$

$$\Pi f := \int_{\mathbb{S}^1} f\,\frac{\mathrm{d}\alpha}{2\pi}\,,$$

and the *mass* M_f of a given distribution $f \in L^2(\mathrm{d}\mu_\kappa)$,

$$M_f := \int_{\mathbb{R}^2\times\mathbb{S}^1} f\,\frac{\mathrm{d}x\mathrm{d}\alpha}{2\pi}\,.$$

Integrating (1.2) over $\mathbb{R}^2 \times \mathbb{S}^1$ shows that the mass of solutions of (1.2) is conserved over time, and standard maximum principle arguments show that it remains non-negative for non-negative initial data. The collision operator Q is symmetric and satisfies

$$\forall\, f \in \mathcal{C}, \quad \langle \mathsf{Q}f, f\rangle_0 = -D\,\|\partial_\alpha f\|_0^2 \leqslant 0\,,$$

i.e. Q is dissipative in $L^2(\mathrm{d}\mu_0)$. Further, we have $\mathsf{T}\Pi f = e^{-V}\tau \cdot \nabla_x u_f$ for $f \in \mathcal{C}$, with $u_f := e^V \Pi f$, which implies $\Pi\mathsf{T}\Pi = 0$ on $\mathcal{C}$. Since the transport operator T is skew-symmetric with respect to $\langle \cdot\,, \cdot \rangle_0$,

$$\langle \mathsf{L}_\kappa f, f\rangle_0 = \langle \mathsf{Q} f, f\rangle_0 + \langle \mathsf{P}_\kappa f, f\rangle_0$$

for any f in $\mathcal{C}$. In the case $\kappa = 0$, if the entropy dissipation $-\langle \mathsf{Q} f, f\rangle_0$ was coercive with respect to the norm $\|\cdot\|_0$, exponential decay to zero would follow as $t \to \infty$. However, such a coercivity property cannot hold since Q vanishes on the set of local equilibria. Instead, Dolbeault et al. [135] applied a strategy called *hypocoercivity* (as theorised in [298]) and developed by several groups in the 2000s, see for instance [185, 178, 225, 129, 130]. The full hypocoercivity analysis of the long time behaviour of solutions to this kinetic model in the case of a stationary conveyor belt, $\kappa = 0$, is completed in [134]. For technical applications in the production process of non-wovens, one is interested in a model including the movement of the conveyor belt, and our aim is to extend the results in [134] to small $\kappa > 0$.

We follow the approach of hypocoercivity for linear kinetic equations conserving mass developed in [135], with several new difficulties. Considering the case $\kappa = 0$, Q and T are closed operators on $L^2(\mathrm{d}\mu_0)$ such that $\mathsf{Q} - \mathsf{T}$ generates the $\mathcal{C}_0$-semigroup $e^{(\mathsf{Q}-\mathsf{T})t}$ on $L^2(\mathrm{d}\mu_0)$. When $\kappa > 0$, we use the additional weight function $g > 0$ to control the perturbative term P_κ in the case of unbounded potential gradients; and show the existence of a $\mathcal{C}_0$-semigroup for $\mathsf{L}_\kappa = \mathsf{Q} - \mathsf{T} + \mathsf{P}_\kappa$ (see Section 4.1). Unless otherwise specified, all computations are performed on the operator core $\mathcal{C}$, and can be extended to $L^2(\mathrm{d}\mu_\kappa)$ by density arguments.

When $\kappa = 0$, the hypocoercivity result in [135, 134] is based on: *microscopic coercivity*, which assumes that the restriction of Q to $(\operatorname{Ker}\mathsf{Q})^\perp$ is coercive, and *macroscopic coercivity*, which is a spectral gap-like inequality for the operator obtained when taking a parabolic drift-diffusion limit, in other words, the restriction of T to $\operatorname{Ker}\mathsf{Q}$ is coercive. The two properties are satisfied in the case of a stationary conveyor belt:

- The operator Q is symmetric and the Poincaré inequality on $\mathbb{S}^1$,

$$\frac{1}{2\pi}\int_{\mathbb{S}^1} |\partial_\alpha f|^2 \,\mathrm{d}\alpha \geqslant \frac{1}{2\pi}\int_{\mathbb{S}^1} \left(f - \frac{1}{2\pi}\int_{\mathbb{S}^1} f\,\mathrm{d}\alpha\right)^2 \mathrm{d}\alpha,$$

  implies that $-\langle \mathsf{Q} f, f\rangle_0 \geqslant D\,\|(1-\Pi)f\|_0^2$.

- The operator T is skew-symmetric and for any $h \in L^2(\mathrm{d}\mu_0)$ such that $u_h = e^V \Pi h \in H^1(e^{-V}\mathrm{d}x)$ and $\int_{\mathbb{R}^2\times\mathbb{S}^1} h\,\mathrm{d}\mu_0 = 0$, **(H3)** implies

$$\|\mathsf{T}\Pi h\|_0^2 = \frac{1}{4\pi}\int_{\mathbb{R}^2\times\mathbb{S}^1} e^{-V}|\nabla_x u_h|^2 \,\mathrm{d}x\,\mathrm{d}\alpha \geqslant \frac{\Lambda}{4\pi}\int_{\mathbb{R}^2\times\mathbb{S}^1} e^{-V} u_h^2 \,\mathrm{d}x\,\mathrm{d}\alpha = \frac{\Lambda}{2}\,\|\Pi h\|_0^2\,.$$

In the case $\kappa = 0$, the unique global normalised equilibrium distribution $F_0 = e^{-V}$ lies in the intersection of the null spaces of T and Q. When $\kappa > 0$, F_0 is not in the kernel of P_κ and we are not able to find the global Gibbs state of (1.5) explicitly. However, the hypocoercivity theory is based on a priori estimates [135] that are, as we shall prove, to some extent stable under perturbation.

Our main result reads:

Theorem 1.4. *Let $f_{\text{in}} \in L^2(\mathrm{d}\mu_\kappa)$ and let **(H1-2-3-4-5)** hold. For $0 < \kappa < 1$ small enough (with a quantitative estimate) and $\zeta > 0$ large enough (with a quantitative estimate), there exists a unique non-negative stationary state $F_\kappa \in L^2(\mathrm{d}\mu_\kappa)$ with unit mass $M_{F_\kappa} = 1$. In addition, for any solution f of (1.2) in $L^2(\mathrm{d}\mu_\kappa)$ with mass M_f and subject to the initial condition $f(t=0) = f_{\text{in}}$, we have*

$$\|f(t,\cdot) - M_f F_\kappa\|_\kappa \leqslant C \|f_{\text{in}} - M_f F_\kappa\|_\kappa \, e^{-\lambda_\kappa t}\,, \tag{1.8}$$

where the rate of convergence $\lambda_\kappa > 0$ depends only on κ, D and V, and the constant $C > 0$ depends only on D and V.

In the case of a stationary conveyor belt $\kappa = 0$ considered in [134], the stationary state is characterised by the eigenpair (Λ_0, F_0) with $\Lambda_0 = 0$, $F_0 = e^{-V}$, and so $\operatorname{Ker} \mathsf{L}_0 = \langle F_0 \rangle$. This means that there is an isolated eigenvalue $\Lambda_0 = 0$ and a spectral gap of size at least $[-\lambda_0, 0]$ with the rest of the spectrum $\Sigma(\mathsf{L}_0)$ to the left of $-\lambda_0$ in the complex plane. Adding the movement of the conveyor belt, Theorem 1.4 shows that $\operatorname{Ker} \mathsf{L}_\kappa = \langle F_\kappa \rangle$ and the exponential decay to equilibrium with rate λ_κ corresponds to a spectral gap of size at least $[-\lambda_\kappa, 0]$. Further, it allows to recover an explicit expression for the rate of convergence λ_0 for $\kappa = 0$ (see Step 5 in Section 2.1). In general, we are not able to compute the stationary state F_κ for $\kappa > 0$ explicitly, but F_κ converges to $F_0 = e^{-V}$ weakly as $\kappa \to 0$ (see Remark 4.2). Let us finally emphasize that a specific contribution of this work is to introduce *two* (and not one as in [135, 134]) modifications of the entropy: 1) we first modify the *space itself* with the coercivity weight g, then 2) we change the norm with an auxiliary operator following the hypocoercivity approach.

The rest of the chapter deals with the case $\kappa > 0$ and is organised as follows. In Section 2, we prove the main hypocoercivity estimate. This allows us to establish the existence of solutions to (1.2) using semigroup theory and to deduce the existence and uniqueness of a steady state in Section 4 by a contraction argument. In Section 3, we give a detailed definition of the weight function g that is needed for the hypocoercivity estimate in Section 2.

2 Hypocoercivity estimate

Following [135] we introduce the auxiliary operator

$$\mathsf{A} := (1 + (\mathsf{T}\Pi)^*(\mathsf{T}\Pi))^{-1}(\mathsf{T}\Pi)^* ,$$

and a modified entropy, i.e. a *hypocoercivity functional* G on $L^2(\mathrm{d}\mu_\kappa)$:

$$\mathsf{G}[f] := \frac{1}{2}\|f\|_\kappa^2 + \varepsilon_1 \langle \mathsf{A}f, f\rangle_0 , \quad f \in L^2(\mathrm{d}\mu_\kappa)$$

for some suitably chosen $\varepsilon_1 \in (0,1)$ to be determined later. It follows from [135] that $|\langle \mathsf{A}f, f\rangle_0| \leqslant \|f\|_0^2$. Also, $\|f\|_0^2 \leqslant \|f\|_\kappa^2$ by construction of μ_κ, and hence $\mathsf{G}[\cdot]$ is norm-equivalent to $\|\cdot\|_\kappa^2$:

$$\forall\, f \in L^2(\mathrm{d}\mu_\kappa), \quad \left(\frac{1-\varepsilon_1}{2}\right) \|f\|_\kappa^2 \leqslant \mathsf{G}[f] \leqslant \left(\frac{1+\varepsilon_1}{2}\right) \|f\|_\kappa^2 , \tag{2.9}$$

In this section, we prove the following hypocoercivity estimate:

Proposition 2.1. *Assume that hypothesis* ***(H1-2-3-4-5)*** *hold and that $0 < \kappa < 1$ is small enough (with a quantitative estimate). Let $f_{\mathrm{in}} \in L^2(\mathrm{d}\mu_\kappa)$ and $f = f(t,x,\alpha)$ be a solution of (1.2) in $L^2(\mathrm{d}\mu_\kappa)$ subject to the initial condition $f(t=0) = f_{\mathrm{in}}$. Then f satisfies the following Grönwall type estimate:*

$$\frac{\mathrm{d}}{\mathrm{d}t}\mathsf{G}[f(t,\cdot)] \leqslant -\gamma_1 \mathsf{G}[f(t,\cdot)] + \gamma_2 M_f^2, \tag{2.10}$$

where $\gamma_1 > 0, \gamma_2 > 0$ are explicit constants only depending on κ, D and V.

Note that the estimate (2.10) is stronger than what is required for the uniqueness of a global Gibbs state, and represents an extension of the estimate given in [134]. When applied to the difference of two solutions with the same mass, (2.10) gives an estimate on the exponential decay rate towards equilibrium.

2.1 Proof of Proposition 2.1

Differentiate in time $\mathsf{G}[f]$ to get

$$\frac{\mathrm{d}}{\mathrm{d}t}\mathsf{G}[f] = \mathsf{D}_0[f] + \mathsf{D}_1[f] + \mathsf{D}_2[f] + \mathsf{D}_3[f] ,$$

where the *entropy dissipation functionals* D_0, D_1, D_2 and D_3 are given by

$$\begin{aligned}
\mathsf{D}_0[f] &:= \langle \mathsf{Q}f, f\rangle_0 - \varepsilon_1 \langle \mathsf{AT}\Pi f, \Pi f\rangle_0 - \varepsilon_1 \langle \mathsf{AT}(1-\Pi)f, \Pi f\rangle_0 \\
&\qquad + \varepsilon_1 \langle \mathsf{TA}f, (1-\Pi)f\rangle_0 + \varepsilon_1 \langle \mathsf{AQ}f, \Pi f\rangle_0 , \\
\mathsf{D}_1[f] &:= \varepsilon_1 \langle \mathsf{AP}_\kappa f, \Pi f\rangle_0 + \varepsilon_1 \langle \mathsf{P}_\kappa^* \mathsf{A}f, \Pi f\rangle_0 , \\
\mathsf{D}_2[f] &:= \langle \mathsf{P}_\kappa f, f\rangle_0 , \\
\mathsf{D}_3[f] &:= \kappa\zeta \int_{\mathbb{R}^2\times\mathbb{S}^1} \mathsf{L}_\kappa(f) f g \, \frac{\mathrm{d}x\,\mathrm{d}\alpha}{2\pi} .
\end{aligned}$$

Note that the term $\langle \mathsf{LA}f, f\rangle_0$ vanishes since it has been shown in [135] that $\mathsf{A} = \Pi\mathsf{A}$ and hence $\mathsf{A}f \in \operatorname{Ker}\mathsf{Q}$. Further, $\langle \mathsf{T}f, f\rangle = 0$ since T is skew-symmetric. We estimate the entropy dissipation of the case $\kappa = 0$ as in [134]:

 # Step 1: Estimation of $\mathsf{D}_0[f]$.

We will show the boundedness of D_0, which is in fact the dissipation functional for a stationary conveyor belt. We thus recall without proof in the following lemma some results from [134].

Lemma 2.2 (Dolbeault et al. [134]). *The following estimates hold:*

$$\langle \mathsf{Q}f, f\rangle_0 \leqslant -\left\|(1-\Pi)f\right\|_0^2, \qquad \left\|\mathsf{AT}(1-\Pi)f\right\|_0 \leqslant C_V \left\|(1-\Pi)f\right\|_0,$$

$$\left\|\mathsf{AQ}f\right\|_0 \leqslant \frac{D}{2}\left\|(1-\Pi)f\right\|_0, \qquad \left\|\mathsf{TA}f\right\|_0 \leqslant \left\|(1-\Pi)f\right\|_0.$$

In order to control the contribution $\langle \mathsf{AT}\Pi f, \Pi f\rangle_0$ in D_0, we note that

$$\mathsf{AT}\Pi = \left(1 + (\mathsf{T}\Pi)^*\mathsf{T}\Pi\right)^{-1}(\mathsf{T}\Pi)^*\mathsf{T}\Pi$$

shares its spectral decomposition with $(\mathsf{T}\Pi)^*\mathsf{T}\Pi$, and by *macroscopic coercivity*

$$\langle (\mathsf{T}\Pi)^*\mathsf{T}\Pi f, f\rangle_0 = \left\|\mathsf{T}\Pi f\right\|_0^2 = \left\|\mathsf{T}\Pi(f - M_f e^{-V})\right\|_0^2 \geqslant \frac{\Lambda}{2}\left\|\Pi(f - M_f e^{-V})\right\|_0^2.$$

Hence,

$$\langle \mathsf{AT}\Pi f, f\rangle_0 \geqslant \frac{\Lambda/2}{1+\Lambda/2}\left\|\Pi(f - M_f e^{-V})\right\|_0^2.$$

Now, recalling Lemma 2.2 and using $\left\|\Pi(f - M_f e^{-V})\right\|_0^2 = \left\|\Pi f\right\|_0^2 - M_f^2$, we estimate

$$\mathsf{D}_0[f] \leqslant (\varepsilon_1 - D)\left\|(1-\Pi)f\right\|_0^2 + \varepsilon_1\lambda_2\left\|(1-\Pi)f\right\|_0\left\|\Pi f\right\|_0 - \varepsilon_1\gamma_2\left(\left\|\Pi f\right\|_0^2 - M_f^2\right),$$

with $\lambda_2 := C_V + D/2 > 0$ and $\gamma_2 := \frac{\Lambda/2}{1+\Lambda/2} > 0$.

 # Step 2: Estimation of $\mathsf{D}_1[f]$.

We now turn to the entropy dissipation functional D_1, which we will estimate using elliptic regularity. Instead of bounding AP_κ, we apply an elliptic regularity strategy to its adjoint, as for $\mathsf{AT}(1-\Pi)$ in [134]. Let $f \in L^2(\mathrm{d}\mu_0)$ and define $h := \left(1 + (\mathsf{T}\Pi)^*\mathsf{T}\Pi\right)^{-1} f$ so that $u_h = e^V \Pi h$ satisfies

$$\Pi f = e^{-V}u_h + \Pi\mathsf{T}^*\mathsf{T}\left(e^{-V}u_h\right) = e^{-V}u_h - \frac{1}{2}\nabla_x \cdot \left(e^{-V}\nabla_x u_h\right).$$

We have used here the fact that in the space $L^2(\mathrm{d}\mu_0)$:

$$\begin{cases} \mathsf{T} = \tau\cdot\nabla_x - \partial_\alpha\left[\left(\tau^\perp\cdot\nabla_x V\right)\right], \\ \mathsf{T}^* = -\tau\cdot\nabla_x + \left(\tau^\perp\cdot\nabla_x V\right)\partial_\alpha - \left(\tau\cdot\nabla_x V\right). \end{cases}$$

Then

$$\mathsf{A}^* f = \mathsf{T}\Pi h = e^{-V}\tau \cdot \nabla_x u_h \,,$$

and since the adjoint for $\langle \cdot, \cdot \rangle_0$ of the perturbation operator P_κ is given by

$$\mathsf{P}_\kappa^* = -\mathsf{P}_\kappa - \mathsf{P}_\kappa V \,,$$

it follows that

$$\begin{aligned}
\|(\mathsf{A}\mathsf{P}_\kappa)^* f\|_0^2 &= \left\|\kappa\, \tau \cdot \nabla_x (e_1 \cdot \nabla_x u_h) e^{-V}\right\|_0^2 \\
&= \frac{\kappa^2}{2} \int_{\mathbb{R}^2 \times \mathbb{S}^1} e^{-V} |\tau \cdot \nabla_x \left(e_1 \cdot \nabla_x u_h\right)|^2 \, \mathrm{d}\mu_0 \\
&= \frac{\kappa^2}{2} \int_{\mathbb{R}^2} e^{-V} |\nabla_x \left(e_1 \cdot \nabla_x u_h\right)|^2 \, \mathrm{d}x \\
&\leqslant \frac{\kappa^2}{2} \left\|\nabla_x^2 u_h\right\|^2_{L^2(e^{-V}\,\mathrm{d}x)} \\
&\leqslant \frac{\kappa^2}{2} C_V^2 \|\Pi f\|_0^2 \,,
\end{aligned}$$

where in the last inequality we have used an elliptic regularity estimate. This estimate turns out to be a particular case of [134, Proposition 5 and Sections 2-3], where the positive constant C_V is the same as in Lemma 2.2 reproduced from [134]. This concludes the boundedness of $\mathsf{A}\mathsf{P}_\kappa$,

$$\|\mathsf{A}\mathsf{P}_\kappa f\|_0 \leqslant \kappa \frac{C_V}{\sqrt{2}} \|\Pi f\|_0 \leqslant \kappa \frac{C_V}{\sqrt{2}} \|f\|_0 \,. \tag{2.11}$$

Using a similar approach for the operator $\mathsf{P}_\kappa^* \mathsf{A}$, we rewrite its adjoint as

$$\mathsf{A}^* \mathsf{P}_\kappa f = \mathsf{T}\Pi \tilde{h} \,,$$

where we define $\tilde{h} := (1 + (\mathsf{T}\Pi)^* \mathsf{T}\Pi)^{-1} \mathsf{P}_\kappa f$ for a given $f \in L^2(\mathrm{d}\mu_0)$, or equivalently

$$e^{-V} u_{\tilde{h}} - \frac{1}{2} \nabla_x \cdot \left(e^{-V} \nabla_x u_{\tilde{h}}\right) = \Pi \mathsf{P}_\kappa f = \mathsf{P}_\kappa \Pi f \,.$$

Multiplying by $u_{\tilde{h}}$ and integrating over $\mathbb{R}^2$, we have

$$\begin{aligned}
\|u_{\tilde{h}}\|^2_{L^2(e^{-V}\,\mathrm{d}x)} + \frac{1}{2} \|\nabla_x u_{\tilde{h}}\|^2_{L^2(e^{-V}\,\mathrm{d}x)} &= -\kappa \int_{\mathbb{R}^2} \mathbf{e}_1 \cdot \nabla_x \left(\Pi f\right) u_{\tilde{h}} \, \mathrm{d}x \\
&= \kappa \int_{\mathbb{R}^2} \left(\Pi f\right) \mathbf{e}_1 \cdot \nabla_x u_{\tilde{h}} \, \mathrm{d}x \\
&\leqslant \kappa \int_{\mathbb{R}^2} \left|\nabla_x u_{\tilde{h}} e^{-V/2}\right| \left|\Pi f e^{V/2}\right| \, \mathrm{d}x \\
&\leqslant \kappa \left\|\nabla_x u_{\tilde{h}}\right\|_{L^2(e^{-V}\,\mathrm{d}x)} \|\Pi f\|_0 \\
&\leqslant \frac{1}{4} \|\nabla_x u_{\tilde{h}}\|^2_{L^2(e^{-V}\,\mathrm{d}x)} + \kappa^2 \|\Pi f\|_0^2 \,.
\end{aligned}$$

This inequality is a $H^1(e^{-V}\,\mathrm{d}x) \to H^{-1}(e^{-V}\,\mathrm{d}x)$ elliptic regularity result. Hence,

$$\|\mathsf{A}^* \mathsf{P}_\kappa f\|_0^2 = \|\mathsf{T}\Pi h\|_0^2 = \frac{1}{2} \|\nabla_x u_{\tilde{h}}\|^2_{L^2(e^{-V}\,\mathrm{d}x)} \leqslant 2\kappa^2 \|\Pi f\|_0^2 \,,$$

and so we conclude

$$\|\mathsf{P}_\kappa^* \mathsf{A} f\|_0 \leqslant \sqrt{2}\kappa \,\|(1-\Pi)f\|_0 \leqslant \sqrt{2}\kappa \,\|f\|_0 \,. \tag{2.12}$$

Combining (2.11) and (2.12), the entropy dissipation functional D_1 is bounded by

$$\mathsf{D}_1[f] \leqslant \kappa\varepsilon_1 \left(\frac{C_V}{\sqrt{2}} + \sqrt{2}\right) \|f\|_0^2 = 2\kappa\lambda_1 \,\|f\|_0^2,$$

where we defined $\lambda_1 := \frac{1}{2}\left(\frac{C_V}{\sqrt{2}} + \sqrt{2}\right)$.

 # Step 3: Estimation of $\mathsf{D}_2[f]$.

Using integration by parts, we have

$$\langle \mathsf{P}_\kappa f, f\rangle_0 = \frac{\kappa}{2}\int_{\mathbb{R}^2\times\mathbb{S}^1} (e_1\cdot\nabla_x V)\, f^2 e^V \,\frac{\mathrm{d}x\,\mathrm{d}\alpha}{2\pi}\,.$$

The estimation of this term goes differently depending on the boundedness of $\nabla_x V$.

If $\nabla_x V$ is bounded, we write

$$\mathsf{D}_2[f] \leqslant |\langle \mathsf{P}_\kappa f, f\rangle_0| \leqslant \frac{\kappa}{2}\|\nabla_x V\|_\infty \|f\|_0^2 = \frac{\kappa}{2}\|\nabla_x V\|_\infty \|f\|_\kappa^2,$$

where we have used $\|f\|_\kappa = \|f\|_0$, since $g \equiv 0$.

Assume now that $|\nabla_x V| \to \infty$ as $|x| \to \infty$. Thanks to the choice of g, we have the estimate

$$\mathsf{D}_2[f] \leqslant |\langle \mathsf{P}_\kappa f, f\rangle_0| \leqslant \frac{\kappa}{2}\int_{\mathbb{R}^2\times\mathbb{S}^1} |\nabla_x V| f^2 e^V \,\frac{\mathrm{d}x\,\mathrm{d}\alpha}{2\pi} \leqslant \frac{\kappa}{2} C_3 \int_{\mathbb{R}^2\times\mathbb{S}^1} f^2 g \,\frac{\mathrm{d}x\,\mathrm{d}\alpha}{2\pi}, \tag{2.13}$$

with

$$C_3 := \sup_{x\in\mathbb{R}^2} \left(|\nabla_x V| e^V g^{-1}\right),$$

which is finite by **(H5)**.

 # Step 4: Estimation of $\mathsf{D}_3[f]$.

We start by recalling that this estimate is only relevant when $\nabla_x V$ is unbounded. Indeed, in the opposite case, $\mathsf{D}_3[f] = 0$ since $g \equiv 0$ by definition. By the identity

$$\int_{\mathbb{R}^2\times\mathbb{S}^1} \mathsf{L}_\kappa(f) f g \,\mathrm{d}x\,\mathrm{d}\alpha = \frac{1}{2}\int_{\mathbb{R}^2\times\mathbb{S}^1} \mathcal{L}_\kappa(g) f^2 \,\mathrm{d}x\,\mathrm{d}\alpha - D\int_{\mathbb{R}^2\times\mathbb{S}^1} |\partial_\alpha f|^2 \, g \,\mathrm{d}x\,\mathrm{d}\alpha$$

with $\mathcal{L}_\kappa$ as defined in (1.7), we have

$$\mathsf{D}_3[f] \leqslant \kappa\zeta \left(\frac{1}{2}\int_{\mathbb{R}^2\times\mathbb{S}^1} \mathcal{L}_\kappa(g) f^2 \,\frac{\mathrm{d}x\,\mathrm{d}\alpha}{2\pi}\right). \tag{2.14}$$

Proposition 1.3 allows us to control the g-weighted L^2-norm outside some fixed ball. More precisely, take $R > 0$ in (1.6) large enough s.t. $|\nabla_x V| \geqslant 1$ for all $|x| > R$, then

$$\begin{aligned}
&\int_{\mathbb{R}^2\times\mathbb{S}^1} \mathcal{L}_\kappa(g) f^2 \,\frac{\mathrm{d}x\,\mathrm{d}\alpha}{2\pi} \\
&\quad\leqslant \int_{\mathbb{S}^1}\int_{|x|<R} \mathcal{L}_\kappa(g) f^2 \,\frac{\mathrm{d}x\,\mathrm{d}\alpha}{2\pi} - c\int_{\mathbb{S}^1}\int_{|x|>R} |\nabla_x V| f^2 g \,\frac{\mathrm{d}x\,\mathrm{d}\alpha}{2\pi} \\
&\quad\leqslant \int_{\mathbb{S}^1}\int_{|x|<R} \left((\mathcal{L}_\kappa(g) + cg)\, e^{-V}\right) f^2 e^V \,\frac{\mathrm{d}x\,\mathrm{d}\alpha}{2\pi} - c\int_{\mathbb{R}^2\times\mathbb{S}^1} f^2 g \,\frac{\mathrm{d}x\,\mathrm{d}\alpha}{2\pi} \\
&\quad\leqslant C_4(R)\|f\|_0^2 - c\int_{\mathbb{R}^2\times\mathbb{S}^1} f^2 g \,\frac{\mathrm{d}x\,\mathrm{d}\alpha}{2\pi}\,,
\end{aligned} \tag{2.15}$$

where $C_4(R) := \sup_{|x|\leqslant R}\left(|\mathcal{L}_\kappa(g) + cg|e^{-V}\right)$.

Remark 2.3. *Observe here that one could take advantage of the growth of $\nabla_x V$ by playing with the cut-off parameter R and keeping track of $\min_{|x|\geqslant R}|\nabla_x V|$ in the negative term. It could lead to more optimal constants but we chose instead to vary the parameter ζ in front of the coercivity weight g in the measure μ_κ for simplicity.*

 # Step 5: Putting the four previous steps together.

Combine the previous steps into

$$\begin{aligned}
\mathsf{D}_0[f] + \mathsf{D}_1[f] \leqslant&(\varepsilon_1 - D)\,\|(1-\Pi)f\|_0^2 + \varepsilon_1\lambda_2\,\|(1-\Pi)f\|_0\,\|\Pi f\|_0 \\
&- \varepsilon_1\gamma_2\left(\|\Pi f\|_0^2 - M_f^2\right) + 2\kappa\lambda_1\,\|f\|_0^2 \\
=&-(D - \varepsilon_1 - 2\kappa\lambda_1)\,\|(1-\Pi)f\|_0^2 + \varepsilon_1\lambda_2\,\|(1-\Pi)f\|_0\,\|\Pi f\|_0 \\
&-(\varepsilon_1\gamma_2 - 2\kappa\lambda_1)\,\|\Pi f\|_0^2 + \varepsilon_1\gamma_2 M_f^2 \\
\leqslant&-\left(D - \varepsilon_1 - 2\kappa\lambda_1 - \frac{\varepsilon_1\lambda_2 b}{2}\right)\|(1-\Pi)f\|_0^2 \\
&-\left(\varepsilon_1\gamma_2 - 2\kappa\lambda_1 - \frac{\varepsilon_1\lambda_2}{2b}\right)\|\Pi f\|_0^2 + \varepsilon_1\gamma_2 M_f^2 \\
\leqslant&-2\xi(\kappa)\|f\|_0^2 + \varepsilon_1\gamma_2 M_f^2\,,
\end{aligned}$$

by Young's inequality with the choice $b = \lambda_2/\gamma_2$, and where we used the fact that $\|(1-\Pi)f\|_0^2 + \|\Pi f\|_0^2 = \|f\|_0^2$. Here, $\xi(\kappa)$ is explicit, and given by

$$\begin{aligned}
\xi(\kappa) :=&\frac{1}{2}\min\left\{D - \varepsilon_1\left(1 + \frac{\lambda_2^2}{2\gamma_2}\right)\,,\ \frac{\varepsilon_1\gamma_2}{2}\right\} - \kappa\lambda_1 \\
=&\frac{D\gamma_2^2}{2\left(\gamma_2^2 + 2\gamma_2 + \lambda_2^2\right)} - \kappa\lambda_1\,,
\end{aligned}$$

since the minimum in the first term is realised when the two arguments are equal, fixing $\varepsilon_1 = 2D\gamma_2/\left(\gamma_2^2 + 2\gamma_2 + \lambda_2^2\right)$. Note that this choice of ε_1 satisfies $\varepsilon_1 < D$ and $\varepsilon_1 < 1$. Choosing κ small

enough ensures $\xi(\kappa) > 0$. From this analysis we conclude

$$\mathsf{D}_0[f] + \mathsf{D}_1[f] \leqslant -2\xi(\kappa)\|f\|_0^2 + \varepsilon_1\gamma_2 M_f^2 \,. \tag{2.16}$$

Let us now add the control of $\mathsf{D}_2 + \mathsf{D}_3$. If $\nabla_x V$ is bounded, $g \equiv 0$ and $\mathsf{D}_3 = 0$:

$$\begin{aligned}\frac{\mathrm{d}}{\mathrm{d}t}\mathsf{G}[f] &= \mathsf{D}_0[f] + \mathsf{D}_1[f] + \mathsf{D}_2[f] \\ &\leqslant -\left(4\xi(\kappa) - \kappa\|\nabla_x V\|_\infty\right)\frac{1}{2}\|f\|_\kappa^2 + \varepsilon_1\gamma_2 M_f^2 \\ &\leqslant -\gamma_1 \mathsf{G}[f] + \varepsilon_1\gamma_2 M_f^2\end{aligned}$$

by the norm equivalence (2.9). Here, we defined

$$\gamma_1 := \frac{4\xi(\kappa) - \kappa\|\nabla_x V\|_\infty}{1+\varepsilon_1} > 0\,.$$

When $\nabla_x V$ is unbounded, (2.13)-(2.14)-(2.15)-(2.16) imply

$$\begin{aligned}\frac{\mathrm{d}}{\mathrm{d}t}\mathsf{G}[f] =& \mathsf{D}_0[f] + \mathsf{D}_1[f] + \mathsf{D}_2[f] + \mathsf{D}_3[f] \\ \leqslant& -2\xi(\kappa)\|f\|_0^2 + \varepsilon_1\gamma_2 M_f^2 + \frac{\kappa}{2}C_3\int_{\mathbb{R}^2\times\mathbb{S}^1} f^2 g\,\frac{\mathrm{d}x\,\mathrm{d}\alpha}{2\pi} \\ &+ \frac{\kappa\zeta}{2}\left(C_4(R)\|f\|_0^2 - c\int_{\mathbb{R}^2\times\mathbb{S}^1} f^2 g\,\frac{\mathrm{d}x\,\mathrm{d}\alpha}{2\pi}\right) \\ =& -\frac{1}{2}\left(4\xi(\kappa) - \kappa\zeta C_4(R)\right)\|f\|_0^2 - \frac{\kappa\zeta}{2}\left(c - \frac{C_3}{\zeta}\right)\int_{\mathbb{R}^2\times\mathbb{S}^1} f^2 g\,\frac{\mathrm{d}x\,\mathrm{d}\alpha}{2\pi} + \varepsilon_1\gamma_2 M_f^2 \\ \leqslant& -\frac{1}{2}\min\left\{4\xi(\kappa) - \kappa\zeta C_4(R), c - \frac{C_3}{\zeta}\right\}\|f\|_\kappa^2 + \varepsilon_1\gamma_2 M_f^2 \\ \leqslant& -\gamma_1\,\mathsf{G}[f] + \varepsilon_1\gamma_2 M_f^2\end{aligned}$$

again by norm equivalence (2.9), and where we defined

$$\gamma_1 := \frac{1}{1+\varepsilon_1}\min\left\{4\xi(\kappa) - \kappa\zeta C_4(R), c - \frac{C_3}{\zeta}\right\} > 0\,.$$

This requires $\zeta > 0$ to be large enough, and the upper bound for κ should be chosen accordingly:

$$\zeta > \frac{C_3}{c}\,, \qquad 4\xi(\kappa) - \kappa\zeta C_4(R) > 0\,.$$

In order to maximise the rate of convergence to equilibrium given κ, D and V, one can optimise γ_1 over ζ whilst respecting the above constraints.

Remark 2.4. *The condition $\gamma_1 > 0$ translates into an explicit upper bound on κ. More precisely, we require $\xi(\kappa) > \kappa u/4$ where $u := \|\nabla_x V\|_\infty$ in the case of a bounded potential gradient, and $u := \zeta C_4(R)$ otherwise. This condition is satisfied for small enough κ:*

$$0 \leqslant \kappa < \frac{\varepsilon_1\gamma_2}{(4\lambda_1 + u)} = \frac{2D\gamma_2^2}{(4\lambda_1+u)(\gamma_2^2 + 2\gamma_2 + \lambda_2^2)}$$

which also implies $\xi(\kappa) > 0$. Recall that Proposition 1.3 requires $\kappa < 1/3$ in the case of unbounded potential gradients. These conditions provide a range of κ for which Proposition 2.1 holds.

3 The coercivity weight g

In this section, we define the function g in such a way that it allows us to control the loss of weight in the perturbation operator P_κ. When $\nabla_x V$ is bounded, we do not need any extra weight since then we may control the perturbation thanks to the stationary weight e^V, and so we set $g \equiv 0$ in that case. When it is not, Proposition 1.3 provides a suitable weight function g by constructive methods.

3.1 Proof of Proposition 1.3

The proof is strongly inspired from [206], however our weight is different since we work in an L^2-framework rather than in an L^1 one. Assuming $\nabla_x V$ is unbounded, we seek a weight g of the form

$$g(x,\alpha) = \exp\left(\beta V(x) + |\nabla_x V(x)|\Gamma\left(\tau(\alpha)\cdot\frac{\nabla_x V(x)}{|\nabla_x V(x)|}\right)\right),$$

where the parameter $\beta > 1$ and the function $\Gamma \in C^1([-1,1])$, $\Gamma > 0$ are to be determined. We define

$$Y(x,\alpha) := \tau(\alpha)\cdot\frac{\nabla_x V(x)}{|\nabla_x V(x)|}, \qquad Y^\perp(x,\alpha) := \tau^\perp(\alpha)\cdot\frac{\nabla_x V(x)}{|\nabla_x V(x)|},$$

and split the proof into four steps: 1) we rewrite statement (1.6) using the explicit expression of the weight g, 2) we simplify the obtained expression using assumption **(H5)**, 3) we prove the equivalent statement obtained in Step 2 by defining a suitable choice of $\Gamma(\cdot)$ and β, and 4) we demonstrate that it is indeed possible to choose suitable parameters for the calculations in Step 3 to hold, fixing explicit expressions where possible.

 # Step 1: Rewriting the weight estimate (1.6).

Applying the operator $\mathcal{L}_\kappa$ defined in (1.7) to g, we can compute explicitly

$$\begin{aligned}\frac{\mathcal{L}_\kappa(g)}{g} =& D\left(|\nabla_x V|\partial_{\alpha\alpha}\Gamma(Y) + |\nabla_x V|^2|\partial_\alpha\Gamma(Y)|^2\right)\\ &+ (\tau(\alpha)+\kappa e_1)\cdot\left(\beta\nabla_x V + \nabla_x\left(|\nabla_x V|\Gamma(Y)\right)\right)\\ &- |\nabla_x V|^2 Y^\perp\partial_\alpha\Gamma(Y) - |\nabla_x V| Y\,.\end{aligned}$$

Since

$$\partial_\alpha\Gamma = Y^\perp\Gamma'(Y) \quad\text{and}\quad \partial_{\alpha\alpha}\Gamma = \partial_\alpha\left(Y^\perp\Gamma'(Y)\right) = -Y\Gamma'(Y) + |Y^\perp|^2\Gamma''(Y),$$

we get

$$\begin{aligned}\frac{\mathcal{L}_\kappa(g)}{g} =& D\left(|\nabla_x V|\left(-Y\Gamma'(Y)+|Y^\perp|^2\Gamma''(Y)\right)+|\nabla_x V|^2|Y^\perp|^2\left(\Gamma'(Y)\right)^2\right)\\ &+(\tau(\alpha)+\kappa e_1)\cdot(\beta\nabla_x V+\nabla_x(|\nabla_x V|\Gamma(Y)))\\ &-|\nabla_x V|^2|Y^\perp|^2\Gamma'(Y)-|\nabla_x V|Y\\ =&(\beta-1-D\Gamma'(Y))|\nabla_x V|Y+\kappa\beta e_1\cdot\nabla_x V+(\tau(\alpha)+\kappa e_1)\cdot\nabla_x(|\nabla_x V|\Gamma(Y))\\ &+|Y^\perp|^2\left(D|\nabla_x V|\Gamma''(Y)+|\nabla_x V|^2\left[D\left(\Gamma'(Y)\right)^2-\Gamma'(Y)\right]\right).\end{aligned}$$

In order to see which Γ to choose, let us divide by $|\nabla_x V|$ and denote the diffusion and transport part by

$$\mathrm{diff}(x,\alpha):=(\tau(\alpha)+\kappa e_1)\cdot\frac{\nabla_x(|\nabla_x V|\Gamma(Y))}{|\nabla_x V|}\,,\qquad \mathrm{tran}(x):=\frac{e_1\cdot\nabla_x V}{|\nabla_x V|}\,.$$

Now, we can rewrite the statement of Proposition 1.3: we seek a positive constant $c>0$ and a radius $R>0$ such that for any $\alpha\in\mathbb{S}^1$ and $|x|>R$,

$$\begin{aligned}&(\beta-1-D\Gamma'(Y))Y+\kappa\beta\mathrm{tran}(x)+\mathrm{diff}(x,\alpha)\\ &\qquad+|Y^\perp|^2\left(D\Gamma''(Y)+|\nabla_x V|\left[D\left(\Gamma'(Y)\right)^2-\Gamma'(Y)\right]\right)\leqslant -c\,.\end{aligned}$$

To achieve this bound, note that $|Y|\leqslant 1$ and $|\mathrm{tran}|\leqslant 1$ for all $(x,\alpha)\in\mathbb{R}^2\times\mathbb{S}^1$.

 # Step 2: Simplifying the weight estimate.

Further, the diffusion term $\mathrm{diff}(\cdot)$ can be made arbitrarily small outside a sufficiently large ball. Indeed,

$$\mathrm{diff}(x,\alpha)=(\tau+\kappa e_1)\cdot\left[\Gamma'(Y)\,\nabla_x Y+\Gamma(Y)\,\frac{\nabla_x(|\nabla_x V|)}{|\nabla_x V|}\right],$$

and both $|\nabla_x Y|$ and $|\nabla_x(|\nabla_x V|)|/|\nabla_x V|$ converge to zero as $|x|\to\infty$ by assumption **(H5)**, and Γ is bounded. In other words, using the fact that the potential gradient is unbounded, it remains to show that we can find constants $\gamma>\kappa\beta>0$ and a radius $r_1>0$ such that

$$\forall|x|>r_1,\quad(\beta-1-D\Gamma')Y+|Y^\perp|^2\left(D\Gamma''+|\nabla_x V|\left[D\left(\Gamma'\right)^2-\Gamma'\right]\right)\leqslant-\gamma\,.\tag{3.17}$$

Then we can choose $r_2>0$ such that

$$|x|>r_2\quad\Longrightarrow\quad\forall\alpha\in\mathbb{S}^1,\quad\mathrm{diff}(x,\alpha)\leqslant\frac{\gamma-\kappa\beta}{2}\,,$$

and we conclude for the statement of Proposition 1.3 with $R:=\max\{r_1,r_2\}$ and $c:=(\gamma-\kappa\beta)/2>0$.

 # Step 3: Proof of the weight estimate.

Proving (3.17) can be done by an explicit construction. We define $\Gamma'\in C^0([-1,1])$ piecewise,

$$\Gamma'(Y) = \begin{cases} \delta^+ & \text{if } Y > \varepsilon_0\,, \\ \frac{\delta^+ - \delta^-}{2\varepsilon_0}\,(Y + \varepsilon_0) + \delta^- & \text{if } |Y| \leqslant \varepsilon_0\,, \\ \delta^- & \text{if } Y < -\varepsilon_0\,, \end{cases}$$

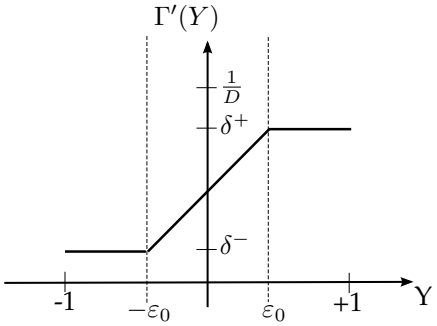

Figure 5.1: Derivative of Γ

where $0 < \delta^- < \delta^+ < 1/D$ and $\varepsilon_0 \in (0,1)$ are to be determined. With this choice of Γ', we can ensure that Γ is strictly positive in the interval $[-1,1]$. Now, let us show that there exist suitable choices of γ and β for the bound (3.17) to hold. More precisely, we choose a suitable β such that $(\beta-1)/D \in (\delta^-, \delta^+)$ and $0 < \gamma < \tilde{\gamma}$, defining $\gamma := \varepsilon_0\,(1 + D\delta^+ - \beta)$ and $\tilde{\gamma} := \varepsilon_0\,(\beta - 1 - D\delta^-)$. We split our analysis into cases:

- Assume $Y > \varepsilon_0$. Then the LHS of (3.17) can be bounded as follows:

$$(\beta - 1 - D\delta^+)Y + \delta^+\left(D\delta^+ - 1\right)|\nabla_x V||Y^\perp|^2 < (\beta - 1 - D\delta^+)\varepsilon_0 = -\gamma\,.$$

- Assume $Y < -\varepsilon_0$. Then the LHS of (3.17) can be bounded as follows:

$$(\beta - 1 - D\delta^-)Y + \delta^-\left(D\delta^- - 1\right)|\nabla_x V||Y^\perp|^2 < -(\beta - 1 - D\delta^-)\varepsilon_0 = -\tilde{\gamma}\,.$$

- Assume $|Y| \leqslant \varepsilon_0$. Since $1 = |Y|^2 + |Y^\perp|^2$, we have $|Y^\perp|^2 \geqslant 1 - \varepsilon_0^2$. Further, setting

$$h = aY + b \in (\delta^-, \delta^+)\,, \quad a := \frac{\delta^+ - \delta^-}{2\varepsilon_0}\,, \quad b := \frac{\delta^+ + \delta^-}{2}\,,$$

  we have $\Gamma' = h$ and $Dh^2 - h \leqslant D\delta^-(\delta^+ - 1/D)$. Now, using the fact that the potential gradient is unbounded, we can find a radius $r_1 > 0$ large enough such that for all $|x| > r_1$,

$$\frac{D(\delta^+ - \delta^-)}{2\varepsilon_0} - D\delta^-\left(\frac{1}{D} - \delta^+\right)|\nabla_x V| < -\frac{2\tilde{\gamma}}{(1-\varepsilon_0^2)}\,.$$

  Putting these estimates together, we obtain for $|x| > r_1$:

$$\begin{aligned} &(\beta - 1 - Dh)Y + |Y^\perp|^2\left(\frac{D(\delta^+ - \delta^-)}{2\varepsilon_0} + |\nabla_x V|\left[Dh^2 - h\right]\right) \\ &\leqslant (\beta - 1 - D\delta^-)\varepsilon_0 + |Y^\perp|^2\left(\frac{D(\delta^+ - \delta^-)}{2\varepsilon_0} + |\nabla_x V|\left[D\delta^-\left(\delta^+ - \frac{1}{D}\right)\right]\right) \\ &\leqslant \tilde{\gamma} + (1-\varepsilon_0^2)\left(\frac{D(\delta^+ - \delta^-)}{2\varepsilon_0} + |\nabla_x V|\left[D\delta^-\left(\delta^+ - \frac{1}{D}\right)\right]\right) \leqslant -\tilde{\gamma}\,. \end{aligned}$$

 # Step 4: Choice of parameters.

We now come back to the choice of $\delta^-, \delta^+, \varepsilon_0, \beta$ such that $\kappa\beta < \gamma$ and $0 < \gamma < \tilde{\gamma}$ hold true. More precisely, these two constraints translate into the following bound on β:

$$1 + D\left(\frac{\delta^+ + \delta^-}{2}\right) < \beta < \left(\frac{\varepsilon_0}{\kappa + \varepsilon_0}\right)\left(1 + D\delta^+\right) . \tag{3.18}$$

It is easy to see that this bound also implies $1 + D\delta^- < \beta < 1 + D\delta^+$ as required. However, for this to be possible we need to choose ε_0 such that $LHS < RHS$, in other words,

$$\kappa\left(\frac{2 + D\left(\delta^+ + \delta^-\right)}{D\left(\delta^+ - \delta^-\right)}\right) < \varepsilon_0 . \tag{3.19}$$

Since ε_0 has to be less than 1 and $D(\delta^+ - \delta^-)/(2 + D\left(\delta^+ + \delta^-\right)) < 1/3$, this bound is only possible if $\kappa \in (0, 1/3)$; then it remains to choose $0 < \delta^- < \delta^+ < 1/D$ such that

$$\kappa < \frac{D\left(\delta^+ - \delta^-\right)}{2 + D\left(\delta^+ + \delta^-\right)} \in \left(0, \frac{1}{3}\right) . \tag{3.20}$$

To satisfy all these constraints, we make the choice of parameters (for $\kappa < 1/3$):

$$\delta^+ := \frac{3(1+\kappa)}{4D}, \qquad \delta^- := \frac{(1-3\kappa)}{4D} .$$

Then (3.20) holds true, and we can fix $\varepsilon_0 \in (0, 1)$ to satisfy (3.19):

$$\varepsilon_0 := \frac{1}{2}\left(1 + \kappa\left(\frac{2 + D\left(\delta^+ + \delta^-\right)}{D\left(\delta^+ - \delta^-\right)}\right)\right) = \frac{1}{2}\left(\frac{1+9\kappa}{1+3\kappa}\right) .$$

Finally, we choose β satisfying (3.18) as follows:

$$\begin{aligned}\beta &:= \frac{1}{2}\left[1 + D\left(\frac{\delta^+ + \delta^-}{2}\right) + \left(\frac{\varepsilon_0}{\kappa + \varepsilon_0}\right)\left(1 + D\delta^+\right)\right] \\ &= \frac{3}{4} + \frac{(1+9\kappa)(7+3\kappa)}{8(6\kappa^2 + 11\kappa + 1)} \in (1, 2) .\end{aligned}$$

4 Existence and uniqueness of a steady state

4.1 Existence of a $\mathcal{C}_0$-semigroup

Proving existence of solutions to the perturbed equation (1.2) relies on the a priori estimates from Section 2:

Theorem 4.1. *The linear operator $\mathsf{L}_\kappa : \mathcal{D}(\mathsf{L}_\kappa) \to L^2(\mathrm{d}\mu_\kappa)$ defined in (1.5) is the infinitesimal generator of a $\mathcal{C}_0$-semigroup $(S_t)_{t\geqslant 0}$ on $L^2(\mathrm{d}\mu_\kappa)$.*

Proof. Let us denote by L_κ^* the adjoint of L_κ in $L^2(\mathrm{d}\mu_\kappa)$. Both domains $\mathcal{D}\left(\mathsf{L}_\kappa\right)$ and $\mathcal{D}\left(\mathsf{L}_\kappa^*\right)$ contain the core $\mathcal{C}$ and are dense. The operator L_κ is closable in $L^2(\mathrm{d}\mu_\kappa)$. To see this, take a sequence

$(f_n)_{n\in\mathbb{N}} \in \mathcal{D}(\mathsf{L}_\kappa)$ converging to zero in $L^2(\mathrm{d}\mu_\kappa)$ such that the sequence $(\mathsf{L}_\kappa f_n)_{n\in\mathbb{N}}$ converges to some limit $h \in L^2(\mathrm{d}\mu_\kappa)$. Then for any test function $\varphi \in \mathcal{C}$,

$$\left\langle \varphi \,,\, \mathsf{L}_\kappa f_n \right\rangle_\kappa = \left\langle \mathsf{L}_\kappa^* \varphi \,,\, f_n \right\rangle_\kappa \to 0 \qquad \text{as } n \to \infty \,.$$

Since the left-hand side converges to $\left\langle \varphi \,,\, h \right\rangle_\kappa$ for all $\varphi \in \mathcal{C}$, we conclude $h \equiv 0$ a.e., and so L_κ is closable. Similarly, L_κ^* is closable. We denote by $\tilde{\mathsf{L}}_\kappa$ and $\tilde{\mathsf{L}}_\kappa^*$ some closed extensions of L_κ and L_κ^*, respectively. Lumer-Phillips Theorem in the form [254, Corollary 4.4] states that an operator $\tilde{\mathsf{L}}$ generates a $\mathcal{C}_0$-semigroup if $\tilde{\mathsf{L}}$ is closed and both $\tilde{\mathsf{L}}$ and $\tilde{\mathsf{L}}^*$ are dissipative. Since the core $\mathcal{C}$ is dense in both $\mathcal{D}(\tilde{\mathsf{Q}}_\kappa)$ and $\mathcal{D}(\tilde{\mathsf{Q}}_\kappa^*)$, which in turn are both dense in $L^2(\mathrm{d}\mu_\kappa)$, then for any constant $C > 0$, $\tilde{\mathsf{L}}_\kappa - C\mathsf{Id}$ is dissipative if and only if $\tilde{\mathsf{L}}_\kappa^* - C\mathsf{Id}$ is dissipative. Therefore, it remains to show that $\tilde{\mathsf{L}}_\kappa - C\mathsf{Id}$ is dissipative for some $C > 0$. Since the restriction of $\tilde{\mathsf{L}}_\kappa$ to $\mathcal{C}$ is L_κ, it is enough to prove that $\mathsf{L}_\kappa - C\mathsf{Id}$ is dissipative on $\mathcal{C}$ for some constant $C > 0$. The estimates in Section 2 show that there exists $C > 0$ s.t.

$$\forall f \in \mathcal{C}, \qquad \left\langle \mathsf{L}_\kappa f \,,\, f \right\rangle_\kappa \leqslant C \|f\|_\kappa^2$$

for some explicit constant $C > 0$, which concludes the proof. □

4.2 Proof of Theorem 1.4

Proposition 2.1 is the key ingredient to deduce existence of a unique steady state. The set

$$\mathcal{B} := \left\{ f \in L^2(\mathrm{d}\mu_\kappa) \,:\, \mathsf{G}[f] \leqslant \frac{\gamma_2}{\gamma_1},\, f \geqslant 0,\, M_f = 1 \right\}$$

is convex and bounded in $L^2(\mathrm{d}\mu_\kappa)$ by the norm equivalence (2.9). By Theorem 4.1, the operator L_κ generates a $\mathcal{C}_0$-semigroup $(S_t)_{t\geqslant 0}$. Then let us show that $\mathcal{B}$ is invariant under the action of $(S_t)_{t\geqslant 0}$. Integrating in time the hypocoercivity estimate (2.10) in Proposition 2.1 for any $f_{\mathrm{in}} \in L^2(\mathrm{d}\mu_\kappa)$ with mass 1, we obtain the bound

$$\mathsf{G}[f(t)] \leqslant \mathsf{G}[f_{\mathrm{in}}] e^{-\gamma_1 t} + \frac{\gamma_2}{\gamma_1} \left(1 - e^{-\gamma_1 t}\right) \,,$$

and thus

$$\forall\, t > 0, \qquad \mathsf{G}[f(t)] \leqslant \max\left\{ \mathsf{G}[f_{\mathrm{in}}], \frac{\gamma_2}{\gamma_1} \right\}.$$

Since in addition, $(S_t)_{t\geqslant 0}$ conserves mass and positivity, we conclude $S_t(\mathcal{B}) \subset \mathcal{B}$ for all times.

Integrate again the hypocoercivity estimate (2.10) in Proposition 2.1, now for the difference of two solutions with same mass, to get

$$\mathsf{G}[S_t f - S_t h] \leqslant e^{-\gamma_1 t} \mathsf{G}[f - h]$$

for any $t > 0$ and $f, h \in \mathcal{B}$. It follows by Banach's fixed-point theorem that there exists a unique $u^t \in \mathcal{B}$ such that $S_t(u^t) = u^t$ for each $t > 0$. Let $t_n := 2^{-n}$, $n \in \mathbb{N}$, and $u_n := u^{t_n}$. Then $S_{2^{-n}}(u_n) =$

u_n, and by repeatedly applying the semigroup property,

$$\forall\, k \in \mathbb{N},\ \forall\, m \leqslant n \in \mathbb{N}, \quad S_{k2^{-m}}(u_n) = u_n\,. \tag{4.21}$$

Let us prove that $\mathcal{B}$ is weakly compact in $L^2(\mathrm{d}\mu_\kappa)$. Consider a sequence $(f_n)_{n\in\mathbb{N}} \in \mathcal{B}$. It has a cluster point f for the weak convergence since $\mathcal{B}$ is bounded in $L^2(\mathrm{d}\mu_\kappa)$, and the corresponding subsequence is still denoted f_n for simplicity. By lower semi-continuity of the equivalent norm G:

$$\mathsf{G}[f] \leqslant \liminf_{n\to\infty} \mathsf{G}[f_n] \leqslant \gamma_2/\gamma_1\,.$$

Further, since $f_n \geqslant 0$ for all $n \in \mathbb{N}$, it follows that $f \geqslant 0$ (the set of non-negative functions is a strongly closed convex set, hence weakly closed). It remains to show that the limit f has mass 1 by preventing loss of mass at infinity. Use Cauchy-Schwarz's inequality and the norm equivalence (2.9) to get for $r > 0$

$$\begin{aligned}
(1+\kappa\zeta)\left(\int_{|x|>r} \Pi f_n\, dx\right)^2 &\leqslant \left(\int_{|x|>r}\int_{\mathbb{S}^1} f_n^2\, e^V\, \frac{\mathrm{d}x\mathrm{d}\alpha}{2\pi}\right)\left(\int_{|x|>r}\int_{\mathbb{S}^1} e^{-V}\, \frac{\mathrm{d}x\mathrm{d}\alpha}{2\pi}\right)\\
&\quad + \kappa\zeta\left(\int_{|x|>r}\int_{\mathbb{S}^1} f_n^2\, g\frac{\mathrm{d}x\mathrm{d}\alpha}{2\pi}\right)\left(\int_{|x|>r}\int_{\mathbb{S}^1} g^{-1}\, \frac{\mathrm{d}x\mathrm{d}\alpha}{2\pi}\right)\\
&\leqslant \|f_n\|_\kappa^2 \left(\int_{|x|>r}\int_{\mathbb{S}^1} \left(e^{-V}+g^{-1}\right)\, \frac{\mathrm{d}x\mathrm{d}\alpha}{2\pi}\right)\\
&\leqslant \left(\frac{2}{1-\varepsilon_1}\right)\frac{\gamma_2}{\gamma_1}\left(\int_{|x|>r}\int_{\mathbb{S}^1} 2e^{-V}\, \frac{\mathrm{d}x\mathrm{d}\alpha}{2\pi}\right)\,.
\end{aligned}$$

This shows that

$$\begin{aligned}
&\sup_{n\in\mathbb{N}}\left(\int_{|x|>r} \Pi f_n\, dx\right)\\
&\quad\leqslant \left(\left(\frac{4}{(1-\varepsilon_1)(1+\kappa\zeta)}\right)\left(\frac{\gamma_2}{\gamma_1}\right)\right)^{1/2}\left(\int_{|x|>r}\int_{\mathbb{S}^1} e^{-V}\, \frac{\mathrm{d}x\mathrm{d}\alpha}{2\pi}\right)^{1/2} \to 0 \quad \text{as } r\to\infty\,,
\end{aligned}$$

since $\int_{\mathbb{R}^2\times\mathbb{S}^1} e^{-V}\,\frac{\mathrm{d}x\mathrm{d}\alpha}{2\pi} = 1$. Together with $M_{f_n} = 1$ for all $n \in \mathbb{N}$, it follows that $M_f = 1$. Hence $f \in \mathcal{B}$. The weak compactness of $\mathcal{B}$ implies the existence of a subsequence u_{n_j} of u_n and a function $u \in \mathcal{B}$ such that u_{n_j} converges weakly to u in $L^2(\mathrm{d}\mu_\kappa)$. Letting $n_j \to \infty$ in (4.21) implies that (since S_t is a continuous operator)

$$\forall\, m \in \mathbb{N},\ \forall\, k \in \mathbb{N}, \quad S_{k2^{-m}}(u) = u\,.$$

Finally the density of the dyadic rationals $\{k2^{-m} : k \in \mathbb{N}, m \in \mathbb{N}\}$ in $(0,+\infty)$ and continuity of $S_t(u)$ in t for all $u \in \mathcal{B}$ imply that

$$\forall\, t \geqslant 0, \quad S_t(u) = u\,.$$

This shows the existence and uniqueness of a global stationary state $F_\kappa := u \in \mathcal{B}$.

To complete the proof of Theorem 1.4, we apply the hypocoercivity estimate Proposition 2.1 to the difference between a solution $f \in L^2(\mathrm{d}\mu_\kappa)$ and the unique stationary state of the same mass, $M_f F_\kappa$, to show exponential convergence to equilibrium in $\|\cdot\|_\kappa$: first of all, we deduce from the contraction estimate (2.10) that

$$\mathsf{G}[f(t) - M_f F_\kappa] \leqslant \mathsf{G}[f_{\mathrm{in}} - M_f F_\kappa]\, e^{-\gamma_1 t}\,,$$

which allows then to estimate the difference to equilibrium in the $L^2(\mathrm{d}\mu_\kappa)$-norm. Indeed, by norm equivalence, we obtain

$$\|f(t) - M_f F_\kappa\|_\kappa^2 \leqslant \frac{1+\varepsilon_1}{1-\varepsilon_1}\|f_{\mathrm{in}} - M_f F_\kappa\|_\kappa^2\, e^{-\gamma_1 t}\,.$$

Hence, we obtain (1.8) with rate of convergence $\lambda_\kappa := \gamma_1/2$.

Remark 4.2. *From our previous estimates, we have that $\mathsf{G}(F_k)$ is uniformly bounded in κ for κ sufficiently small. As a consequence, $(F_\kappa)_{\kappa>0}$ is a relatively weakly compact family in $L^2(\mathrm{d}\mu_\kappa)$, and by uniqueness of the stationary state in the case $\kappa = 0$, we deduce that $F_\kappa \to F_0$ as $\kappa \to 0$. It could also be proved with further work that the optimal (spectral gap) relaxation rate is continuous as $\kappa \to 0$.*

Part III

Scaling Approaches for Social Dynamics

Thinking Fluids

Do you remember the last time you saw birds in the sky?
Thousands of birds, moving in coordinated patterns?
Often, each bird can only see the birds right next to it,
and yet they manage to create an emerging collective behaviour.
How do they do it?
What if we consider that each bird is reacting according to 3 simple rules:

1. Repulsion – they don't want to be too close to each other,
2. Attraction – they don't want to loose the group,
3. Alignment – they want to go in the same direction as their neighbours.

If we put these 3 simple rules into a mathematical model,
we can recreate the same patterns that we observe in nature.

Now, why should we care about birds?
In fact, what matters is
how we can predict the behaviour of a large group of individuals
by knowing only how each one of them reacts to its neighbours.
Imagine zooming out and looking at many many birds from far away,
it looks like a continuous fluid.
Mathematically,
this can be described by a partial differential equation,
or PDE.
PDEs encode the physical laws about how a quantity changes with
time, position and velocity.
Often, these models are so complicated,
that there is no hope of finding explicit solutions.
However, sometimes,
we are able to read the important properties from the model itself.
My research is about proving these properties
and trying to explain the longterm behaviour of solutions
without knowing these solutions explicitly.
The exact same PDE that models the behaviour of birds
can also model many other organisms
from schools of fish, to colonies of bacteria.

But what about us humans?
You would think that
human communication is far too complicated
to be reduced into function,
right?
Well, actually, in certain situations,
people react instinctively,
and we can use the same type of PDE
to model the motion of pedestrian crowds.
A famous example of dangerous overcrowding
is the Jamarat Bridge in Saudi-Arabia,
where hundreds died during pilgramage.
We can model these disasters
by treating the crowd as a THINKING FLUID,
just like birds, fish or bacteria.
This will allow us to make predictions for panic situations
such as earthquakes and fire escapes,
and hopefully it will help us
to prevent crowd disasters in the future.

What is so fascinating
is that all these different applications
are just special cases of the same class of PDEs.
If we understand more about the general structure of these models,
we will have added a timeless piece of wisdom
to our understanding of the world.

Text for 3-Minute-Thesis Competition
by Franca Hoffmann
Imperial College London, April 2016

Chapter 6

Non-local models for self-organised animal aggregation

This chapter follows in most parts the article "Non-local kinetic and macroscopic models for self-organised animal aggregations" written in collaboration with José A. Carrillo[1] and Raluca Eftimie[2], and published in *Kinetic and Related Models* **8** (2015), no. 3, 413 - 441. Section 2.2 was contributed by Raluca Eftimie and Section 3.2 was contributed by José A. Carrillo. Some of the results presented in this chapter were already part of my master thesis, namely: (1) a special case of the parabolic scaling for the kinetic 1D model (2.1) under assumption (2.14) with $\lambda_1 = 0$ (Remark 2.2), (2) the parabolic drift-diffusion limit of the 2D kinetic model (3.18) with $\lambda_1 = 0$ (Section 3.1), and (3) a theoretical development of the AP scheme (Section 4) for the 1D kinetic model (2.1) under scaling assumption (2.14) with $\lambda_1 = 0$. These parts have been included here to allow for a comprehensive and self-contained presentation of the chapter.

Chapter Summary

The last two decades have seen a surge in kinetic and macroscopic models derived to investigate the multi-scale aspects of self-organised biological aggregations. Because the individual-level details incorporated into the kinetic models (e.g., individual speeds and turning rates) make them somewhat difficult to investigate, one is interested in transforming these models into simpler macroscopic models, by using various scaling techniques that are imposed by the biological context. However, not many studies investigate how the dynamics of the initial models are preserved via these scalings. Here, we consider two scaling approaches (parabolic and grazing collision limits) that can be used to reduce a class of non-local 1D and 2D models for biological aggregations to simpler models existent in the literature. Then, we investigate how some of the spatio-temporal patterns exhibited by the original kinetic models are preserved via

[1]Department of Mathematics, Imperial College London, South Kensington Campus, London SW7 2AZ, UK.
[2]Division of Mathematics, University of Dundee, Dundee, UK.

these scalings. To this end, we focus on the parabolic scaling for non-local 1D models and apply asymptotic preserving numerical methods, which allow us to analyse changes in the patterns as the scaling coefficient ϵ is varied from $\epsilon = 1$ (for 1D transport models) to $\epsilon = 0$ (for 1D parabolic models). We show that some patterns (describing stationary aggregations) are preserved in the limit $\epsilon \to 0$, while other patterns (describing moving aggregations) are lost. To understand the loss of these patterns, we construct bifurcation diagrams.

Chapter Content

Milima haikutani,
lakini binadamu hukutana.

Mountains don't meet,
but human beings do[3].

Kiswahili Proverb

[3] Do not say that you will never meet somebody.

1 Introduction

Over the past 10-20 years a multitude of kinetic and macroscopic models have been introduced to investigate the formation and movement of various biological aggregations: from cells [22, 5] and bacteria [257] to flocks of birds, schools of fish and even human aggregations (see, for example, [290, 83, 251, 86, 124, 27, 112] and the references therein). The use of kinetic or macroscopic approaches is generally dictated by the problem under investigation: (i) kinetic (transport) models focus on changes in the density distribution of individuals that have a certain spatial position, speed and movement direction (or are in some activity state [24]); (ii) macroscopic models focus on changes in the averaged total density of individuals [87, 144].

Generally, these kinetic and macroscopic models assume that individuals, particles, or cells can organise themselves in the absence of a leader. The factors that lead to the formation of self-organised aggregations are the interactions among individuals as a result of various social forces: repulsion from nearby neighbours, attraction to far-away neighbours (or to roosting areas [93]) and alignment/orientation with neighbours positioned at intermediate distances. These interaction forces are usually assumed to act on different spatial ranges, depending on the communication mechanisms used by individuals; e.g., via acoustic long-range signals, or via chemical/visual short-range signals. The non-locality of the attractive and alignment/orientation interactions is supported by radar tracking observations of flocks of migratory birds, which can move with the same speed and in the same direction despite the fact that individuals are 200-300 meters apart from each other [209]. For the repulsive forces some models consider non-local effects generated by decaying interactions with neighbours positioned further and further away [146], while other models consider only local effects [282]. In the case of continuous mesoscopic and macroscopic models, the non-local interactions are modelled by interaction kernels (see Figure 6.1 for 2D and 1D kernels). The most common choices for these kernels are Morse potential-type kernels [87, 83, 86, 91] (see Figure 6.1(b)) and Gaussian kernels [147, 146, 144, 237] (see Figure 6.1(c)).

Due to their complex structure, kinetic models are difficult to investigate. Although progress has been made in recent years, mainly regarding the existence and stability of various types of solutions and the analytic asymptotic methods that allow transitions from kinetic (mesoscopic) to macroscopic models (see, for example, [189, 190, 23, 83, 59, 124, 123, 42, 28, 179] and the references therein), it is still difficult to study analytically and numerically the spatial and spatio-temporal aggregation patterns exhibited by the kinetic models. For example, there are very few studies that investigate the types of spatio-temporal patterns obtained with 2D and 3D kinetic models (see the review in [144]). Moreover, the presence of non-local interaction terms increases the complexity of the models, leading to a larger variety of patterns that are more difficult to analyse. While

numerical and analytical studies have been conducted to investigate the patterns in 1D non-local models [146, 145, 56], such an investigation is still difficult in the 2D non-local case (see [153]).

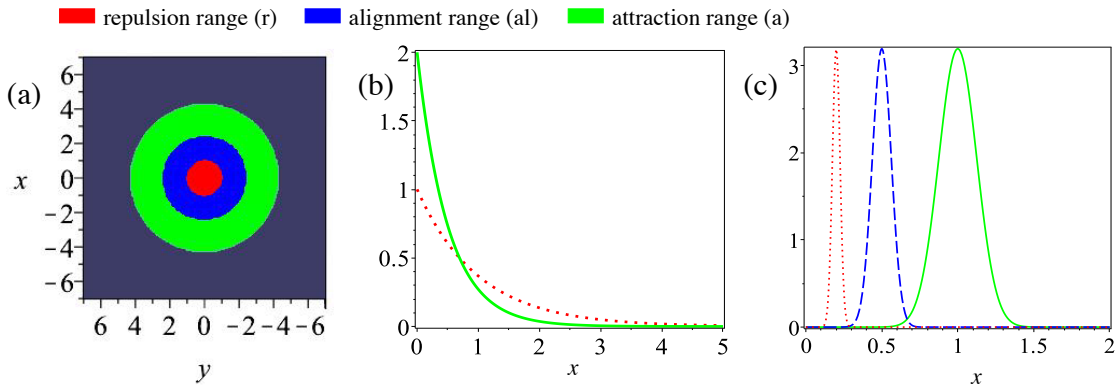

Figure 6.1: 2D and 1D spatial kernels for social interactions. (a) 2D: Attractive (K_a), repulsive (K_r) and alignment (K_{al}) kernels described by equation (3.21); (b) 1D: Morse-type kernels: $K_{r,a}(x) = e^{-|x|/s_{r,a}}$. (c) 1D: Translated Gaussian kernels K_j as defined in (2.3) with $j = r, al, a$.

The first goal of this chapter is to start with a class of 1D and 2D non-local kinetic models for self-organised aggregations that incorporate all three social interactions, and to show, through different parabolic scaling approaches, that these models can be reduced to known non-local parabolic models for swarming; see Figure 6.2 for a diagram illustrating this approach. For the 1D case, similar analytical scalings have been done in the context of bacterial chemotaxis [265] and for the kinetic model (2.1) for individuals moving along a line [143].

The next aim is to investigate the numerical preservation of patterns between the mesoscopic and macroscopic scales. We use asymptotic preserving numerical methods [201, 202, 88, 102], to obtain a better understanding of what happens with the 1D patterns via the parabolic scaling. With the help of these methods, we investigate numerically the preservation of stationary aggregations (that arise via steady-state bifurcations) and moving aggregations (that arise via Hopf bifurcations), as the scaling parameter ε is varied from large positive values ($\varepsilon = 1$) corresponding to the kinetic models to zero values corresponding to the limiting parabolic models. To visualise the transitions between different patterns as $\varepsilon \to 0$, we construct bifurcation diagrams for the amplitude of the solutions. For the 2D kinetic models, we focus on two analytical scalings that lead to two different non-local parabolic models. Our final target is to show that by considering such scaling approaches, we may lose certain aspects of the model dynamics - as emphasised by the numerical simulations in the 1D case.

The chapter is structured as follows. Section 2 contains a detailed description of the 1D non-local models for animal aggregations, followed by the parabolic scaling of these models. We also

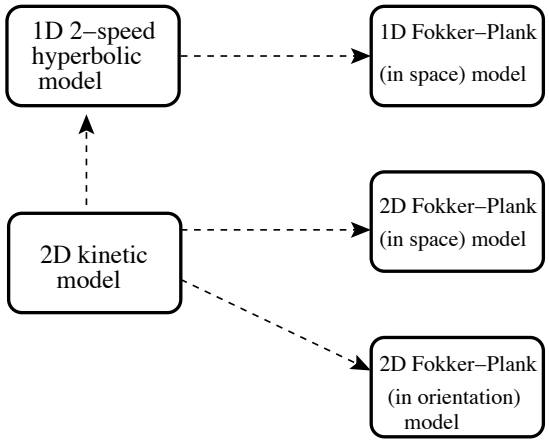

Figure 6.2: Schematic diagram of the scaling and reductionist approaches taken here.

investigate analytically the steady states of the kinetic and corresponding parabolic models. Section 3 contains a description of the 2D non-local models, followed by a parabolic limit and a "grazing collision" limit, which lead to different types of macroscopic models of parabolic type. Section 4 focuses on asymptotic preserving methods for 1D models, and shows the spatial and spatio-temporal patterns obtained with the parabolic and kinetic models, for some specific parameter values. Here, we come back to the steady states of the 1D kinetic and parabolic models, and investigate them numerically. We conclude in Section 5 with a summary and discussion of the results.

2 Description of 1D models

The following one-dimensional model was introduced in [147, 146] to describe the movement of the densities of left-moving (u^-) and right-moving (u^+) individuals that interact with conspecifics via social interactions:

$$\frac{\partial u^+}{\partial t} + \gamma \frac{\partial u^+}{\partial x} = -u^+\lambda^+[u^+,u^-] + u^-\lambda^-[u^+,u^-], \tag{2.1a}$$

$$\frac{\partial u^-}{\partial t} - \gamma \frac{\partial u^-}{\partial x} = u^+\lambda^+[u^+,u^-] - u^-\lambda^-[u^+,u^-], \tag{2.1b}$$

$$u^\pm(x,0) = u_0^\pm(x). \tag{2.1c}$$

Here γ is the constant speed and λ^+ is the rate at which right-moving individuals turn left. Similarly λ^- is the rate at which left-moving individuals turn right. To model the turning rates, we recall the observation made by Lotka [227]: "the type of motion presented by living organisms [...] can be regarded as containing both a systematically directed and also a random component". Since the rates $\lambda^\pm$ are related to the probability of turning (see the derivation of model (2.1) in [144]),

they are positive functions defined as:

$$\begin{aligned}\lambda^{\pm}[u^+,u^-] =&\lambda_1+\lambda_2 f(y_N[u^+,u^-])+\lambda_3 f(y_D^{\pm}[u^+,u^-])\\ =&\lambda_1+\lambda_3\Big(\lambda_2^0 f(y_N[u^+,u^-])+f(y_D^{\pm}[u^+,u^-])\Big),\end{aligned} \tag{2.2}$$

where we denote by $u=u^++u^-$ the total population density and all other terms will be defined below. In this chapter, we generalise the turning rates in [147, 146, 144] and assume that:

- individuals can turn randomly at a constant rate approximated by λ_1 [147];
- individuals can turn randomly in response to the perception of individuals inside any of the repulsive/attractive/alignment ranges (and independent of the movement direction of their neighbours). These *non-directed interactions* with neighbours are described by the term $y_N[u^+,u^-]$ with turning rate λ_2;
- individuals can turn in response to interactions with neighbours positioned within the repulsive (r), attractive (a) and alignment (al) zones, respectively (see Figure 6.1(a)) [147]. This turning is *directed towards or away* from neighbours, depending on the type of interaction (attractive or repulsive). For alignment interactions, individuals turn to move in the same direction as their neighbours. The non-local *directed interactions* with neighbours are described by terms $y_D^{\pm}[u^+,u^-]$ with turning rate λ_3.

If $\lambda_3\neq 0$, we denote by λ_2^0 the quotient of the turning rates λ_2/λ_3. This choice of notation is motivated by the corresponding 2D model (Section 3). The connection between the 1D model (2.1) and the 2D model (3.18) will be made clearer in Remarks 3.1, 3.2, 3.3 and 3.4. The turning function $f(\cdot)$ is a non-negative, increasing, bounded functional of the interactions with neighbours. An example of such function is $f(Y)=0.5+0.5\tanh(Y-y_0)$ (see [146]), where y_0 is chosen such that when $Y=0$ (i.e., no neighbours around), then $f(0)\approx 0$ and the turning is mainly random.

To model the long-distance social interactions that lead to turning behaviours, we define the interaction kernels in 1D, see Figure 6.1, as decreasing functions of the distance between the reference position x (of the population density) and the mid of the interaction ranges s_j, $j=r,al,a$,

$$K_j(x)=\frac{1}{\sqrt{2\pi m_j^2}}e^{-(x-s_j)^2/(2m_j^2)}, \tag{2.3}$$

for $x>0$ and zero otherwise, with $j=r,al,a$ denoting short-range repulsion (K_r), medium-range alignment (K_{al}) and long-range attraction (K_a) interaction kernels. Here, $m_j=s_j/8$ controls the width of the interaction range j.

For the non-directed density-dependent turning we define the turning kernel, $K^N(x)=\hat{\mathbf{K}}^N(x)+\hat{\mathbf{K}}^N(-x)$ with $\hat{\mathbf{K}}^N=q_rK_r+q_{al}K_{al}+q_aK_a$ obtained by superimposing the kernels K_j, $j=r,al,a$.

Here q_r, q_{al} and q_a represent the magnitudes of the repulsive, alignment and attractive social interactions. Note that in [146], $\lambda_2^0 = 0$ and the density-dependent non-directed turning term does not exist. However, in 2D, this term appears naturally when we incorporate random turning behaviour (as discussed in Section 3). With these notations we may define

$$y_N[u] = K^N * u, \quad \text{with } u = u^+ + u^-,$$

for the *non-directed* turning mechanisms. We assume here that individuals turn randomly whenever they perceive other neighbours around (within the repulsive, alignment and attractive ranges).

For the *directed* density-dependent turning, we define

$$y_D^{\pm}[u^+, u^-] = y_r^{\pm}[u^+, u^-] - y_a^{\pm}[u^+, u^-] + y_{al}^{\pm}[u^+, u^-]. \tag{2.4}$$

Here, $y_j^{\pm}[u^+, u^-]$, $j = r, al, a$, describe the directed turning in response to neighbours within the repulsive (r), alignment (al) and attractive (a) social ranges (as in [147]). As we will explain shortly, the direction of the turning will be given by incorporating movement direction towards or away conspecifics. For this reason, $y_a^{\pm}$ and $y_r^{\pm}$ enter equation (2.4) with opposite signs.

The density-dependent turnings depend greatly on how individuals communicate with each other, namely whether they can emit (perceive) signals to (from) *all* or *some* of their neighbours. Two particular situations, described by models called M2 and M4 as in [146] (see Figure 6.3) are considered:

- *Model M2:* Individuals communicate via omni-directional communication signals, and thus they can perceive *all* their neighbours positioned around them within all social interaction ranges. For instance, the majority of mammals communicate via a combination of visual, chemical and auditory signals, which allows them to receive/send information from/to all their neighbours. With this assumption (see Figure 6.3(a)), the terms $y_{r,a,al}^{\pm}$ are defined as follows:

$$y_{r,a}^{\pm}[u^+, u^-] = q_{r,a} \int_0^{\infty} K_{r,a}(s)\big(u(x \pm s) - u(x \mp s)\big)ds, \tag{2.5a}$$

$$y_{al}^{\pm}[u^+, u^-] = q_{al} \int_0^{\infty} K_{al}(s)\big(u^{\mp}(x \mp s) + u^{\mp}(x \pm s) - u^{\pm}(x \mp s) - u^{\pm}(x \pm s)\big)ds. \tag{2.5b}$$

  Here, q_j describe the magnitudes of the social interactions associated to the interaction kernels defined in (2.3). To understand the effect of these terms on the turning rates, let us focus on y_r^+, for example. If $u(x+s) > u(x-s)$, then y_r^+ enters λ^+ with positive sign, suggesting a higher likelihood of turning, to avoid collision with neighbours ahead at $x+s$. If, on

the other hand, $u(x+s) < u(x-s)$, then y_r^+ enters λ^+ with a negative sign, suggesting a lower likelihood of turning. In this case, the individuals at x will keep moving in the same direction, to avoid collision with neighbours behind at $x-s$. Note that the directionality of neighbours influences only the alignment interactions (the attractive and repulsive interactions being defined in terms of the total density u). Also, for this particular model, the random density-dependent terms are given by

$$y_N[u] = \int_0^\infty \hat{\mathbf{K}}^N(s)\big(u(x+s)+u(x-s)\big)ds. \tag{2.6}$$

- *Model M4:* Individuals communicate via unidirectional communication signals, and thus they can perceive only those neighbours moving towards them. For example, birds communicate via directional sound signals, and to ensure an effective transmission of their signals they orient themselves towards their targeted receivers [52]. With this assumption (see Figure 6.3(b)), the terms $y^{\pm}_{r,a,al}$ are defined as follows:

$$y^{\pm}_{r,a,al}[u^+,u^-] = q_{r,a,al}\int_0^\infty K_{r,a,al}(s)\big(u^{\mp}(x\pm s)-u^{\pm}(x\mp s)\big)ds. \tag{2.7}$$

Here, the directionality of neighbours influences all three social interactions. Moreover, for this model, the random density-dependent terms are given by

$$y_N[u^+,u^-] = \int_0^\infty \hat{\mathbf{K}}^N(s)\big(u^-(x+s)+u^+(x-s)\big)ds. \tag{2.8}$$

In this equation, we assume that individuals turn randomly in response to u^- and u^+ individuals (i.e., in (2.8) we add all perceived individuals; this is in contrast to equation (2.7), where we subtract individuals positioned ahead from individuals positioned behind, to impose directionality in the turning behaviour). Note that in (2.8), y_N does not depend anymore on $u = u^+ + u^-$ (as in (2.6)), since the individuals at x cannot perceive all their neighbours at $x \pm s$.

We focus on these two particular models because: (i) the model (2.1)+(2.2)+(2.5)+(2.6) assuming $\lambda_1 = 0$ has been generalised to 2D; (ii) the model (2.1)+(2.2)+(2.7)+(2.8) assuming $\lambda_2 = 0$ has been investigated analytically and numerically, and showed that it can exhibit Hopf bifurcations (even when $q_{al} = 0$), which give rise to spatio-temporal patterns such as rotating waves and modulated rotating waves [56]. In contrast, model (2.1)+(2.2)+(2.5)+(2.6) with $\lambda_2 = 0$ does not seem to exhibit rotating waves when $q_{al} = 0$, see [146].

To complete the description of the model, we need to specify the domain size and the boundary conditions. Throughout most of this chapter, we will consider an infinite domain. However, for the purpose of numerical simulations, in Sections 2.2 and 4 we will consider a finite domain of length L (i.e., $[0, L]$) with periodic boundary conditions: $u^+(L,t) = u^+(0,t), \quad u^-(0,t) = u^-(L,t)$.

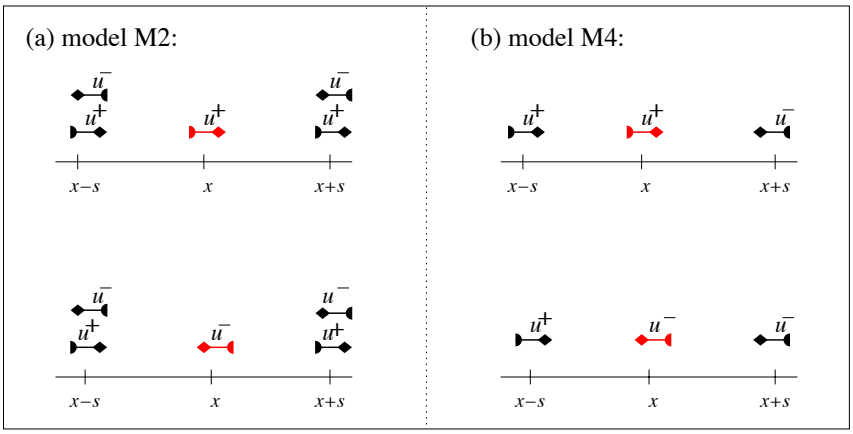

Figure 6.3: Diagram describing the mechanisms through which a reference individual positioned at x (right-moving – top; left-moving – bottom) perceives its neighbours positioned at $x - s$ and $x + s$. The reference individual can perceive (a) all its neighbours (model M2 in [146]); (b) only its neighbours moving towards it (model M4 in [146]).

This assumption will also require wrap-around conditions for the kernels describing the non-local social interactions, see Section 4. For large L, this assumption approximates the dynamics on an infinite domain.

In the following, we show how this hyperbolic 2-velocity model can be reduced to a parabolic equation by considering suitable scalings, which depend on the biological assumptions. Of course, to be useful in practice, these parameters have to be calibrated and adapted to particular species as in [183, 188]. The scaling arguments are classically obtained by writing a dimensionless formulation of the problem. We refer to [265] in bacterial chemotaxis and [6] in semiconductor modelling for a detailed description. After this dimensionless rescaling, we typically end up with two different time scales whose balance determines our small parameter: the drift time and the diffusion time.

We start in Subsection 2.1 with a parabolic scaling, which describes the situation where the drift time of a population is much smaller than its diffusion time. To this end, we discuss two separate cases (i.e., social interactions described by non-linear or linear functions $f(y)$ in (2.2)), which lead to two different parabolic equations.

2.1 Parabolic limit for non-linear interactions

Next, we focus only on model M2 (i.e., equations (2.1)+(2.2)+(2.5)+(2.6)), since the results for model M4 are similar. The scaling argument applied in [189] transforms the hyperbolic system (2.1) into a parabolic equation. One can scale the space and time variables ($x = x^*/\varepsilon, t = t^*/\varepsilon^2$, with $\varepsilon \ll 1$), or can scale the speed (γ) and the turning rates ($\lambda_{1,2,3}$). In both cases, we consider the rescaled interaction kernels $K_j^*(x^*) = \frac{1}{\varepsilon} K_j(\frac{x^*}{\varepsilon})$ in the expressions for $y_j^{\pm}$, $j = r, al, a$. Here, we scale the time and space variables to be consistent with the approach in Section 3.1. As mentioned above,

the scaling parameter ε depends on the biological problem modelled. For example, in [189] the authors connect ε to the ratio of the drift (τ_{drift}) and diffusion (τ_{diff}) times observed in bacteria such as *E. coli*, where $\tau_{drift} \approx 100$ seconds and $\tau_{diff} \approx 10^4$ seconds, and thus $\varepsilon \approx O(10^{-2})$. Similar scaling arguments are used in [265, Appendix] to analyse the ability of parabolic scalings to describe travelling pulses.

To perform the scaling, let us re-write model (2.1) in terms of the total density $u(x,t)$ and the flux $v(x,t) = \gamma(u^+(x,t) - u^-(x,t))$ of individuals (see also [189, 192]):

$$\varepsilon^2 \frac{\partial u}{\partial t} + \varepsilon \frac{\partial v}{\partial x} = 0, \tag{2.9a}$$

$$\varepsilon^2 \frac{\partial v}{\partial t} + \varepsilon\gamma^2 \frac{\partial u}{\partial x} = \gamma u\big(\lambda^-[u,v] - \lambda^+[u,v]\big) - v\big(\lambda^+[u,v] + \lambda^-[u,v]\big), \tag{2.9b}$$

with initial conditions $u(x,0) = u_0(x)$, $v(x,0) = v_0(x)$. For clarity, here we dropped the $*$ from the rescaled space (x*) and time (t*) variables. In addition, we assume that individuals have a reduced perception of the surrounding neighbours for small values of ε, [143]:

$$f_\varepsilon\Big(y_D^\pm[u,v]\Big) = \varepsilon f\Big(y_D^\pm[u, \int_{\frac{x*}{\varepsilon}} \varepsilon \frac{\partial u}{\partial t*}]\Big), \quad f_\varepsilon\Big(y_N[u]\Big) = \varepsilon f\Big(y_N[u]\Big), \tag{2.10}$$

where f enters the turning functions $\lambda^\pm$ (2.2):

$$\begin{aligned} \lambda^+[\cdot] + \lambda^-[\cdot] &= 2\lambda_1 + 2\lambda_2\, \varepsilon f(y_N[\cdot]) + \varepsilon\, \lambda_3 \Big(f(y_D^+[\cdot]) + f(y_D^-[\cdot])\Big), \\ \lambda^-[\cdot] - \lambda^+[\cdot] &= \lambda_3 \varepsilon \Big(f(y_D^-[\cdot]) - f(y_D^+[\cdot])\Big). \end{aligned}$$

By eliminating $v = \varepsilon \int_x \frac{\partial u}{\partial t}$ from equations (2.9), and taking the limit $\varepsilon \to 0$, we obtain the following parabolic equation

$$\frac{\partial u}{\partial t} = \frac{\gamma^2}{2\lambda_1} \frac{\partial}{\partial x}\left(\frac{\partial u}{\partial x}\right) - \frac{\lambda_3 \gamma}{2\lambda_1} \frac{\partial}{\partial x}\left(\left(f(y_D^-[u]) - f(y_D^+[u])\right)u\right). \tag{2.11}$$

We note here that the non-local terms $f(y_D^\pm[u])$ now depend only on the repulsive and attractive interactions. The reason for this is that the alignment interactions are defined in terms of $u^\pm = (u \pm \frac{1}{\gamma} v)/2 = 0.5(u \pm \frac{1}{\gamma} \int_{x/\varepsilon} \varepsilon^2 \partial u/\partial t)$. As $\varepsilon \to 0$, the u terms in (2.5) cancel out, and the integrals approach zero. Equation (2.11) can be re-written as

$$\frac{\partial u}{\partial t} = \frac{\partial}{\partial x}\left(D_0 \frac{\partial u}{\partial x}\right) - \frac{\partial}{\partial x}\Big(S_0\, u\, V(u)\Big), \tag{2.12}$$

with diffusion rate $D_0 = \gamma^2/(2\lambda_1)$ and drift rate $S_0 = \lambda_3\gamma/(2\lambda_1)$. The velocity $V(u)$ depends on the communication mechanism incorporated. For example, for model M2 we have $y_D^\pm[u] = \pm K * u$, and so the velocity is given by

$$V[u] = f\big(-K * u\big) - f\big(K * u\big)$$

where we define

$$K * u = \bar{K}^+ * u - \bar{K}^- * u, \quad \bar{K}^\pm * u = \int_0^\infty \bar{K}(s) u(x \pm s) ds,$$

$$\bar{K} = q_r K_r - q_a K_a. \tag{2.13}$$

For model M4, we have $y_D^{\pm}[u] = \pm 0.5K * u$, and so the velocity is quite similar: $V[u] = f\big(-0.5K * u\big) - f\big(0.5K * u\big)$, the factor 0.5 appearing from $u^{\pm} = 0.5(u \pm \frac{1}{\gamma}v)$.

Remark 2.1. *We observe that the random density-dependent turning $f(y_N[u])$ does not appear in this parabolic limit. This is the result of the scaling assumptions (2.10).*

Remark 2.2. *Here, the turning functions $f(\cdot)$ were chosen to be bounded, since individuals cannot turn infinitely fast when subject to very strong interactions with neighbours [146, 145]. However, for simplicity, many models consider linear functions: $f(z) = z$ (see, for example, [237, 239, 153]). The choice of having bounded or non-bounded turning functions $f(\cdot)$ has further implications on the models. In particular, for linear functions, the argument $y_D^{\pm} = y_r^{\pm} - y_a^{\pm} + y_{al}^{\pm}$ can be either positive or negative (depending on the magnitudes of the social interactions), with $y_D^{+} = -y_D^{-}$. For very small constant and non-directional turning rates ($\lambda_1, \lambda_2 \approx 0$), this can lead to $\lambda^+ < 0$ and $\lambda^- > 0$, or vice versa. Now the $u^+\lambda^+$ terms add to the $u^-\lambda^-$ terms, causing both u^+ and u^- populations to decide very fast to move in the same direction (in fact, one of the populations is reinforced to keep its moving direction). This is different from the case with bounded turning functions, where if $y_D^{+} = -y_D^{-} \ll 0$, then $0 < \lambda^+ \approx \lambda_1 + \lambda_2 f\left(y_N[u^+, u^-]\right) < \lambda^-$. So if $\lambda_1, \lambda_2 \approx 0$, then $u^+\lambda^+ \approx 0$ and hence population u^+ is not reinforced to keep its movement direction.*
Because the 2D kinetic model that we will investigate in Section 3 assumes f to be a linear function, with a very weak directed turning behaviour ($\varepsilon\lambda_3$), we now consider the case $f(y_N[u]) = y_N[u] = K^N * u$ and $f(y_D^{\pm}[u]) = \varepsilon y_D^{\pm}[u]$, and so the turning rates can be written as

$$\lambda^{\pm}[u^+, u^-] = \lambda_1 + \lambda_2\, K^N * u + \varepsilon\, \lambda_3 y_D^{\pm}[u]\,. \tag{2.14}$$

By taking the limit $\varepsilon \to 0$ in (2.9), we obtain the following parabolic equation with density-dependent coefficients:

$$\frac{\partial u}{\partial t} = \frac{\partial}{\partial x}\left(D[u]\frac{\partial u}{\partial x}\right) - \frac{\partial}{\partial x}\Big(S[u]u\big(y_D^-[u] - y_D^+[u]\big)\Big), \tag{2.15a}$$

$$D[u] = \frac{\gamma^2}{2(\lambda_1 + \lambda_2 K^N * u)} \quad \text{and} \quad S[u] = \frac{\lambda_3\gamma}{2(\lambda_1 + \lambda_2 K^N * u)}. \tag{2.15b}$$

This expression is similar to the asymptotic parabolic equation (3.30) for the 2D model. We will return to this aspect in Section 3.1.

2.2 The preservation of steady states and their stability as $\varepsilon \to 0$

The spatially homogeneous steady states describe the situation where individuals are evenly spread over the whole domain. In the following we investigate how these steady states and their linear stability are preserved in the parabolic limit. To this end, we focus on the more general case of non-linear social interactions (the case with linear interactions is similar). For simplicity we assume here that $\lambda_2 = 0$ and $q_{al} = 0$. To calculate these spatially homogeneous states we need to

define $A = \int_0^L (u^+ + u^-)\, dx$ the total population density. For simplicity, throughout this section we assume that $A = 2$; similar results can be obtained for different values of A.

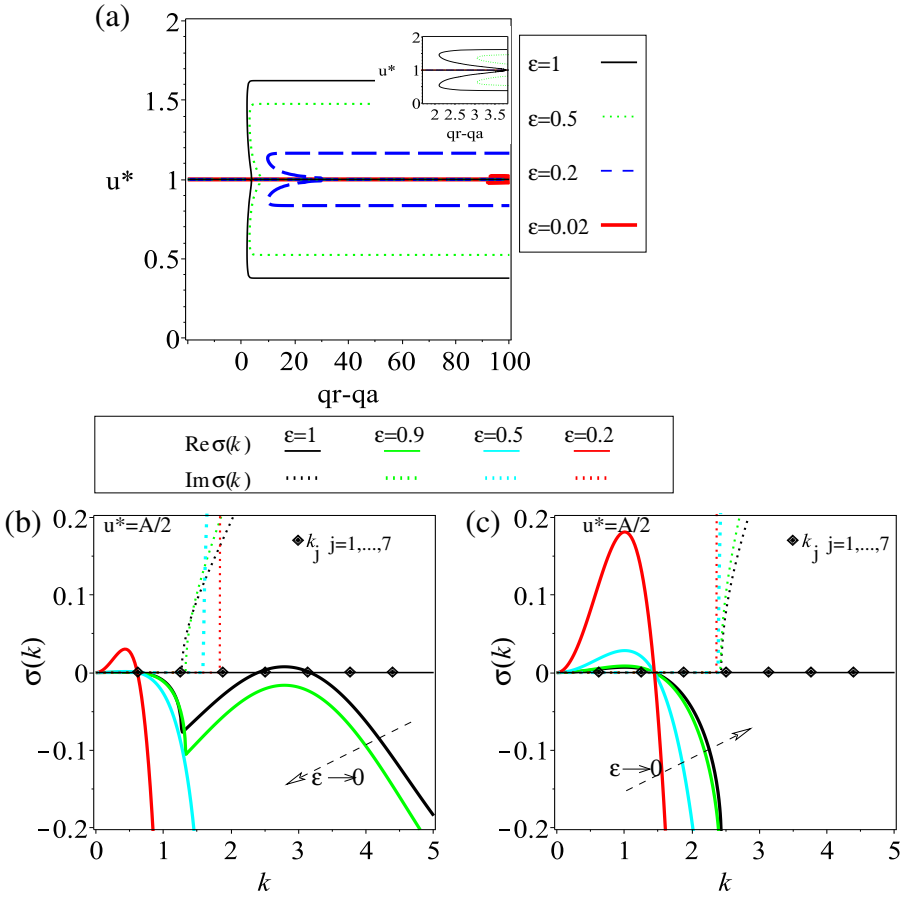

Figure 6.4: (a) Spatially homogeneous steady states u^* for model (2.9) with communication signals (2.7) and (2.8) (communication mechanism M4), for different values of ε. The small inset figure shows the 5 possible steady states occurring for $\varepsilon = 1$ and $q_r - q_a \in (2, 3.7)$ (see the black continuous curve); (b) Dispersion relation $\sigma(k_j)$ for M4 (given by (2.16)), showing the stability of the spatially homogeneous steady state $u^* = A/2$, for different values of ε; (c) Dispersion relation $\sigma(k_j)$ for M2, for the stability of the spatially homogeneous steady state $u^* = A/2$, for different values of ε. The continuous curves describe Re $\sigma(k_j)$, while the dotted curves describe Im $\sigma(k_j)$. The small diamond-shaped points show the discrete wavenumbers $k_j, j = 1, ..., 7$, with $k_j = 2\pi j/L$ (and thus $k_j \in (0, 5)$ for $j = 1, .., 7$ and $L = 10$). The parameter values are: (b) $q_a = 1.545$, $q_r = 2.779$; (c) $q_a = 1.5$, $q_r = 0.93$. The rest of parameters are: $q_{al} = 0$, $\lambda_1 = 0.2$, $\lambda_2 = 0$, $\lambda_3 = 0.9$, $A = 2$.

Figure 6.4(a) shows the number and magnitude of the steady states u^* displayed by (2.9)-(2.10) with communication mechanism M4, for different values of ε, as one varies the difference in the magnitude of the repulsive and attractive social interactions, $q_r - q_a$. For medium ε, the model can display up to 5 different steady states: one "unpolarised" state $(u^+, u^-) = (u^*, u^*) = (A/2, A/2)$ (where half of the individuals are facing left and half are facing right), and two or four "polarised" states $(u^*, A - u^*), (A - u^*, u^*)$ characterised by $u^* < A/2$ or $u^* > A/2$. Two of these "polarised"

states exist only in a very narrow parameter range: e.g., for $\varepsilon = 1$, they exist when $q_r - q_a \in (2, 3.7)$. The other two "polarised" states exist for any $q_r - q_a > 2$. For a calculation of the threshold values of $q_r - q_a$ that ensure the existence of 3 or 5 steady states see [147]. As ε decreases, the magnitude of the polarised states decreases (i.e., the differences between the number of individuals facing right and those facing left are decreasing). Moreover, for small ε, these polarised states appear only when repulsion becomes much stronger than attraction (i.e., $q_r - q_a \gg 10$). When $\varepsilon = 0$ there is only one steady state $u^* = A/2$. Since this state exists for all $\varepsilon \geqslant 0$, from now on we will focus our attention only on this state. Note that for $q_{al} = 0$ and for the communication mechanism M2 (not shown here), the non-local attractive-repulsive terms vanish, and there is only one steady state, $u^* = A/2 = 1$, which does not depend on ε.

Models (2.1) and (2.9) do exhibit a large variety of local bifurcations: codimension-1 Steady-state and Hopf bifurcations [145] as well as codimension-2 Hopf/Hopf, Hopf/Steady-state and Steady-state/Steady-state bifurcations [56]. Next we focus on the parameter region where two such bifurcations can occur. We choose a Hopf/steady-state bifurcation for M4 (Figure 6.4(b)) and a steady-state bifurcation for M2 (Figure 6.4(c)), and investigate what happens when $\varepsilon \to 0$. To identify the parameter regions where these bifurcations occur, we consider a finite domain of length L, and investigate the growth of small perturbations of spatially homogeneous solutions. We assume $u^{\pm} \propto u^* + a_{\pm}\exp(\sigma t + ik_j x)$, with $k_j = 2\pi j/L, j \in \mathbb{N}^+$, the discrete wave-numbers, and $|a_{\pm}| \ll 1$. We substitute these solutions into the linearised system (2.9), and by imposing that the determinant of this system is zero, we obtain the following dispersion relation, which connects σ (the growth/decay of the perturbations) with the wave-numbers k_j:

$$\varepsilon^2\sigma^2 + \sigma(2L_1^{\varepsilon} - R_2^{\varepsilon}\mathrm{Re}(\hat{\mathbf{K}}^+)) + \gamma^2 k_j^2 - \gamma k_j R_2 \mathrm{Im}(\hat{\mathbf{K}}^+) = 0, \tag{2.16}$$

where $L_1^{\varepsilon} = \lambda_1 + \varepsilon\lambda_3 f(0)$, $R_2^{\varepsilon} = 2\varepsilon u^* \lambda_3 f'(0)$, and $\hat{\mathbf{K}}^+ = \mathrm{Re}(\hat{\mathbf{K}}^+) + i\mathrm{Im}(\hat{\mathbf{K}}^+)$ the Fourier transforms of $\bar{K}^+ * u$ described in equations (2.13). Note that the wave numbers k_j that become unstable (i.e., for which $\mathrm{Re}(\sigma(k_j)) > 0$) determine, at least for a short time, the number of "peaks" j that emerge in the spatial distribution of the density.

Figure 6.4(b) shows the stability of the spatially homogeneous steady state $u^* = A/2$ for model M4 as given by the dispersion relation (2.16). Even if the wave-numbers k_j are discrete (see the diamond-shaped points on the x-axis of Figure 6.4(b)), we plot $\sigma(k_j)$, $j > 0$ as a continuous function of k_j for clarity. To discuss what happens with a Hopf bifurcation as $\varepsilon \to 0$, we focus in Figure 6.4(b) on a parameter space where such a bifurcation occurs (i.e., where $\mathrm{Re}(\sigma(k_j)) = 0$ in (2.16)): $q_a = 1.545$, $q_r = 2.779$, $\lambda_1 = 0.2$, $\lambda_2 = 0$, $\lambda_3 = 0.9$ and $\varepsilon = 1$ (see also [57]). For these parameter values, three modes become unstable at the same time: a steady-state mode k_1 ($\mathrm{Im}(\sigma(k_1)) = 0$; associated with stationary patterns with 1 peak) and two Hopf modes k_4 and k_5 ($\mathrm{Im}(\sigma(k_{4,5})) > 0$; associated with travelling patterns with 4 or 5 peaks). As $\varepsilon \to 0$, the steady-state

mode persists while the Hopf modes disappear (i.e., $0 < \text{Re}(\sigma(k_1)) \ll 1$ and $\text{Re}(\sigma(k_{4,5})) < 0$; see Figure 6.4(b).) This can be observed also from equation (2.16): as $\varepsilon \to 0$, we have $\sigma \in \mathbb{R}$. A similar investigation of the local stability of the spatially homogeneous steady states associated with the non-local parabolic equation (2.12) shows that this equation cannot have complex eigenvalues (i.e., $\text{Im}(\sigma(k_j)) = 0$ for all $j > 0$), and thus cannot exhibit local Hopf bifurcations [58].

Figure 6.4(c) shows the stability of the spatially homogeneous steady state $u^* = A/2$, for model M2, as given by the dispersion relation $\sigma(k_j)$:

$$\varepsilon^2\sigma^2 + \sigma(2L_1^\varepsilon) + \gamma^2 k_j^2 - 2\gamma k_j R_2 \text{Im}(\hat{\mathbf{K}}^+) = 0. \tag{2.17}$$

For $q_a = 1.5$, $q_r = 0.93$, $\lambda_1 = 0.2$, $\lambda_2 = 0$, $\lambda_3 = 0.9$ and $\varepsilon = 1$, model M2 exhibits a steady-state bifurcation, i.e., $\text{Re}(\sigma(k_j)) = \text{Im}(\sigma(k_j)) = 0$ in (2.17). In particular, two steady-state modes are unstable at the same time: k_1 and k_2 (both associated with stationary patterns). As $\varepsilon \to 0$, the two modes remain unstable. Hence, we expect that the spatial patterns generated by these modes will persist as $\varepsilon \to 0$. We will return to this aspect in Section 4.4, when we will investigate numerically the mechanisms that lead to the disappearance of the Hopf modes and the persistence of the steady-state modes, as $\varepsilon \to 0$.

3 Description of 2D models

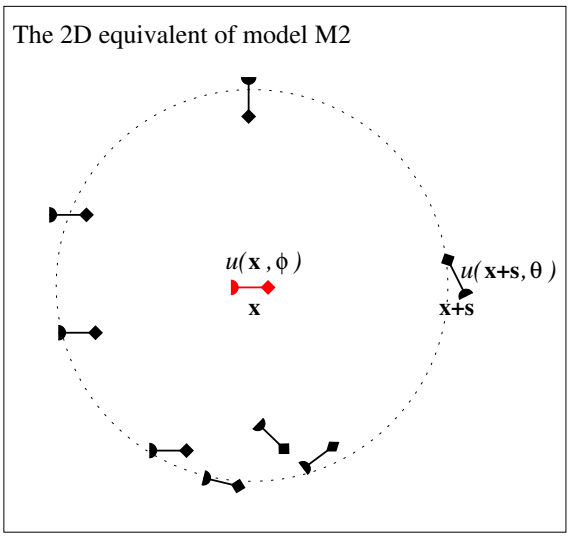

Figure 6.5: Caricature description of the M2 mechanism in 2D (where individuals can perceive *all* their neighbours within a certain interaction range). We assume that a reference individual is positioned at $\mathbf{x} = (x, y)$ and moves in direction ϕ. Its neighbours are at various spatial positions $\mathbf{x} + \mathbf{s}$ within a certain interaction range (e.g., alignment range). The interaction ranges are described by the 2D kernels (3.21); see also Figure 6.1(a).

An attempt to generalise a specific case of the 1D model (2.1)-(2.2)-(2.5)-(2.6) to two dimensions was made by Fetecau [153]. The Boltzman-type model described in [153] incorporates the non-local social interactions in the re-orientation terms:

$$\frac{\partial u}{\partial t} + \gamma \mathbf{e}_\phi \cdot \nabla_{\mathbf{x}} u = -\lambda(\mathbf{x}, \phi)u + \int_{-\pi}^{\pi} T(\mathbf{x}, \phi', \phi)u(\mathbf{x}, \phi', t)d\phi'. \tag{3.18}$$

Here, $u(\mathbf{x}, \phi, t)$ is the total population density of individuals located at $\mathbf{x} = (x, y)$, moving at a constant speed $\gamma > 0$ in direction ϕ. The term $\mathbf{e}_\phi = (\cos(\phi), \sin(\phi))$ gives the movement direction of individuals. The re-orientation terms, $\lambda(\mathbf{x}, \phi)$ and $T(\mathbf{x}, \phi', \phi)$ depend on the non-local interactions with neighbours, which can be positioned in the repulsive, attractive, and alignment ranges depicted in Fig. 6.1(a). Thus, these terms have three components each, corresponding to the three social interactions:

$$T(\mathbf{x}, \phi', \phi) = T_{al}(\mathbf{x}, \phi', \phi) + T_a(\mathbf{x}, \phi', \phi) + T_r(\mathbf{x}, \phi', \phi).$$

In contrast to the model in [153], here we assume that the re-orientation terms

$$\lambda_j(\mathbf{x}, \phi') = \int_{-\pi}^{\pi} T_j(\mathbf{x}, \phi', \phi)\mathrm{d}\phi, \quad j = r, a, al$$

have both a constant and a density-dependent component:

$$T_{al}(\mathbf{x}, \phi', \phi) = \frac{\eta_{al}}{2\pi} + \tag{3.19a}$$
$$\lambda_3\, q_{al} \int_{-\pi}^{\pi} \int_{\mathbb{R}^2} K^d_{al}(\mathbf{x} - \mathbf{s}) K^o_{al}(\theta, \phi') \omega_{al}(\phi' - \phi, \phi' - \theta) u(\mathbf{s}, \theta, t) ds d\theta,$$
$$T_{r,a}(\mathbf{x}, \phi', \phi) = \frac{\eta_{r,a}}{2\pi} + \tag{3.19b}$$
$$\lambda_3\, q_{r,a} \int_{-\pi}^{\pi} \int_{\mathbb{R}^2} K^d_{r,a}(\mathbf{x} - \mathbf{s}) K^o_{r,a}(\mathbf{s}, \mathbf{x}, \phi') \omega_{r,a}(\phi' - \phi, \phi' - \psi) u(\mathbf{s}, \theta, t) ds d\theta.$$

Therefore, the turning rate $\lambda(\mathbf{x}, \phi) = \lambda_{al}(\mathbf{x}, \phi) + \lambda_a(\mathbf{x}, \phi) + \lambda_r(\mathbf{x}, \phi)$ is defined by

$$\lambda = \lambda_1 + \lambda_3 \bar{\lambda}[u(\mathbf{x}, \phi)]\,, \tag{3.20}$$

with $\lambda_1 = \eta_r + \eta_{al} + \eta_a$ and with $\bar{\lambda}[u(\mathbf{x}, \phi)]$ being given as the integral over $\phi' \in [-\pi, \pi]$ of the sum of non-local terms in (3.19) with ϕ and ϕ' interchanged.

Remark 3.1. *By defining the constant basic turning rate to be $\lambda_1 = \eta_r + \eta_{al} + \eta_a$, we generalised the model in [153] (where $\lambda_1 = 0$). Note that the turning rates here are linear functions of the non-local interactions with neighbours. This is in contrast to the more general non-linear turning function f we considered in Section 2.1 for the 1D hyperbolic model. In what follows, we are interested in non-constant turning rates $\lambda_j(\mathbf{x}, \phi')$, $j = r, a, al$, and so we will henceforth assume $\lambda_3 \neq 0$.*

As in [153], λ_j, $j = r, a, al$, are defined in terms of both distance kernels and orientation kernels. The 2D distance kernels K^d_j, $j = r, a, al$ are given by

$$K^d_j(\mathbf{x}) = \frac{1}{A_j} e^{-(\sqrt{x^2+y^2} - d_j)/m_j^2}, \quad j = r, a, al, \tag{3.21}$$

where constants A_j are chosen such that the kernels integrate to one. The orientation kernels K_j^o measure the likelihood of turning in response to the movement direction of neighbours (for alignment interactions) or in response to the position of neighbours (for repulsive and attractive interactions):

$$\begin{aligned} K_{al}^o(\theta,\phi) &= \frac{1}{2\pi}(1-\cos(\phi-\theta))\,, \\ K_r^o(\mathbf{s},\mathbf{x},\phi) &= \frac{1}{2\pi}(1+\cos(\phi-\psi))\,, \\ K_a^o(\mathbf{s},\mathbf{x},\phi) &= \frac{1}{2\pi}(1-\cos(\phi-\psi))\,, \end{aligned}$$

where ψ is the angle between the positive x-axis and the relative location $\mathbf{s}-\mathbf{x}$ of the neighbours at $\mathbf{s}$ with respect to the reference individual at $\mathbf{x}$. Finally, ω describes the tendency to turn from direction ϕ' to direction ϕ, as a result of interactions with individuals moving in direction θ:

$$\omega(\phi'-\phi,\phi'-\theta) = g(\phi'-\phi-R(\phi'-\theta))\,,$$

for some suitable choice of g. Note that in the case $\lambda_1 = 0$, the function ω describes the probability of re-orientation in the sense discussed in [167] and thus we require $\int \omega(\phi'-\phi,\phi'-\theta)\,d\phi = 1$. For example, g could be a periodic function that integrates to one:

$$g(\theta) = \frac{1}{\sqrt{\pi}\sigma}\sum_{z\in\mathbb{Z}} e^{-(\frac{\theta+2\pi z}{\sigma})^2}\,, \quad \theta\in(-\pi,\pi)\,,$$

with σ a parameter measuring the uncertainty of turning (with small σ leading to exact turning) [153, 167]. Another typical choice could be the von Mises distribution, as in Vicsek-type models [120].

On the other hand, when $\lambda_1 > 0$, then g can be interpreted as a small re-orientation perturbation from the random turning behaviour and so ω satisfies $\int \omega(\phi'-\phi,\phi'-\theta)\,d\phi = 0$ and therefore g is required to be odd.

Remark 3.2. *Fetecau [153] showed that by imposing the turning angle to have only two possible values $\phi = \pm\pi$, the 2D model (3.18) can be reduced to the 1D model (2.1) for a specific choice of turning rates $\lambda^{\pm}[u^+,u^-]$. More precisely, considering the more general turning operators (3.19a) and (3.19b), we recover (2.2) with $\lambda_1,\lambda_3 \geqslant 0$, $\lambda_2 = 0$ for a linear turning function $f(z) = z$, and with the communication mechanism*

$$\begin{aligned} y_D^{\pm}[u^+,u^-] = \frac{1}{\pi}q_{al}\int_{-\infty}^{\infty} K_{al}(x-s)\left(u^{\mp}(s,t)\right)\mathrm{d}s \\ + \frac{1}{\pi}q_a\int_{-\infty}^{x} K_a(x-s)\left(u^{+}(s,t)+u^{-}(s,t)\right)\mathrm{d}s \\ + \frac{1}{\pi}q_r\int_{x}^{\infty} K_r(x-s)\left(u^{+}(s,t)+u^{-}(s,t)\right)\mathrm{d}s..\end{aligned}$$

This is a similar turning behaviour to model M2 in [146], since individuals receive and emit omni-directional communication signals, but with the function f linear. Moreover, as we will show in the next section, even if the 2D model (3.18) can be reduced to a special case of the 1D model (2.1) without λ_2 in (2.2), the parabolic scaling of the 2D model reduces to a special case of the parabolic scaling of the 1D model, which includes a λ_2 term for non-directed turning. As we will see shortly, this 2D parabolic scaling leads to the natural appearance of a non-directed interaction contribution, suggesting that there are more subtle differences between the 1D and 2D models.

The diffusion limit (i.e., $x = x^*/\varepsilon$, $t = t^*/\varepsilon^2$) of a transport model similar to (3.18), but with constant turning rates λ was discussed in [189, 190]. In the following we consider the parabolic limit for model (3.18) with density-dependent turning rates.

3.1 Parabolic drift-diffusion limit

We focus on the case where individuals are only influenced slightly by the presence of neighbours, i.e., the turning mechanism can be assumed to be a small perturbation of a uniform turning probability. In this case, we will show that the Boltzmann-type equation (3.18) can be reduced to a drift-diffusion equation in the macroscopic regime.

We consider the scaling $t = t^*/\varepsilon^2$, $\mathbf{x} = \mathbf{x}^*/\varepsilon$, where $\varepsilon \ll 1$ is a small parameter. Since the velocity in the new variables is of order $1/\varepsilon$, then we make the scaling assumption that an individual's turning behaviour is only influenced slightly by the presence of neighbours:

$$T[u](\mathbf{x}, \phi', \phi) = \frac{\lambda_1}{2\pi} + \frac{\lambda_2}{2\pi} K^d * \rho(\mathbf{x}, t) + \varepsilon\, \lambda_3\, B[u](\mathbf{x}, \phi', \phi)\,, \tag{3.22}$$

with $\rho(\mathbf{x}, t) = \int_{-\pi}^{\pi} u(\mathbf{x}, \phi, t)\, \mathrm{d}\phi$, and where we define

$$K^d(\mathbf{x}) := q_{al} K^d_{al}(\mathbf{x}) + q_a K^d_a(\mathbf{x}) + q_r K^d_r(\mathbf{x})$$

to be the *social distance kernel*. As we have done in the 1D case, we have separated the non-directed and directed turning rates.

If $\lambda_3 \neq 0$, we factorise again the turning rate λ_3 corresponding to the directed interactions and write $\lambda_2^0 = \lambda_2/\lambda_3$ the quotient of turning rates. With this notation, $\bar{\lambda}[u(\mathbf{x}, \phi)]$ in (3.20) can be written as

$$\bar{\lambda}[u(\mathbf{x}, \phi)] = \lambda_2^0\, K^d * u(\mathbf{x}, \phi, t) + \varepsilon\, y_D[u(\mathbf{x}, \phi, t)]\,, \tag{3.23}$$

with $y_D[u] = \int B[u](\mathbf{x}, \phi', \phi) \mathrm{d}\phi'$. Note that the turning rate λ given by (3.20)-(3.23) corresponds to the 1D turning rates (2.14) with this specific choice of $y_D[u]$. The scaling assumption (3.22) can be derived by introducing reduced perception of directionality of neighbours into the re-orientation

function ω and into the orientation kernels K_j^o,

$$\begin{aligned} g_j(\vartheta) &= \lambda_2^0 + \varepsilon G_j(\vartheta)\,, \\ K_{al}^o(\theta,\phi) &= \frac{1}{2\pi}\left(1-\varepsilon\,\cos\left(\phi-\theta\right)\right)\,, \\ K_r^o(\mathbf{s},\mathbf{x},\phi) &= \frac{1}{2\pi}\left(1+\varepsilon\,\cos\left(\phi-\psi\right)\right)\,, \\ K_a^o(\mathbf{s},\mathbf{x},\phi) &= \frac{1}{2\pi}\left(1-\varepsilon\,\cos\left(\phi-\psi\right)\right)\,, \end{aligned}$$

where $G_j(\vartheta)$, $j=r,a,al$ are *signal response functions* to be chosen according to the biological context. Substituting these expressions into the re-orientation terms (3.19), we define $\lambda_1=\eta_{al}+\eta_r+\eta_a$ and we obtain (3.22) with a precise expression for the *social response function* $B[u]$.

If $\lambda_1=0$, we further have $\lambda_2=\lambda_3/2\pi$ and $\int_{-\pi}^{\pi} G_j(\phi'-\phi-R(\phi'-\theta))\mathrm{d}\phi=0$, $j=r,a,al$ as the probability to turn to any new angle is 1. In addition, we want the turning function $R(\vartheta)$ to be close to an unbiased turning mechanism. This can be expressed by taking $R(\vartheta)=\varepsilon\vartheta$, which indeed corresponds to weak interaction between individuals, [167]. We obtain $B[u]=B_{al}[u]+B_a[u]+B_r[u]$ with

$$\begin{aligned} B_{al}[u](\phi',\phi) =& \frac{1}{2\pi}\,q_{al}\,G_{al}(\phi'-\phi)\,K_{al}^d * \rho(\mathbf{x},t) \\ &- \frac{\lambda_2^0}{2\pi}\,q_{al}\int_{\mathbb{R}^2} K_{al}^d(\mathbf{x}-\mathbf{s})\int_{-\pi}^{\pi}\cos\left(\phi'-\theta\right)\,u(\mathbf{s},\theta,t)\,\mathrm{d}\theta\,\mathrm{d}\mathbf{s}\,, \end{aligned} \tag{3.24}$$

$$\begin{aligned} B_{r,a}[u](\phi',\phi) =& \frac{1}{2\pi}\,q_{r,a}\,G_{r,a}(\phi'-\phi)\,K_{r,a}^d * \rho(\mathbf{x},t) \\ &\pm \frac{\lambda_2^0}{2\pi}\,q_{r,a}\int_{\mathbb{R}^2} K_{r,a}^d(\mathbf{x}-\mathbf{s})\cos\left(\phi'-\psi\right)\,\rho(\mathbf{s},t)\,\mathrm{d}\mathbf{s}\,. \end{aligned} \tag{3.25}$$

Remark 3.3. *Note that in 2D, λ_2^0 is introduced as the relative strength of non-directed and directed turning kernels. This is part of the scaling assumption in 2D, whereas in 1D, we introduced it as part of the model (2.1)-(2.2) before rescaling. Note that $\lambda_2^0=1/2\pi$ in Fetecau's model where no distinction is made between directed and non-directed turning.*

Let us introduce

$$K_*^d(\mathbf{x}^*)=\frac{1}{\varepsilon}K^d\left(\frac{\mathbf{x}^*}{\varepsilon}\right),\quad B_*(\mathbf{x}^*,\phi',\phi)=\frac{1}{2\pi}B\left(\frac{\mathbf{x}^*}{\varepsilon},\phi',\phi\right)\,.$$

Simplifying the notation by dropping $*$, system (3.18) writes in the new variables as

$$\begin{aligned} \varepsilon^2\partial_t u+\varepsilon\,\gamma\,\mathbf{e}_\phi\cdot\nabla_{\mathbf{x}}u =& \frac{1}{2\pi}\left(\lambda_1+\lambda_2\,K^d*\rho\right)(\rho-2\pi u) \\ &+\varepsilon\,\lambda_3\,2\pi\int_{-\pi}^{\pi}B(\mathbf{x},\phi',\phi)\,u(\mathbf{x},\phi',t)\,\mathrm{d}\phi' \\ &-\varepsilon\,\lambda_3\,2\pi\;u(\mathbf{x},\phi,t)\int_{-\pi}^{\pi}B(\mathbf{x},\phi,\phi')\mathrm{d}\phi'\,. \end{aligned} \tag{3.26}$$

Using a Hilbert expansion approach, $u=u_0+\varepsilon u_1+\varepsilon^2u_2+\ldots$, and defining the macroscopic densities $\rho_i=\int_{-\pi}^{\pi}u_i\,\mathrm{d}\phi$ for $i\in\mathbb{N}_0$, we obtain at leading oder a relaxation towards a uniform

angular distribution at each position:

$$u_0(\mathbf{x},\phi,t) = \rho_0(\mathbf{x},t)F(\phi), \qquad F(\phi) = \frac{1}{2\pi}\mathbb{1}_{\phi\in(-\pi,\pi]}. \tag{3.27}$$

Integrating (3.26) with respect to the direction of motion ϕ, we obtain the continuity equation

$$\partial_t\rho_0 + \gamma\int_{-\pi}^{\pi}\mathbf{e}_\phi\cdot\nabla_{\mathbf{x}}\,u_1\mathrm{d}\phi = 0. \tag{3.28}$$

Comparing orders of ε and using (3.27), we can derive an expression for u_1 in terms of u_0,ρ_0,ρ_1,

$$\begin{aligned}u_1 =& \frac{1}{2\pi}\rho_1 - \gamma\,\frac{\mathbf{e}_\phi\cdot\nabla_{\mathbf{x}}u_0}{\lambda_1+\lambda_2\,K^d*\rho_0}\\ &+\rho_0\,\frac{\lambda_3}{\lambda_1+\lambda_2\,K^d*\rho_0}\int_{-\pi}^{\pi}B[\rho_0](\mathbf{x},\phi',\phi)-B[\rho_0](\mathbf{x},\phi,\phi')\,\mathrm{d}\phi'.\end{aligned}$$

Substituting into (3.28), we arrive at a macroscopic drift-diffusion equation of the form

$$\partial_t\rho_0 = \nabla_{\mathbf{x}}\,.\,(D[\rho_0]\,\nabla_{\mathbf{x}}\rho_0 - \rho_0\mathbf{k}[\rho_0])\,,$$

where the macroscopic diffusion coefficient $D[\rho_0] = \gamma^2/(2(\lambda_1+\lambda_2\,K^d*\rho_0))$ and the social flux

$$\mathbf{k}[\rho_0] = \frac{\lambda_3\,\gamma}{\lambda_1+\lambda_2\,K^d*\rho_0}\int_{-\pi}^{\pi}\int_{-\pi}^{\pi}(\mathbf{e}_\phi-\mathbf{e}_{\phi'})\,B[\rho_0](\mathbf{x},\phi',\phi)\mathrm{d}\phi'\mathrm{d}\phi \tag{3.29}$$

are both described in terms of microscopic quantities. In the context of collective behaviour of animal groups, we make two further assumptions:

(i) Individuals can process information in a similar manner for all three types of social interactions:

$$G_{al}(\vartheta) = G_r(\vartheta) = G_a(\vartheta) =: G(\vartheta) \quad \forall\vartheta\,.$$

(ii) Individuals have symmetric perception, in other words, they can process information equally well from left and right. Then the turning probability function ω is bisymmetric,

$$\omega(-\alpha,-\beta) = \omega(\alpha,\beta)\,,$$

which implies symmetry of the signal response function G.

Under these assumptions, the first term of the social response functions $B_j[u]$ in (3.24) and (3.25) cancels when substituted into the social flux (3.29). The second term contains the factor λ_2^0 which cancels with λ_3 in (3.29), leaving us with a factor of λ_2 in the social flux. Using (3.27), we can simplify the social flux even further and obtain the drift-diffusion equation

$$\partial_t\rho = \nabla_{\mathbf{x}}\,.\,(D_0[\rho]\nabla_{\mathbf{x}}\rho) - \nabla_{\mathbf{x}}\,.\,(\rho\,\mathbf{k}[\rho])\,, \tag{3.30a}$$

$$D_0[\rho] = \frac{\gamma^2}{2(\lambda_1+\lambda_2\,K^d*\rho)}\,, \tag{3.30b}$$

$$\mathbf{k}[\rho](\mathbf{x},t) = \frac{\lambda_2\pi\gamma}{\lambda_1+\lambda_2\,K^d*\rho}\left(q_r\,K_r^d(\mathbf{x})\,\frac{\mathbf{x}}{|\mathbf{x}|} - q_a\,K_a^d(\mathbf{x})\,\frac{\mathbf{x}}{|\mathbf{x}|}\right)*\rho\,. \tag{3.30c}$$

For notational convenience, we dropped the zero in ρ_0. Note that this equation is similar to the 1D drift-diffusion equation (2.15) obtained via the parabolic limit for linear social interactions.

Remark 3.4. *Integrating the 2D scaling assumption (3.22), we have*

$$\lambda(\mathbf{x},\phi') = \lambda_1 + \lambda_2\, K^d * \rho(\mathbf{x},t) + \varepsilon\,\lambda_3 \int B[u](\mathbf{x},\phi',\phi)\mathrm{d}\phi\,,$$

which is a particular case of the 1D scaling assumption (2.14). More precisely, the 2D turning rate $\lambda(\mathbf{x},\phi')$ corresponds to (2.2) on the projected velocity set $\{0,\pi\}$, with a linear turning function $f(z)=z$ and with the non-directed and directed communication mechanisms given by

$$\begin{aligned} y_N[u] =& K^d * \rho(\mathbf{x},t),\\ y_D^{\pm}[u^+,u^-] =& \frac{G(0)+G(\pi)}{2} K^d * \rho(\mathbf{x},t)\\ &\mp \lambda_2^0 \int_{\mathbb{R}} q_{al} K_{al}^d(\mathbf{x}-\mathbf{s})\left(u^+(s_1,t)-u^-(s_1,t)\right)\mathrm{d}s_1\\ &\mp \lambda_2^0 \int_{-\infty}^{x_1} \left(q_r K_r^d(\mathbf{x}-\mathbf{s}) - q_a K_a^d(\mathbf{x}-\mathbf{s})\right)\rho(\mathbf{s},t)\mathrm{d}s_1\\ &\pm \lambda_2^0 \int_{x_1}^{\infty} \left(q_r K_r^d(\mathbf{x}-\mathbf{s}) - q_a K_a^d(\mathbf{x}-\mathbf{s})\right)\rho(\mathbf{s},t)\mathrm{d}s_1\,, \end{aligned} \tag{3.31}$$

where $\mathbf{x}=(x_1,0)$, $\rho(\mathbf{x},t)=u^+(x_1,t)+u^-(x_1,t)=u(x_1,t)$, and where we used assumptions (i) and (ii). Hence, model (2.1)-(2.14) with communication mechanism (3.31) corresponds exactly to the 2D non-local kinetic model (3.18)-(3.22)-(3.24)-(3.25). This means, for instance, that the macroscopic 2D model (3.30) reduces to the heat equation for $\lambda_2=0$, which is not the case in the parabolic limit (2.15) of the corresponding 1D hyperbolic model (2.1) with the turning rates given by (2.2). In fact, our 2D scaling assumption $g_j(\vartheta)=\lambda_2^0+\varepsilon G_j(\vartheta)$, $j=al,r,a$, introduces the relative strength of directed and non-directed turning kernels into the expression of the social response function $B[u]$, which is responsible for the appearance of a factor λ_2 in the drift of the macroscopic 2D model (3.30).

Remark 3.5. *For some particular choices of distance kernels, the limiting parabolic model (3.30) can be reduced to well known equations. Let us assume, for example, that the distance kernels are constant on the whole domain,*

$$K_j^d(\mathbf{x}) = 1, \quad j=al,a,r\,. \tag{3.32}$$

This assumption corresponds to a setting in which individuals interact equally well with all other individuals present in the entire domain. This is true locally for example if we have many individuals packed in little space. Under assumption (3.32) together with $\lambda_1=0$, model (3.30) simplifies to

$$\partial_t\rho = \frac{C_0}{\lambda_2}\,\Delta\rho + C_1\,\nabla\cdot\left(\rho\int_{\mathbb{R}^2}\mathbf{e}_\psi\rho(\mathbf{s})\,\mathrm{d}\mathbf{s}\right)\,,$$

where

$$\mathbf{e}_\psi = \frac{\mathbf{s}-\mathbf{x}}{|\mathbf{s}-\mathbf{x}|}\,,$$

and C_0, C_1 are constants depending only on γ, q_{al}, q_a, q_r and the total mass $\int \rho \, \mathrm{d}\mathbf{x}$. If $q_a = q_r$, then the attraction and repulsion forces cancel out ($C_1 = 0$) and we obtain the heat equation. Let us henceforth assume $q_a \neq q_r$. Furthermore, we can write the social flux as

$$\mathbf{k}[\rho] = \nabla W * \rho \,, \tag{3.33}$$

where the interaction potential $W : \mathbb{R}^2 \longrightarrow \mathbb{R}$ is given by $W(\mathbf{x}) = C_1|\mathbf{x}|$. In fact, for the more general distance kernels (3.21) the social flux can also be written in the form (3.33), with the interaction potential W behaving like $|\mathbf{x}|$ close to zero and decaying exponentially fast as $|\mathbf{x}| \longrightarrow \infty$ (e.g. Morse potentials). Therefore, we recover the diffusive aggregation equation

$$\partial_t \rho = \Delta \rho + \nabla \,.\, (\rho \, (\nabla W * \rho)) \,, \tag{3.34}$$

which models the behaviour of particles interacting through a pairwise potential while diffusing with Brownian motion. This type of equation has received a lot of attention in recent years because of its ubiquity in modelling aggregation processes, such as collective behaviour of animals [237, 240, 28, 114] and bacterial chemotaxis [41] (see also the references therein). In fact, model (3.34) is part of the family of aggregation-diffusion equations presented in Part I. Here, we have linear diffusion $m = 1$ and a non-singular interaction kernel with power $k = 1$ (using the notation of Part I). This means (3.34) falls into the diffusion-dominated regime discussed in Chapter 4, see Definition 3.1 in Chapter 1.

3.2 Grazing collision limit

In the following, we consider another type of scaling that leads to parabolic equations, by focusing on the case where individuals turn only a small angle upon interactions with neighbours. This is biologically realistic as, for example, many migratory birds follow favourable winds or magnetic fields [244] and social interactions with neighbours might not have a considerable impact on directional changes of individuals. The so-called *grazing collisions*, i.e. collisions with small deviation, correspond to this assumption. In this case, we show that the Boltzmann-type equation (3.18) can be reduced to a Fokker–Planck equation with non-local advective and diffusive terms in the orientation space.

For simplicity, the 2D kinetic model (3.18) can be re-written as

$$\frac{\partial u}{\partial t} + \gamma e_\phi \nabla_x u = -Q^-[u] + Q^+[u,u]$$

with

$$Q^-[u] = Q_r^-[u] + Q_a^-[u] + Q_{al}^-[u], \quad Q^+[u,u] = Q_r^+[u,u] + Q_a^+[u,u] + Q_{al}^+[u,u] \,,$$
$$Q_j^-[u] = \lambda_j(x,\phi)u, \quad Q_j^+[u,u] = \int_{-\pi}^{\pi} T_j(x,\phi',\phi)u(x,\phi',t)d\phi' \,, \quad \text{for } j = r, al, a.$$

Let us focus for now only on the alignment interactions, the analysis of attraction and repulsion interactions is similar. The grazing collision assumption suggests that we can rescale the probability of re-orientation as follows:

$$\omega_{al}^{\varepsilon}\left(\phi-\phi',\phi-\theta\right)=\frac{1}{\varepsilon}g_{\varepsilon}\Big(\frac{\phi-\phi'-\varepsilon R(\phi-\theta)}{\varepsilon}\Big)\,.$$

Here, the parameter ε is related to the small re-orientation angle following interactions with neighbours moving in direction θ. If we denote by $\varepsilon\beta=\phi-\phi'-\varepsilon R(\phi-\theta)$, then since ω_ε integrates to 1, we obtain:

$$1=\int_{-\pi}^{\pi}\omega_{al}^{\varepsilon}(\phi-\phi',\phi-\theta)d\phi'=\int_{-\pi+\phi-R(\phi-\theta)}^{\pi+\phi-R(\phi-\theta)}g_{\varepsilon}(\beta)d\beta=\int_{-\pi}^{\pi}g_{\varepsilon}(\beta)d\beta\,,$$

by periodicity of g_ε.

Generally, when an interaction kernel in the Boltzmann equation presents a singularity point, the troubles are avoided by considering a weak formulation of the Boltzmann operator [173, 87]. Expanding $Q_{al}[u]:=-Q_{al}^{-}[u]+Q_{al}^{+}[u,u]$, we obtain for all $\psi\in C_c^\infty([-\pi,\pi])$,

$$\begin{aligned}\int_{-\pi}^{\pi}Q_{al}[u]\psi(\phi)d\phi=\eta_{al}\int_{-\pi}^{\pi}\Big(\frac{1}{2\pi}\rho(x,t)-u(x,\phi,t)\Big)\psi(\phi)d\phi\\+\int_{-\pi}^{\pi}\int_{-\pi}^{\pi}\int_{\mathbb{R}^2}\lambda_3 q_{al}K_{al}^{d}(x-s)K_{al}^{0}(\theta,\phi)u(x,\phi,t)u(s,\theta,t)\cdot\\\int_{-\pi}^{\pi}\omega_{al}^{\varepsilon}(\phi-\phi',\phi-\theta)\big[\psi(\phi')-\psi(\phi)\big]d\phi' ds d\theta d\phi\,.\end{aligned}\tag{3.36}$$

By substituting $\phi'=\phi-\varepsilon\beta-\varepsilon R(\phi-\theta)$ into the $\psi(\phi')$ term in (3.36), and then expanding in Taylor series about ϕ we obtain:

$$\begin{aligned}\int_{-\pi}^{\pi}\omega_{al}^{\varepsilon}(\phi-\phi',\phi-\theta)\Big[\psi(\phi')-\psi(\phi)\Big]d\phi'\approx\\\int_{-\pi}^{\pi}g_{\varepsilon}(\beta)\Big[\big(-\varepsilon\beta-\varepsilon R(\phi-\theta)\big)\frac{\partial\psi}{\partial\phi}+\frac{\varepsilon^2}{2}\big(\beta+R(\phi-\theta)\big)^2\frac{\partial^2\psi}{\partial\phi^2}\Big]d\beta\,.\end{aligned}$$

Equation (3.36) can thus be approximated by

$$\begin{aligned}\int_{-\pi}^{\pi}Q_{al}[u]\psi(\phi)d\phi=\eta_{al}\int_{-\pi}^{\pi}\Big(\frac{1}{2\pi}\rho(x,t)-u(x,\phi,t)\Big)\psi(\phi)d\phi\\-\int_{-\pi}^{\pi}\frac{\partial}{\partial\phi}\Big[u(x,\phi,t)C_{al}^{\varepsilon}[u,x,\phi]\Big]\psi(\phi)d\phi\\+\int_{-\pi}^{\pi}\frac{\partial^2}{\partial\phi^2}\Big[u(x,\phi,t)D_{al}^{\varepsilon}[u,x,\phi]\Big]\psi(\phi)d\phi\end{aligned}$$

with the definitions

$$\begin{aligned}C_{al}^{\varepsilon}[u,x,\phi]&:=\int_{-\pi}^{\pi}\int_{\mathbb{R}^2}\lambda_3 q_{al}K_{al}^{d}(x-s)K_{al}^{0}(\theta,\phi)A_{al}^{\varepsilon}(\phi-\theta)u(s,\theta,t)d\theta ds,\\D_{al}^{\varepsilon}[u,x,\phi]&:=\int_{-\pi}^{\pi}\int_{\mathbb{R}^2}\lambda_3 q_{al}K_{al}^{d}(x-s)K_{al}^{0}(\theta,\phi)B_{al}^{\varepsilon}(\phi-\theta)u(s,\theta,t)d\theta ds\,,\end{aligned}$$

where

$$A^{\varepsilon}_{al}(\phi-\theta) := -\varepsilon\big(M_1(\varepsilon)+M_0(\varepsilon)R(\phi-\theta)\big)\,,$$
$$B^{\varepsilon}_{al}(\phi-\theta) := \frac{\varepsilon^2}{2}\big(M_2(\varepsilon)+2M_1(\varepsilon)R(\phi-\theta)+M_0(\varepsilon)R(\phi-\theta)^2\big)\,,$$

and $M_n(\varepsilon) := \int_{-\pi}^{\pi}\beta^n g_\varepsilon(\beta)\,d\beta$, $n=0,1,2$, denote the moment generating functions of $g_\varepsilon(\beta)$. In a similar manner we can approximate the attractive and repulsive non-local terms:

$$\begin{aligned}\int_{-\pi}^{\pi} Q_{r,a}[u]\psi(\phi)d\phi = \eta_{r,a}\int_{-\pi}^{\pi}\left(\frac{1}{2\pi}\rho(x,t)-u(x,\phi,t)\right)\psi(\phi)d\phi\\ -\int_{-\pi}^{\pi}\frac{\partial}{\partial\phi}\Big(u(x,\phi,t)C^{\varepsilon}_{r,a}[u,x,\phi]\Big)\psi(\phi)d\phi\\ +\int_{-\pi}^{\pi}\frac{\partial^2}{\partial\phi^2}\Big(u(x,\phi,t)D^{\varepsilon}_{r,a}[u,x,\phi]\Big)\psi(\phi)d\phi\,,\end{aligned}$$

where

$$\begin{aligned}C^{\varepsilon}_{r,a}[u,x,\phi] &= \int_{-\pi}^{\pi}\int_{\mathbb{R}^2}\lambda_3 q_{r,a}K^d_{r,a}(x-s)K^0_{r,a}(s,x,\phi)A^{\varepsilon}_{r,a}(s,x,\phi)u(s,\theta,t)dsd\theta\,,\\ D^{\varepsilon}_{r,a}[u,x,\phi] &= \int_{-\pi}^{\pi}\int_{\mathbb{R}^2}\lambda_3 q_{r,a}K^d_{r,a}(x-s)K^0_{r,a}(s,x,\phi)B^{\varepsilon}_{r,a}(s,x,\phi)u(s,\theta,t)dsd\theta\,,\\ A^{\varepsilon}_{r,a}(s,x,\phi) &= -\varepsilon(M_1(\varepsilon)M_0(\varepsilon)R(\phi-\psi_s)),\\ B^{\varepsilon}_{r,a}(s,x,\phi) &= \frac{\varepsilon^2}{2}\Big[M_2(\varepsilon)+2M_1(\varepsilon)R(\phi-\psi_s)+M_0(\varepsilon)R(\phi-\psi_s)^2\Big]\,.\end{aligned}$$

Therefore, the kinetic model (3.18) in the strong formulation can be approximated (when individuals turn only by a small angle upon interactions with their neighbours) by the following Fokker–Planck model that contains all three social interactions:

$$\begin{aligned}\frac{\partial u}{\partial t}+\gamma e_\phi\cdot\nabla_x u = \lambda_1\left(\frac{1}{2\pi}\rho(x,t)-u(x,\phi,t)\right)\\ +\frac{\partial}{\partial\phi}\Big[-uC^{\varepsilon}[u,x,\phi]+\frac{\partial}{\partial\phi}(uD^{\varepsilon}[u,x,\phi])\Big]\,,\end{aligned}\tag{3.37}$$

with $\lambda_1=\eta_a+\eta_{al}+\eta_r$, and

$$\begin{aligned}C^{\varepsilon}[u,x,\phi] &= C^{\varepsilon}_{al}[u,x,\phi]+C^{\varepsilon}_{r}[u,x,\phi]+C^{\varepsilon}_{a}[u,x,\phi]\,,\\ D^{\varepsilon}[u,x,\phi] &= D^{\varepsilon}_{al}[u,x,\phi]+D^{\varepsilon}_{r}[u,x,\phi]+D^{\varepsilon}_{a}[u,x,\phi]\,.\end{aligned}$$

While non-local 2D Fokker–Planck models have been introduced in the past years in connection with self-organised aggregations, the majority of these models consider local diffusion [123, 12]. If we neglect the ε^2 terms (i.e., $B^{\varepsilon}\approx 0$) and assume $\lambda_1=0$, equation (3.37) reduces to a Vlasov-type flocking equation:

$$\frac{\partial u}{\partial t}+\gamma e_\phi\cdot\nabla_x u+\frac{\partial}{\partial\phi}\Big[uC^{\varepsilon}[u,x,\phi]\Big]=0\,.$$

These type of models have been previously derived from individual-based models (Vicsek or Cucker–Smale models) with or without noise [123, 179, 87].

4 Asymptotic preserving methods for 1D models

The kind of diffusion asymptotics we employed in the previous sections have been numerically investigated in [88] using so-called asymptotic preserving (AP) schemes. The AP methods, which improve the scheme already proposed in [169], are a fully explicit variation of the methods introduced in [201, 202]. They are a powerful tool to investigate how patterns are preserved in the parabolic limit by providing numerical schemes for all intermediate models of a scaling process given some scaling parameter $\varepsilon > 0$, and naturally produce a suitable numerical method for the limiting model as $\varepsilon \to 0$. Here, we apply these schemes only to the 1D models introduced in Section 2, since the numerics become much more complex in two dimensions. Taking advantage of our understanding of the limit process, we base our scheme on a splitting strategy with a convective-like step involving the transport part of the operator and an explicitly solvable ODE step containing stiff sources (see Section 4.2).

4.1 Odd and even parity

We consider the 1D kinetic model (2.1) written as an odd-even decomposition,

$$\begin{cases} \partial_t r + \gamma \partial_x j &= 0\,, \\ \partial_t j + \gamma \partial_x r &= -2\lambda^+[r,j](r+j) + 2\lambda^-[r,j](r-j)\,, \end{cases}$$

with the equilibrium part (macro part/even part) r and the non-equilibrium part (micro part/odd part) j given by

$$r(x,t) = \frac{1}{2}\left(u^+(x,t) + u^-(x,t)\right)\,, \quad j(x,t) = \frac{1}{2}\left(u^+(x,t) - u^-(x,t)\right)\,.$$

Under scaling assumption (2.10) for (2.2), this model reads in the new variables $x = \tilde{x}/\varepsilon, t = \tilde{t}/\varepsilon^2$ as follows:

$$\begin{aligned} \varepsilon\partial_{\tilde{t}}\tilde{r} + \gamma\partial_{\tilde{x}}\tilde{j} &= 0 \\ \varepsilon\partial_{\tilde{t}}\tilde{j} + \gamma\partial_{\tilde{x}}\tilde{r} &= \tilde{r}\lambda_3(f[\tilde{y}^-] - f[\tilde{y}^+]) \\ &\quad - \frac{1}{\varepsilon}\tilde{j}\left(2\lambda_1 + 4\varepsilon\lambda_2 f\left(\tilde{K}^N * \tilde{r}\right) + \varepsilon\lambda_3(f[\tilde{y}^+] + f[\tilde{y}^-])\right)\,, \end{aligned}$$

where $\tilde{K}^N(\tilde{x}) = \frac{1}{\varepsilon}K^N(\frac{\tilde{x}}{\varepsilon})$. Rearranging the terms and dropping "$\sim$" for notational convenience, we obtain for r and $J := \frac{1}{\varepsilon}j$:

$$\begin{cases} \partial_t r + \gamma\partial_x J = 0 \\ \partial_t J + \gamma\partial_x r = \dfrac{1}{\varepsilon^2} r\lambda_3(f[y^-] - f[y^+]) + \left(1 - \dfrac{1}{\varepsilon^2}\right)\gamma\partial_x r \\ \qquad\qquad - \dfrac{1}{\varepsilon^2} J\left(2\lambda_1 + 4\varepsilon\lambda_2 f\left(K^N * r\right) + \varepsilon\lambda_3(f[y^+] + f[y^-])\right)\,. \end{cases} \tag{4.38}$$

4.2 Operator splitting

We can now employ an operator splitting method on (4.38), separating the stiff source part, which can be treated by an implicit Euler method, and the transport part, which we can solve by an explicit method such as upwinding:

1. **Stiff source part:**

$$\begin{aligned}\partial_t r &= 0,\\ \partial_t J &= \frac{1}{\varepsilon^2} r\lambda_3(f[y^-] - f[y^+]) + \left(1 - \frac{1}{\varepsilon^2}\right)\gamma\partial_x r\\ &\quad -\frac{1}{\varepsilon^2} J\left(2\lambda_1 + 4\,\varepsilon\,\lambda_2 f\left(K^N * r\right) + \varepsilon\,\lambda_3(f[y^+] + f[y^-])\right).\end{aligned} \tag{4.39}$$

2. **Transport part:**

$$\begin{aligned}\partial_t r + \gamma\,\partial_x J &= 0,\\ \partial_t J + \gamma\,\partial_x r &= 0\,.\end{aligned} \tag{4.40}$$

It can easily be verified that, in the limit $\varepsilon \to 0$, we recover indeed the macroscopic model (2.11) for $u = 2r$.

4.3 Alternated upwind discretisation

In the following, we are interested in the numerical implementation of model (2.1) with the turning rates (2.2) depending on a non-linear turning function f without a non-directed density-dependent turning term (i.e. $\lambda_2 = 0$). As shown in Section 2.1, in this case, the parabolic limit yields the drift-diffusion equation (2.11)

$$\partial_t u = D_0\partial_{xx} u - S_0\partial_x\left(u(f^-[u] - f^+[u])\right),$$

with $D_0 = \gamma^2/(2\lambda_1)$ and $S_0 = \lambda_3\gamma/(2\lambda_1)$. Note the shorthand $f^\pm[u] = f(y_D^\pm[u])$. We propose an alternated upwind discretisation with the even part r evaluated at full grid points $x_i = i\,\Delta x$, and the odd part J evaluated at half grid points $x_{i+\frac{1}{2}} = (i+\frac{1}{2})\,\Delta x$. First, we discretise the stiff source part (4.39) using an implicit Euler discretisation and respecting the direction of the drift. We obtain an explicit expression for J^*,

$$\begin{aligned}J^*_{i+\frac{1}{2}} &= \frac{\varepsilon^2 J^n_{i+\frac{1}{2}} + \gamma\frac{\Delta t}{\Delta x}\left(\varepsilon^2 - 1\right)\left(r^n_{i+1} - r^n_i\right)}{\varepsilon^2 + 2\lambda_1\Delta t + \varepsilon\lambda_3\Delta t\left(f^+[r^n] + f^-[r^n]\right)_{i+\frac{1}{2}}}\\ &\quad + \frac{\lambda_3\Delta t\left((f^-[r^n] - f^+[r^n])^+_{i+\frac{1}{2}}\, r^n_i + (f^-[r^n] - f^+[r^n])^-_{i+\frac{1}{2}}\, r^n_{i+1}\right)}{\varepsilon^2 + 2\lambda_1\Delta t + \varepsilon\lambda_3\Delta t\left(f^+[r^n] + f^-[r^n]\right)_{i+\frac{1}{2}}},\end{aligned}$$

with $r^* = r^n$. Here, r^n and J^n are the numerical solutions of r and J at time $t_n = n\Delta t$. We use the $*$-notation for half steps in time. Since J is evaluated at half grid point, the discretisation of the transport part (4.40) can be chosen independently of the sign of the drift,

$$\frac{1}{\Delta t}\left(r_i^{n+1} - r_i^*\right) + \frac{1}{\Delta x}\left(J^*_{i+\frac{1}{2}} - J^*_{i-\frac{1}{2}}\right) = 0\,,$$
$$\frac{1}{\Delta t}\left(J^{n+1}_{i+\frac{1}{2}} - J^*_{i+\frac{1}{2}}\right) + \frac{1}{\Delta x}\left(r^*_{i+1} - r^*_i\right) = 0\,.$$

Taking the limit $\varepsilon \to 0$ in the expression for $J^*_{i+\frac{1}{2}}$ and substituting into the first equation of the transport part, we obtain the following discretisation of the one-dimensional macroscopic model (2.11):

$$\begin{aligned}\frac{u_i^{n+1} - u_i^n}{\Delta t} &= \frac{D_0}{(\Delta x)^2}\left(\partial^{(c)}_{xx} u^n\right)_i \\ &- \frac{S_0}{\Delta x}\left(u_i^n \left(f^-[r^n] - f^+[r^n]\right)^+_{i+\frac{1}{2}} - u^n_{i-1}\left(f^-[r^n] - f^+[r^n]\right)^+_{i-\frac{1}{2}}\right) \\ &- \frac{S_0}{\Delta x}\left(u^n_{i+1}\left(f^-[r^n] - f^+[r^n]\right)^-_{i+\frac{1}{2}} - u_i^n\left(f^-[r^n] - f^+[r^n]\right)^-_{i-\frac{1}{2}}\right)\,.\end{aligned}$$

Here, $\partial^{(c)}_{xx} u^n$ denotes the standard central difference discretisations. This illustrates how the choice of discretisation for (4.39) directly induces a discretisation of model (2.11). We will now use this scheme to investigate how some of the patterns observed in model (2.1)-(2.2) change as $\varepsilon \to 0$.

Remark 4.1. *The stability restriction for the proposed AP scheme is less clear. We can expect that the time steps size Δt needs to be sufficiently small, with an upper stability bound depending on the space step size Δx, the diffusion coefficient D_0, and the social interaction kernels via the terms $K^N * u$ and $f^{\pm}[u]$.*

4.4 Simulation results

In Section 2.2 we have seen that for model M4, the two Hopf bifurcations that occurred for the k_4 and k_5 modes have disappeared as $\varepsilon \to 0$. In this Section, we start with a rotating wave pattern (i.e., travelling pulses) that arises at $\varepsilon = 1$ through a Hopf bifurcation (i.e., for the same parameter values as in Figure 6.4: $q_a = 1.545$, $q_r = 2.779$, $\lambda_1 = 0.2$, $\lambda_2 = 0$, $\lambda_3 = 0.9$, $\gamma = 0.1$, $A = 2$). Then, we investigate numerically what happens with this pattern as $\varepsilon \to 0$. The initial conditions for the simulations are random perturbations of maximum amplitude 0.2 of the spatially homogeneous steady state $u^* = A/2 = 1$. We start with $\varepsilon = 1$, and run the numerical simulations up to $t = 1000$. Then we decrease ε, and choose the new initial condition to be the final solution obtained with the previous ε value.

Figure 6.6(a) shows the amplitude of the patterns obtained when $\varepsilon \in [0, 1]$, for the particular parameter values mentioned before. Since some of these amplitudes show time-oscillations between different values, we graph their maximum and minimum values for each ε. As we decrease ε from 1.0 towards 0.64 (region III), the amplitude undergoes some very small temporal oscillations (see

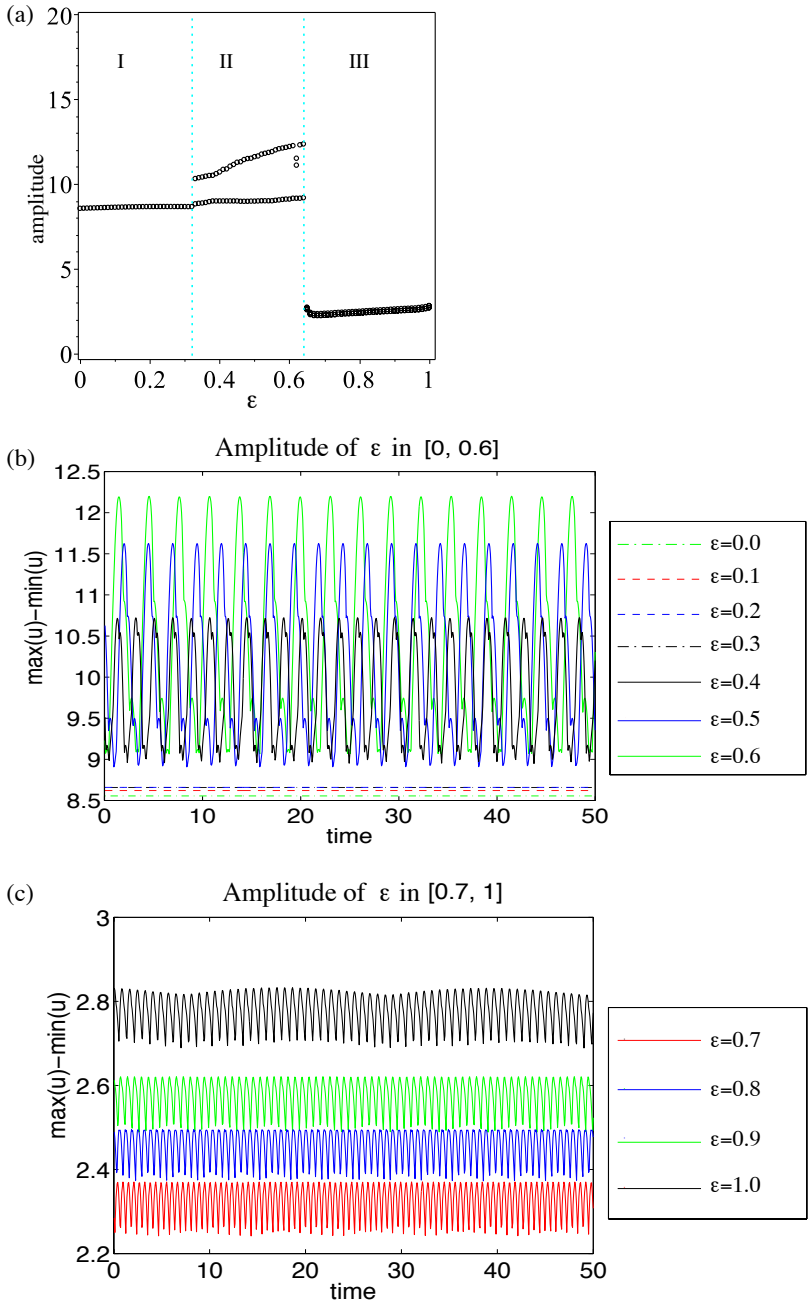

Figure 6.6: The amplitude and density profile of the patterns obtained for $q_a = 1.545$, $q_r = 2.779$, $q_{al} = 0$, $\lambda_1 = 0.2$, $\lambda_2 = 0$, $\lambda_3 = 0.9$ with model M4, as ε is decreased from 1.0 to 0.0. (a) Bifurcation diagram for the amplitude of the patterns as a function of ε. For $\varepsilon \leqslant 0.32$ (region I), the amplitude is constant. For $\varepsilon \in (0.32, 0.64)$ (region II) the amplitude oscillates between two different values. For $\varepsilon \geqslant 0.64$ (region III) there are some very small oscillations in the amplitude, however due to the scale of the plot these oscillations are almost unobservable. (b) Amplitude of the patterns for $\varepsilon \in [0, 0.6]$ and for $t \in (0, 50)$. We show here $\max_{x\in[0,L]} u(x,t) - \min_{x\in[0,L]} u(x,t)$, with $u = u^+ + u^-$. (c) Amplitude of the patterns for $\varepsilon \in [0.7, 1.0]$ and for $t \in (0, 50)$.

also panel (c)), corresponding to the rotating wave patterns (with a small time-modulation) shown in Figure 6.7(c). For $\varepsilon \in (0.32, 0.64)$ (region II), the amplitude oscillates between two large values. This corresponds to the "inside-group" zigzagging behaviour shown in Figure 6.7(b) near $x = 6$, where the group as a whole does not move in space but individuals inside the group move between the left and right edges of the group. We also note a period-doubling bifurcation at $\varepsilon = 0.61$ (region II, Figure 6.6(a); see the two dots that appear between the main branches), which leads to a slight decrease in the amplitude. Finally, as ε is decreased below 0.32 (region I), the movement inside the group is lost and the pattern is described by stationary pulses with fixed amplitude (see Figure 6.6(a) and Figure 6.7(a)). Figures 6.6(b),(c) show the time-variation of the amplitudes of the spatial and spatio-temporal patterns obtained for $\varepsilon \in [0, 1]$. Figures 6.7(a')-(c') show the density profiles of the patterns observed in regions I-III.

Because the macro-scale models ($\varepsilon = 0$) seem to exhibit stationary pulses (as shown in Figure 6.7(a)), we now start with these stationary pulses (for $\varepsilon = 1$) and investigate whether they change in any way as $\varepsilon \to 0$. We focus here on model M2 (see Figure 6.3). Figure 6.8 shows the amplitude of the stationary pulses obtained with model M2 in a particular parameter region ($q_a = 2.2, q_r = 0.93$, $q_{al} = 0$; see also Figure 6.4), as we decrease the scaling parameter ε. We observe that in this case, the scaling does not affect the patterns or their amplitudes.

Remark 4.2. *Note that the rotating wave pattern shown in Figure 6.7(c) for $\varepsilon = 1$ is obtained near a Hopf/steady-state bifurcation (with k_5 the Hopf wavenumber), and hence the 5 rotating peaks that form this pattern. However, as $\varepsilon \to 0$, the wavenumber k_3 seems to become unstable (hence the 3 peaks for the patterns shown in Figure 6.7(a),(b)), even if the dispersion relation shown in Figure 6.4(b) suggests that k_3 should be stable.*

5 Summary and discussion

In this chapter, we investigated the connections between a class of 1D and 2D non-local kinetic models and their limit macroscopic models for self-organised biological aggregations. The non-locality of these models was the result of the assumptions that individuals can interact with neighbours positioned further away, but still within their perception range. To simplify the kinetic models that incorporate microscopic-level interactions (such as individuals' speed and turning rates), we focused on two types of scalings, namely a parabolic and a grazing collision limit, which lead to parabolic models described in terms of average speed and average turning behaviour. We showed that while for the kinetic models the non-local interactions influence the turning rates (i.e., individuals turn to approach their neighbours, to move away from them or to align with them), for the limit parabolic models the non-local interactions influence the dispersion and the drift of the

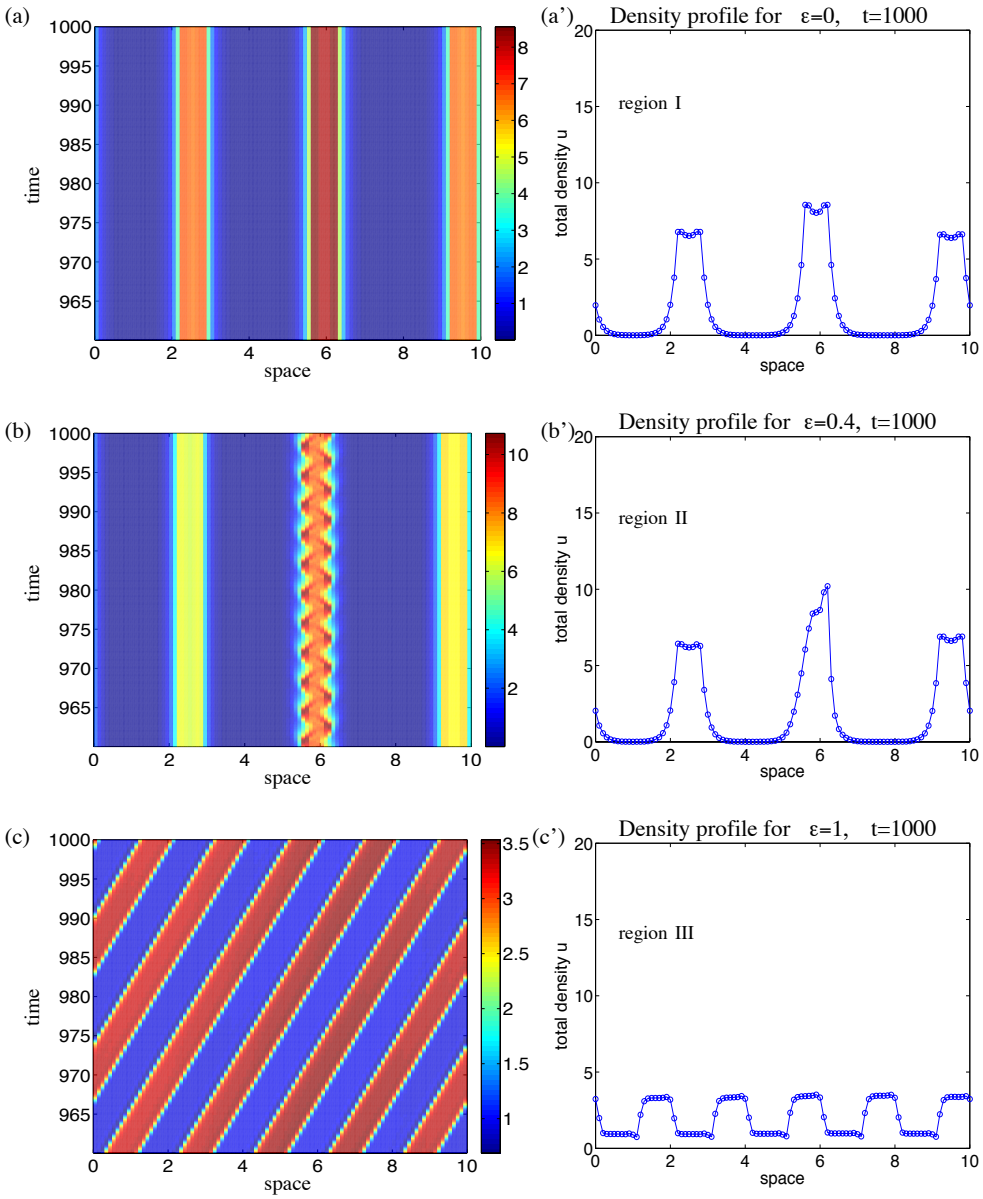

Figure 6.7: The spatial and spatio-temporal patterns obtained with model M4, for $q_a = 1.545$, $q_r = 2.779$, $q_{al} = 0$, $\lambda_1 = 0.2$, $\lambda_2 = 0$, $\lambda_3 = 0.9$, as ε is decreased from 1 to 0, using model M4. (a) Stationary pulse patterns observed in region I: $\varepsilon \leqslant 0.32$; (b) "Inside-group" zigzag patterns observed in region II: $\varepsilon \in (0.32, 0.64)$; (c) Rotating wave (travelling pulse) patterns observed in region III: $\varepsilon \geqslant 0.64$. Panels (a')-(c') show the density profiles corresponding to patterns in panels (a)-(c), at time $t = 1000$.

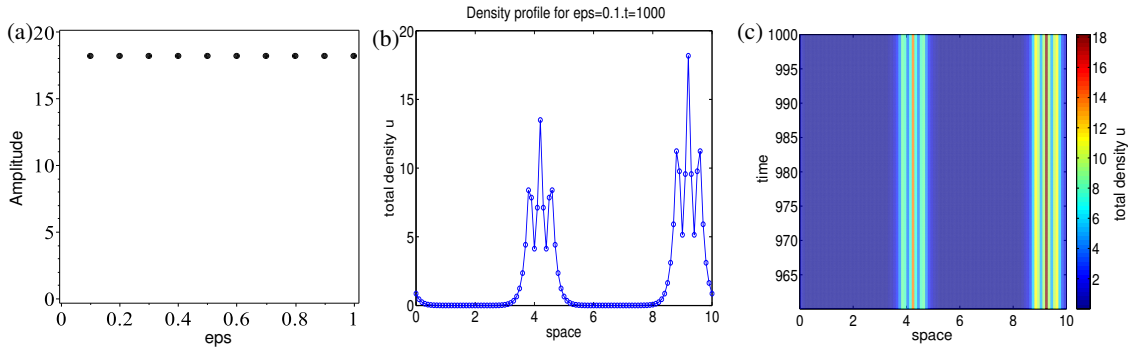

Figure 6.8: The amplitude and density of the patterns obtained for model M2 with $q_a = 2.2$, $q_r = 0.93$, $q_{al} = 0$, $\lambda_1 = 0.2$, $\lambda_2 = 0$, $\lambda_3 = 0.9$, as ε is decreased from 1 to 0. (a) Bifurcation diagram for the amplitude of the patterns as a function of ε. (b) Density profile for the stationary patterns. (c) Time-space plot of the density.

aggregations. In particular, we showed that the assumption that individuals can turn randomly following the non-directional perception of neighbours around them leads, in the macroscopic scaling, to density-dependent diffusion. Moreover, this diffusion decreased with the increase in the population density. Biologically, this means that larger animal groups are less likely to spread out. This phenomenon has been observed for various species. For example, studies have shown that aggregations of locusts [55] or ants [21] can persist only if the number of individuals is above a certain threshold.

The introduction in (2.2) of the term y_N describing random non-directional turning (which generalised the turning rates in [147]) was required by the comparison of the parabolic limit models in 1D and 2D. In particular, the 2D parabolic limit lead to the natural appearance of this term, which is absent from the 1D parabolic model. Therefore, to obtain similar parabolic models in 1D and 2D, we had to explicitly add y_N in equation (2.2). This suggests that even if the 2D model (3.18) can be reduced to a special case of the 1D model (2.1) (as shown in [153]) there are more subtle differences between these non-local 1D and 2D models. These differences can impact the types of patterns displayed by the 2D models – an aspect that would be interesting to study in the future.

Next, we investigated how two types of patterns (i.e., travelling and stationary aggregations) displayed by the 1D kinetic models, were preserved in the limit to macroscopic parabolic models. To this end, we first investigated the local stability of spatially homogeneous patterns characterised by individuals spread evenly over the domain, and showed that local Hopf bifurcations are lost in the parabolic limit. These Hopf bifurcations give rise to travelling aggregations (i.e., rotating waves). We then tested this observation numerically, with the help of asymptotic preserving methods. We started with a rotating wave pattern obtained near a Hopf/Steady-state bifurcation for $\varepsilon = 1$ (1D kinetic model; see Figure 6.7(c)), and studied numerically how does this pattern change

when $\varepsilon \to 0$ (1D parabolic model; see Figure 6.7(a)). By graphing in Figure 6.6(a) the amplitude of the resulting patterns as the scaling parameter ε is decreased from $\varepsilon = 1$ to $\varepsilon = 0$, we showed that there were two major transitions. The first transition occurred around $\varepsilon = 0.64$, when the travelling (rotating) groups stopped moving. We note, however, that while the group as a whole was stationary, the individuals inside the group were still moving between the left- and right-edges of the group, leading to an "inside-group" zigzagging behaviour. The second transition occurred around $\varepsilon = 0.32$, when the individuals inside the groups stopped moving, leading to stationary pulses.

We emphasise here that this study is one of the first in the literature to investigate numerically the transitions between different aggregation patterns, as a scaling parameter ε is varied from values corresponding to mesoscale dynamics ($\varepsilon = 1$) to values corresponding to macroscale dynamics ($\varepsilon = 0$). Understanding these transitions is important when investigating biological phenomena that occur on multiple scales, since it allows us to make decisions regarding the models that are most suitable to reproduce the observed dynamics.

In this study we investigated the preservation of patterns via the 1D parabolic limit, but similar investigations could be performed for the grazing collision limit. Moreover, as shown previously [146], model (2.1) can display many more types of complex spatio-temporal patterns than the two types of patterns investigated here. We focused on travelling and stationary aggregations since our aim here was not to investigate how all possible patterns are preserved by all these different scaling approaches. Rather, it was to show that by taking these asymptotic limits, some patterns could be lost. Therefore, even if the macroscopic models are simpler to investigate, they might not exhibit the same patterns as the kinetic models. Our analysis aimed at highlighting the usefulness of asymptotic preserving numerical methods to understand the bifurcation of the solutions as one investigates the transition from mesoscopic-level to macroscopic-level aggregation dynamics.

Conclusions and Perspectives

Adding to the conclusions drawn in each of the previous chapters, let me comment on the main goals, challenges and results of this thesis, as well as interesting questions and perspectives moving forward.

When tackling the question of long-time asymptotics in Parts I and II, the main challenges we encounter are structural, and the main goal of this thesis is to develop new methods and analytical tools that allow to overcome these challenges. The motivation of our approach is not only to tackle the models considered here, but to derive ideas that can then be applied to different problems with similar structural challenges.

More precisely, in Part I, the main structural challenge is the interplay between non-linear diffusion and non-local interaction creating a rich set of possible behaviour of solutions. The main goal is to obtain a complete characterisation for the asymptotic behaviour of solutions in all possible parameter regimes. This thesis represents a step towards that goal. However, here, we mainly focus on the fair-competition regime and make some investigations in the diffusion-dominated regime. In short, for the fair-competition regime, we see that the behaviour of solutions is very different depending on the sign of k. If $k < 0$ (hence $m > 1$) we observe a dichotomy similar to the critical mass phenomenon of the classical Keller-Segel model, whereas for $k > 0$ (hence $m < 1$), no such criticality exists. For both the fair-competition regime and the diffusion-dominated regime, this family of models has not been analysed for the case of smooth potentials $k > 0$ despite the fact that there are interesting applications for this class of potentials.

To obtain the results presented in Part I, we made use of the special gradient flow structure of the equation, as well as related functional inequalities by making the connection between stationary states of the equation and global minimisers of the associated free energy functional. Further, in one dimension, we used tools from optimal transportation to derive suitable functional inequalities and obtain formally convergence to equilibrium in Wasserstein-2 distance.

Moving forward, I would like to contribute to a more general understanding of the behaviour of solutions for this class of models, and the methods and tools developed in this thesis are the necessary ground work to do that. In particular, the natural candidates amongst which to look for asymptotic profiles are the equilibrium states of the system, and the first logical step towards understanding the asymptotic behaviour of solutions is therefore to study the stationary problem instead, which is our focus in Chapters 2, 3 and 4. Thanks to the analysis of the stationary problem for the fair-competition regime and certain cases of the diffusion-dominated regime presented in Part I, we are now able to advance a more rigorous analysis of the dynamical problem including the time evolution of solutions.

Moreover, looking at the results we obtain, the question of the convexity properties of the energy functionals $\mathcal{F}_k$ and $\mathcal{F}_{k,\textbf{resc}}$ arises. In fact, our analysis indicates that the behaviour of $\mathcal{F}_k$ or $\mathcal{F}_{k,\textbf{resc}}$ is that of convex functionals in certain regimes in the sense that existence of a global minimiser implies its uniqueness (here only proven in one dimension). However, the overall convexity properties of $\mathcal{F}_k$ and $\mathcal{F}_{k,\textbf{resc}}$ are not known and there is certainly a bigger picture to be understood there.

Finally, another important direction of future research is of course to investigate the parameter regimes not considered in this thesis, such as the diffusion-dominated regime for $k > 0$ and the aggregation-dominated regime.

Part II is concerned with a different application and a different equation, however, the question we seek to answer is the same: What is the asymptotic behaviour of solutions? The main goal is the development of a suitable method to show convergence to equilibrium for certain types of kinetic equations where the equilibrium state is not known a priori. We develop such a method in the context of a specific industrial application: modelling part of the production process of non-woven textiles. In the case of a stationary conveyor belt $\kappa = 0$, a hypocoercivity strategy has recently been applied successfully to this kinetic fibre lay-down model to show exponential convergence to equilibrium. In this case, the equilibrium distribution is known explicitly and the collision and transport parts of the operator satisfy the necessary assumptions in an L^2-framework. Adding the movement of the belt however, we encounter two new structural challenges. First of all, we do not know the equilibrium distribution a priori which is usually the case when applying a hypocoercivity method. Secondly, as the perturbation of the moving belt only acts in one direction, it breaks the symmetry of the problem. As a result, even if the existence of an equilibrium F_κ, $\kappa > 0$, could be guaranteed a priori, the collision and transport parts of the operator would not satisfy the good assumptions in $L^2(F_\kappa^{-1}\,\mathrm{d}x\mathrm{d}\alpha)$, and so the standard hypocoercivity strategy cannot be applied.

The good news however is that hypocoercivity as a method is based on a priori estimates and is therefore stable under perturbation. Our approach here is therefore to treat the system as a small

perturbation of the case $\kappa = 0$. In order to control the perturbative term, we introduce not one, but *two* modifications of the 'natural' entropy: 1) we first modify the *space itself* with a well-chosen coercivity weight, then 2) we change the norm with an auxiliary operator following the standard hypocoercivity approach, recovering the missing decay in the space variable. Further, in order to overcome the structural difficulty of the hypocoercivity theory when the equilibrium distribution is not known a priori, we derive a stronger hypocoercivity estimate for the generalised entropy dissipation which holds on any solution and involving an additional mass term, instead of an estimate on fluctuations around the equilibrium only. This hypocoercivity estimate is the key ingredient from which existence and uniqueness of a stationary state can be derived. Applied to the difference between this stationary state and a solution of the same mass, it allows to deduce exponential decay to equilibrium with an explicit rate.

There are several ways in which one could seek to improve the results in Part II. For example, one could try to push the convergence result to larger values of κ using bifurcation techniques. More precisely, for a path $p : \kappa \mapsto F_k$ mapping κ to the unique stationary state F_κ, our results in Part II ensure that p is defined on a small interval $[0, \kappa_0)$ for some $0 < \kappa_0 \ll 1$. It may be possible to extend this interval by showing that the implicit equation $P(\kappa, F_\kappa) = 0$ defining the stationary state F_κ is non-degenerate, i.e. that $\partial_2 P(\kappa, F_\kappa) \neq 0$.

Another future avenue would be to apply the techniques developed here to other models where the global equilibrium is not known a priori.

Finally, Part III is centred around the idea of understanding the relationship between different kinetic and macroscopic models for collective animal behaviour using multiscale analysis. Animal groups are able to form beautiful patterns in the absence of a leader. We want to understand how these patterns arrise and which are the driving factors behind the dynamics. In particular, the goal of Part III is to understand how the different patterns are affected by the choice of modelling scale. Understanding the transitions is important when investigating biological phenomena that occur on multiple scales since it allows us to make decisions regarding the choice of models that are most suitable to reproduce the observed dynamics. To achieve this, we use both analytical and numerical tools.

Firstly, we develop a common framework for a class of collective animal behaviour models, making the connection between non-local kinetic 1D and 2D models with the corresponding macroscopic models via parabolic and grazing collision limits. We observe that if we allow individuals to turn randomly following the non-directional perception of neighbours produces a density-dependent diffusion in the 1D and 2D parabolic limit. This diffusion decreases with increasing population density, a phenomenon which makes biological sense since larger groups are less likely to spread out. Taking a grazing collision limit in 2D, we obtain a Fokker-Planck equation with non-local

advective and diffusive terms in orientation space, whereas the majority of non-local 2D Fokker-Planck models concerned with self-organised aggregations consider local diffusion only. A further simplification of the limiting equation reduces it to a Vlasov-type flocking equation, a class of models that have previously been derived from individual-based models directly (Vicsek or Cucker–Smale models). The analysis of this limiting equation would be another interesting avenue for further research.
Secondly, we investigate how some of the kinetic spatio-temporal patterns are preserved via these scalings using asymptotic preserving numerical methods. We observe that certain patterns such as stationary aggregations are preserved, while others, e.g. moving aggregations, are lost. Therefore, even if the macroscopic models are simpler to investigate, they might not exhibit the same patterns as the kinetic models. This is an important information for choosing a modelling scale that is well adapted to the dynamics one would like to capture. It also serves to demonstrate the usefulness of AP schemes in understanding the bifurcation of solutions as $\varepsilon \to 0$ as they are able to simulate the models on all the intermediate scales as well using one single scheme. AP schemes have only recently been applied to investigate multiscale aspects of biological aggregations and they provide a useful tool for further analysis of pattern formations on different scales.

The process of writing this thesis made me realise that what I am interested in are research questions leading to the development of new methods and tools and that allow for a better understanding of the bigger picture around a certain problem. It is exciting how mathematical ideas can draw connections between very different subject areas and can therefore contribute to advances across disciplines.

Bibliography

[1] R. Alonso, T. Goudon, and A. Vavasseur. Damping of particles interacting with a vibrating medium. *Annales de l'Institut Henri Poincare (C) Non Linear Analysis*, 2017.

[2] W. Alt. Biased random walk models for chemotaxis and related diffusion approximations. *J. Math. Biol.*, 9(2):147–177, 1980.

[3] L. A. Ambrosio, N. Gigli, and G. Savaré. *Gradient flows in metric spaces and in the space of probability measures*. Lectures in Mathematics. Birkhäuser, 2005.

[4] G. E. Andrews, R. Askey, and R. Roy. *Special functions*, volume 71 of *Encyclopedia of Mathematics and its Applications*. Cambridge University Press, Cambridge, 1999.

[5] E. D. Angelis and B. Lods. On the kinetic theory for active particles: a model for tumor-immune system competition. *Mathematical and Computer Modeling*, 47:196–209, 2008.

[6] A. Arnold, J. A. Carrillo, I. Gamba, and C.-w. Shu. Low and high field scaling limits for the vlasov- and wigner-poisson-fokker-planck systems. *Transp. Theory Stat. Phys.*, 30:121–153, 2001.

[7] D. G. Aronson. The porous medium equation. In *Nonlinear diffusion problems (Montecatini Terme, 1985)*, volume 1224 of *Lecture Notes in Math.*, pages 1–46. Springer, Berlin, 1986.

[8] A. A. Arsen'ev and O. E. Buryak. On a connection between the solution of the Boltzmann equation and the solution of the Landau-Fokker-Planck equation. *Mat. Sb.*, 181(4):435–446, 1990.

[9] D. Bakry and M. Émery. Diffusions hypercontractives. In *Séminaire de probabilités, XIX, 1983/84*, volume 1123 of *Lecture Notes in Math.*, pages 177–206. Springer, Berlin, 1985.

[10] D. Balagué, J. A. Carrillo, T. Laurent, and G. Raoul. Dimensionality of local minimizers of the interaction energy. *Arch. Ration. Mech. Anal.*, 209(3):1055–1088, 2013.

[11] D. Balagué, J. A. Carrillo, T. Laurent, and G. Raoul. Nonlocal interactions by repulsive-attractive potentials: radial ins/stability. *Phys. D*, 260:5–25, 2013.

[12] A. Barbaro and P. Degond. Phase transition and diffusion among socially interacting self-propelled agents. *Discrete Cont Dyn Syst B. In Press*, 2013.

[13] C. Bardos, R. Santos, and R. Sentis. Diffusion approximation and computation of the critical size. *Trans. Amer. Math. Soc.*, 284(2):617–649, 1984.

[14] G. I. Barenblatt. On some unsteady motions of a liquid and gas in a porous medium. *Akad. Nauk SSSR. Prikl. Mat. Meh.*, 16:67–78, 1952.

[15] G. I. Barenblatt. *Scaling, self-similarity, and intermediate asymptotics*, volume 14 of *Cambridge Texts in Applied Mathematics*. Cambridge University Press, Cambridge, 1996. With a foreword by Ya. B. Zeldovich.

[16] G. I. Barenblatt and P. Makinen. *Dimensional Analysis*. Gordon & Breach Publishing Group, 1987.

[17] F. Barthe. Inégalités de Brascamp-Lieb et convexité. *C. R. Math. Acad. Sci. Paris*, 324:885–888, 1997.

[18] F. Barthe. On a reverse form of the Brascamp-Lieb inequality. *Invent. Math.*, 310:685–693, 1998.

[19] W. Beckner. Sharp Sobolev inequalities on the sphere and the Moser-Trudinger inequality. *Ann. of Math.*, 138:213–242, 1993.

[20] J. Bedrossian, N. Rodríguez, and A. L. Bertozzi. Local and global well-posedness for aggregation equations and Patlak-Keller-Segel models with degenerate diffusion. *Nonlinearity*, 24(6):1683–1714, 2011.

[21] M. Beekman, D. J. T. Sumpter, and F. L. W. Ratnieks. Phase transitions between disordered and ordered foraging in pharaoh's ants. *Proc. Natl. Acad. Sci.*, 98(17):9703–9706, 2001.

[22] N. Bellomo, E. D. Angelis, and L. Preziosi. Multiscale modeling and mathematical problems related to tumor evolution and medical therapy. *Journal of Theoretical Medicine*, 5(2):111–136, 2003.

[23] N. Bellomo, A. Bellouquid, J. Nieto, and J.Soler. Multicellular biological growing systems: hyperbolic limits towards macroscopic description. *Mathematical Models and Methods in Applied Sciences*, 17:1675–1693, 2007.

[24] N. Bellomo, C. Bianca, and M. Delitala. Complexity analysis and mathematical tools towards the modelling of living systems. *Physics of Life Reviews*, 6:144–175, 2009.

[25] P. Bénilan and M. G. Crandall. The continuous dependence on φ of solutions of $u_t - \Delta\varphi(u) = 0$. *Indiana Univ. Math. J.*, 30(2):161–177, 1981.

[26] A. Bensoussan, J.-L. Lions, and G. C. Papanicolaou. Boundary layers and homogenization of transport processes. *Publications of the Research Institute for Mathematical Sciences*, 15(1):53–157, 1979.

[27] M. G. Bertotti and M. Delitala. Conservation laws and asymptotic behavior of a model of social dynamics. *Nonlinear Analysis RWA*, 9:183–196, 2008.

[28] A. L. Bertozzi, J. A. Carrillo, and T. Laurent. Blow-up in multidimensional aggregation equations with mildly singular interaction kernels. *Nonlinearity*, 22(3):683–710, 2009.

[29] A. L. Bertozzi, T. Kolokolnikov, H. Sun, D. Uminsky, and J. von Brecht. Ring patterns and their bifurcations in a nonlocal model of biological swarms. *Commun. Math. Sci.*, 13(4):955–985, 2015.

[30] A. L. Bertozzi and T. Laurent. Finite-time blow-up of solutions of an aggregation equation in $\mathbf{R}^n$. *Comm. Math. Phys.*, 274(3):717–735, 2007.

[31] A. L. Bertozzi, T. Laurent, and J. Rosado. L^p theory for the multidimensional aggregation equation. *Comm. Pure Appl. Math.*, 64(1):45–83, 2011.

[32] S. Bian and J.-G. Liu. Dynamic and steady states for multi-dimensional Keller-Segel model with diffusion exponent $m > 0$. *Comm. Math. Phys.*, 323(3):1017–1070, 2013.

[33] P. Biler, G. Karch, P. Laurençot, and T. Nadzieja. The 8π-problem for radially symmetric solutions of a chemotaxis model in the plane. *Math. Methods Appl. Sci.*, 29(13):1563–1583, 2006.

[34] P. Biler and T. Nadzieja. Existence and nonexistence of solutions for a model of gravitational interaction of particles. *Colloq. Math.*, 66:319–334, 1994.

[35] A. Blanchet, M. Bonforte, J. Dolbeault, G. Grillo, and J.-L. Vázquez. Asymptotics of the fast diffusion equation via entropy estimates. *Arch. Ration. Mech. Anal.*, 191(2):347–385, 2009.

[36] A. Blanchet, V. Calvez, and J. A. Carrillo. Convergence of the mass-transport steepest descent scheme for the subcritical Patlak-Keller-Segel model. *SIAM J. Numer. Anal.*, 46(2):691–721, 2008.

[37] A. Blanchet, E. A. Carlen, and J. A. Carrillo. Functional inequalities, thick tails and asymptotics for the critical mass Patlak-Keller-Segel model. *J. Funct. Anal.*, 262(5):2142–2230, 2012.

[38] A. Blanchet and G. Carlier. From Nash to Cournot-Nash equilibria via the Monge-Kantorovich problem. *Philos. Trans. R. Soc. Lond. Ser. A Math. Phys. Eng. Sci.*, 372(2028):20130398, 11, 2014.

[39] A. Blanchet, J. A. Carrillo, and P. Laurençot. Critical mass for a Patlak-Keller-Segel model with degenerate diffusion in higher dimensions. *Calc. Var. Partial Differential Equations*, 35(2):133–168, 2009.

[40] A. Blanchet, J. A. Carrillo, and N. Masmoudi. Infinite time aggregation for the critical Patlak-Keller-Segel model in $\mathbb{R}^2$. *Comm. Pure Appl. Math.*, 61(10):1449–1481, 2008.

[41] A. Blanchet, J. Dolbeault, and B. Perthame. Two dimensional Keller-Segel model in $\mathbb{R}^2$: optimal critical mass and qualitative properties of the solution. *Electron. J. Differential Equations*, 2006(44):1–33 (electronic), 2006.

[42] M. Bodnar and J. J. L. Velazquez. Derivation of macroscopic equations for individual cell-based models: a formal approach. *Math. Meth. Appl. Sci.*, 28:1757–1779, 2005.

[43] M. Bodnar and J. J. L. Velázquez. Friction dominated dynamics of interacting particles locally close to a crystallographic lattice. *Math. Methods Appl. Sci.*, 36(10):1206–1228, 2013.

[44] F. Bolley, I. Gentil, and A. Guillin. Uniform convergence to equilibrium for granular media. *Arch. Ration. Mech. Anal.*, 208(2):429–445, 2013.

[45] L. Boltzmann. *Lectures on gas theory*. Translated by Stephen G. Brush. University of California Press, Berkeley-Los Angeles, Calif., 1964.

[46] L. Boltzmann. *Weitere Studien über das Wärmegleichgewicht unter Gasmolekülen*, pages 115–225. Vieweg+Teubner Verlag, Wiesbaden, 1970.

[47] M. Bonforte, J. Dolbeault, G. Grillo, and J. L. Vázquez. Sharp rates of decay of solutions to the nonlinear fast diffusion equation via functional inequalities. *Proc. Natl. Acad. Sci. USA*, 107(38):16459–16464, 2010.

[48] M. Bonforte and J. L. Vazquez. Global positivity estimates and Harnack inequalities for the fast diffusion equation. *J. Funct. Anal.*, 240(2):399–428, 2006.

[49] E. Bouin, F. Hoffmann, and C. Mouhot. Exponential decay to equilibrium for a fibre laydown process on a moving conveyor belt. *Preprint arXiv:1605.04121v3*.

[50] D. P. Bourne and S. M. Roper. Centroidal power diagrams, Lloyd's algorithm, and applications to optimal location problems. *SIAM J. Numer. Anal.*, 53(6):2545–2569, 2015.

[51] V. Boussinesq. *Recherches théoriques sur l'écoulement des nappes d'eau infiltrées dans le sol et sur le débit des sources*, volume 10 of *Comptes Rendus Acad. Sci. / Journal de mathématiques pures et appliquées*.

[52] R. Breitwisch and G. Whitesides. Directionality of singing and non-singing behaviour of mated and unmated Northern Mockingbirds, *Mimus polyglottos*. *Anim. Behav.*, 35:331–339, 1987.

[53] Y. Brenier. Polar factorization and monotone rearrangement of vector-valued functions. *Comm. Pure Appl. Math.*, 44:375–417, 1991.

[54] F. Brock and A. Y. Solynin. An approach to symmetrization via polarization. *Trans. Amer. Math. Soc.*, 352(4):1759–1796, 2000.

[55] J. Buhl, D. J. T. Sumpter, I. D. Couzin, J. J. Hale, E. Despland, E. R. Miller, and S. J. Simpson. From disorder to order in marching locusts. *Science*, 312:1402–1406, 2006.

[56] P.-L. Buono and R. Eftimie. Analysis of Hopf/Hopf bifurcations in nonlocal hyperbolic models for self-organised aggregations. *Math. Models Methods Appl. Sci.*, 24:327, 2014.

[57] P.-L. Buono and R. Eftimie. Codimension-two bifurcations in animal aggregation models with symmetry. *SIAM J. Appl. Dyn. Syst.*, 2014.

[58] P.-L. Buono and R. Eftimie. Symmetries and pattern formation in hyperbolic versus parabolic models for self-organised aggregations. *J. Math. Biol.*, 2014.

[59] M. Burger, V. Capasso, and D. Morale. On an aggregation model with long and short range interactions. *Nonlinear Analysis: Real World Applications*, 8:939–958, 2007.

[60] L. A. Caffarelli and P. R. Stinga. Fractional elliptic equations, Caccioppoli estimates and regularity. *Ann. Inst. H. Poincaré Anal. Non Linéaire*, 33(3):767–807, 2016.

[61] V. Calvez and J. A. Carrillo. Volume effects in the Keller-Segel model: energy estimates preventing blow-up. *J. Math. Pures Appl.*, 86:155–175, 2006.

[62] V. Calvez and J. A. Carrillo. Refined asymptotics for the subcritical Keller-Segel system and related functional inequalities. *Proc. Amer. Math. Soc.*, 140(10):3515–3530, 2012.

[63] V. Calvez, J. A. Carrillo, and F. Hoffmann. Equilibria of homogeneous functionals in the fair-competition regime. *Nonlinear Anal.*, 159:85–128, 2017.

[64] V. Calvez, J. A. Carrillo, and F. Hoffmann. The geometry of diffusing and self-attracting particles in a one-dimensional fair-competition regime. In *Nonlocal and Nonlinear Diffusions and Interactions: New Methods and Directions*, volume 2186 of *Lecture Notes in Math.* Springer, [Cham], 2017.

[65] V. Calvez and L. Corrias. Blow-up dynamics of self-attracting diffusive particles driven by competing convexities. *Discrete Contin. Dyn. Syst. Ser. B*, 18(8):2029–2050, 2013.

[66] V. Calvez and T. O. Gallouët. Blow-up phenomena for gradient flows of discrete homogeneous functionals. *Preprint arXiv:1603.05380v2*.

[67] V. Calvez and T. O. Gallouët. Particle approximation of the one dimensional Keller-Segel equation, stability and rigidity of the blow-up. *Discrete Contin. Dyn. Syst.*, 36(3):1175–1208, 2016.

[68] V. Calvez, B. Perthame, and M. Sharifi tabar. Modified Keller-Segel system and critical mass for the log interaction kernel. In *Stochastic analysis and partial differential equations*, volume 429 of *Contemp. Math.*, pages 45–62. Amer. Math. Soc., Providence, RI, 2007.

[69] V. Calvez, G. Raoul, and C. Schmeiser. Confinement by biased velocity jumps: aggregation of Escherichia coli. *Kinet. Relat. Models*, 8(4):651–666, 2015.

[70] J. F. Campos and J. Dolbeault. A functional framework for the Keller-Segel system: logarithmic Hardy-Littlewood-Sobolev and related spectral gap inequalities. *C. R. Math. Acad. Sci. Paris*, 350(21-22):949–954, 2012.

[71] J. F. Campos and J. Dolbeault. Asymptotic estimates for the parabolic-elliptic Keller-Segel model in the plane. *Comm. Partial Differential Equations*, 39(5):806–841, 2014.

[72] J. A. Cañizo, J. A. Carrillo, and F. S. Patacchini. Existence of compactly supported global minimisers for the interaction energy. *Arch. Ration. Mech. Anal.*, 217(3):1197–1217, 2015.

[73] E. A. Carlen. Duality and stability for functional inequalities. *Preprint arXiv:1609.00936*.

[74] E. A. Carlen, J. A. Carrillo, and M. Loss. Hardy-Littlewood-Sobolev inequalities via fast diffusion flows. *Proc. Natl. Acad. Sci. USA*, 107(46):19696–19701, 2010.

[75] E. A. Carlen and A. Figalli. Stability for a GNS inequality and the log-HLS inequality, with application to the critical mass Keller-Segel equation. *Duke Math. J.*, 162(3):579–625, 2013.

[76] E. A. Carlen, R. L. Frank, and E. H. Lieb. Stability estimates for the lowest eigenvalue of a Schrödinger operator. *Geom. Funct. Anal.*, 24(1):63–84, 2014.

[77] E. A. Carlen and M. Loss. Competing symmetries, the logarithmic HLS inequality and Onofri's inequality on $\mathbb{S}^n$. *Geom. Funct. Anal.*, 2:90–104, 1992.

[78] J. A. Carrillo, D. Castorina, and B. Volzone. Ground states for diffusion dominated free energies with logarithmic interaction. *SIAM J. Math. Anal.*, 47(1):1–25, 2015.

[79] J. A. Carrillo, M. Chipot, and Y. Huang. On global minimizers of repulsive-attractive power-law interaction energies. *Philos. Trans. R. Soc. Lond. Ser. A Math. Phys. Eng. Sci.*, 372(2028):20130399, 13, 2014.

[80] J. A. Carrillo, Y.-P. Choi, and M. Hauray. The derivation of swarming models: mean-field limit and Wasserstein distances. In *Collective dynamics from bacteria to crowds*, volume 553 of *CISM Courses and Lect.*, pages 1–46. Springer, Vienna, 2014.

[81] J. A. Carrillo, M. G. Delgadino, and A. Mellet. Regularity of local minimizers of the interaction energy via obstacle problems. *To appear in Comm. Math. Phys., preprint arXiv:1406.4040 [math.AP]*, 2014.

[82] J. A. Carrillo, M. DiFrancesco, A. Figalli, T. Laurent, and D. Slepcev. Global-in-time weak measure solutions and finite-time aggregation for nonlocal interaction equations. *Duke Math. J.*, 156(2):229–271, 2011.

[83] J. A. Carrillo, M. R. D'Orsogna, and V. Panferov. Double milling in self-propelled swarms from kinetic theory. *Kinetic and Related Models*, 2:363–378, 2009.

[84] J. A. Carrillo, R. Eftimie, and F. Hoffmann. Non-local kinetic and macroscopic models for self-organised animal aggregations. *Kinet. Relat. Models*, 8(3):413–441, 2015.

[85] J. A. Carrillo, L. C. F. Ferreira, and J. C. Precioso. A mass-transportation approach to a one dimensional fluid mechanics model with nonlocal velocity. *Adv. Math.*, 231(1):306–327, 2012.

[86] J. A. Carrillo, M. Fornasier, J. Rosado, and G. Toscani. Asymptotic flocking dynamics for the kinetic Cucker-Smale model. *SIAM J. Math. Anal.*, 42:218–236, 2010.

[87] J. A. Carrillo, M. Fornasier, G. Toscani, and F. Vecil. Particle, kinetic, and hydrodynamic models of swarming. In *Mathematical modeling of collective behavior in socio-economic and life sciences*, Model. Simul. Sci. Eng. Technol., pages 297–336. Birkhäuser Boston, Inc., Boston, MA, 2010.

[88] J. A. Carrillo, T. Goudon, P. Lafitte, and F. Vecil. Numerical schemes of diffusion asymptotics and moment closures for kinetic equations. *J. Sci. Comput.*, 36(1):113–149, 2008.

[89] J. A. Carrillo, S. Hittmeir, B. Volzone, and Y. Yao. Nonlinear aggregation-diffusion equations: Radial symmetry and long time asymptotics. *Preprint arXiv:1603.07767*.

[90] J. A. Carrillo, F. Hoffmann, E. Mainini, and B. Volzone. Ground states in the diffusion-dominated regime. *Preprint arXiv:1705.03519*.

[91] J. A. Carrillo, Y. Huang, and S. Martin. Explicit flock solutions for Quasi-Morse potentials. *European J. Appl. Math.*, 25(5):553–578, 2014.

[92] J. A. Carrillo, A. Jüngel, P. A. Markowich, G. Toscani, and A. Unterreiter. Entropy dissipation methods for degenerate parabolic problems and generalized Sobolev inequalities. *Monatsh. Math.*, 133(1):1–82, 2001.

[93] J. A. Carrillo, A. Klar, S. Martin, and S. Tiwari. Self-propelled interacting particle systems with roosting force. *Math. Models Methods Appl. Sci.*, 20:1533, 2010.

[94] J. A. Carrillo, S. Lisini, and E. Mainini. Uniqueness for Keller-Segel-type chemotaxis models. *Discrete Contin. Dyn. Syst.*, 34(4):1319–1338, 2014.

[95] J. A. Carrillo, S. Martin, and V. Panferov. A new interaction potential for swarming models. *Phys. D*, 260:112–126, 2013.

[96] J. A. Carrillo, R. J. McCann, and C. Villani. Kinetic equilibration rates for granular media and related equations: entropy dissipation and mass transportation estimates. *Rev. Mat. Iberoamericana*, 19:1–48, 2003.

[97] J. A. Carrillo, R. J. McCann, and C. Villani. Contractions in the 2-Wasserstein length space and thermalization of granular media. *Arch. Ration. Mech. Anal.*, 179:217–263, 2006.

[98] J. A. Carrillo and D. Slepcev. Example of a displacement convex functional of first order. *Calc. Var. Partial Differential Equations*, 36(4):547–564, 2009.

[99] J. A. Carrillo and Y. Sugiyama. Compactly supported stationary states of the degenerate keller-segel system in the diffusion-dominated regime. *Preprint arXiv:1612.05375*.

[100] J. A. Carrillo and G. Toscani. Asymptotic L^1-decay of solutions of the porous medium equation to self-similarity. *Indiana Univ. Math. J.*, 49(1):113–142, 2000.

[101] J. A. Carrillo and J. L. Vázquez. Fine asymptotics for fast diffusion equations. *Comm. Partial Differential Equations*, 28(5-6):1023–1056, 2003.

[102] J. A. Carrillo and B. Yan. An asymptotic preserving scheme for the diffusive limit of kinetic systems for chemotaxis. *Multiscale Model. Simul.*, 11(1):336–361, 2013.

[103] C. Cercignani, R. Illner, and M. Pulvirenti. *The mathematical theory of dilute gases*, volume 106 of *Applied Mathematical Sciences*. Springer-Verlag, New York, 1994.

[104] F. Chalub, P. Markowich, B. Perthame, and C. Schmeiser. Kinetic models for chemotaxis and their drift-diffusion limits. *Monatsh. Math.*, 142:123–141, 2004.

[105] S. Chandrasekhar. *Principles of stellar dynamics*. Enlarged ed. Dover Publications, Inc., New York, 1960.

[106] P.-H. Chavanis, P. Laurençot, and M. Lemou. Chapman-Enskog derivation of the generalized Smoluchowski equation. *Phys. A*, 341(1-4):145–164, 2004.

[107] P. H. Chavanis and R. Mannella. Self-gravitating Brownian particles in two dimensions: the case of $N = 2$ particles. *Eur. Phys. J. B*, 78(2):139–165, 2010.

[108] P.-H. Chavanis and C. Sire. Anomalous diffusion and collapse of self-gravitating langevin particles in d dimensions. *Phys. Rev. E*, 69:016116, Jan 2004.

[109] L. Chen, J.-G. Liu, and J. Wang. Multidimensional degenerate Keller-Segel system with critical diffusion exponent $2n/(n + 2)$. *SIAM J. Math. Anal.*, 44(2):1077–1102, 2012.

[110] L. Chen and J. Wang. Exact criterion for global existence and blow up to a degenerate Keller-Segel system. *Doc. Math.*, 19:103–120, 2014.

[111] S. Chen, R. Frank, and T. Weth. Remainder terms in the fractional Sobolev inequality. *Indiana Univ. Math. J.*, 62:1381–1397, 2013.

[112] A. Chertock, A. Kurganov, A. Polizzi, and I. Timofeyev. Pedestrian flow models with slowdown interactions. *Math Models Methods Appl. Sci.*, 24(2):249–275, 2014.

[113] S. Childress and J. K. Percus. Nonlinear aspects of chemotaxis. *Math. Biosciences*, 56:217–237, 1981.

[114] Y.-L. Chuang, M. R. D'Orsogna, D. Marthaler, A. L. Bertozzi, and L. S. Chayes. State transitions and the continuum limit for a 2d interactiong, self-propelled particle system. *Physica D*, 232:33–47, 2007.

[115] T. Cieślak and P. Laurençot. Looking for critical nonlinearity in the one-dimensional quasilinear Smoluchowski-Poisson system. *Discrete Contin. Dyn. Syst.*, 26(2):417–430, 2010.

[116] T. Cieślak and P. Laurençot. Global existence vs. blowup in a one-dimensional Smoluchowski-Poisson system. In *Parabolic problems*, volume 80 of *Progr. Nonlinear Differential Equations Appl.*, pages 95–109. Birkhäuser/Springer Basel AG, Basel, 2011.

[117] D. Cordero-Erausquin, B. Nazaret, and C. Villani. A mass-transportation approach to sharp Sobolev and Gagliardo-Nirenberg inequalities. *Adv. Math.*, 182(2):307–332, 2004.

[118] L. Corrias, B. Perthame, and H. Zaag. Global solutions of some chemotaxis and angiogenesis systems in high space dimensions. *Milan J. Math.*, 72:1–28, 2004.

[119] K. Craig. Nonconvex gradient flow in the wasserstein metric and applications to constrained nonlocal interactions. *Preprint arXiv:1512.07255v1*.

[120] P. Degond, G. Dimarco, and T. Mac. Hydrodynamics of the Kuramoto-Vicsek model of rotating self-propelled particles. *Mathematical Models and Methods in Applied Sciences*, 24:277–325, 2014.

[121] P. Degond, T. Goudon, and F. Poupaud. Diffusion limit for nonhomogeneous and non-micro-reversible processes. *Indiana Univ. Math. J.*, 49(3):1175–1198, 2000.

[122] P. Degond and B. Lucquin-Desreux. The Fokker-Planck asymptotics of the Boltzmann collision operator in the Coulomb case. *Math. Models Methods Appl. Sci.*, 2(2):167–182, 1992.

[123] P. Degond and S. Motsch. Macroscopic limit of self-driven particles with orientation interaction. *C.R. Acad. Sci. Paris Ser. I*, 345:555–560, 2007.

[124] P. Degond and S. Motsch. Large scale dynamics of the persistent turning awlker model of fish behaviour. *J. Stat. Phys.*, 131:989–1021, 2008.

[125] M. Del Pino and J. Dolbeault. Best constants for Gagliardo-Nirenberg inequalities and applications to nonlinear diffusions. *J. Math. Pures Appl. (9)*, 81(9):847–875, 2002.

[126] F. Demengel and G. Demengel. *Functional spaces for the theory of elliptic partial differential equations*. Universitext. Springer, London; EDP Sciences, Les Ulis, 2012. Translated from the 2007 French original by Reinie Erné.

[127] L. Desvillettes. On asymptotics of the Boltzmann equation when the collisions become grazing. *Transport Theory Statist. Phys.*, 21(3):259–276, 1992.

[128] L. Desvillettes. Plasma kinetic models: the Fokker-Planck-Landau equation. In *Modeling and computational methods for kinetic equations*, Model. Simul. Sci. Eng. Technol., pages 171–193. Birkhäuser Boston, Boston, MA, 2004.

[129] L. Desvillettes and C. Villani. On the trend to global equilibrium in spatially inhomogeneous entropy-dissipating systems: the linear Fokker-Planck equation. *Comm. Pure Appl. Math.*, 54(1):1–42, 2001.

[130] L. Desvillettes and C. Villani. On the trend to global equilibrium for spatially inhomogeneous kinetic systems: the Boltzmann equation. *Invent. Math.*, 159(2):245–316, 2005.

[131] R. L. Dobrushin. Vlasov equations. *Funktsional. Anal. i Prilozhen.*, 13(2):48–58, 96, 1979.

[132] J. Dolbeault. Sobolev and Hardy-Littlewood-Sobolev inequalities: duality and fast diffusion. *Math. Res. Lett.*, 18(6):1037–1050, 2011.

[133] J. Dolbeault and G. Jankowiak. Sobolev and Hardy-Littlewood-Sobolev inequalities. *J. Differential Equations*, 257(6):1689–1720, 2014.

[134] J. Dolbeault, A. Klar, C. Mouhot, and C. Schmeiser. Exponential rate of convergence to equilibrium for a model describing fiber lay-down processes. *Appl. Math. Res. Express. AMRX*, (2):165–175, 2013.

[135] J. Dolbeault, C. Mouhot, and C. Schmeiser. Hypocoercivity for linear kinetic equations conserving mass. *Trans. Amer. Math. Soc.*, 367(6):3807–3828, 2015.

[136] J. Dolbeault and B. Perthame. Optimal critical mass in the two-dimensional Keller-Segel model in $\mathbb{R}^2$. *C. R. Math. Acad. Sci. Paris*, 339(9):611–616, 2004.

[137] J. Dolbeault and G. Toscani. Improved interpolation inequalities, relative entropy and fast diffusion equations. *Ann. Inst. H. Poincaré Anal. Non Linéaire*, 30(5):917–934, 2013.

[138] H. Dong. The aggregation equation with power-law kernels: ill-posedness, mass concentration and similarity solutions. *Comm. Math. Phys.*, 304(3):649–664, 2011.

[139] M. R. D'Orsogna, Y.-L. Chuang, A. L. Bertozzi, and L. S. Chayes. Self-propelled particles with soft-core interactions: patterns, stability, and collapse. *Phys. Rev. Lett.*, 96(10):104302, 2006.

[140] I. Drelichman. *Weighted inequalities for fractional integrals of radial functions and applications*. PhD thesis, Universidad de Buenos Aires, 2010.

[141] J.-P. Eckmann and M. Hairer. Uniqueness of the invariant measure for a stochastic PDE driven by degenerate noise. *Comm. Math. Phys.*, 219(3):523–565, 2001.

[142] M. P. Edgington and M. J. Tindall. Understanding the link between single cell and population scale responses of escherichia coli in differing ligand gradients. *Computational and Structural Biotechnology Journal*, 13:528 – 538, 2015.

[143] R. Eftimie. *Modeling group formation and activity patterns in self-organizing communities of organisms*. PhD thesis, University of Alberta, 2008.

[144] R. Eftimie. Hyperbolic and kinetic models for self-organized biological aggregations and movement: a brief review. *J. Math. Biol.*, 65(1):35–75, 2012.

[145] R. Eftimie, G. de Vries, and M. Lewis. Weakly nonlinear analysis of a hyperbolic model for animal group formation. *J. Math. Biol.*, 59:37–74, 2009.

[146] R. Eftimie, G. de Vries, and M. A. Lewis. Complex spatial group patterns result from different animal communication mechanisms. *Proc. Natl. Acad. Sci.*, 104(17):6974–6979, 2007.

[147] R. Eftimie, G. de Vries, M. A. Lewis, and F. Lutscher. Modeling group formation and activity patterns in self-organizing collectives of individuals. *Bull. Math. Biol.*, 69(5):1537–1566, 2007.

[148] G. Egaña-Fernández and S. Mischler. Uniqueness and long time asymptotic for the Keller-Segel equation: the parabolic-elliptic case. *Arch. Ration. Mech. Anal.*, 220(3):1159–1194, 2016.

[149] M. Eisenbach, J. Lengeler, M. Varon, D. Gutnick, R. Meili, R. Firtel, J. Segall, G. Omann, A. Tamada, and F. Murakami. *Chemotaxis*. Imperial College Press, London, 2004.

[150] R. Erban and H. G. Othmer. From individual to collective behavior in bacterial chemotaxis. *SIAM J. Appl. Math.*, 65(2):361–391, 2004/05.

[151] K. Fellner and G. Raoul. Stable stationary states of non-local interaction equations. *Math. Models Methods Appl. Sci.*, 20(12):2267–2291, 2010.

[152] K. Fellner and G. Raoul. Stability of stationary states of non-local equations with singular interaction potentials. *Math. Comput. Modelling*, 53(7-8):1436–1450, 2011.

[153] R. Fetecau. Collective behavior of biological aggregations in two dimensions: a nonlocal kinetic model. *Math. Model. Method. Appl. Sci.*, 21(07):1539, 2011.

[154] R. C. Fetecau and Y. Huang. Equilibria of biological aggregations with nonlocal repulsive-attractive interactions. *Phys. D*, 260:49–64, 2013.

[155] R. C. Fetecau, Y. Huang, and T. Kolokolnikov. Swarm dynamics and equilibria for a nonlocal aggregation model. *Nonlinearity*, 24(10):2681–2716, 2011.

[156] J. Fourier. *Théorie analytique de la chaleur*. Éditions Jacques Gabay, Paris, 1988. Reprint of the 1822 original.

[157] N. Fournier and D. Godinho. Asymptotic of grazing collisions and particle approximation for the Kac equation without cutoff. *Comm. Math. Phys.*, 316(2):307–344, 2012.

[158] N. Fournier and H. Guérin. On the uniqueness for the spatially homogeneous Boltzmann equation with a strong angular singularity. *J. Stat. Phys.*, 131(4):749–781, 2008.

[159] H. Gajewski and K. Zacharias. Global behavior of a reaction-diffusion system modelling chemotaxis. *Math. Nachr.*, 195:77–114, 1998.

[160] V. A. Galaktionov and L. A. Peletier. Asymptotic behaviour near finite-time extinction for the fast diffusion equation. *Arch. Rational Mech. Anal.*, 139(1):83–98, 1997.

[161] V. A. Galaktionov and J. L. Vázquez. *A stability technique for evolution partial differential equations*, volume 56 of *Progress in Nonlinear Differential Equations and their Applications*. Birkhäuser Boston, Inc., Boston, MA, 2004. A dynamical systems approach.

[162] I. Gallagher, T. Gallay, and F. Nier. Spectral asymptotics for large skew-symmetric perturbations of the harmonic oscillator. *Int. Math. Res. Not. IMRN*, (12):2147–2199, 2009.

[163] R. J. Gardner. The Brunn-Minkowski inequality. *Bull. Amer. Math. Soc.*, 39:355–405, 2002.

[164] J. Garnier, G. Papanicolaou, and T.-W. Yang. Large deviations for a mean field model of systemic risk. *SIAM J. Financial Math.*, 4(1):151–184, 2013.

[165] J. Garnier, G. Papanicolaou, and T.-W. Yang. Consensus convergence with stochastic effects. *Vietnam J. Math.*, 45(1-2):51–75, 2017.

[166] M. G. D. Geers, R. H. J. Peerlings, M. A. Peletier, and L. Scardia. Asymptotic behaviour of a pile-up of infinite walls of edge dislocations. *Arch. Ration. Mech. Anal.*, 209(2):495–539, 2013.

[167] E. Geigant, K. Ladizhansky, and A. Mogilner. An integrodifferential model for orientational distributions of F-actin in cells. *SIAM J. Appl. Math.*, 59(3):787–809, 1998.

[168] T.-E. Ghoul and N. Masmoudi. Stability of infinite time blow up for the Patlak–Keller–Segel system, 2016.

[169] P. Godillon-Lafitte and T. Goudon. A coupled model for radiative transfer: Doppler effects, equilibrium, and nonequilibrium diffusion asymptotics. *Multiscale Model. Simul.*, 4(4):1245–1279, 2005.

[170] F. Golse. The mean-field limit for the dynamics of large particle systems. In *Journées "Équations aux Dérivées Partielles"*, pages Exp. No. IX, 47. Univ. Nantes, Nantes, 2003.

[171] L. Gosse and G. Toscani. Lagrangian numerical approximations to one-dimensional convolution-diffusion equations. *SIAM J. Sci. Comput.*, 28(4):1203–1227 (electronic), 2006.

[172] T. Götz, A. Klar, N. Marheineke, and R. Wegener. A stochastic model and associated Fokker-Planck equation for the fiber lay-down process in nonwoven production processes. *SIAM J. Appl. Math.*, 67(6):1704–1717, 2007.

[173] T. Goudon. On Boltzmann equations and Fokker-Plank asymptotics: influence of grazing collisions. *J. Stat. Phys.*, 89(3-4):751–776, 1997.

[174] T. Gowers, J. Barrow-Green, and I. Leader, editors. *The Princeton companion to mathematics*. Princeton University Press, Princeton, NJ, 2008.

[175] H. Grad. Asymptotic theory of the Boltzmann equation. II. In *Rarefied Gas Dynamics (Proc. 3rd Internat. Sympos., Palais de l'UNESCO, Paris, 1962), Vol. I*, pages 26–59. Academic Press, New York, 1963.

[176] S. Graf and H. Luschgy. *Foundations of quantization for probability distributions*, volume 1730 of *Lecture Notes in Mathematics*. Springer-Verlag, Berlin, 2000.

[177] M. Grothaus, A. Klar, J. Maringer, and P. Stilgenbauer. Geometry, mixing properties and hypocoercivity of a degenerate diffusion arising in technical textile industry. *Preprint arXiv/1203.4502*, 2012.

[178] Y. Guo. The Landau equation in a periodic box. *Comm. Math. Phys.*, 231(3):391–434, 2002.

[179] S.-Y. Ha and E. Tadmor. From particle to kinetic and hydrodynamic descriptions of flocking. *Kinetic and Related Models*, 1(3):415–435, 2008.

[180] G. H. Hardy and J. E. Littlewood. Some properties of fractional integrals. I. *Math. Z.*, 27(1):565–606, 1928.

[181] G. H. Hardy and J. E. Littlewood. Notes on the Theory of Series (XII): On Certain Inequalities Connected with the Calculus of Variations. *J. London Math. Soc.*, S1-5(1):34, 1930.

[182] B. Helffer and F. Nier. *Hypoelliptic estimates and spectral theory for Fokker-Planck operators and Witten Laplacians*, volume 1862 of *Lecture Notes in Mathematics*. Springer-Verlag, Berlin, 2005.

[183] C. K. Hemelrijk and H. Kunz. Density distribution and size sorting in fish schools: an individual-based model. *Behav. Ecol.*, 16(1):178–187, 2004.

[184] F. Hérau. Hypocoercivity and exponential time decay for the linear inhomogeneous relaxation Boltzmann equation. *Asymptot. Anal.*, 46(3-4):349–359, 2006.

[185] F. Hérau and F. Nier. Isotropic hypoellipticity and trend to equilibrium for the Fokker-Planck equation with a high-degree potential. *Arch. Ration. Mech. Anal.*, 171(2):151–218, 2004.

[186] M. A. Herrero and M. Pierre. The Cauchy problem for $u_t = \Delta u^m$ when $0 < m < 1$. *Trans. Amer. Math. Soc.*, 291(1):145–158, 1985.

[187] M. A. Herrero and J. J. L. Velázquez. A blow-up mechanism for a chemotaxis model. *Ann. Scuola Norm. Sup. Pisa Cl. Sci. (4)*, 24(4):633–683 (1998), 1997.

[188] H. Hildenbrandt, C. Carere, and C. K. Hemelrijk. Self-organised complex aerial displays of thousands of starlings: a model. *Behavioral Ecology*, 107(21):1349–1359, 2010.

[189] T. Hillen and H. G. Othmer. The diffusion limit of transport equations derived from velocity jump process. *SIAM J.Appl.Math.*, 61(3):751–775, 2000.

[190] T. Hillen and H. G. Othmer. The diffusion limit of transport equations. II. Chemotaxis equations. *SIAM J. Appl. Math.*, 62(4):1222–1250, 2002.

[191] D. D. Holm and V. Putkaradze. Formation of clumps and patches in self-aggregation of finite-size particles. *Phys. D*, 220(2):183–196, 2006.

[192] E. E. Holmes. Are diffusion models too simple? A comparison with telegraph models of invasion. *Am. Nat.*, 142:779–795, 1993.

[193] L. Hörmander. Hypoelliptic second order differential equations. *Acta Math.*, 119:147–171, 1967.

[194] W. Jäger and S. Luckhaus. On explosions of solutions to a system of partial differential equations modelling chemotaxis. *Trans. Amer. Math. Soc.*, 329:819–824, 1992.

[195] R. Jordan, D. Kinderlehrer, and F. Otto. The variational formulation of the Fokker-Planck equation. *SIAM J. Math. Anal.*, 29(1):1–17, 1998.

[196] E. F. Keller and L. A. Segel. Initiation of slime mold aggregation viewed as an instability. *J. Theor. Biol.*, 26(3):399 – 415, 1970.

[197] E. F. Keller and L. A. Segel. Model for chemotaxis. *J. Theor. Biol.*, 30:225–234, 1971.

[198] S. Kesavan. *Topics in functional analysis and applications*. John Wiley & Sons, Inc., New York, 1989.

[199] I. Kim and Y. Yao. The Patlak-Keller-Segel model and its variations: properties of solutions via maximum principle. *SIAM Journal on Mathematical Analysis*, 44(2):568–602, 2012.

[200] J. R. King. Extremely high concentration dopant diffusion in silicon. 40:163 – 181, 1988.

[201] A. Klar. An asymptotic-induced scheme for nonstationary transport equations in the diffusive limit. *SIAM J. Numer. Anal.*, 35(3):1073–1094 (electronic), 1998.

[202] A. Klar. An asymptotic preserving numerical scheme for kinetic equations in the low Mach number limit. *SIAM J. Numer. Anal.*, 36(5):1507–1527 (electronic), 1999.

[203] A. Klar, J. Maringer, and R. Wegener. A 3D model for fiber lay-down in nonwoven production processes. *Math. Models Methods Appl. Sci.*, 22(9):1250020, 18, 2012.

[204] B. Kloeckner. Approximation by finitely supported measures. *ESAIM Control Optim. Calc. Var.*, 18(2):343–359, 2012.

[205] M. Kolb, M. Savov, and A. Wübker. Geometric ergodicity of a hypoelliptic diffusion modelling the melt-spinning process of nonwoven materials. *Preprint arXiv/1112.6159*, 2011.

[206] M. Kolb, M. Savov, and A. Wübker. (Non-)ergodicity of a degenerate diffusion modeling the fiber lay down process. *SIAM J. Math. Anal.*, 45(1):1–13, 2013.

[207] T. Kolokolnikov, J. A. Carrillo, A. Bertozzi, R. Fetecau, and M. Lewis. Emergent behaviour in multi-particle systems with non-local interactions [Editorial]. *Phys. D*, 260:1–4, 2013.

[208] L. Landau. Die kinetische gleichung für den fall coulombscher wechselwirkung. *Phys. Z. Sowjet.*, 154(10), 1936.

[209] R. Larkin and R. Szafoni. Evidence for widely dispersed birds migrating together at night. *Integrative and comparative biology*, 48(1):40–49, 2008.

[210] E. W. Larsen and J. B. Keller. Asymptotic solution of neutron transport problems for small mean free paths. *Journal of Mathematical Physics*, 15:75–81, 1974.

[211] C. Lattanzio and A. E. Tzavaras. Relative entropy in diffusive relaxation. *SIAM J. Math. Anal.*, 45(3):1563–1584, 2013.

[212] S. Lattimore. *The Peloponnesian War*. Cassell, 1998.

[213] T. Laurent. Local and global existence for an aggregation equation. *Comm. Partial Differential Equations*, 32(10-12):1941–1964, 2007.

[214] N. N. Lebedev. *Special Functions and Their Applications*. Prentice-Hall, 1965.

[215] J. M. Lee and T. H. Parker. The Yamabe problem. *Bull. Amer. Math. Soc. (N.S.)*, 17(1):37–91, 1987.

[216] L. S. Leibenzon. The motion of a gas in a porous medium. *Complete works*, 2, 1953 (Russian). First published in *Neftanoe i slantsevoe khozyastvo*, **10**, 1929, and *Neftanoe khozyastvo*, **8-9**, 1930 (Russian).

[217] E. H. Lieb. Sharp constants in the Hardy-Littlewood-Sobolev and related inequalities. *Ann. of Math.*, 118:349–374, 1983.

[218] E. H. Lieb and M. Loss. *Analysis*, volume 14 of *Graduate Studies in Math.* Amer. Math. Soc., Providence, RI, second edition, 2001.

[219] E. M. Lifschitz and L. P. Pitajewski. *Lehrbuch der theoretischen Physik ("Landau-Lifschitz"). Band X.* Akademie-Verlag, Berlin, second edition, 1990. Physikalische Kinetik. [Physical kinetics].

[220] P.-L. Lions. The concentration-compactness principle in the calculus of variations. The locally compact case. I. *Ann. Inst. H. Poincaré Anal. Non Linéaire*, 1(2):109–145, 1984.

[221] P.-L. Lions. The concentration-compactness principle in the calculus of variations. The locally compact case. II. *Ann. Inst. H. Poincaré Anal. Non Linéaire*, 1(4):223–283, 1984.

[222] P.-L. Lions. The concentration-compactness principle in the calculus of variations. The limit case. I. *Rev. Mat. Iberoamericana*, 1(1):145–201, 1985.

[223] P.-L. Lions. The concentration-compactness principle in the calculus of variations. The limit case. II. *Rev. Mat. Iberoamericana*, 1(2):45–121, 1985.

[224] J.-G. Liu and J. Wang. A note on L^∞-bound and uniqueness to a degenerate Keller-Segel model. *Acta Appl. Math.*, 142:173–188, 2016.

[225] T.-P. Liu, T. Yang, and S.-H. Yu. Energy method for Boltzmann equation. *Phys. D*, 188(3-4):178–192, 2004.

[226] C. Liverani and S. Olla. Toward the Fourier law for a weakly interacting anharmonic crystal. *J. Amer. Math. Soc.*, 25(2):555–583, 2012.

[227] A. Lotka. *Elements of physical biology*. Williams & Wilkins Company, 1925.

[228] E. Mainini, P. Piovano, and U. Stefanelli. Finite crystallization in the square lattice. *Nonlinearity*, 27(4):717–737, 2014.

[229] E. Mainini and U. Stefanelli. Crystallization in carbon nanostructures. *Comm. Math. Phys.*, 328(2):545–571, 2014.

[230] N. Marheineke and R. Wegener. Fiber dynamics in turbulent flows: general modeling framework. *SIAM J. Appl. Math.*, 66(5):1703–1726 (electronic), 2006.

[231] N. Marheineke and R. Wegener. Fiber dynamics in turbulent flows: specific Taylor drag. *SIAM J. Appl. Math.*, 68(1):1–23 (electronic), 2007.

[232] J. C. Maxwell. On the dynamical theory of gases. *Philosophical Transactions of the Royal Society of London*, (157):49–88, 1867.

[233] R. J. McCann. Existence and uniqueness of monotone measure-preserving maps. *Duke Math. J.*, 80:309–323, 1995.

[234] R. J. McCann. A convexity principle for interacting gases. *Adv. Math.*, 128:153–179, 1997.

[235] Q. Mérigot. A multiscale approach to optimal transport. In *Computer Graphics Forum*, volume 30, pages 1583–1592. Wiley Online Library, 2011.

[236] P. Mironescu. Superposition with subunitary powers in Sobolev spaces. *C. R. Math. Acad. Sci. Paris*, 353(6):483–487, 2015.

[237] A. Mogilner and L. Edelstein-Keshet. A non-local model for a swarm. *J. Math. Biol.*, 38(6):534–570, 1999.

[238] A. Mogilner, L. Edelstein-Keshet, L. Bent, and A. Spiros. Mutual interactions, potentials, and individual distance in a social aggregation. *J. Math. Biol.*, 47(4):353–389, 2003.

[239] A. Mogilner, L. Edelstein-Keshet, and G. B. Ermentrout. Selecting a common direction. II. Peak-like solutions representing total alignment of cell clusters. *J. Math. Biol.*, 34:811–842, 1996.

[240] D. Morale, V. Capasso, and K. Oelschläger. An interacting particle system modelling aggregation behavior: from individuals to populations. *J. Math. Biol.*, 50(1):49–66, 2005.

[241] M. M. Muskat. *The flow of homogeneous fluids through porous media*. International Human Resources Development Corporation, 1982, Boston, 1937.

[242] T. Nagai. Blow-up of radially symmetric solutions to a chemotaxis system. *Adv. Math. Sci. Appl.*, 5:581–601, 1995.

[243] V. Nanjundiah. Chemotaxis, signal relaying and aggregation morphology. *J. Theor. Biol.*, 42:63–105, 1973.

[244] I. Newton. *The migration ecology of birds*. Academic Press, Elsevier, 2008.

[245] K. Oelschläger. Large systems of interacting particles and the porous medium equation. *J. Differential Equations*, 88(2):294–346, 1990.

[246] H. Okuda and J. M. Dawson. Theory and nunmerical simulation on plasma diffusion across a magnetic field. 16:408 – 426, 1973.

[247] H. G. Othmer, S. R. Dunbar, and W. Alt. Models of dispersal in biological systems. *J. Math. Biol.*, 26(3):263–298, 1988.

[248] F. Otto. The geometry of dissipative evolution equations: the porous medium equation. *Comm. Partial Differential Equations*, 26(1-2):101–174, 2001.

[249] J. Parker. *Flicker to Flame: Living with Purpose, Meaning, and Happiness*. Morgan James Publishing, 2006.

[250] J. K. Parrish and L. E. Keshet. Complexity, Pattern, and Evolutionary Trade-Offs in Animal Aggregation. *Science*, 284(5411):99–101, 1999.

[251] R. D. Passo and P. de Mottoni. Aggregative effects for a reaction-advection equation. *J. Math. Biology*, 20:103–112, 1984.

[252] C. Patlak. Random walk with persistence and external bias. *Bull. Math. Biophys.*, 15:311–338, 1953.

[253] R. E. Pattle. Diffusion from an instantaneous point source with a concentration-dependent coefficient. *Quart. J. Mech. Appl. Math.*, 12:407–409, 1959.

[254] A. Pazy. *Semigroups of linear operators and applications to partial differential equations*, volume 44 of *Applied Mathematical Sciences*. Springer-Verlag, New York, 1983.

[255] L. A. Peletier. The porous media equation. In *Applications of nonlinear analysis in the physical sciences (Bielefeld, 1979)*, volume 6 of *Surveys Reference Works Math.*, pages 229–241. Pitman, Boston, Mass.-London, 1981.

[256] B. Perthame. *Transport equations in biology*. Frontiers in Mathematics. Birkhäuser Verlag, Basel, 2007.

[257] B. Pfistner. A one dimensional model for the swarming behaviour of Myxobacteria. In *Biological Motion, Lecture Notes on Biomathematics, 89*, pages 556–563. Springer, 1990.

[258] F. Poupaud and J. Soler. Parabolic limit and stability of the Vlasov-Fokker-Planck system. *Math. Models Methods Appl. Sci.*, 10(7):1027–1045, 2000.

[259] M. Pulvirenti. The weak-coupling limit of large classical and quantum systems. In *International Congress of Mathematicians. Vol. III*, pages 229–256. Eur. Math. Soc., Zürich, 2006.

[260] P. Raphaël and R. Schweyer. On the stability of critical chemotactic aggregation. *Math. Ann.*, 359(1-2):267–377, 2014.

[261] X. Ros-Oton and J. Serra. Regularity theory for general stable operators. *J. Differential Equations*, 260(12):8675–8715, 2016.

[262] W. Rudin. *Real and complex analysis*. McGraw-Hill Book Co., New York, third edition, 1987.

[263] L. Saint-Raymond. *Hydrodynamic limits of the Boltzmann equation*, volume 1971 of *Lecture Notes in Mathematics*. Springer-Verlag, Berlin, 2009.

[264] S. G. Samko, A. A. Kilbas, and O. I. Marichev. *Fractional integrals and derivatives*. Gordon and Breach Science Publishers, Yverdon, 1993. Theory and applications, Edited and with a foreword by S. M. Nikol′skiĭ, Translated from the 1987 Russian original, Revised by the authors.

[265] J. Saragosti, V. Calvez, N. Bournaveas, A. Buguin, P. Silberzan, and B. Perthame. Mathematical description of bacterial traveling pulses. *PLoS Comput. Biol.*, 6(8):e1000890, 12, 2010.

[266] R. L. Schilling and L. Partzsch. *Brownian motion*. De Gruyter Graduate. De Gruyter, Berlin, second edition, 2014. An introduction to stochastic processes, With a chapter on simulation by Björn Böttcher.

[267] S. Serfaty. Large systems with Coulomb interactions: variational study and statistical mechanics. *Port. Math.*, 73(4):247–278, 2016.

[268] W. Sickel. Composition operators acting on Sobolev spaces of fractional order—a survey on sufficient and necessary conditions. In *Function spaces, differential operators and nonlinear analysis (Paseky nad Jizerou, 1995)*, pages 159–182. Prometheus, Prague, 1996.

[269] D. Siegel and E. Talvila. Pointwise growth estimates of the riesz potential. *Dynamics of Continuous, Discrete and Impulsive Systems*, 5:185–194, 1999.

[270] L. Silvestre. Regularity of the obstacle problem for a fractional power of the Laplace operator. *Comm. Pure Appl. Math.*, 60(1):67–112, 2007.

[271] C. Sire and P.-H. Chavanis. Critical dynamics of self-gravitating Langevin particles and bacterial populations. *Phys. Rev. E (3)*, 78(6):061111, 22, 2008.

[272] E. M. Stein. *Singular integrals and differentiability properties of functions*. Princeton Mathematical Series, No. 30. Princeton University Press, Princeton, N.J., 1970.

[273] G. Ströhmer. Stationary states and moving planes. In *Parabolic and Navier-Stokes equations. Part 2*, volume 81 of *Banach Center Publ.*, pages 501–513. Polish Acad. Sci. Inst. Math., Warsaw, 2008.

[274] D. W. Stroock. Some stochastic processes which arise from a model of the motion of a bacterium. 28(4):305–315, 1974.

[275] Y. Sugiyama. Global existence in sub-critical cases and finite time blow-up in super-critical cases to degenerate Keller-Segel systems. *Differential Integral Equations*, 19(8):841–876, 2006.

[276] Y. Sugiyama. Application of the best constant of the Sobolev inequality to degenerate Keller-Segel models. *Adv. Differential Equations*, 12(2):121–144, 2007.

[277] Y. Sugiyama. The global existence and asymptotic behavior of solutions to degenerate quasi-linear parabolic systems of chemotaxis. *Differential Integral Equations*, 20(2):133–180, 2007.

[278] Y. Sugiyama and H. Kunii. Global existence and decay properties for a degenerate Keller-Segel model with a power factor in drift term. *J. Differential Equations*, 227(1):333–364, 2006.

[279] F. Theil. A proof of crystallization in two dimensions. *Comm. Math. Phys.*, 262(1):209–236, 2006.

[280] M. J. Tindall, P. K. Maini, S. L. Porter, and J. P. Armitage. Overview of mathematical approaches used to model bacterial chemotaxis. ii. bacterial populations. *Bull. Math. Biol.*, 70(6):1570–1607, 2008.

[281] C. M. Topaz and A. L. Bertozzi. Swarming patterns in a two-dimensional kinematic model for biological groups. *SIAM J. Appl. Math.*, 65(1):152–174, 2004.

[282] C. M. Topaz, A. L. Bertozzi, and M. A. Lewis. A nonlocal continuum model for biological aggregation. *Bull. Math. Bio.*, 68:1601–1623, 2006.

[283] G. Toscani. Entropy production and the rate of convergence to equilibrium for the Fokker-Planck equation. *Quart. Appl. Math.*, 57(3):521–541, 1999.

[284] G. Toscani. One-dimensional kinetic models of granular flows. *RAIRO Modél. Math. Anal. Numér.*, 34:1277–1291, 2000.

[285] J. Tugaut. Phase transitions of McKean-Vlasov processes in double-wells landscape. *Stochastics*, 86(2):257–284, 2014.

[286] J. L. Vázquez. An introduction to the mathematical theory of the porous medium equation. In *Shape optimization and free boundaries (Montreal, PQ, 1990)*, volume 380 of *NATO Adv. Sci. Inst. Ser. C Math. Phys. Sci.*, pages 347–389. Kluwer Acad. Publ., Dordrecht, 1992.

[287] J. L. Vázquez. *Smoothing and decay estimates for nonlinear diffusion equations*, volume 33 of *Oxford Lecture Series in Mathematics and its Applications*. Oxford University Press, Oxford, 2006. Equations of porous medium type.

[288] J. L. Vázquez. Perspectives in nonlinear diffusion: between analysis, physics and geometry. In *International Congress of Mathematicians. Vol. I*, pages 609–634. Eur. Math. Soc., Zürich, 2007.

[289] J. L. Vázquez. *The porous medium equation*. Oxford Mathematical Monographs. The Clarendon Press, Oxford University Press, Oxford, 2007. Mathematical theory.

[290] F. Venuti, L. Bruno, and N. Bellomo. Crowd dynamics on a moving platform: mathematical modelling and application to lively footbridges. *Mathematical and Computer Modelling*, 45(3-4):252–269, 2007.

[291] C. Villani. On a new class of weak solutions to the spatially homogeneous Boltzmann and Landau equations. *Arch. Rational Mech. Anal.*, 143(3):273–307, 1998.

[292] C. Villani. On the spatially homogeneous Landau equation for Maxwellian molecules. *Math. Models Methods Appl. Sci.*, 8(6):957–983, 1998.

[293] C. Villani. Limites hydrodynamiques de l'équation de Boltzmann (d'après C. Bardos, F. Golse, C. D. Levermore, P.-L. Lions, N. Masmoudi, L. Saint-Raymond). *Astérisque*, (282):Exp. No. 893, ix, 365–405, 2002. Séminaire Bourbaki, Vol. 2000/2001.

[294] C. Villani. A review of mathematical topics in collisional kinetic theory. In *Handbook of mathematical fluid dynamics, Vol. I*, pages 71–305. North-Holland, Amsterdam, 2002.

[295] C. Villani. *Topics in optimal transportation*, volume 58 of *Graduate Studies in Mathematics*. American Mathematical Society, Providence, RI, 2003.

[296] C. Villani. Hypocoercive diffusion operators. In *International Congress of Mathematicians. Vol. III*, pages 473–498. Eur. Math. Soc., Zürich, 2006.

[297] C. Villani. *Optimal transport, old and new*. Lecture Notes for the 2005 Saint-Flour summer school. Springer, 2007.

[298] C. Villani. Hypocoercivity. *Mem. Amer. Math. Soc.*, 202(950):iv+141, 2009.

[299] J. von Goethe, W. von Biedermann, and G. Sophie. *Goethes Briefe: Anfang 1804-9. Mai 1805*. Goethes Briefe. H. Böhlau, 1895.

[300] D. V. Widder. *The heat equation*. Academic Press [Harcourt Brace Jovanovich, Publishers], New York-London, 1975. Pure and Applied Mathematics, Vol. 67.

[301] C. Xue, H. J. Hwang, K. J. Painter, and R. Erban. Travelling waves in hyperbolic chemotaxis equations. *Bull. Math. Biol.*, 73(8):1695–1733, 2011.

[302] Y. Yao. Asymptotic behavior for critical Patlak-Keller-Segel model and a repulsive-attractive aggregation equation. *Ann. Inst. H. Poincaré Anal. Non Linéaire*, 31(1):81–101, 2014.

[303] I. Zel'dovich and Y. Raizer. *Physics of Shock Waves and High-Temperature Hydrodynamic Phenomena*. Dover Books on Physics. Dover Publications, 2002.

[304] Y. B. Zel'dovich and A. Kompaneets. Towards a theory of heat conduction with thermal conductivity depending on the temperature. *Collection of papers dedicated to 70th Anniversary of A. F. Ioffe*, pages 61–72, 1950.